# Controls on fluvial sedimentary architecture and sediment fill-state in salt-walled mini-basins

Steven Gordon Banham

Submitted in accordance with the requirements for the degree of Doctor of Philosophy

University of Leeds
School of Earth and Environment
October 2013

## Intellectual Property and Publication Statements

The candidate confirms that the work submitted is his own and that appropriate credit has been given where reference has been made to the work of others.

This copy has been supplied on the understanding that it is copyright material and that no quotation from the thesis may be published without proper acknowledgement.

© 2013 The University of Leeds and Steven G. Banham

# Acknowledgements

Firstly I would like to thank my supervisors Dr Nigel Mountney, and Prof. Bill McCaffrey for giving me this opportunity to do a PhD, and for their support and encouragement throughout the duration. I would like to give Nige additional thanks for the untold hours he spent proof reading then correcting (and re-correcting) my poor English.

Additionally, I thank my viva panel, Stephen Flint (University of Manchester) and Jeffrey Peakall (University of Leeds) for their feedback, candour, and making the task pain-free.

I would like to thank the sponsors of the Fluvial Research Group (Areva, BHP Billiton, ConocoPhillips, Nexen, Saudi Aramco, Shell & Woodside) and the University of Leeds for providing me with the funding to carry out this research.

I wish to give my gratitude to the people who I spent time with in the field with over the 6 months I spent in Utah. Their abundant humour and tolerance made field work a memorable experience. Jo Venus, Layla Cartwright, Hollie Romain, Tom Randles, Luca Colombera, Sally Molyneux, Stu Clarke, and Austin Shock all made this field work memorable. I wish to give special thanks to: Jo Venus, who seemed to know everyone in Moab, for initial guidance plus the hours of entertainment with various “songs” and memorable experiences throughout the duration of field work; and Layla Cartwright for acting as my field assistant during my first field season.

I am grateful to all the geologist that we met in the field, particularly to Bruce Trudgill, who knows how to operate a barbeque! Additional thanks is given to the people of Castle Valley, the Rancher in Fisher Valley, and the various people in Moab who allowed us to access outcrop through their properties.

Thanks to the Level 7 & SCR people who made the non-field work side of the PhD interesting and certainly humors: Alan Wood, Jess Ross, Rachael Dale, Kat Hunter, and Team Pembroke – Graham McLeod and James Witts. Julie Boyce is thanked for proof reading papers and “chatting science”.

Finally, I could not have completed this PhD without the support of my parents, Christopher and Patricia, who have tolerated my being an “idle student for plenty long enough” and supported me financially throughout my extremely long education.

## Preface

Each of the main chapters within this thesis (Chapters 2, 3, and 4) were written as papers which were submitted to various geoscience journals for publication, and thus they are stand alone pieces of work. The literature review and background sections within these chapters are focused at a particular aspect relating to the study (e.g. sedimentology, or halokinesis), and as a result of the common theme of the papers, do overlap. This should assist the reader by presenting the most relevant information pertaining to the subject to be discussed.

## Publications (at time of submission):

**Banham, S.G., and Mountney, N.P.** (2013): "Controls on fluvial sedimentary architecture and sediment fill state in salt walled mini basins: Triassic Moenkopi Formation, Salt Anticline Region, SE Utah, USA." *Basin Research*. Article first published online: 25 MAY 2013. DOI: 10.1111/bre.12022.

**Banham, S.G., and Mountney, N.P.** (2013) "Climatic versus halokinetic control on sedimentation in a dryland fluvial succession." *Sedimentology*. Article first published online: 24 AUG 2013. DOI: 10.1111/sed.12064

**Banham, S.G., and Mountney, N.P.** (2013) "Evolution of fluvial systems in salt-walled mini-basins: A review and new insights." *Sedimentary Geology*. Volume 296, 15 October 2013, 142–166.

# Abstract

Halokinesis and climate can exert strong controls on the accumulation of fluvial stratigraphy within a series of salt walled mini-basins, which can be expressed as a number subtle features within the preserved stratigraphic record:

- Control of drainage networks entering the region of halokinetic influence. Drainage pathway can be diverted or deflected by uplifted salt walls, or alternatively, become entrenched in areas of enhanced subsidence.
- Drainage diversion can lead to drainage isolation of mini-basins, resulting in the accumulation of sand-poor basin-fill styles within mini-basins isolated from the main drainage pathways. Conversely, basins which act as the main conduit to drainage may become preferentially sand-prone relative to adjacent basins
- The interplay of sediment supply rates and subsidence rates can control the accumulating stratigraphic style, where the interplay between subsidence rates and sediment supply rate can result in the accumulation of sand-prone or sand-poor basin-fills.
- The interplay between halokinesis and climate can be delineated by local (inter- to intra-basin scale) and regional (halokinetic province scale) variations of sediment distribution and accumulation: halokinesis redistributes drainage pathways and sediments between basins, where as climate is expressed as variations in sediment accumulation style across the halokinetic region.

This study uses the Triassic Moenkopi Formation which accumulated within the Salt Anticline Region of southeast Utah, USA, to demonstrate the extent to which halokinesis and climate controlled the ensuing stratigraphic accumulation of a low relief dryland fluvial system within a series of actively subsiding salt-walled mini-basins. This knowledge can be used for predicting distribution of fluvial elements within subsurface halokinetic provinces for the purpose of hydrocarbon exploration.

# Contents


**1. Introduction** **1**

1.1 Project Rationale 1
1.2 Aims and Objectives: Key Research Questions 2
1.3 Data Collection & Field Techniques 3
1.3.1 Database 3
1.3.2 Field Techniques 3
1.3.2.1 Vertical Graphical Profiles: Sedimentary Logs 3
1.3.2.2 Architectural Diagrams 6
1.3.2.3 Paleocurrent Analysis 6
1.4 Brief overview of the Paradox Basin, Salt Anticline Region & White Canyon Region 6
1.5 Outcrop expression of the Moenkopi Formation 10
1.5.1 Outcrop Expression: Salt Anticline Region 14
1.5.2 Outcrop Expression: White Canyon Region 19
1.6 Thesis Structure 23

**2. Evolution of fluvial systems in salt-walled mini-basins: a review and new insights** **28**

2.0 Abstract 28
2.1 Introduction 29
Terminology 32
2.3 Controls on the style of stratigraphic in-fill of salt-walled mini-basins 35
2.3.1 Initiation of salt-walled mini-basins 35
2.3.2 Parameters controlling subsidence and sedimentation rate 40
Static parameters 40
Dynamic parameters 44
Fluvial Interactions 46
Mini-basin sediment-fill style 48
2.4 Case Studies 51
2.4.1 Salt Anticline Region, SE Utah 51
The Cutler Group 54
The Moenkopi Formation 58
The Chinle Formation 60
2.4.2 Pre-Caspian Basin 62
2.4.3 North Sea – J Block/Skagerrak Formation 66
2.4.4 La Popa Basin 70
2.5 Discussion 74
Evolution of Fluvial Systems in salt-walled mini-basins 76
Gaps in understanding 86
2.6 Conclusions 87

**3. Climatic versus halokinetic control on sedimentation in a dryland fluvial succession 89**

3.0 Abstract 89
3.1 Introduction 90
3.2 Background 97
3.3 Geological Setting 98
3.4 Data and Methods 101
3.5 Sedimentology and Stratigraphy 102
3.5.1 Lithofacies 102
3.5.2 Architectural Elements 102
Multi-storey, multi-lateral channel-fill elements (F1) 110
Single-storey, multi-lateral channel-fill elements (F2) 114
Single-storey unilateral (isolated) channel-fill elements with abundant infraformational clasts (F3) 116
Massive & horizontally laminated channel elements (F4) 119
Sheet-like heterolithic elements (F5) 119
Gypsum-clast-bearing elements (F6) 120
Partly confined over-spill element (F7) 121
Chute elements with coarse-grained fill (F8) 122
Floodplain pond elements (F9) 123
3.6 Spatial & Temporal Variations in Sedimentary Architecture 123
3.6.1 Salt Anticline Region 124
Tenderfoot Member 125
Ali Baba Member 126
Sewemup Member 128
Parriott Member 128
Palaeocurrent data and sediment provenance 130
3.6.2 White Canyon Region 132
Hoskinnini Member 135
Torrey Member 135
Palaeocurrent data and sediment provenance 136
3.7 Discussion 136
Environment of deposition 137
Halokinetic control on sediment accumulation 139
Climatic Control on sediment accumulation 140
3.8 Conclusions 142
3.9 Facies Annex 145

**4. Controls on fluvial sedimentary architecture and sediment-fill state in salt-walled mini-basins: Triassic Moenkopi Formation, Salt Anticline Region, SE Utah, USA 163**

4.0 Abstract 163
4.1 Introduction 164
4.2 Background and Geological Setting 167
4.3 Methods and Data Collection 174
4.4 Styles of mini-basin fill 174
4.4.1 The Fisher Basin 194
4.4.2 The Parriott Basin 198
4.4.3 The Big Bend Basin 201
4.5 Styles of salt-wall and sediment interaction 198
4.5.1 The Fisher Valley salt wall and Onion Creek salt diapir 203
4.5.2 The Castle Valley salt wall 204
4.5.3 Cache Valley salt-wall 208
4.6 Tectono-stratigraphic model 208
4.6.1 Tenderfoot Member 221
4.6.2 Ali Baba Member 222
4.6.3 Sewemup Member 222
4.6.4 Parriott Member 223
4.7 Discussion 224
4.8 Conclusions 229

**5. Discussion 232**

5.0 Overview1 332
5.1 Moenkopi Formation and Paradox Basin 232
5.2.1 Paradox Basin Geometry 233
5.2.2 Cutler (Pre-Moenkopi) Basin Fill 233
5.2.3 Moenkopi Basin Fill Evolution 236
5.3 Generic Implications 245
5.3.1 Basin Fill 246
5.3.2 Basin-fill geometries 246
5.3.3 Basin fill style 248
5.4 Basin segregation 251
5.5 Climatic Signature 259
5.6 Expression of Climate and Halokinesis 259
5.7 Applications to industry 267
5.7.1 Predicting sand distribution 268
5.7.2 Climate change in wells 271
5.8 Conclusions 273

**6. Conclusions & Further Work** **275**
6.1 Research Questions 275
6.1.1 What is the sedimentary expression of the Moenkopi Formation of SE Utah: a low relief dryland fluvial system which accumulated in an arid to hyper-arid continental setting? 277
6.1.2 What influence did syn-sedimentation halokinesis have on the distribution of the drainage pathways and the ensuing preserved stratigraphic accumulation of the fluvial system? 277
6.1.3 Can the signature of climatic variations be discerned from that of the signature of halokinesis? 278
6.1.4 Can the synthesis of data from questions 1-3, plus the synthesis of other studies be used to develop a reliable model for both axial and transverse draining fluvial systems accumulating in salt-walled mini-basins? 279
6.2 Final Conclusions 280
6.3 Further Work 282

**7. Reference** **286**

**8. Appendix** **307**

# 1. Introduction

---

*This chapter sets out the aims and objectives of the thesis, and describes its structure. The key research questions that are used to meet the specific work objectives are introduced, and the methods used to address these research questions are also introduced.*
*Brief introductory summaries regarding the geological evolution of the Paradox Basin and the outcrop expression of the Moenkopi Formation in the Salt Anticline Region and White Canyon Region are presented.*

---

## *1.1 Project Rationale*

The majority of studies concerned with the style of interaction between halokinesis and sediment accumulation have, to date, focused principally on basin-scale fill geometries and large-scale stratal architectural relationships within successions accumulated within salt-bounded mini-basins (e.g. Barde *et al.*, 2002a; Kluth & DuChene, 2009; Trudgill, 2011). Typically, such studies include only limited primary sedimentological data and these are chiefly derived from seismic and well data, which restricts the resolution of the study in terms of detailed observations regarding sedimentological relationships (Hodgson *et al.*, 1992; Barde *et al.*, 2002b). Subsurface seismic and well-log data are typically of rather low spatial resolution and this has historically had a limiting effect on understanding key aspects of salt-basin evolution, such as the development of predictive models for lithofacies and architectural-element distributions and the styles of interaction between active fluvial systems and coevally uplifting salt walls at mini-basin margins. Furthermore, the majority of past studies have typically focused on a single mini-basin, limiting the understanding of sediment routing throughout broader halokinetic provinces.

The aim of this study is to address these shortcomings through a detailed analysis of the preserved expression of a fluvial system that accumulated in a series of adjoining mini-basins within a major halokinetic

province, and compare the succession to that of the same fluvial system preserved in an area outside the region of salt deformation to determine the role played by halokinesis in influencing accumulated fluvial style. In addition, this study demonstrates the preserved sedimentary signature of climatic controls that acted upon the fluvial system and presents a series of observations with which to discern the relative roles of halokinesis and climate as primary allogenic controls on fluvial sedimentation. To achieve these aims, a set of detailed sedimentary vertical graphic profiles (logs) and architectural-element analysis panels have been recorded across a halokinetic province to better understand the spatial distribution of preserved fluvial elements and their relationship to bounding salt walls.

This project investigates the sedimentology of the Triassic Moenkopi Formation within the Salt Anticline Region of south eastern Utah to understand the relationship between halokinesis and sediment supply and how the interaction of these two factors control the distribution of axial-draining fluvial systems within salt-walled mini-basins and the ensuing succession preserved in the stratigraphic record. This project complements a recent study conducted by Joanne Venus (2013), which investigated the evolution of the underlying Undifferentiated Cutler Group in response to halokinesis where fluvial systems drained transverse to the uplifting salt walls.

## *1.2 Aims and Objectives: Key Research Questions*

The aim of this study is to demonstrate the influence of ongoing halokinesis and the controls it can exert on accumulating fluvial stratigraphy. In addition, this study considers the influence of climate on sediment accumulation, and how this can be delineated from the expression of halokinesis. Specifically, this project seeks to address these research issues through consideration of the following specific research questions:

1. What is the sedimentary expression of the fluvial deposits of the Triassic Moenkopi Formation of SE Utah, a succession that records the depositional history of a low-relief, dryland fluvial system that accumulated in an arid to hyper-arid continental setting?
2. What influence did syn-sedimentary halokinesis have on the distribution of the drainage pathways and the ensuing preserved

stratigraphic accumulation of the fluvial system represented by the Moenkopi Formation?

3. Can the signature of climatic variations be discerned from the effects of halokinesis?
4. Can the synthesis of data arising from analysis of questions 1-3 be combined with a suite of data derived from other similar studies to develop a reliable set of models for predicting likely preserved depositional architectures in both axial- and transverse-draining fluvial systems accumulating in salt-walled mini-basins?
5. How can a stochastic modelling workflow be designed and implemented to predict fluvial sand-body connectivity within a series of salt-walled mini-basins?

## *1.3 Data Collection & Field Techniques*

### 1.3.1 Database

Data for this project were collected during 4 separate field seasons between 2010 and 2011, totalling approximately 6 months of work in the field. Field work was carried out in South East Utah, in both the Salt Anticline Region and in the White Canyon Region (Fig 1.1).

Additional literature-derived data related directly to the Salt Anticline Region, together with that related to case studies of other halokinetic provinces are reviewed and presented in Chapter 2. These additional data complement the primary field-derived data set collected as an integral part of this study.

### 1.3.2 Field Techniques

*1.3.2.1 Vertical Graphical Profiles: Sedimentary Logs*

In total, 52 sections were measured across the Salt Anticline Region, recording a total of approximately 9000 m of sedimentary succession. Of these logs, 38 sections were measured within the main study area centred on exposures of the Moenkopi Formation around the Fisher Valley, Castle Valley, and Cache Valley salt walls (Fig 1.2). The remaining 14 logs were collected around the Cane Creek Anticline, and south west of the Moab Valley Salt Wall. Of the 38 logs recorded in the Main Salt Anticline Region study area, 22

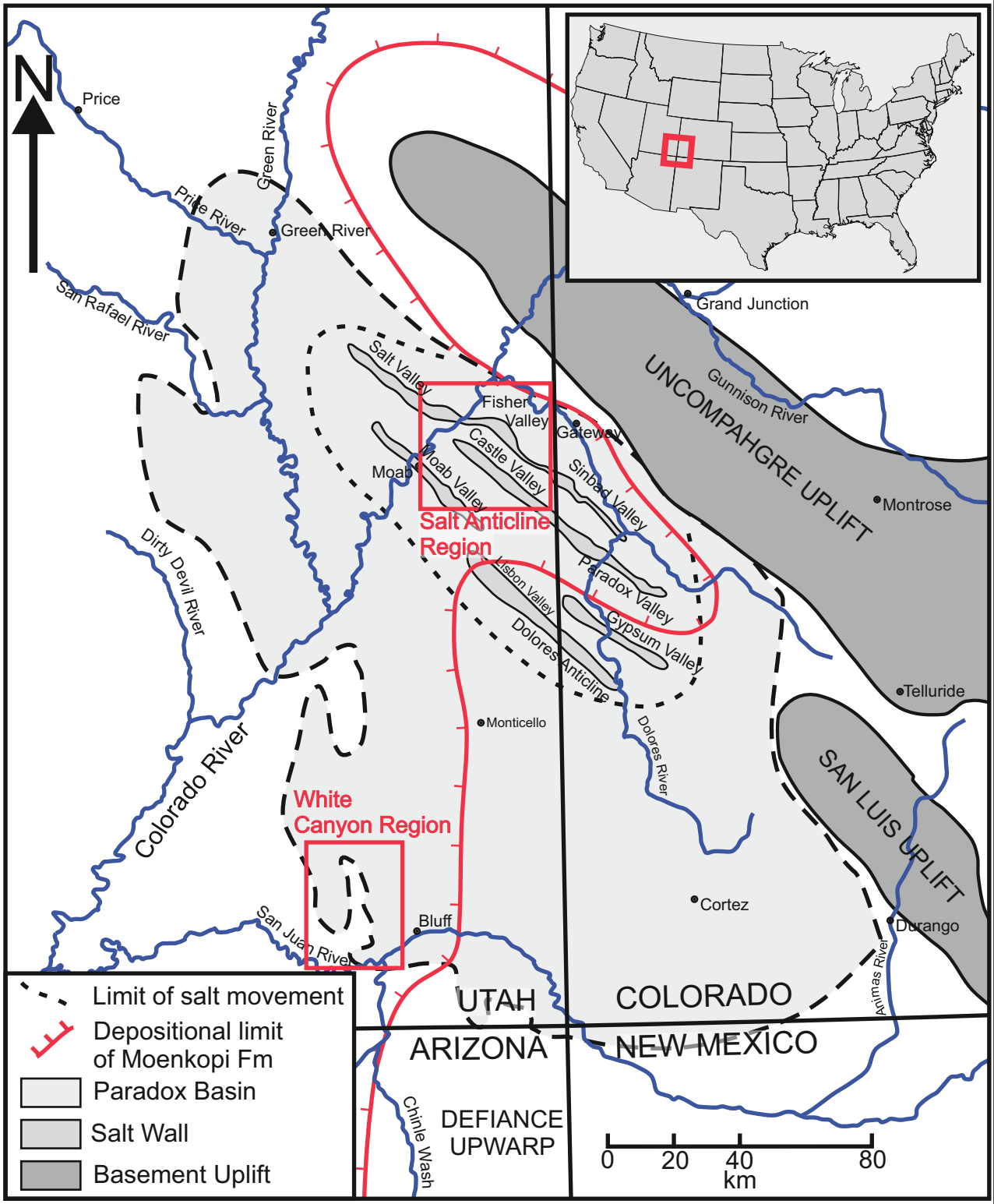


**Figure 1.1**: Overview map of the Paradox Basin, the location of the Salt Anticline Region and the two study areas referred to in this work. (After Trudgill, 2011).

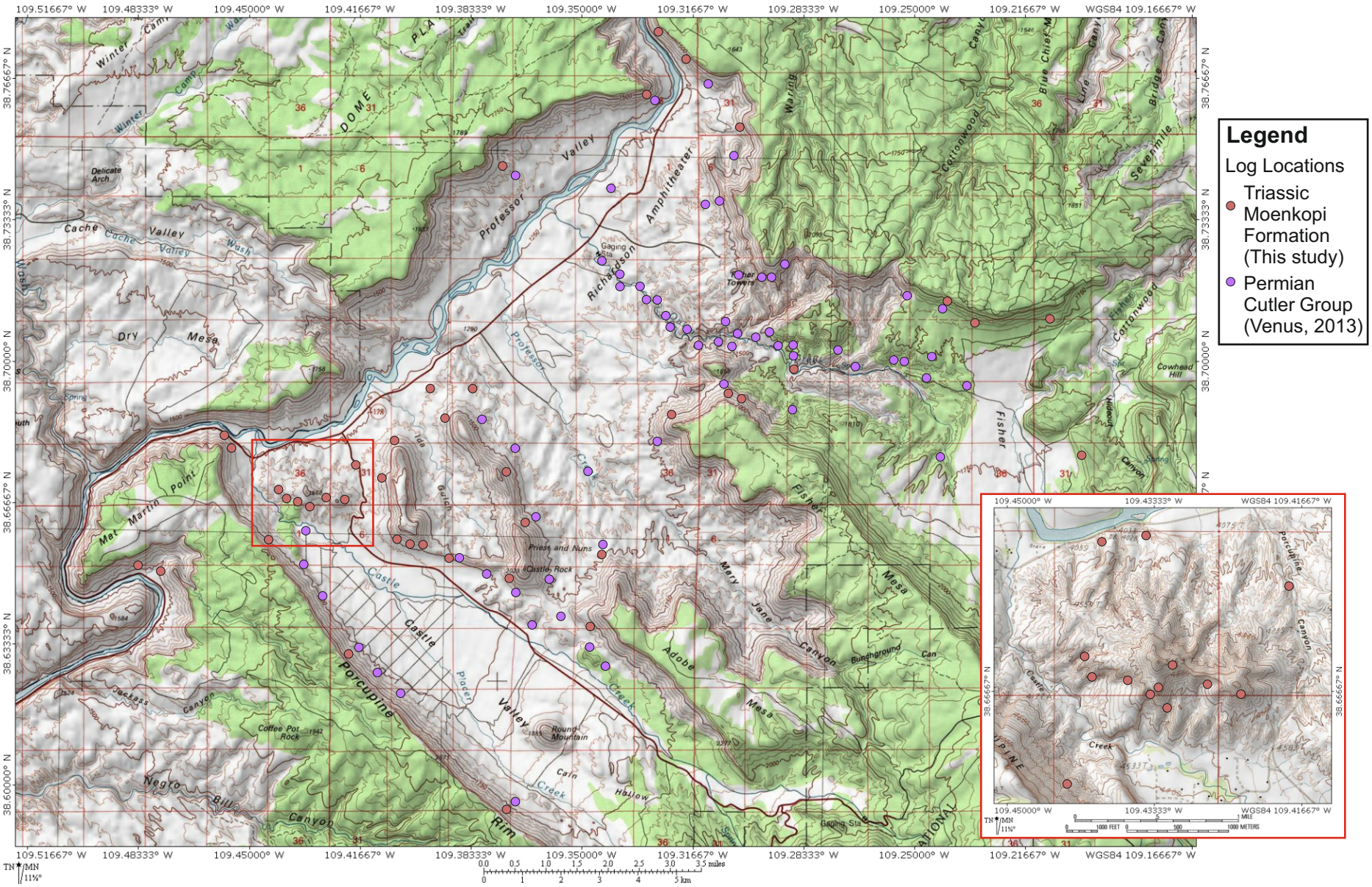


**Figure 1.2**: Map of the Salt Anticline Region displaying log locations collected by Banham (Moenkopi Formation) and Venus (Cutler Group) in 2010 and 2011. These logs form only a subset of the total dataset collected from the wider Paradox Basin region (See appendix for logs).

measured sections recorded the full succession of the Moenkopi Formation from the basal contract with the underlying Permian Cutler Group, through to the unconformable contact with the overlaying Upper Triassic Chinle Formation.

In addition, 11 sedimentary logs were measured in the White Canyon Region of SE Utah, all of which recorded the full succession of the Torrey Member of the Moenkopi Formation from the basal contact with the underlying Hoskinnini Member, or Organ Rock Formation (where the Hoskinnini Member was absent) through to the overlying Chinle Formation (Fig 1.3).

*1.3.2.2 Architectural Diagrams*

Architectural panels have been generated from photographs and photomontages to determine the distribution and relations of fluvial architectural elements both within the Salt Anticline Region and in the White Canyon Region. These panels have been constructed by lateral tracing and correlation of key surfaces in the field by walking out key stratal surfaces; such observations are supported by analyses of high-resolution photomontages. Architectural panels have been tied to measured sections to enable the generation of a series of models with which to depict important tectono-stratigraphic relationships.

*1.3.2.3 Palaeocurrent Analysis*

Palaeocurrent data have been collected to determine spatial and temporal trends in drainage direction within both the principal study areas. One-hundred and seventy-seven palaeocurrent indicators were collected within the Salt Anticline Region and 56 were recorded from the White Canyon Region. These palaeocurrent data were collected from a range of sedimentary structures including ripple crests, climbing-ripple strata, cross-bedding foreset azimuths and channel axes.

## *1.4 Brief overview of the Paradox Basin, Salt Anticline Region & White Canyon Region*

The Salt Anticline Region formed within the Paradox Basin which is located across the present day Utah-Colorado border. The Paradox Basin, is interpreted to be an asymmetric basin which developed in response to loading

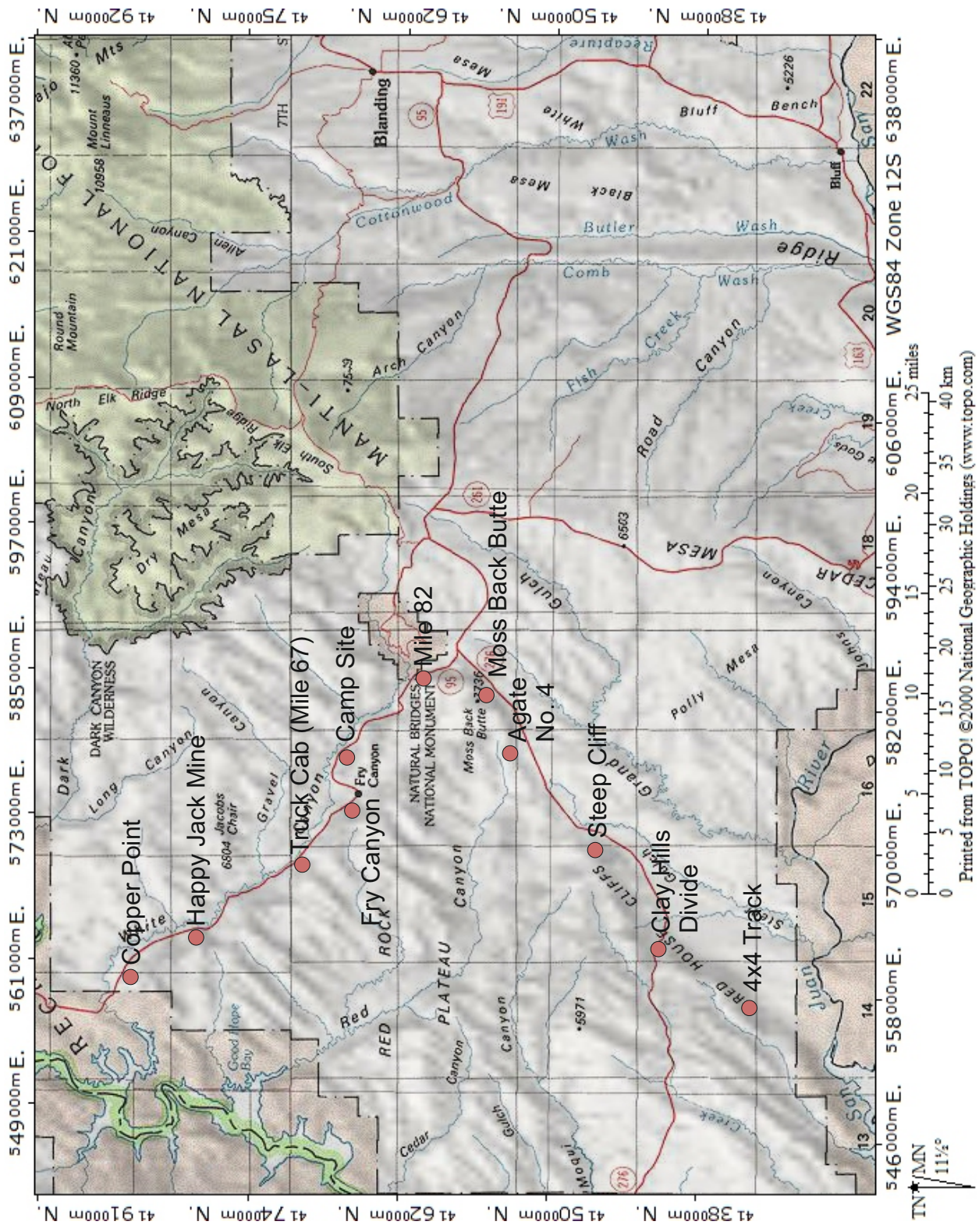


**Figure 1.3**: Location map of White Canyon study area displaying log locations collected in November 2010. These logs form only a subset of the total dataset collected from the wider Paradox Basin region. See Fig 1.1 for location in relation to the SAR. See appendix for logs.

of the lithosphere by the uplifting Uncompahgre Front (Fig 1.4, Trudgill, 2011). The Uncompahgre Uplift formed during the Pennsylvanian-Permian Ancestral Rocky Mountain orogenic event as one of several late Palaeozoic features developed across what is now the southwest United States (Baker *et al.*, 1933; Ohlen & McIntyre, 1965; Kluth & Coney, 1981; Baars, 1986; Barbeau, 2003). The Paradox Basin developed in response to loading and downwarping of the crust by the mass of the Uncompahgre Front. The Uncompahgre Uplift was approximately 145 km long, and elongate in a northwest to southeast orientation over an area that straddled the Colorado–Utah Border (Elston *et al.,* 1962). During this initial phase of evolution, the Paradox Basin was repeatedly flooded by a series of marine incursions associated with eustatic sea-level changes, and these resulted in the accumulation of mixed continental and marine deposits of the Hermosa Group (Goldhammer, *et al.*, 1991, Blakey & Ranney, 2008). During this time, the basin became repeatedly isolated from the regional sea-way, resulting in a progressive increase in salinity in response to on-going progressive desiccation and episodic recharge, culminating in the accumulation of a 2000-2500 m thick succession of mixed salt, carbonate and black shales of the Paradox Formation (Doelling, 1988; Trudgill, 2011). During the early Permian a growing alluvial wedge prograded southwest-wards into the basin as detritus was shed from the growing Uncompahgre Uplift. However, growth of this large alluvial megafan (distributive fluvial system, *sensu* Hartley *et al.*, 2010; Weissmann *et al.*, 2011) was periodically interrupted by marine incursions into the basin, as recorded within deposits of the Honaker Trail Formation of the Hermosa Group, and the overlying lower Cutler beds (Blakey, 2009; Jordan & Mountney, 2010). During the late Permian, degradation of the Uncompahgre Uplift resulted in the shedding of a large volume of detritus southwest-ward into the foredeep of the developing Paradox Basin, and this accumulated to in excess of 4,000 m thickness, to form deposits of the south-westerly prograding Cutler Undivided Megafan, (Eliston *et al.*, 1962; Barbeau, 2003).

Initial movement of salt of the Paradox Formation occurred in response to loading by the Honaker Trail Formation and lower Cutler Beds during the late-Pensylvanian or early Permian (Trudgill, 2004). Halokinesis continued

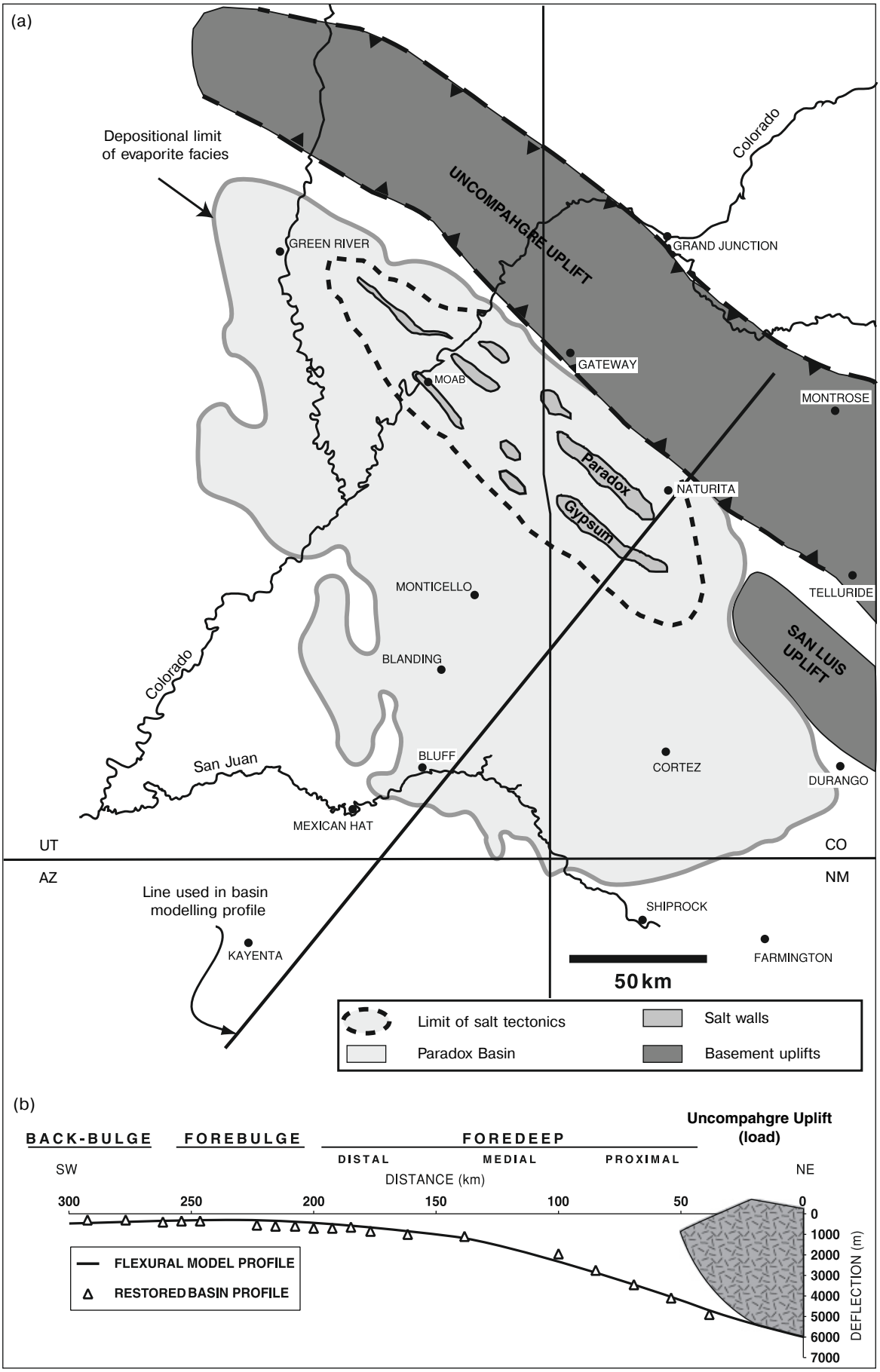


**Figure 1.4**: Overview map and cross section depicting the geometry of the Paradox Basin (Trudgill, 2011).

throughout the Permian, controlling the pattern of sedimentation in the accumulating Undivided Cutler Group (Venus, 2013). Salt movement continued throughout the Triassic, albeit at an apparently diminished rate, influencing accumulation of the Lower Triassic Moenkopi Formation (Banham & Mountney, 2012a) and the Upper Triassic Chinle Formation (Matthews *et al.*, 2007) before largely abating during the Jurassic, after influencing deposition of the Kayenta Formation to only a modest extent (Bromley, 1981; Kluth & DuChene, 2009; Trudgill, 2011). Salt deformation was most prevalent in the foredeep of the basin, where the preserved thickness of salt of the Paradox Formation attained a maximum (~4000 m) and overburden was greatest (Jones, 1959).

Accumulation of the so-called undivided Cutler Group (Newberry, 1861) plays an important role in subsidence potential and distribution of depocentres during the later deposition of the Moenkopi Formation in the Salt Anticline Region. Within the White Canyon Region, in the more distal parts of the Paradox Basin, the Moenkopi Formation overlays the distal part of the Cutler Group which consists of the Organ Rock Formation and the White Rim sandstone (Fig. 1.5).

## *1.5 Outcrop expression of the Moenkopi Formation*

The Moenkopi Formation, which was first described by Ward (1901), has been recorded across wide area of the mid-west and southwest of the United States (Ward, 1901; Darton, 1910; Gregory, 1917; Stewart, 1959; Cater, 1970; Stewart *et al.*, 1972; Blakey, 1974, 1989). Outcrops of the Moenkopi Formation, and related lateral equivalents, are known from the States of Colorado, New Mexico, Arizona, Nevada, California, Utah and Wyoming (Stuart *et al.*, 1972). In total there are in excess of 20 formally defined members of the Moenkopi Formation (Stuart *et al.*, 1972; Blakey, 1974, 1989), of which several are defined based on spatial and temporal relationships and changes in characteristic lithofacies compositions related to subtle variations in the palaeoenvironments of deposition during the early Triassic, which varied from marine facies (e.g. Sinbad Limestone), through to fluvial-dominated continental red beds (e.g. Parriott Member). This study focuses on two specific areas: the Salt Anticline Region, central and eastern

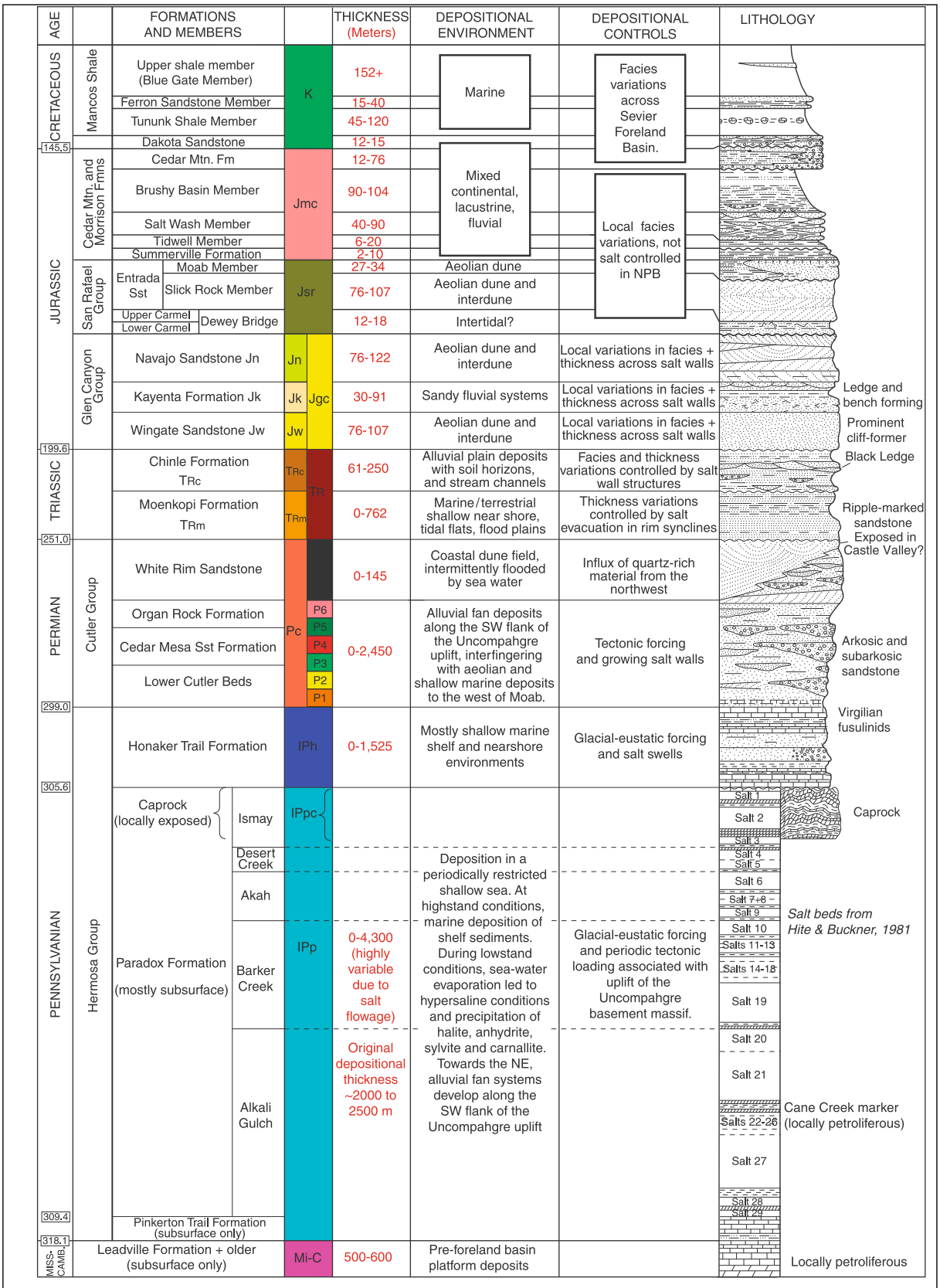


**Figure 1.5**: Stratigraphic column depicting the units and the depositional environments which accumulated within the Paradox basin (Trudgill, 2011).

Utah; and the White Canyon Region, southeast Utah. The preserved thickness of the Moenkopi Formation varies dramatically within the Salt Anticline Region, with maximum thickness observed within a single mini-basin ranging from 125 m to 245 m thick, and diminishing to <20 m over the crests of some salt walls, where only preserved remnants of the formation have been observed. The preserved thickness of the Moenkopi Formation varies to a lesser extent within the White Canyon Region, where it ranges from 45 to 64 m (excluding the Hoskinnini Member, which was not logged due to time constraints during the White Canyon Region field season, which is 30 m thick where present). Deposits of the Moenkopi Formation in both the Salt Anticline Region and the White Canyon regions are interpreted to be fully continental, with no convincing evidence for marine influence (Blakey & Raney, 2008; Banham & Mountney, 2013a) (Fig 1.6).

Key members of the Moenkopi Formation observed in this study include: the Tenderfoot, Ali Baba, Sewemup and Parriott members within the Salt Anticline Region, and the Hoskinnini and Torrey members in the White Canyon Region. The Tenderfoot Member and Hoskinnini Member have been demonstrated to share many common features, and have been interpreted to be lateral equivalents (Stewart, 1959; Doelling & Chisney, 2008) although the nature of the association has been disputed (Blakey, 1974). Correlation between the other members of the Moenkopi Formation between the two regions are tentative, at best, because each is characterised by significantly different lithofacies assemblages, architectural styles, preserved thicknesses and sediment provenance. A tentative correlation could be extended between the Ali Baba Member in the Salt Anticline Region to the informal (Stewart *et al., 1972)* lower-slope forming member and cliff-forming member within the White Canyon Region, due in part to their similar outcrop expression. Palaeocurrents determined from analysis of sedimentary structures preserved in sandy macro- and micro-bedforms indicate a general palaeodrainage direction of the fluvial systems of the Moenkopi Formation from the southeast, and towards the northwest.

Given that the Moenkopi Formation is characterised by many common lithofacies, architectural elements, and architectural arrangements across both the Salt Anticline Region and the White Canyon Region, both can be

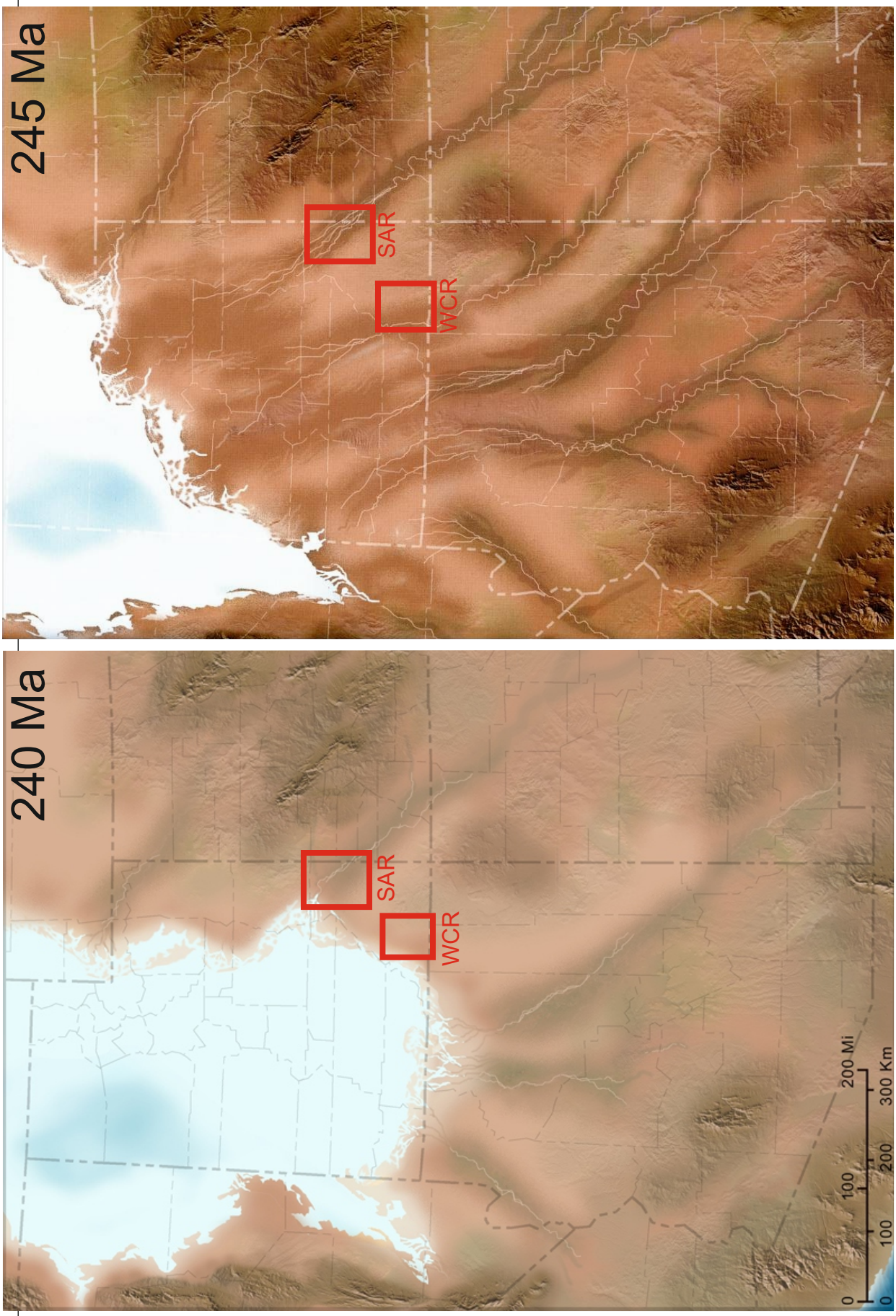


**Figure 1.6**: Palaeogeographic map of the Four Corners region. Early and late Anisian times (245 Ma and 240 Ma): Broad low-relief alluvial plains are present in the southwest of Utah; these alluvial systems pass northwestwards into a series of broad coastal plains and a marine embayment. The maps depict the gradual retreat of the Kaibab sea-way throughout deposition of the Moenkopi Formation. After Blakey & Ranney (2009).

compared to discern the influence of halokinesis on the preserved expression of a dryland fluvial system.

### 1.4.1 Outcrop Expression: Salt Anticline Region

For this study, The Moenkopi Formation was studied in the three mini basins closest to the Uncompahgre front: the Fisher Basin, Parriott Basin, and the Big Bend Basin. These basins were chosen due to their continuity, the abundance of outcrop exposure within them due to sparse vegetation, and because the amplitude of the salt walls increased the chance of drainage diversion and basin isolation. The Moenkopi Formation within the Salt Anticline Region is divided into four Members (in stratigraphic order): the Tenderfoot; Ali Baba; Sewemup; and Parriott members (Fig 1.7). The Moenkopi Formation unconformably overlies the Undivided Cuter Group, typically with an angular discordance, which can be up to 30° adjacent to salt-wall margins. In mini-basin centres, the angular discordance is usually less, and can be difficult to distinguish in outcrop (Fig 1.8). A diagnostic feature at the base of the Tenderfoot is a distinctive gypsum bed, which is present across three studied salt-walled mini-basins, although is heavily denuded and degraded in the Fisher Basin (Fig 1.9). Within the Fisher Valley – Cache Valley salt wall transition zone, the Tenderfoot Member contains a number of enigmatic dewatering structures which form a polygonal network across several discrete horizons.

The expression of the basal Tenderfoot Member is variable across the basins, and is typically characterised by a thicker cliff-forming succession in the Fisher Basin (Fig 1.10) and a thinner slope-forming unit within the Parriott Basin. Within the Big Bend Basin, the Tenderfoot Member exhibits both slope-forming, and cliff-forming characteristics. The Tenderfoot as a whole has a characteristic orange colour, which contrasts with the underlying purple colour of the Undivided Cutler Group. The Ali Baba Member has a variable expression across the Salt Anticline Region: the base of this member within the Fisher Basin is delineated by the accumulation of amalgamated channel-fill elements, which are typically cliff forming (Figs 1.10, 1.11). Within the Parriott Basin, the Ali Baba Member is expressed as a cliff-forming succession consisting of heterolithic sheet-like elements, with a laterally

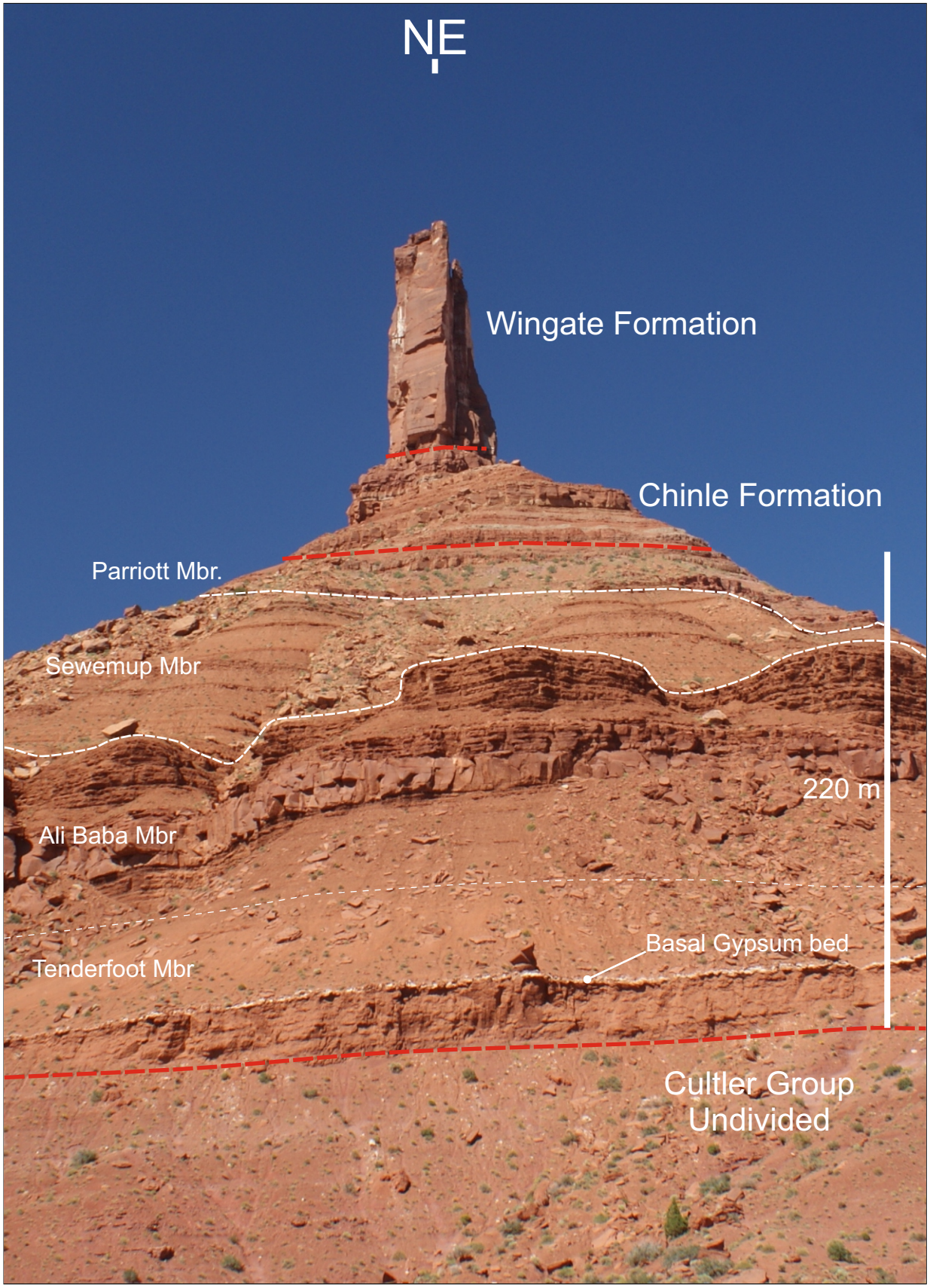


**Figure 1.7**: Outcrop expression of the stratigraphy in the Paradox Basin at Castleton Tower, Castle Valley. The various members of the Moenkopi Formation are clearly recognisable in this region.

Location: 38.645294°, -109.373744°

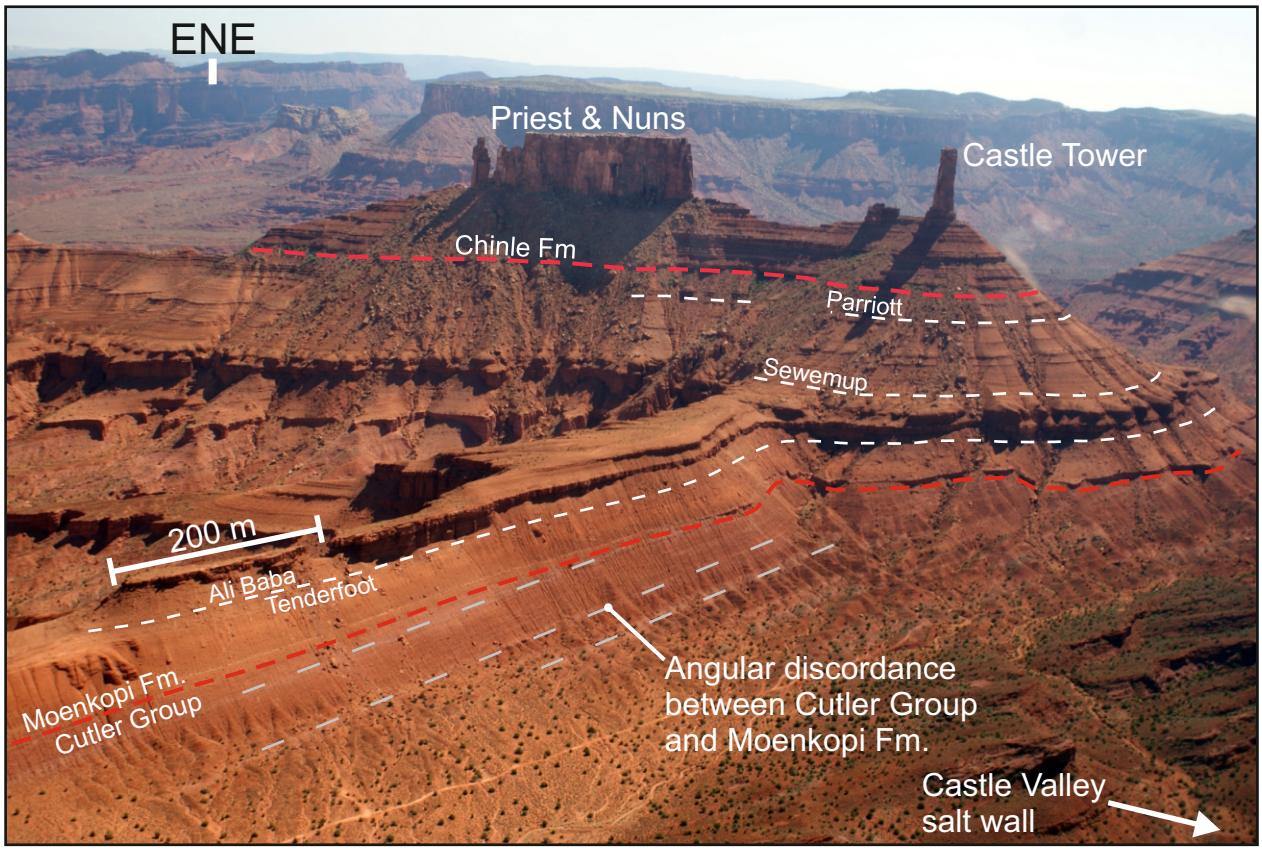


**Figures 1.8**: Angular unconformity between the Cutler Group and Moenkopi Formation Location: 38.648361°, -109.396768°, facing NW.

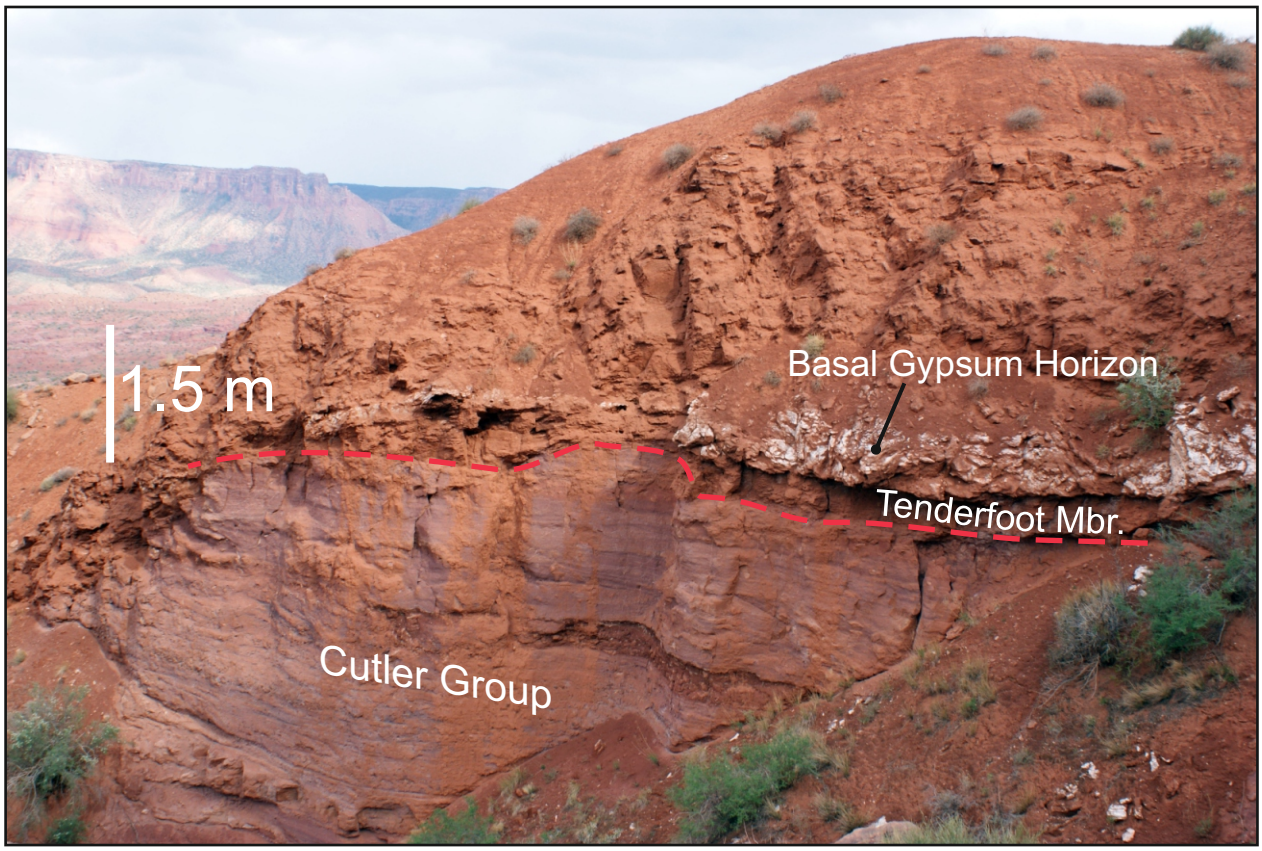


**Figure 1.9**: Typical outcrop expression of the Basal Gypsum Bed within the Parriott Basin.

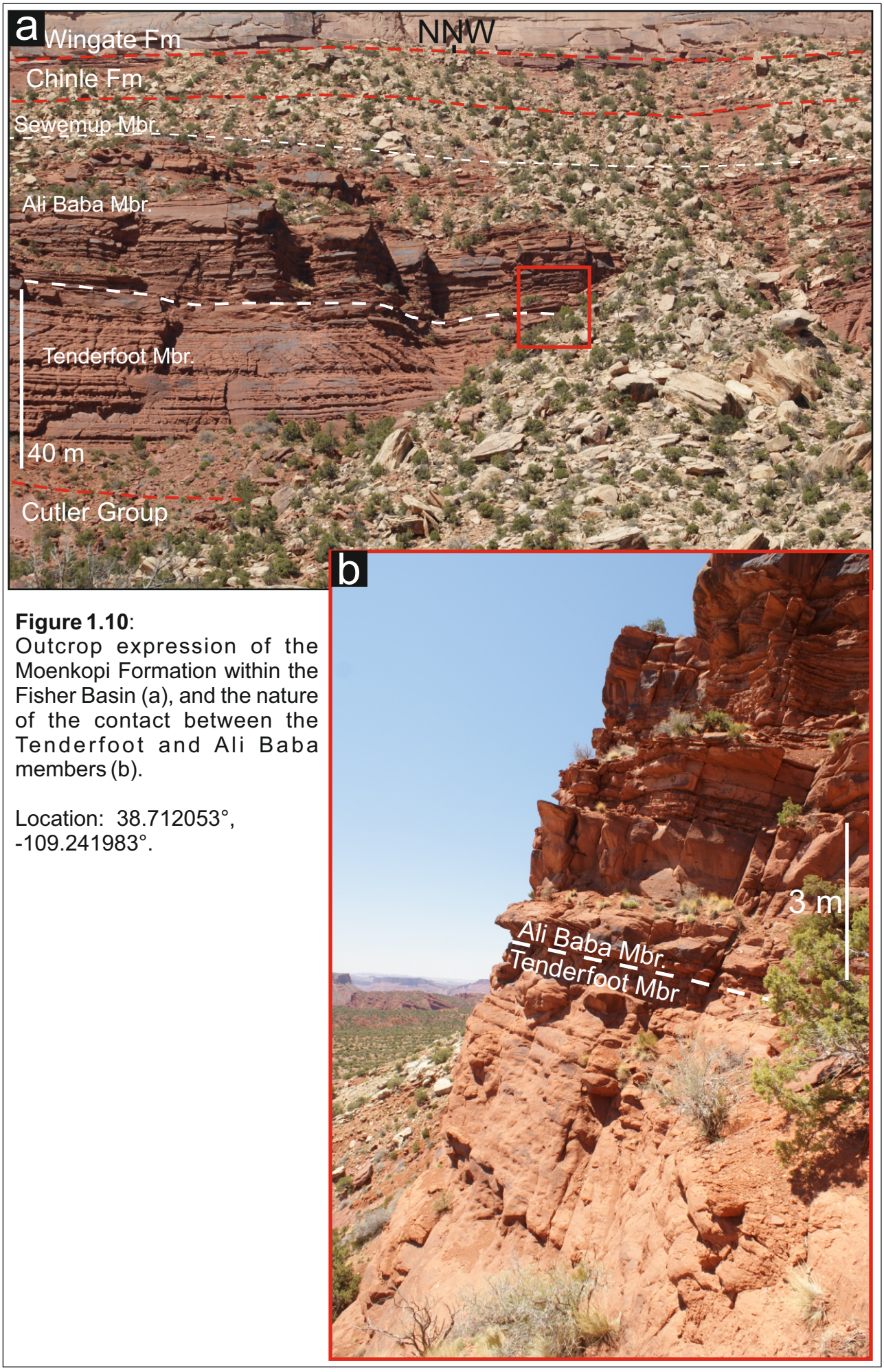


**Figure 1.10**:
Outcrop expression of the Moenkopi Formation within the Fisher Basin (a), and the nature of the contact between the Tenderfoot and Ali Baba members (b).

Location: 38.712053°, -109.241983°.

**Figure 1.11**: Outcrop expression of Channel complex within the Ali Baba Member, Fisher Basin. Location: 38.709442°, -109.209175°. Facing east.

extensive channelised succession within the central part of the member (Fig 1.7). Within the Big Bend Basin the Ali Baba Member is characterised by amalgamated channel-fill elements and sheet-like heterolithic elements (Fig 1.12). The member is characterised by a “chocolate brown” hue, although some of the channelised elements can exhibit a purple colour, reminiscent of that of the older Cutler Group deposits.

The Sewemup Member is characterised across all three basins by a slope-forming heterolithic sheet-like succession (Figs 1.7, 1.10). A particular diagnostic feature of this Member is the inclusion of gypsum-clast-bearing beds in the succession adjacent to the Castle Valley salt wall in both the Parriott and Big Bend Basin.

The Parriott Member is absent from the Fisher Basin (Fig 1.10), but is present in the Parriott and Big Bend Basins (Figs 1.7, 1.8, 1.13, 1.14). In the Parriott Basin, this member is denoted by an increase in the occurrence of channelized fluvial elements, although overall the succession retains its slope-forming characteristic. Within the Big Bend Basin, the Parriott Member is typically cliff forming adjacent to the Castle Valley salt wall, however in other areas, it can take on a slope-forming expression. The base of the Parriott Member is recognised by the uppermost occurrence of the gypsum-clast-bearing beds. The Moenkopi Formation is overlain unconformably by the Chinle Formation across the Salt Anticline Region The unconformity is typically expressed by the presence of grey coarse to very coarse-grained channel elements (Figs 1.15, 1.16) with extraformational clasts, and which are associated with a mottled coloured palaeosol that exhibits a distinct yellow and purple colour. In some parts of the region, this mottled palaeosol is associated with the presence of Crayfish burrows.

### 1.4.2 Outcrop Expression: White Canyon Region

The Moenkopi Formation within the studied parts of White Canyon Region is formally divided into the Hoskinnini Member and the Torrey Member (Blakey, 1974), although the Torrey Member was originally informally subdivided into a lower slope-forming member, a ledge-forming member, and an upper slope-forming member, and an uppermost cliff-forming member (Stewart *et al.*, 1972).

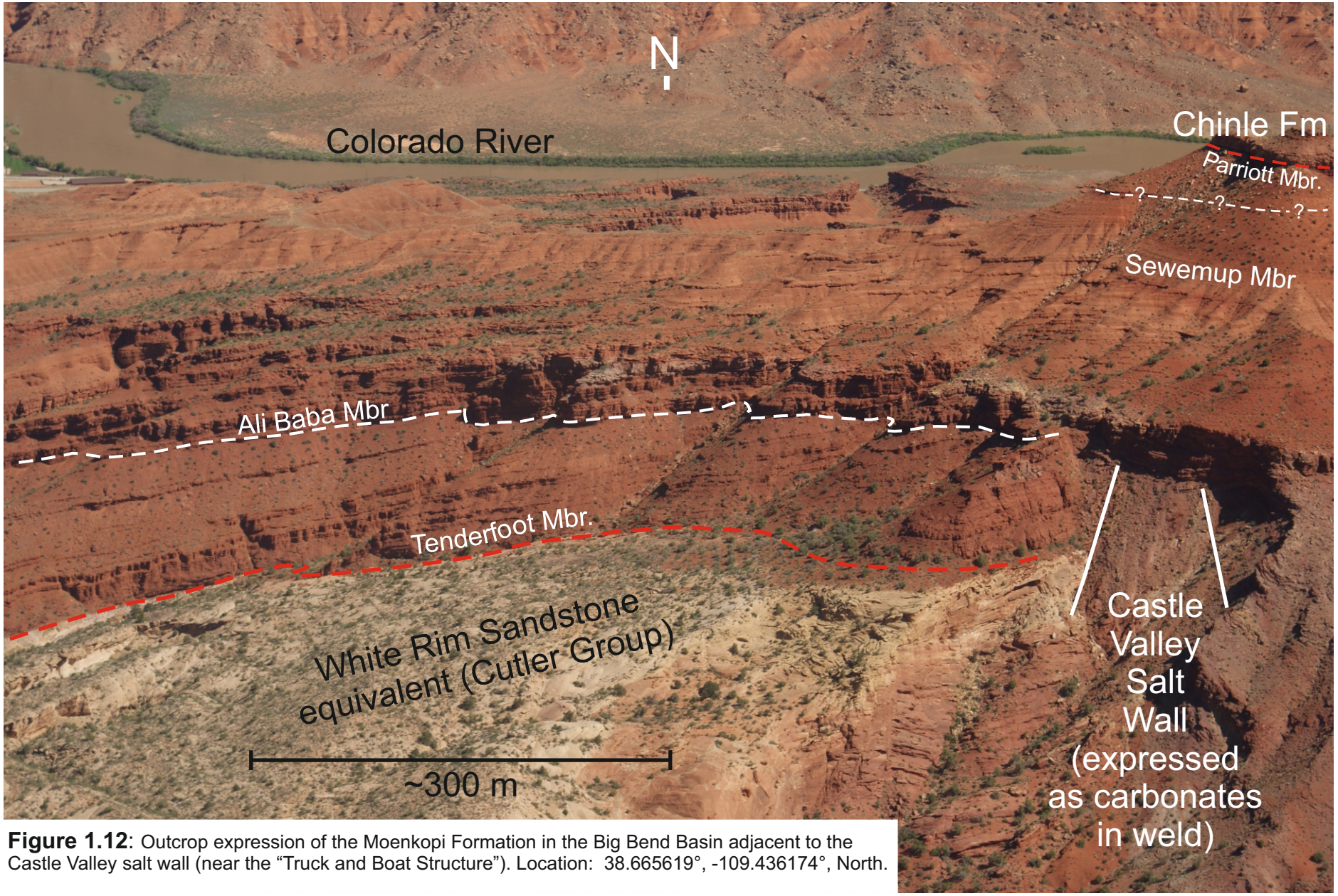


**Figure 1.12**: Outcrop expression of the Moenkopi Formation in the Big Bend Basin adjacent to the Castle Valley salt wall (near the "Truck and Boat Structure"). Location: 38.665619°, -109.436174°, North.

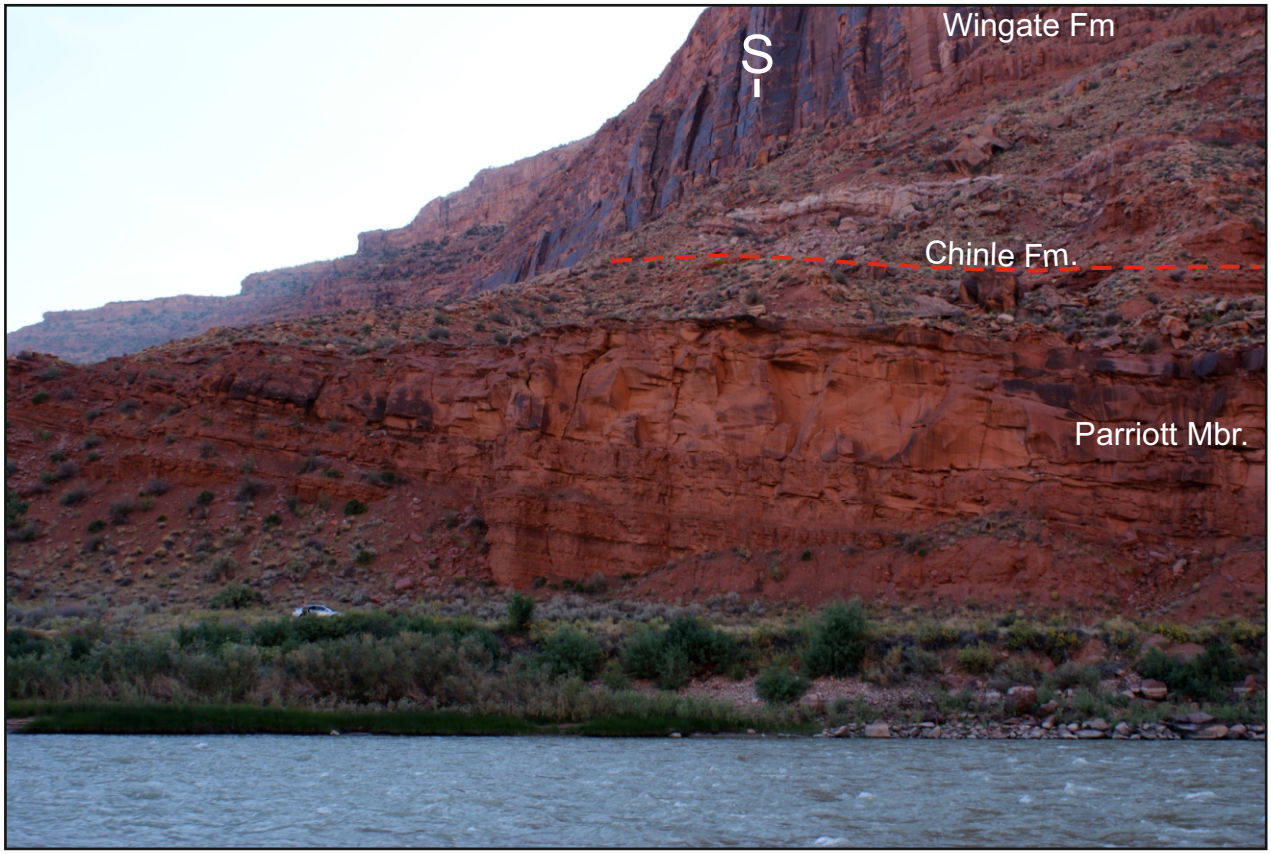


**Figure 1.13**: Outcrop expression of the Parriott Member in the rim-syncline south west of the Castle Valley salt wall. Note car for scale. Location: 38.683061°, -109.455290°, facing south.

**Figure 1.14**: Outcrop expression of the Parriott Member at Big Bend Campsite C. Location: 38.651, -109.477, facing south.

**Figure 1.15**: Typical expression of the unconformable relationship between the Moenkopi Formation and the overlying Chinle Formation within the Fisher Basin.

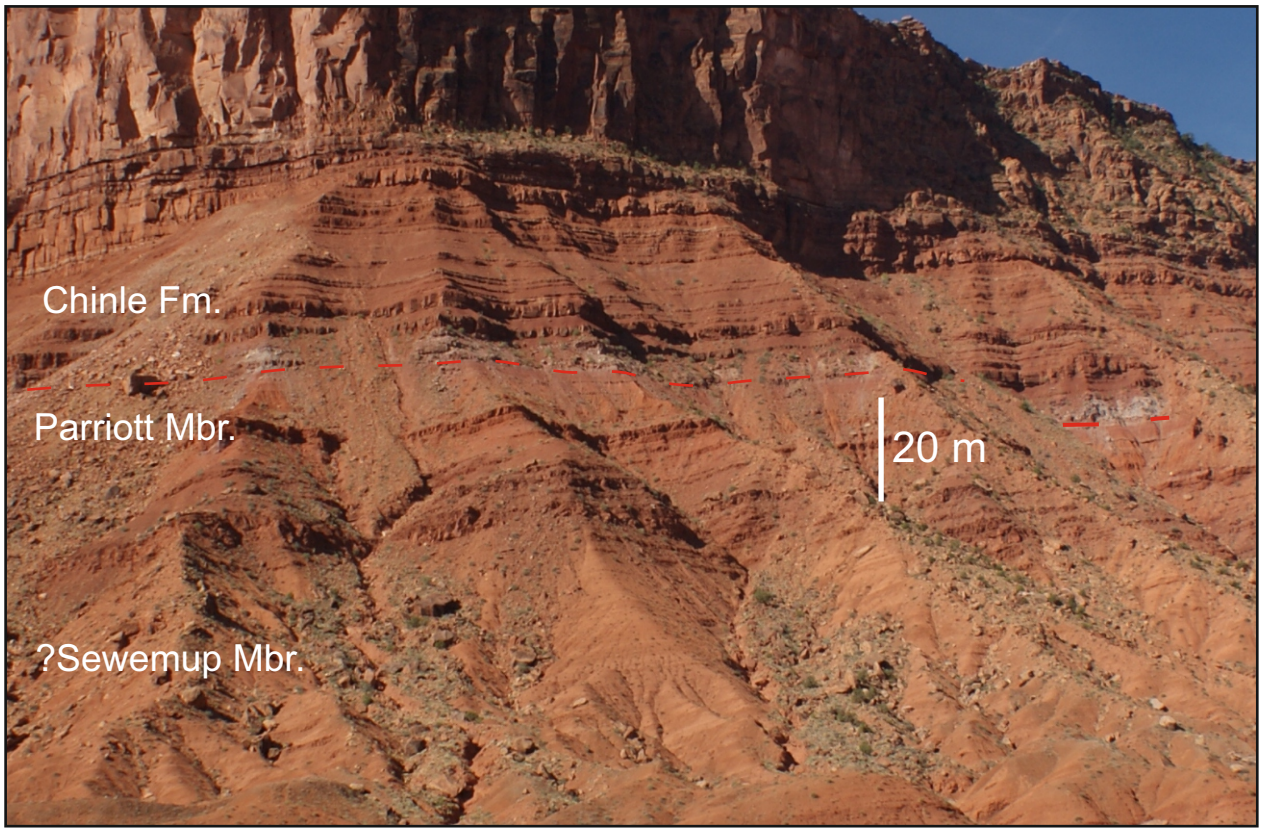


**Figure 1.16**: Representative outcrop expression of the unconformable relationship between the Moenkopi Formation and the overlying Chinle Formation. White weathered horizon demarks the base Chinle Unconformity.

The Hoskinnini Member shares similar characteristics with that of the Tenderfoot Member within the Salt Anticline Region, particularly the occurrence of distinct cliff-forming sandstones and the orange colour (Fig 1.17). The Hoskinnini Member also contains enigmatic dewatering structures similar to those in the Tenderfoot Member. Elsewhere, the Hoskinnini Member exhibits distinctive wavy structures on a bed-scale. A 1 to 2 m-thick gypsum bed has been identified within the basal section of the Moenkopi Formation in the Clay Hills Area (Fig 1.18), however the exact stratigraphic position within the Formation is unclear.

The Torrey Member is characterised by a mix of styles of channelised elements, which are typically cliff-forming units, together with heterolithic sheet-like elements, which are typically slope-forming units. The channel complexes forming the cliff-forming units can be traced for 10s km both parallel and perpendicular to palaeoflow (Fig 1.19).

## *1.5 Thesis Structure*

This thesis represents a discussion based around four papers submitted for publication in internationally recognised academic journals, and the structure of this thesis reflects this. As a result, parts of the various chapters contain modest overlap where key background information is reiterated. The reader should also note that the publications on which the chapters in this thesis have been based were not written in a chronological order that reflects the order of chapters included in the thesis.

### Chapter 2: *Literature Review*

(***Evolution of fluvial systems in salt-walled mini-basins: a review and new insights****: Paper 3, Published: Sedimentary Geology, 17 August 2013,* ***296****, 15 October 2013, 142–166*)

Chapter 2 discusses the current state of the science with regard to our understanding of fluvial interactions within salt-walled mini-basins. This chapter introduces a set of common terminology, it discusses causes of the initiation of halokinesis and mini-basin development, it considers parameters that control subsidence and sedimentation in salt-walled mini-basins, and it presents a series of case studies (Salt Anticline Region, Utah; Pre Caspian

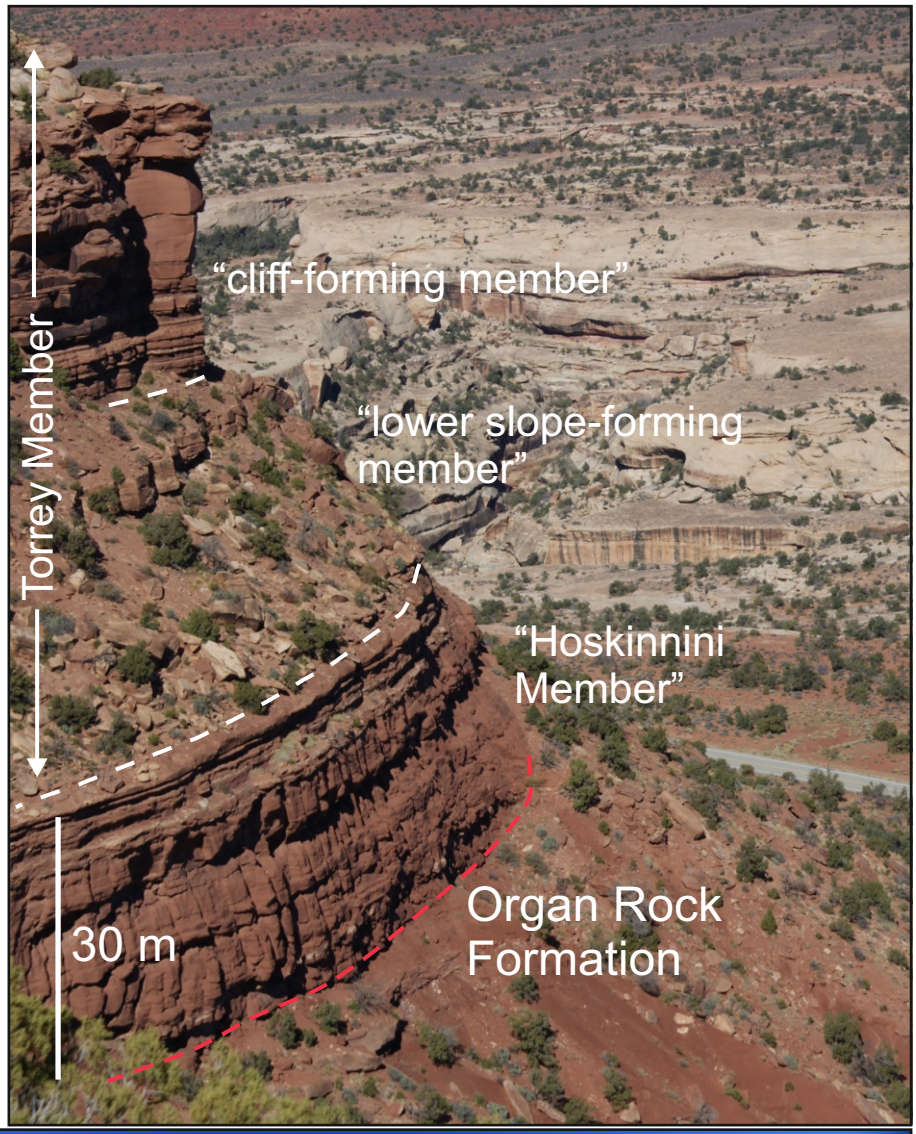


**Figure 1.17**: Outcrop expression of the Moenkopi Formation in near "Campsite", White Canyon Region. Location 37.638°, -110.170°, facing north.

**Figure 1.18**: Outcrop expression of Moenkopi Formation in the Clay Hill area of the White Canyon Region. Location: 37.347°, -110.350°, facing NNW.

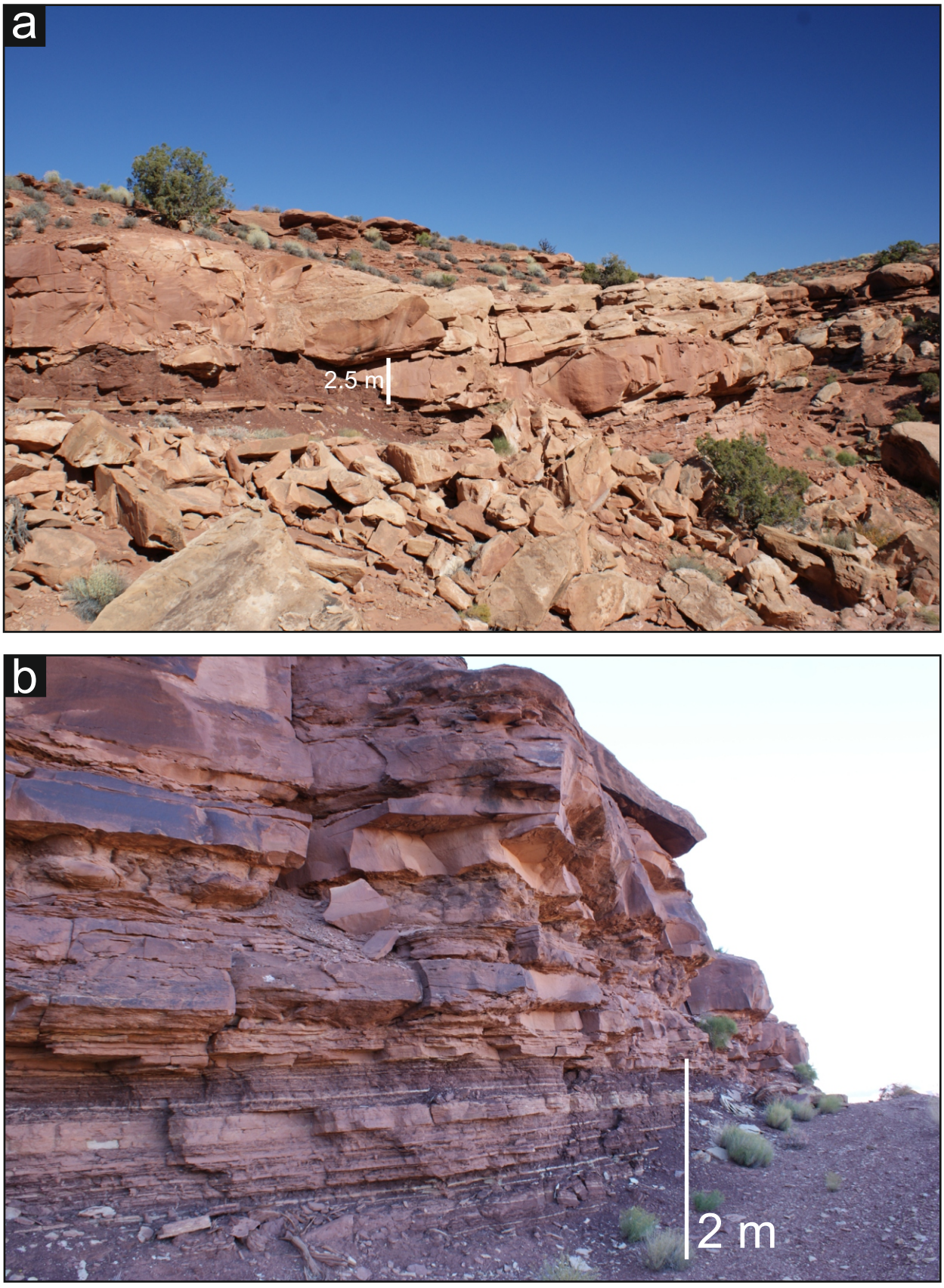


**Figure 1.19**: Typical expression of the Moenkopi Formation in the White Canyon Region. Both pictures demonstrate confined and non-confined flow units: confined units are typically the thick sandstone beds, and non-confined flow units are the thin sheet-like heterolithic elements.

Basin, Kazakhstan; Central North Sea; La Popa Basin, Mexico; additional examples). This chapter concludes with the presentation of a suite of tectono-stratigraphic models with which to account for the evolution of fluvial systems in salt-walled mini-basins.

### Chapter 3: Sedimentology of the Moenkopi Formation

(***Climatic versus halokinetic control on sedimentation in a dryland fluvial succession****: Paper 2, Published Online: Sedimentology, 24 August, 2013. DOI: 10.1111/sed.12064*)

Chapter 3 describes the facies and architectural composition of the Moenkopi Formation, and the spatial and temporal distribution of these components firstly in an area influenced by halokinesis, the Salt Anticline Region, and secondly from an area beyond the influence of halokinetic deformation in the White Canyon Region of south east Utah. This chapter also describes and discusses how the stratigraphic expression of the influence of halokinesis can be differentiated from that of variations in the climatic regime.

### Chapter 4: Halokinetic controls on sediment accumulation

(***Controls on fluvial sedimentary architecture and sediment-fill state in salt-walled mini-basins: Triassic Moenkopi Formation, Salt Anticline Region, SE Utah, USA****: Paper 1, Published Online: Basin Research, 25 May 2013. DOI: 10.1111/bre.12022*)

Chapter 4 describes the influence of ongoing halokinesis on the accumulation of the Moenkopi Formation within the Salt Anticline Region, and considers how such activity controlled the spatial and temporal distribution of facies within the three observed and adjacent salt-walled mini-basins. This chapter presents a detailed model with which to account for the evolution of the preserved expression of the Moenkopi Formation, and for the various factors governing this.

### Chapter 5: Discussion: Synthesis of Research, generic implications and application to industry

Chapter 6 synthesises chapters 2, 3, and 4, and discusses the wider implications of this study before discussing how these findings can be used

for the benefit of industry. This chapter details conceptual models which demonstrate how the stratigraphic expression of fluvial systems accumulating in salt-walled mini-basins can vary depending on the interplay between the controlling factors, including sediment supply, rate of subsidence, rate of uplift, and drainage distribution. The chapter presents a series of models depicting how climatic variations and subsidence rates are depicted in a series of mini-basins, and demonstrates how this knowledge can be used for hydrocarbon exploration.

## Chapter 6: Conclusions

Chapter 6 provides a concise overview of the thesis and re-considers the original questions posed in the introduction to this work. Additionally, this chapter concludes the thesis by postulating a set of additional research questions that could be used to further advance our present understanding of fluvial systems (and indeed other sedimentary systems) accumulating in salt-walled mini-basins.

# 2. Evolution of fluvial systems in salt-walled mini-basins: a review and new insights

*This chapter is a review of the current literature pertaining to the current understanding the accumulation of fluvial systems in salt-walled mini-basins. This chapter discusses terminology defining key aspects of the nature of basin-fill, and the parameters that control sediment supply, halokinesis, and the distribution of fluvial elements.*

*The chapter then goes on to review 4 key case studies and how the various parameters controlling sediment supply and halokinesis control the accumulation of sediments within the evolving mini-basins.*

*Finally, a series of generic evolution models are developed from the synthesis of data from the case studies, describing likely basin fill states throughout the development of both linear salt-walled mini-basins and polygonal salt-walled mini-basins.*

## *2.0 Abstract*

The preserved sedimentary expression of fluvial successions accumulated in salt-walled mini-basins records the complex history of basin subsidence, the style of sediment supply, and the pattern of sediment distribution in response to a range of fluvial processes throughout the evolution of such basins. Temporal and spatial variations in the rate of basin subsidence govern the generation of accommodation space, whereas the rate and style of sediment supply govern how available accommodation is filled; together these parameters act as principal controls that dictate the gross-scale pattern of fluvial sedimentation. Additional factors that influence fluvial stratigraphic architecture in salt-walled mini-basins are: (i) the trend and form of inherited basement lineations and faults that control the geometry, orientation and spacing of salt walls that develop in response to halokinesis; (ii) salt thickness and composition that dictate both the maximum potential basin-fill thickness within a developing mini-basin and the rate of evacuation (migration) of salt from beneath evolving mini-basins, leading to the growth of confining salt

walls, uplift of which may generate surface topographic expression that influences fluvial drainage patterns; (iii) climate that dictates fluvial style and the processes by which sediment is distributed; and (iv) the inherited direction of drainage relative to the trend of elongate salt walls and locus of sediment supply that dictates how sediments are distributed both within a single mini-basin and between adjacent basins.

Examples of fluvial sedimentary architectures preserved in salt-walled mini-basins from a number of geographic regions are used to illustrate and document the primary controls that influence patterns of fluvial sediment accumulation. The distribution of fluvial architectural elements preserved within mini-basins follows a predictable pattern, both within individual basin depocentres and between adjoining basins: drainage pathways preferentially migrate to topographic lows within basins, such as developing rim-synclines, and away from topographic highs, such as uplifting salt walls or developing turtle-back structures.

This paper demonstrates a range of fluvial-halokinetic interactions through consideration of a series of case studies, which demonstrate current understanding of fluvial response to salt-walled mini-basin evolution and which highlight gaps in current understanding.

## *2.1 Introduction*

Globally, there exist in excess of 120 provinces in which evaporite basins are known to have been influenced by salt deformation (Hudec and Jackson, 2007; Fig. 2.1). Numerous studies have been previously conducted to demonstrate how various sedimentary environments are influenced by coeval halokinesis that results in high rates of basin subsidence (e.g., Prather *et al.*, 1998), diversion of sediment transport pathways by uplifting topography (e.g., Kneller and McCaffrey, 1995; Banham and Mountney, 2013a), and reworking of uplifted sediments or diapir-derived detritus (e.g., Lawton and Buck, 2006). Studies show how the effects of these phenomena are expressed in the preserved stratigraphic record: in deep-water environments, turbidity currents can be deflected, diverted or reflected by uplifting salt topography resulting in a complex arrangement of turbidite deposits (Kelling *et al.*, 1979; Kneller and

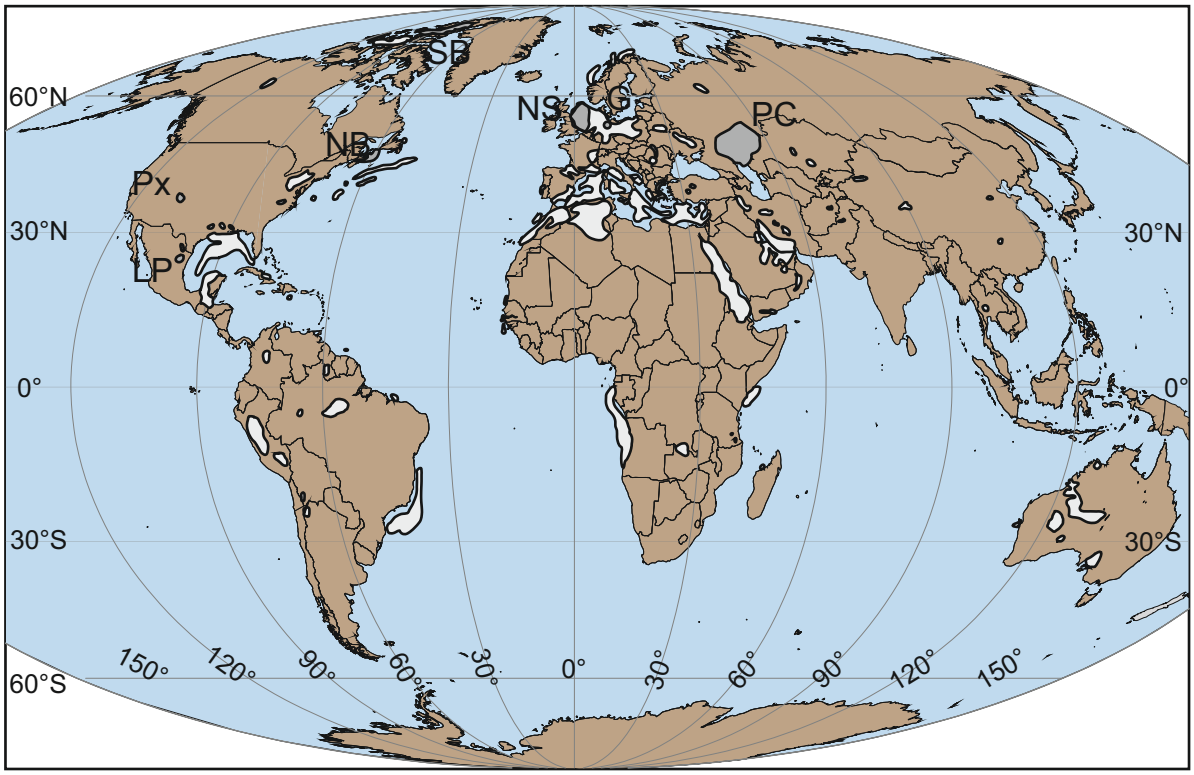


**Figure 2.1**: Overview of halokinetic provinces world-wide. Light grey indicates halokinetic provinces not covered in this study. Dark grey denotes provinces mentioned in this study. G: German case studies; LP: La Popa Basin; NB: New Brunswick; NS: North Sea; PC: Precaspian Basin; Px: Paradox Basin; SB: Sverdrup Basin. Modified after Hudec and Jackson (2007).

McCaffrey, 1995; Byrd et al., 2004; Kane et al., 2012); in shallow-marine environments, enhanced rates of subsidence can locally increase sediment accumulation rates (Dyson, 2004; Kernen et al. 2012); and in aeolian environments, surface topography arising from salt-wall growth can encourage dune-field construction, accumulation and preservation by shielding such environments from reworking by fluvial processes (Venus, 2013). Of these and other studies, only a modest number have attempted to document and account for the style of accumulation of fluvial successions in salt-walled mini-basins and show how fluvial systems can be diverted by salt-wall-generated topography. Despite having hitherto been the attention of only relatively few studies, understanding the detailed sedimentology and stratigaphy of fluvial successions preserved in salt-walled mini-basins is important since such successions act as economically important hydrocarbon reservoirs in several salt-basin provinces globally (Smith et al., 1993; Barde et al., 2002a; Newell et al., 2012).

The aim of this paper is to review the current state of literature regarding controls on the style of accumulation of fluvial successions in salt-walled mini-basins and to highlight gaps in current understanding. Specific objectives are as follows: (i) to establish a standard set of terminology for the description of various attributes associated with the spatial and temporal evolution of salt-walled mini-basins; (ii) to highlight the numerous ways in which halokinetic and sedimentary processes can interact; (iii) to illustrate how these different styles of interaction are known to be expressed through examination of a series of reviewed case studies; (iv) to present a series of summary tectono-stratigraphic models with which to relate preserved fluvial stratigraphic architecture present in mini-basins to the principal halokinetic and sedimentary controls; (v) to show how such models can be used as predictive tools; and (vi) to discuss potential approaches to future research which will address issues that currently remain unresolved in this field of research.

This work is of broad appeal for the following reasons: (i) the terminology describing the attributes and style of infill of salt-walled mini-basins are currently poorly defined and this study provides clarification and discussion through development of a generic classification framework; (ii) this

work identifies and discusses a series of controls that operate to determine the style of evolution of salt-walled mini-basins and the manner by which these basins become filled by fluvial successions; and (iii) this work distils our current understanding into a series of generic models that describe the influence of key controls on fluvial sedimentation for a variety of types of basin fill.

## *2.2 Terminology*

The terminology required for the description of basin subsidence, gross-style of basin fill and basin-fill state at any given time during the evolution of a series of salt-walled mini-basins is inherently complex because many dependent and independent variables are known to interact during the evolution of such systems. To resolve this issue, terminology describing the primary variables that govern mini-basin evolution and their fill states are defined here in an attempt to standardise descriptions of basin attributes (Fig. 2.2).

**Basin-fill thickness (T)** describes the current total thickness of accumulated sediment within a subsiding mini-basin. This thickness may vary across a single basin in cases where differential subsidence has generated variable accommodation; for example, a rim syncline structure (R) will locally increase accommodation, whereas accommodation will be less above a turtle-back structure (Tb).

**Maximum basin-fill thickness (M)** describes the maximum potential thickness of fill that can be accommodated by continued subsidence and accumulation within a mini-basin This is governed by both basement geometry and by the original thickness of salt present at the location of mini-basin formation. Where a mini-basin grounds on pre-salt basement strata, further subsidence is no longer possible and T = M, if the effects of additional sediment compaction are ignored.

**Remaining basin-fill potential (P)** describes the remaining thickness of salt beneath a subsiding mini-basin at a given point, and the maximum remaining distance the mini-basin can subside before it grounds on the sub-salt basement. Where a basin or part thereof grounds on the pre-salt basement, a

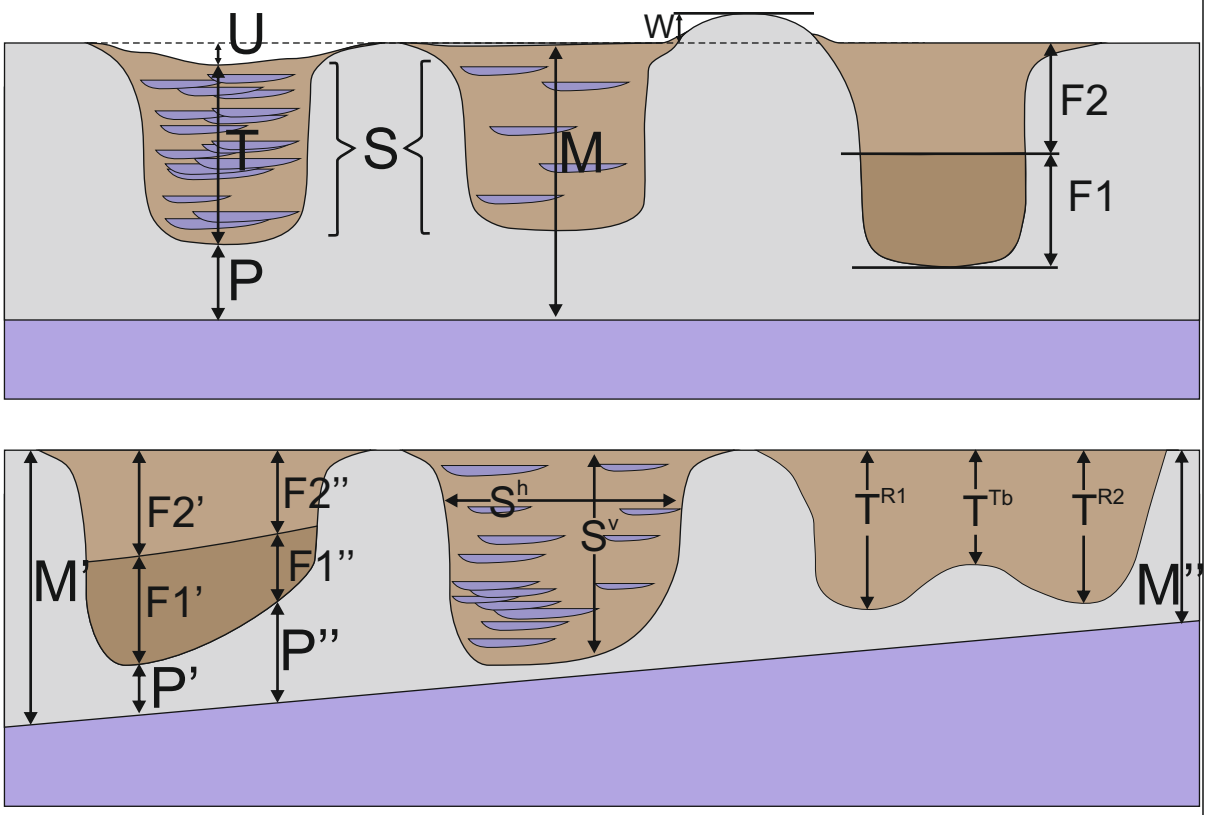


**Figure 2.2**: Description of basin-fill attributes defining basin-fill thickness, fill style, pre-existing basin fill, and remaining subsidence potential of the basin. These parameters can vary both between mini-basins and within a single mini-basin.
**T = Basin-fill thickness**, which can vary within a single basin, e.g., features such as turtle-back structures & rim synclines.
**F = Fill inheritance**, which records the state of basin-fill at the onset of a subsequent episode of deposition, and which can vary spatially across a mini-basin due to variations in differential subsidence rate or existing basin fill-thickness.
**M = Maximum basin-fill level** (fill potential) is determined by the original thickness of salt and can vary due to the presence of a dipping basement or the presence of pre-salt basement structures.
**P = Remnant basin-fill potential**, describes the salt remaining beneath an evolving mini-basin and can vary across a basin due to differential subsidence or due to sub-salt basement geometries.
**S = Basin-fill style** is a general concept describing the overall nature of the sediment fill (e.g. sand-prone or sand-poor). Sh = horizontal fill style; Sv = vertical fill style.
**U = Available accommodation** (space remaining unfilled) and can be negative if the basin fill becomes elevated above a "baseline of erosion".
**W= Salt-wall height** above "regional" elevation.

salt weld is formed and remnant basin-fill potential (potential accommodation space) for that location is theoretically zero.

**Fill inheritance (F)** describes the pre-existing basin-fill thickness at the onset of a new sequence of sediment delivery, where the inherited fill state is described in relation to the onset of accumulation of a new stratigraphic sequence. Differential rates of subsidence within a single mini-basin can lead to spatial variation in inherited basin-fill thickness at the onset of accumulation of a later stratigraphic sequence. Such a situation might arise in response to the early grounding of one side of a mini-basin while the other side remains actively subsiding and able to accumulate additional strata. This can result in the development of a so-called “heel-toe” sediment-fill geometry (Kluth and DuChene, 2009), a common style of architectural expression. The sum of all inherited basin-fill is equal to basin-fill thickness (T).

**Available unfilled accommodation space (U)** refers to the vertical thickness of accommodation within a mini-basin that remains unfilled by sediment at a given point and for a specified time period, but which could potentially be filled with sediment without additional subsidence occurring. This can be a negative value if the basin-fill rises locally or temporarily above the regional base level.

**Basin-fill style (S)** describes the nature of the basin-fill and the distribution of fluvial elements in general, qualitative terms; for example, whether the basin-fill is relatively sand-prone or sand-poor. The distribution of fluvial elements may be heterogeneous at the scale of a mini-basin, giving rise to variations in the style of accumulated strata, potentially in orientations parallel or perpendicular to the trend of elongate basins, or vertically within the overall fill of a mini-basin. For example, the arrangement of stratal packages may exhibit heterogeneity such that groups of channel-fill elements might be clustered at certain stratigraphic intervals or at only one side of a mini-basin.

**Salt-wall height (W)** describes the relief of the salt-wall (or its directly overlying cover sediment) relative to that of the sediment fill-level in the adjoining mini-basin(s). When a salt wall (or its cover sediment) rises above the height of the surrounding basin plain to generate a topographic expression, it will be prone to erosion and reworking, potentially acting as a source for the generation of clastic detritus derived from reworked cover sediment, and diapir-derived detritus reworked from the salt wall itself. Such

detritus may be reworked into the surrounding accumulating stratigraphy as part of the basin fill and recorded as lithofacies characterised by lithic clasts of local intraformational origin (e.g., mudstone rip-ups) or by clasts of reworked evaporite material (e.g., gypsum).

**Basin subsidence rate (R)** refers specifically to the rate at which the floor of the mini-basin subsides into the underlying salt. This value may vary in orientations both parallel and transverse to the axis of elongate mini-basins, as well as temporally.

**Salt-wall uplift rate (U)** refers to the rate at which a salt wall (or its directly overlying cover sediment) is uplifted above the sediment fill-level of the adjoining mini-basin. This rate of uplift may be modified by dissolution of the salt in the subsurface, effectively reducing the rate of uplift.

**Salt-weld formation or basin grounding** refers to the time that basin subsidence effectively ceases because the remaining thickness of salt beneath a subsiding mini-basin is insufficient to allow further flow because the remaining basin-fill potential (P) is effectively zero (cf., Hudec and Jackson, 2009) and a salt weld forms. The ability of salt to deform and flow is dependent on the thickness of salt, with shear rates in the salt tending to reduce with decreasing thickness of salt: the conditions that dictate the timing of salt-weld formation vary and are mainly dependent on the composition of the salt layers (Hudec and Jackson, 2009).

## *2.3 Controls on the style of stratigraphic in-fill of salt-walled mini-basins*

### 2.3.1 Initiation of salt-walled mini-basins

The initiation of mini-basin subsidence requires a number of prerequisites: (i) the presence of a salt layer (or layers) of sufficient thickness to allow halokinesis to occur (Trusheim, 1960; Hudec *et al.,* 2009); and (ii) a mechanism to initiate halokinesis (Fig. 2.3), such as extension (Hodgson et al., 1992), compression (Jackson and Talbot, 1986; Brun and Fort, 2003), differential loading (Ings and Beaumont, 2010), or buoyancy (Trusheim, 1960). Where salt thickness is sufficient to allow the development of salt-walled mini-basins, the presence of pre-salt basement structures, including

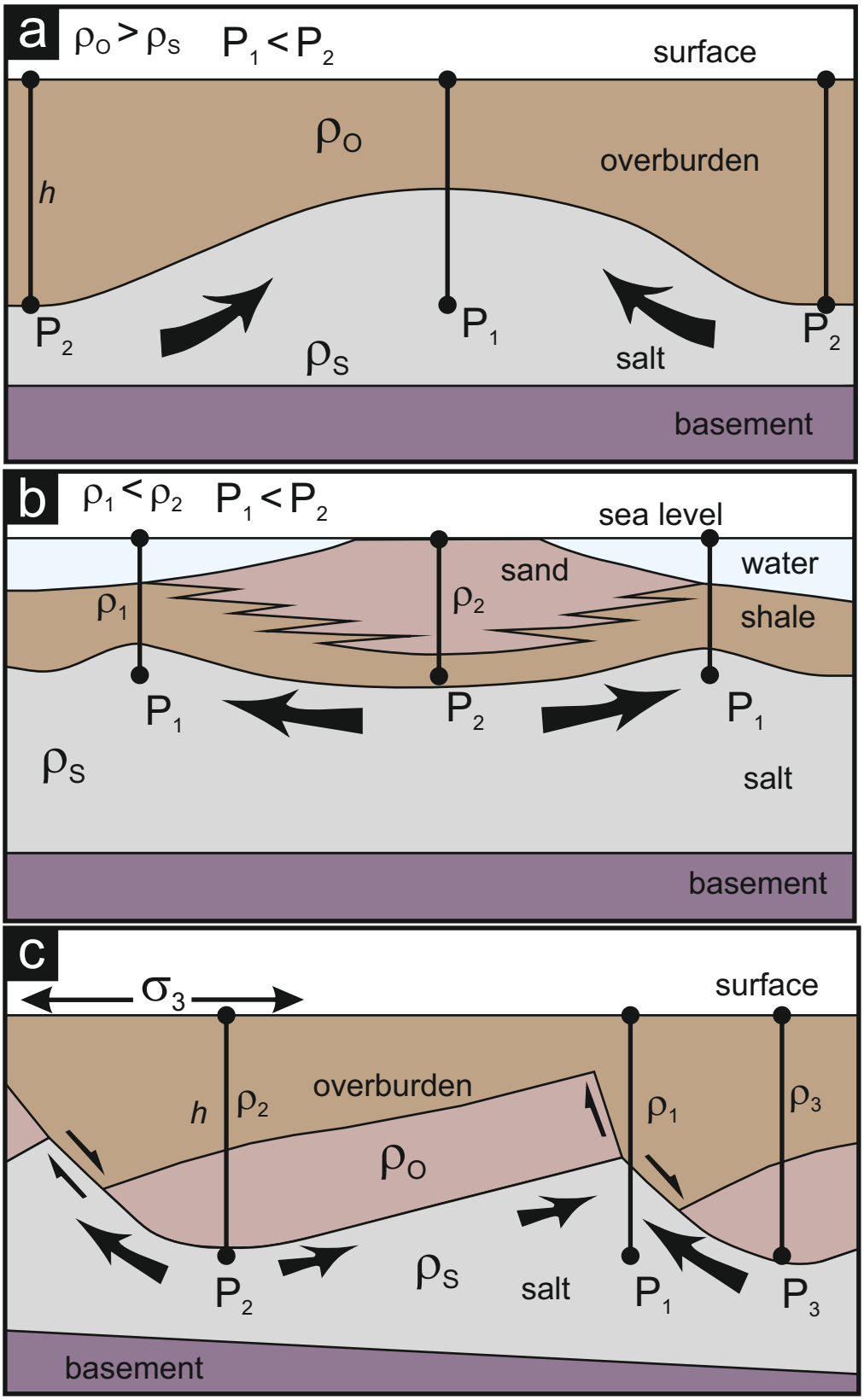


**Figure 2.3**: Common mechanisms for the initiation of halokinesis. ρ signifies density of material. (a) Buoyancy-driven halokinesis, where density of the overburden initiates and drives halokinesis. (b) Differential loading, where halokinesis is driven by varying thickness and density of overburden, created by features such as accumulation of a prograding alluvial wedge. (c) Initiation of halokinesis due to extension, where thin-skinned tectonics creates differential thicknesses of salt. Modified after Jackson and Talbot (1986).

their geometry, trend, spacing and along-strike continuity commonly exert a significant control on the location and style of salt-wall growth (Doelling, 1988; Barde et al., 2002a; Trudgill, 2011). Sites of initiation of salt-wall growth and the orientation of such salt walls have been related to the distribution and orientation of various types of basement feature, including horst-and-graben structures or relict topography, which generate variations in the thickness of salt, of which triggers the onset of halokinesis (Hodgson et al., 1992; Smith et al., 1993). Salt walls typically form above horst and graben structures, although a differential thickness of salt may not itself be the sole factor responsible for the initiation of the growth of salt walls. Additionally, differential loading may exert a control on the spacing of salt walls, as a function of salt viscosity, salt thickness, and overburden density (Ings and Beaumont, 2010). Mini-basin size varies, in part as a function of initiation mechanism, with individual basins typically being 8 – 15 km wide, whereas intervening salt walls typically have widths of 1 to 2 km (Barde et al., 2002a; Goldsmith et al., 2003; Trudgill, 2011; Banham and Mountney, 2013a).

The ongoing growth of salt-walled mini-basins is maintained and driven by a buoyancy imbalance (Rayleigh-Taylor instability), where the overlying sediment has a greater density than that of the underlying salt (Hudec et al., 2009; Ings and Beaumont, 2010; Fig. 2.3). This density-driven process typically requires sediments to have a density of ~2500 kg $m^{-3}$, which equates to a burial depth of ~1000 – 2300 m to generate the mechanical compaction required to achieve this density for most clastic sediments (Jackson and Talbot, 1986; Hudec et al., 2009).

Initiation of salt-wall growth by other mechanisms has also been described by Hudec et al. (2009), including: (i) lateral shortening of the salt layer due to the application of compressive stress, thereby creating a bathymetric high where salt is forced up and a bathymetric low in the top surface of the adjacent salt; (ii) thinning of the salt layer due to extensional stress, whereby stretching of the salt layer causes it to sag, forming a bathymetric low (Fig. 2.3); or (iii) flow of salt via creep down-dip under the influence of gravity, thereby creating a bathymetric low at the head of the original salt body; (iv) sediment loading, whereby overlying strata of variable thickness generates a significant differential load at a point on the underlying

salt layer (Fig. 2.3); or (v) sub-salt deformation, such as the creation of a roll-over basin by extension or folding by compression. Each of these mechanisms relies on the generation of a bathymetric low in the salt to allow for the accumulation of sediment, progressive accumulation of which, in turn, generates additional loading and enables buoyancy-driven withdrawal and lateral salt migration at depth, thereby leading to additional subsidence at the site of loading.

An alternative mechanism for the initiation of mini-basin generation is the viscous pressure ridge model proposed by Ings and Beaumont (2010), in which flow of overburden and underlying salt – driven by, for example, collapse of a continental margin or progradation of a delta or alluvial mega-fan – can result in the formation of a pressure ridge due to differential rates of flow within the underlying salt. The trapping of sediment by the formation of these viscous pressure ridges culminates in the development of a sediment succession that is sufficiently thick to create a Rayleigh-Taylor instability, allowing conventional buoyancy-driven subsidence to take over.

Once a sufficient density contrast threshold has been attained, whereby compaction of the overlying sediment has resulted in a mean sediment density that is greater than that of the underlying salt, load-driven displacement of the salt from beneath the incipient mini-basins will commence as salt flows into neighbouring growing salt walls (Ings and Beaumont, 2010).
The evolution of salt-walled mini-basins (or ‘pods’) was described previously by Hodgson et al (1992) (Fig. 2.4). Initiation of salt-wall growth can be triggered by any one of the aforementioned mechanisms, before sediment loading of the salt eventually takes over as the driving mechanism of basin subsidence and salt wall growth (Hudec et al., 2009; Ings and Beaumont, 2010). Sediment accumulation in these basins continues by the process of down-building (Barton, 1933) until the basin grounds on the sub-salt basement, effectively preventing additional accumulation of sediments within the mini-basin. Later, axial migration or dissolution of salt from an uplifted swell, wall or stock can cause the salt uplift to collapse, thereby allowing secondary mini-basins to form over the crests of the former salt-wall highs (Colman et al., 1986; Hodgson et al., 1992; Hudec, 1995).

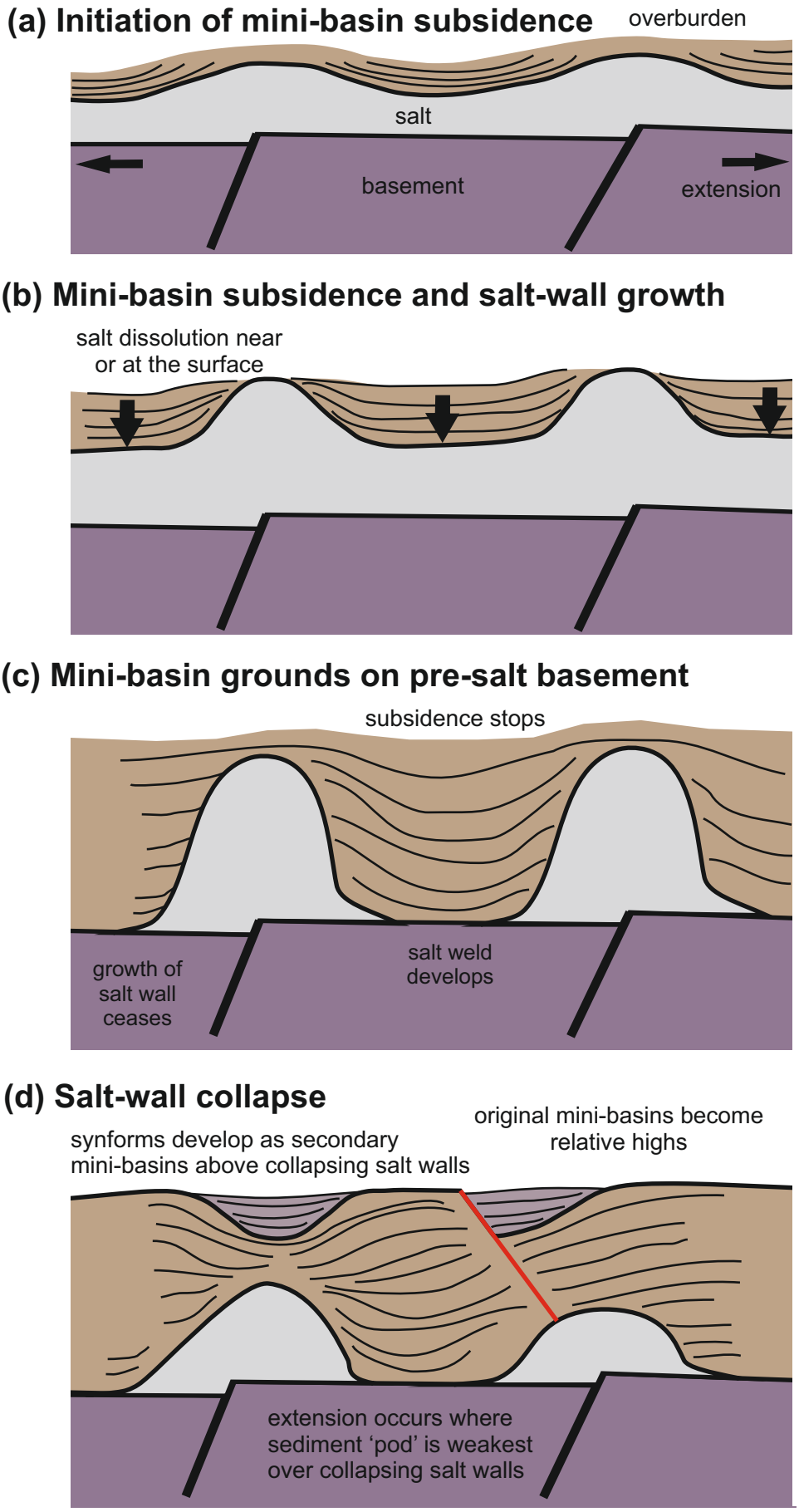


**Figure 2.4**: Model demonstrating the evolution of salt-walled mini-basins throughout various stages of evolution. Modified after Hodgson et al. (1992).

Once initiated, mini-basins can subside at sustained rates of >1 km/Ma for several million years: for example, some Pliocene and Pleistocene examples have fills that are up to 8 km thick (Hudec et al., 2009). In some instances, rates of up to 10 km/Ma have been recorded in the Gulf of Mexico (Prather, 2000).

### 2.3.2 Parameters controlling subsidence and sedimentation rate

Many parameters are known to influence the style of sediment accumulation in salt-walled mini-basins: some are static (e.g., original salt thickness and composition) in that they do not vary throughout the episode of mini-basin subsidence; others are dynamic variables (e.g., climate and sediment delivery rate) that change over the course of mini-basin subsidence (Banham and Mountney 2013a; Fig. 2.5) Understanding these parameters is key to determining the history of subsidence and sedimentation within a salt mini-basin province, and for showing how this may have controlled fluvial drainage pathways, and subsequently how this influenced basin-fill evolution.

#### Static parameters

Static parameters are controls that remain constant (i.e., temporally invariable) throughout the evolution of a mini-basin; such parameters typically exert a basin-scale control on system evolution and are normally set prior to the onset of halokinesis.

***Basement geometries.*** The trends of faults in the pre-salt basement, their spacing and geometry, together with the average dip of the pre-salt basement, act to control the spatial pattern of development and temporal sequence of evolution of growing salt walls (Fig. 2.6). Salt walls tend to develop at a site of change in salt thickness, such as commonly occurs across fault offsets (Doelling, 1988; Smith et al., 1992; Trudgill, 2011). Alternatively changes in salt thickness may occur where salt overlies buried topography, or may result from facies variations within the evaporite-bearing depositional units. Where basement trends are simple and follow a single trend, salt walls tend to evolve as elongate, linear and parallel features (e.g., Salt Anticline Region of the Paradox Basin, Utah; La Popa Basin, Mexico; parts of the

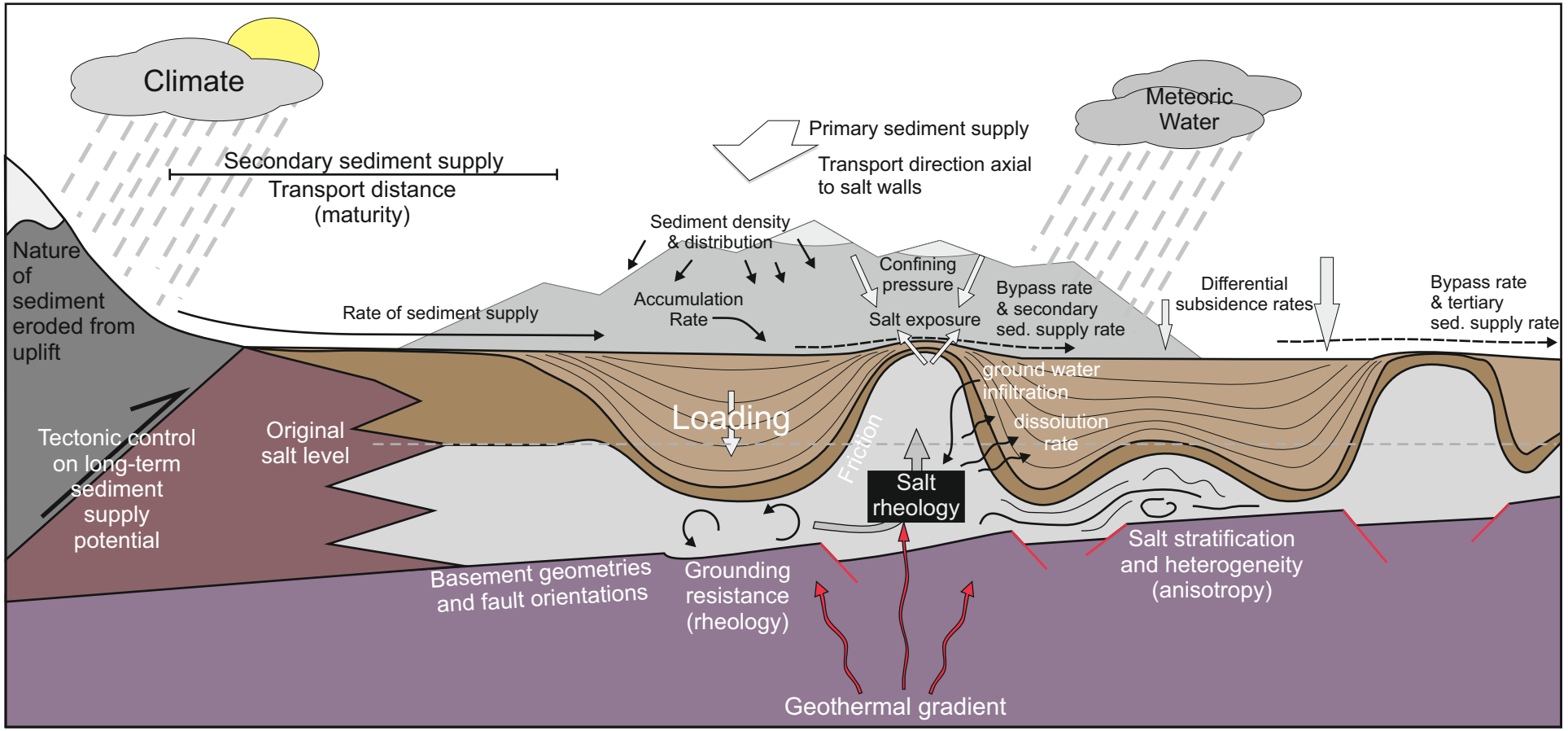


**Figure 2.5**: Schematic depiction of the action of a suite of controlling parameters to dictate the geometry and style of infill of salt-walled mini-basins. These factors govern rates of sediment accumulation and basin subsidence. Modified after Banham and Mountney (2013a).

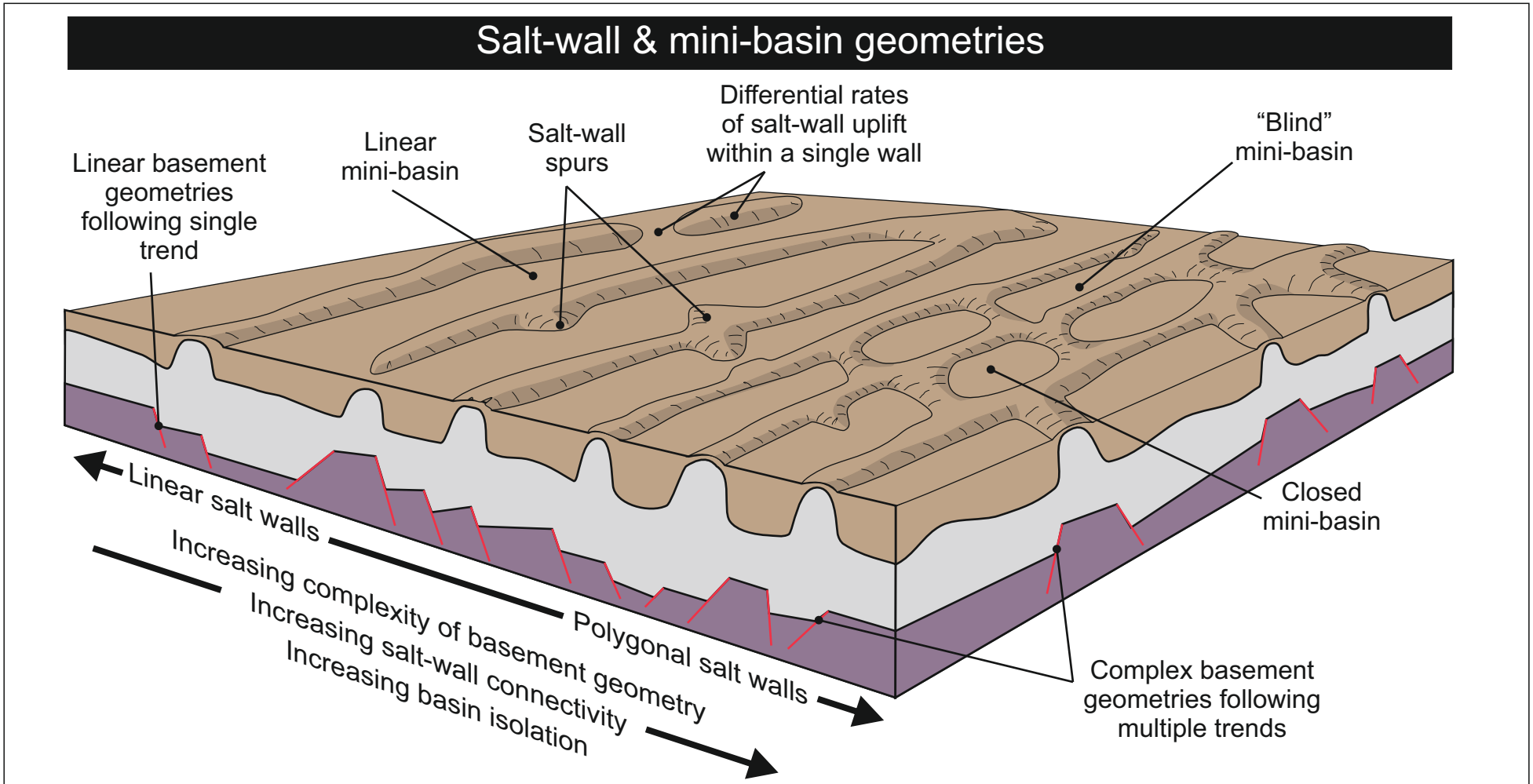


**Figure 2.6**: Common salt wall and mini-basin geometries. Geometries of developing salt walls are controlled by factors, including: the trend of pre-existing basement faults and topography; the direction of tectonic extension or shortening; the direction of differential loading. Where a single basement trend exists, linear salt walls tend to develop and these separate elongate, linear mini-basins. Where multiple basement trends exist or where tectonism occurs in an orientation that is oblique to the trend of pre-existing basement structures, polygonal walled mini-basins tend to develop.

Central Graben in the subsurface of the North Sea). By contrast, in situations where basement features are present that trend in different orientations, more complex pre-salt basement geometries tend to favour the evolution of salt walls arranged in polygonal patterns and with varying continuity (e.g., Pre-Caspian Basin, Kazakhstan) (Fig. 2.6). Basement dip, which can result in a variable basement depth across a basin, may determine basin-scale regional changes in the thickness of salt that accumulates. This in turn determines the maximum potential basin-fill thickness during the later development of salt-walled mini-basins.

***Total thickness of salt.*** The thickness of salt ultimately controls the maximum distance a mini-basin can subside before it grounds on the pre-salt basement. The total thickness of salt can vary across the basin (e.g., Paradox Basin, Trudgill, 2011; Central North Sea, Hodgson et al., 1992, Smith et al., 1993), resulting in adjacent mini-basins grounding at different times during the evolution of a mini-basin province. Mini-basin grounding results in a cessation of generation of further accommodation in that basin and once local available accommodation has been filled, sediment bypass into neighbouring basins will commence leading to a relative increase in sedimentation rate in mini-basins that may formerly have been relatively sediment-starved. Furthermore, thicker successions of salt tend to deform and flow at faster rates than thinner successions, meaning that higher rates of subsidence tend to occur in mini-basin provinces for which evaporite thicknesses are greatest (Hudec and Jackson, 2007).

***Evaporite properties.*** The composition and style of stratification of the evaporate-bearing units undergoing halokinesis exert a control on the shear rate of the salt as it deforms and flows within the subsurface. The presence of clastic or carbonate lithologies within an otherwise evaporite-dominated succession will tend to reduce the flow rate (Hite, 1968; Jackson and Talbot, 1986), thereby directly influencing the rate of subsidence of overlying mini-basins and the rate of uplift of adjacent salt walls. The composition of the evaporites undergoing deformation will also influence the timing of salt-weld formation because the presence of clastic and carbonate lithologies acts to hamper the ability of salt to flow, especially where the thickness of salt is substantially reduced.

**Dynamic parameters**

Dynamic parameters are controls that vary either spatially within or between mini-basins, or temporally through the evolution of one or a series of mini-basins. These factors can be allogenic or autogenic in origin and can influence the style of sedimentation at a range of scales.

***Geothermal controls.*** Geothermal gradient dictates the viscosity and density of salt (Jackson and Talbot, 1986). An increase in the geothermal gradient will act to reduce salt viscosity, thereby enabling it to flow at a faster rate. Decreasing the density of the salt will reduce the threshold required to allow buoyancy-driven subsidence to occur (Srivastava and Merchant, 1973; Jackson and Talbot, 1986).

***Climate.*** Climate controls the evolution of salt walled mini-basins in several ways. Where meteoric water percolates into subsurface salt layers, “softening” of the salt ensues, leading to increased flow rates, enhanced rates of subsurface dissolution, a reduction in the overall rate of salt-wall uplift, or enhanced rates of mini-basin subsidence (Jackson and Talbot, 1986; Senseny et al., 1992). Climate is also a fundamental control that influences rates of weathering and erosion in fluvial catchments, fluvial discharge regime, style of sediment transport, and fluvial form at downstream sites of sediment deposition. Thus, climate exerts a significant influence on the ensuing style of fluvial sedimentation and generation of preserved sedimentary architecture.

***Sediment delivery direction.*** The orientation of inherited sediment delivery networks relative to the orientation of the trend of evolving salt walls exerts a fundamental control on the style of stratigraphic architecture preserved both within a single mini-basin and between neighbouring mini-basins. In situations where preferred drainage is aligned transverse to the trend of growing salt walls – and especially in cases where salt-wall uplift has been sufficient to generate a surface topographic expression – the style of fill of a series of adjacent mini-basins will tend to be manifest as a systematic proximal-to-distal fining away from the sediment source (Venus, 2013). By contrast, fluvial drainage systems aligned parallel to the trend of salt walls tend to result in basin-fill architectures that can change from sand-prone to sand-poor between neighbouring mini-basins, in situations where topography associated

with growing salt walls is effective in confining fluvial fairways to a particular mini-basin, leaving others relatively sediment-starved (Banham and Mountney, 2013 a, b).

***Sediment delivery rate.*** The rate of sediment delivery, which is significantly controlled by external factors such as climate regime and bedrock geology in the catchment area, exerts a direct control on the rate at which accommodation in mini-basins becomes filled; evidence for such control is recorded in the architectural fill-style of the developing mini-basins. Furthermore, the rate of sediment delivery and infilling of accommodation also exerts an indirect control on the generation of new accommodation by driving additional subsidence due to loading that enhances rates of subsurface salt withdrawal from beneath evolving mini-basins. High rates of sediment delivery tend to favour rapid infilling of available accommodation, leading to significant reworking of earlier deposits by fluvial systems that migrate dynamically across alluvial plains and undertake repeated avulsions. Such activity tends to preserve fluvial expressions that are dominated by relatively coarse-grained lower parts of fluvial channel-fill elements, with reworking leading to considerable bypass of detritus farther downstream (Hardgrove et al., 2010). Such conditions favour the accumulation of relatively sand-prone basin-fill styles with the associated preservation of multi-storey channel complexes (Banham and Mountney, 2013a). By contrast, low rates of sediment delivery favour the accumulation and preservation of more complete fluvial depositional cycles arising from the cut, fill and migration of channels and the accumulation of surrounding floodplain elements since accommodation will more likely be available to promote preservation. Such conditions tend to favour the development of relatively sand-poor basin fills in which a greater proportion of argillaceous floodplain sediments are preserved and where channel-belts will tend to be isolated in otherwise overbank-dominated successions (cf. Bristow and Best, 1993; Banham and Mountney, 2013a).

***Dissolution rate.*** Salt dissolution by meteoric waters tends to enhance rates of mini-basin subsidence and retard rates of salt-wall growth. A reduction or even reversal of salt-wall uplift may result in the diminishment or elimination of surface topographic expression, resulting in a reduction in the amount of incision required by a fluvial system to maintain a drainage pathway across an

actively uplifting salt wall and potentially eventually leading to the linkage of neighbouring mini-basins and a cessation of basin isolation.

These parameters can interact dynamically creating both positive and negative feed-back cycles, which can enhance, or retard the rate of sediment accumulation within this basins.

## Fluvial Interactions

Surface topography generated by the combination of growth of salt walls with subsidence of adjacent mini-basins exerts a fundamental control on fluvial drainage pathways and therefore also on the resultant accumulated stratigraphic succession. The effect of this control is manifest in a number of different ways (Fig. 2.7). Preferred or inherited orientation of drainage networks relative to the trend of salt walls acts to determine the type and geometrical arrangement of preserved fluvial elements and their distribution both within and between mini-basins. Topography associated with uplifted salt walls can divert or deflect transverse-draining fluvial systems, or induce localised accumulation of sediment while fluvial systems attempt to incise across uplifted salt-walls. This can ultimately lead to drainage capture or diversion and the development of antecedent drainage networks. Sediment input into neighbouring basins, may then be reduced which inturn can lead to the formation of relatively sand-poor basins adjacent to relatively sand-prone basins. Where drainage pathways cross salt-wall-generated topography, the potential rate of fluvial incision must be greater than the rate of salt-wall uplift for the fluvial course to be maintained.

Active channels draining parallel to or across salt-wall-generated topography can migrate and encroach on to and rework sediment derived from the flanks of salt walls leading to the accumulation of beds composed of locally reworked intraformational clasts or, in some cases, diapir-derived detritus such as reworked clasts of gypsum, carbonate or clastic material associated with surface exposure of the uplifted salt (Lawton and Buck, 2006; Banham and Mountney, 2013a).

In the case of axial-draining fluvial systems for which confining salt-wall-generated topography is linear, elongate and continuous, individual mini-basins tend to be isolated from their neighbours, even where surface relief

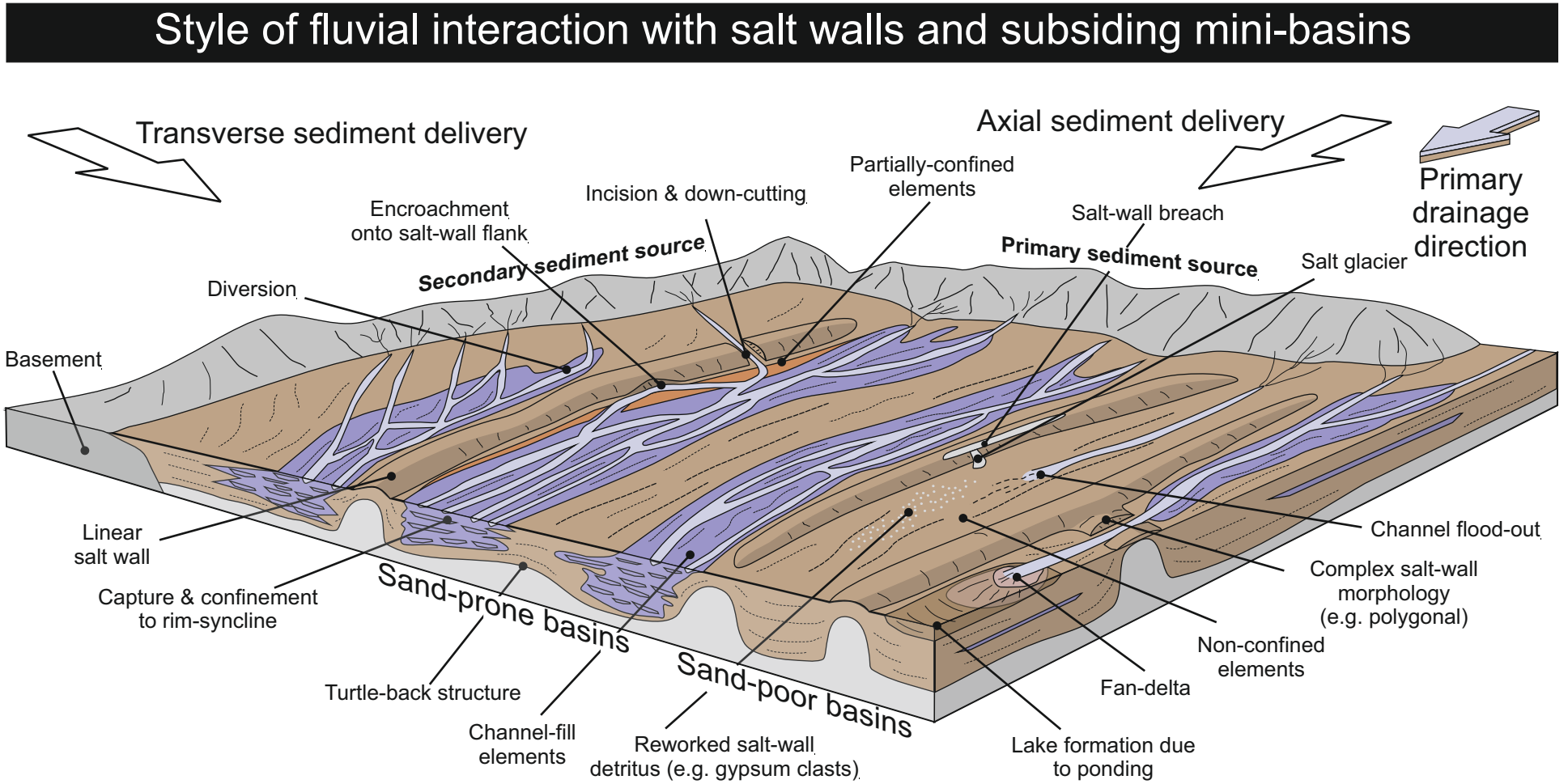


**Figure 2.7**: Fluvial interactions with uplifted salt walls and subsiding mini-basins. Sediments can be delivered transversely or axially into the mini-basins and this may act to dictate the ensuing basin-fill style. The development of polygonal salt walls can further add to stratigraphic complexity.

over the salt wall is minimal. This configuration potentially allows significantly different successions to accumulate between neighbouring basins, in terms of sediment and rate of accumulation.

Generation of topographic lows associated with the development of rim-synclines by the preferential withdrawal of salt from beneath the margins of mini-basins adjacent to salt walls (Barde et al., 2002b; Banham and Mountney, 2013a) can result in the capture of fluvial systems and their confinement to the edges of a single mini-basin (Fig. 2.7). As such, the distribution of preserved fluvial elements in areas close to the flanks of salt walls can vary markedly from those present in the central part of the same mini-basin (Andrie et al., 2012; Banham and Mountney, 2013a, b). Salt trapped beneath the centre of a mini-basin can result in formation of a turtle-back structure (sensu Barde et al., 2002a), where subsidence rates are reduced relative to those of adjacent rim-synclines (Fig. 2.7). This can result in the generation of a relative high in the centre of a mini-basin that may limit the rate of sedimentation in such regions and may even potentially isolate two marginal rim-synclines to form sub-basins.

In isolated basins, where fluvial activity is limited due to preferential drainage into adjacent basins, active fluvial processes tend to be dominated by: (i) localised reworking and redistribution of sediment from uplifted salt-wall topography; (ii) delivery of sediment via the overspill of drainage pathways from adjacent basins; and (iii) the development of minor drainage pathways within the basin via supply along the basin axis, in some cases in the form of episodic non-confined flow rather than channelised flow (Abdullatif, 1989; Banham and Mountney, 2013b*)*. Non-confined flows that give rise to depositional sediment bodies with thin but laterally extensive sheet-like elements and only minor channel elements are especially common in relatively isolated, sediment-starved basins under semi-arid climates (Rahn, 1967; Williams 1970; Benvenuti *et al.*, 2005; Banham and Mountney, 2013a, b).

## Mini-basin sediment-fill style

The interplay between the rates of sediment supply and accommodation generation due to subsidence is a key factor that dictates basin-fill style (S) in

evolving mini-basins (Fig. 2.8). For example, for a relatively high and constant rate of sediment supply (Fig. 2.8), fluvial strata within a slowly-subsiding basin will experience significant reworking as fluvial systems avulse and migrate laterally, preserving only the lower parts of channel-fill elements that become vertically stacked to form multi-storey channel complexes dominated by coarse-grained clastic deposits. In such cases, aggradation rates are relatively low and the middle and upper parts of channel-fill elements, including the sandy bedforms that typically characterise the middle parts of fluvial depositional cycles (Miall, 1996), will be prone to reworking as later channels migrate across the flood plain. In cases like this, where the rate of sediment delivery outpaces the rate of accommodation generation, an ***over-filled basin*** tends to develop, the fill of which is dominated by channel lag and gravel sheet elements arranged into multiple, vertically stacked thin sets and cosets separated by complex arrangements of erosional bounding surfaces (Fig. 2.8). Bypass of sediment farther downstream within the system as sand-dominated bedload and mud- and silt-dominated suspended load is significant.

In cases where the rate of sediment delivery is broadly in equilibrium with the rate of accommodation generation due to on-going subsidence, fluvial depositional cycles will tend to preserve a relatively complete record of the cut, infill, lateral migration and final abandonment of channel systems (Fig. 2.8). Such fluvial cycles tend to have an erosional base, a lower part dominated by gravel sheet elements, a middle part dominated by cross-bedded sand-dominated bedform elements, and an upper part dominated by ripple cross-laminated fine-grained sandstone elements (often with climbing-ripple strata) and argillaceous floodplain elements. In some cases, the down-cutting associated with the emplacement and lateral accretion of later channel elements will result in reworking of overbank (floodplain) elements and the transport of argillaceous sediment farther downstream. Over time, this will culminate in the formation of a ***filled basin***, the fill of which will tend to be dominated by a sand-prone basin fill style in which fining-upward depositional cycles are evident.

In cases where the rate of sediment delivery is outpaced by the rate of accommodation generation due to subsidence, the potential vertical

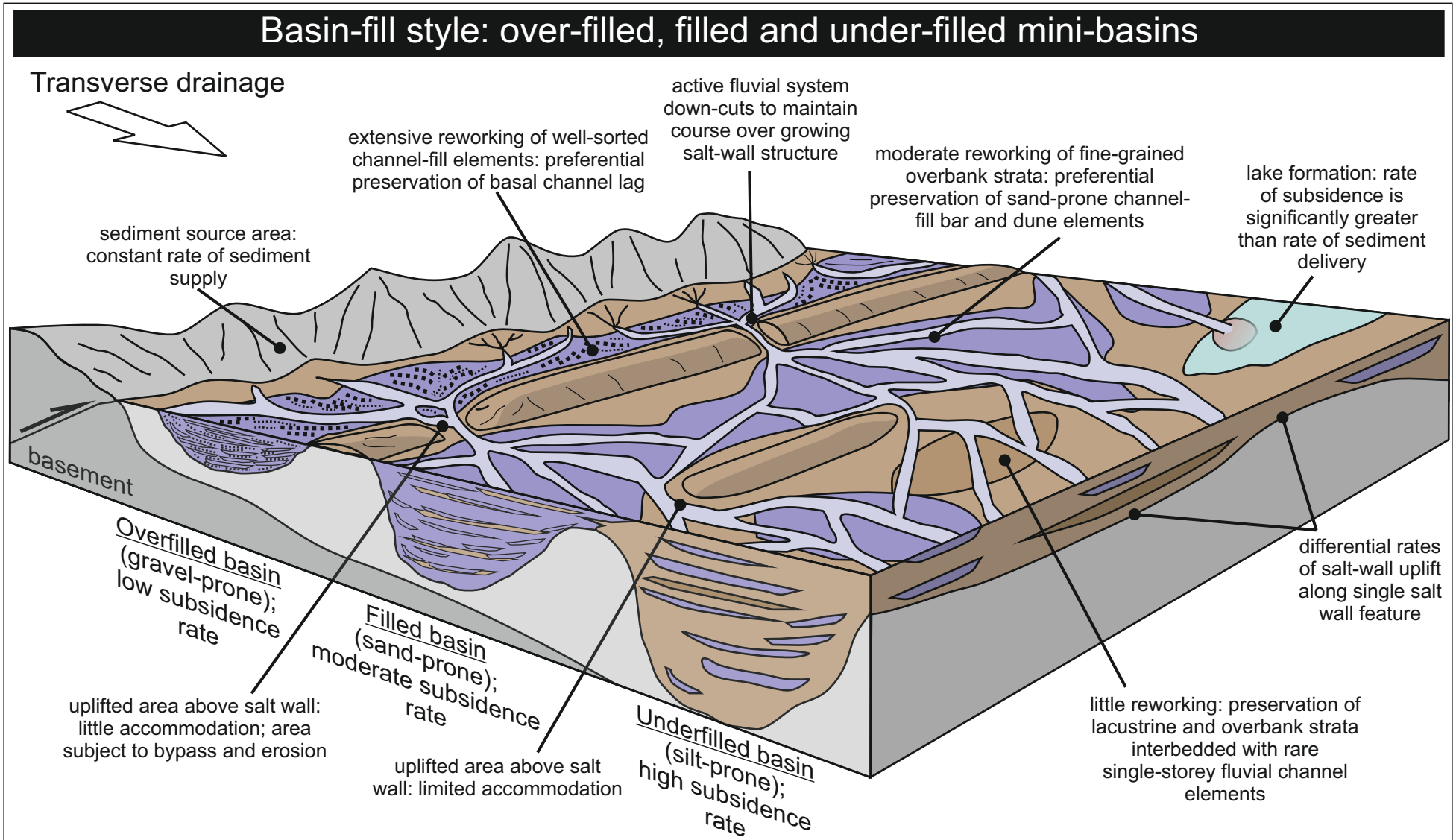


**Figure 2.8**: Basin-fill style, demonstrating the development of over-filled, filled, and under-filled basin styles. The model depicts a system subject to a constant rate of sediment supply rate, but for adjacent mini-basins that undertake variable rates of subsidence.

aggradation rate will be high but if sedimentation rate does not fill available accommodation an ***under-filled basin*** will develop, the fill of which will be dominated by channelised fluvial elements encased within finer-grained elements of floodplain and overbank origin (Fig. 2.8). The preservation potential of floodplain packages is greatest in these types of basins, and relatively silt-prone and sand-poor basin-fill styles tend to accumulate as a consequence. Fluvial successions in under-filled basins are commonly intercalated with lacustrine successions, especially in humid-climate settings (Prochnow et al., 2006; Matthews et al., 2007). By contrast, in arid-climate settings, accommodation may remain unfilled and sabkha and playa systems may develop (Banham and Mountney 2013a).

## *2.4 Case Studies*

The expression of fluvial systems accumulating in salt-walled mini-basins varies dramatically, both between and within halokinetic provinces (c.f., Bromley, 1991; Matthews et al., 2007; Venus, 2013; Banham and Mountney, 2013 a, b). The various styles of basin fill are herein explored through studies (Table 2.1) which demonstrate how the interplay between various controlling factors (Fig. 2.5) act to dictate drainage pathways, the generation of localised depocentres, and the style of fluvial system accumulation and preservation.

### 2.4.1 Salt Anticline Region, SE Utah

The Salt Anticline Province of SE Utah is located in the foredeep of the Paradox Basin, which developed as a flexural foreland basin during the Pennsylvanian in response to loading of the continental plate by the Uncompahgre Uplift of the Ancestral Rocky Mountains (Barbaeu, 2003; Fig. 2.9). The Uncompahgre Uplift formed the northwest margin of the basin, adjacent to the foredeep, and acted as a source of sediment throughout much of the Pennsylvanian and Permian (Kluth and Coney, 1981; Barbeau, 2003), eventually leading to the progradation and accumulation of the alluvial mega-fan of the Cutler Group (Barbaeu, 2003; Cain and Mountney, 2009, 2011). A series of transgressive-regressive cycles driven by eustatic sea-level changes during the Pennsylvanian (Goldhammer et al., 1991) resulted in the periodic partial isolation of the foredeep region from a larger epeiric sea-way by the

| Case Study | Age | Drainage Orientation | Climate | Type | Sed Supply Rate | Subsidence Rate | Fill Style | Key References |
|---|---|---|---|---|---|---|---|---|
| **Paradox Basin** | | | | | | | | Barbeau, 2003; Trudgill, 2011 |
| **Cutler Group** | Permian | Transverse | Arid | Braided | High | High | Gravel Prone | Venus, 2013 |
| **Moenkopi Fm** | Triassic (Lower) | Axial | Hyperarid | Braided/Nonconfined | Low | Moderate | Basin Dependent (Silt Prone) | Stuart *et al.* , 1972; Lawton & Buck, 2006; Banham & Mountney, 2013a&b |
| **Chinle Fm** | Triassic (Upper) | Axial | Subhumid - Arid | L. Meandering U. Braided | High | Low | Sand Prone | Hazel, 1994; Protchnow, 2006; Matthews *et al.,* 2007 |
| **Kayenta Fm** | Jurassic | Tangental | Arid | Braided | High | Low | Sand Prone | Bromley, 1991 |
| **Precaspian Basin** | | | | | | | | Volozh, 1997; Barde *et al.,* 2002a |
| **Tatarian** | Permian | Transverse | Arid | Braided, Evaporitic | - | - | Basin Dependent | Barde *et al.* , 2002b; Newell *et al.* , 2012 |
| **Triassic** | Triassic | Transverse | Semiarid | Braided, Lacustrine, Detaic | High | Moderate | Basin Dependent | Barde *et al.,* 2002b; Newell *et al.,* 2012 |
| **Central Graben, CNS** | | | | | | | | |
| **Skaggerak Fm** | Triassic | Axial | Arid | Braided/NonConfined Terminal splay | Low-Mod. | Moderate | Basin Dependent (Sand Prone) | Hodgson *et al.,* 1992; Smith *et al.* , 1993; McKie, 2011 |
| **La Popa Basin** | | | | | | | | Rowan *et al.,* 2012 |
| **Carroza Fm** | Eocene | Axial | Arid | Braided | Moderate | - | - | Buck *et al.,* 2010; Andrie *et al.,* 2012 |
| **Germany** | | | | | | | | |
| **Weisselster Basin** | Eocene | | Temperate | Meandering | - | Low | - | Halfar *et al.* 1998 |
| **River Weser & Aller** | Recent | Axial | Temperate | Meandering | - | Low | - | Sirocko *et al.* , 2002 |
| **Canada** | | | | | | | | |
| **New Brunswick** | Carboniferous | - | - | - | - | - | - | Waldron & Rygel, 2010; Craggs *et al.* , 2013 |
| **Severdrup Basin** | Juras. - Cret. | - | ?Temperate | - | - | - | - | Harrison & Jackson, 2013 |

**Table 2.1:** Global examples of halokinetic provinces where fluvial systems accumulated during evolution of the province

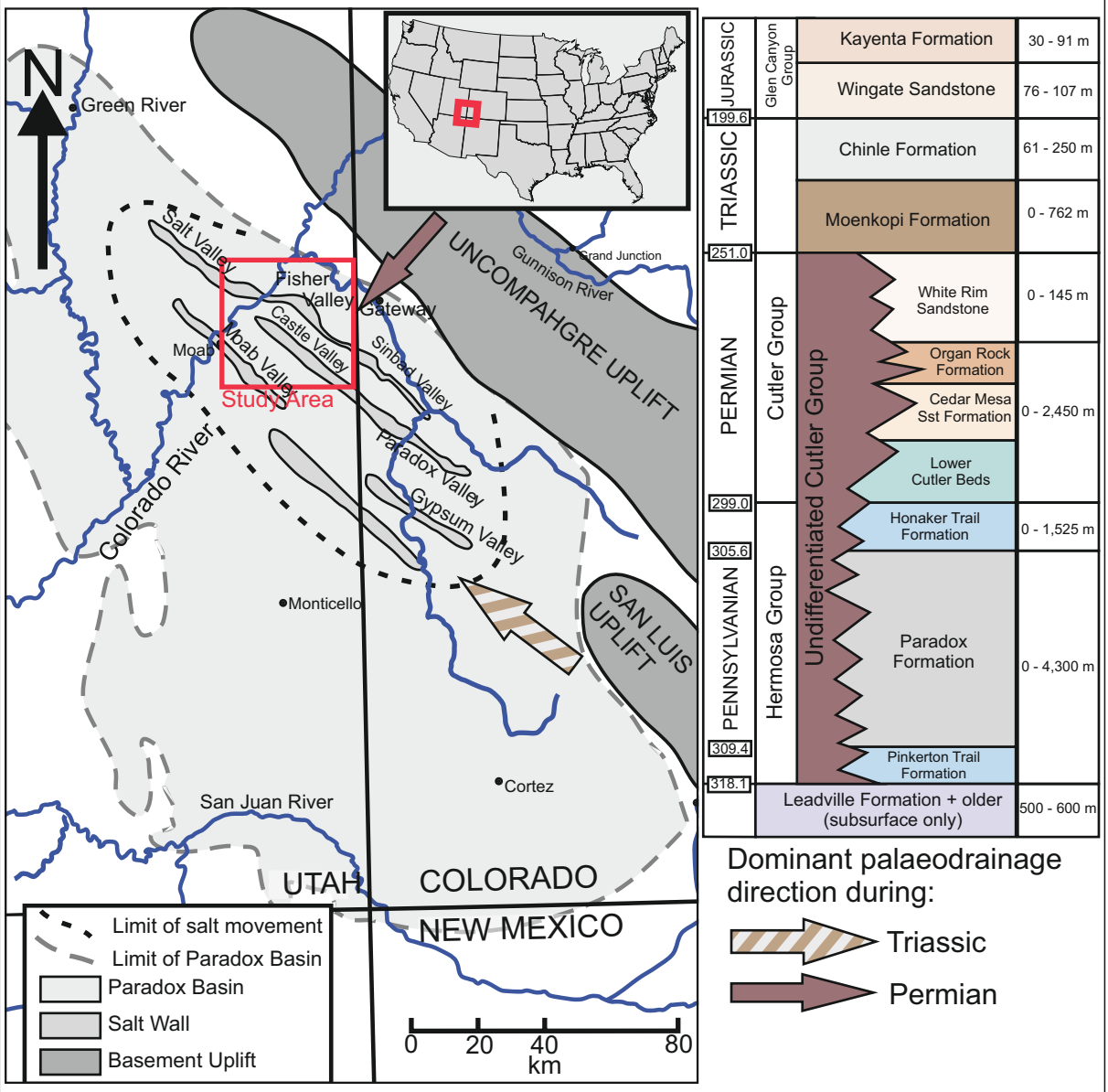


**Figure 2.9**: Salt Anticline Region, southeastern Utah. Overview of map and stratigraphy of the Paradox Basin.

forebulge of the Paradox Basin, and this repeated isolation resulted in the accumulation of a thick succession of evaporites (the Paradox Formation).

Pre-salt basement faults generated by brittle deformation associated with flexural down-warping are aligned northwest-to-southeast, parallel to the elongate trend of the uplifted Uncompahgre Front (Doelling, 1988; Barbeau, 2003; Trudgill, 2011). The accumulation of differential salt thicknesses across these basement faults, combined with differential loading of the salt by the Cutler Undivided mega-fan likely initiated salt movement and controlled the location and orientation of the resultant salt walls, which grew to form linear features along the same northwest-southeast trend (Prommel 1923; Shoemaker and Newman, 1959; Doelling, 2002). Halokinesis and mini-basin development commenced in response to loading of salt of the Paradox Formation by accumulating fluvial strata of the overlying Honaker Trail Formation and Cutler Group during the late Pennsylvanian and Permian (Kluth and DuChene, 2009; Trudgill, 2011). Throughout the duration of sedimentation in the Salt Anticline Region, both the direction and rate of sediment supply varied substantially. These changes are recorded by significant differences in the style of fill of the mini-basins by fluvial (see below). Mini-basin subsidence and sediment accumulation continued throughout Permian (Venus, 2013), Triassic (Matthews et al., 2007; Banham and Mountney, 2013a), and locally into the Jurassic (Doelling, 1988; Bromley, 1991). Four fully developed salt-walled mini-basins developed between the Uncompahgre Front and the Paradox fore-bulge: the Fisher; Parriott; Big Bend (Matthews et al., 2007; Banham and Mountney, 2013a,b); and Shafer basins (Venus, 2013). Additional mini-basins not described here are present elsewhere in the region, most notably along-strike from these primary basins (Trudgill, 2011).

**The Cutler Group**

The Undifferentiated Cutler Group, of predominantly Permian age, accumulated in the mini-basins of the Salt Anticline Region during a protracted episode characterised by relatively high rates of sediment delivery. Sediment was principally sourced from the eroding Uncompahgre Uplift, a region of significant regional elevation on the northeast flank of the Paradox

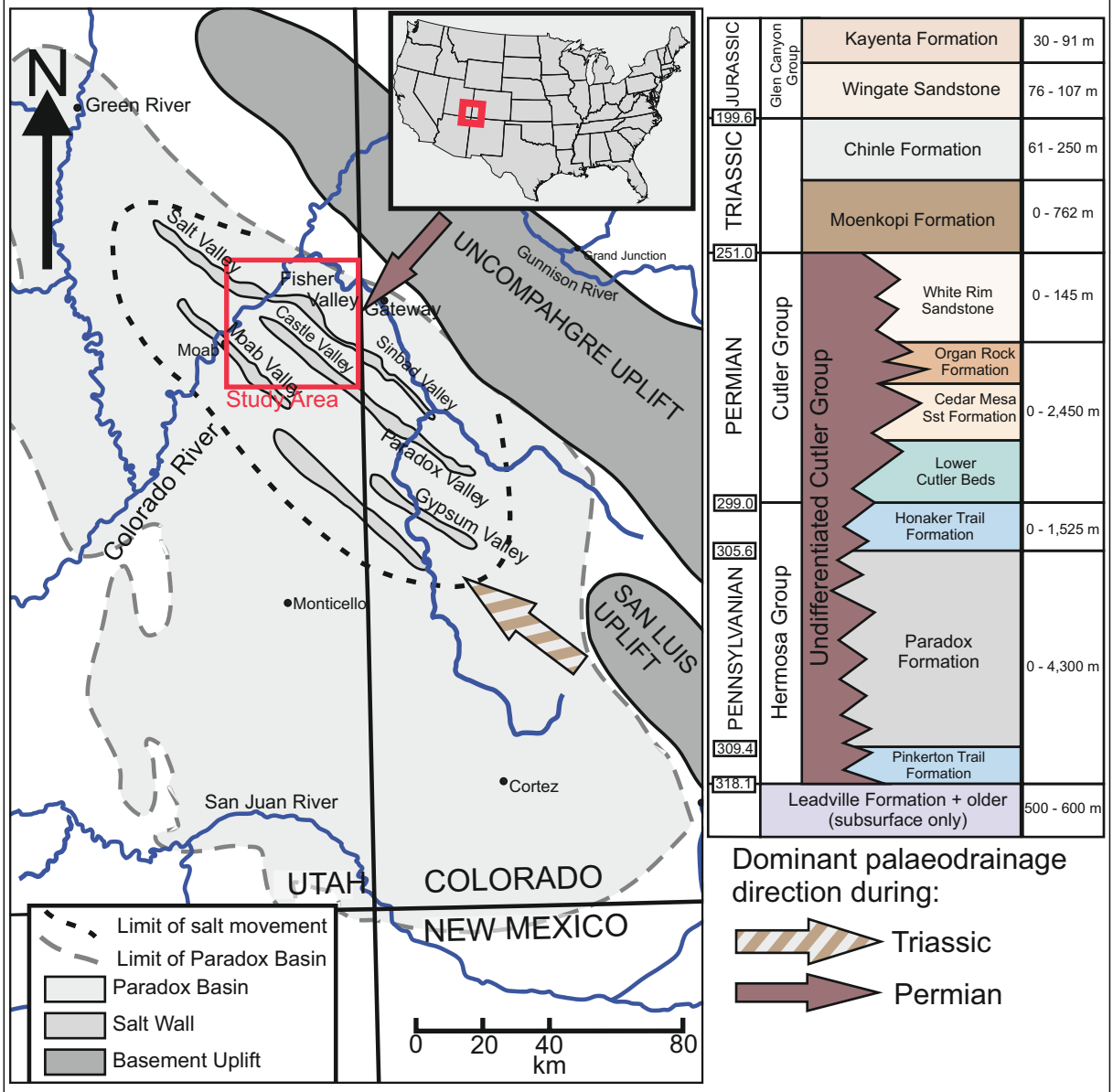


**Figure 2.9**: Salt Anticline Region, southeastern Utah. Overview of map and stratigraphy of the Paradox Basin.

Basin, and delivered southwest-wards into the Salt Anticline Region, perpendicular to the northwest- southeast trend of the evolving salt walls (Werner, 1974; Mack and Rasmussen, 1984; Cain and Mountney, 2009; Venus, 2013; Fig. 2.10). The prevailing climate at this time was dominantly semi-arid (Werner, 1974; Cain and Mountney, 2009), though with evidence for more humid episodes at times (Cain and Mountney, 2009, 2011; Soreghan et al., 2009). Evidence for these climatic variations are recorded in part by the progradation and retrogradation of the Organ Rock Formation, a ~100 m-thick wedge of alluvial strata, which is the lateral equivalent of the Undivided Cutler Group and which interacts with an aeolian dune field in the distal part of the Paradox Basin, beyond the margin of the Salt Anticline Region (Cain and Mountney, 2009).

The transverse drainage orientation relative to the trend of the actively uplifting salt walls resulted in initial preferential deposition and accumulation of fluvial strata in the Fisher mini-basin that developed adjacent to the frontal thrust of the Uncompahgre Uplift, most proximal to the sediment source (Venus, 2013). Throughout most of the episode of accumulation of strata of the Cutler Group, the rate of delivery of sediment significantly outpaced the rate of subsidence, and an over-filled basin state developed in which the accumulating fluvial system was able to rapidly fill available accommodation in the developing mini-basins, sequentially from the most proximal Fisher Basin, and latterly into the Parriott and Big Bend basins (Kluth and DuChene, 2009; Trudgill, 2011). During the late Permian, the fluvial systems were episodically able to deliver sediment beyond the distal limits of the Salt Anticline Region, leading to progradation of the Organ Rock Formation (Cain and Mountney, 2009).

The styles of fluvial sediment fill within the subsiding mini-basins document an architectural expression which records high rates of sediment delivery that resulted in an over-filled basin state and the preservation of a sand- and gravel-prone fill-style (Venus, 2013). The total thickness of accumulated Cutler Group sediments in each mini-basin systematically decreases from the more proximal Fisher Basin to the more distal Shafer Basin across the Salt Anticline Region (Paz and Trudgill, 2009; Trudgill, 2010). Basin-fill styles demonstrate a progressive fining trend from the

proximal Fisher Basin into the Parriott, Big Bend and finally into the Shafer basins (Cain and Mountney, 2009, 2011; Venus, 2013). This occurred, in-part, due to systematic fining of the sediment in transport with increasing distance down-steam, and implies a decrease in fluvial energy and transport capacity that is typical of alluvial mega-fans or distributive fluvial systems, due to radial spreading and transmissions loss (Fisher and Nichols, 2007; Hartley et al., 2010; Weissmann et al., 2010). Additionally, downstream fining of the calibre of accumulated sediment was also influenced by episodic salt-wall uplift, which episodically resulted in repeated diversion of fluvial drainage pathways to orientations parallel to the trend of the salt walls and the ponding of flood-water and sediment behind growing salt-wall topography (Venus, 2013). These “pond” elements are characterised by non-channelised elements containing high proportions of mica, suggesting an episodic damming of flood-waters that resulted in the accumulation of deposits from slow-flowing or standing water in areas directly upstream of uplifted salt-wall topography.

The damming of floodwater required the emergence of localised relief associated with growing salt-wall topography and such episodes record the episodic transition to a temporarily under-filled basin-fill style. Ponding of sediment behind salt walls likely corresponded to episodes of decreased fluvial activity at times of heightened climatic aridity: fluvial deposits indicative of such conditions are characterised by surfaces with desiccation cracks in fine-grained strata and sedimentary structures such as climbing ripples and trough cross-bedding which record palaeoflow indicators that are diverted or even reversed compared to the dominant south-westerly trend (Venus, 2013). Despite evidence to show that salt-wall topography influenced fluvial drainage pathways, few salt clasts are preserved in the Cutler Group accumulations that form the main fill of the mini-basins, and this demonstrates that the salt walls themselves were unlikely to have breached the land surface.

Episodic resurgence of fluvial activity led to overtopping of salt walls and such events likely corresponded to more humid climatic episodes. For such events, palaeoflow indicators record transport directly across buried salt walls suggesting the burial of any earlier surface topographic expression. Localised reworking of fluvial strata from atop salt walls is demonstrated by an increase in the occurrence of intraformational rip-up clasts in sediment

accumulations directly downstream from the buried but slowly growing salt walls (Cain and Mountney, 2009; Venus, 2013).

**The Moenkopi Formation**

The resumption of fluvial accumulation in the Salt Anticline Region of the Paradox Basin in the early Triassic coincided with a significant change in the climatic and drainage regime of the region. Sediment accumulation during this period occurred under the influence of an arid to hyper-arid regime (Blakey and Ranney, 2008; Banham and Mountney, 2013b). Palaeodrainage from the Uncompahgre Highlands had diminished significantly by the onset of deposition of the Moenkopi Formation, and instead a new dominant drainage pathway had become established that was sourced in the San Luis and Defiant Upwarp region to the southwest (Fig. 2.11), and which drained north-westward through the Salt Anticline Region (Stuart et al., 1972; Blakey, 1974; Banham and Mountney, 2013b). Sediment was delivered axially into what was by then a series of well-developed northwest-southeast-trending mini-basins: the Fisher, Parriott and Big Bend Basins, each of which was apparently isolated from its neighbouring basins in terms of drainage pathways.

Subsidence rates between the basins varied throughout accumulation of the Moenkopi Formation, in part due to the inheritance of basin-fill geometries from the previously accumulated deposits of the Cutler Group. These inherited basin-fill geometries, where the basin-fill thicknesses varied both within and between basins, were important in controlling the style, timing and rate of mini-basin subsidence throughout accumulation of the Moenkopi Formation. The basin-fill thickness was thinnest adjacent to the Uncompahgre Uplift (where Cutler Group sediments were preferentially deposited in the earlier phase of basin fill) and thickened towards more central parts of the Paradox Basin (Banham and Mountney, 2013a). Variable rates of both subsidence and sediment supply resulted in the accumulation of both sand-prone (filled) and sand-poor (under-filled) basin-fill styles in neighbouring basins for the same stratigraphic levels. The Fisher Basin, which had little remaining remnant basin-fill potential (i.e., available accommodation) due to its imminent grounding by the onset of the early Triassic, experienced low rates of subsidence (Banham and Mountney, 2013a). This, coupled with high

rates of sediment delivery (both from the San-Luis Uplift region and from the remnant Uncompahgre Highlands as a secondary source), resulted in the accumulation of a sand-prone basin-fill style, apparently early in the history of accumulation of the Moenkopi Formation. As the basins evolved during the early Triassic, the rate of sediment delivery to the Fisher Basin progressively diminished, in-part due to the final denudation of the Uncompahgre Uplift, resulting in the basin-fill style becoming progressively less sand-prone upwards.

In the adjacent Parriott Basin, the basin-fill potential varied spatially, due to the variable thickness of the inherited basin-fill: basin-fill potential was least on the side of the basin closest to the Uncompahgre Front where a thick succession of Cutler Group sediments had accumulated, and greatest on the distal margin of the basin. This resulted in preferential subsidence on the distal margin of the Parriott Basin, culminating in the formation of a rim-syncline in the latter stages of accumulation of the Moenkopi Formation. This rim-syncline, which formed a locus of subsidence and which apparently formed a topographic low, acted as a preferential drainage corridor, leading to the accumulation of stacked fluvial channel-fill elements during the final phases. During accumulation of the middle and upper parts of the Moenkopi Formation, high rates of salt-wall uplift, combined with an increase in climatic aridity resulted in a relative reduction in the of rate sediment supply (Banham and Mountney, 2013a) which allowed the Castle Valley Salt Wall, separating the Parriott and Big Bend basins, to breach the land-surface (Lawton and Buck, 2006). Detritus derived from surface exposure of this salt wall was subsequently reworked into discrete gypsum-clast-bearing units, which are preserved in the succession around the flanks of the Castle Valley salt wall, in both the Parriott and Big Bend basins. The Big Bend Basin, which occupied a position further from the Uncompahgre Uplift, had the greatest basin-fill potential at the onset of accumulation of the Moenkopi Formation and the rate of sediment supply to this basin is interpreted to have been slightly higher than that to the Parriott Basin because a greater proportion of channel elements are preserved throughout the stratigraphic succession, especially in the upper part where the in-fill of a pronounced rim-syncline is dominated by

amalgamated channel-fill elements, indicating preferential concentration of drainage pathways in this topographic low.

**The Chinle Formation**

By onset of accumulation of the Chinle Formation, the Fisher and Parriott Basins had all but effectively grounded, allowing only very limited additional accumulation in these basins. The palaeodrainage direction remained axial to the salt walls, towards the northwest. The final burial of the remnants of the Uncompahgre Uplift signified a final cessation of sediment derived from the northeast (Trudgill, 2011). Climate during accumulation of the Chinle Formation changed from humid to semi-arid (Prochnow et al., 2006; Fig. 2.9d). This shift in climate is recorded by a change in fluvial style: architectural elements in the lower part of the formation are characterised by thick and well-developed palaeosols that are intercalated with thick channel-fill elements, the internal fill of which is dominated by asymptotic-based cross-stratified sets indicative of accumulation of a coarse-grained meandering river system in which lateral accretion processes dominated (Hazel, 1994); the upper part of the formation, records laminated sand sheet elements and sandy bedforms containing crudely-bedded conglomerate and coarse-grained sandstone trough cross-stratified sets and scour fills, indicative of accumulation of a gravelly low-sinuosity fluvial system (Hazel, 1994).

Preferential accumulation of fluvial deposits of the Cutler Group and Moenkopi Formation in the basins closest to the Uncompahgre Uplift limited the remnant basin-fill potential of the Fisher and Parriott Basins, which by the Late Triassic had effectively grounded. However, in the Big Bend Basin, lower rates of subsidence throughout evolution of this basin, and the retention of residual salt beneath this basin, allowed continued localised subsidence into the Late Triassic. This is reflected by variations in thickness in units of the lower part of the Chinle Formation, which vary from <10 m thick in the northern-most part of the Paradox Basin, to over 50 m thick in localised depocentres, such as parts of the Big Bend Basin, and near the Cane Creek Anticline of the Shafer Basin to the southwest of the town of Moab (Matthews et al., 2007; Fig. 2.12). These localised depocentres record the final phases of subsidence associated with salt displacement from beneath mini-basins

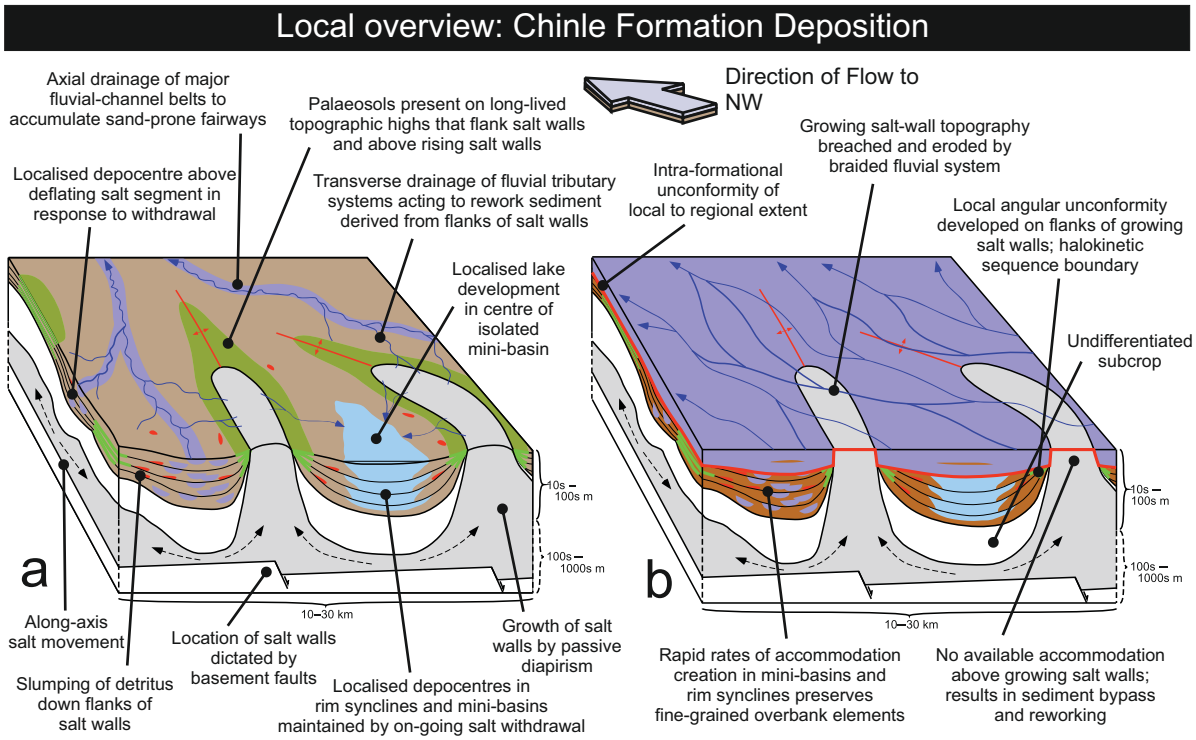


**Figure 2.12**: Salt Anticline Region, southeastern Utah. General depositional model depicting the style of fluvial accumulation in the Upper Triassic Chinle Formation, where episodic uplift of salt walls influenced sediment accumulation across the region. In addition, climate variation during influenced fluvial style and preserved stratigraphic expression. (Matthews et al., 2007)

where axial variations of salt thickness or rate of salt flow resulted in localised grounding relatively late in the history of evolution of the Salt Anticline Region and the concomitant accumulation of a thicker succession.

In addition to variations in preserved thickness, angular discordances between the Chinle and Moenkopi formations, together with intraformational unconformities within the Chinle Formation, indicate ongoing tilting of strata by halokinesis in some parts of the succession (Matthews et al., 2007). Areas of relatively high rates of subsidence in basin centres were typically poorly drained, resulting in accumulation of lacustrine elements, especially during the lower part of the Chinle Formation (Matthews et al., 2007). Multi-storey channel elements and palaeosols accumulated toward the basin margins during episodes of halokinetic quiescence, with higher proportions of channel elements and palaeosol maturity apparently increasing with the duration of quiescence (Prochnow et al., 2006; Matthews et al., 2007). In the upper part of the Chinle Formation, an increase in aridity is recorded by a change from a meandering to a braided system (Hazel, 1994). During this episode palaeodrainage was oblique to salt-wall axes; aggradation of the basin fill to the level where available accommodation was filled temporarily allowed cross-salt-wall drainage, before renewed uplift of the salt walls resulted in deflection of the drainage pathways parallel to salt walls (Matthews et al., 2007).

### 2.4.2 Pre-Caspian Basin

Salt-walled mini-basins of the Pre-Caspian salt tectonic province, Pre-Caspian Basin developed in a rift basin which formed during the Devonian (Pairazian, 1999; Barde et al., 2002a; Fig. 2.13). Throughout the Carboniferous, approximately 2000 m of carbonate strata recording reef development accumulated in the basin at a time when it was largely starved of clastic sediment input (Schamel, 1995). This episode of carbonate accumulation ceased when the Pre-Caspian Basin became partially isolated from the regional sea due to uplift of the developing Ural Mountains to the east during the Late Carboniferous (Barde et al., 2002a; Volozh et al., 2003). This restriction of marine water circulation resulted in repeated desiccation of the basin, culminating in the accumulation of up to 4500 m of salt during the Kungurian to Kazanian (Permian) (Garalla and Marsky, 2000; Barde et al.,

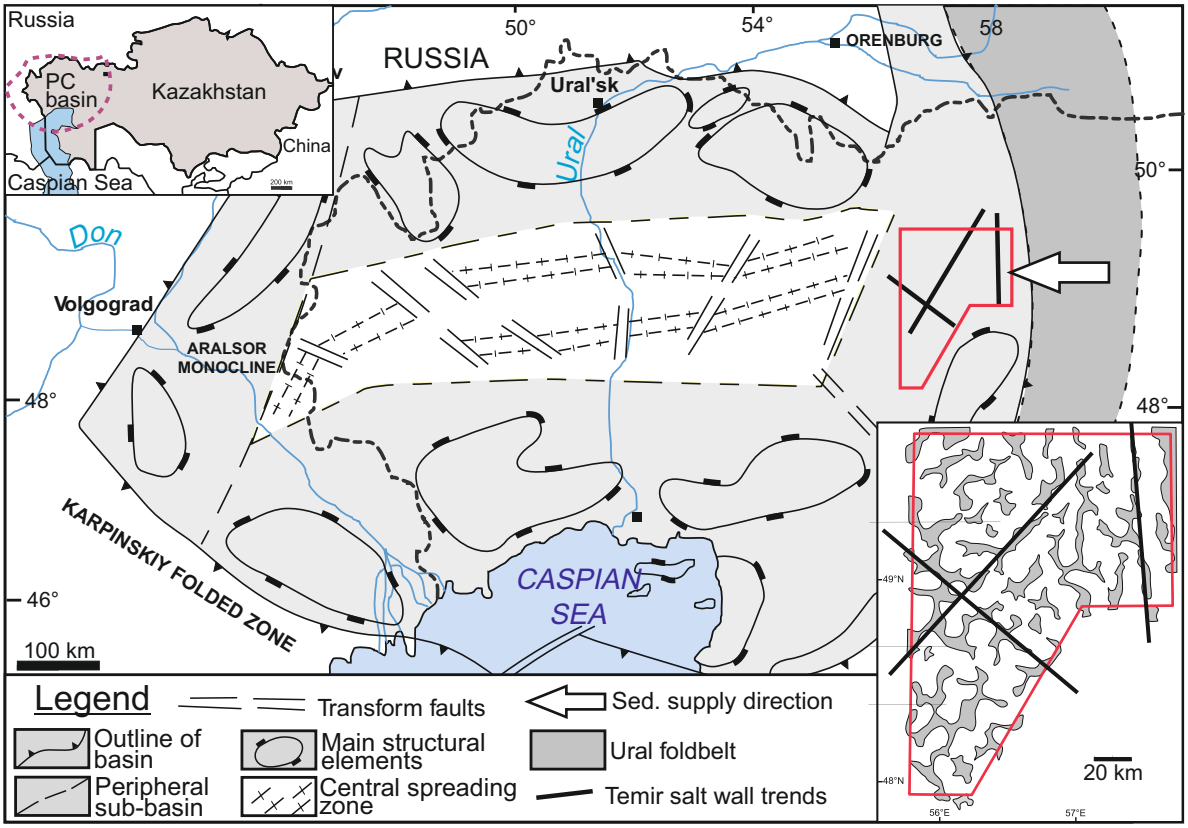


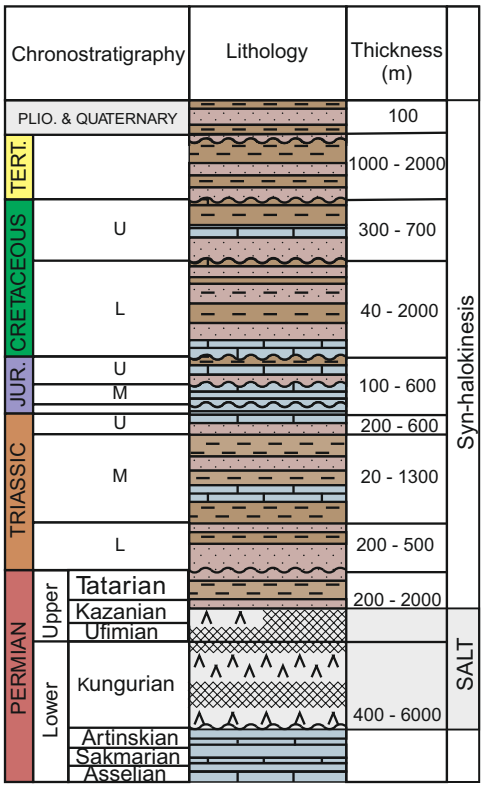


**Figure 2.13**: Pre-Caspian Basin, Kazakhstan. Overview map and stratigraphic column (After Barde et al., 2002a, b).

2002a). Onset of halokinesis was linked to further uplift of the Urals, either by lateral shortening and orogenic collapse (Ings and Beaumont, 2010; Newell et al., 2012) or by sediment loading induced by accumulation of clastic sediments derived from the Urals. The orientation of the developing salt walls was controlled either by pre-existing basement trends inherited from the original onset of the Pre-Caspian Basin or from the ensuing uplift of the Urals (Barde et al., 2002a; Brown et al., 2004). These events resulted in the development of complex basement trends, which are expressed by the distribution of salt-wall geometries: linear salt walls with a north-south trend typically developed in the east and these follow basement faults sympathetic to the trend of the Urals. In the rest of the Pre-Caspian Basin, basement faults are typically oriented northeast-southwest and southeast-northwest, having been generated during the initial evolution of the basin (Barde et al., 2002a). These competing basement trends resulted in the generation of salt walls with polygonal geometries throughout the rest of the basin (Barde et al., 2002a; Volozh et al., 2003).

Sediment accumulation within the mini-basins occurred from the Late Permian through to present, with rates of halokinesis having decreased significantly since the Triassic. Up to 6 km of sediment accumulated in the western mini-basins (Barde et al., 2002; Newell et al., 2012). Most subsurface studies have focused on the Permian and Triassic parts of the basin fill since these host significant hydrocarbon plays (Barde et al., 2002a; O'Hearn et al., 2003, Volozh, et al., 2003); more recently, field-based studies have additionally been undertaken where outcrop allows (Newell et al., 2012).

Sediment was delivered into the Pre-Caspian Basin by fluvial systems emanating from the Ural Mountains (Newell et al., 2012) that drained transverse to the north-south trend of the linear mini-basins in the eastern part of the region. Climate during the Tatarian (Upper Permian) was semi-arid to sub-humid, whereas Triassic strata accumulated under a more arid climatic regime (Newell et al., 1999). The polygonal salt walls in much of the basin exerted a significant control on fluvial pathways and sediment distribution, resulting in the evolution of multiple of sedimentary environments within adjacent basins (Fig. 2.14). Where fluvial systems incised into uplifting salt walls and maintained their drainage pathways, braided river and associated

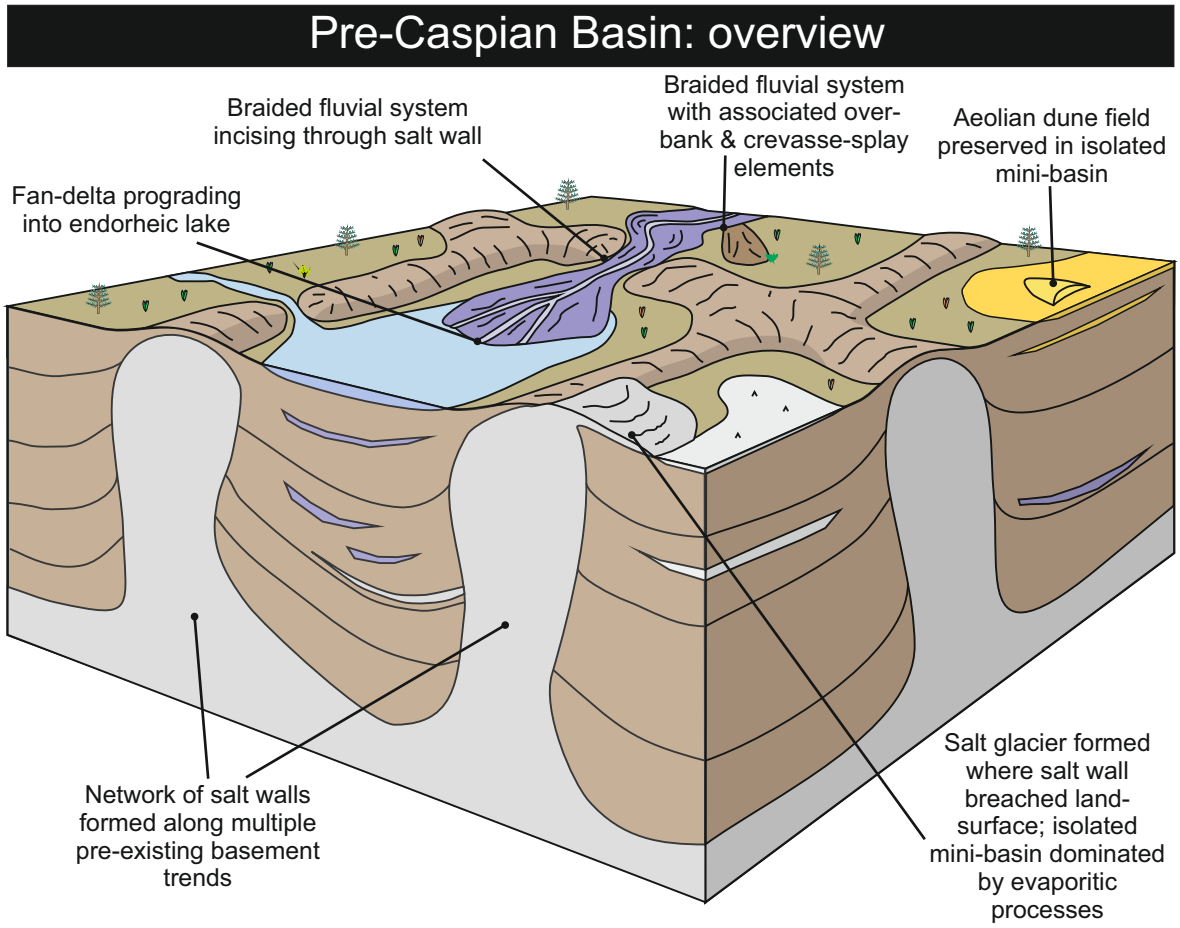


**Figure 2.14**: Pre-Caspian Basin, Kazakhstan. General depositional model depicting fluvial sediment accumulation in a series of polygonal salt-walled mini-basins in the Pre-Caspian Basin. Basin-fill style is highly variable: drainage pathways can become entrenched in some mini-basins, thereby preventing sediment delivery into neighbouring basins. Sediment-starved basins tend to be characterised by evaporitic or lacustrine sedimentation. Modified after Barde et al. (2002b).

facies dominated the basin fill (Barde et al., 2002b). Where mini-basins became endorheic, due to uplift of a salt wall on the downstream margin of the basin, intra-basin lakes developed, with the fluvial systems terminating as lacustrine fan-deltas (cf., Nichols and Fisher, 2007). This is expressed as a basin-fill style that is sand-prone at its upstream margin but which is dominated by heterolithic siltstone, mudstone and potentially lacustrine organic-rich argillaceous strata in its central part. Where mini-basins remained isolated due to diversion of drainage pathways or high rates of salt-wall uplift driven by displacement of salt from beneath adjacent basins, the resulting accumulation is dominated by a sediment-starved basin-fill style characterised by the accumulation of continental evaporites. Locally, diapir-derived detritus from salt-glaciers (salt-wall segments that breached the ground surface before undergoing gravity collapse) and conglomerate horizons (reworked from clastic material forming the flank of the uplifting salt wall) contributed to coarse detritus filling these basins (cf., Lawton and Buck, 2006; Buck *et al.*, 2010).

Basin-fill style between the mini-basins varies dramatically, as recorded by subsurface well-log data (Barde et al., 2002b). This is a function of several factors: inheritance and capture of pre-existing drainage pathways as mini-basins developed; maintenance of salt-wall height at a rate of uplift that preserved a long-lived topographic expression capable of effectively partitioning neighbouring mini-basins and localised differences in the rate of sediment delivery and accumulation to fill available accommodation in adjacent mini-basins. Presently, there is a lack of detailed sedimentological description for the basin-fill styles of the mini-basins in the Pre-Caspian Basin.

### 2.4.3 North Sea – J Block/Skagerrak Formation

During the Middle Permian, ongoing subsidence of the northern Rotliegend Basin (located in the subsurface beneath the present-day North Sea) allowed the Zechstein Sea to flood into the basin from the north via a sill or narrow inlet (Ziegler, 1975). Repeated closure of this inlet, coupled with prevailing arid conditions and high evaporation rates, led to restricted recharge of the fluids circulating in the basin and culminated in accumulation of a series of thick evaporate sequences of the Zechstein Group (Smith and Taylor, 1992). The total thickness of these evaporite layers in the Central Graben region

exceeds 1.5 km (Stewart and Clarke, 1999; Glennie et al., 2004; Fig. 2.15). Initiation of halokinesis occurred during the Early Triassic in response to differential loading of the salt by prograding clastic fluvial wedges from the north, and by thin-skinned extension causing reactive diapirism (Stewart and Clarke, 1999). It is likely that basement faults exerted a fundamental control on the orientation and distribution of salt walls, which follow the primary NNW-SSE-oriented fault trends of the Central Graben (Hodgson et al., 1992; Peacock, 2004; Fig 2.15). The duration of halokinesis in the Central Graben was dictated by the thickness of salt beneath the mini-basins, with basins developed over palaeo-highs where the salt was thinner, typically grounding on the pre-salt basement during the Early- to Middle-Triassic, and salt basins formed over thicker successions of salt grounding in the late Triassic or Jurassic (Smith et al., 1993). In some instances, salt walls began to collapse due to secondary axial migration away from the wall or in response to dissolution after grounding of the adjacent mini-basins. These processes led to the development of secondary mini-basins over the original salt-wall crests (Smith et al., 1993).

The Triassic fill of the Central Graben consists of two main formations: the Lower Triassic Smith Bank Formation, which is of fluvio-lacustrine origin (Smith et al., 1993; Goldsmith et al., 2004); and the Middle- to Upper-Triassic Skagerrak Formation, which is divided into the Judy, Joanne, and Josephine sandstone members, and the Julius, Jonathan and Joshua mudstone members (Goldsmith et al., 1995; Fig 2.15). Provenance of the lower parts of the Skagerrak Formation demonstrates a sediment source almost exclusively from the Shetland Platform, with sediments in the upper parts of the formation having been sourced from both Scotland and Fennoscandia (Mange-Rajetzkey, 1995). This temporal change in sediment provenance could have arisen in response to a change in climate, a change in tectonic regime on the Fennoscandian margin, or a change in rate of halokinesis that could have resulted in a change of configuration of sediment supply (cf., Moenkopi Formation). The Judy and Joanne sandstone members form two of the main hydrocarbon plays of the Triassic syn-halokinetic sequence in the Central Graben of the North Sea (Goldsmith et al., 1995; McKie, 2011).

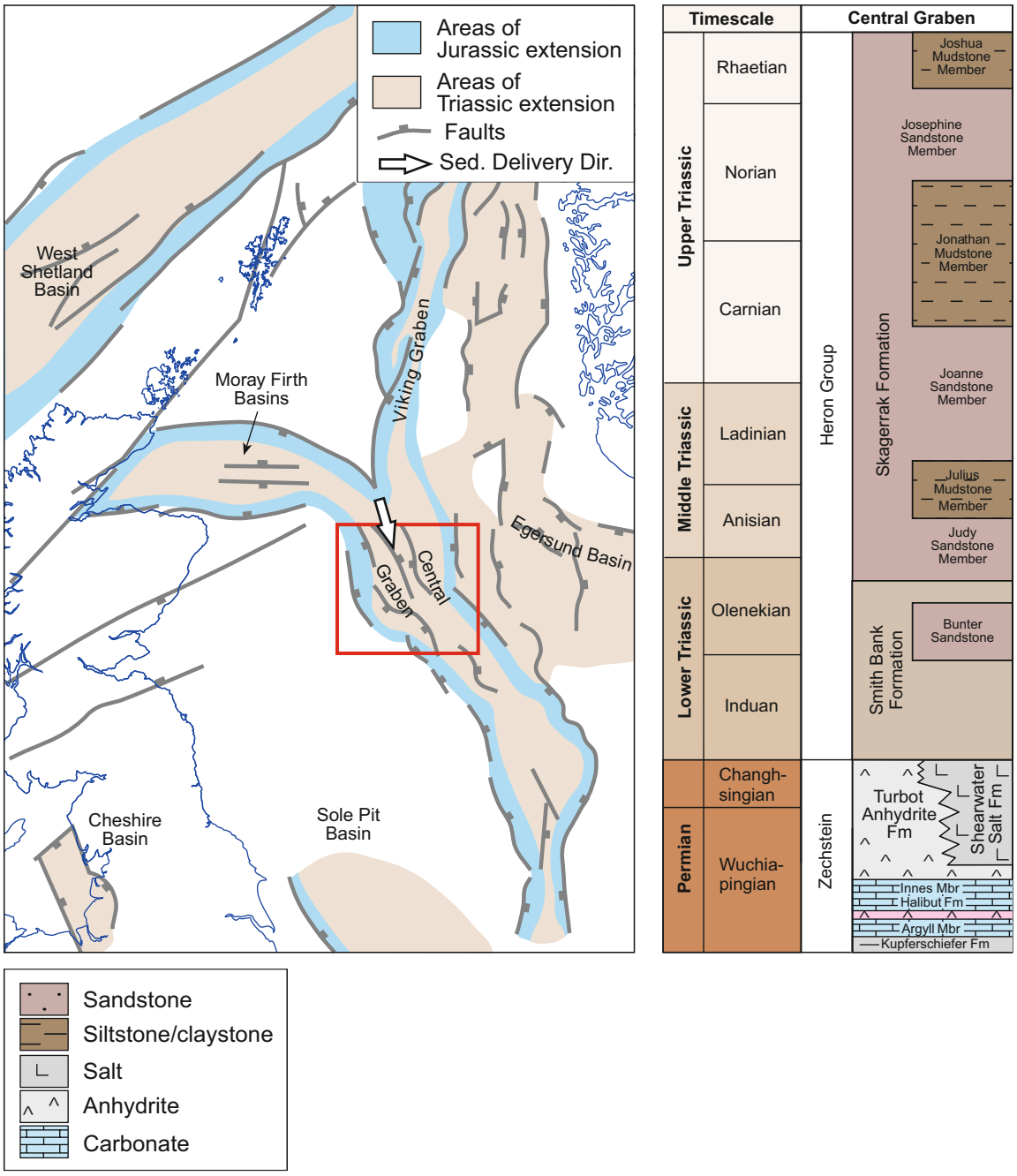


**Figure 2.15**: Central Graben, North Sea. Overview map of Central Graben & stratigraphic column (Modified after Goldsmith et al., 1995; Glennie et al, 2003; Goldsmith et al., 2003).

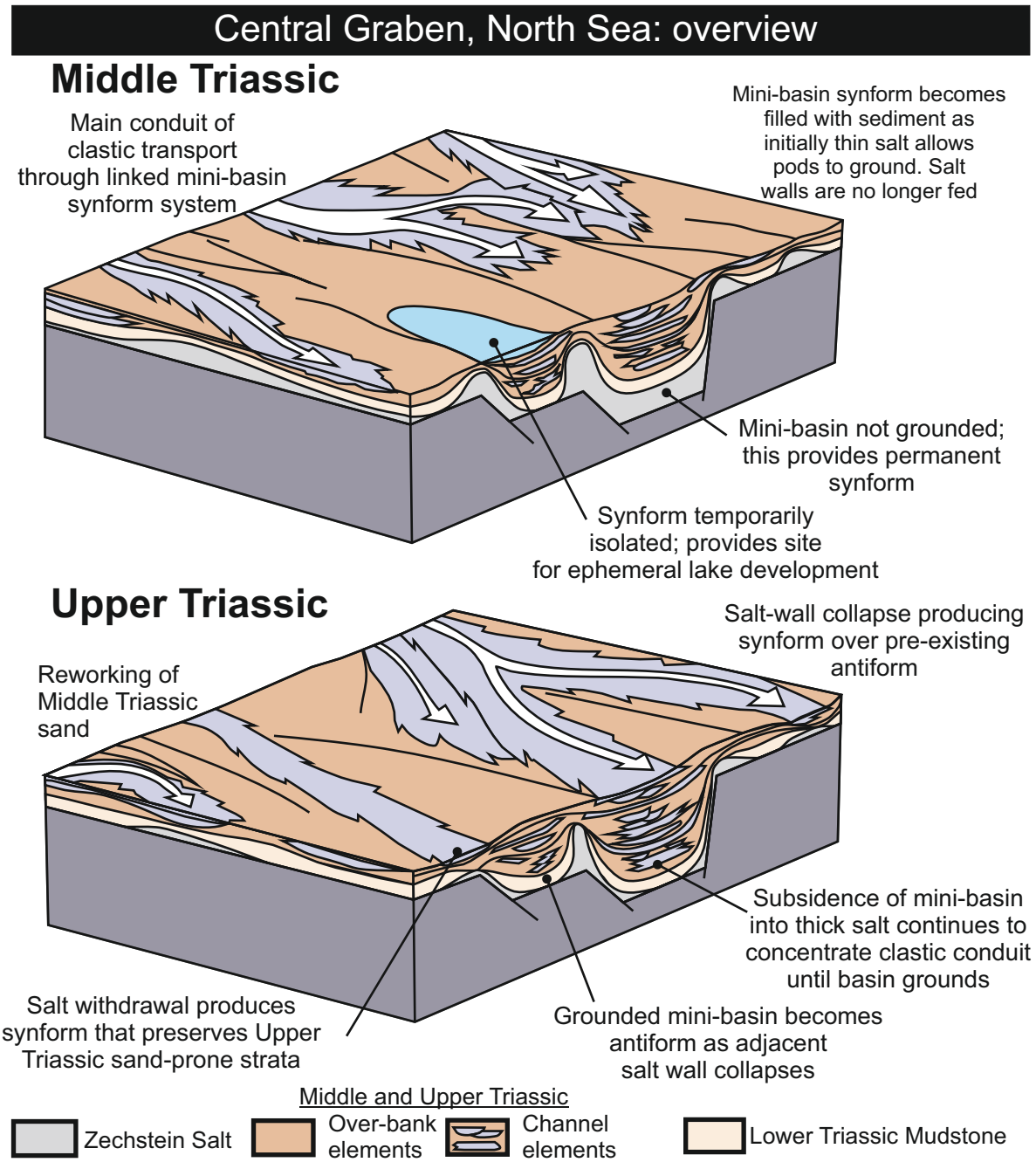


**Figure 2.16**: Central Graben, North Sea. General depositional model depicting fluvial sediment accumulation during the Middle and Late Triassic in the Central Graben of the North Sea. Drainage pathways may bifurcate or become isolated as a result of salt-wall uplift, which controls the developing stratigraphic succession. Differential subsidence rates may lead to the development of lacustrine intervals within the succession. Modified after Hodgson et al. (1992).

The Judy Sandstone Member is interpreted to be a dryland terminal fluvial system, characterised by: stacked, low-sinuosity, high width-depth ratio channel-fill elements; terminal splay and flood-out elements; and ephemeral playa lake elements (McKie et al., 2010; McKie, 2011). Throughout the Middle- to Late-Triassic, sediment was delivered axially in an orientation parallel to the uplifted salt walls, with surface topography above growing salt walls apparently causing neighbouring mini-basins to develop in isolation. This resulted in contrasting styles of basin fill between adjacent mini-basins (Hodgson et al., 1992; Smith et al., 1993; Fig. 2.16). Temporary closure of basins resulted in the accumulation of ephemeral lakes or salt pans, with much of the fill characterised by argillaceous heterolithic facies, the total thickness of which was partly dependent on the duration of isolation. During these episodes of drainage diversion, fluvial pathways were apparently concentrated preferentially along the axes of some basins, resulting in the coeval development of sand-prone basin fill styles in certain mini-basins, yet notably sand-poor fill-styles in neighbouring mini-basins.

### 2.4.4 La Popa Basin

La Popa Basin, northern Mexico, developed during the Late Jurassic as a pull-apart basin associated with movement on the Coahuila-Tamaulipas transform and roll-back and eventual foundering of the Mezcalera Plate (Dickinson and Lawton, 2001; Andrie *et al.*, 2012), in which the Minas Viejas evaporite accumulated (Rowan et al., 2012; Fig. 2.17). The onset of halokinesis occurred during the Late Jurassic, though the initiation mechanism remains unresolved, with (i) extension, thermal and loading subsidence that caused tilting, or (ii) differential loading by sediments derived from the Coahuila Platform each having been proposed as the likely cause (Rowan et al., 2012). Sediment accumulation continued in La Popa Basin from the Late Jurassic to the Eocene, with the Cretaceous and Palaeocene stratigraphy being dominated by marine sedimentation (Lawton et al., 2001). The Hidalgoan Orogeny (Cretaceous-Palaeogene) generated the Sierra Madre Fold-Thrust belt, which was the principal source region of sediment to the La Popa Basin to the south (Rowan et al., 2012). The fluvial Carroza Formation accumulated during the late Eocene at the end of a major marine

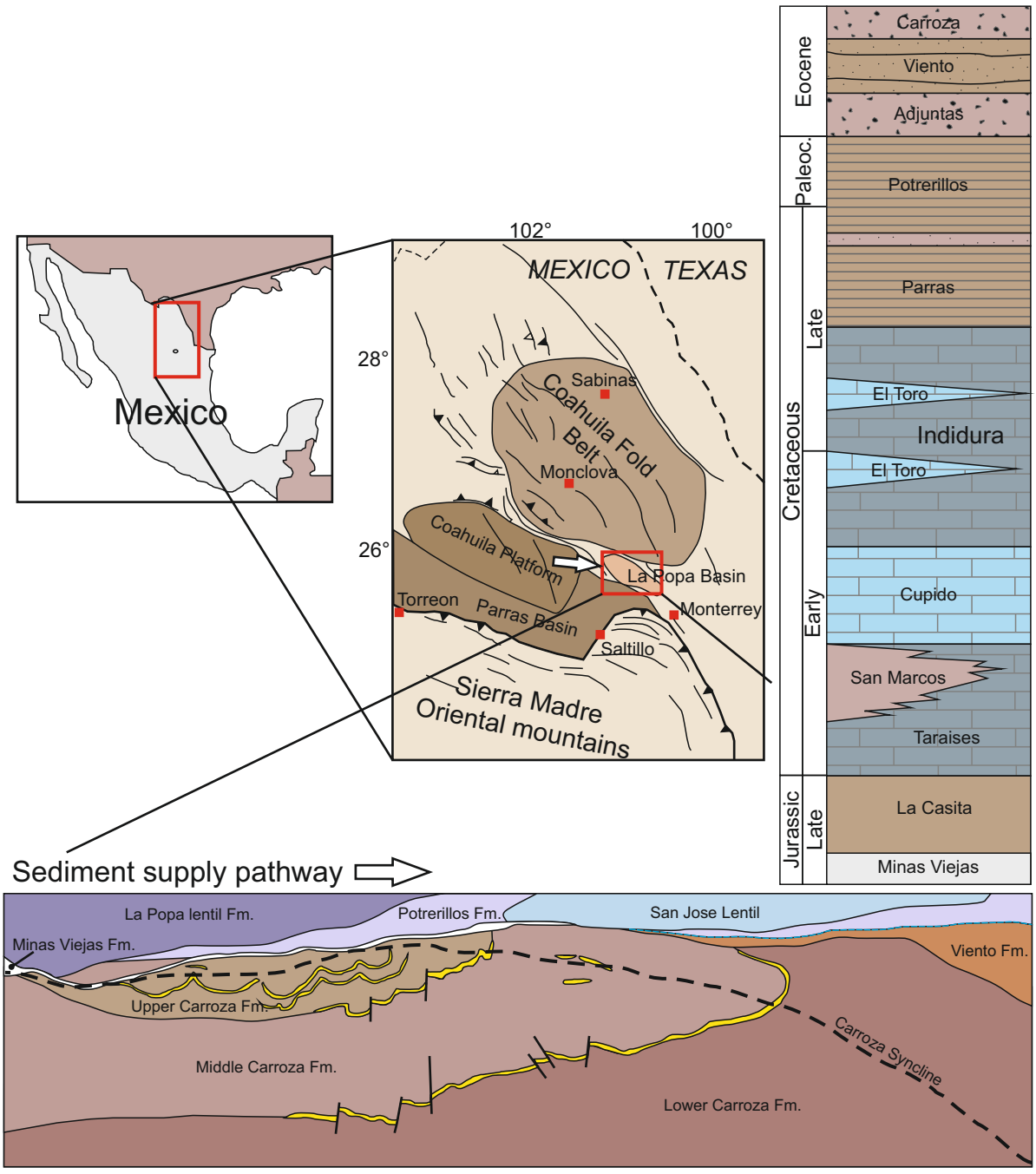


**Figure 2.17:** La Popa Basin, Mexico. Overview maps of La Popa Basin and stratigraphic column (After Dickinson and Lawton, 2001; Andrie et al., 2012). For more accurate maps, see Andrie et al., 2012.

regression (Andrie et al., 2012), and was later deformed during formation of the Carroza syncline by continued salt displacement and crustal shortening by the Hidalgoan Orogenic event (Rowan et al., 2012).

The distribution of fluvial elements in the Carroza Formation demonstrates how halokinetic processes can control the position of drainage pathways adjacent to uplifting salt walls, and study of these has led to development of models with which to predict the distribution of sand bodies and the reservoir potential (Andrie et al., 2012; Fig. 2.18). The Lower Member of the Carroza Formation is characterised by wide but isolated channel-fill complexes, with varying palaeocurrents (Andrie et al., 2012). Sedimentation rates were relatively high compared to subsidence rates during the initial phase of deposition, allowing for unconfined migration of the fluvial system across the basin. During accumulation of the Middle Carroza Member, fluvial elements began preferentially stacking around the position of the Carroza syncline hinge, which by this time had migrated toward the flank of La Popa salt wall. Palaeodrainage direction became preferentially aligned parallel to this northwest-southeast trending salt wall, indicating that sufficient topography had been generated to capture drainage pathways. The topographic expression eventually became sufficient to trigger debris flows from salt-wall flanks. Alignment and stacking of fluvial channel elements indicates that drainage pathways were confined to the developing rim syncline adjacent to the salt wall at this time. During accumulation of Upper Carroza Member, the channel elements became restricted to the immediate flank of the salt wall, as controlled by the migrating axis of the Carroza Syncline. The progressive migration of the Carroza syncline axis and associated development and migration of a rim-syncline controlled the locus of drainage and the progressive shift of the accumulation of fluvial channel elements towards the flank of La Popa salt wall over time.

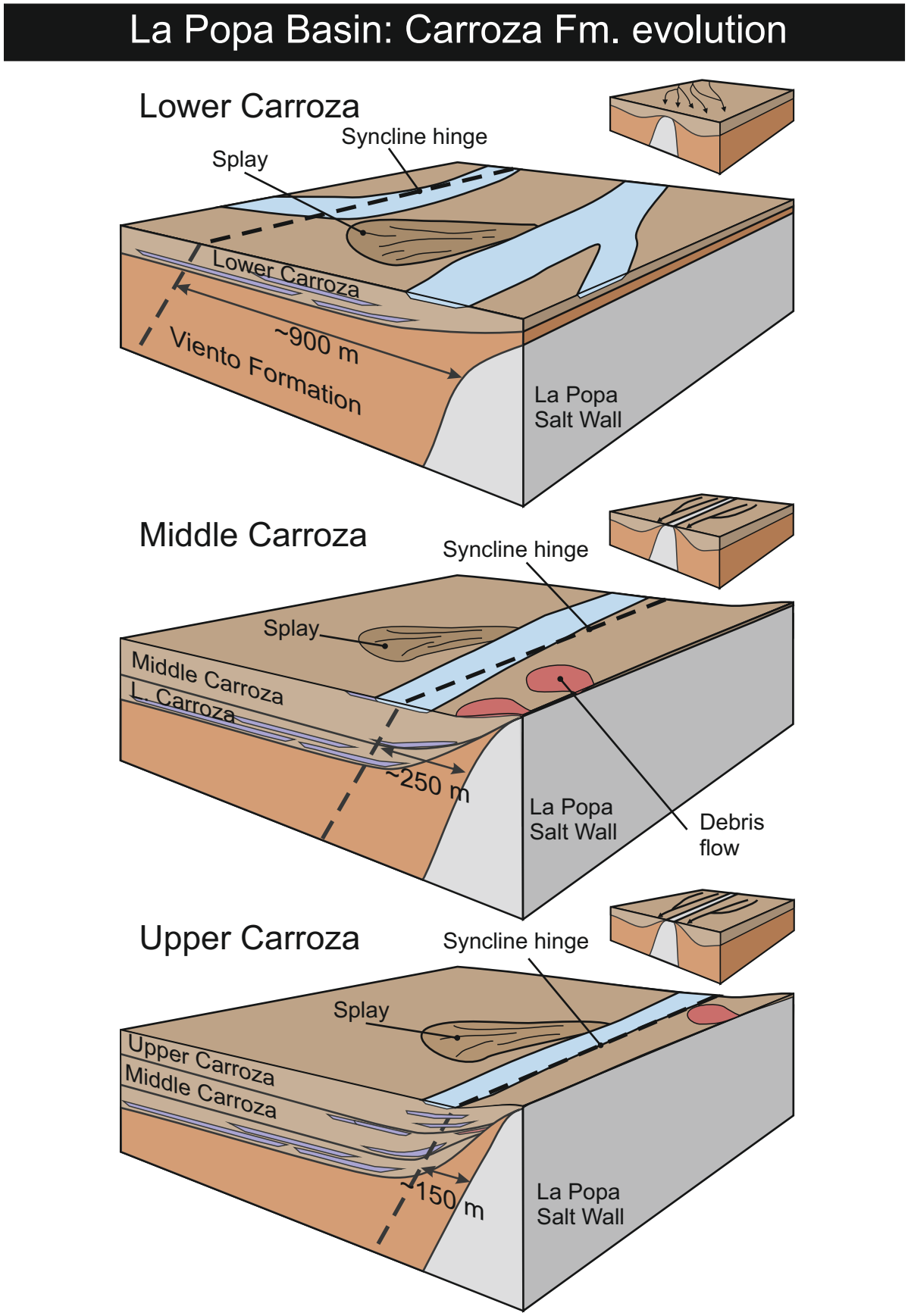


**Figure 2.18**: La Popa Basin, Mexico. General depositional model depicting fluvial sediment accumulation in the Carroza Formation, La Popa Basin, Mexico. Development of a rim-syncline adjacent to La Popa salt wall controlled the location of drainage pathways throughout the latter stages of deposition of the Carroza Formation. Modified after Andrie et al. (2012).

## 2.5 Discussion

The interplay between the rate of mini-basin subsidence and the rate of sediment accumulation, including variation in these over space and time, is a key control on the development of fluvial systems and their preserved successions in salt-walled mini-basins. Mini-basin subsidence rates are determined by the rate of underlying salt evacuation, which will vary over time in response to changes of sediment loading and proximity to grounding on the pre-salt basement, typically resulting in a non-linear subsidence history. Rates of sediment delivery, which are themselves partly controlled by external factors such as climate and source area, dictate sediment type, composition, availability and delivery rate. Dominant drainage pathway and the nature of any sediment bypassing that may occur (itself controlled by subsidence rates) can result in significant variations in the style of sediment delivery and rate of accumulation between and within mini-basins. Figure 2.19 demonstrates how the interplay between sediment supply rate and subsidence rate can control basin-fill style.

In cases where rate of sediment delivery and subsidence are balanced, avulsion coupled with lateral migration of channels tends to rework and remove the majority of fine-grained overbank elements, resulting in high proportions of sand-prone channel-fill elements. Where the rate of subsidence outpaces sediment delivery, the fluvial system will aggrade to preserve near-complete fluvial fining-upward cycles, and avulsion and lateral migration are less likely to rework or remove these overbank elements. Such conditions result in sandy channel-fill elements becoming vertically isolated from each other. Such a situation may culminate in the formation of perennial lakes, which can lead to accumulation of thick lacustrine successions. Conversely, where the rate of sediment delivery significantly outpaces the rate of subsidence, lack of available accommodation means that deposited strata are prone to reworking, thereby preserving only the lowermost parts of fluvial depositional cycles, such as pebbly basal lags. Many such deposits have poor reservoir potential. Where rates of sediment delivery greatly exceed rates of subsidence, fluvial systems can potentially overspill confining salt walls, resulting in drainage diversion into adjacent basins, especially where salt

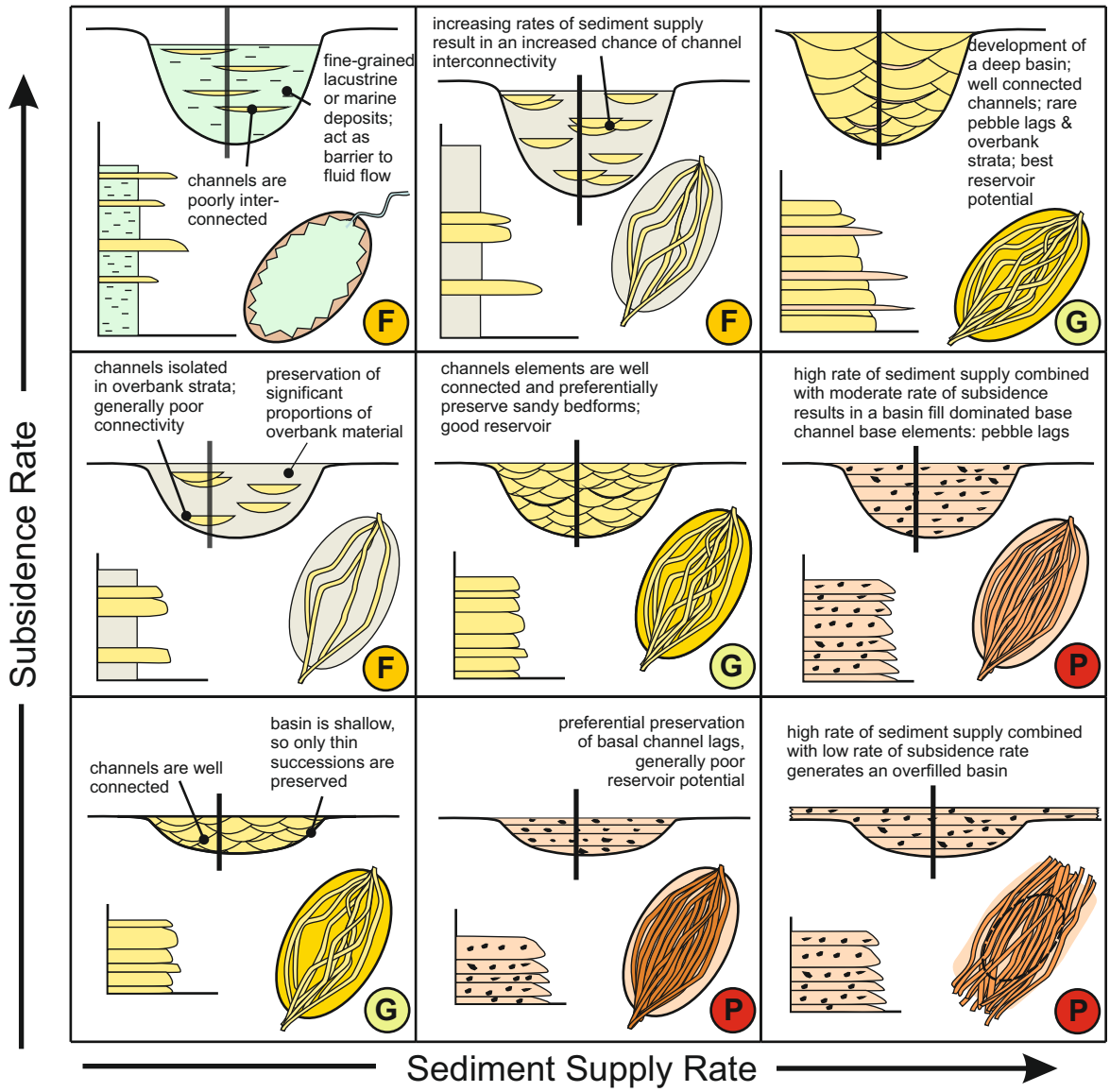


very poorly sorted; clay-pebble

moderately to well sorted; sand

poor to moderately sorted; clay-silt

moderately sorted; silt-fine sand

G good reservoir potential

F fair reservoir potential

P poor reservoir potential

Matrix displays likely basin-fill architectures associated with various rates of sediment supply and subsidence.

Overfilled basins tend to occur when rates of sedimentation outpace rates of subsidence

Underfilled basins tend to occur when rates of subsidence outpace rates of sediment supply and the available accommodation space remains partly unfilled.

Filled Basins occur when the rates of sediment supply and subsidence are balanced.

**Figure 2.19**: Conceptual model demonstrating how the interplay between rates of subsidence and sediment supply act to control the developing basin-fill style. Balanced rates of subsidence and sediment supply generate filled (sand-prone) basins; in cases where the rate of subsidence outpaces the rate of sediment supply, under-filled basins with argillaceous fills tend to develop and available accommodation may remain partially unfilled; in cases where the rate of sediment supply outpaces the rate of subsidence, over-filled basins with gravel-prone fills tend to develop and accommodation is filled leading to downstream bypassing of excess sediment.

walls are arranged in polygonal patterns. Alternatively, where growing salt walls generate a long-lived surface expression, fluvial systems may become confined within a single mini-basin, leaving adjacent basins isolated from the primary source of sediment input. These isolated mini-basins can potentially become dominated by evaporitic processes and salt flats might form (Goodall *et al*., 2000), whereas thick palaeosols and possibly coal swamps may develop in more humid settings. Eventual overtopping of salt walls by fluvial systems will result in incision and diversion of drainage into adjacent under-filled mini-basins; such events may either temporarily or permanently change the fill-style of the neighbouring basin.

## Evolution of Fluvial Systems in salt-walled mini-basins

Consideration of various case-studies has allowed for a series of generic evolutionary models to be proposed for both linear and polygonal salt-walled mini-basins, and these depict the expected sequence of basin-scale sedimentary architectures (Figs 2.20, 2.21).

### Linear basins

**Initiation** of salt-walled mini-basin growth (Fig. 2.20a) triggered by sediment loading in combination with a tectonic mechanism results in initial diversion of fluvial systems in cases where they are unable to respond sufficiently quickly to downcut through growing salt highs. Mini-basins closest to the sediment source will tend to fill quicker and therefore tend to be sand- or gravel-prone; conversely, more distal mini-basins may develop relatively sand-poor basin-fill styles.

**Rapid subsidence** may occur due to a rapid influx of sediment, which will act to load the salt beneath the developing basin (Fig. 2.20b). A reduction in the rate of sediment supply, for example due to a change to a more arid climatic regime, may contribute to fluvial diversion during episodes when the rate of sediment delivery is outpaced by subsidence and salt wall uplift. Mini-basins may become isolated for short episodes, developing under-filled basin segments, or for longer episodes where the style of basin infill may record isolation (e.g., evaporite basins). The development of turtle-back structures and rim synclines may act to partition drainage pathways within a single mini-basin.

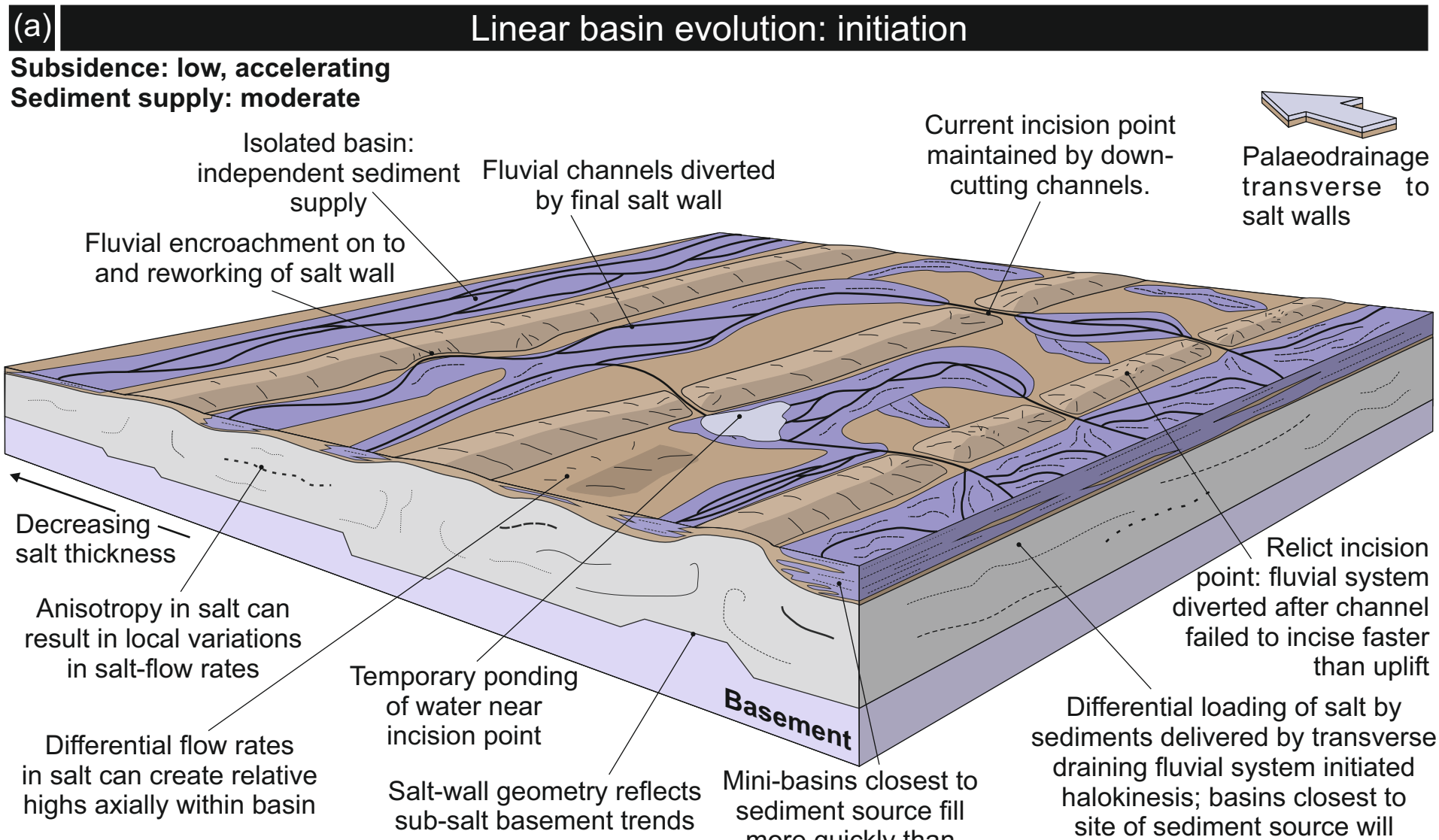


**Figure 2.20**: Models depicting the evolution of linear salt-walled mini-basins. See text for further explanation.

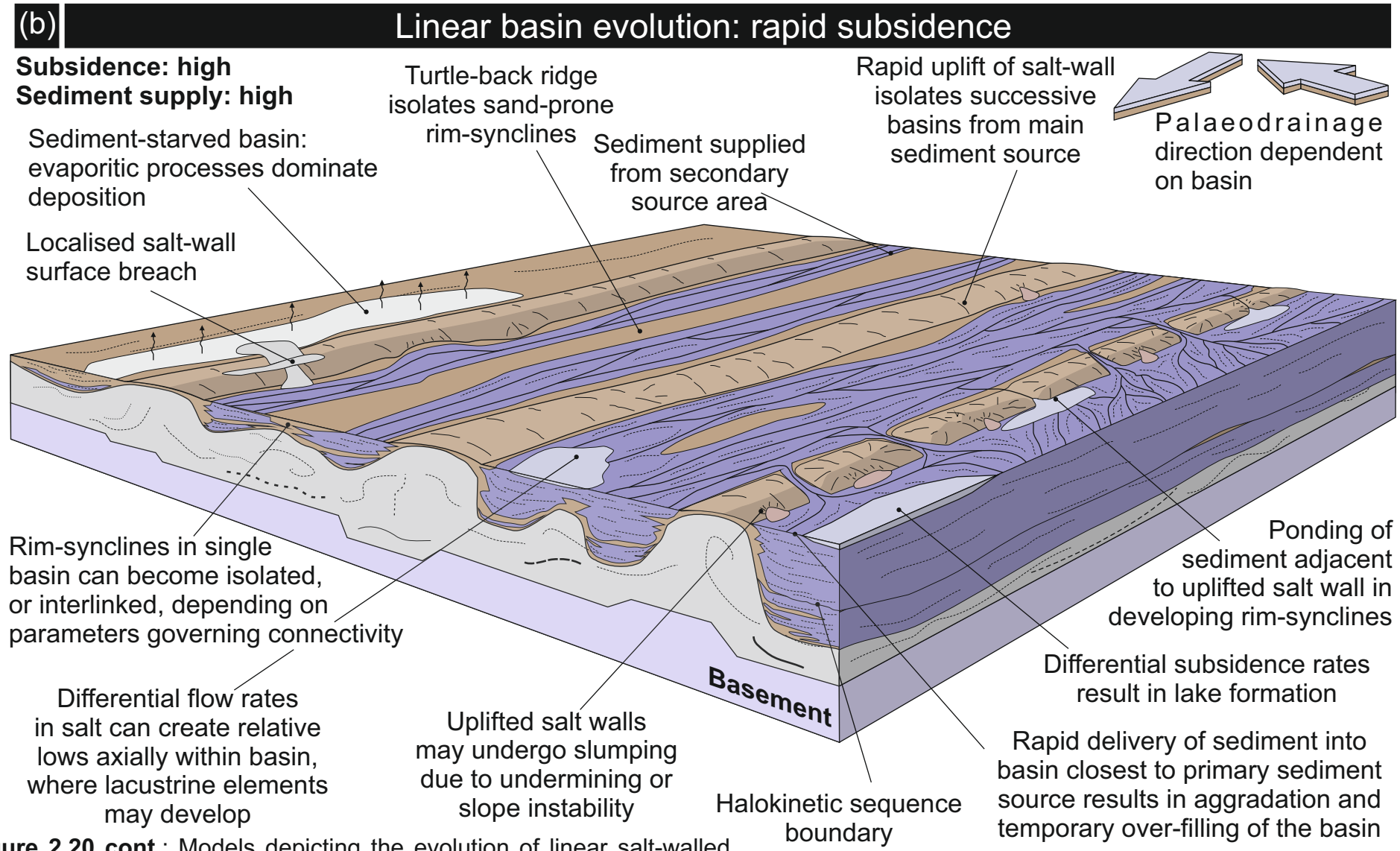


**Figure 2.20 cont.**: Models depicting the evolution of linear salt-walled mini-basins. See text for further explanation.

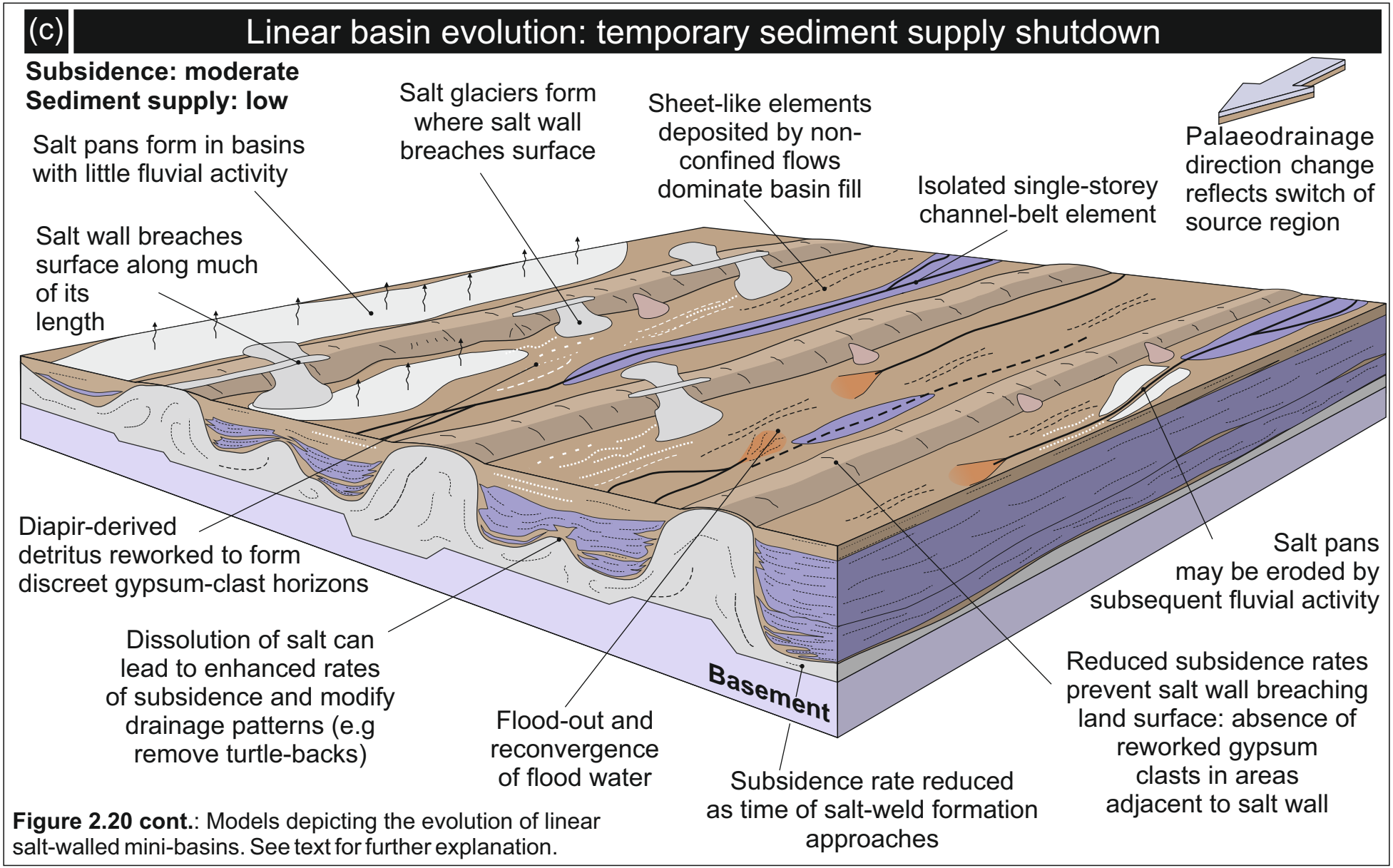


**Figure 2.20 cont.**: Models depicting the evolution of linear salt-walled mini-basins. See text for further explanation.

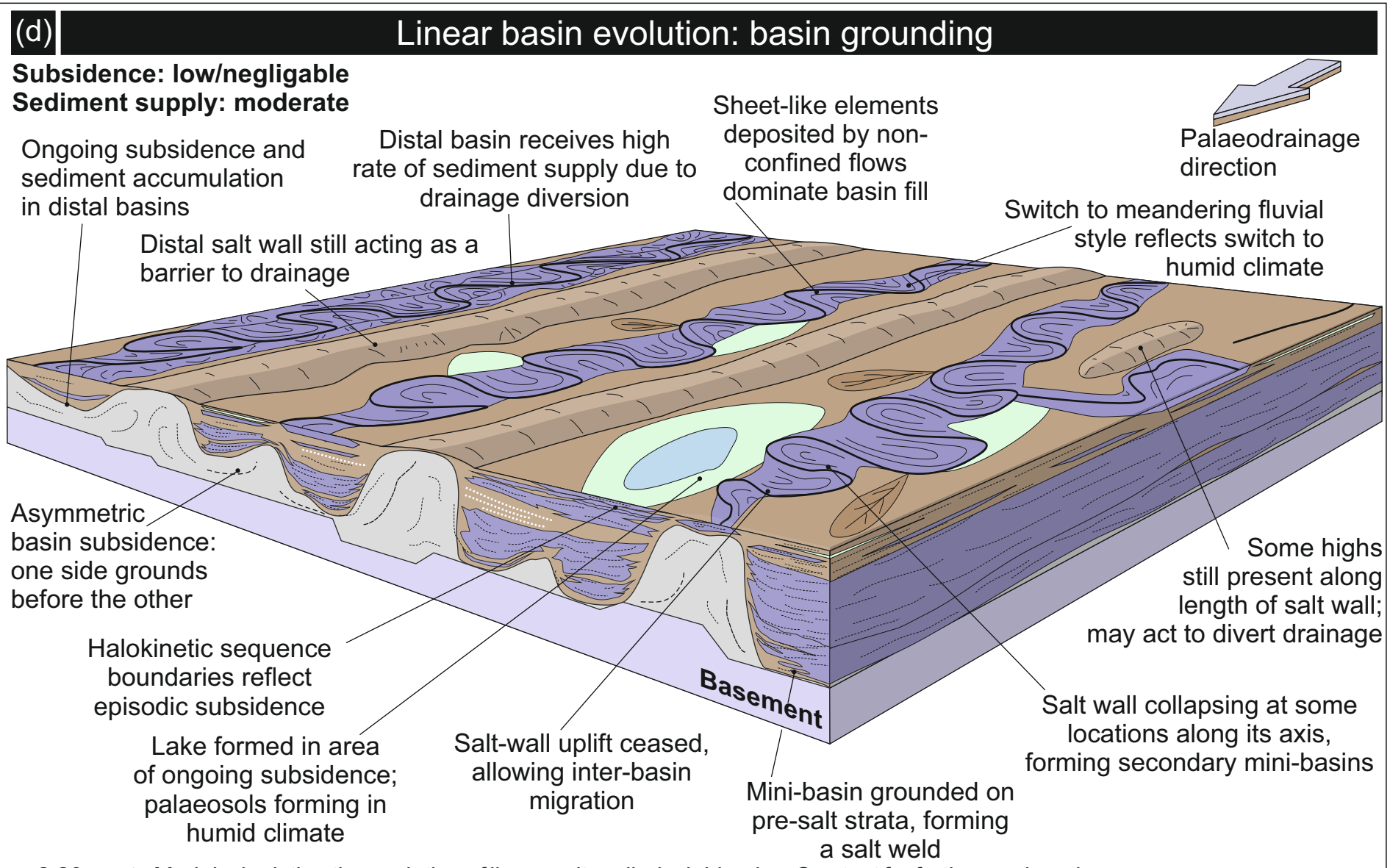


**Figure 2.20 cont.**: Models depicting the evolution of linear salt-walled mini-basins. See text for further explanation.

**Temporary sediment supply shutdown** driven by a region-wide shift in climatic regime may significantly reduce fluvial activity resulting in reduced sediment accumulation rates in all mini-basins across a province (Fig. 2.20c). Such a climate change may also coincide with a change of sediment source region. Such a change may account for the development of adjacent sand-prone and sand-poor basins. When salt wall uplift rates outpace sediment accumulation, salt walls may breach the land surface, creating a source of detritus that may be locally reworked.

**Basin grounding** will eventually occur once subsiding mini-basins have effectively displaced the underlying salt, and this will prevent further subsidence (Fig. 2.20d). Due to the differential subsidence history of adjacent mini-basins or the onset of salt-wall collapse, subsidence may continue locally and may lead to the development of secondary basin atop collapsing salt walls. A shift to more humid conditions can result in the development of meandering fluvial systems, with ephemeral or perennial lakes developing in some basins.

**Polygonal basins**

**Initiation** of polygonal salt walls in response to multiple basement trends can lead to development of blind or closed (i.e., isolated) mini-basins, with fluvial systems becoming confined to a series of adjacent basins (Fig. 2.21a). Blind basins can be characterised by lacustrine elements with deltas developing on lake margins.

**Rapid subsidence** and ensuing salt-wall uplift can disrupt drainage through the region, with previously open basins becoming closed or blind (Fig. 2.21b). Some isolated basins can become dominated by evaporitic or aeolian processes, especially those distal to sediment source area in arid settings.

**Drainage diversion** may occur when sediment accumulation in a closed basin out-strips subsidence rates, allowing the fluvial system to breach a salt wall and incise a new drainage pathway into a neighbouring basin (Fig. 2.21c).

**Onset of basin grounding** will tend to occur first in those mini-basins that experienced high rates of sediment delivery and therefore rapid subsidence (Fig. 2.21d). Partial collapse of certain salt walls in the aftermath of grounding

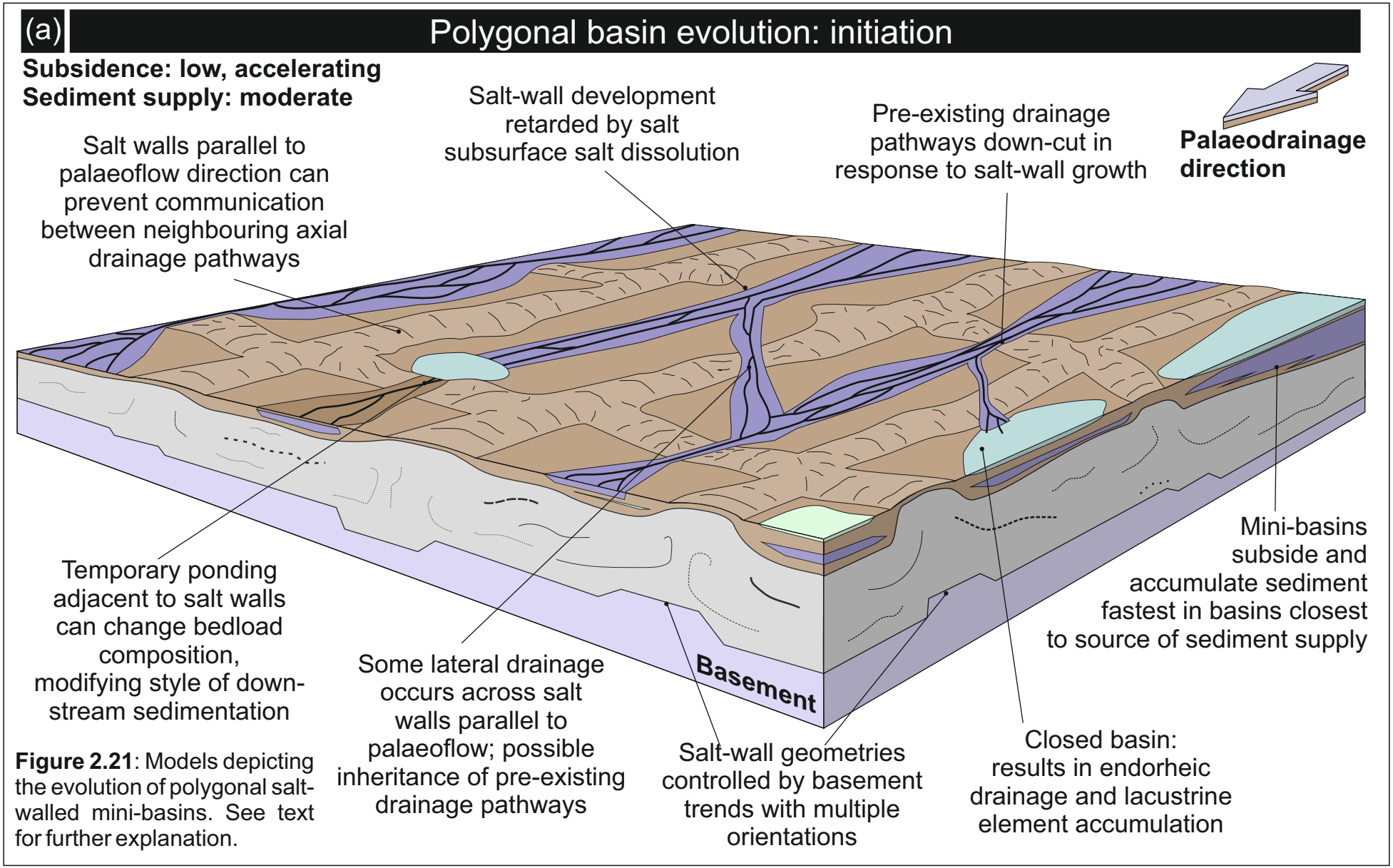


**Figure 2.21**: Models depicting the evolution of polygonal salt-walled mini-basins. See text for further explanation.

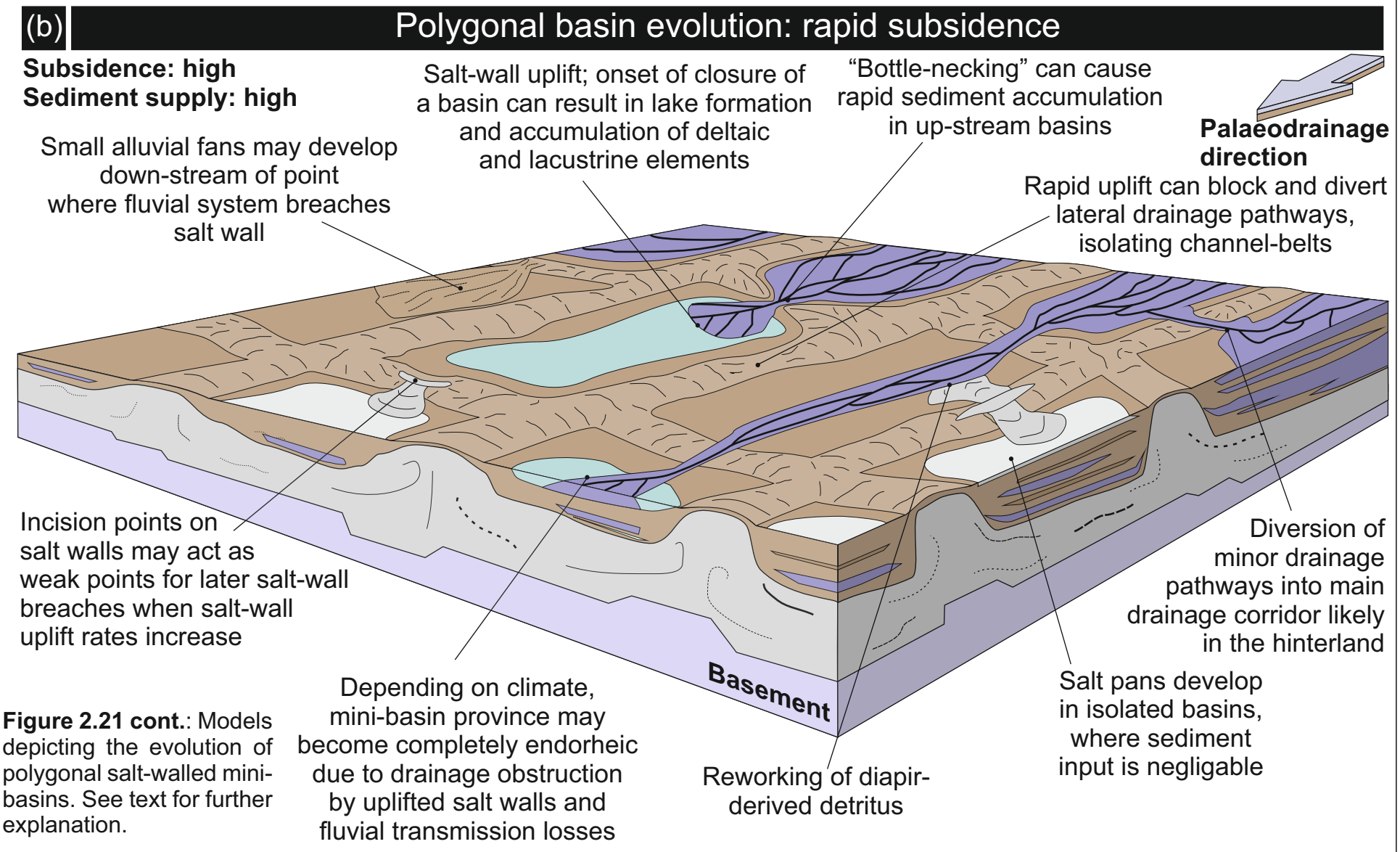


**Figure 2.21 cont.**: Models depicting the evolution of polygonal salt-walled mini-basins. See text for further explanation.

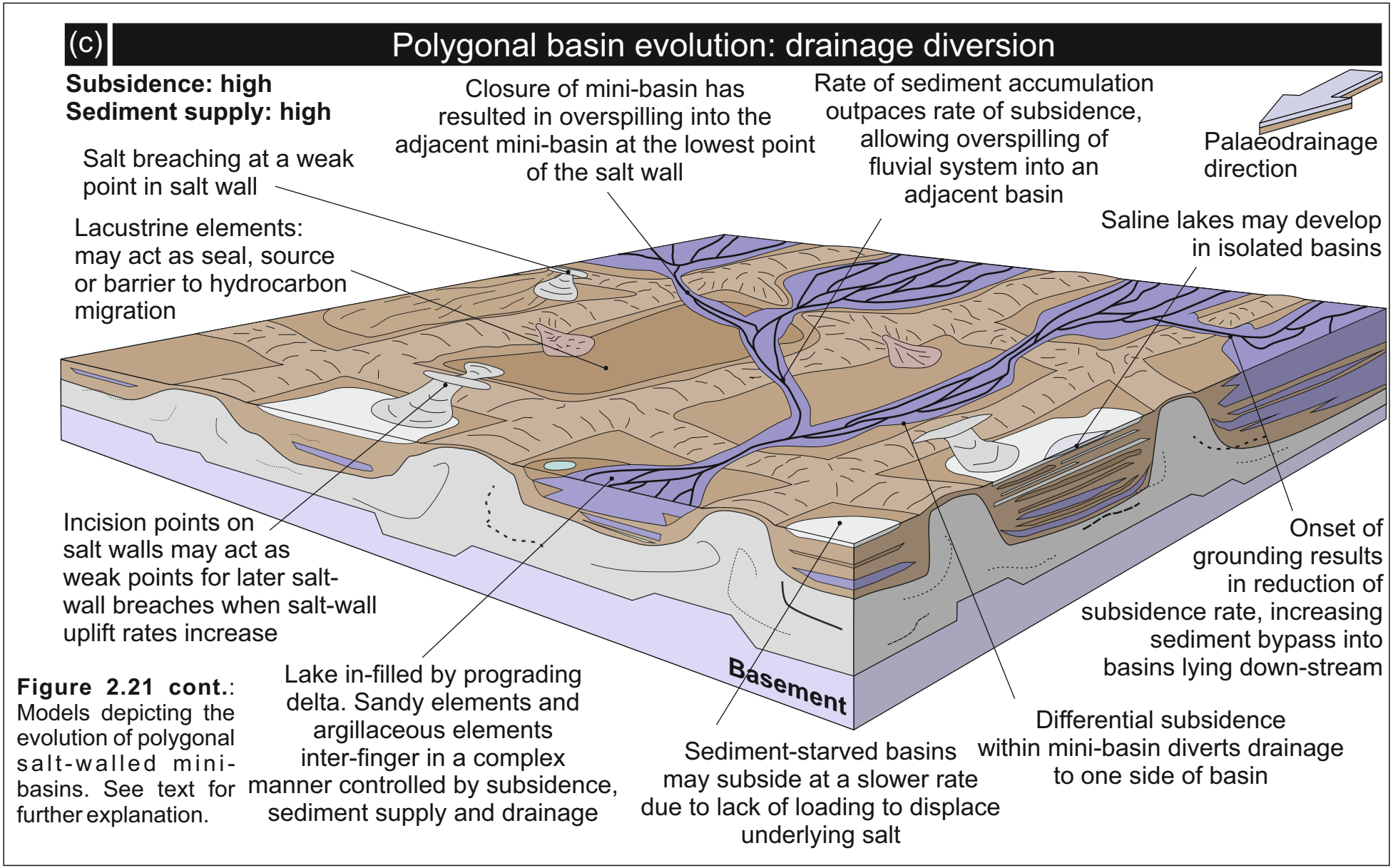


**Figure 2.21 cont.**: Models depicting the evolution of polygonal salt-walled mini-basins. See text for further explanation.

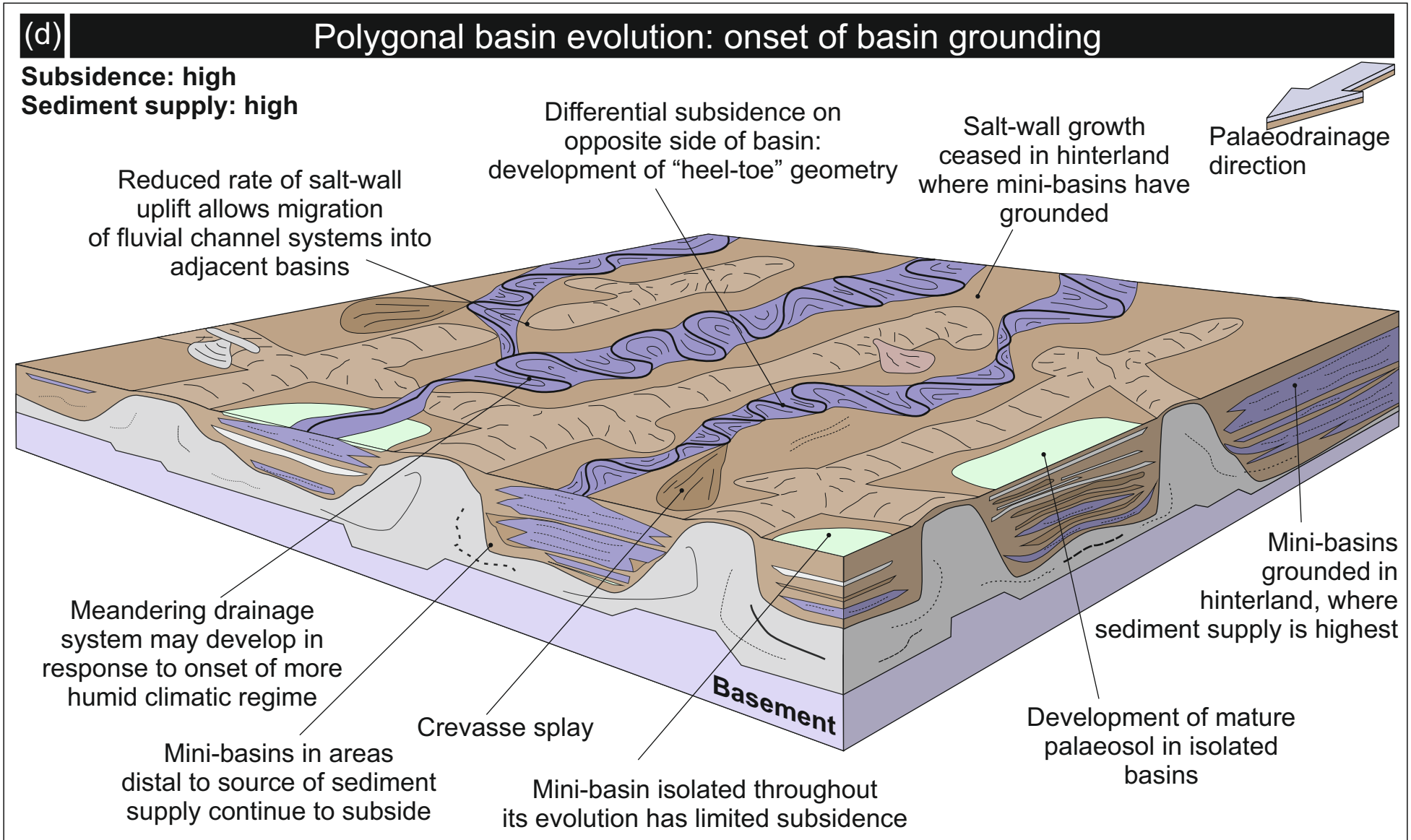


**Figure 2.21 cont.**: Models depicting the evolution of polygonal salt-walled mini-basins. See text for further explanation.

will tend to promote unrestricted inter-basin drainage, whilst other salt walls may continue to grow and therefore prevent sediment delivery to adjacent basins. Heel-toe geometries with intraformational unconformities may develop where subsidence switches from one side of a single mini-basin to the other.

## Gaps in understanding

Despite having been the subject of numerous studies since the early 1990s (e.g., Bromley, 1991), there remain significant gaps in our understanding of the mechanisms governing the accumulation of fluvial stratigraphy in salt-walled mini-basins. Of the 120 evaporite provinces documented by Hudec and Jackson (2007) that are known to have undergone salt deformation, many examples that demonstrate syn-halokinetic evolution of fluvial systems exist, both in the subsurface and in outcrop. The majority of recent detailed outcrop studies have been conducted in the Paradox Basin of Utah, with fewer studies undertaken in other outcropping basins, such as the Pre-Caspian Basin, or La Popa Basin.

Of the case studies considered in this study, 7 examples accumulated under semi-arid or arid climates, which are reflected by a dominance of braided fluvial networks, with evidence for evaporitic processes and development of calcisols and aridisols. This may reflect the fact that most outcropping salt basins, which were later mobilised to form salt-walled mini-basin provinces, developed between the late Pennsylvanian and Permian, with fluvial sediment accumulation occurring during the globally arid periods of the Permian and Triassic. Studies of meandering fluvial systems preserved in ancient salt mini-basins are under-represented in the literature, in part due to a lack of recognition of suitable outcrops for study.

Spatial variations in rates of subsidence along mini-basin axes and the creation of local depocentres have yet to be studied in detail. Such spatial variations could result in local accumulation of lacustrine deposits, or could act as a mechanism for controlling the location of nodal avulsions, flood-outs or points of convergence of high-aspect-ratio channels, thereby controlling the distribution of sand-prone channel-fill elements or thin sheet-like heterolithic elements.

Detailed analysis of the controls on drainage pathways in polygonal salt-walled mini-basins also requires further study. Switching of drainage pathways and total or partial isolation of certain mini-basins reflects local changes in sediment delivery. Locally increased rates of accumulation can lead to accelerated rates of subsidence. This may drive positive feed-back cycles that promotes or accelerates mini-basin development.

## *2.6 Conclusions*

Evolution of salt-walled mini-basins and the ensuing accumulation of fluvial strata within these basins is an inherently complex process with multiple factors controlling sediment distribution, both within and between mini-basins. The style of basin fill can evolve independently between neighbouring mini-basins of equivalent age, most notably where drainage networks are aligned parallel to elongate salt walls such that they become partitioned from each other by growth of salt-related surface topography. Alternatively, where the preferred orientation of fluvial drainage is transverse to linear salt walls, mini-basins between salt walls may fill sequentially with increasing distance from the sediment source. Polygonal networks of salt walls for which surface topographic expression is present may result in the development of partially closed mini-basins occupied by lacustrine systems and fed by fan deltas.

Where rates of salt-wall uplift and mini-basin subsidence, which in combination define the rate of generation of accommodation, are matched or exceeded by the sediment delivery and accumulation, mini-basins become filled and surface topographic expression is overwhelmed, allowing fluvial systems to flow without significant interference and potentially allowing for correlation between separate mini-basin stratigraphic fills.

By reviewing a series of case studies, common examples of fluvial stratigraphic response to different types of salt-walled mini-basins have been identified; a series of generic models have been synthesised that demonstrate the expected evolutionary history for linear and polygonal salt-walled mini-basins. Generic basin evolution models demonstrate the inherent complexities present within mini-basins separated by elongate, linear salt walls and how basin-fill style might vary over time and space depending on sediment delivery

(Fig. 2.20a-d). Such controls dictate how fluvial architectural elements are distributed throughout the course of basin evolution. Figure 2.21a-d demonstrates a typical evolutionary sequence for a polygonal arrangement of salt-walled mini-basins, showing the predicted distribution of fluvial architectural elements and how drainage pathways can be diverted by various controls operating within the mini-basin province.

These case studies demonstrate that fluvial facies and architectural-element distributions can be predicted both within and between mini-basins. The predictive models presented here are of value in assessing the distribution of sand-prone elements within subsurface reservoirs. However, improved techniques for understanding architectural-element distribution and prediction of climate regimes will require good well control and high-quality seismic to predict the probable locations of sand fairways for systems known only from the subsurface.

# 3. Climatic versus halokinetic control on sedimentation in a dryland fluvial succession

*This chapter is aimed at describing the sedimentology of a dryland fluvial system which accumulated across a low-relief alluvial plain. This chapter contains a review on the literature of other dryland fluvial systems, and their expression within the stratigraphic record. The chapter then gives a detailed description of the sedimentology of the Moenkopi Formation throughout the Paradox Basin (from both the Salt Anticline Region and the White Canyon Region), describing the facies and their arrangement within common architectural elements observed throughout the formation. This chapter then goes on to discuss the spatial distribution of these architectural elements, and discusses the palaeoenvironment in which the Moenkopi Formation was deposited.*

*Finally, this chapter examines at the signature of climate on the Moenkopi Formation, and how it can be differentiated from the signature of halokinesis.*

## *3.0 Abstract*

Fluvial systems and their preserved stratigraphic expression as the fill of evolving basins are controlled by multiple factors, which can vary both spatially and temporally, including prevailing climate, sediment provenance, localised changes in the rates of creation and infill of accommodation in response to subsidence, and diversion by surface topographic features. In basins that develop in response to halokinesis, mobilised salt tends to be displaced by sediment loading to create a series of rapidly subsiding mini-basins, each separated by growing salt walls. The style and pattern of fluvial sedimentation governs the rate at which accommodation becomes filled, whereas the rate of growth of basin-bounding salt walls governs whether an emergent surface topography will develop that has the potential to divert and modify fluvial drainage pathways and thereby influence the resultant fluvial stratigraphic architecture. Discerning the relative roles played by halokinesis

and other factors such as climate-driven variations in the rate and style of sediment supply, is far from straightforward. Diverse stratigraphic architectures present in temporally equivalent, neighbouring salt-walled mini-basins demonstrate the effectiveness of topographically elevated salt walls as agents that partition and guide fluvial pathways and thereby control the loci of accumulation of fluvial successions in evolving mini-basins: drainage pathways can be focused into a single mini-basin to preserve a sand-prone fill style, whilst leaving adjoining basins relatively sand-starved. By contrast, over the evolutionary history of a suite of salt-walled mini-basins, region-wide changes in fluvial style can be shown to have been driven by changes in palaeoclimate and sediment-delivery style.

The Triassic Moenkopi Formation of the south-western USA represents the preserved expression of a dryland fluvial system that accumulated across a broad, low-relief alluvial plain, in a regressive continental to paralic setting. Within south-eastern Utah, the Moenkopi Formation accumulated in a series of actively subsiding salt-walled mini-basins, ongoing evolution of which exerted a significant control on the style of drainage and resultant pattern of stratigraphic accumulation. Drainage pathways developed axial (parallel) to salt walls, resulting in compartmentalised accumulation of strata whereby neighbouring mini-basins record significant variations in sedimentary style at the same stratigraphic level. Despite the complexities created by halokinetic controls, the signature of climate-driven sediment delivery can be deciphered from the preserved succession by comparison with the stratigraphic expression of part of the system that accumulated beyond the influence of halokinesis, and this approach can be used to demonstrate regional variations in climate-controlled styles of sediment delivery.

## *3.1 Introduction*

Ephemeral fluvial systems that develop under the influence of arid climatic conditions are common as both present-day active alluvial systems and as successions preserved in the ancient rock record (Williams, 1971; Picard & High, 1973; Rust, 1981; Jones *et al.*, 2005; McKie *et al.*, 2010; McKie 2011). In addition to climate, basin setting, tectonic regime and rates of sediment

delivery from upstream catchment areas are all important extrinsic factors that influence the style of drainage and pattern of sedimentation in ephemeral fluvial systems (Hampton & Horton, 2007; Thamo-Bozso *et al.*, 2002). As a result of the interplay between these variables, a range of different channelised and non-channelised (typically sheet-like) architectural elements – each characterised by a varied range of internal facies compositions – are recognized as the constituent geometrical bodies that comprise the accumulations of ephemeral fluvial successions (e.g. Hubert & Hyde, 1982; Nichols and Fisher, 2007; Cain & Mountney 2009, 2011). Understanding lateral and vertical arrangements of architectural elements in terms of their style of juxtaposition relative to one another is the key to building robust models with which to demonstrate the relative significance of the varied external controls that can potentially act to dictate the gross-scale architecture of such fluvial systems (Miall, 1985; Bridge and Tye, 2000; Gibling, 2006; Colombera *et al.*, 2012a, b).

The Triassic Moenkopi Formation (Olenekian to Anisian) is present across much of the south-western United States and has been interpreted to represent the preserved accumulation of a series of genetically-related deltaic, shoreline, tidal-flat and continental alluvial and fluvial palaeoenvironments (Stuart *et al.*, 1972; Blakey & Ranney, 2008). In the southeast Utah region (Fig. 3.1), the Moenkopi Formation records the preserved expression of a dryland fluvial system for which the style of sedimentation was influenced to a considerable extent by long-lived and widespread arid climatic conditions that prevailed across a broad, low-relief and largely non-confined alluvial plain (Stuart *et al.*, 1972; Blakey, 1973, 1974, 1977; Dubiel, 1994). In the Salt Anticline Region (Elston *et al.*, 1962*;* Carter, 1970) around the town of Moab, Utah, (Fig. 3.2a) the fluvial systems represented by the Moenkopi Formation were significantly influenced by syn-sedimentary halokinesis, which involved the growth of salt walls and the occasional sub-areal breaching of the surface landscape by salt diapirs (Lawton & Buck, 2006; Trudgill, 2011). Areas directly adjacent to growing salt walls experienced mini-basin subsidence (Kluth & DuChene, 2009; Rasmussen & Rasmussen, 2009; Trudgill, 2011) and the sedimentary expression of the Moenkopi Formation can be shown to have been controlled

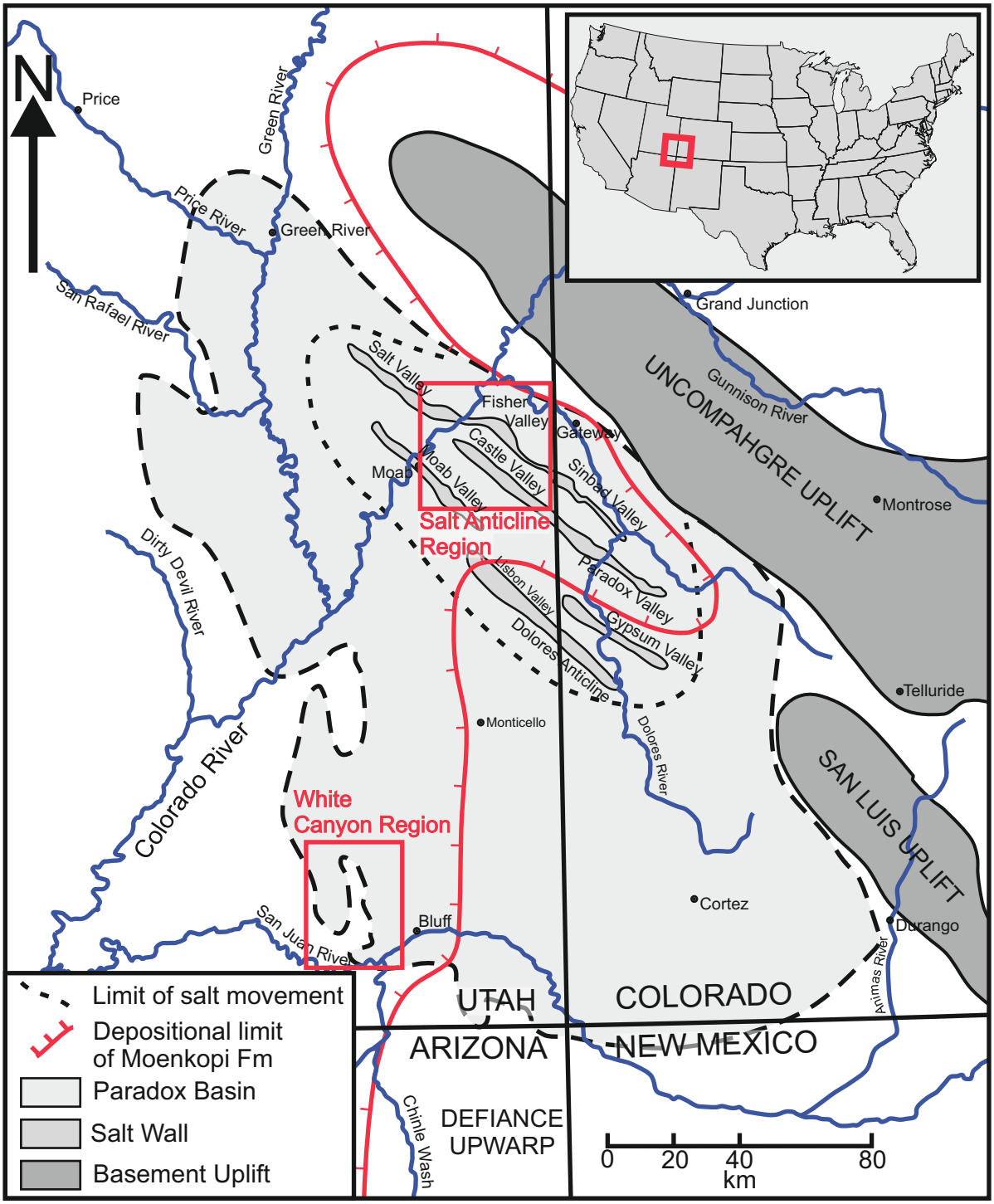


**Figure 3.1 (a)**: Paradox Basin Overview. Regional map of the Paradox Basin and location of the study areas in relation to areas of likely sediment provenance of the Moenkopi Formation. Modified after Trudgill, 2011; Banham & Mountney (2013a).

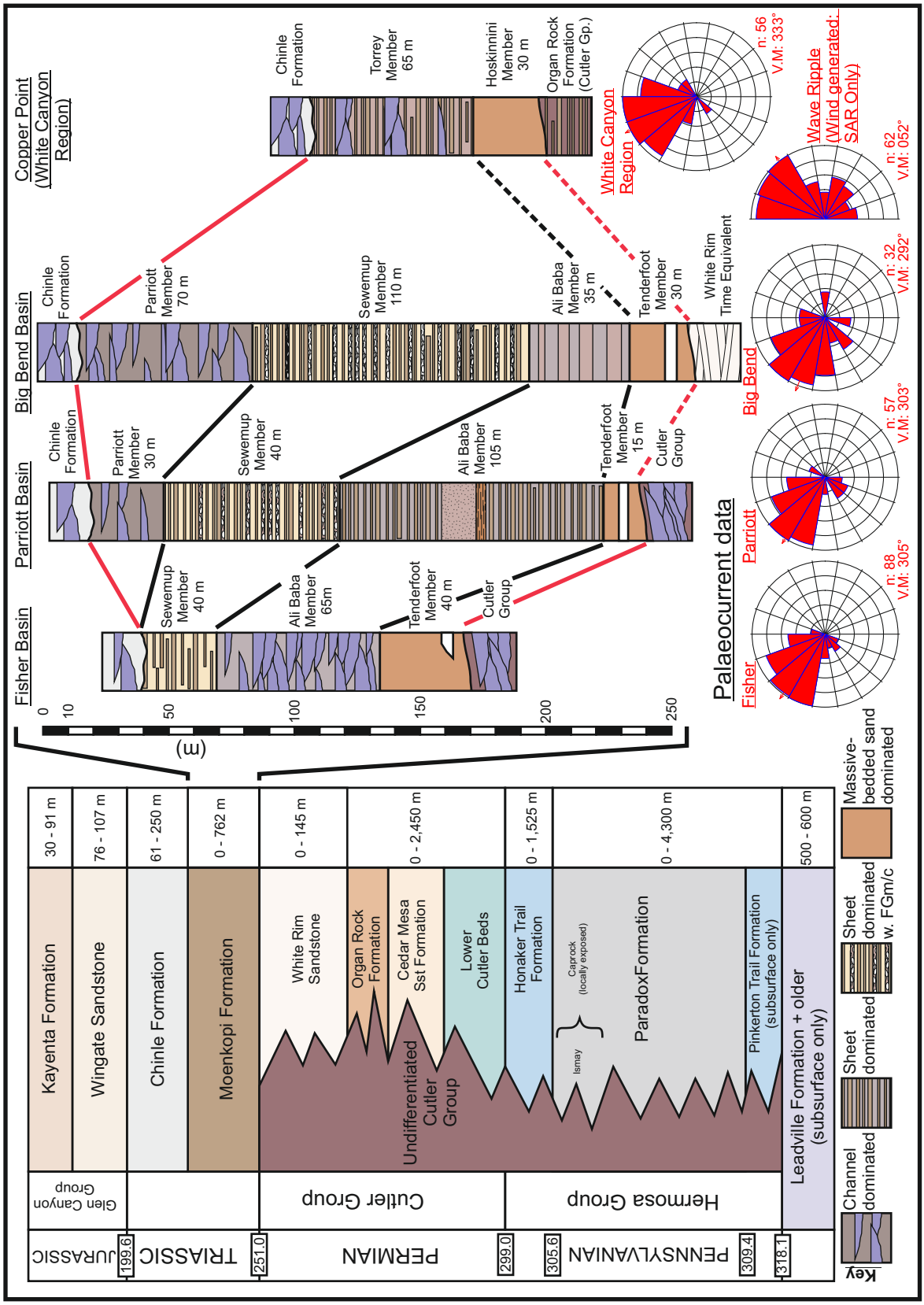


**Figure 3.1 (b)**: Paradox Basin Overview. Regional stratigraphic column and palaeocurrent summary data. Column depicts the average thickness of the various stratigraphic units within the Paradox Basin, and average thickness of the Moenkopi Formation in the three studied basins of the Salt Anticline Region and Copper Point, White Canyon Region. Palaeocurrent summary data for each studied mini-basin and White Canyon Region are plotted as a rose diagram vector mean (Vm) and vector magnitude (Vg) are: Fisher Basin, Vm= 305°, Vg=0.91, n=88; Parriott Basin, Vm=303°, Vg=0.85, n=57; Big Bend, Vm= 292°, Vg=0.77, n=32; Wave Ripples, SAR, Vm=052°, Vg=0.73, n=62; Copper Point, WCR, Vm=333°, Vg=0.89, n-56. After Trudgill (2011) and Banham & Mountney, 2013a

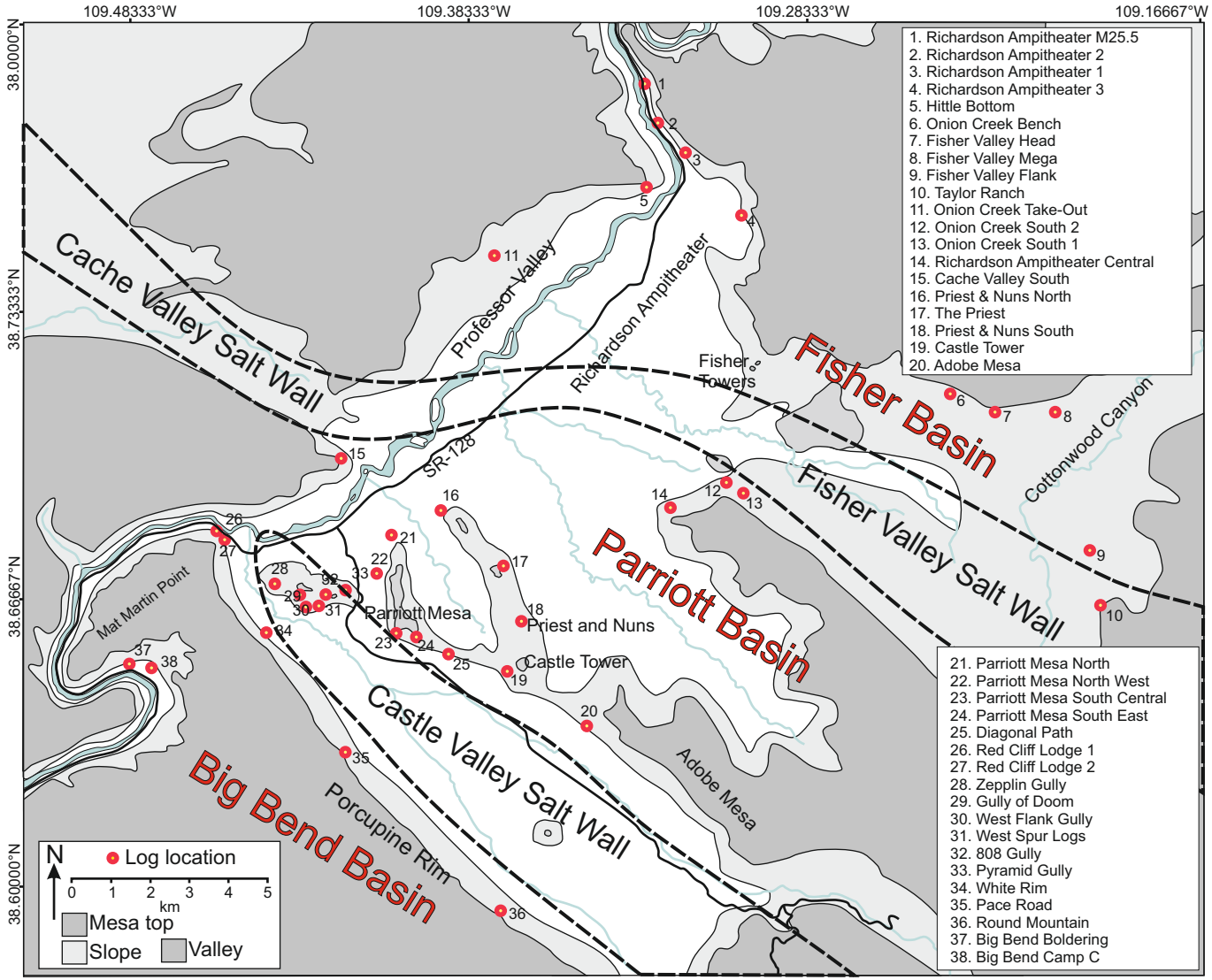


**Figure 3.2 (a)**: Overview location maps. Salt Anticline Region study area map depicting the location of salt walls and mini-basins in relation to the present-day topography. Map centre: 38.70°N, 109.324°W, geodesic system: WGS 84 (modified after Banham & Mountney, 2013a).

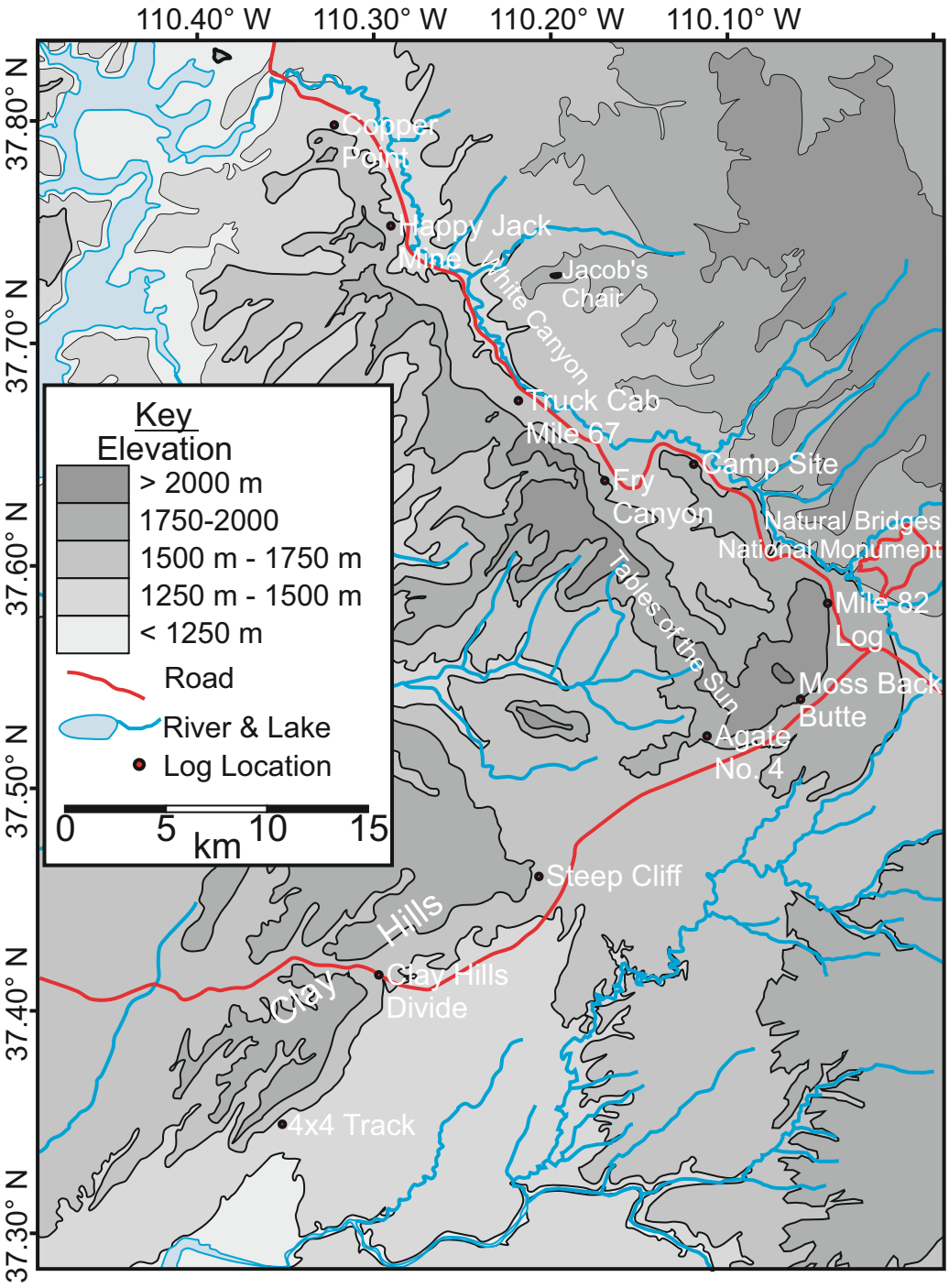


**Figure 3.2 (b)**: Overview location maps. White Canyon Region study area map. Map centre 37.566°N, 110.233°W, geodesic system: WGS 84. The location of measured vertical log profiles is indicated.

by both salt-wall growth and mini-basin subsidence (Lawton & Buck, 2006; Banham & Mountney, *2013a*), resulting in a complex preserved sedimentary architectural style. By contrast, in areas outside the Salt Anticline Region – including the White Canyon region of far-south Utah (Fig 3.2b) – the preserved succession of the Moenkopi Formation was not influenced by subsurface halokinesis and the sedimentology was principally controlled by intrinsic fluvial processes moderated by episodic climatic trends (Mullens, 1960; Thaden *et al.*, 1964; Johnson & Thordarson, 1966; Stewart *et al.*, 1972; Blakey, 1974).

The aim of this study is to compare and contrast the processes by which the detailed facies and architectural elements preserved as deposits of a low-relief, dryland fluvial system accumulated in both a part of the system controlled dominantly by active salt tectonics (halokinesis) and a part of the system controlled by a combination of non-tectonic factors including the prevailing climatic regime, the style of sediment delivery from upstream catchment areas and intrinsic (autogenic) behaviour of the fluvial system itself. Specific objectives are as follows: (i) to interpret the processes by which lithofacies and architectural elements preserved in a low-relief, dryland fluvial system accumulated and became preserved; (ii) to describe how halokinesis in the form of salt-wall uplift and ensuing mini-basin isolation acted to control the generation and distribution of fluvial facies and architectural elements; (iii) to develop a predictive model with which to account for spatial variations in the distribution and geometrical arrangement of architectural elements both within and away from areas of halokinetic influence; (iv) to demonstrate how variations in climate and fluvial-discharge regime influence the preserved stratigraphic architecture of dryland fluvial systems.

This work is important for the following reasons: (i) it enables development of an improved understanding of the controls that govern the formation and distribution of architectural elements in dryland fluvial systems; (ii) it enables the relative roles of external (allogenic) halokinetic and climatic controls on fluvial basin-fill architecture to be identified and examined; (iii) it provides a series of detailed depositional models with which to predict sand-body distribution in analogous settings, including economically important subsurface reservoirs such as the Triassic Skagerrak Formation (Hodgson *et*

*al.,* 1992; Smith *et al.,* 1993) of the Central North Sea, and the Pre-Caspian Basin of the Urals region (Barde *et al., 2002a;* Newell *et al.*, 2012).

## *3.2 Background*

Fluvial systems draining regions influenced by syn-sedimentary halokinesis and their accumulated deposits preserved in the stratigraphic record have been the focus of relatively few detailed studies at the scale whereby relationships between individual architectural elements can be determined. Early studies of fluvial successions developed in salt-walled mini-basins are those from subsurface studies of Hodgson *et al.* (1992) and Smith *et al.* (1993) regarding the economically important, hydrocarbon-bearing Triassic Joanne & Judy sandstones of the Central North Sea. McKie & Audretsch (2005); McKie & Williams (2009) and McKie (2011) undertook detailed studies on the Skagerrak Formation of the Central North Sea, specifically of the Herron Cluster (UKCS Quad 22), to determine how the preserved sedimentary architecture and drainage behaviour of a dryland fluvial succession that accumulated in a salt-withdrawal mini-basin was influenced by halokinesis. More recently, Barde *et al.* (2002a,b) and Newell *et al.* (2012) investigated the influence of halokinesis on Permo-Triassic fluvial successions in the Pre-Caspian Basin of the Urals region of Kazakhstan using a range of techniques including analysis of seismic reflection data and interpretation of satellite, wireline-log and core data to delineate depositional environments. However, the subsurface nature of each of these studies precluded analysis of detailed relationships between architectural elements.

The Chinle Formation of the Salt Anticline Region, South East Utah, has been the subject of several studies of halokinetic influence on fluvial sedimentation (Blakey & Gubitosa 1984; Hazel, 1994; Prochnow *et al.*, 2006; Matthews *et al.*, 2007). Climate during accumulation of this Triassic fluvial succession is considered to have been humid, with a monsoonal component (Blakey & Ranney, 2008), and rates of sediment supply were high relative to slow rates of subsidence that arose as a consequence of the grounding of mini-basins due to complete salt withdrawal. As a consequence, fluvial

architectures in the Chine Formation are characterised by high proportions of channel fill-complexes, containing coarse-grained sandstone.

Venus (2013) undertook a detailed study of the proximal part of the Cutler Group, which accumulated as an alluvial mega-fan distributive fluvial system (Barbeau, 2003; Cain & Mountney, 2009, 2011; cf. Hartley *et al.*, 2010; cf. Weismann *et al.*, 2011) succession in the Salt Anticline Region of SE Utah. This succession represents the preserved expression of a braided fluvial system for which high rates of sediment supply were sufficient to fill accommodation developed in a series of salt-walled mini-basins, thereby allowing drainage pathways to pass largely undiverted across several blind salt walls throughout much of their evolution. As drainage progressed over the crests of the salt walls, the fluvial systems apparently evolved in a manner whereby subtle changes in facies and architectural-element distributions are recorded: mean grain size systematically decreases with increasing distance from the salt walls; ponded, finer-grained elements accumulated on the upstream side of salt-walls; palaeodrainage direction in some areas was temporarily deflected from the general trend in response to episodes of salt-wall growth; aeolian elements accumulated in the sheltered lee of salt-wall generated topography. Indeed, Venus (2012) demonstrate that drainage networks of fluvial systems represented by the Cutler Group were unlikely to have been isolated in separate mini-basins due to the high rate of sediment delivery to the system that allowed drainage to occur transverse to salt wall orientation.

Basin isolation is an important factor that dictates preserved fluvial architectural expression in salt-walled mini-basins: where mini-basins are physically isolated from each other, sediment supply rates can vary significantly between adjacent basins, giving rise to the development of adjoining sand-prone and sand-poor basins, potentially in close proximity to each other (Hodgson *et al*., 1992; Banham & Mountney, *2013a*).

## *3.3 Geological Setting*

The Paradox Basin in which the Moenkopi Formation studied here accumulated, is a Pennsylvanian to Permian foreland basin in which more than 4000 m of strata were accumulated in the foredeep adjacent to the

Uncompahgre Uplift of the Ancestral Rocky Mountains (Barbeau, 2003). During the late-stage filling of the Paradox Basin, the Uncompahgre Uplift remained an active source of clastic detritus and was a major sediment source for the Permian Cutler Group. By the early Triassic, the largely denuded uplift likely contributed only localised sources of sediment for accumulation of the Moenkopi Formation (Dubiel *et al*., 1996; Nuccio & Condon, 1997; Banham & Mountney, 2013a), before the last remnants of the palaeo-high were buried by deposits of the Upper Triassic Chinle Formation (Blakey & Ranney, 2008; Trudgill, 2011).

The Moenkopi Formation crops out in parts of the present-day states of Arizona (Ward, 1901), New Mexico, Colorado, Utah, and Nevada (Darton, 1910; Gregory, 1917; Stewart, 1959, Carter, 1970; Blakey 1973, 1974, 1989; Hintze & Axen, 1995). This formation accumulated in a mixed fluvial, coastal plain and paralic setting, in which the shoreline underwent a gradual but prolonged marine regression throughout the Early Triassic, such that marine-influenced environments, including tidal flats, retreated to the northwest to become replaced further south by continental fluvial environments (Blakey, 1974; Blakey & Ranney, 2008). The Moenkopi Formation is divided into at least 20 formally recognized members (Blakey, 1974, 1989; Stuart *et al.*, 1972), each reflecting regional changes in depositional sub-environment.

Halokinesis initiated by differential sediment loading of the salt-bearing Pennsylvanian Paradox Formation by the Pennsylvanian-aged Honaker Trail Formation and Permian-aged Cutler Group continued from late Pennsylvanian in to the Jurassic (Doelling, 1988; Trudgill, 2011). This influenced deposition in the Salt Anticline Region of the foredeep of the Paradox Basin where accumulated salt was most thickly developed and overburden greatest (Kluth & DuChene, 2009; Rasmussen & Rasmussen, 2009; Paz *et al.*, 2009; Trudgill & Paz 2009; Venus, 2012). Salt-induced deformation extended into the Lower Triassic Moenkopi Formation (Banham & Mountney, 2013) and Upper Triassic Chinle Formation (Hazel 1994; Prochnow *et al.*, 2006; Matthews *et al.* 2007), as well as the Jurassic Wingate Sandstone and Kayenta Formation (Doelling, 1988; Bromley, 1989), albeit to a lesser extent than that experienced during the Permian (Fig. 3.1b).

The Moenkopi Formation in the Salt Anticline Region was originally described by Shoemaker and Newman (1959) and has been studied more recently by Lawton & Buck (2006) and Dodd & Clarke (2011). In the Salt Anticline Region, the formation is divided into 4 members: the Tenderfoot (lowermost), Ali-Baba, Sewemup, and Parriott (Shoemaker & Newman, 1959) (Fig. 3.1b). The lowermost three members are each laterally traceable both within and between a series of salt-walled mini-basins in the Richardson Amphitheater, Castle Valley, Big Bend, Moab, Potash and Shafer Basin areas (Fig. 3.1; Doelling & Chidsey, 2009), whereas the uppermost Parriott Member is restricted to the flanks of the Castle Valley salt wall (Shoemaker & Newman, 1959; Stuart *et al.*, 1972). The four members are delineated by distinct and mappable variations in architectural style and associated facies: the Tenderfoot Member; the Ali-Baba; the Sewemup; and the Parriott.

The Moenkopi Formation in the White Canyon region, southern Utah, is divided into 2 members: the Torrey and Hoskinnini (Blakey, 1974) (Fig 3.1b). The Hoskinnini Member was originally named by Baker & Reeside (1929) and was interpreted as part of the Cutler Group, before being re-interpreted as a basal member of the Moenkopi Formation (Stuart, 1959). This unit was later re-interpreted again as a separate formation by Blakey (1974), who considered it to have accumulated in a separate isolated basin, therefore representing a transitional unit between the Permian and Triassic successions. The Hoskinnini Member shares many similar characteristics with that of the Tenderfoot Member observed in the Salt-Anticline Region (especially in the Fisher basin), and has previously been considered a lateral equivalent (Stuart, 1959). The Torrey Member (referred to as the lower slope-forming, cliff-forming and upper ledge-forming members by Stuart *et al.*, 1972) was considered in detail in this study, with basic observations being made for the Hoskinnini Member. The depositional limit of the Sinbad Limestone, Black Dragon and Moody Canyon Members each pinch out near Hite Crossing beyond the limit of this study (Blakey, 1974; O'Sullivan & MacLachlan, 1975).

The palaeoclimate of the Moenkopi Formation has long been considered to have been arid (Stuart *et al.*¸1972; Blakey, 1974; Morales, 1987; Stokes 1987; Blakey & Ranney, 2008), with the palaeoenvironment having formed an extremely low-relief, low-gradient alluvial plain, based on

analysis of mineral composition and textural maturity of the accumulated sandstone and the sheet-like preserved architectural expression of fluvial elements (Blakey, 1974).

## *3.4 Data and Methods*

For this study, 49 vertical profiles were measured: 38 from the Salt Anticline Region and 11 from the White Canyon area. To complement these data, drawn architectural panels and photomontages depicting the distribution and style of juxtaposition of architectural elements and lithofacies were used to generate a series of correlation panels and architectural element models. Stratigraphic surfaces of significant lateral extent and which bound major architectural elements were traced between measured profiles to aid correlation; oblique aerial photography was used to assist tracing of key stratal surfaces where outcrop was inaccessible or difficult to observe from on the ground.

Of the 38 measured vertical profiles from the Salt Anticline Region, which collectively record >9000 m of stratigraphic succession, 22 measured sections record continuous profiles through the entire thickness of the Moenkopi Formation from the basal contact with the underlying Cutler Group or White Rim Sandstone (a capping formation of the Cutler Group), to the unconformable base of the overlying Chinle Formation (Fig. 3.1b). The total preserved thickness of the Moenkopi Formation varies from 125 m to 245 m, with significant variations both within and between salt-walled mini-basins. The majority of the remaining measured sections from the Salt Anticline Region record either the basal or top unconformities that bound the formation. For all measured sections, the stratigraphic position of the bases of the various members can be identified with confidence.

Each of the 11 measured vertical profiles from the White Canyon study area record the full thickness of the Torrey Member of the Moenkopi Formation, from the contact with the underlying Hoskinnini Member (as defined by Blakey, 1974), through to the unconformity that defines the contact with the overlying Chinle Formation (Fig. 3.1b). The preserved thickness of Moenkopi Formation varies from 60 to 110 m.

Palaeocurrent analysis was undertaken in all of the mini-basins observed within the Salt Anticline Region and White Canyon Region to determine the drainage direction and potential regions of sediment supply. Statistics including the vector mean and vector magnitude were calculated using methods described by Lindholm (1987). In total, 233 indicators of palaeoflow were measured from sedimentary structures including ripple-crests, climbing-ripple strata, cross bedding foreset azimuths and channel axes.

## *3.5 Sedimentology and Stratigraphy*

### 3.5.1 Lithofacies

Fifteen distinct and commonly occurring lithofacies types are identified throughout the study areas (Salt Anticline Region, SAR; White Canyon Region, WCR) (Table 1; Fig. 3.3), with the majority of lithofacies being demonstrably of fluvial origin; the remainder are a product of evaporitic or aeolian processes, though examples of such types occur as accumulations of only local extent and limited thickness. Representative vertical profiles for both the Salt Anticline Region (Fig. 3.4a) and White Canyon Region (Fig. 3.4b) demonstrate the typical stratigraphic styles preserved in the study areas. Vertical profiles for the Salt Anticline Region (Fig. 3.4a) portray representative parts of the succession for each of three separate mini basins studied: the Fisher, Parriott and Big Bend basins (Fig 3.2a). The profiles demonstrate variations in preserved fluvial expression between neighbouring mini-basins. Vertical profiles for the White Canyon area (Fig 3.4b) portray representative parts of the succession across the southern-most study area.

In addition, detailed facies diagrams highlighting key sedimentary features are annexed at the end of this chapter in section 3.9.

### 3.5.2 Architectural Elements

Representative examples of fluvial architectures present in both study areas depict common architectural elements in the Salt Anticline Region and White Canyon Region (Fig. 3.5). Fluvial facies are grouped into 2 facies associations corresponding to (i) channelised deposition and (ii) non-confined, sheet-like deposition. Four distinct architectural elements (F1 to F4) are associated with

| Code | Facies | Description | Interpretation |
|---|---|---|---|
| Fce | Extraformational conglomerate | Crudely-bedded (sometimes trough cross-bedded), matrix or clast supported, poorly sorted with rounded clasts. Matrix is medium sand to granule grade. Clasts composed of crystaline basement rocks. | Represents immature material derived from the Uncompahgre Highlands. |
| Fci | Intraformational conglomerate | Crudely bedded, matrix or clast supported, very poorly sorted with angular clasts. Matrix can be fine- to coarse-sand. Clasts are composed of locally derived siltstone or sandstone. | Represents the entrainment and reworking of locally derived sediment. Can occur as basal lags or as channel fill. |
| Fxt | Trough cross-bedded sandstone | Fine-sand to granule grade, moderate- to poorly-sorted and sub-angular to sub-rounded. Beds are typically 0.3 to 2 m thick. Sets can have coarse-grained lags of gravel. | Represents down-channel migration of sinuous-crested sand or gravel meso-forms (dune scale). |
| ha Fxp | High-angle trough cross-bedded sandstone | Fine-sand to granule grade, moderate- to poorly-sorted and sub-angular to sub-rounded. Beds are typically 0.3 m to 1 m thick. This facies is defined by planar-tabular sets that are tangential to the set base. Subcritical angle of climb. | Represents sinuous- or straight-crested sand (rarely gravel) meso-forms (dune scale) migrating down channel. |
| la Fxp | Low-angle trough cross-bedded sandstone | Fine-sand to granule grade, moderate- to poorly-sorted and sub-angular to sub-rounded. Beds are typically 0.3 m to 1 m thick. This facies is defined by planar-tabular sets that are asymptotic to the set base. | Represents cross-flow migration of sandy, laterally accreting macro-forms (either point bars, or mid-channel bars). |
| Frc/Fxl | Climbing-ripple strata and trough cross-laminated sandstone | Very-fine to medium sand, moderate- to well-sorted, sub-rounded to rounded. Beds typically 50 mm to 2 m thick. Ripple strata typically climb at angles <10° (subcritical), but can climb at supercritical angles (>15°). Ripple forms are sinuous-crested (Fxl) or straight-crested (Frc). | Represents down-flow migration of sandy micro-forms in either channelised or non-confined environments in waning flow regimes. |
| Fh | Horizontally laminated sandstone | Very-fine to fine sand, moderate to well-sorted, sub-rounded to rounded. Some examples are medium- to coarse-sand and angular grains. 2 to 7 mm laminations in sets > 50 mm thick. Primary current lineation on bedding surfaces. | Deposited under upper-flow regiemes either in channelised or partially/non-confined sheet-like units. Coarse-grained examples are associated with partially confined flows. |
| Fm | Massive (structureless) sandstone | Fine- to medium-sand, moderate- to poorly-sorted, sub-angular to rounded. Bed thickness ranges from 0.1 to 2 m thick. Beds may be normally graded. | Represents rapid deposition of sand from suspension. Grading (where present) indicates gradual waining of flow velocity. |

**Table 3.1: Table of lithofacies**

| Code | Facies | Description | Interpretation |
|---|---|---|---|
| Fd | Deformed bedding | Very-fine to medium-sand, moderately sorted, sub-angular to sub-rounded. Set thickness ranges from 0.1 to 1.7 m. Deformed bedding includes structures such as slumps and water escape structures. | Water escape structures represent water loss via infiltration through less permeable layers in responce to increase in pore-water pressure caused by sediment loading. Slump structures may indicate sediment movement down-slope. |
| FGm/c | Gypsum clast horizon (Matrix and clast supported) | 10 to 150 mm diametre clasts with fine-grained sand matrix. Generally very-poorly sorted, with rounded gypsum clasts that can be either matrix or clast supported. Gypsum clasts are rarely mixed with intraformational clasts and very rarely with extraformational clasts. | Discrete beds of gypsum-clast-bearing strata; indicate episodic reworking of diapir-derived detritus. These strata record episodes when salt walls had breached the land surface, resulting in the availability of gypsum material for reworking. |
| Fhiss | Horizontally interbedded siltstone and sandstone | Fine- to coarse-sand, moderately sorted, interbedded with homogeneous or laminated siltstone. Sandstone may be characteriesed by sedimentary strucures seen in facies **Fh, Fm, Frc/Fxl, WR** and rarely **Fci**. Desiccation cracks in-filled with homogeneous sandstone are common. | Represents multiple non-confined flow events where a waning flow resulted in accumulation of progresively finer-grained sediment, with associated sedimentary structures. |
| WR | Wave-rippled sandstone | Very-fine to fine-sand, poorly- to moderately-sorted, sub- angular to sub-rounded. Occurs in sets 10 mm to 0.3m thick. Typically symmetrical ripple forms but can co-exist with asymmetric ripples. Ripple crests are generally parralel and continuous over long distances relative to wavelength. | Represents micro-forms generated in response to oscillating water in puddles or shallow ponds, usually in response to wind action. Slight asymmetry of some ripple forms may indicate slight current modification. |
| GC | Crystalline gypsum | 1 to 2.5 m-thick homogenious or laminated gypsum bed (laminations may be convoluted). Gypsum may have a saccaroidal form or occur as flakey sheets. Some layers near the top of the bed can contain clinoforms. | Accumulation of gypsum by precipitation of saline water, potentially in a restricted basin. Clinoforms are interpreted to have been generated by aeolian dune-form migration (Lawton & Buck 2006) in the aftermath of episodes of desiccation. |
| Scls | Crenulated sandstone | Fine- to medium-sand, sub-angular to sub-rounded. Beds are characterised by discordant "crinkly" laminations. | Represents disruption of pre-existing sedimentary structures by water movement driven by capillary action (cf. Goodall *et al.,* 2000). |
| SGb | Gypsum-bound sandstone | Typically fine- to medium-sand (rarely coarse), poorly-sorted. Gypsum-bound sandstone is typically massively bedded and has a pervasive gypsum cement. | Origin is linked to throughflow of saline fluid and subsiquent precipitation of gypsum in the pore space as water evaporated at the ground surface. |

**Table 3.1 cont.: Table of lithofacies**

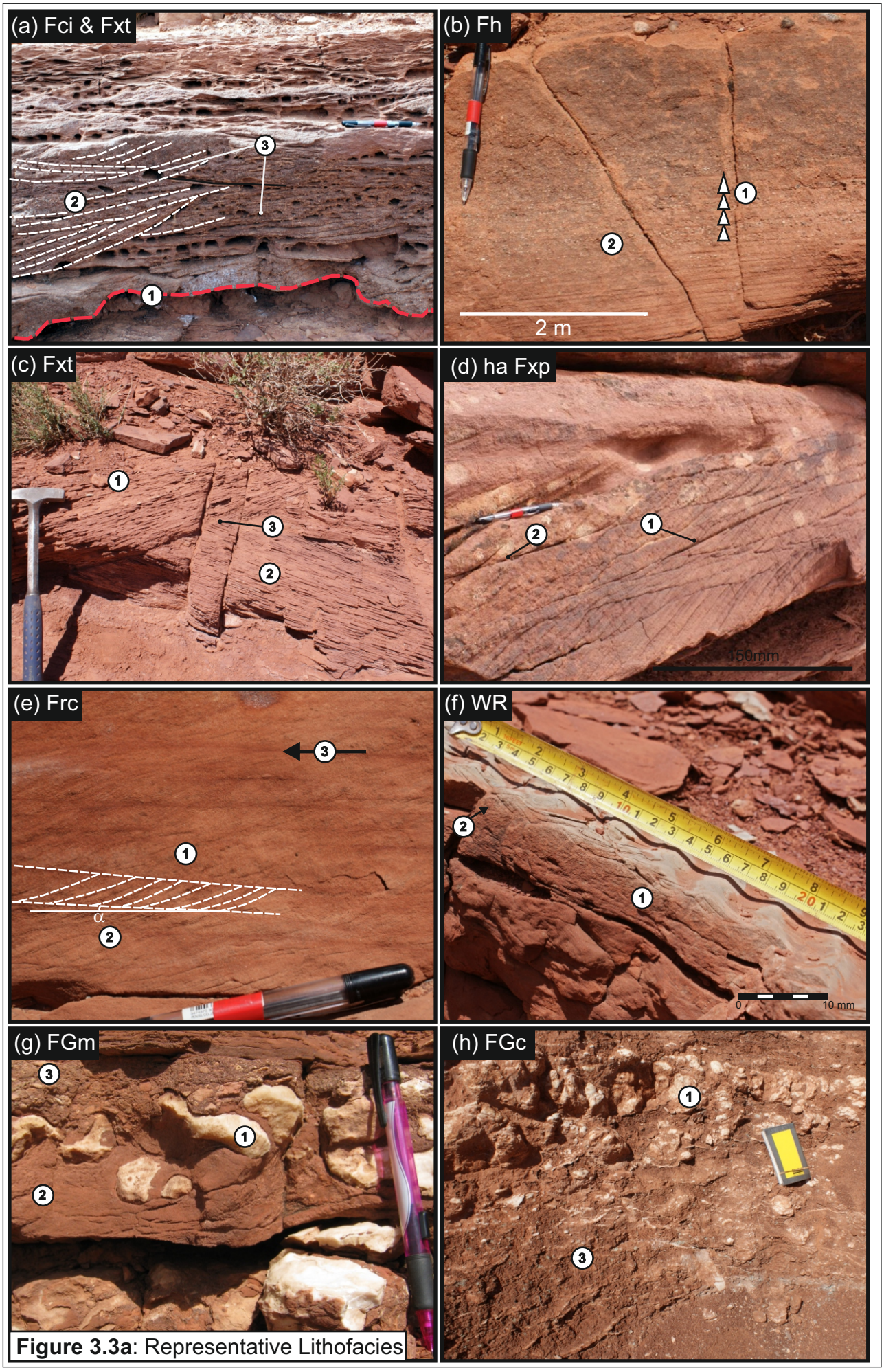


**Figure 3.3a**: Representative Lithofacies

***Figure.3.3**. Representative lithofacies of the Moenkopi Formation in the Salt Anticline Region (SAR) and White Canyon Region (WCR). See Table 1 for explanation of lithofacies codes. Black borders indicate photograph was taken in SAR, green border indicate WCR. Note that all depicted facies occur commonly in both areas, unless otherwise stated. (a) Trough cross-bedded sandstone (Fxt) with intraformational clasts (Fci). 1: Erosive base 2: Medium- to coarse- grained trough cross-bedded sandstone with a high proportion of intraformational clasts (which are mostly removed by erosion) 3: Intraformational clasts are angular to sub-rounded and <30 mm in size. (b) Horizontally laminated sandstone (Fh). 1: repeating small-scale fining upwards cycles 2: coarse-grained base of fining-up cycle. (c) Trough cross-bedded sandstone (Fxt). 1: Large scale cross-bedding is indicative of larger bedforms that typically develop in main channels. 2: Thin foresets within trough. 3: Grain size is typically medium-grained, although sporadic floating pebbles do occur (both intra- and extraformational). (d) High-angle planar cross-bedding (ha Fxp). 1: High angle tangential terminating foresets indicate direction of palaeoflow. 2: Erosive base foresets result from successive dunes migrating over the previous dune at sub-critical angles of climb. (e) Climbing ripple-strata (Frc) 1: Climbing ripple stratification in sets composed of fine- to medium-grained sandstone. 2: Positive, subcritical angle of climb. 3: Direction of Palaeoflow. (f) Wave-ripple laminated sandstone (WR). 1: Ripple forms preserved on upper bedding surfaces. In section these can exhibit combinations of chevron up-building, and draping of foresets onto ripple crests. 2: Some examples of asymmetric ripples indicate mixed uni- and bi-directional flow regime, which are typical of wind shear influence on shallow water. (g) Gypsum-clast-bearing unit; matrix supported (FGm). 1: Gypsum clasts are sub-angular: indicative of short transport distance. 2: Matrix-supported nature of sets indicates deposition by debris flow or water flow. 3: Pebble-grade clast horizon overlain by coarse-grained granulestone of gypsum micro-conglomerate, indicating disaggregation of larger clasts in higher energy flows, or possibly indicative of longer transport distances. (h) Gypsum-clast-bearing unit; clast supported (FGc). 1: Clast-supported gypsum horizon indicates close proximity to the source of gypsum detritus. 2: Gypsum clast-bearing intervals are discrete in nature, indicating episodic availability of diaper-derived detritus. (i) Preserved ripple. 1: Preserved asymmetric ripple crest, exhibiting a stoss and lee side of ripple. 2: Internal lamination, indicating direction of ripple migration. 3: Erosive base where successive migrating ripple has eroded and reworked pre-existing ripple strata. (j) Trough cross-bedded sandstone (Fxt). 1: lee side of dunes preserved as laminations which terminate tangentially to against coset beneath. 2: bounding surface defining top and base of coset. 3: coset, composed of cross-strata. (k) Subcritical to critical angle climbing-ripple strata (Frc). 1: Variable angle of climb indicates changing rate in sediment accumulation. 2: sigmoidal laminations indicate complete preservation of migrating ripple forms. 3: Critical angle of climb, where stoss-sides of ripples are preserved. (l) Massively bedded, graded sandstone (Fm). 1: Coarse, poorly-sorted, angular sand grains 2: Fining up cycles, indicating multiple phases of deposition from waning flows, or a single pulsing flow. (m) Horizontal interbedded siltstone and sandstone (Fhiss) 1: thicker sand lens (composed of massive bedded sandstone) preserved within a succession of heterolithic strata. 2: typical expression of heterolithic strata composed of interbedded sandstones and argillites, representing a deposition from a waning flow. (n) Horizontal interbedded siltstone and sandstone (Fhiss) 1: Sand-prone Fhiss, characterised by a higher proportion of sand preserved. 2: Sand-poor Fhiss, characterised by lower proportion of sand preserved. Both represent variations in sediment supply to this specific location, which can be controlled by sediment supply rates or autocyclic processes. (o) Horizontal interbedded siltstone and sandstone (Fhiss) 1: Climbing-ripple strata preserved in heterolithic succession, indicating bed-load transport. 2: succeeding siltstone horizon indicates progressive decrease in flow velocity after accumulation of climbing-ripple strata during initial stage of sediment deposition. 3: Palaeocurrent direction. (p) Crystaline gypsum horizon (GC) Crystalline gypsum horizon, in weathered form.*

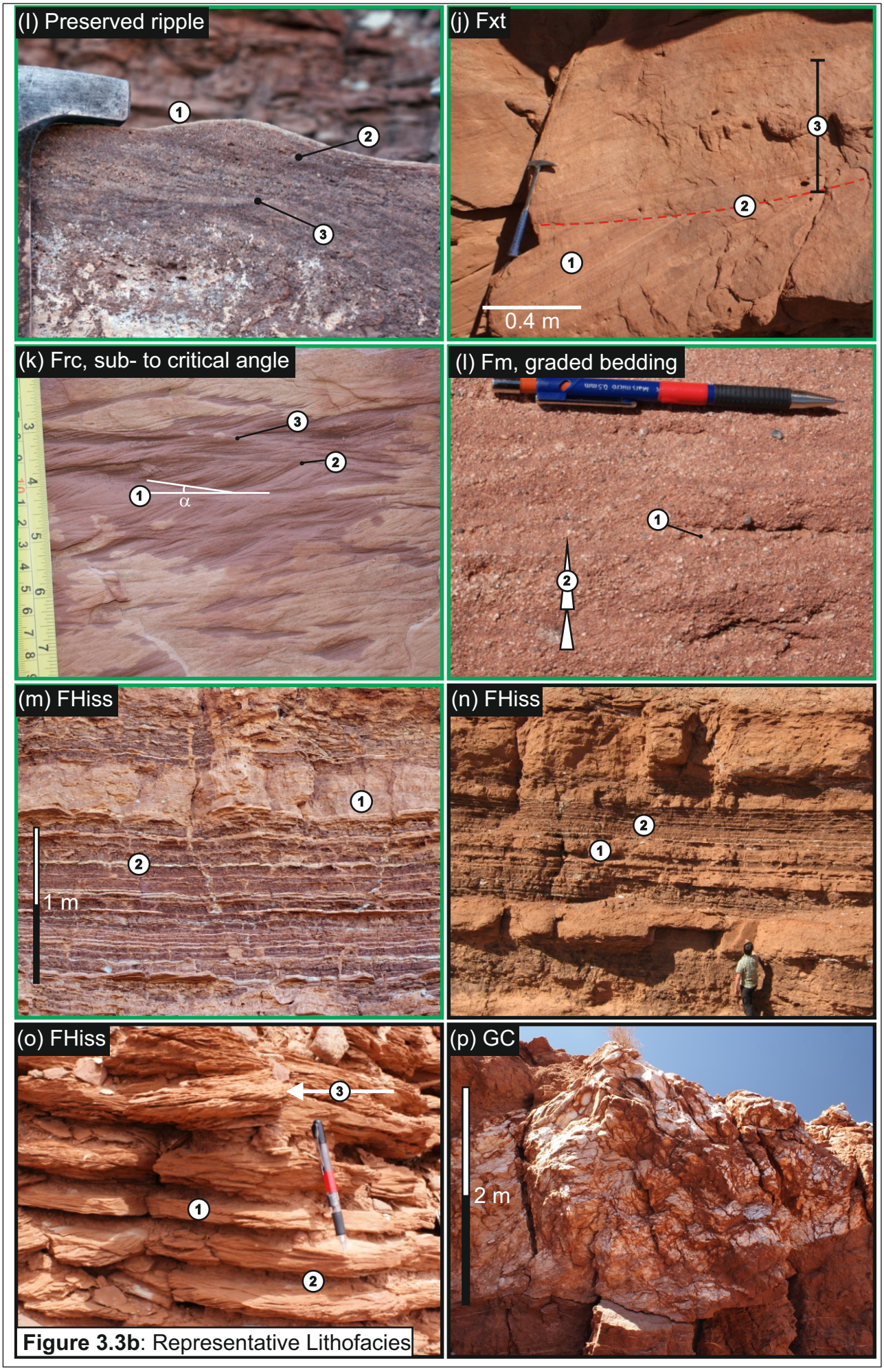


**Figure 3.3b**: Representative Lithofacies

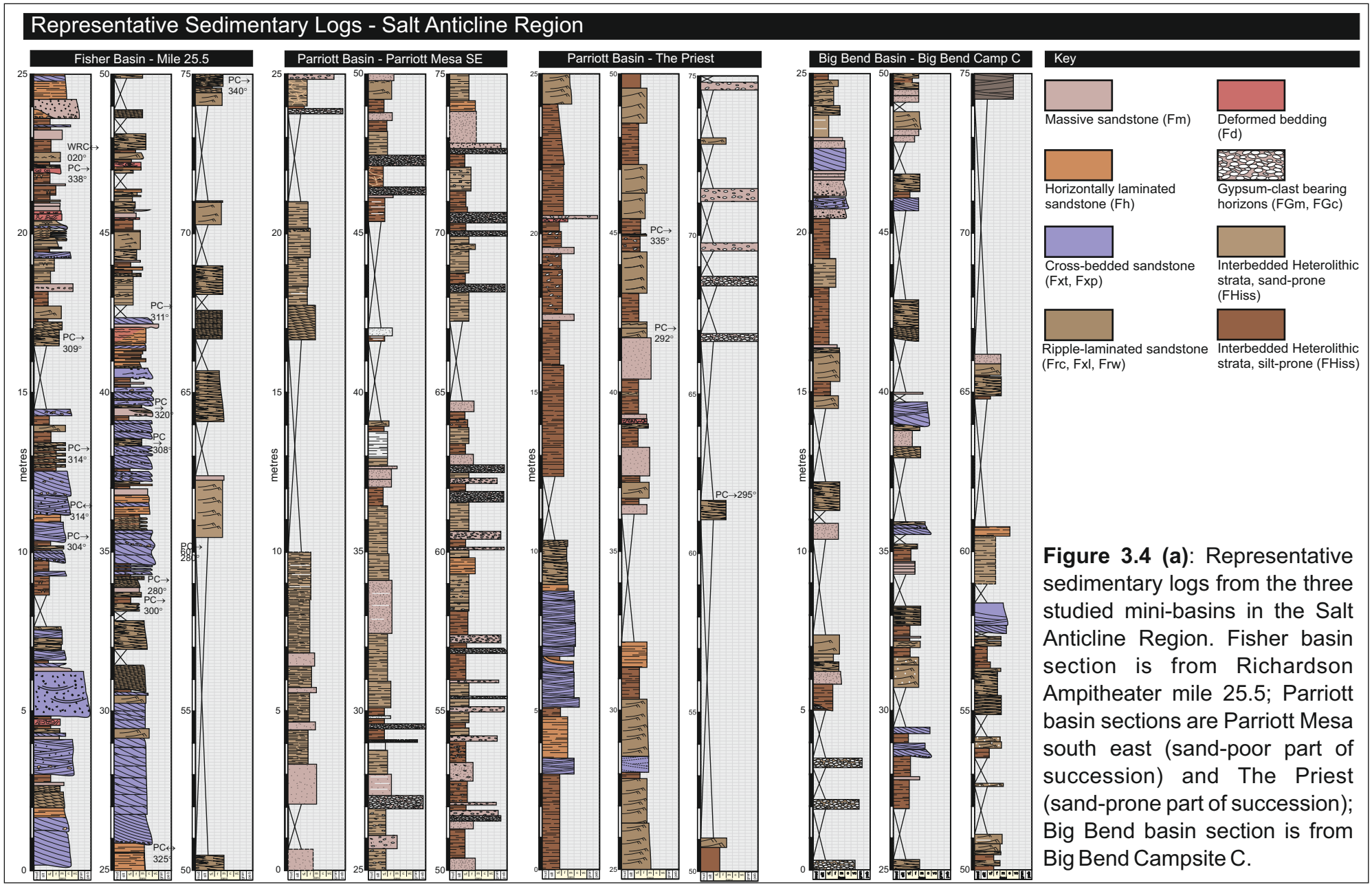


**Figure 3.4 (a)**: Representative sedimentary logs from the three studied mini-basins in the Salt Anticline Region. Fisher basin section is from Richardson Ampitheater mile 25.5; Parriott basin sections are Parriott Mesa south east (sand-poor part of succession) and The Priest (sand-prone part of succession); Big Bend basin section is from Big Bend Campsite C.

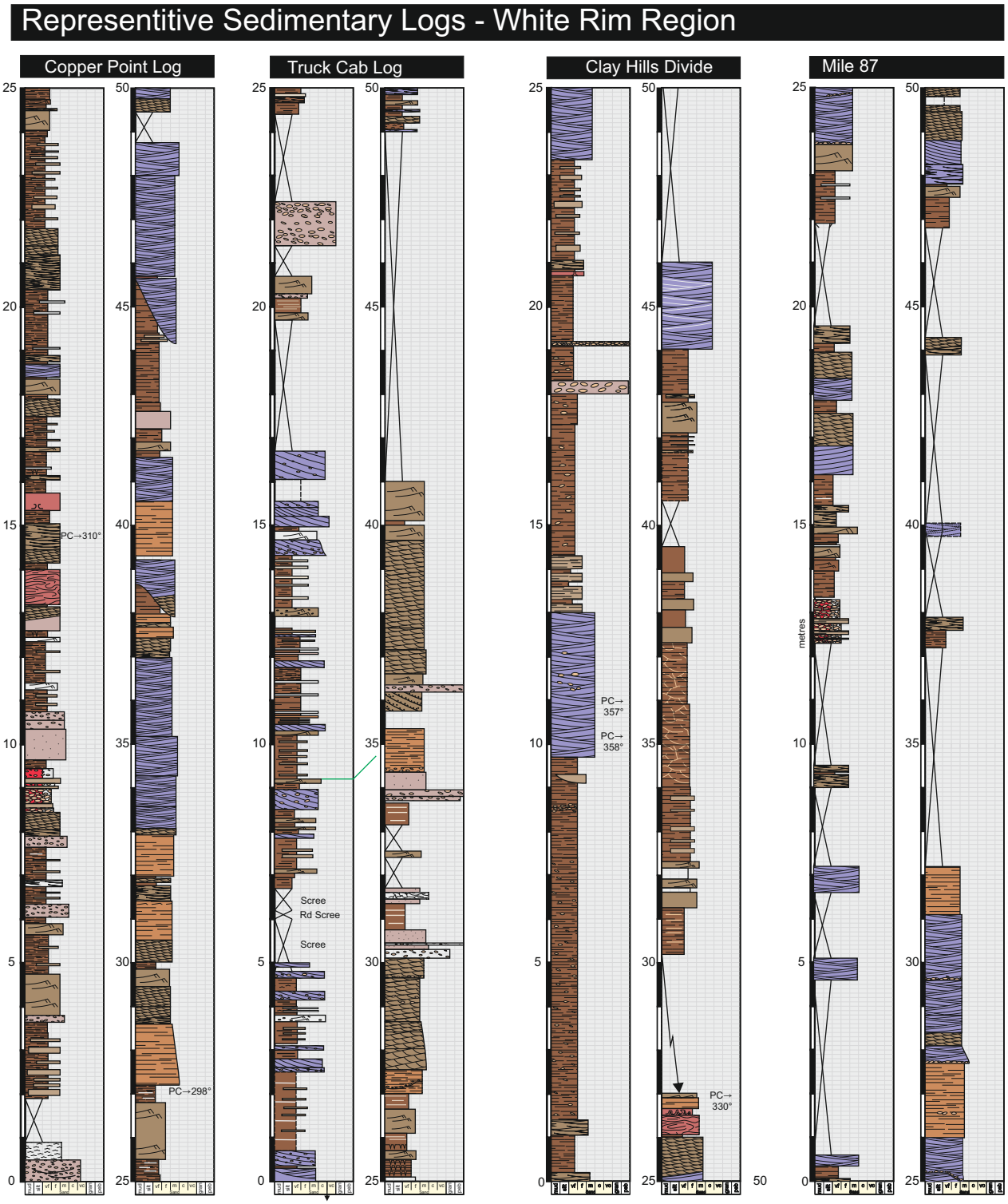


**Figure 3.4 (b)**: Representative sedimentary logs from the White Canyon

channelised deposition; five other distinct architectural elements (F5 to F9) are associated with non-confined deposition. Each architectural element is composed internally of lithofacies assemblages that typically occur as predictable vertical or lateral successions, and each element type exhibits distinctive geometric properties (Fig. 3.6) and styles of juxtaposition to neighbouring elements.

### Multi-storey, multi-lateral channel-fill elements (F1)

*Description:* F1 elements (Fig. 3.5a,e,f,g) are typically 3 to 10 m thick and comprise laterally and vertically amalgamated packages of strata. A representative vertical succession through an F1 element consists of a series one or more 0.2 to 2 m-thick cosets. Each coset is defined at its base by a $5^{th}$-order erosional bounding surface (Fig. 3.5a; Miall, 1996), commonly with a pebble-lag of either intra- or extra-formational clasts (typically no more than 0.3 m thick but rarely up to 0.6 m thick) lying directly upon it. The lowermost basal unit in each coset is succeeded upwards by multiple stacked sets of trough- or high-angle-inclined planar cross-bedding (Fxt/ha Fxp), the two forms being difficult to differentiate in cases where the outcrop trend is parallel to the original bedform migration direction. Cross-bedded sandstone sets rarely pass gradationally upward into sets of climbing-ripple-stratified sandstone (Frc/Fxl) or homogeneous siltstone (Fhiss), but in most cases, such successions are not fully preserved because the base of the overlying coset erodes into the upper part of the underlying one. Individual storeys represented by cosets of strata can be traced laterally for 50 to 300 m; their erosional basal surfaces exhibit up to 0.5 m of relief and they are typically cut-out laterally by adjacent storeys. Groups of laterally or vertically amalgamated storeys collectively characterize a single F1 element, examples of which can be traced in directions perpendicular and parallel to regional palaeoflow for up to 2 km and 10 km, respectively. Although relief due to incision is present at the base of F1 elements in the form of a $6^{th}$ order bounding surfaces of significant lateral extent (Miall, 1996), it rarely exceeds 1 m.

*Interpretation:* Multi-storey multi-lateral channel-fill elements represent the deposits of laterally extensive, aggrading braid-belts (Fig. 3.7a; cf. Flores &

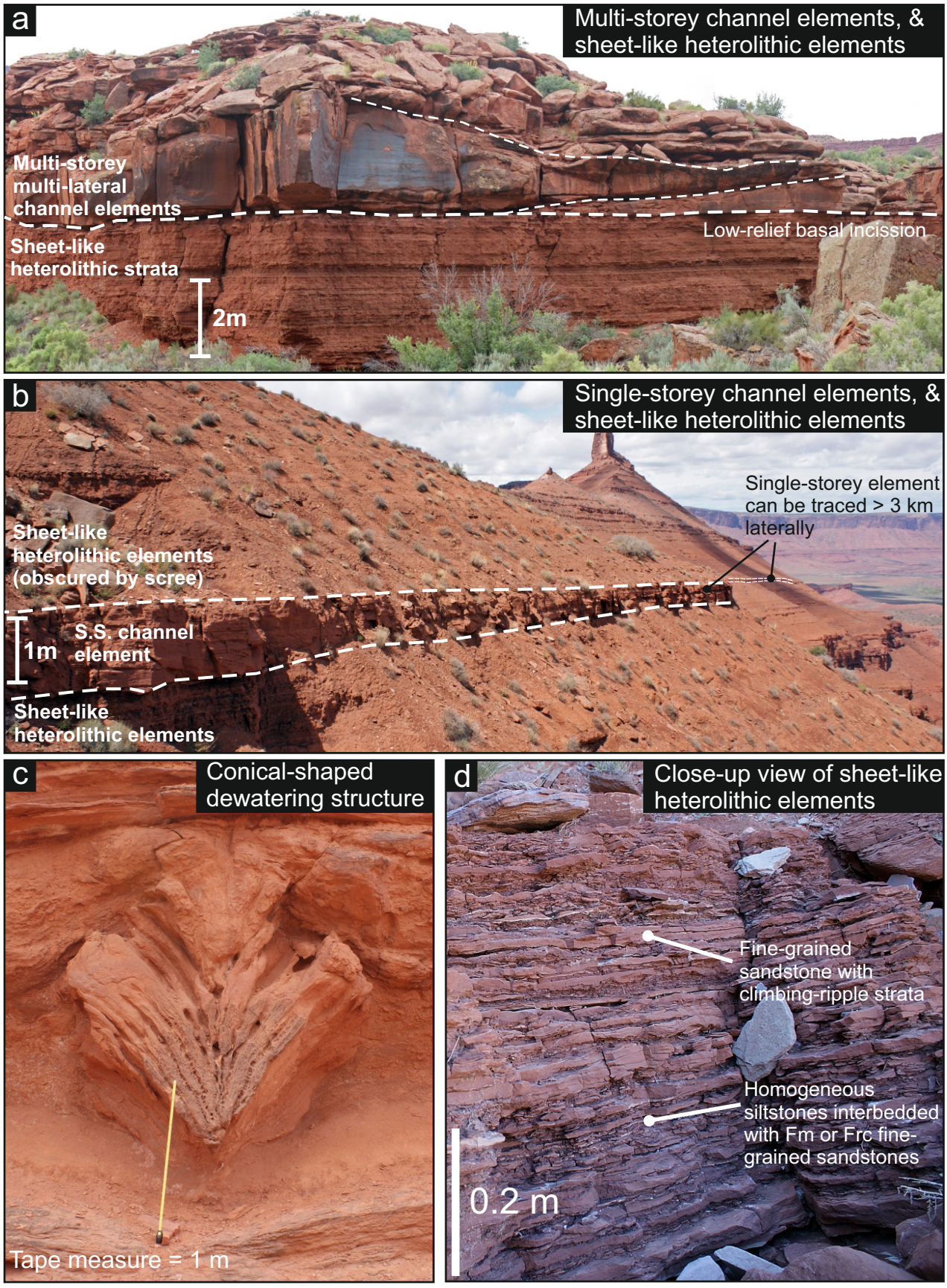


**Figure 3.5**: Representative architectural elements from the Salt Anticline Region (SAR). (a) Multi-storey, multi-lateral elements with heterolithic sheet-like elements. (b) Single-store, multi-lateral channel element. (c) Conical de-watering structure. Tape measure is 1 m. (d) Close-up view of sheet-like heterolithic strata.

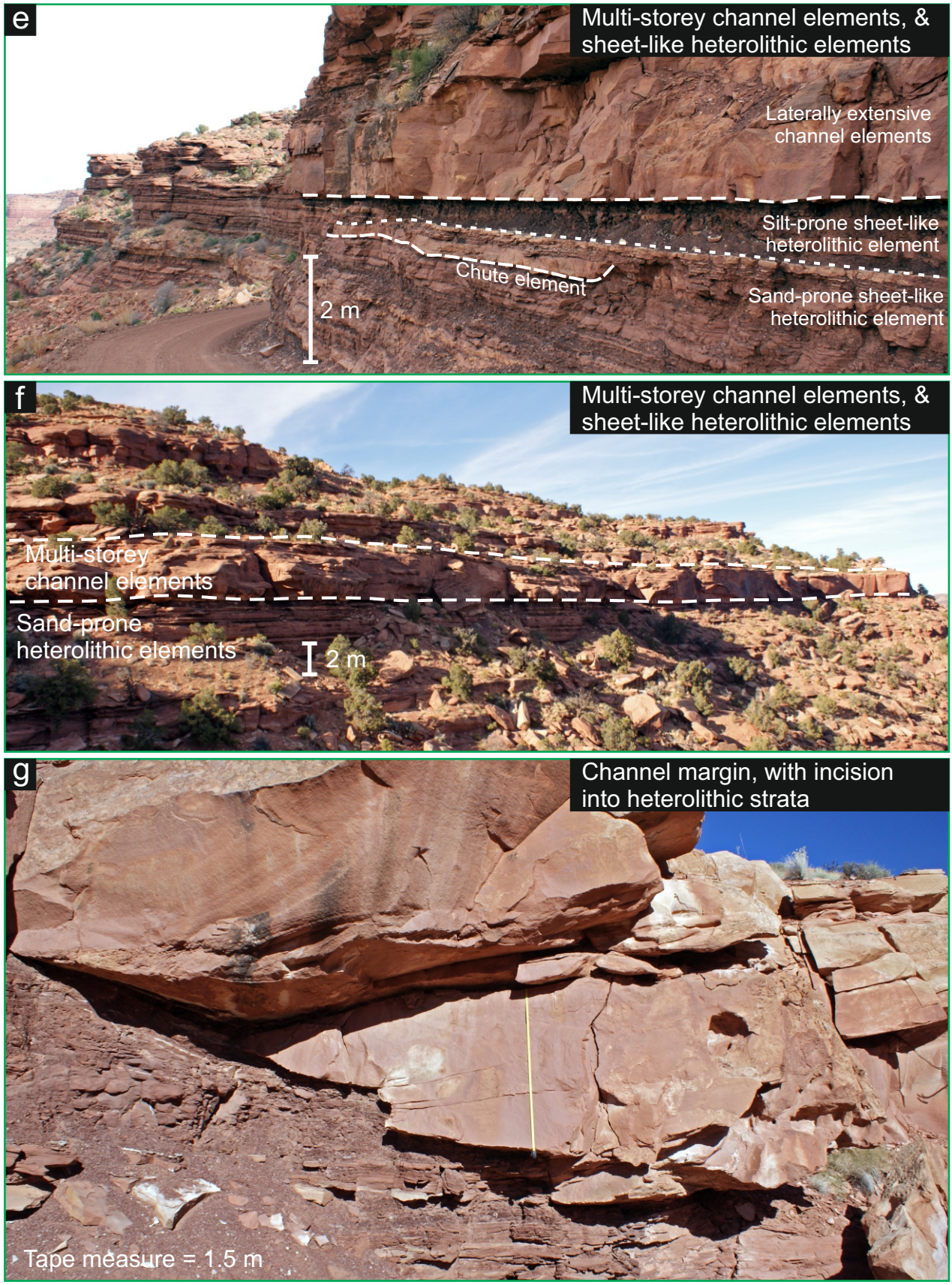


**Figure 3.5**: Representative architectural elements from the White Canyon Region. Representative architectural elements from the White Canyon Region (WCR). (e) Multi-storey, multi-lateral elements with heterolithic sheet-like elements. Note chute element nested in sand-prone portion of sheet-like heterolithic element. (f) Multi-storey, multi-lateral channel elements nested in sand-prone sheet-like heterolithic channel elements. (g) Margin of a channel element, where the channel element has incised into the underlying sheet-like heterolithic element.

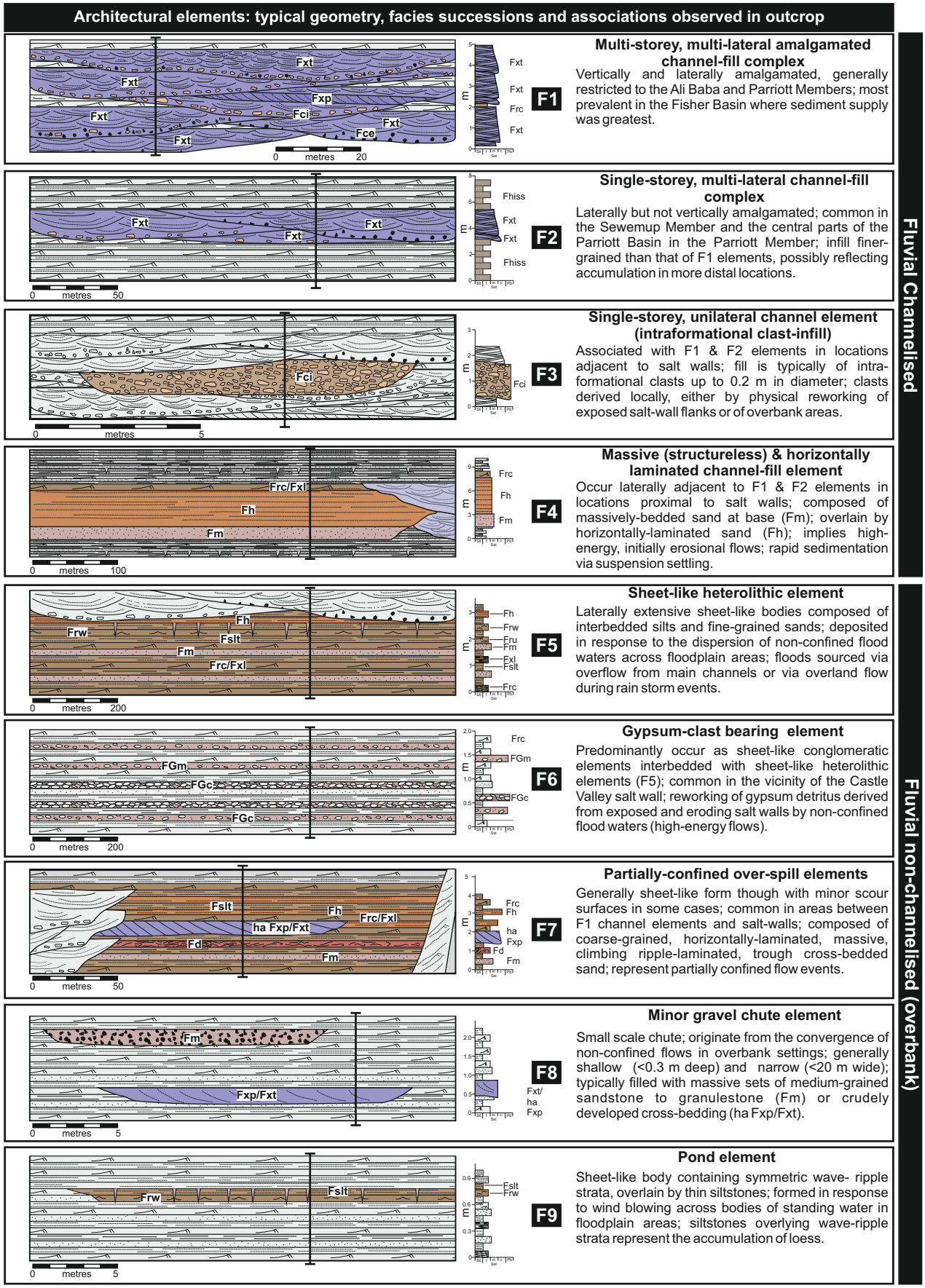


**Figure 3.6**: Representative architectural elements, depicting generalised geometries and internal facies composition of the principal architectural elements of the Moenkopi Formation.

Pillmore, 1987; Gibling, 2006). These elements are the preserved expression of sandy macro-forms that migrated axially within channels, which themselves formed part of a wider active braided channel complex (cf. Miall.1996; McKie 2011). The occurrence of gravel lags in association with erosively based channel storeys indicates high-energy flow where stream power was sufficiently high to result in incision into the underlying substrate, followed by localized transport of pebble-grade material (mostly mud-chip rip-up clasts) prior to deposition as a basal lag, probably in the immediate aftermath of peak-flood discharge on the falling limb of the hydrograph (cf. McKie, 2011). A combination of rapid downstream and lateral barform migration and expansion, frequent localized channel avulsion and high rates of sediment delivery over a protracted period generated multiple laterally amalgamated and vertically stacked storeys (cf. Cain & Mountney 2009); the erosional surfaces that bound each storey could have arisen either through lateral channel migration, barform migration or barform expansion within a broad channel (cf. Picard & High, 1973; Miall, 1996; Bridge, 2003). The repeated stacking of multiple storeys resulted in the generation of a laterally extensive sheet-like body of composite channel-fill elements to form the F1 element. Internally, although erosional bounding surfaces that define storeys are numerous, few such surfaces define distinct channel margins. These multi-storey multi-lateral elements were preserved through a combination of lateral avulsion of channels, possible lateral migration of the entire channel belt and by the aggradation of the system to allow the vertical accumulation and stacking of later storeys of channel-fills (Gibling, 2006). The considerable overprinting of vertically-stacked storeys could indicate a relatively low rate of generation of accommodation space or might alternatively indicate a high frequency of avulsion (Bristow & Best, 1993). The multi-storey and multi-lateral nature of these composite channel-fill elements indicates a significant and possibly long-lived episode of fluvial activity in a localized area to allow the accumulation of these stacked sheet-like bodies (Cain & Mountney, 2009).

### Single-storey, multi-lateral channel-fill elements (F2)

*Description:* F2 elements are composed internally of laterally but not vertically amalgamated channel-fill storeys that are each 0.5 to 2 m thick (Fig. 3.5b).

The basal surfaces of these elements are sharp and many exhibit incision (up to 1 m of relief, though typically no more than a few decimetres). Vertical facies successions in these elements are encapsulated within a single coset of cross strata that forms a storey, though storeys are stacked laterally adjacent to each other, with their bounding surfaces typically showing local lateral incision into neighbouring storeys. Cosets representing storeys are delineated by a basal erosion surface that commonly has pebble (and rarely cobble) intraformational clasts (Fci) associated with it. These lags are overlain by sets of trough or high-angle-inclined planar cross-bedded strata (Fxt/ha Fxp). Rarely, sets of low-angle-inclined sandstone (la Fxp) are observed but these never comprise more than a few percent of the element. Cross-bedded sets present in F2 elements are typically overlain by F5 elements (sheet-like heterolithic bodies) containing sets of climbing-ripple strata (Frc/Fxl), overlain by horizontally interbedded sandstone and siltstone (Fhiss). These elements are typically laterally extensive and many can be traced for over 2 km in orientations perpendicular to regional palaeoflow.

*Interpretation:* Single-storey, multi-lateral channel-fill elements represent non-aggrading laterally extensive and laterally mobile braid-belts which were succeeded by non-confined sheet-like elements (Fig. 3.7b). These elements are dominated by bedload transport processes, with cross-bedded sets representing the downstream migration of dune-scale mesoforms (Miall 1996). The only rare presence of low-angle-inclined Fxt lithofacies indicates that these elements did not migrate laterally to any significant degree; rather, sedimentation occurred predominantly as a result of down-channel migration of sandy bedforms (Miall, 1996). The laterally extensive “sheet-like” nature of these amalgamated channel complexes arose from repeated avulsion of active channels at a single stratigraphic horizon to form a channel belt (Martinsen *et al.*, 1999; Gibling 2006). Original channel width is difficult to determine from outcrop study, but is likely to have been several hundred metres to possibly in excess of 1 km (cf. Tunbridge 1981a). The style of termination of F2 elements, which are overlain by non-channelised elements of various types, indicates that the braid-belt either avulsed abruptly to an alternative location elsewhere on the alluvial plain (cf. Mackey & Bridge, 1995;

Bridge 2003), else a cessation of channelised fluvial activity occurred throughout the region in favour of non-confined sedimentation, possibly in response to a change to a more arid climate (Blum & Tornqvist, 2000) or to a shut-down in sediment delivery (Leeder *et al*., 1998).

### Single-storey unilateral (isolated) channel-fill elements with abundant infraformational clasts (F3)

*Description:* Isolated F3 channel elements typically occur embedded within F1 and F2 elements, although they also occur as isolated forms encased in non-confined elements. F3 elements are discernable from F1 & F2 elements by virtue of their distinctive fill of pebble-grade clasts of intraformational origin. F3 elements are typically defined by steep-sided channel margins inclined up to 50°; channel fills are 0.5 to 1.5 m thick and up to 15 m wide. F3 elements are overlain either by non-confined elements or are partly eroded by channelised elements. Clasts are angular, composed of argillaceous siltstone and (more rarely) mudstone that was apparently derived from the local vicinity, and have diameters from 10 mm to 0.4 m. The style of fill of these F3 elements by intraformational clasts may give rise to either a massive (structureless) fabric (Fci) or result in the preservation of crude cross-bedding (Fxt with Fci). The matrix present between the clasts is fine-grained sand.

*Interpretation:* Isolated, intraformational clast-filled elements represent the preserved product of erosion and reworking of argillaceous material derived locally from the surrounding alluvial plain and the subsequent deposition of this material in thread-like channels, probably in a single cut-and-fill event related to an individual flood (Fig. 3.7a; Billi, 2007; Cain & Mountney, 2009). A possible variation on this mechanism for the generation of these elements could have arisen where locally active fluvial systems encroached onto the flanks of a pre-existing topographic high, resulting in localised erosion, entrainment, transport and deposition through incision (c.f. Rodríguez-López *et al.*, 2012) and collapse at the outer bank of the channel (Gomez-Gras & Alonso-Zarza, 2002). In places, F3 elements can be shown to be associated with locations proximal to topographic features on the alluvial plain, including topography generated by salt-wall uplift (discussed later).

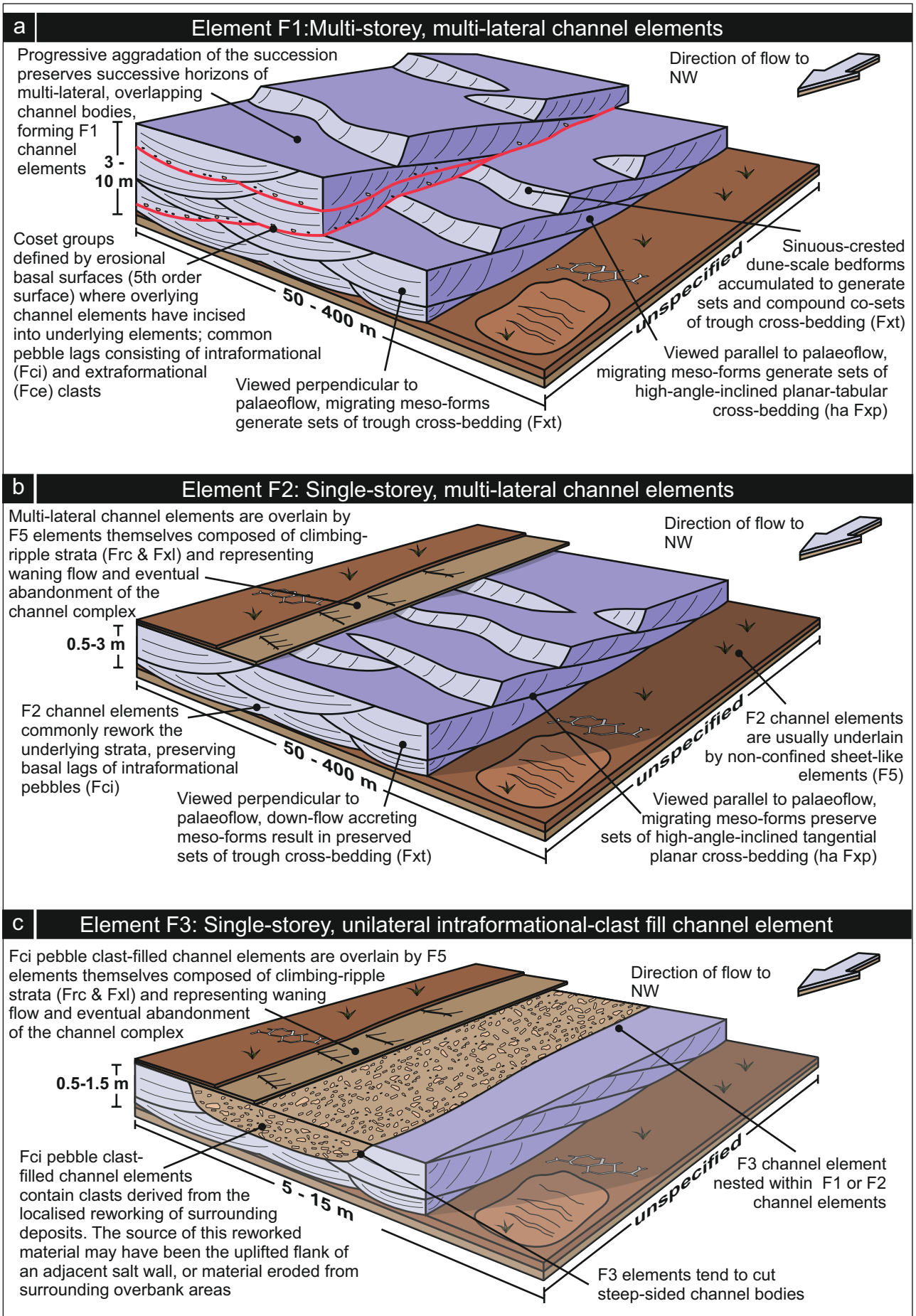


**Figure. 3.7**: Three-dimensional multi-element deposition models depicting confined- and non-confined flow architectural elements.

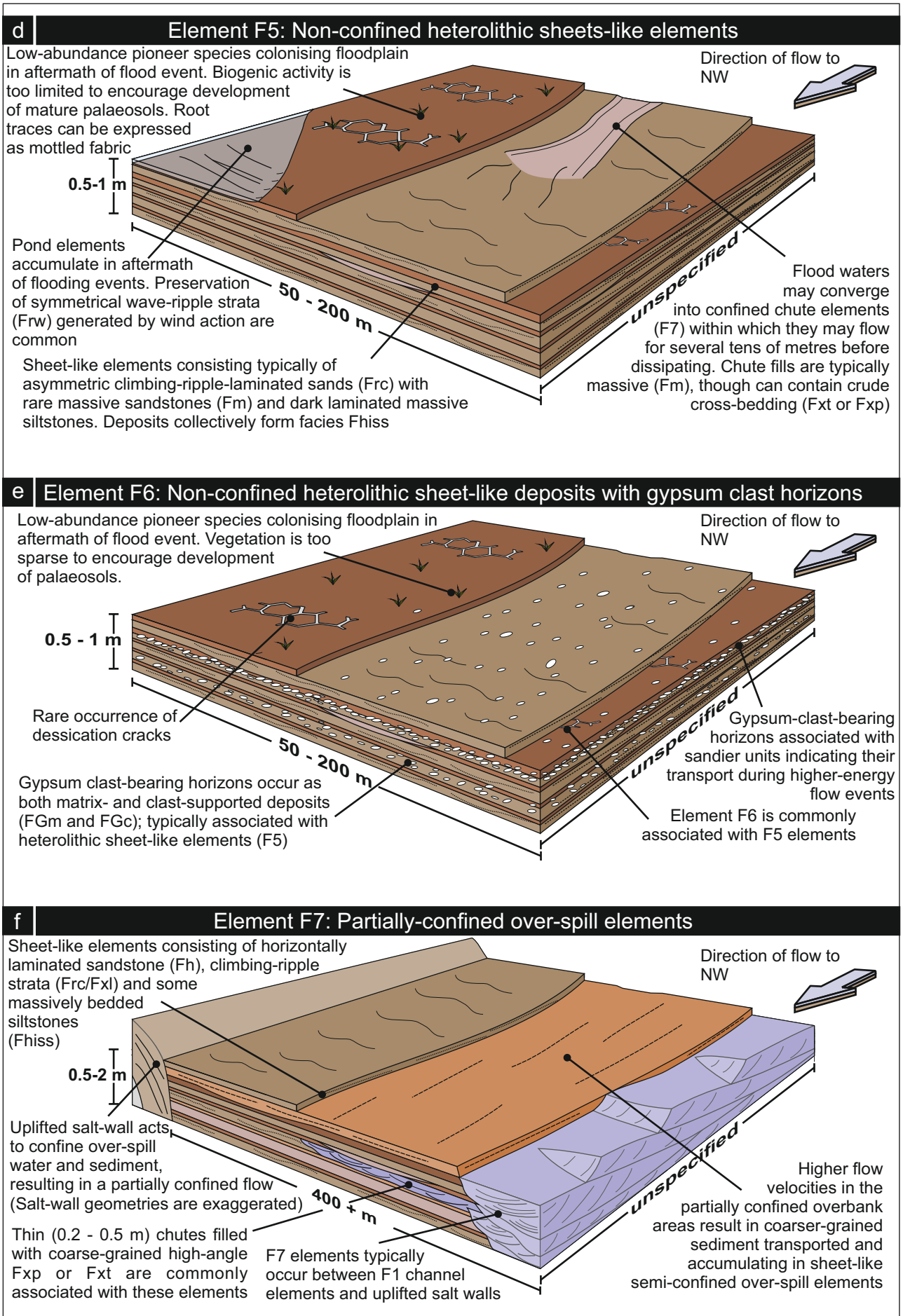


**Figure 3.7 cont.:** Generalised deposition model depicting relationships between confined & non-confined fluvial elements.

### Massive (structureless) & horizontally laminated channel elements (F4)

*Description:* F4 elements are typically up to 8 m thick, and are characterised at their base by a 1 to 2 m-thick set of massive bedded sandstone (Fm), overlain by a 6 to 7 m-thick set of horizontally bedded sandstone (Fh), bedding surfaces of which reveal primary current lineation. Basal incision typically exhibits modest relief that rarely exceeds 1 to 2 m. These elements typically occur adjacent to multi-storey (F1), and single storey (F2) multi-lateral channel-fill elements and in close proximity to the flanks of salt walls, notably in the vicinity of the Castle Valley salt wall in the Parriott basin.

*Interpretation*: Massive (structureless) and horizontally laminated sandstone channel-fill elements (Fig. 3.6) most likely represent rapid incision and subsequent fill during a single flood event. The basal part of the channel-fill association represents rapid deposition from suspension, before flow velocities waned and upper plane-bed conditions prevailed (Ashley *et al.*, 1990). The presence of a single facies succession, most of which was horizontally laminated sandstone (Fh) with primary current lineation demonstrates accumulation from a fast-moving flow arising from a single flood event (McKee *et al.*, 1966).

### Sheet-like heterolithic elements (F5)

*Description:* Elements composed of heterolithic strata are laterally extensive and can be typically be traced laterally over many square kilometres; they comprise >75% of the total vertical succession in some areas. A typical vertical facies succession within this element may include a basal massive-bedded (Fm) sandstone sheet, which may have a coarse-grained sandstone lag and erosive relief of up to a few tens of millimetres. Massive sandstone (where present) is overlain by sets of climbing-ripple strata (Frc/Fxl), within which ripple trains usually climb at a subcritical angle (Fig 3.6). These pass gradationally upward into sets of homogenous or laminated siltstone (Fhiss) at the top of the succession. Single examples of these sheet-like elements are typically only 0.1 to 0.4 m thick, but can occur in repeating cycles that are collectively >20 m thick (Figs. 3.5d,e). Sheet-like elements can occur juxtaposed laterally with channelised elements (F1 to F4) (Fig. 3.5g), or

vertically (Figs 3.5a,b,e,f), where successive channelised elements have incised into the pre-existing sheet-like heterolithic elements.

*Interpretation:* These heterolithic sheet-like elements are the preserved expression of repeated non-confined flood events that distributed thin sheets of sediment across the alluvial plain during episodes of elevated discharge (Fig. 3.7d). Each element, defined by a fining-upward cycle, likely represents an individual flood event, where a predictable facies succession is deposited, corresponding to deposition from a waning flow. The lowermost massive sandstone sets, which typically possess a low-relief and a sharp erosional base, represent the passage of an initial flood bore, which possessed sufficient energy to entrain sediment from underlying flood deposits before depositing them either through progressive accretion or via rapid suspension settling as the flood-front passed (Blair, 2000). The facies succession in the upper part of the element is characteristic of a progressive reduction of flow competence, with the relatively thick accumulations of bed-load generated structures such as climbing-ripple strata being diagnostic (Benvenuti *et al.*, 2005; Hampton & Horton, 2007). Water depth of the sheet-like flood waters was likely between 0.07 and 0.8 m (Rahn, 1967; Bentham *et al.*, 1993; Tooth, 1999a; Blair, 2000), although water depth may have increased where chute elements (F8) occur. Radial spreading of water over a considerable area (cf. Fisher *et al.*¸ 2008) and transmission losses would have resulted in dissipation of the flood water and eventual deposition of lower-stage plane beds and the settling of argillaceous siltstone from suspension during the final phase of the flood when flow velocity decreased to approach zero (Hampton & Horton, 2007). Repeated, stacked cycles of these elements demonstrate that sheet-flood events were a dominant process in parts of the Moenkopi Formation.

### Gypsum-clast-bearing elements (F6)

*Description:* Gypsum-clast-bearing elements are restricted to the Sewemup Member and are characterised by 0.1 to 0.4 m-thick accumulations that can either be clast-supported (FGc) or matrix-supported (FGm), with a fine sand matrix. Such clast-rich sets can typically be traced laterally for several hundred metres. Clasts are composed predominantly of detrital gypsum,

although intra-formational clasts of reworked argillaceous silt and fine sand and extremely rare extra-formational clasts are also typically present. Gypsum-clast-bearing sets are typically overlain by sets of climbing-ripple strata (Frc/Fxl), which are capped by a siltstone set (Fhiss) (Fig. 3.6). These gypsum clast elements are only observed within 5 to 8 kilometres of the Castle Valley salt wall.

*Interpretation:* Gypsum clast horizons represent the preserved expression of fluvial erosion and entrainment of diapir-derived gypsum detritus (Figs 3.7e; Lawton & Buck, 2006). During episodes where salt-wall uplift exceeded the rate of sedimentation, actively uplifting salt walls breached the land surface, forming salt glaciers (cf. Ala, 1974; Talbot & Rogers, 1980) which acted as an episodic source of detritus that was subsequently reworked by fluvial activity (Banham & Mountney, 2013a). These clasts were transported up to several km from the flank of the salt wall by flood waters before being deposited as clast-bearing units. The proportion of clasts-to-matrix in such units is a function of transport distance from the salt wall and gypsum availability (itself a function of the ratio of salt-wall uplift and sedimentation rate).

### Partly confined over-spill element (F7)

*Description:* These elements, which are typically several 100 metres wide, are characterised by a sheet-like geometry and occur in close association with chute elements (F8), typically embedded within them in areas adjacent to channel-fill complexes (F1 & F2) (Fig. 3.6). Characteristic vertical facies successions of these elements comprise coarse-grained, horizontally-laminated sandstone (Fh), within which F8 chute elements may be embedded, overlain by typically climbing-ripple strata (Frc) and interbedded very-fine sand and silt (Fhiss). These sheet-like successions are each typically 0.5 to 2 m thick and may occur vertically stacked as repeating cycles of fining-upward facies successions. These elements typically occur nested within a succession composed of other sheet-like elements, including sheet-like heterolithic and pond elements (F5 and F9). Significantly, these elements typically only occur in close proximity (within 500 m) of uplifted salt walls.

*Interpretation:* Partly confined over-spill elements represent the deposits of non-channelised flows that originated as splays from channels during flood episodes when bank-full capacity was exceeded and flow spread across the floodplain in an unconfined manner (Fig. 3.7f). Rather than radially dissipating across the floodplain as for conventional non-confined flows, an elevated feature, such as salt-wall-generated topography, acted to partially confine the flow. Such partial confinement resulted in water depth and velocity locally increasing, enabling the flow to erode and transport relatively coarse-grained sediment across the floodplain before depositing this load either as chute elements in locations where floodwaters converged to form a small channelised feature (F8) filled with crudely cross-bedded deposits, or as a coarse-grained, horizontally laminated sandstone in a non-confined setting (F7). As flood waters subsided and flow velocity waned, the falling-stage sedimentary succession (typically climbing-ripple strata) accumulated, followed by suspension settling of very-fine sand and silt (Tunbridge 1981b; Miall 1985).

### Chute elements with coarse-grained fill (F8)

*Description:* These elements occur as 0.1 to 0.4 m thick, medium-grained sandstone to granulestone lenses, with erosive relief of up to 0.1 m on their basal surface. These elements can typically be traced laterally for up to 20 m before they pass abruptly into sheet-like heterolithic elements (F5). The fill of these chute elements is either of massive sandstone (Fm), or crude trough cross-bedding (Fxt), and is normally overlain by a heterolithic sheet-element succession of climbing-ripple laminated strata (Frc/Fxl) and siltstone (Fhiss).

*Interpretation:* Chute elements represent the preserved expression of the convergence of non-confined floodwater on the floodplain to form minor channels (Fig 3.7d; Abdullatif, 1989; Field, 2001; Benvenuti, 2005; Cain & Mountney 2009, 2011). The localized convergence of flood waters induced local deepening and increased flow velocity (cf. Field, 2001), which encouraged incision and the local entrainment and transport of coarser-grained sediment via bed-load transport, possibly with the winnowing of finer-grained material (Hjulstrom, 1935; Sundborg 1956). Rapid deposition of

coarse-grained material from suspension resulted in the accumulation of structureless sandstone, whereas gradual waning of the late-stage flow induced deposition from bed-load transport and the formation of crude cross-bedding (Fxt). These chute elements likely carried flow for no more than a few hundred metres before passing back into a non-confined flow (cf. Cain & Mountney, 2011).

### Floodplain pond elements (F9)

*Description:* Pond elements are characterised internally by associations of wave-rippled sandstones (WR) and homogeneous or horizontally laminated siltstone, with fine-grained deposits commonly possessing well developed and distinctive desiccation cracks that are up to 0.6 m deep and filled with structureless siltstone or fine sandstone. Sandstone in these elements is commonly reduced to a grey colour. Individual pond elements are 0.2 to 0.5 m thick, and can typically be traced for 10 to 40 m laterally, though the largest example has been traced over an area of 25,000 $m^2$.

*Interpretation:* Pond elements record sedimentation in the aftermath of flood events. Floodwaters accumulated in very shallow depressions on the floodplain and formed shallow ponds of standing water, which may have persisted for several days or weeks (cf. Picard & High, 1973; Fisher *et al.*, 2008). Wind blowing over the surface of these ponds generated surface waves, which in turn allowed symmetrical ripple-forms to develop on the fine-grained sandy substrate (Allen, 1968). Silt settled from suspension. Loess transported by aeolian processes in the arid environment was likely trapped to form an additional sediment component. Evaporation and infiltration of water caused the surface to dry out and resulted in the generation of desiccation cracks, with larger cracks indicative of slower rates of desiccation.

## *3.6 Spatial & Temporal Variations in Sedimentary Architecture*

This study considers the Moenkopi Formation in two distinct geographical areas, each with their own tectonic and provenance history. The Moenkopi Formation in the Salt Anticline Region was influenced by ongoing salt tectonics throughout the period of deposition (Rasmussen & Rasmussen,

2009; Kluth & DuChene, 2009; Trudgill & Paz, 2009; Trudgill, 2011). As a result of this halokinetic influence, the Moenkopi Formation accumulated in a series of isolated salt-walled mini-basins, each with a unique sediment supply and subsidence regime (Banham & Mountney, 2013a). The effects of this isolation resulted in the preservation of significantly different styles of fluvial architecture. By contrast, the Moenkopi Formation in the White Canyon area lacks evidence for a tectonic control but instead records a strong climatic signature that is additionally modified by the impact of spatial variations in accumulation style that arose as a result of autogenic fluvial processes.

### *3.6.1 Salt Anticline Region*

Within the Salt Anticline Region, the Moenkopi Formation accumulated in three distinct mini-basins (Fig. 3.2a): the Fisher basin between the Uncompahgre Front and the Fisher Valley salt wall, the Parriott Basin between the Fisher Valley and Castle Valley salt walls, and the Big Bend Basin (Banham & Mountney, 2013a) between the Castle Valley and Moab (Lisbon) Valley salt wall. The preserved thickness of the Moenkopi Formation varies between the studied mini-basins, as a function of both the subsidence history of individual basin segments and location within individual mini-basins (e.g. depocentre versus flank); the thickest preserved succession (245 m) occurs in the Big Bend Basin.

The Moenkopi Formation in the Salt Anticline Region is separated from the underlying Permian Cutler Group by an angular unconformity that accounts for approximately 25 Ma of non-deposition and erosion (Rasmussen and Rasmussen, 2009), with the angular nature of the unconformity having developed in response to continued and progressive salt movement between the cessation of Cutler Group sedimentation and the onset of Moenkopi Formation sedimentation (Trudgill, 2011). Although the sedimentary character of the four members of the Moenkopi Formation tends to vary between each studied mini-basin (Fig. 3.9), the preserved fluvial successions in each mini-basin share a common association of lithofacies and architectural-element types (Figs 3.6 and 3.7a/b). Throughout accumulation of the Moenkopi Formation, the fluvial system drained from southeast to northwest, parallel to the trend of the linear salt walls (Fig. 3.9).

## Tenderfoot Member

The basal Tenderfoot Member attains a maximum thickness of 70 m at the Fisher Valley Head locality in the Fisher basin (Fig. 3.10) but thins to only 40 m at the Mile 25 locality in Richardson Amphitheater. In the Parriott Basin, the maximum recorded thickness is 40 m at Castle Tower and the member is generally slope forming. The basal-most part of this member is characterised by fluvial strata with embedded clasts apparently derived from localised reworking of the uppermost strata of the underlying Cutler Group. A prominent feature of this member is a 1 to 2.5 m-thick gypsum bed (GC) that is laterally continuous throughout the Parriott Basin (Fig. 3.10), and which is also present in the north-eastern part of the Big Bend Basin, though has apparently been largely eroded along the southern margin of the Fisher Basin. This gypsum bed is characterised by a saccharoidal, crystalline texture that has been interpreted previously to have accumulated either in a restricted tidal-flat (sabkha) setting within a large embayment (Stuart *et al.*, 1972; Baldwin, 1973) or as an aeolianite (Lawton & Buck, 2006).

Although poorly exposed in the Parriott and Big-Bend basins, the beds overlying the gypsum horizon, which are locally composed of coarse-grained sandstone with distinctive angular grains and a gypsum cement, weather to a distinctive orange colour making them a useful marker unit. In the Fisher Basin, the Tenderfoot Member forms distinct cliffs, which are brown-orange in colour and beds have a predominantly rounded profile. As a result, the beds are better exposed and can be characterised by distinctive wavy or crinkly-laminated sandstones (facies Scls), considered to be indicative of repeated salt precipitation and dissolution in a sabkha-like environment (Goodall *et al.*, 2000). Fluvial-channel elements are generally absent. Conical-shaped de-watering structures (Fig. 3.5A) similar to those observed in the Hoskinnini Member (Stuart, 1959; Chan, 1989; Dubiel *et al.*, 1996) occur at one locality in the transfer zone between the Cache Valley salt wall and the Fisher Valley salt wall (Fig 3.2: 3 km northwest of Log 16). These features are typically 1 to 2 m in height and occur as “megapolygons” (Chan, 1989; Dubiel *et al.*, 1996) that are traceable over an area of 100 $m^2$ but are apparently confined both spatially and temporally to this single area in the Salt Anticline Region, with no other examples observed in this study area.

## Ali Baba Member

The cliff-forming Ali Baba Member has a sedimentary character that differs significantly between the Fisher and Parriott basins (Fig. 3.10). In the Fisher Basin, the member is ~50 m thick, and is characterised by medium- to coarse-grained sandstone with localised pebble lags and rare beds of pebble-grade orthoconglomerate (Fce). Metre-thick sets of tabular and trough cross-bedding (Fxp/Fxt) are common. In the Parriott Basin the member is 25 to 40 m thick and is characterised by interbedded siltstone and fine- to medium-grained sandstone (Fhiss) in both the basal- and upper-most parts. By contrast, the middle part of the member is characterised by a prominent 8 to 10 m-thick cliff-forming sandstone composite bedset composed of dual-storey, multilateral channel-fill elements (F1) and massive & horizontally laminated channel-fill elements (F4), which are well exposed along the flanks of the Castle Valley and along the side of Parriott Mesa and the Priest and Nuns mesas. This prominent, laterally extensive bedset is largely massively bedded (Fm) in the Castle Tower area, but exhibits trough (Fxt) and planar-tabular (Fxp) cross-bedding near Adobe Mesa and the Priest & Nuns mesas. Associated lithofacies present in this member include, ripple forms (both current and wave ripples) and ripple cross-lamination (Frc & WR), structureless sandstone beds (Fm), primary current lineation (Fh), lags of mud-chip rip-up clasts of intraformational origin (Fci), plus bedding surfaces preserving obstacle scours and desiccation cracks.

Fluvial architectural elements in the Ali-Baba Member are dominantly characterised by 1 to 2 m-thick single-storey multi-lateral channel-elements (F2) in the Parriott and Big Bend basins, but are additionally characterised by 6 to 10 m-thick, vertically-stacked and amalgamated multi-storey channel elements (F1) in the Fisher Basin, and up to 8 m thick massive & horizontally laminated channel-fill elements (F4) in the Parriott Basin. Larger multi-storey channel-element complexes can be traced laterally for distances in excess of 10 km in orientations parallel to palaeoflow (i.e. in orientations parallel to the strike of the linear salt walls). Heterolithic units of interbedded siltstones and sandstones in the Parriott Basin form sheet-like fluvial elements (F3) that are each laterally continuous for at least 200 m, with some examples extending for in excess of 1 km.

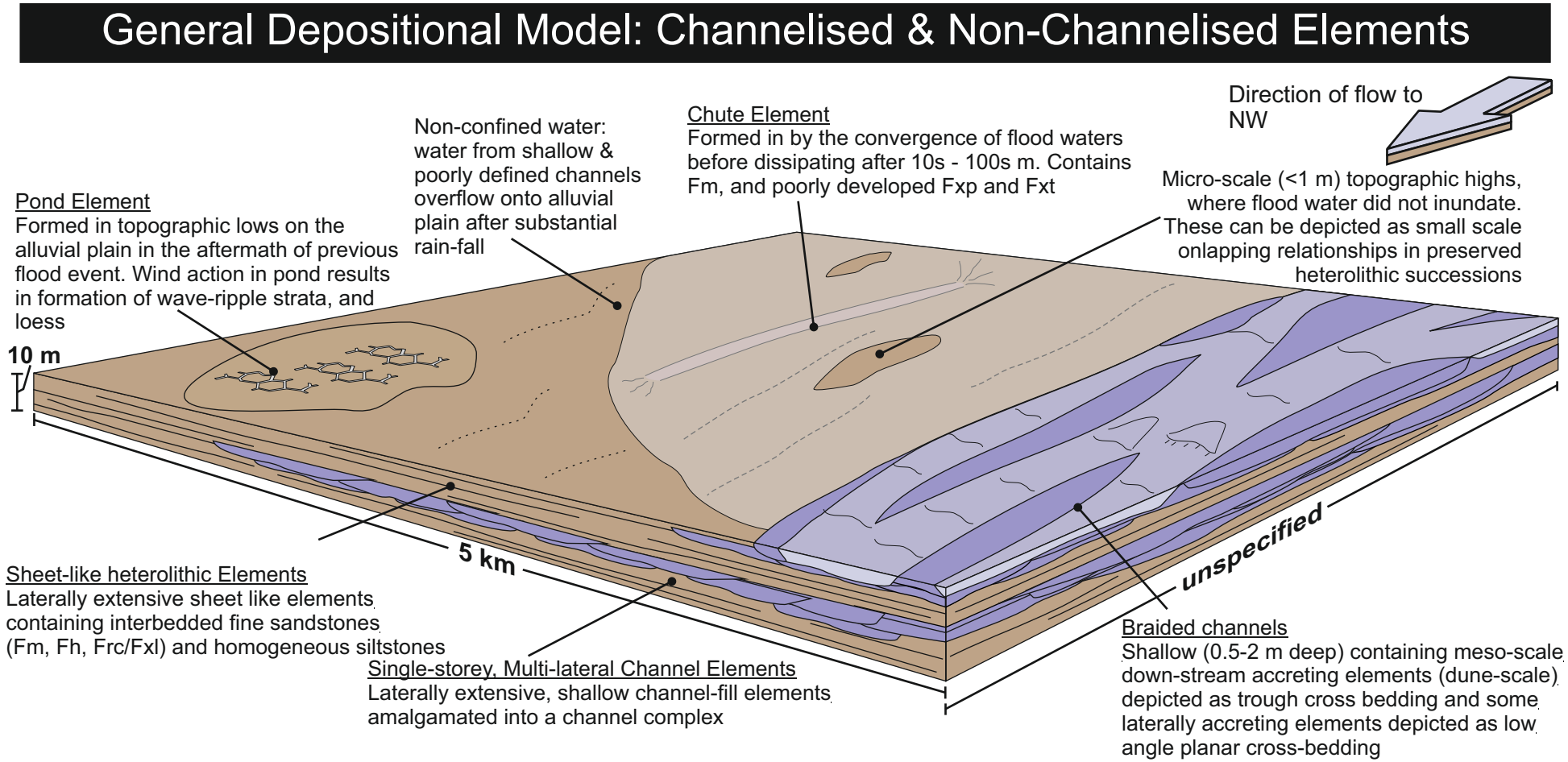


**Figure 3.8**: Generalised deposition model depicting relationships between confined & non-confined fluvial elements.

## Sewemup Member

The sedimentary character of the Sewemup Member varies between each studied mini-basin, but the member as a whole is slope forming (Fig. 3.10). The maximum preserved thickness is 110 m at Castle Tower and elsewhere along the southwest side of the Parriott Basin. The member thins to the northeast toward the Onion Creek–Fisher Valley salt wall in the Parriott Basin.

One diagnostic feature of the Sewemup Member adjacent to the Castle Valley salt wall is the widespread occurrence of several distinctive gypsum-clast-bearing beds (Fig 3.3) (clasts 10 to 200 mm diameter; mean 100 mm), each up to 1 m thick (FGc/m). These beds tend to be orthoconglomerates (FGc) in areas within 2000 m of the Castle Valley salt wall but are paraconglomerates (FGm) in areas toward the centre of the mini-basins. Gypsum clasts are absent from the Fisher Basin and from parts of the Parriott Basin adjacent to the Onion Creek-Fisher Valley salt wall. Common sedimentary structures in the Sewemup Member include desiccation cracks, small gutter channels (0.1 m-deep) (F8), a range of dewatering structures including load casts and flame structures, overturned, and convolute bedding (Fd).

Common architectural elements of the Sewemup Member include laterally extensive bodies with sheet-like geometries that are composed internally of heterolithic siltstone and sandstone beds (Fhiss, F6) and which are traceable for distances in excess of 1000 metres. Single-storey channel-fill elements (F2) are rare and, where present, they are relatively small (0.3 to 1 m thick; mean 0.4 m), with width:thickness ratios that range from 25:1 to over 250:1, and with fills that are characterised by trough cross-bedding (Fxt) and massive (structureless) fine-grained sandstone (Fm). High-angle inclined fractures (10-30 mm wide) filled with fibrous gypsum and typically arranged in an anastomosing pattern are a distinctive non-sedimentrary feature of this member.

## Parriott Member

The Parriott Member attains a maximum thickness of 40 m adjacent to the Castle Valley salt wall and thins toward the Onion Creek – Fisher Valley salt wall, pinching out over the crest of this salt wall. Typically, the member is 15

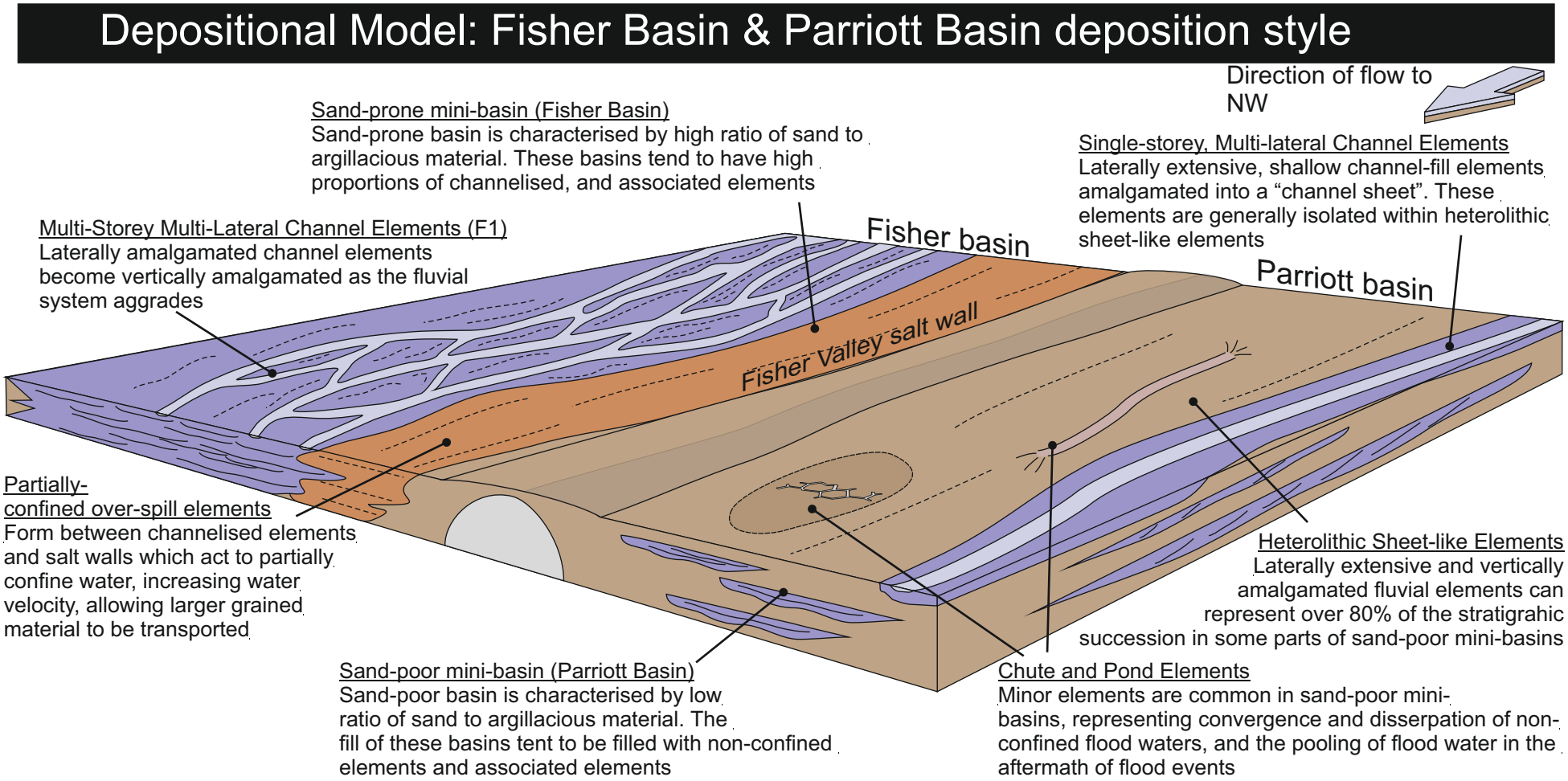


**Figure 3.9**: Generalised deposition model for the Salt Anticline Region. Model depicts the relationship of fluvial elements to the uplifted Fisher Valley salt wall, which acted to isolate the neighbouring Fisher and Parriott mini-basins.

to 30 m thick but is mostly absent over the crests of the salt walls, either due to non-deposition on the highs created by salt-wall uplift, or uplift and erosion prior to the onset of the accumulation of the overlying Chinle Formation. An exception to this is a 10 m-thick succession preserved on the nose of the Castle Valley salt wall (in the Red Hills area; Fig. 3.10).

The Parriott Member is characterised by an absence of gypsum clasts (FGc/m), with the succession containing a high proportion of multi-storey channel-fill elements (F1) around the flanks of the Castle Valley salt wall, and single-storey channel-fill (F2) & heterolithic sheet-like elements (F5) elsewhere in the basins. The central and north-eastern parts of the Parriott Basin are characterised by rare and isolated occurrences of single-storey multi-lateral channel elements (F2), each 1 to 2 m thick and several hundred metres wide. Adjacent to the nose of the Castle Valley salt-wall in the Parriott Basin (at the so called Truck-and-Boat structure; Fig. 3.10) a dual-storey fluvial channel-fill element (F1) forms a distinctive feature, which is laterally continuous for 950 m before it is cut-out by recent erosion. In the Big Bend Basin adjacent to the Castle Valley salt wall, the Parriott Member is characterised by multi-lateral and multi-storey channel elements (F1) that collectively form a major fluvial-channel complex that extends laterally for in excess of 1000 m.

The boundary between the Moenkopi Formation and the overlying Chinle Formation is marked by a disconformity across much of the Salt Anticline Region, although locally this boundary is represented by a distinctive angular unconformity in areas immediately adjacent to the salt-walls, indicating uplift of the salt-walls during or after the latter stages of deposition of the Moenkopi Formation but prior to the onset of accumulation of the Chinle Formation.

## Palaeocurrent data and sediment provenance

Analyses of palaeocurrent data from the orientations of ripple crests and lee-slope azimuths in climbing-ripple strata, trough and high-angle planar cross-bedded sandstone in the Salt Anticline Region indicate dominant palaeo-drainage that was consistently toward the northwest throughout accumulation of the Moenkopi Formation (Fig. 3.1b) (vector mean = 302°; vector magnitude

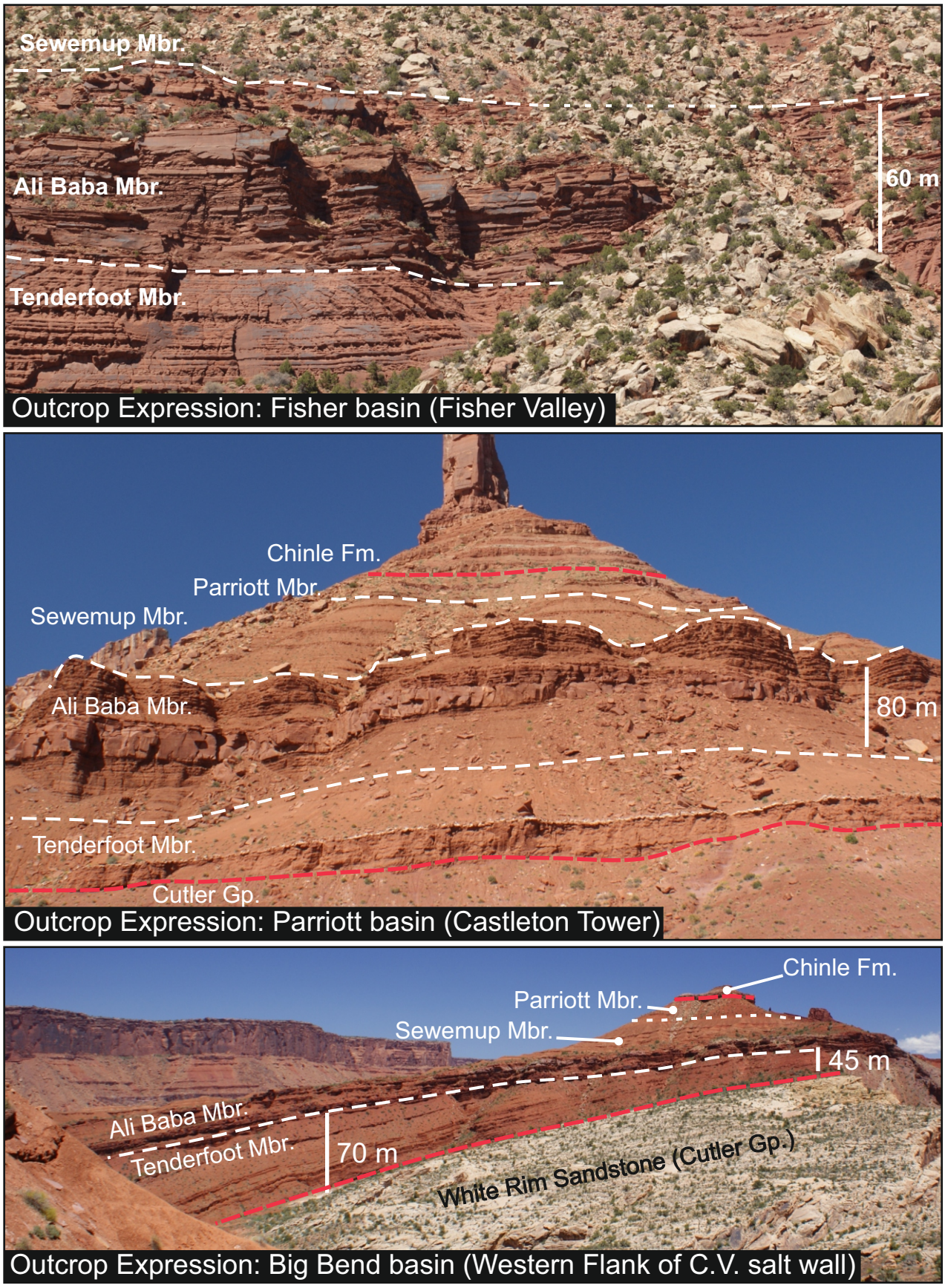


**Figure 3.10**: Changes in stratigraphic expression between different mini-basins for members of the Moenkopi Formation in the Salt Anticline Region. See figure 2 for locations.

= 0.86; n = 177). Data from individual mini-basins also reflect this overall trend (Fisher Basin: vector mean = 305°; vector magnitude = 0.91; n = 88. Parriott Basin: vector mean = 303°; vector magnitude = 0.85; n = 57. Big Bend Basin: vector mean = 292°; vector magnitude = 0.77; n = 32). Crests of wave ripples on exposed bedding surfaces created by bi-oscillating currents in bodies of standing water (F9: pond elements) throughout the Salt Anticline Region have a vector mean trend of 052° (vector magnitude = 0.73; n = 62), a trend that suggests a NW- or SE-oriented prevailing palaeowind (Fig 3.1b).

Provenance and petrographic analyses (Stuart *et al.*, 1972) suggest a dominant sediment source for the Moenkopi Formation in the Salt Anticline Region from the San Luis Uplift. However, the abundance of extraformational conglomerates of Uncompahgre affinity in the Ali-Baba Member in the Fisher Basin indicates a dual source of sediment during the initial phase of accumulation in this mini-basin. The confinement of this secondary source of extraformational clasts solely to the Fisher Basin suggests that salt-wall-generated surface topography acted to prevent the transverse delivery of sediment from the Uncompahgre Uplift into the Parriott or Big Bend basins (Banham & Mountney, 2013a). The Tenderfoot Member contains an abundance of reworked sediment, which has been interpreted as a reworked remnant of the White Rim Sandstone (Dubiel *et al.*, 1996).

### *3.6.2 White Canyon Region*

The White Canyon study area in southeast Utah extends from Copper Point in the north to Moss Back Butte in the southeast, and across to Whirlwind Draw in the Clay Hills region to the southwest of the study area (Fig. 3.2). The only member of the Moenkopi Formation studied in this area is the Torrey Member (Blakey, 1974). In the southern part of the study area, the Moenkopi Formation lies apparently conformably on top of the Hoskinnini Member (Fig 3.11 & 3.12, the boundary being differentiated by a change in colour and bedding style: the Hoskinnini is generally a deeper orange colour, is thicker-bedded, has a rounded weathering profile and exhibits undulatory bedding; Stewart, 1959; Dubiel, 1992). The outcrop expression of the Hoskinnini Member shares many characteristics observed in the Tenderfoot Member of the Salt Anticline Region, including crenulated wavy laminations (Fig. 3.12;

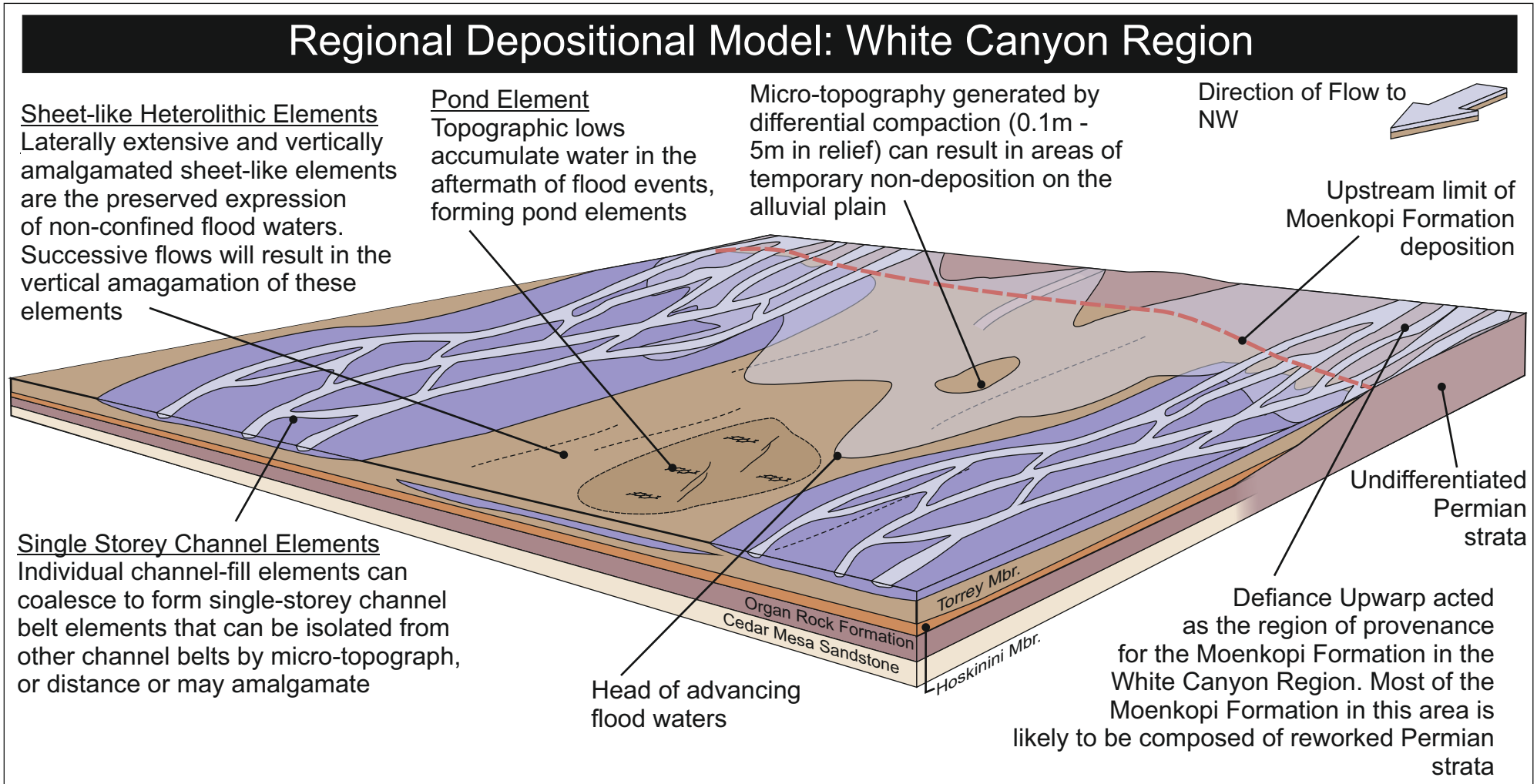


**Figure 3.11**: Generalised deposition model for White Canyon area. Model depicts the relationship of fluvial elements beyond the region of halokinetic influence.

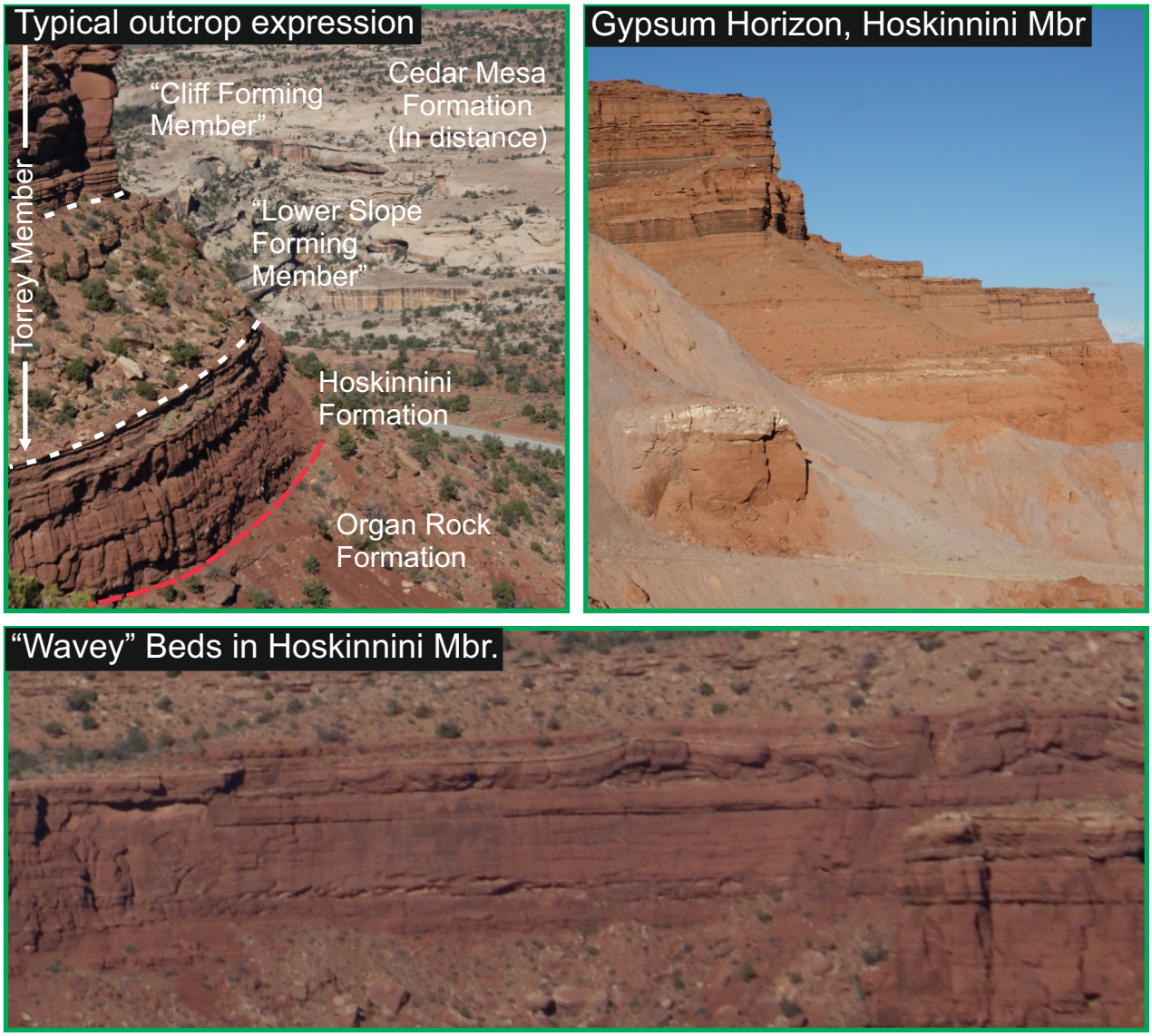


**Figure 3.12**: Stratigraphic features of the Moenkopi Formation in the White Canyon Region.

Stuart, 1959). Where the Hoskinnini Member is absent, the Moenkopi Formation lies disconformably on the Permian Organ Rock Formation (Cain & Mountney, 2009). The Moenkopi Formation throughout this study area is disconformably overlain by the Chinle Formation, which is differentiated from the Moenkopi Formation by a marked increase in grain-size (from very-fine sand and silt to very-coarse sand and pebbles where the basal Shinramup conglomerate is present). Incision of up to 8 m into the underlying Moenkopi Formation by channelised elements of the overlying Chinle Formation is indicated by the presence of distinctive yellow, purple or grey mottling in the basal 10 m of the Chinle Formation and, in some localities, an abundance of petrified wood.

### Hoskinnini Member

The Hoskinnini Member, where observed, is typically 30 m thick and forms distinct, orange-coloured cliffs at the base of the Moenkopi Formation (Fig. 3.12). The beds forming these cliffs have a rounded profile, and some exhibit large-scale deformation manifest as low amplitude undulating beds (Fig. 3.12; “Crinkly beds” – Stuart, 1959). In addition, enigmatic conical-shaped fluid-escape structures similar to those observed in the Tenderfoot Member of the Salt Anticline Region have been documented in the region (Stuart, 1959; Chan 1989; Dubiel, 1992; Dubiel *et al.*, 1996). In the Clay Hills area, a 1 to 2 m thick crystalline gypsum bed is present, which exhibits similar characteristics to the gypsum bed of the Tenderfoot Member of the Salt Anticline Region.

### Torrey Member

Within the study area, the Torrey Member varies from 90 m thick in the southwest, to 64 m thick in the north, to only 45 m thick in the southeast, with an overall south-westerly thinning due to progressive erosion at the top of the succession. The member is characterised by a stepped profile that was originally divided into Lower slope-forming, ledge-forming, and upper slope-forming members (Stewart *et al.*, 1972) that correspond generally to slope-forming sheet-like heterolithic elements (F5) and cliff-forming channel fill-complex elements (F1, F2). Spatial variations in sand content are discernable, with a higher proportion of channel elements in the upper third of the member

in the vicinity of Steer Gulch, Happy Jack Mine and Copper Point logs (Figs 3.2b, 3.4b). A distinctive set of 4 or 5 beds containing intraformational-clasts out-crop in the lower 10 to 30 m of the member, and these are typically interbedded with thin siltstone beds (Fig. 3.5b). These useful markers were observed in 8 of the 11 studied sections, spread over an area of 20 by 40 km. Within the overlying 10 to 20 m of the succession, beds disrupted by soft-sediment deformation (Fd) are common, with the deformation style indicative of structures arising due to upward escape of water, including load and flame structures and sand volcanoes, that occur in close proximity to sand lobes and slump structures (cf. Owen, 1987, 1996).

Channelised fluvial architectural elements (F1, F2) can, in nearly all cases, be traced laterally for in excess of 500 m and in some instances for 10 km. Sheet-like heterolithic elements (F5) are highly laterally extensive and can be traced for tens of km in directions both parallel and perpendicular to palaeoflow. Silt-prone sheet-like elements (F5) are particularly prevalent in the upper portion of the succession in the west of the study area, where they account for over 75% of the interval. Gypsum-clast-bearing elements (F6) are rare and are only observed in the south-western part of the study area. A single example of gypsum clasts preserved within trough cross-bedded strata was observed in the Clay Hills region. The origin of these gypsum clasts is uncertain, but may relate to the gypsum bed present in the Hoskinnini Member.

### Palaeocurrent data and sediment provenance

Palaeocurrent direction in the Torrey Member throughout the White Canyon study area has a vector mean of 333° with a magnitude of 0.89 (n = 56). This favours a likely provenance from the Defiance Upwarp (Figs. 3.1 & 3.11), to the southwest of the study area (Stuart *et al.*, 1972, Fillmore, 2011), a region composed of Permian strata, including the distal fringes of the Organ Rock Formation, the undifferentiated Cutler Group, and the De Chelley Sandstone (Stewart *et al.*, 1972; Stanesco *et al*., 2000).

## *3.7 Discussion*

Combined facies and architectural-element analysis demonstrates significant complexity in terms of spatial and temporal variations in the deposits of the

Monekopi Formation. Although a similar set of lithofacies is present in both study areas, which are indicative of the operation of broadly similar sedimentary processes, significant local variations in the spatial (lateral) and temporal (vertical) arrangement of architectural elements composed of these facies are recognised. Such variations are here shown to have arisen in response to the impact of different sets of allogenic controls including: (i) tectonic (halokinetic) regime, which dictated the rate of generation of accommodation space, the width of basin floor over which the fluvial systems could spread and the location of the salt walls; (ii) climatic regime, which was unlikely to have been significantly different between the two study areas but which may have varied temporally; (iii) the rate and pathway of sediment delivery from both the principal and secondary source areas, which themselves are controlled by salt-wall location. Additionally, local variations in sedimentary character likely also reflect the various autogenic processes that operated in the fluvial systems, including avulsion style and frequency and the mechanisms by which bank-full channel capacity was exceeded during floods to result in sheet-like, non-confined overland flow.

## Environment of deposition

Architectural element analysis demonstrates that accumulation of sediment was dominated by relatively thin but laterally extensive bodies: most F1 and F2 channel elements have width-to-thickness ratios greater than 250:1; sheet-like elements (F5, F6) have width-to-thickness ratios greater than 2000:1. These thin but laterally extensive elements demonstrate a broad, low-relief accumulation surface. Architectural elements with distinctive assemblages of lithofacies (Table 1) in both channelised and non-channelised elements indicate sedimentation via repeated, low-frequency, high-magnitude ephemeral flood events (Williams, 1970, 1971; Glennie, 1970; Picard & High, 1973; Gee, 1990). Individual sedimentary components characteristic of an arid environment are as follows: desiccation cracks (up to 0.6m deep) indicative of slow episodes of desiccation in non-confined elements (F6, F7, F8); gypsum-clast-bearing elements (F6), rare teepee structures; the presence of a crystalline gypsum unit, which demonstrates that the region of deposition endured episodes of sustained aridity to allow preservation of such

soluble material. Facies associations of laterally extensive sheet-like elements (F5), including thin, massively bedded sandstones (Fm), climbing-ripple strata (Frc/Fxl) and homogeneous and horizontally laminated siltstone (Fhiss) demonstrate evidence for rapid deposition from a waning flow (Williams 1971). Thin pond elements (F9) mostly of limited lateral extent and with fills of wind-generated wave-ripple strata (Allen, 1968) demonstrate the presence of shallow pools of standing water; the near-ubiquitous presence of desiccation cracks indicates complete desiccation of the pools; in some examples, the presence of desiccation cracks at multiple closely spaced stratigraphic levels demonstrates repeated flooding and desiccation, and the transient nature of the ponds.

Non-confined flows in extra-channel settings are widely documented as a product of episodic, high-energy ephemeral floods in arid alluvial environments (e.g. Rahn, 1967; Glennie, 1970; Williams, 1970, 1971; Tooth, 1999a,b, 2000). Such flows, which are typified by markedly peaked hydrographs (Reid *et al.*, 1998), are generally capable of transporting and distributing large volumes of sediment over relatively short periods (Frostick *et al.*, 1983).

Although channel elements are relatively abundant in the preserved stratigraphy, at any given time channelised forms likely only occupied a small proportion of the surface area, as is common in many ephemeral alluvial systems (just 3% in the examples studied by Rust & Legun, 1983), thereby implying that most sediment transport and deposition occurred as a result of non-confined fluvial processes. It is the increased preservation potential of erosively-based channel elements and their overprinting of non-confined elements (e.g. via lateral accretion and avulsion processes) that results in them comprising a larger proportion of the *preserved* stratigraphic succession.

Hampton & Horton (2007) recognised sheetflow deposits by virtue of their thin and laterally extensive nature, with poorly defined channel banks with low clay content (cf. North *et al*., 2007) characterised by high width-to-depth ratios. Such poorly defined, high aspect ratio channel elements (>300:1) may be extremely difficult to discern in parts of the succession dominated by non-confined elements, especially if they are in-filled by heterolithic facies associations.

A general depositional model depicting the relationship between confined and non-confined architectural elements observed in the Moenkopi Formation and their likely mode of generation is shown in Fig. 3.8. Channel belts consisting of multiple, shallow and potentially poorly defined braided channel networks (cf. North, 2007; Hampton & Horton, 2007) soon exceeded bank-full capacity during rising flood stage, resulting in over-spill of flood waters onto the adjoining alluvial plain. Non-confined flood waters transported and distributed sediment as both bed load and suspended load across a low-relief alluvial plain. As flood waters emanated away from the confined channel networks, the flood-front dissipated radially across the alluvial plain. Transmission losses due to a combination of infiltration and evaporation increased as the flood waters became spread over a larger area, resulting in a progressive reduction in both flow velocity and stream power (Bull, 1979), thereby leading to the sequential accumulation of the succession of facies representative of waning flow characteristic of non-confined elements (F5) and the preservation of pond elements (F9). Occasionally, these non-confined flood waters converged locally, resulting in the formation of minor chute elements (F8), which run for a few tens to hundreds of metres before flooding out and dissipating (cf. Field, 2001; Cain & Mountney, 2009).

## Halokinetic control on sediment accumulation

The style of sedimentary architecture in both the Salt Anticline Region and the White Canyon area is similar: both are characterised by shared facies associations and several similar architectural elements. However, significant differences in the proportions of facies and the arrangement of elements are recognised. Most significantly, the formation is significantly thicker in the mini-basins of the Salt Anticline Region (typically twice as thick).

A number of elements are unique to the Salt Anticline Region: unilateral intraformational clast-filled channel elements (F3); salt-wall-derived gypsum-clast-bearing elements (F6; Lawton & Buck, 2006); partly confined over-spill elements (F7). These elements require the presence of salt-wall generated topography to form, either by acting as a source of clastic material (intraformational clasts or gypsum detritus) or by acting to confine flow and modify fluvial activity.

The main influence of halokinesis on the accumulating succession is recorded by the distribution of fluvial elements within the studied mini-basins, whereby basin isolation induced by salt-wall uplift controlled architectural-element distribution between mini-basins (Banham & Mountney, 2013).

Figure 3.9 depicts a general depositional model to account for the style of accumulation of fluvial elements in areas adjoining uplifting salt walls, whereby the distribution of elements varies between neighbouring mini-basins. The model depicts how the Fisher Valley salt wall isolated the Fisher and Parriott mini-basins, thereby acting as a control on the resultant style of accumulation. The Fisher Basin, which received clastic input form both the Uncompahgre and San Luis Uplifts during the accumulation of the Ali Baba Member, represents a sand-prone interval, where high rates of sand delivery coupled with low rates of subsidence allowed the formation of braid-belts which resulted in the accumulation of single-storey channel-fill complexes (F2) that subsequently amalgamated vertically to form multi-storey channel-fill complexes (F1). Additionally, partly confined over-spill elements (F7) are prevalent in the Fisher Basin, where they onlap onto the uplifted salt wall flank (Fig 3.10).

The Parriott Basin received clastic input solely from the San-Luis uplift, which resulted in accumulation of a sand-poor interval during the accumulation of the Ali Baba Member: fluvial activity in this basin was diminished relative to that of the neighbouring Fisher Basin, resulting in accumulation of a higher proportion of argillaceous elements (Fhiss). The absence of major channel networks in this basin precluded significant reworking of this argillaceous material.

## Climatic Control on sediment accumulation

Evidence for climatic variation in the Moenkopi Formation is recorded as subtle upward (vertical) changes in the overall style of sedimentation that can be discerned and correlated across both study regions. In the Salt Anticline Region, climatic signatures are masked by the preserved effects of other controls, including varying rates of mini-basin subsidence and sediment supply. However, the overall style of sedimentary architecture changes

through the Moenkopi Formation (Fig. 3.10) and this is likely to have occurred as a function of palaeoclimate.

Throughout accumulation of the Tenderfoot, (and the laterally equivalent Hoskinnini Member – Stewart, 1959) conditions were interpreted to be arid and deposition occurred in a sabkha-like setting (Dubiel, 1994), resulting in accumulation of lithofacies Scls in the Fisher Basin, with few channel-fill complexes preserved. The Ali Baba Member in the Salt Anticline Region is characterised by multi-storey channel-fill complexes (F1) in the Fisher Basin, by single-storey channel-fill complexes (F2) with sheet-like heterolithic strata (F5) in the Parriott Basin, and by a mixture of sheet-like heterolithic elements (F5) and rare single-storey channel-fill elements (F2) in the Big Bend Basin. Collectively, this indicates a region-wide increase in humidity relative to the underlying member, resulting in an increased sediment influx into the mini-basins and an increase in channelised fluvial activity (Rumsby & Macklin, 1994). The Sewemup Member in all of the studied basins is characterised by an abundance of sheet-like heterolithic strata (F5) and gypsum-clast-bearing elements (F6), with few single-storey channel-fill complexes (F2). These elements demonstrate a decrease in fluvial activity across all three mini-basins at this stratigraphic level and record an episode when major flood events did not occur. The fluvial reworking and subsequent preservation of highly-soluble gypsum clasts demonstrates the ephemeral nature of the fluvial system and the overall arid climate. During accumulation of the Parriott Member, a higher proportion of single-storey (mainly in the Parriott Basin) and multi-storey channel-fill elements (F2, F1) were preserved, demonstrating a return to relatively less arid climatic conditions.

Climatic signatures recorded in the Moenkopi Formation of the White Canyon area are less obvious, in part due to the preservation of a thinner succession. However, a channel-prone interval in the middle part of the Torrey Member (the so-called Ledge-Forming Member of Stewart *et al.*, 1972) tentatively correlates with the Ali Baba Member of the Salt Anticline Region based on similar sedimentary character. This would suggest that both study regions shared a common climatic regime, resulting in coeval variations in sediment supply and similar stratigraphic expressions.

## *3.8 Conclusions*

The Moenkopi Formation in the Salt Anticline Region and White Canyon area of southern Utah is the preserved expression of a partly channelised and partly non-channelised fluvial succession that accumulated across a low-relief alluvial plain (Fig 3.13). The prevailing palaeoclimate at the time of accumulation was arid, as reflected in the style of the preserved strata. Depositional style is characterised by accumulation of vertically amalgamated, laterally extensive sheet-like bodies throughout most parts of the formation. These sheet-like bodies are either (i) channel-belt complexes that lacked significant basal erosional relief, composed of single- and multi-storey, multi-lateral channel-fill complexes, or (ii) sheet-like elements with heterolithic internal fills that are the preserved expression of non-confined fluvial flow across an extensive alluvial plain.

Both the Salt Anticline Region and White Canyon area share common facies and architectural elements, indicating the action of comparable fluvial processes under similar climatic conditions across the region. The rate of sediment accumulation in the Salt Anticline Region was controlled primarily by rate of accommodation generation via differential rates of mini-basin subsidence, with sediment supply rate and pathways having governed the accumulation of sand-prone and sand-poor styles of basin fill in neighbouring mini-basins. The absence of halokinetic processes controlling the distribution of fluvial elements in the White Canyon Region allowed autocyclic processes (lateral channel migration & avulsion) to act as dominant controls on fluvial element distribution in this region. Although halokinesis did not exert a primary control on fluvial sedimentary architecture, as demonstrated by the presence of common facies and architectural elements in both study areas, salt-wall uplift did however result in the generation of certain unique facies, element types and relationships, including unilateral channel elements with intraclast fills (F3), gypsum-clast-bearing elements, originating from salt glaciers where salt walls breached the land surface (F6), and partially-confined over-spill elements (F7). The direction of sediment delivery, the presence of a single or multiple areas of sediment provenance, and the rate of sediment supply all played important roles in the development of basin-fill style, with higher overall rates of sediment supply favouring the development of sand-prone basins

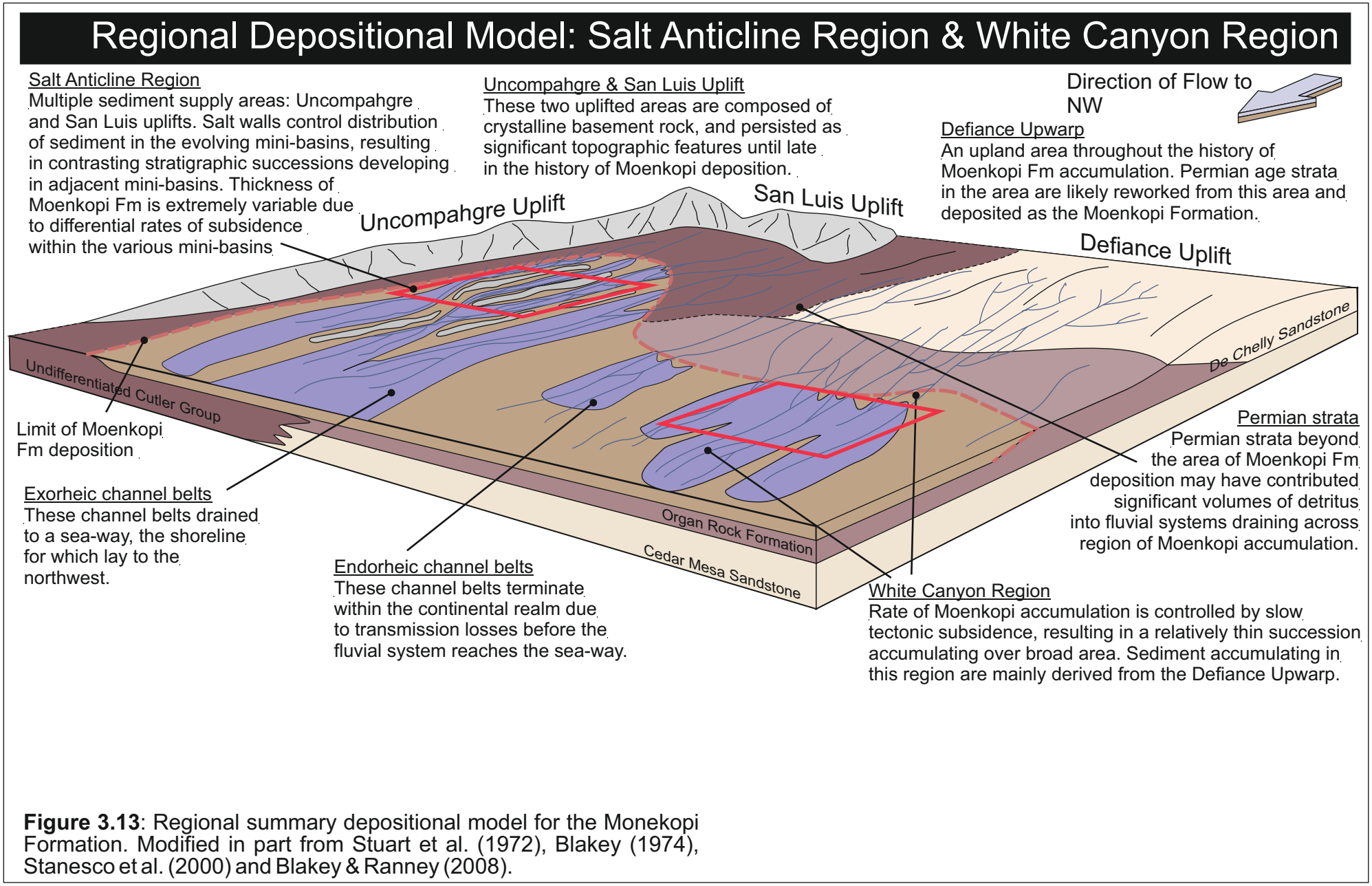


**Figure 3.13**: Regional summary depositional model for the Monekopi Formation. Modified in part from Stuart et al. (1972), Blakey (1974), Stanesco et al. (2000) and Blakey & Ranney (2008).

containing high proportions of channel-fill elements and lower rates of sedimentation favouring the development of sand-poor basins, characterised by elements deposited by non-confined flow. Climatic variations are discerned from changes in sediment supply rate and subsidence rate manifest as coeval variations in the overall style of accumulation, including, for example, the shift in the styles of sedimentation discernable between the Ali Baba Member and the Sewemup Member. By contrast, localised changes in sediment supply rate or basin subsidence rate typically only result in a change in the style of accumulation in a single mini-basin.

The Moenkopi Formation records how the signature of spatial and temporal variations in sediment supply rate, orientation and pathway of sediment delivery, rates of halokinesis, and climate change are manifest in the preserved stratigraphic succession of a dryland fluvial system. The predictable distribution of fluvial elements accumulated in a series of salt-walled mini-basins can be used to develop models to account for the distribution of fluvial elements in subsurface hydrocarbon plays, such as the Central North Sea, or Pre-Caspian Basin of Kazakhstan.

## *3.9 Facies Annex*

# Facies **Fce** - Extraformational Conglomerate

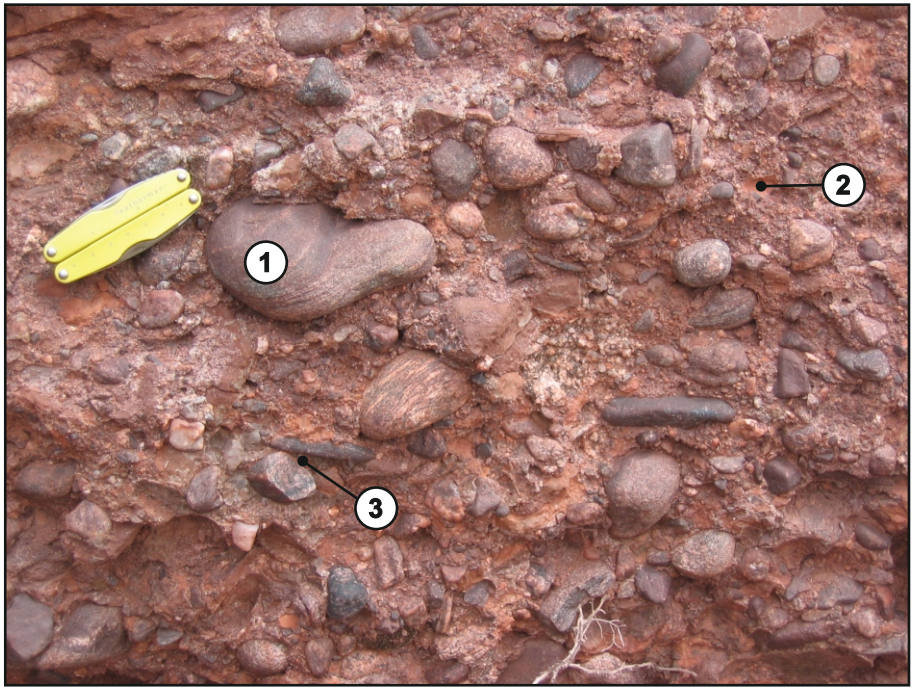


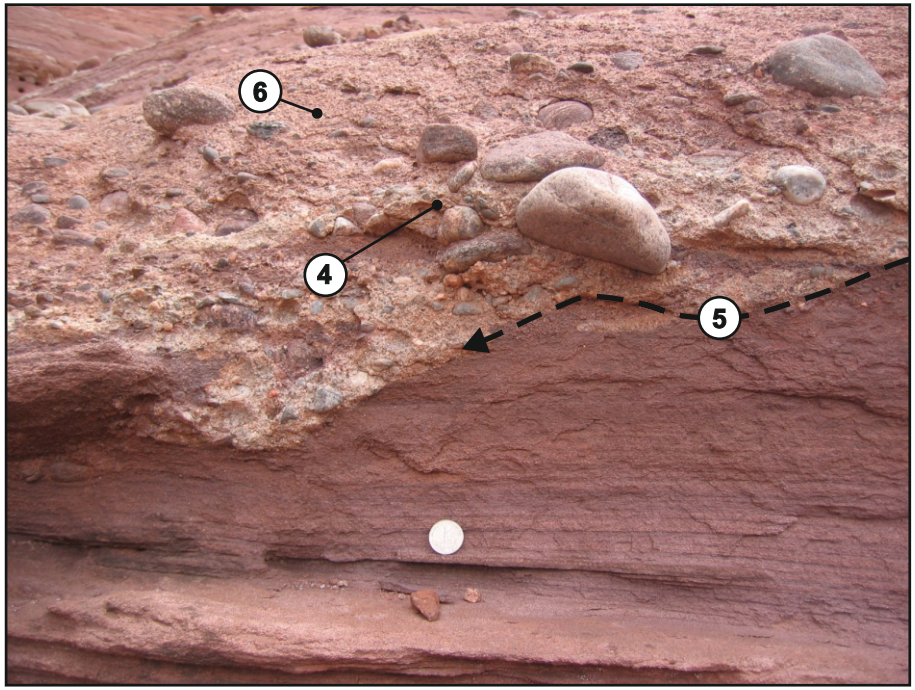


## Key Facies Information

| | |
|---|---|
| Colour | Red-brown - purple-brown |
| Grain-size | Fine-v.coarse sandstone - boulders (0.2 m diameter) |
| Sorting & Texture | Poorly sorted, matrix supported; angular - rounded |
| Set Thickness | 0.1 - 3.0 m sets |
| Facies Association | CF |
| Architectural Elements | F1 |

## Key Facies Characteristics

1. Igneous and metemorphic, basement-derived clasts.
2. Intraclast composed of fine-grained sandstone. Locally derived (reworked channel or overbank sediments).
3. Subtle evidence for imbrication.
4. Poor sorting considered characteristic of this facies.
5. Facies commonly exhibits an erosive lower boundary, indicating fluvial channel incision prior to migration of pebbly bar-forms.
6. Medium-grained sandstone to granule-stone matrix.

## Interpretation

**Extraformational conglomerates represent proximal, downstream and transverse accretionary bars, deposited within high-energy, low sinuosity and laterally unstable fluvial channels. May also represent proximal channel lags.**

**Facies Fce: Extraformational conglomerate lithofacies (Fce).**

# Facies **Fci** - Intraformational Conglomerate

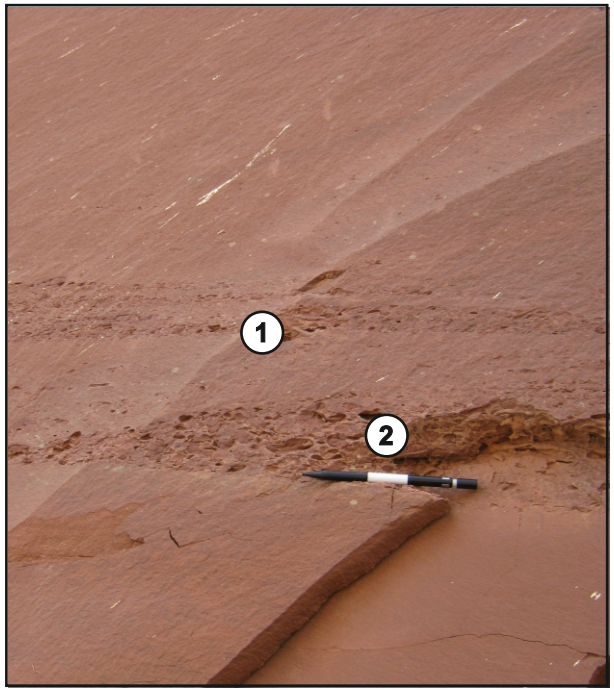


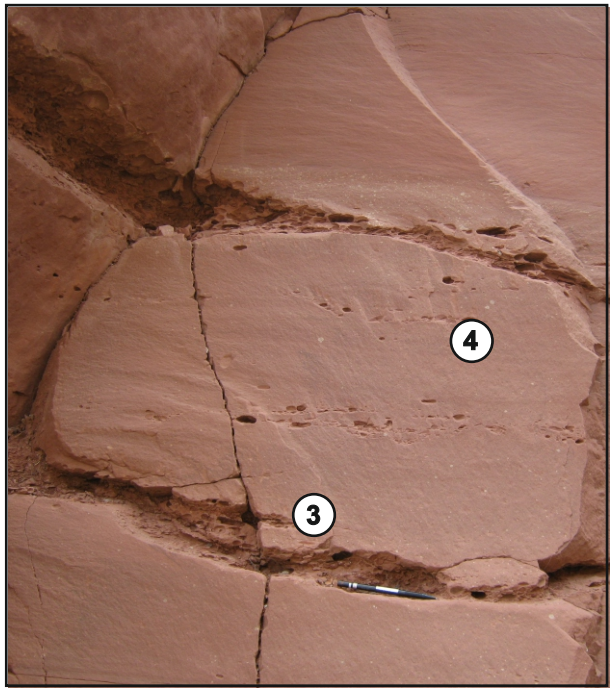


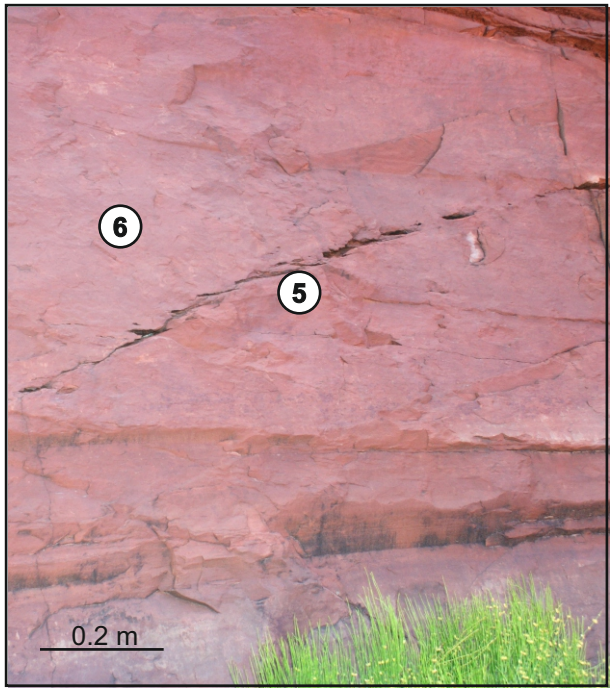


## Key Facies Information

| | |
|---|---|
| Colour | Chocolate brown clasts |
| Grain-size | 5 mm - 50 mm clasts; fine- to medium-grained matrix |
| Sorting & Texture | Poorly sorted, matrix supported; angular - sub-rounded |
| Set Thickness | 0.1 - 0.5 m sets |
| Facies Association | Confined Associations |
| Architectural Elements | Confined Elements |

## Key Facies Characteristics

1. Evidence for subtle fining-up within Fci sets
2. Clast shape varies between equant and bladed, indicating short transport distances
3. Sub-rounded to sub-angular calcrete clasts that lack internal structure
4. Abrupt transition from Fci facies to overlying sandstone facies; rapid changes in flow strength.
5. Siltstone intraclasts exhibiting original depositional structure
6. Anglular, bladed siltstone intraclasts; randomly orientated indicating very short transport distances and rapid deposition

## Interpretation

**Conglomerates and pebbly sandstones with clasts of intraformational origin record erosion and deposition of locally reworked sediments sourced from in-channel and floodplain areas. Rare cross-bedding indicates deposition via bedform migration.**

**Facies Fci**: Intraformational conglomerate lithofacies (Fci).

# Facies **Fci** - Pebbly sandstone with intraformational clasts

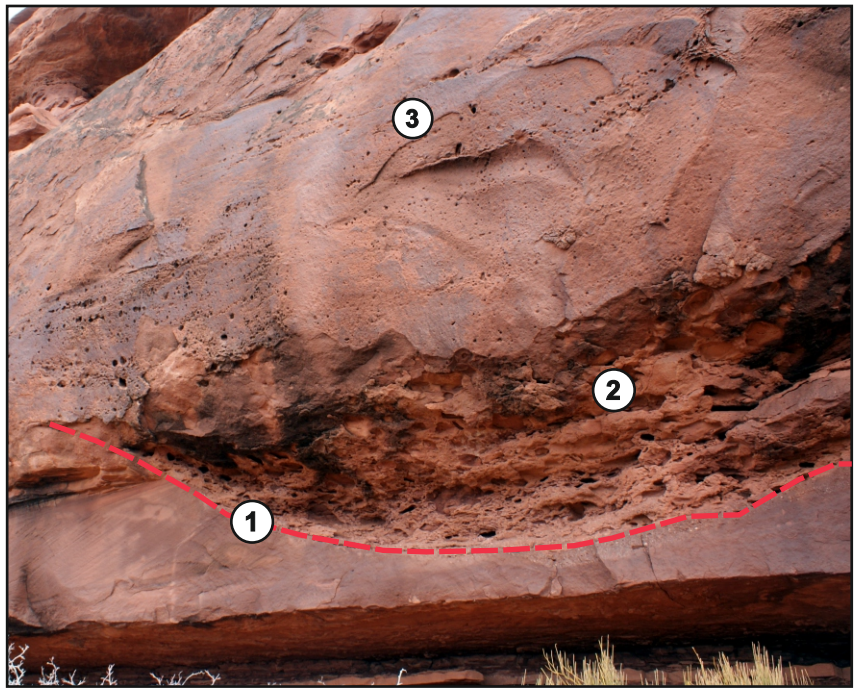


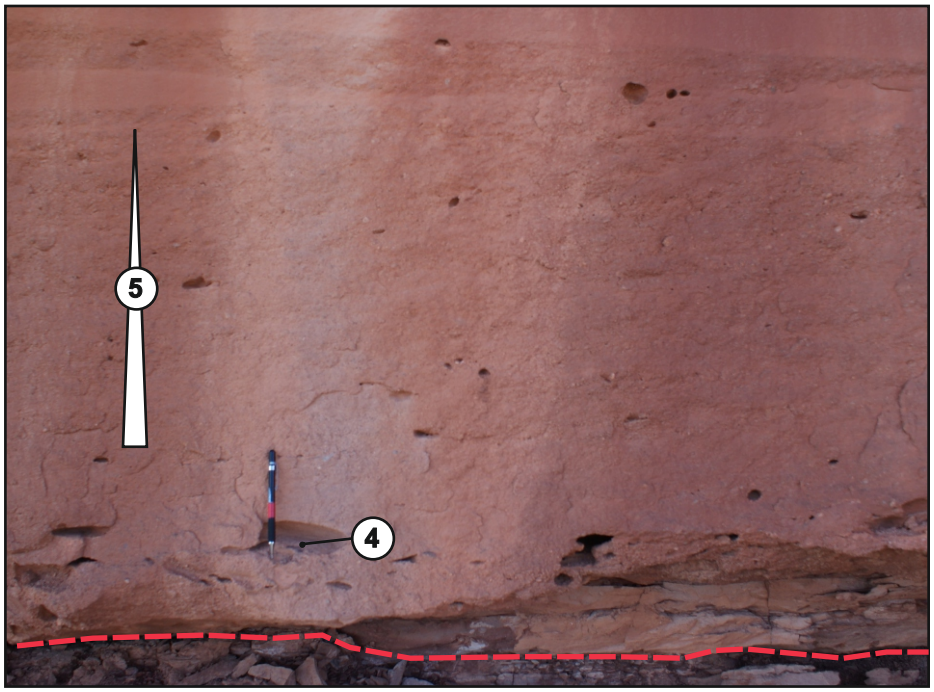


## Key Facies Information

| | |
|---|---|
| Colour | Orange-brown to chocolate-brown |
| Grain-size | 5 mm to 200 mm clasts; matrix is fine to coarse sand |
| Sorting & Texture | Poorly sorted, matrix/clast supported; angular to rounded |
| Thickness | 0.1 m to 1.5 m |
| Facies Association | Confined (channel) associations |
| Architectural Elements | Channel elements |

## Key Facies Characteristics

1. Channel incised into underlying HA Fxp facies
2. Channel infilled with clast-supported Fci facies. Matrix is medium-coarse sandstone
3. Cross-bedded sandstone set containing isolated clasts of intraformational origin
4. Larger intraclasts concentrated immediately above erosional base
5. Intraclast size and frequency decreases upward in set from channel base

## Interpretation

**Intraformational pebbly sandstones & conglomerates (Fci) record the erosion, transport and re-deposition of locally reworked sediments sourced from older in-chanel and floodplain deposits.**

**Facies Fci**: Intraformational conglomerate lithofacies (Fci).

# Facies **Fci** - Pebbly sandstone with intraformational clasts

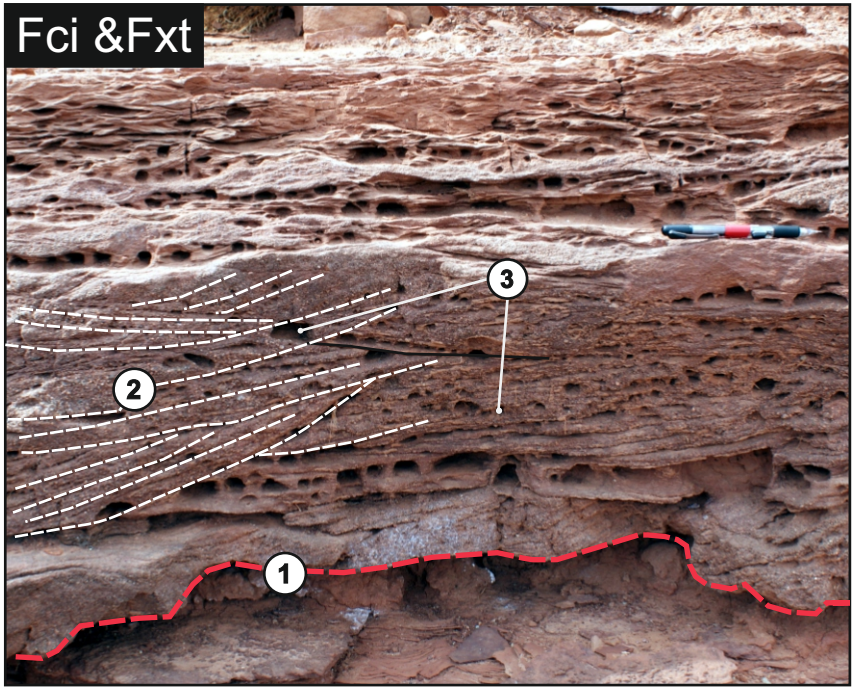


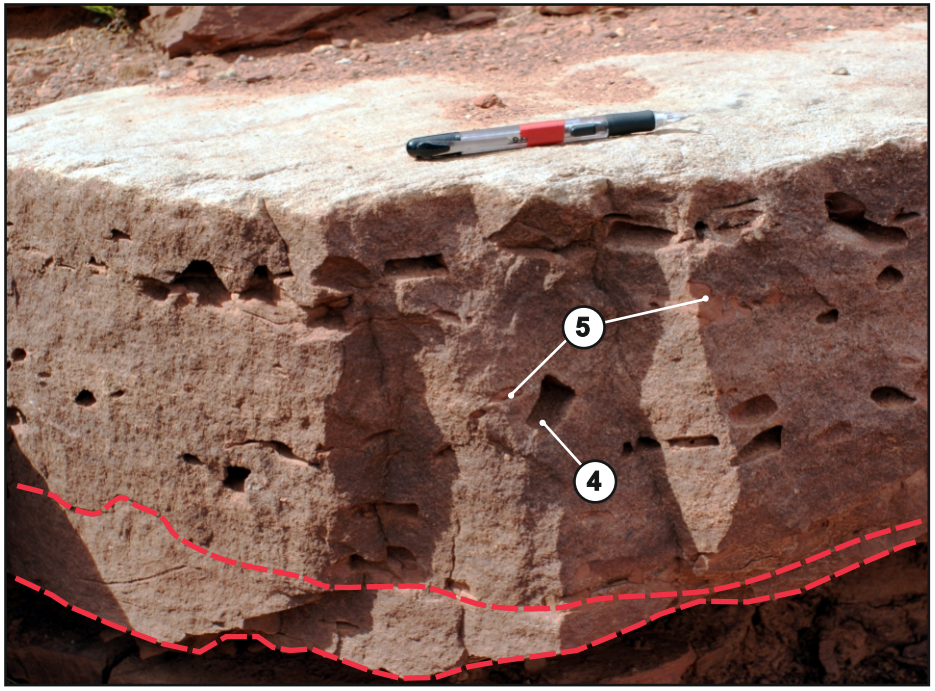


| Key Facies Information | |
|---|---|
| Colour | Orange-brown to chocolate-brown |
| Grain-size | 5 mm to 200 mm clasts; matrix is fine to coarse sand |
| Sorting & Texture | Poorly sorted, matrix/clast supported; angular to rounded |
| Thickness | 0.1 m to 1.5 m |
| Facies Association | Confined (channel) associations |
| Architectural Elements | Channel elements |

## Key Facies Characteristics

1. Channel incised into underlying Fxl facies
2. Medium-to-coarse-grained trough cross-bedded (Fxt) facies with high proportion of intraformational clasts
3. Clasts are angular to sub-rounded
4. Large angular clasts suggest a short transport distance
5. Clasts of softer siltstone have mostly been eroded out from the parent rock, though a few original fragments remain

## Interpretation

**Intraformational pebbly sandstones & conglomerates (Fci) record the erosion, transport and re-deposition of locally reworked sediments sourced from older in-chanel and floodplain deposits.**

**Facies Fci**: Intraformational conglomerate lithofacies (Fci).
Representative facies examples from the Triassic Moenkopi Formation.

# Facies **Fxt** - Trough Cross-Bedded Sandstone

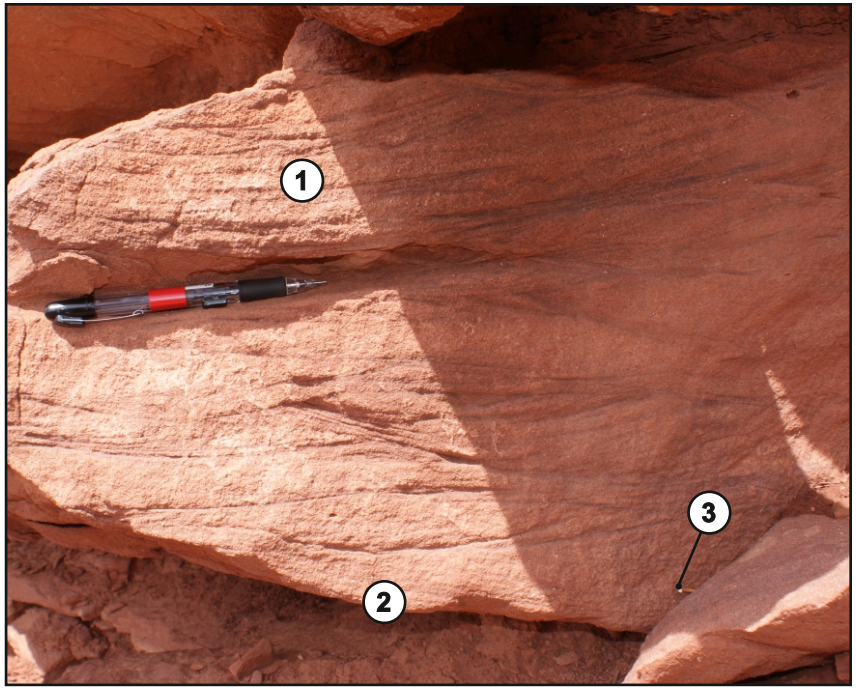


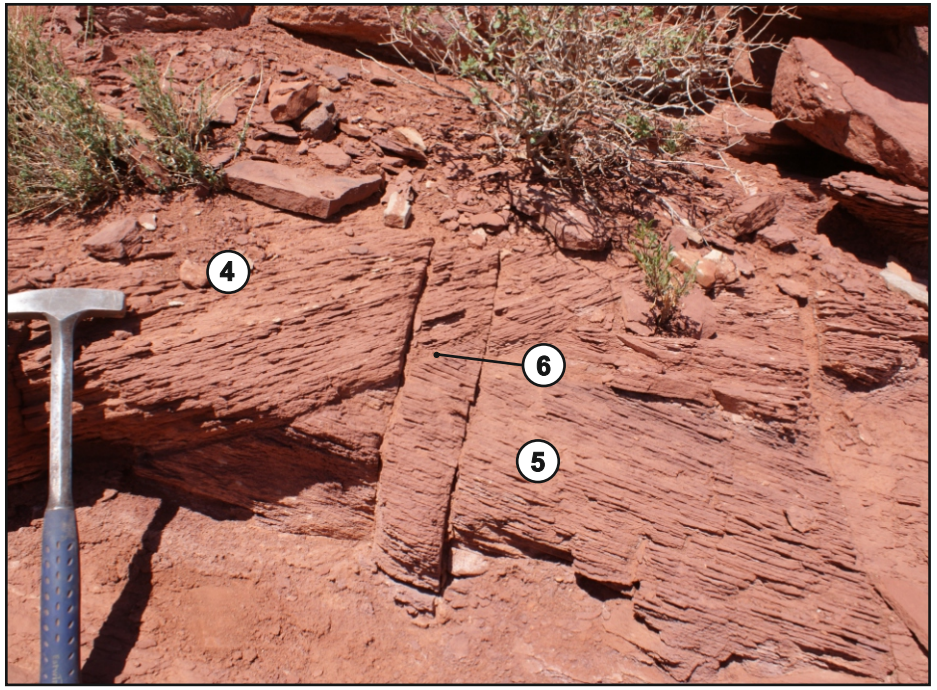


## Key Facies Information

| | |
|---|---|
| Colour | Orange-brown to purple-brown |
| Grain-size | Medium- to coarse-grained sandstone |
| Sorting & Texture | Moderate to poor sorting; sub-angular to sub-rounded |
| Thickness | 0.2 m to 2.5 m |
| Facies Association | Confined Associations |
| Architectural Elements | F1 (Amalgamated), F2 (Single Storey, Multi-lateral) |

## Key Facies Characteristics

1. Small scale (0.3 m) trough cross-beds
2. Sharp boundary between underlying hetrolithic unit and set of Fxt; erosional and incised channel base
3. Sporadic granules to small pebbles near erosive base; traction carpet of granules advancing in front of bedform
4. Larger scale cross-beds suggest greater water depth at time of deposition.
5. Thin laminations within troughs
6. Intersecting trough cut-off in sections perpendicular to flow indicate sinuous, out-of-phase bedform crestlines

## Interpretation

**Trough cross-bedding records the migration of small dunes and larger barform elements within fluvial channels. Troughs demonstrate the passage of bedforms with sinuous crestlines and in these examples, successive crestlines were out-of-phase.**

**Facies Fxt**: Trough cross-bedded sandstone. Representative facies examples from the Triassic Moenkopi Formation.

# Facies **HA Fxp** - High Angle Planar-bedded Sandstone

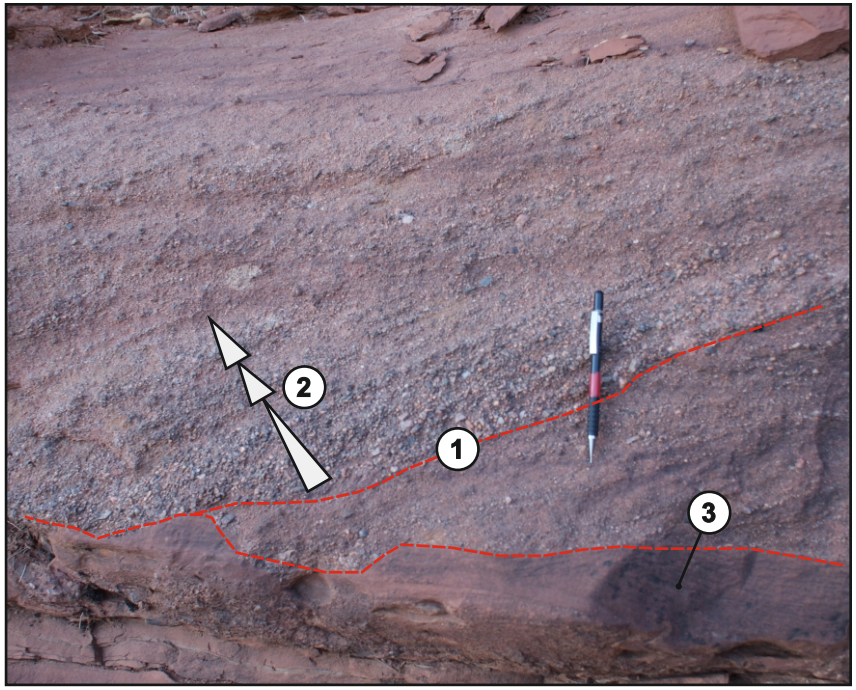


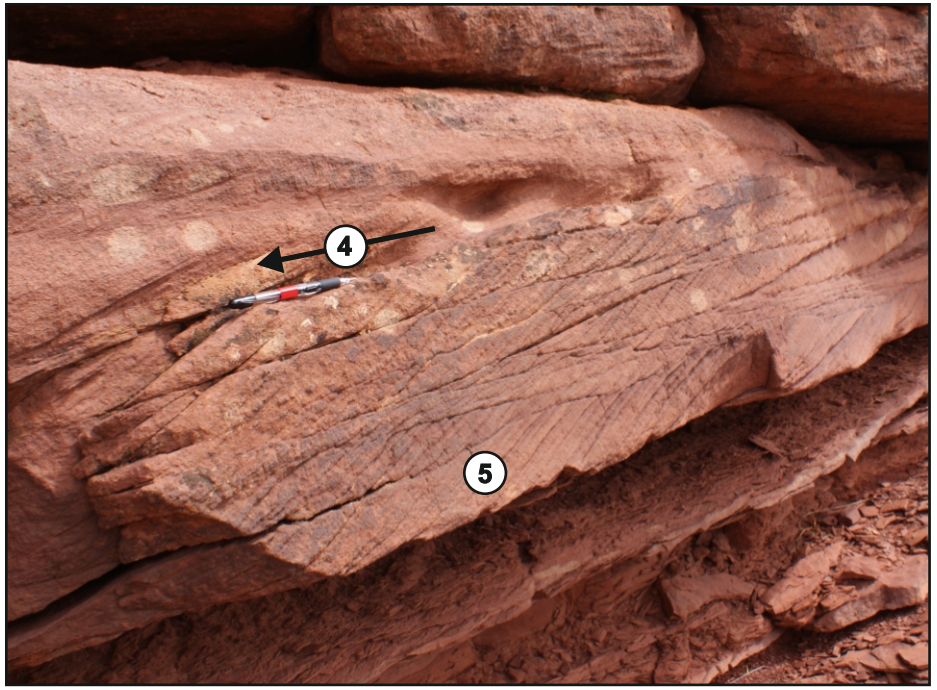


## Key Facies Information

| | |
|---|---|
| Colour | Orange-brown to purple-brown |
| Grain-size | Fine- to coarse-grained sandstone |
| Sorting & Texture | Moderate to poor sorting; sub-angular to sub-rounded |
| Thickness | 0.2 m to 2.5 m |
| Facies Association | Confined Associations |
| Architectural Elements | F1 (Amalgamated), F2 (Single Storey, Multi-lateral) |

## Key Facies Characteristics

1. Sharp, erosive bases indicate initial incision and erosion of underlying channel-fill element
2. Basal granule to pebble fill overlain by fining-upward succession of medium-coarse and granulestone fills; granules and small pebbles common above erosive basal contact; indicative of a gradual waning of flow velocity
3. High-angle-inclined planar bedding can be used to infer general palaeoflow directions
4. Angle of climb vries from near-zero to moderate but still cub-critical
5. Planar-tabular foresets; tangenital to set base

## Interpretation

**High angle planar cross-bedded sandstone and pebbly sandstone sets represent bar forms or variable size migrating within a fluvial channel. Individual sets are simple and rarely exceed 2 m in thickness, suggesting the absence of large, compound bars.**

**Facies ha Fxp**: high angle Plainar Cross Bedding.

# Facies **WR** - Wave-Ripple Laminated Sandstone

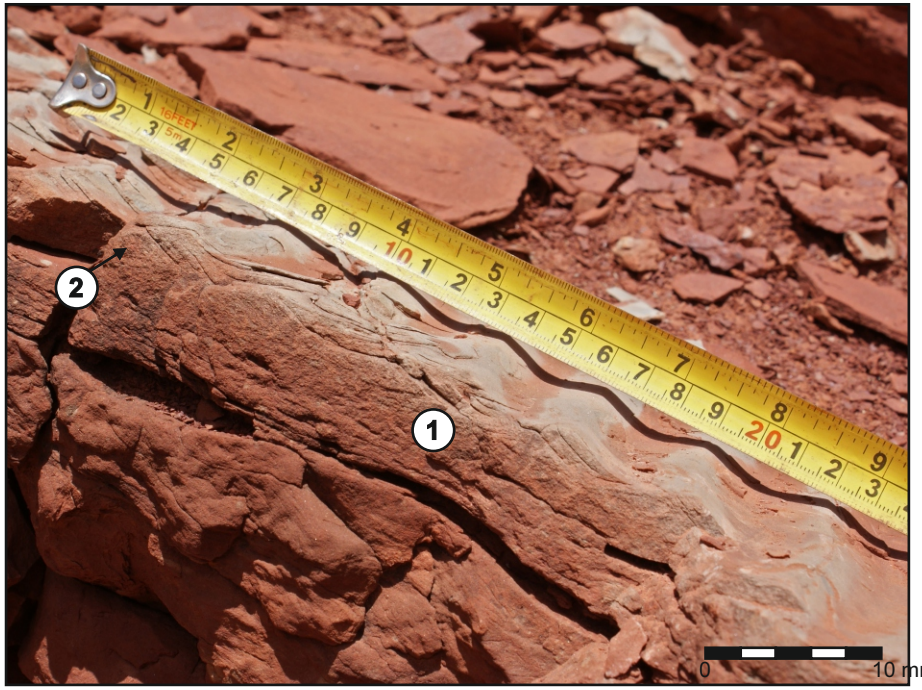


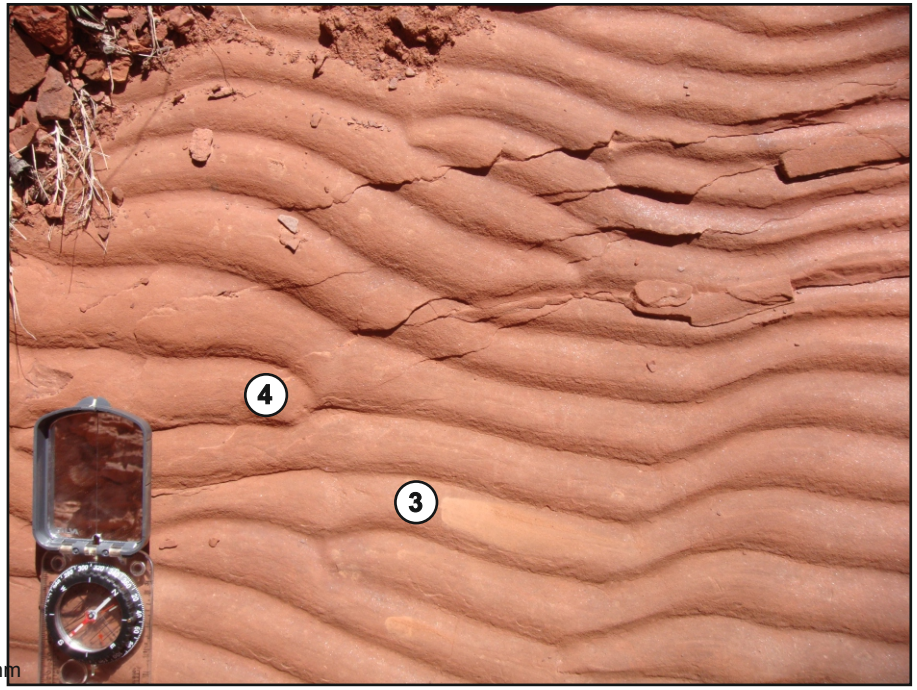


## Key Facies Information

| | |
|---|---|
| Colour | Orange or chocolate brown; some reduced grey |
| Grain-size | Very fine- to fine-grained sandstone |
| Sorting & Texture | Poorly to moderately sorted; sub-angular to sub-rounded |
| Set Thickness | 10 mm to 0.3 m sets |
| Facies Association | Unconfined associations |
| Architectural Elements | Unconfined elements |

## Key Facies Characteristics

1. Ripple forms prsereved on an upper bedding surface seen in section and displaying a combination of chevron upbuilding, and draping on foresets.
2. Some examples of asymmetric ripple foresets indicate a dominant current within the overall bidirectional flow regime
3. Ripple casts in base of block. Note that the rounded forms are troughs
4. Cast of sinuous-crested, bifurcating ripple crest; most ripples crests are parallel and continuous over long distances relative to the wavelength of the rippleforms; crestline sinuosities of successive bedforms are in-phase - common in wave ripples

## Interpretation

**Wave ripple forms and stratification represent ripple generation due to bi-directional flow created by oscillating currents in a standing body of water, such as a pond, shallow lake margin, pool within a drying stream or intertidal flats.**

**Facies WR**: Wave ripple-laminated sandstones. Representative facies examples from

# Facies **Frc/Fxl** - Current Ripple-Laminated / Trough Cross-Laminated Sandstones

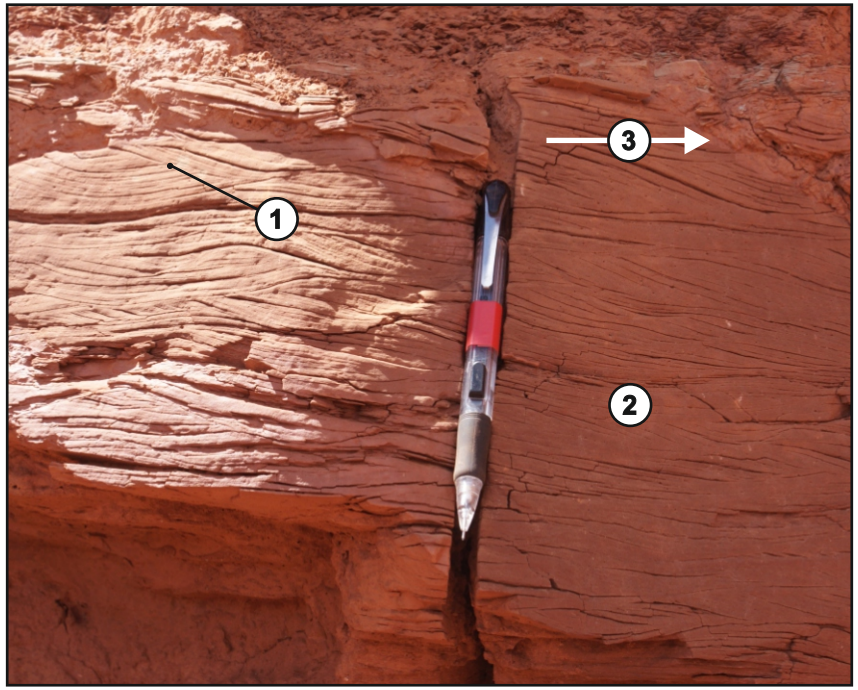


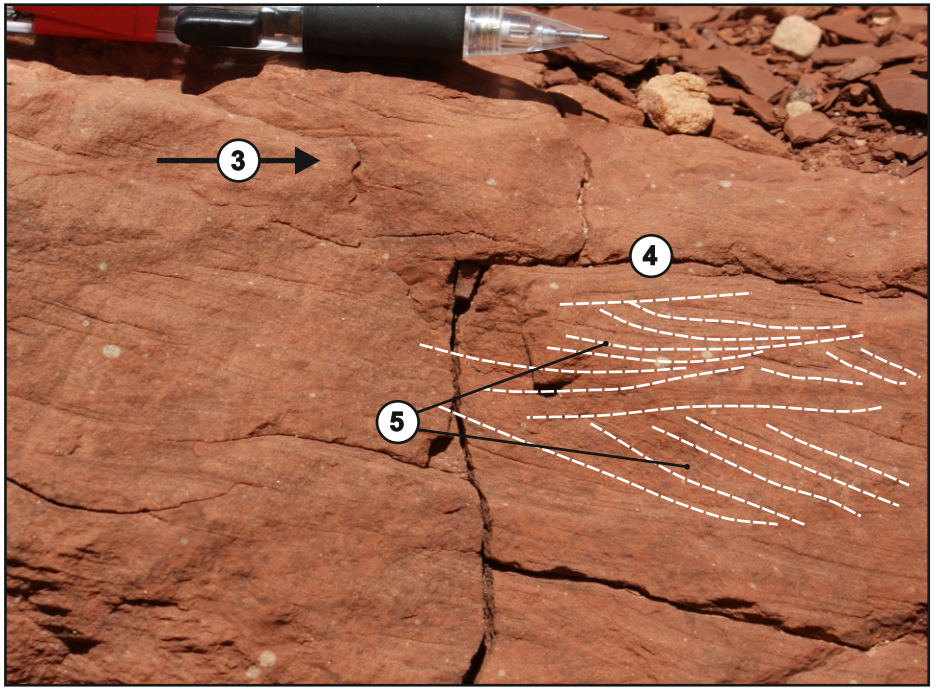


## Key Facies Information

| | |
|---|---|
| Colour | Orange-brown to red-brown |
| Grain-size | Very fine- to medium-grained sandstone |
| Sorting & Texture | Moderately to well sorted; sub-angular to sub-rounded |
| Thickness | 50 mm to 2 m |
| Facies Association | Confined and unconfined associations |
| Architectural Elements | Confined and unconfined elements |

## Key Facies Characteristics

1. Trough cross-lamination; indicative of the migration of sinuous ripple crests
2. Climbing ripple-lamination is observed in faces that deviate more than 20° from perpendicular to the bedform palaeomigration direction
3. Direction of palaeoflow
4. In faces that are not parallel to the palaeoflow direction, a mixture, the preserved expression is a combination of climbing ripple lamination and trough cross-lamination
5. Slight variations in the palaeo-current result in significant changes to the outcrop expression of the ripple stratification

## Interpretation

**Current ripple-laminated and trough cross-laminated sandstones are two expressions of the same sedimentary structure: sinuous-crested climbing ripples. The out-of-phase nature of successive crestlines in a train generate the troughs.**

**Facies Frc/Fxl**: Representative facies examples from the Triassic Moenkopi

# Facies **Frc** - Current-Ripple Laminated Sandstone

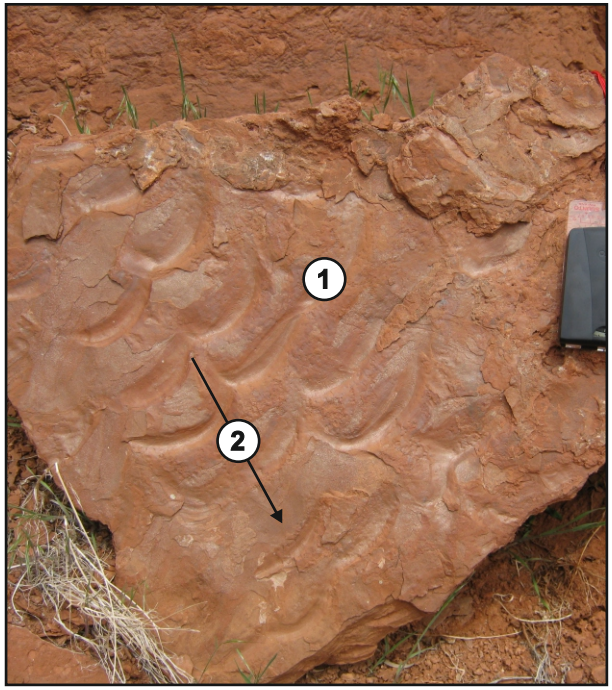


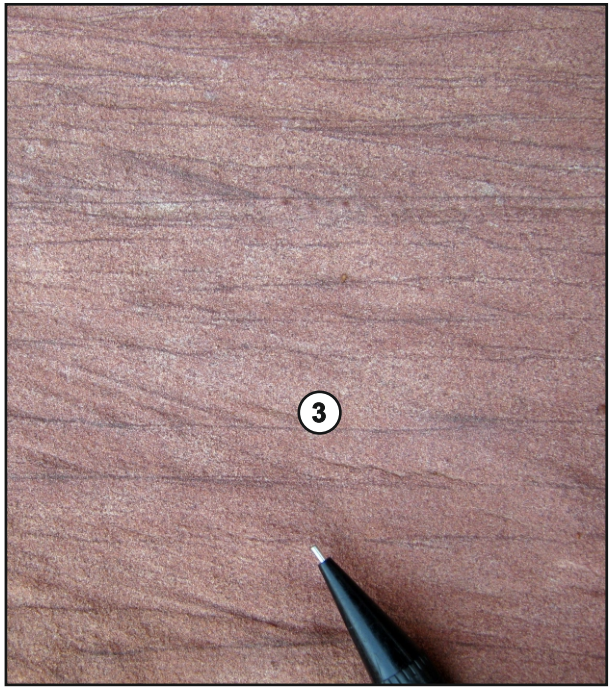


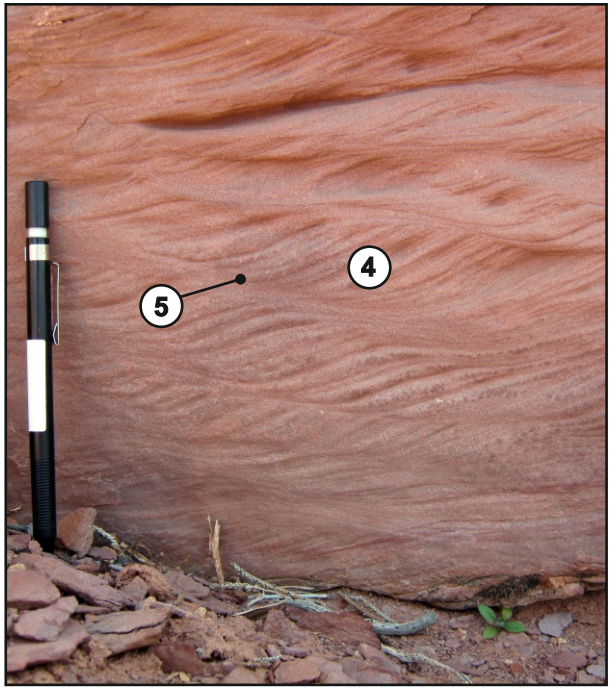


## Key Facies Information

| | |
|---|---|
| Colour | Orange brown to red-brown |
| Grain-size | Very fine- to medium-grained sandstone |
| Sorting & Texture | Moderately sorted; sub-angular to sub-rounded |
| Thickness | 0.05 m to 0.5 m (rarely more than 1 m) |
| Facies Association | Confined and unconfined associations |
| Architectural Elements | Confined and unconfined elements |

## Key Facies Characteristics

1. Bedding surface showing asymmetric, sinuous-crested linguoid ripples
2. Asymmetric ripples indicative of unidirectional flow
3. Sub-critical climbing ripple stratification with mud drapes; indicative of pulsing flow with currents approaching zero to allow suspension settling of mud fraction
4. Critical to super-critical climbing ripples; indicative of episodes of high sediment flux and waning flow to enable rapid accumulation
5. Preserved stoss side of ripples in cases of super-critical climb

## Interpretation

**Represents the unidirectional migration of micro-forms (ripples) via flow within a channel or in an unconfined setting under lower-stage flow regimes. Steeper climb angles indicate rapid accumulation under waning flow. Linguoid ripples form in turbulent flows.**

**Facies Frc**: Representative facies examples from the Triassic Moenkopi Formation.

# Facies **Frc** - Current Ripple Laminated Sandstones

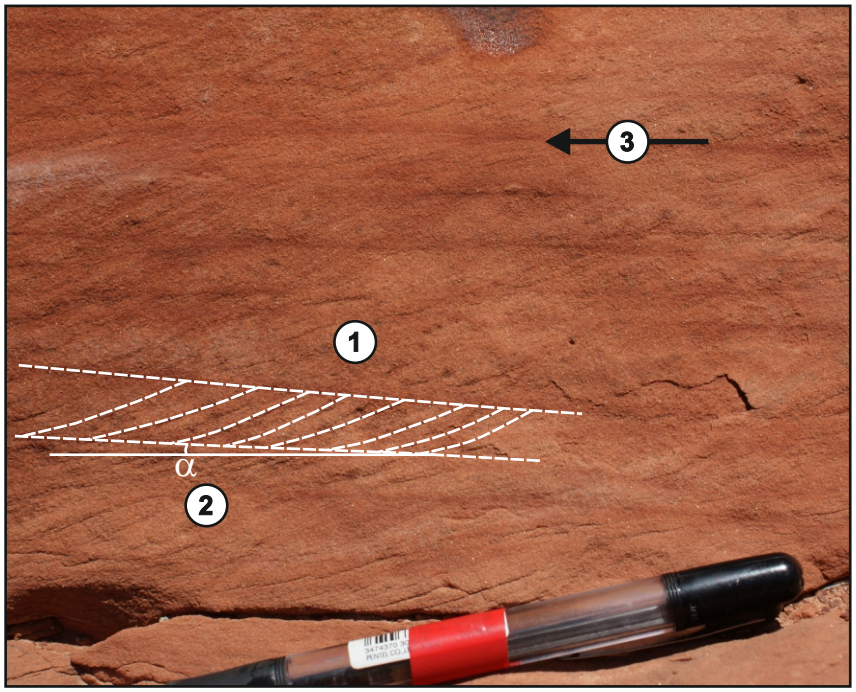


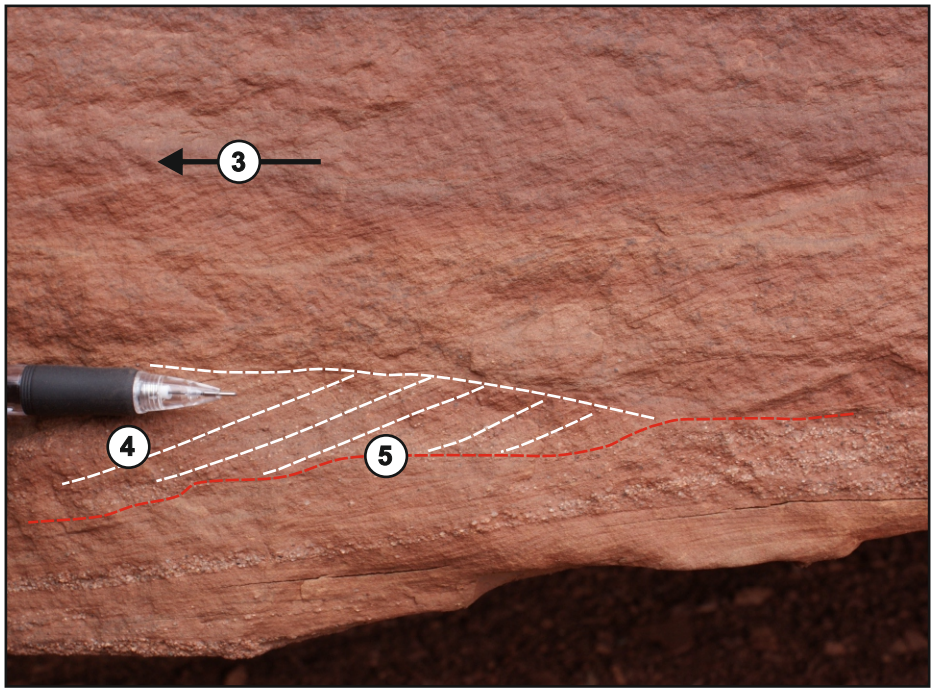


## Key Facies Information

| | |
|---|---|
| Colour | Orange-brown to red brown |
| Grain-size | Very fine- to medium-grained sandstone |
| Sorting & Texture | Well to moderate sorting; sub-angular to sub-rounded |
| Thickness | 0.05 m to 1.5 m (rarely more) |
| Facies Association | Confined flow or unconfined flow |
| Architectural Elements | Confined Flow Elements, Unconfined elements |

## Key Facies Characteristics

1. Sub-critical climbing ripple stratification composed of fine- to medium-grained sandstone
2. Positive angle of climb enables accumulation of ripple-strata; angle of inclination of laminae bounding surfaces relative to lower set bounding surface
3. Direction of Palaeoflow
4. Fine- to medium-grained sand-stone with sporadic upper-medium to coarse sand grains within the matrix
5. Erosional bounding surface down-cutting into pre-existing ripple strata; indicative of episodic cessation in sedimentation

## Interpretation

**Represents the unidirectional migration of micro-forms (ripples) within a fluvial channel or within an unconfined settings under lower-stage flow conditions. Laminations highlighted by the preservation of finer-grained, dark-coloured silt drapes - pulsing flow.**

**Facies Frc**: Representative facies examples from the Triassic Moenkopi Formation.

# Facies **Frc** - Current Ripple Laminated Silt & Sandstones (Overbank Association)

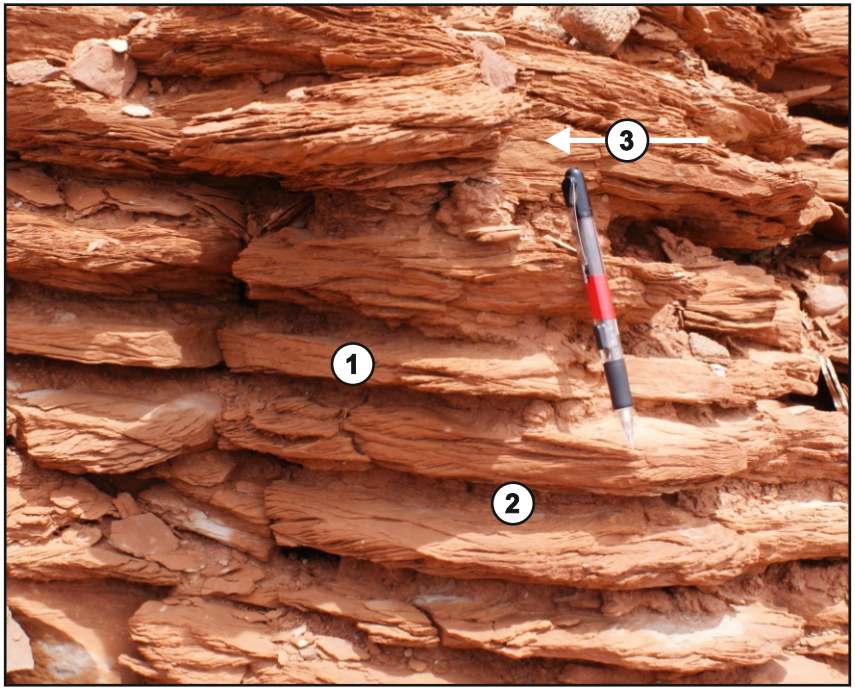


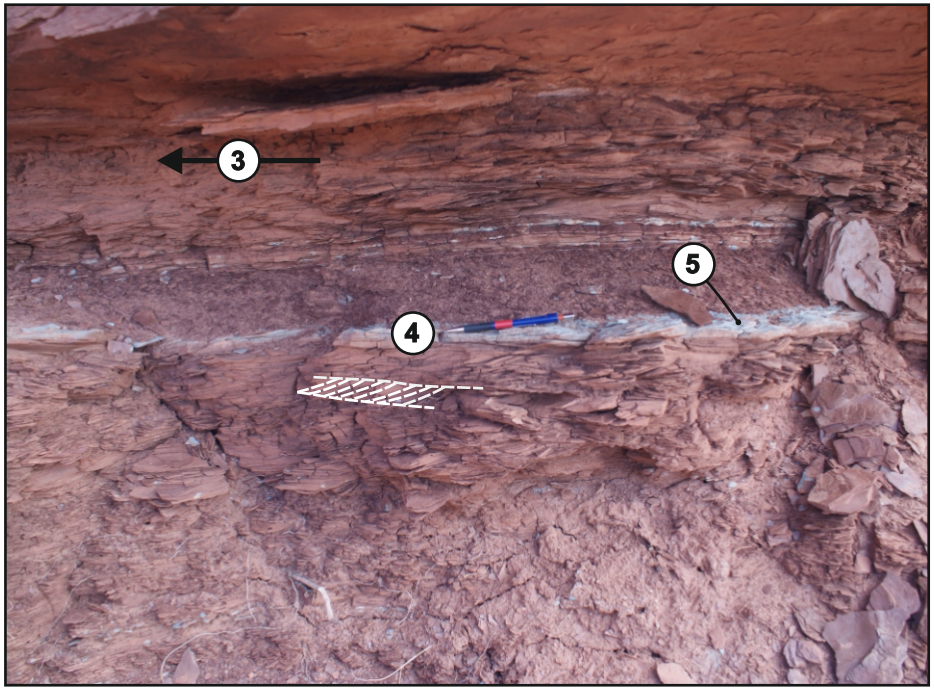


## Key Facies Information

| | |
|---|---|
| Colour | Orange-brown to red brown |
| Grain-size | Very fine- to medium-grained sandstone |
| Sorting & Texture | moderately to well sorting; sub-angular to sub-rounded |
| Thickness | 0.05 m to 0.25 m |
| Facies Association | Unconfined Associations |
| Architectural Elements | Unconfined elements |

## Key Facies Characteristics

1. Sub-critical climbing ripple stratification composed of fine sandstone.
2. Thin sets of climbing ripple strata are interbedded with very thin sets of siltstone.
3. Direction of Palaeoflow.
4. Grey top-surface of ripple strata indicates reduction, possibly caused by stagnation of standing water
5. Linguoidal asymmetric ripple forms preserved on top surface; useful indicator of palaeoflow direction

## Interpretation

**Current-ripple laminated sailtstones and sandstones are common in overbank settings and record the unidirectional migration of micro-forms in an unconfined flow. Interbedded silts and sands represent successive flood events. Common on crevasse splays.**

**Faceis Frc**: Representative facies examples from the Triassic Moenkopi Formation.

# Facies **Fh** - Horizontally Laminated Sandstone

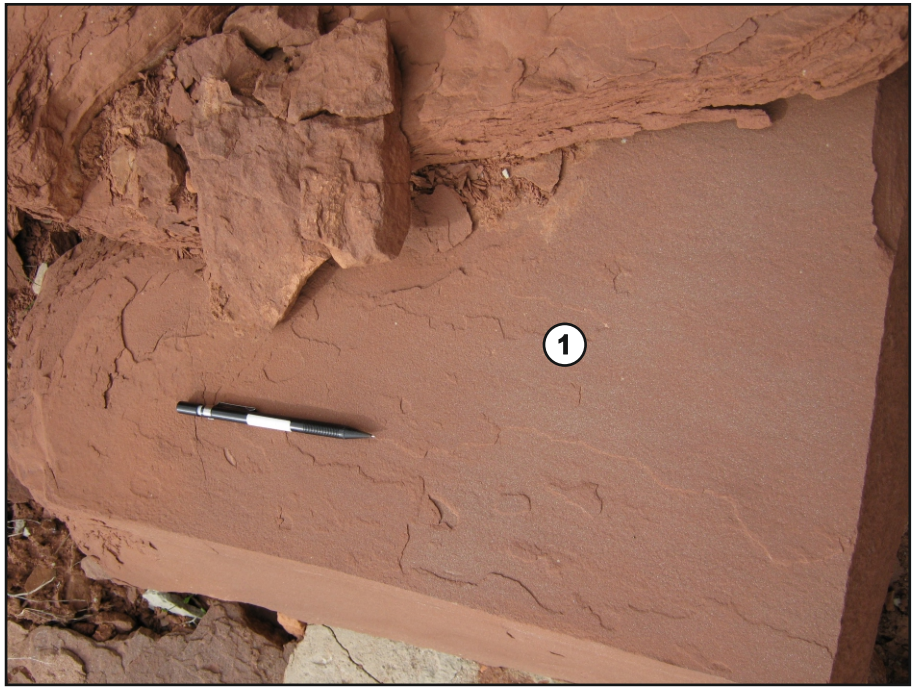


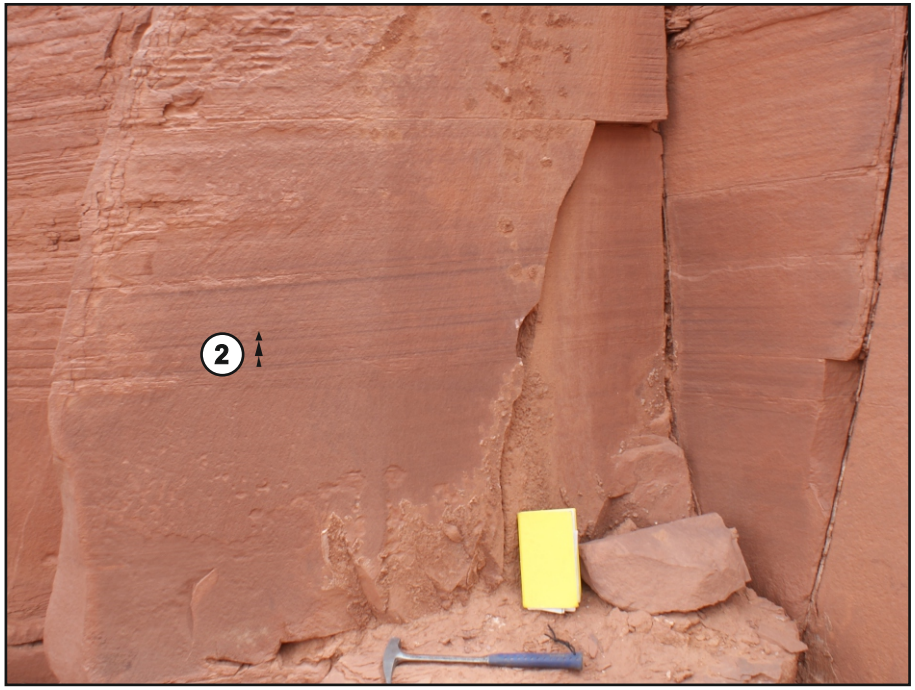


| Key Facies Information | |
|---|---|
| Colour | Variable: orange-brown, red-brown or reduced grey |
| Grain-size | Very fine- to fine-grained sandstone |
| Sorting & Texture | Moderately- to well-sorted; sub-angular to sub-rounded |
| Thickness | 2 mm - 7 mm laminations; > 0.05 m sets |
| Facies Association | Confined and Unconfined Associations |
| Architectural Elements | Confined and Unconfined Elements |

## Key Facies Characteristics

1. Primary current lineations seen on upper bedding surfaces; deposited under upper-flow regime conditions

2. Laminations exhibit normal grading. Fining upward within each lamina from fine-grained sandstone to very fine-grained sandstone.

## Interpretation

**Horizontally laminated sandstones record deposition under either lower- or upper-flow regime conditions within either a fluvial channel or in an unconfined fluvial flow. Primary current lineation on bedding surfaces demonstrates upper-stage flow.**

**Facies Fh**: Horizontally laminated sandstone lithofacies (Fci).

# Facies **Fh** - Horizontally Laminated Sandstone

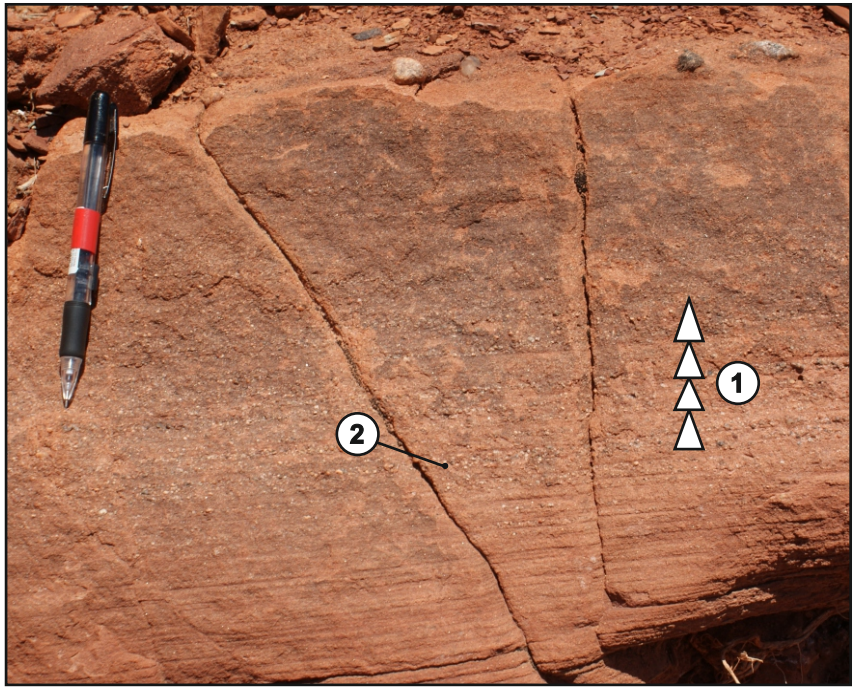


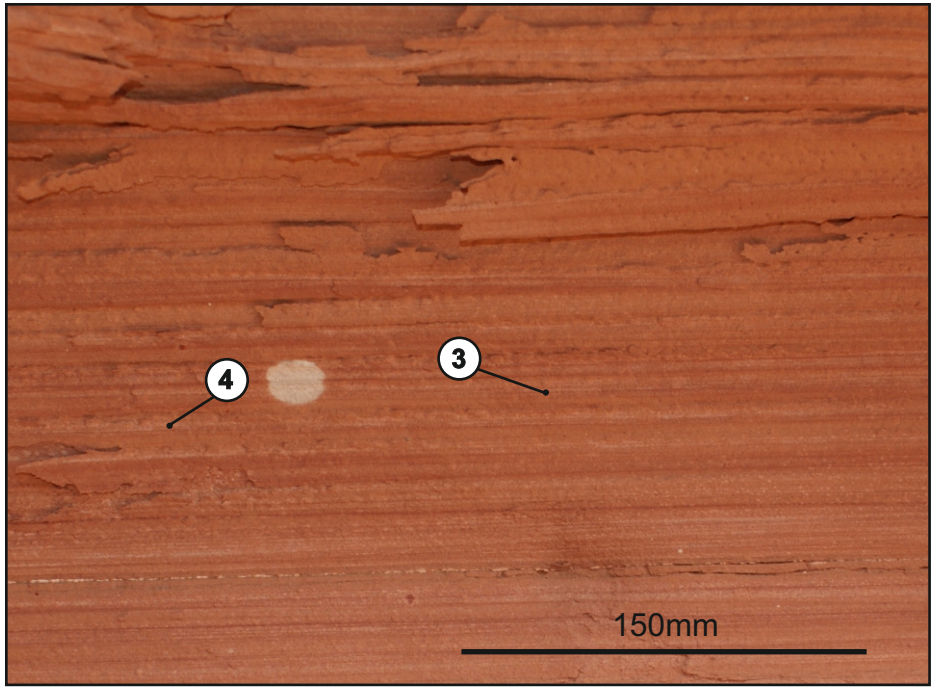


## Key Facies Information

| | |
|---|---|
| Colour | Variable: orange/red-brown or reduced grey |
| Grain-size | Very fine to coarse |
| Sorting & Texture | Poorly to well sorted; sub-angular to rounded |
| Thickness | 50 mm - 5 m |
| Facies Association | Confined and Unconfined associations |
| Architectural Elements | Confined flow elements; Unconfined flow elements |

## Key Facies Characteristics

1. Laminations exhibit normal gradin; likely represent burst-sweep cycles, possibly in a waning flow
2. Base of fining-upward package is coarser-grained
3. Horizontally laminated sandstones composed of fine sand exhibit thinner laminations than in examples composed of coarse sand
4. Thin reduced horizons may indicate reduction associated with slightly less permeable layers

## Interpretation

**Horizontally laminated sandstones represent deposition under either lower- or upper-flow regimes within either a confined flow, or unconfined sheet-like environment. Parting lineation on some bedding surfaces confirms upper stage flow.**

**Facies F**h: Horizontally laminated sandstone facies

# Facies **Fd** - Deformed Bedding & De-Watering Structures

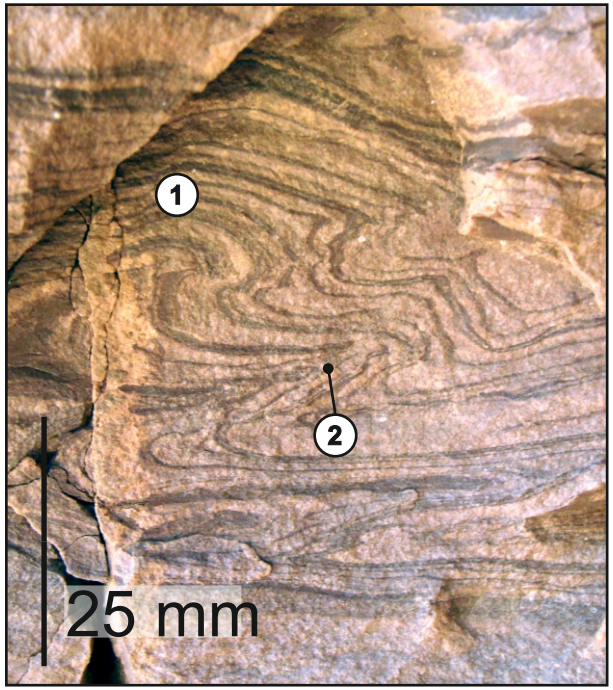


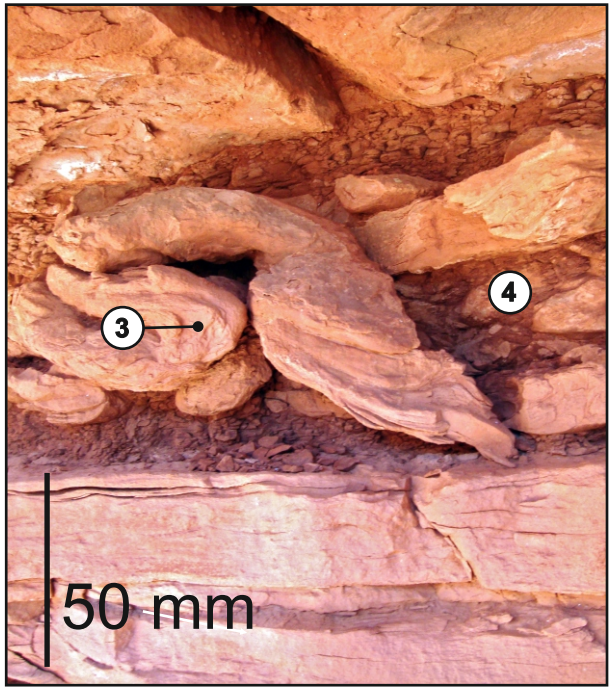


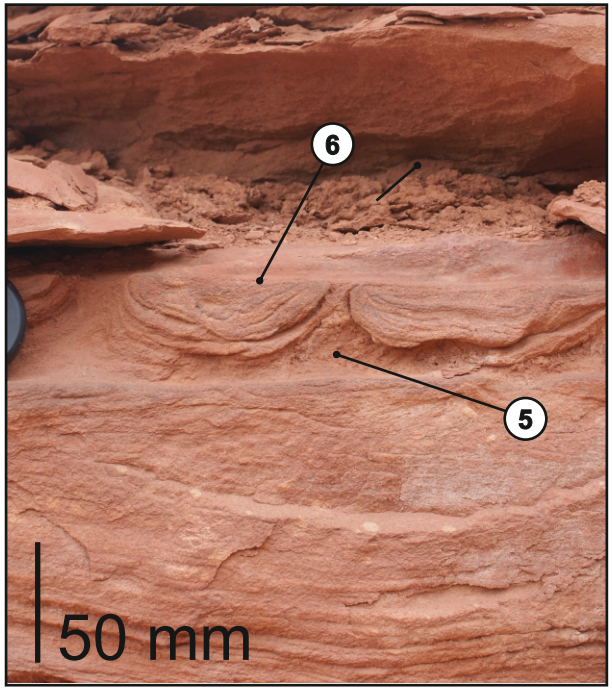


## Key Facies Information

| | |
|---|---|
| Colour | Orange-brown to chocolate-brown |
| Grain-size | Very fine- to medium-grained sandstone |
| Sorting & Texture | Moderate Sorting; sub-angular to sub-rounded |
| Thickness | 0.1 m - 1.7 m |
| Facies Association | Unconfined Associations |
| Architectural Elements | Unconfined Elements |

## Key Facies Characteristics

1. Formerly parallel lamination folded at tight-to-isoclinal angles
2. Folds show common vengeance, indicating direction of shear
3. Thin sandstone beds within incompetent argillaceous units are folded to form recumbent fold structures
4. Sandstone lenses within an argillaceous matrix
5. Water escape structures formed by sediment loading of water saturated sediment
6. Water escape structures later truncated by an erosive channel

## Interpretation

**Various styles of soft sediment deformation resulting from loading of unconsolidated sediment, or via water escape through less permeable sediment. May also indicate sediment movement down an unstable slope created by uplift pre- syn- or post-deposition.**

**Facies Fci**: Intraformational conglomerate lithofacies (Fci).
Representative facies examples from the Triassic Moenkopi Formation.

# Facies **Fhiss** - Horizontally interlaminated siltstones fine sandstones

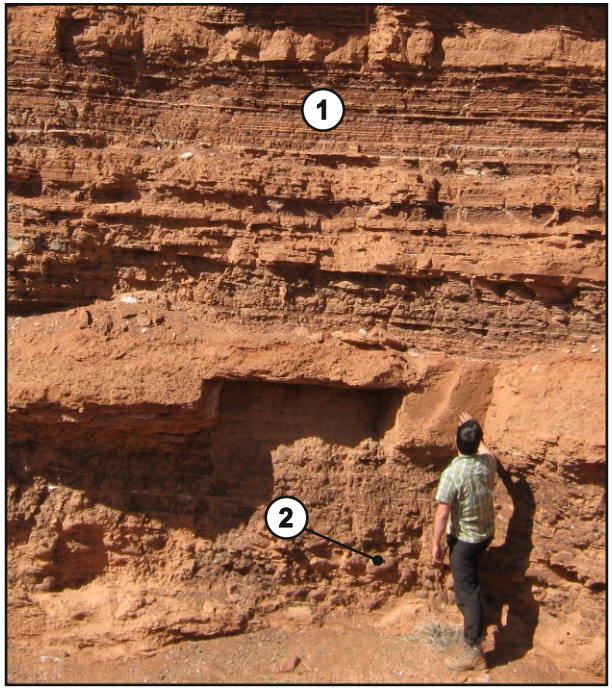


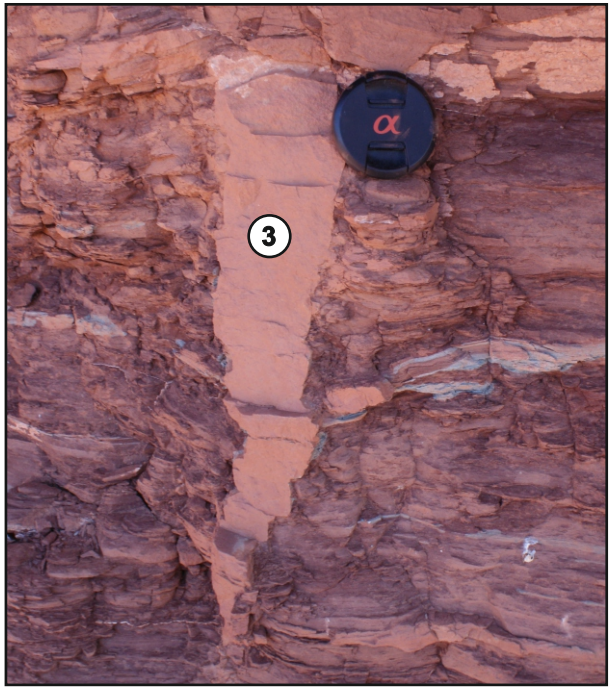


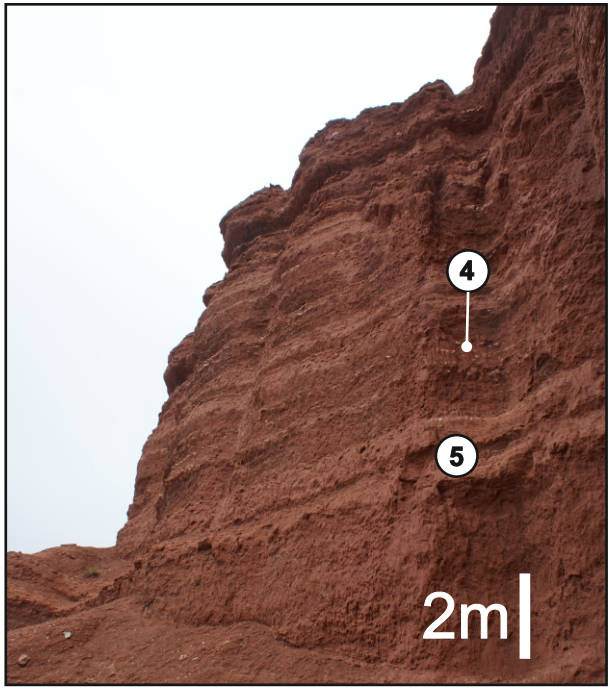


## Key Facies Information

| | |
|---|---|
| Colour | Chocolate-brown & sand brown |
| Grain-size | Mud to very fine sand |
| Sorting & Texture | Moderate sorting within layers |
| Thickness | 0.1 m to > 20 m |
| Facies Association | Unconfined Associations |
| Architectural Elements | Unconfined Elements |

## Key Facies Characteristics

1. Thinly interbedded siltstone and ripple-laminated sandstones. Wave ripples are relatively common
2. Sandstone with a nodular appearance; differential cementation (Ca or Fe?)
3. Sand-filled desiccation cracks indicating repeated episodic drying of a damp substrate
4. Isolated rounded gypsum clasts common in several locations; indicates tractional reworking of salts via ephemeral stream flow in a generally arid environment
5. Thick sand unit accociated with Fhiss units tend to be massive (structureless) and fissile

## Interpretation

**Horizontally interlaminated fines and sands represent deposition from suspension during waning flows within a fluvial floodplain setting. Poorly developed aridisols may be present. Desiccation cracks indicate repeated drying of the substrate.**

**Facies Fhiss**: Horizontally interbedded siltstones and sandstones. Representative facies examples from the Triassic Moenkopi Formation.

# Facies **Fm** - Massive (structureless sandstone)

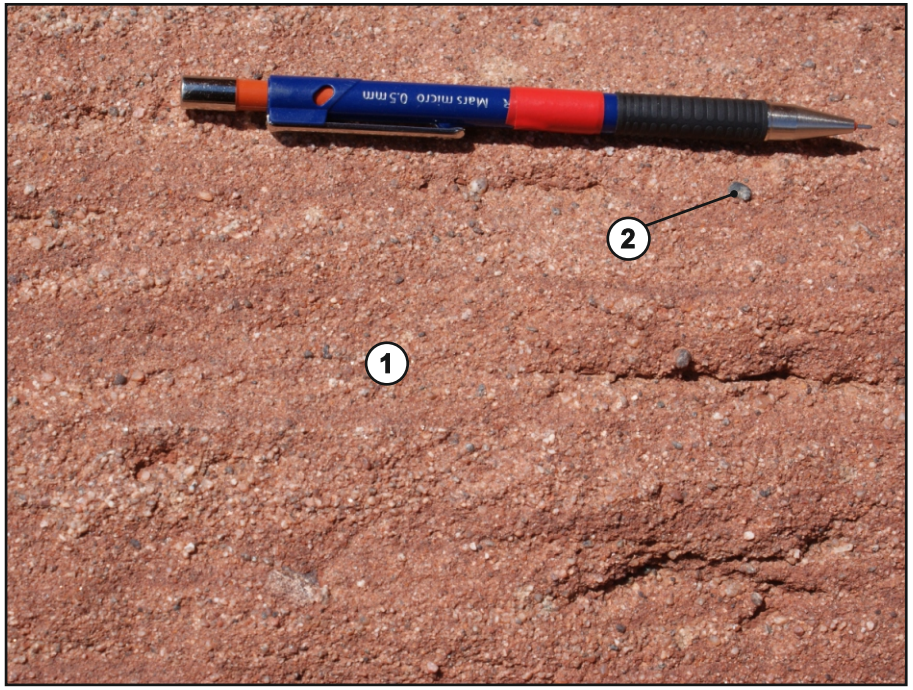


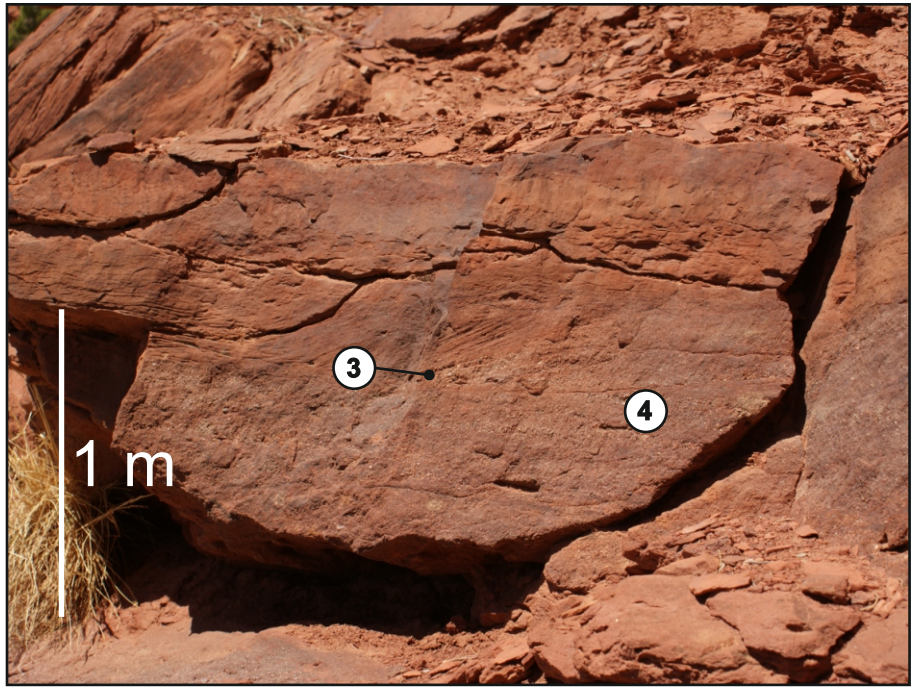


## Key Facies Information

| | |
|---|---|
| Colour | Orange brown to red-brown |
| Grain-size | Very fine- to very coarse-grained sandstone |
| Sorting & Texture | Moderately- to poorly sorted; sub-angular to sub-rounded |
| Thickness | 0.05 m to 2.0 m |
| Facies Association | Confined and unconfined associations |
| Architectural Elements | Confined and unconfined elements |

## Key Facies Characteristics

1. Poorly sorted, medium- to coarse grained sandstones, exhibiting a lack of flow-generated structures
2. Very coarse- to granule-grade floating “pebbles” within matrix
3. Erosive channel base of over-lying channel-fill element.
4. Structureless sandstones filling underlaying channel-fill element

## Interpretation

**Represents rapid deposition of sand from suspension. Grading (where present) indicates gradual waining of flow velocity.**

**Facies Fm**: Representative facies examples from the Triassic Moenkopi Formation.

# Facies Gd - Matrix Supported Gypsum Horizons

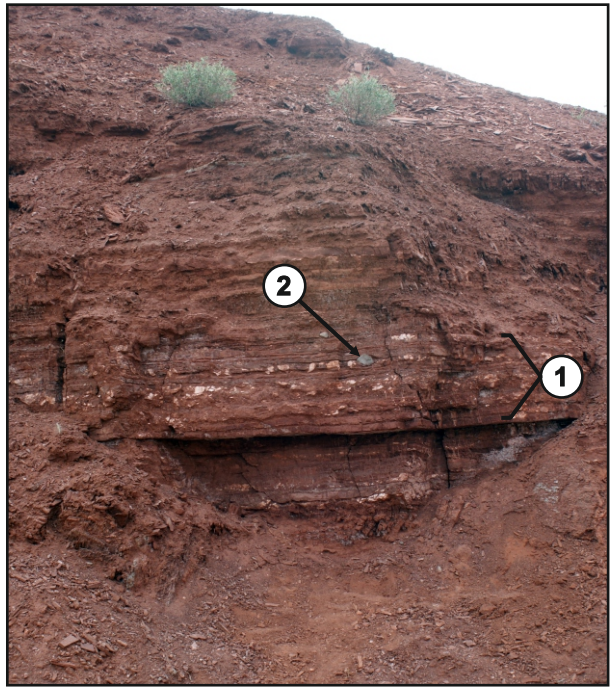


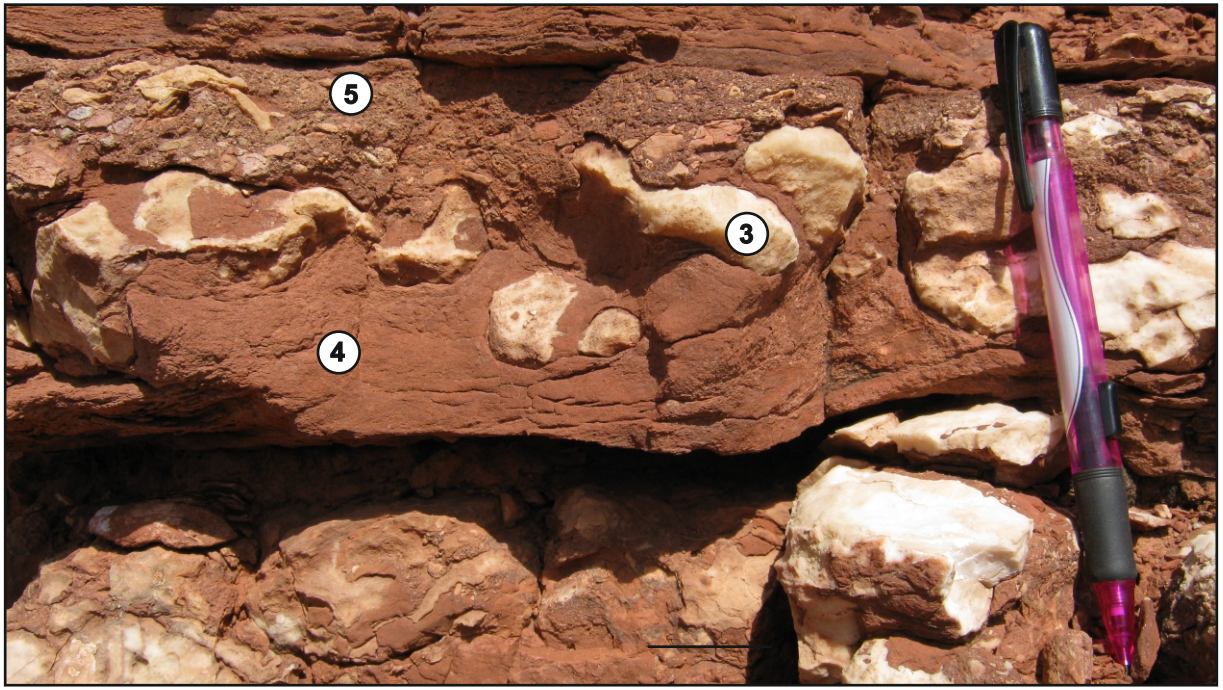


## Key Facies Information

| | |
|---|---|
| Colour | Off-white clasts, typically in a orange-brown sand matrix |
| Grain-size | 10-150 mm diameter clasts; fine-grained sand matrix |
| Sorting & Texture | Poorly sorted; matrix supported; angular |
| Thickness | Clasts occur in 0.1 to 0.4 m-thick beds |
| Facies Association | Unconfined associations; rarely in confined assocs. |
| Architectural Elements | Unconfined element; rarely in confined channels |

## Key Facies Characteristics

1. Discrete bands of gypsum clasts layered in dm-thick sandstone sets
2. Gypsum clast horizons also contain extraformational clasts; indicative of a mixed provenance
3. Gypsum clasts are sub-angular; indicative of a relatively short transport distance
4. Matrix-supported nature of sets indicates deposition of gypsum clasts either by debris flow or water flow
5. Horizon with gypsum clasts overlain by a coarse matrix of gypsum micro-conglomerate within which clasts are smaller; disaggregation and dissolution of clasts in a higher-energy flow or a longer transport distance.

## Interpretation

**Discrete horizons of gypsum clasts indicate that the salt was only available for fluvial transport and reworking episodically, most likely at times when salt diapirs breached the surface. Sub-angular clasts indicate a location close to the salt wall.**

**Facies Gd**: Gypsum clast horizons. Representative facies examples from the Triassic

# 4. Controls on fluvial sedimentary architecture and sediment-fill state in salt-walled mini-basins: Triassic Moenkopi Formation, Salt Anticline Region, SE Utah, USA

---

*This chapter looks specifically at how halokinesis influences the accumulation of fluvial systems within salt-walled mini-basins. A more detailed overview of evolution of the Paradox Basin is described to give insight into the evolution of the Salt Anticline Region preceding deposition of the Moenkopi Formation, which exerts a strong control on the formation of the Moenkopi at the time of Deposition.*

*The Moenkopi Formation within the Salt Anticline Region, and how the thickness and composition varies both between and within the mini basins is described by basin: The Fisher, Parriott and Big Bend Basins, and looks at how rates of subsidence and sediment supply across each of the basins influenced the style of sediment accumulated. In addition, this chapter looks at the style of sediment accumulation on the flanks of the salt-walls to determine how salt-wall uplift influenced drainage pathways at the margins of the basins.*

*Tectonostratigrahic stratigrahic models for the evolution of the Moenkopi Formation are proposed, explaining the observed preserved stratigraphy the basins. Finally, a Barrel diagram which can be used to predict the likely preserved stratigraphy at given locations within the basin is proposed, demonstrating the predictability of fluvial element distribution across these basins.*

---

## *4.0 Abstract*

The Triassic Moenkopi Formation in the Salt Anticline Region, SE Utah represents the preserved record of a low-relief ephemeral fluvial system that accumulated in a series of actively subsiding salt-walled mini-basins. Development and evolution of the fluvial system and its resultant preserved architecture was controlled by: (i) the inherited state of the basin geometry at the time of commencement of sedimentation; (ii) the rate of sediment delivery

to the developing basins; (iii) the orientation of fluvial pathways relative to the salt walls that bounded the basins; (iv) spatially and temporally variable rates and styles of mini-basin subsidence and associated salt-wall uplift, and (iv) temporal changes in regional climate. Detailed outcrop-based tectono-stratigraphic analyses demonstrate how three coevally developing mini-basins and their intervening salt walls evolved in response to progressive sediment loading of a succession of Pennsylvanian salt (the Paradox Formation) by the younger Moenkopi Formation, deposits of which record a dryland fluvial system in which flow was primarily directed parallel to a series of elongate salt walls. In some mini-basins, fluvial channel elements are stacked vertically within and along the central basin axes, in response to preferential salt withdrawal and resulting subsidence. In other basins, rim synclines have developed adjacent to bounding salt walls and these served as loci for accumulation of stacked fluvial channel complexes. Neighbouring mini-basins exhibit different styles of infill at equivalent stratigraphic levels: sand-poor basins dominated by fine-grained, sheet-like sandstone fluvial elements, which are representative of non-channelised flow processes, apparently developed synchronously with neighbouring sand-prone basins dominated by major fluvial channel-belts, demonstrating effective partitioning of sediment route-ways by surface topography generated by uplifting salt walls. Reworked gypsum clasts present in parts of the stratigraphy demonstrate the subaerial exposure of some salt walls, and their partial erosion and reworking into the fill of adjoining mini-basins during accumulation of the Moenkopi Formation. Complex spatial changes in preserved stratigraphic thickness of four members in the Moenkopi Formation, both within and between mini-basins, demonstrates a complex relationship between the location and timing of subsidence and the infill of the generated accommodation by fluvial processes.

## *4.1 Introduction*

Globally, there exist in excess of 120 provinces where the action of salt tectonics has governed basin formation and influenced the style of sediment infill (Hudec & Jackson, 2007). Documented examples record the

development of both passive and reactive salt structures associated with either extension or compression, and the development of structures related to differential loading and flexural buckling of overburden (Vendeville & Jackson, 1992a, b; Jackson *et al.,* 1994, Waltham, 1997). The initiation of salt mobilisation and the onset of salt-related mini-basin development due to subsurface salt withdrawal into adjacent salt walls is triggered by a variety of factors, including buoyancy, differential loading (Ge *et al.*, 1997), thermal convection, and the presence of extensional or contractional tectonic regimes (Jackson & Talbot, 1986; Waltham, 1997; Hudec *et al.*, 2009; Ings & Beaumont, 2010; Fuchs *et al.*, 2011).

The growth and evolution of salt walls in the subsurface can result in a variety of surface topographic expressions, the forms of which are dependent on: (i) the rates and styles of mini-basin subsidence and associated salt-wall uplift, which combine to generate accommodation; and (ii) the rate of sedimentation that serves to fill accommodation. Topographic surface expressions arising from the growth of salt-structures at depth can assume a variety of forms, including subtle swells, ridges and walls, each of which act to deform overlying strata to generate surface expression, and piercement structures where the deforming salt itself breaches the surface (Trusheim, 1960; Ala, 1974; Jackson & Talbot 1986; Jackson *et al.*, 1990; Davison *et al.*, 1996a; Lawton & Buck, 2006). The architecture and location of salt structures at depth are commonly controlled by pre-existing basement structures such as inherited fault arrays, whereby salt-wall development tends to be triggered above or immediately adjacent to points of differential salt thickness (Cater, 1970; Smith *et al.*, 1993; Doelling, 2002a). Evolving salt-walls and adjacent mini-basins therefore develop with a range of planform geometries and surface expressions including parallel, elongate linear ridges such as those present in the Salt Anticline Region of SE Utah (Harrison 1927; Dane, 1935; Trudgill 2011) and the South Urals mini-basins (Newell *et al.*, 2012), or complex interacting polygonal patterns such as those of the Triassic of the Central North Sea (Smith *et al.*, 1993; Stewart, 2007) and the Permo-Triassic Pre-Caspian Basin of Kazakhstan (Barde *et al.*, 2002a; Volozh *et al.*, 2003).

Once salt movement has been initiated, mini-basin subsidence due to salt withdrawal into adjacent, growing salt walls is enhanced by the effects of sediment loading as active depositional systems accumulate strata in evolving mini-basin depocentres (Jackson & Talbot, 1986; Hudec *et al.*, 2009), a process referred to as downbuilding (Barton, 1933). Once initiated, salt-walled mini-basins tend to evolve rapidly with documented subsidence rates up to 10 $km.Myr^{-1}$ (Prather, 2000) allowing thick accumulations of strata to be preserved over relatively short episodes of geological time. Where salt-wall growth generates a surface topographic expression, it dictates processes of sedimentation and styles of accumulation of sedimentary architecture by controlling surface sedimentary processes, including sediment distribution route-ways, and by controlling complex spatial and temporal trends in the rate of creation of accommodation.

Examples of currently active halokinesis include the Zagros Mountain Belt and Qum Kuh of Iran (Ala, 1974; Talbot, 1998; Talbot & Aftabi, 2004), the Gulf of Mexico (Wu *et al.*, 1990), and the Dead Sea (Al-Zoubi & Ten Brink, 2001). Examples of ancient preserved sedimentary successions considered to have been influenced by subsurface salt halokinesis are the shallow-marine Wonoka Formation of the Flinders Range, Australia (Kernen *et al.*, 2012), La Popa Basin, Mexico (Aschoff & Giles, 2005), the deep-marine Bryant Canyon, Garden Banks, Gulf of Mexico (Fiduk, 1995), and Eugene Island and Ship Shoal, Gulf of Mexico (Hall & Thies, 1995). Fluvial successions interpreted to have been influenced and controlled by ongoing halokinesis include those of the Triassic of the Central North Sea (Smith *et al.*, 1993; Jones *et al.*, 2005; McKie & Audretsch, 2005), the Triassic Pre-Caspian Basin, Kazakhstan (Barde *et al.*, 2002b; Hinds *et al.*, 2004), the Eocene Carroza Formation, La Popa Basin, Mexico (Andrie *et al.*, 2012), and the Pennsylvanian-Jurassic Salt Anticline Region of the Paradox Basin, SE Utah (Hudec, 1995; Lawton & Buck, 2006; Prochnow *et al.*, 2006; Matthews, 2007; Trudgill, 2011). The fluvial succession of the Lower Triassic Moenkopi Formation present in the mini-basins of the Salt Anticline Region of the Paradox Basin is the focus of this study.

The aim of this study is to document the mechanisms by which styles of basin subsidence and related salt-wall growth act to directly control fluvial-system type and the form of the stratigraphic architecture preserved in a series of mini-basins. This has been achieved through a detailed analysis of the outcrop pattern of the Triassic Moenkopi Formation, a hybrid braided-channel and non-confined sheet-like fluvial system that developed under the influence of an arid climate across much of what is now the south western United States region (Ward, 1901; Darton, 1910; Gregory, 1917; Stewart, 1959; Stewart *et al.*, 1972; Blakey, 1974). The study accomplishes the following objectives: (i) demonstrates changes in fluvial style between adjacent mini-basins and shows how surface topography generated by salt-wall uplift was able to effectively partition the fluvial system into sand-prone fairways dominated by stacked complexes of channel architectural elements, and extensive areas that were relatively sand-starved and dominated by complexes of fine-grained sheet-like architectural elements; (ii) demonstrates how the distribution of associations of fluvial lithofacies and architectural elements varies predictably from the centre of subsiding mini-basins onto the flanks of bounding salt walls; (iii) illustrates how analysis of the occurrence of associations of fluvial lithofacies and the distribution of architectural elements can be used to infer the relative timing of episodes of salt-wall uplift versus episodes of quiescence through the recognition of styles of onlap and erosional truncation of packages of fluvial elements; (iv) demonstrates how the preserved fluvial succession evolved temporally as accommodation within the evolving mini-basins became progressively infilled.

## *4.2 Background and Geological Setting*

The Paradox Basin developed from the Pennsylvanian to Permian as an intra-foreland flexural basin in response to lithospheric loading by the Uncompahgre Uplift, which formed as part of the so-called Ancestral Rocky Mountains (Fig. 4.1), one of several late Palaeozoic features developed during the Ancestral Rocky Mountain orogenic event (Ohlen & McIntyre, 1965; Kluth & Coney, 1981; Barbeau, 2003). The Uncompahgre Uplift was ~145 km long and elongated in a northwest southeast orientation across southwest Colorado and southeast Utah (Elston *et al.*, 1962). From the mid-

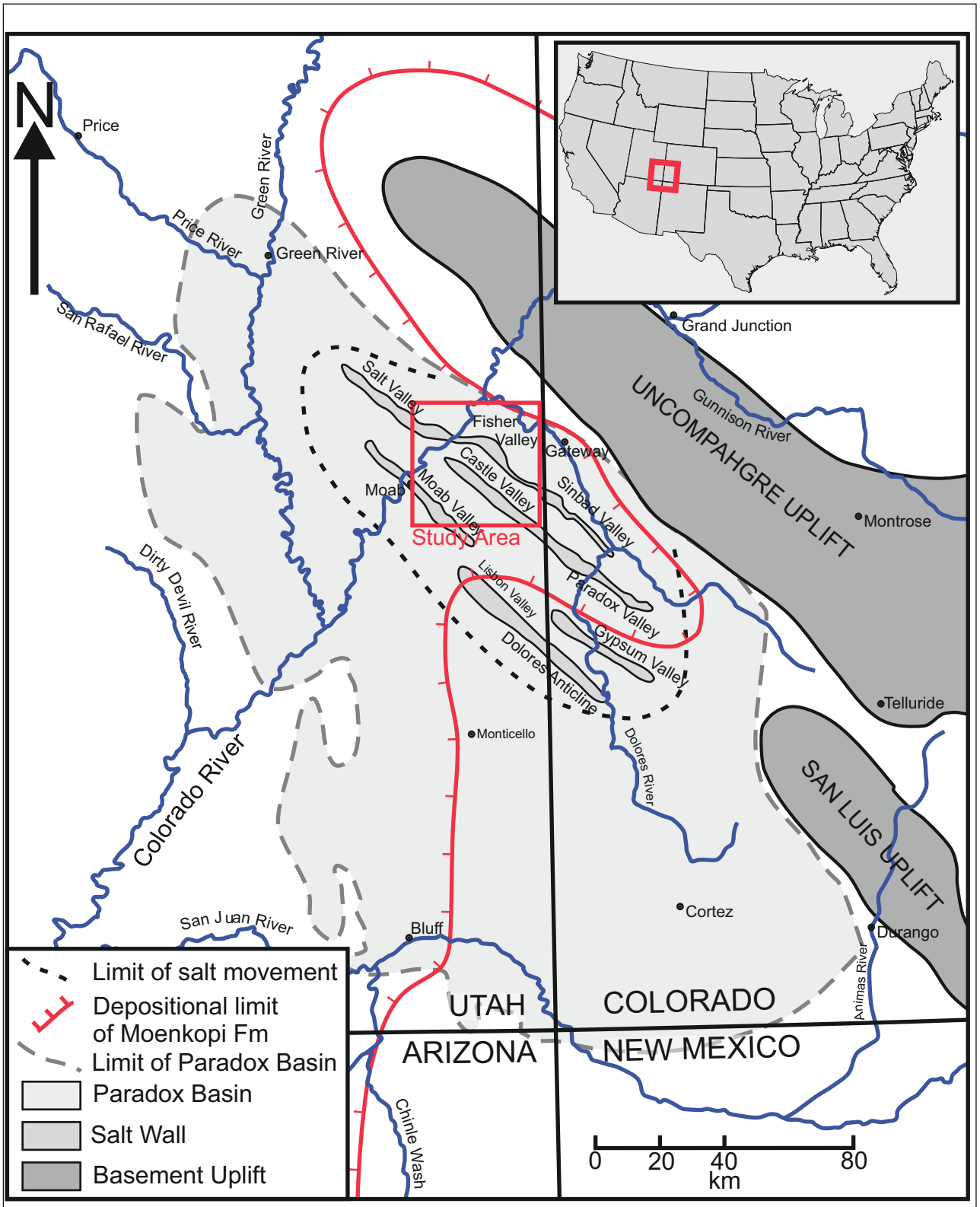


**Figure 4.1**: Regional map of the Paradox Basin and associated Uncompahgre and San Luis uplifts. Map depicts the limits of the Paradox Basin based on the extent of subsurface salt deposits of the Paradox Formation, and the depositional limit of the Moenkopi Formation (modified in part from Barbeau, 2003; Condon, 1997; Shoemaker & Newman, 1959; Stewart *et al.*, 1972).

Pennsylvanian to the late-Permian, in excess of 4000 m of strata accumulated in the foredeep, directly adjacent to the frontal thrust that bounded uplifted Precambrian basement rocks of the Uncompahgre Uplift (Elston *et al.*, 1962). Erosion of the Uncompahgre Uplift yielded much of the clastic detritus that filled the proximal part of the Paradox Basin, resulting in the south westward progradation of a large alluvial clastic wedge (Mack & Rasmussen, 1984; Barbeau, 2003). During the initial stages of formation, the foredeep of the Paradox Basin experienced a series of transgressive-regressive events and cycles accumulated in response to glacio-eustatic sea-level changes recorded by the pattern of sedimentation in the Hermosa Group (Goldhammer *et al.*, 1991; Blakey & Ranney, 2008; Williams, 2009). During episodes of falling relative sea-level, the basin was partially isolated from a regional sea-way by the basin fore-bulge, causing dense brines to develop in the foredeep of the basin. Repeated desiccation and recharging of these brines resulted in accumulation of the Paradox Formation (Doelling, 1988), a unit characterised by cyclic deposits of salts (anhydrite, halite and potash) interbedded with marls and black shales (Hite, 1968; Williams-Stroud, 1994; Rasmussen & Rasmussen, 2009). From the late Pennsylvanian (Missourian to Virgilian) to the early Permian (Wolfcampian), the growing alluvial clastic wedge constructed from detritus derived from the eroding Uncompahgre Uplift prograded further into the foreland basin, though alluvial sedimentation was periodically interrupted by widespread marine incursions that gave rise to the accumulation of thin but laterally extensive shallow-marine carbonate intervals throughout the Missourian to Wolfcampian, as represented by the Honaker Trail Formation (Williams, 1996, 2009) and the overlying lower Cutler beds (Blakey 2009; Jordan & Mountney, 2010, 2012).

Initial movement of the salt layers of the Paradox Formation occurred in response to loading by sediments of the Honaker Trail Formation and lower Cutler beds during late-Pennsylvanian and early Permian (Trudgill *et al.*, 2004), as demonstrated by structural basin modelling (Paz *et al.*, 2009; Rasmussen & Rasmussen, 2009; Kluth & Du Chene, 2009; Trudgill, 2011). The sites of initiation of salt-wall development were controlled by a series of normal faults aligned in an orientation parallel to the Uncompahgre Front:

these faults were activated by flexural downwarping of the developing foredeep (Baars, 1966, Friedman *et al.*, 1994; Doelling, 2002b). Similar basement-fault arrays control the geometries of growing salt-walls in the Central North Sea (Smith *et al.*, 1993; Hodgson *et al.*, 1992). As the effects of sediment loading continued to drive subsurface salt withdrawal and migration into a series of growing salt walls, so a series of salt-walled mini-basins began to develop (Fig. 4.1), initially in the foredeep of the Paradox Basin where the salt layers of the Paradox Formation were thickest and the thickness of overburden greatest (Jones, 1959). Accelerated rates of mini-basin development and ensuing salt-wall growth occurred in the most proximal part of the Paradox Basin in response to additional sediment loading associated with the progradation of a thick alluvial clastic wedge of the Cutler Group, an alluvial mega-fan that prograded south westward into the basin from the Uncompahgre Uplift (Mack & Rasmussen, 1984; Barbeau, 2003; Cain & Mountney, 2009, 2011; Trudgill, 2011). The proximal part of the alluvial clastic wedge of the so-called undifferentiated Cutler Group (Newberry, 1861; Dane, 1935), which accumulated during the main phase of mini-basin evolution, exhibits substantial thickness variation between mini-basins and over salt walls (Trudgill, 2011). Fluvial deposits of this unit demonstrate abrupt and repeated changes in palaeoflow direction that can be shown to have been directly influenced by concomitant salt-wall growth and basin subsidence (Trudgill, 2011; Venus *et al.,* 2014). Salt withdrawal from beneath the basins occurred at the greatest rates adjacent to the developing salt walls, eventually culminating in grounding of the floor of the basins on underlying basement beneath these points and resulting in the trapping of salt remaining beneath the centres of the mini-basins. This resulted in the formation of rim synclines at the basin peripheries (Smith *et al.*, 1992; Doelling, 2002b; Trudgill & Paz, 2009; Trudgill 2011). Salt movement via withdrawal from beneath subsiding mini-basins and its lateral migration to maintain growing salt-walls continued throughout the Triassic and Jurassic, although at a significantly reduced rate compared to that during the Permian (Trudgill, 2011).

Throughout the early Triassic (Induan to Olenekian - Morales, 1987; Rasmussen & Rasmussen, 2009), the Moenkopi Formation accumulated

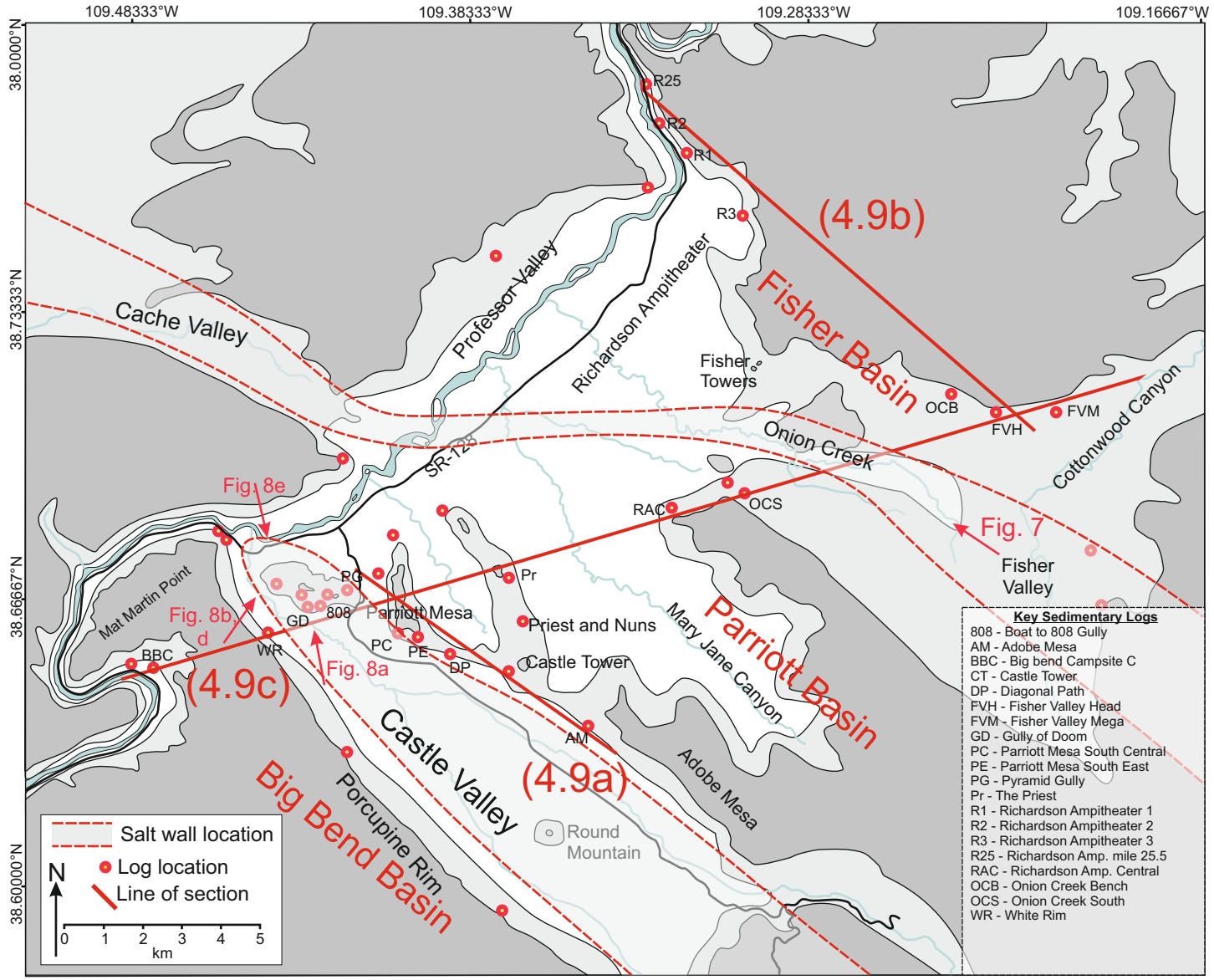


**Figure 4.2**: Overview map of the Salt Anticline Region and study area. Map depicts the location of measured sedimentary sections, and lines of correlation panels. Map centre: 38.70ºN, 109.324ºW; geodetic system: WGS 84. Red arrows indicate location and direction of photographs in diagrams.

across a laterally extensive area now represented by large parts of the states of Arizona, New Mexico, Colorado, Utah and Nevada (Ward, 1901; Darton, 1910; Gregory, 1917; Stewart, 1959; Cater, 1970; Blakey, 1974, 1989; Hintze & Axen, 1995). Regionally, this formation accumulated in an overall mixed fluvial and paralic (coastal) setting, with a region-wide marine regression dictating the style of sedimentation (Blakey, 1973). In the Salt Anticline Region (Fig. 4.2), the Moenkopi Formation has been the subject of several previous studies, most notably by Baker *et al.* (1927), Dane (1935), and Shoemaker & Newman (1959). Here, the Moenkopi Formation consists of four members: the Tenderfoot, Ali Baba, Sewemup and Parriott (Fig. 4.3; Shoemaker & Newman. 1957 & 1959). The name “Parriott” has been used here to reflect the current cartographic convention; this differs from “Pariott” as used by Shoemaker & Newman (1959).

The provenance of sediment for the Moenkopi Formation in the Salt Anticline Region varies between the mini-basins, indicating that uplifted salt walls were effective in partitioning fluvial systems with different source areas. The Uncompahgre and the San Luis uplifts to the northeast and southeast, respectively (Fig. 4.1), were the principal sediment sources and these uplifts represented the only significant upland areas from which palaeo-fluvial systems likely originated (Cadigan & Stewart, 1971; Mattox, 1968; Stewart *et al.*, 1972; Barbeau, 2003). Although at a regional scale the Moenkopi Formation records accumulation in a mixed fluvial and paralic setting, with conditions becoming increasingly marine-influenced towards the northwest (Blakey, 1973), the environment of deposition in the Salt Anticline Region is considered to be that of an arid alluvial plain over which ephemeral streams passed toward a regressing palaeo-shoreline that lay 100 to 300 km the northwest, in the area now occupied by Central Utah (Stewart *et al.*, 1972; Lawton & Buck, 2006; Blakey & Ranney, 2008). The Moenkopi Formation in the study region represents the preserved succession of a largely non-confined alluvial braidplain that preserves a mix of sheet-like and braided-channel fluvial sedimentary architectures.

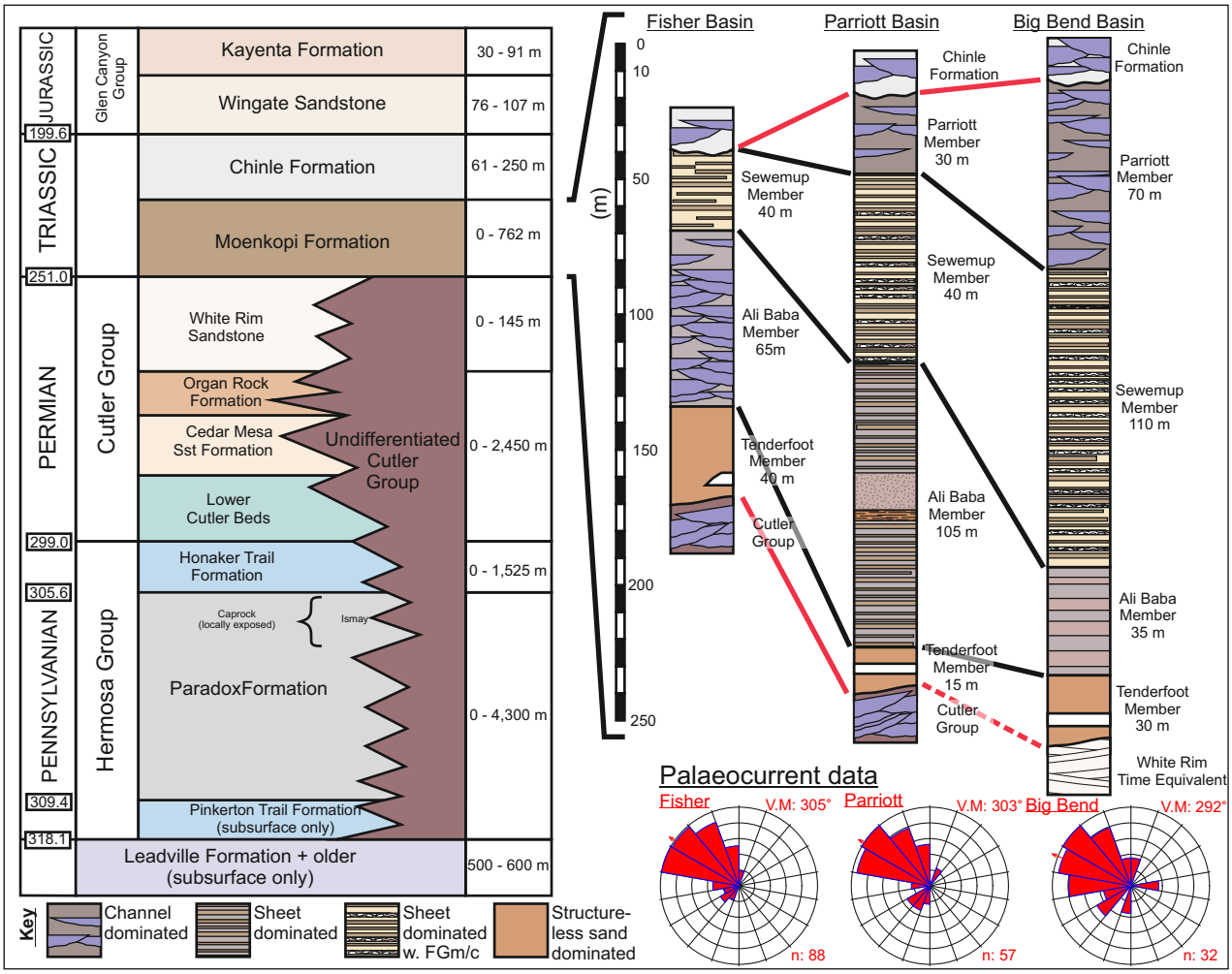


**Figure 4.3**. Regional stratigraphic column and palaeocurrent summary data. Column depicts the average thickness of the various stratigraphic units in the Salt Anticline Region, and average thicknesses of Moenkopi Formation and its constituent members within the individual studied mini-basins. Palaeocurrent summary data for each mini-basin are plotted as rose diagrams for which vector mean, vector magnitude, and number of recorded readings are shown. Regional stratigraphic column after Trudgill (2011).

## *4.3 Methods and Data Collection*

Fifty-two sections were measured in the Salt Anticline Region, recording a total of ~9000 m of succession from the Moenkopi Formation (see Fig. 4.2 for log locations and Fig. 4.4 for representative examples). Of these, 23 measured sections record the entire preserved thickness of the Moenkopi Formation from the top of the underlying Undifferentiated Cutler Group to the base of the overlying Chinle Formation; all other sections record significant proportions of the succession, including either the base or top of the formation in each case.

Sixteen distinct lithofacies are recognised (Table 4.1; Fig. 4.5), of which most are interpreted to have been generated by a range of fluviatile behaviour involving both channelised and non-channelised flow processes (F prefix to facies code); some lithofacies are ascribed to non-fluvial origins in related palaeoenvironmental settings, including shallow, ephemeral lakes and salt flats. Architectural elements (Fig. 4.6) have been defined according to their geometry and their internal lithofacies composition based on the approach described by Miall (1985, 1996). Palaeocurrent data were collected to determine the direction of drainage: 177 indicators of flow direction were taken from asymmetric ripple casts (Frc), climbing ripple strata (Frc/Fxl), trough cross-bedding (Fxt) and high-angle-inclined planar cross-bedding (HA Fxp). From these palaeocurrent data, vector mean and vector magnitude were calculated using the methodology described by Lindholm (1987).

Scaled drawings (panels) depicting the distribution of fluvial architectural elements both within a single mini-basin and between adjacent mini-basins have been constructed by lateral tracing and correlation of key surfaces in the field and supported by analysis of photomontages. Architectural panels have been tied to measured sections to enable the generation of a series of models with which to depict important tectono-stratigraphic relationships.

## *4.4 Styles of mini-basin fill*

The sedimentary record of the style of interaction between mini-basin subsidence and salt-wall growth due to subsurface halokinesis is recorded in

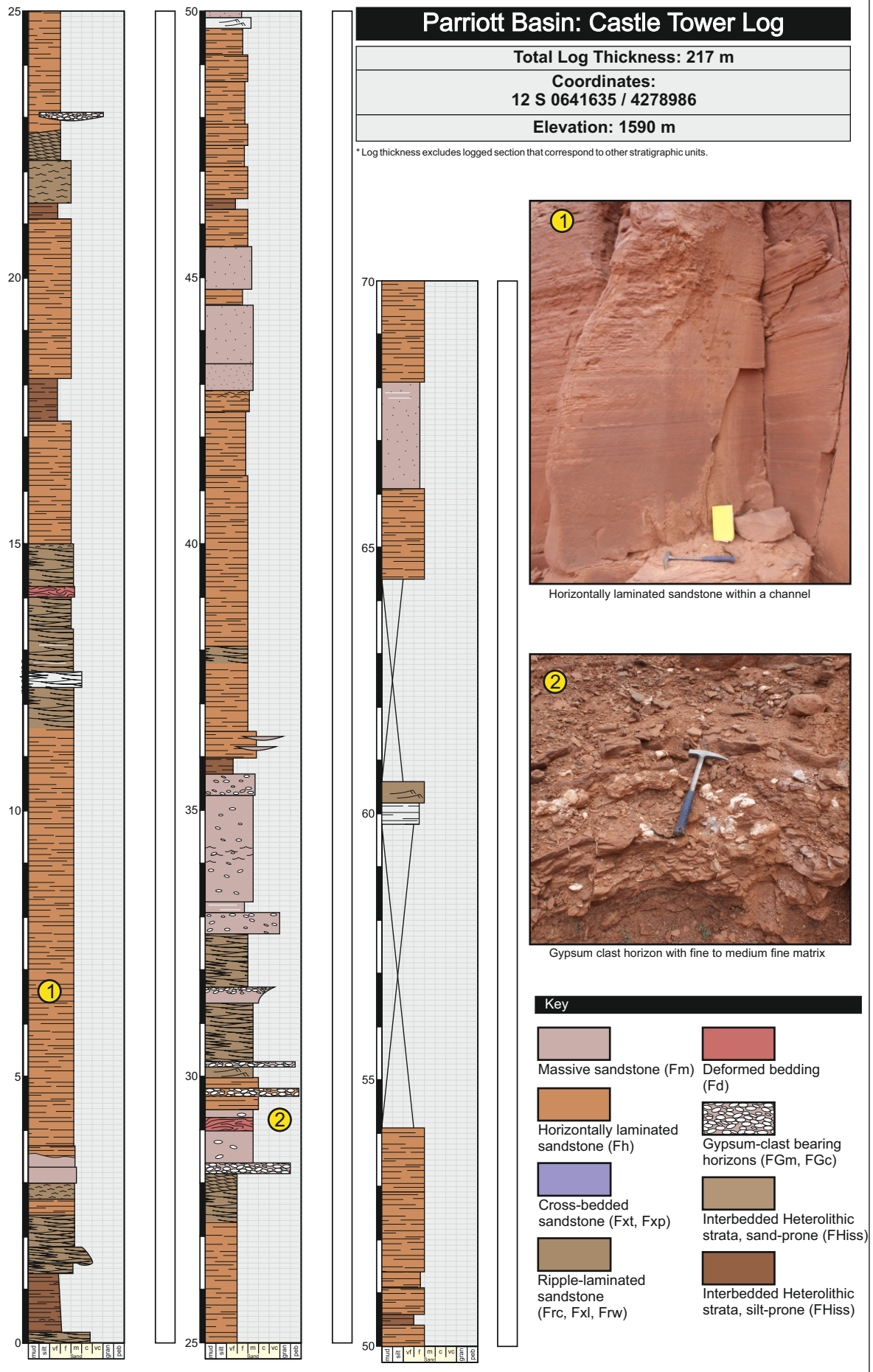


**Figure 4.4**: Representative measured sections from the 3 studied mini-basins

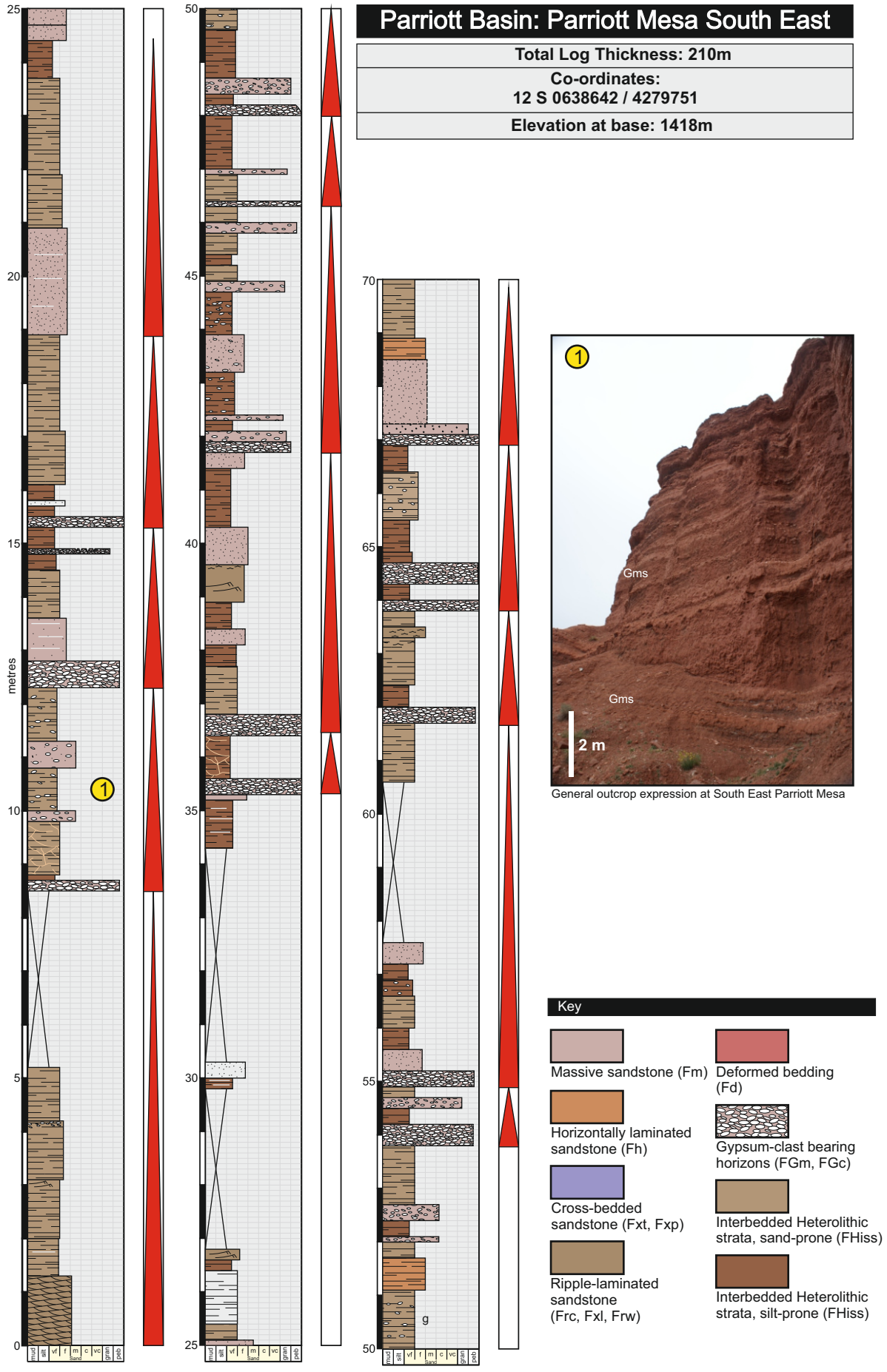


**Figure 4.4 cont.**: Representative sedimentary log section of part of the Moenkopi Formation exposed at South East Pariott Mesa.

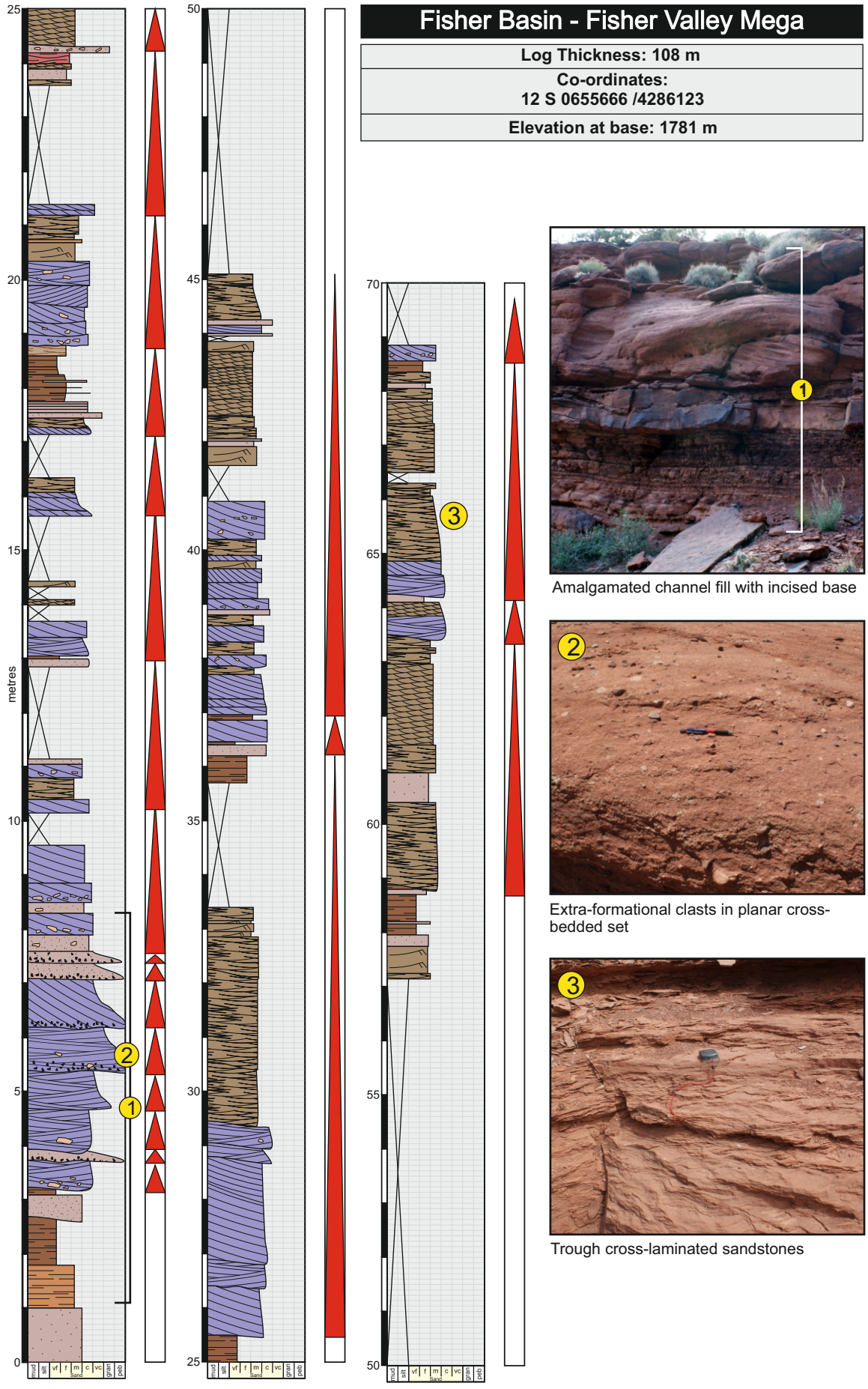


**Figure 4.4 cont**: Representative sedimentary log from the Fisher Valley (Cottonwood) area.

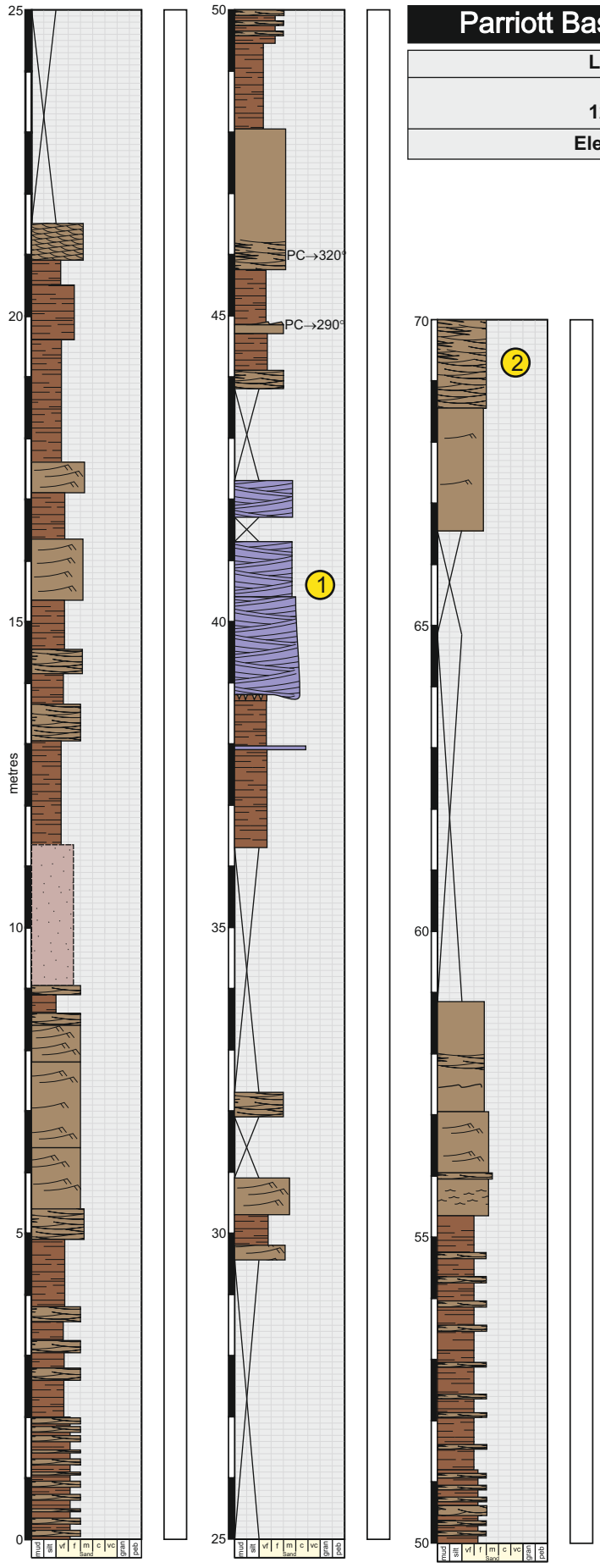

Fluvial channel elements composed of trough cross-bedded sandstones

Trough cross-laminated sandstones, passing into climbing-ripple stratification; indicative of sinuous-crested climbing ripple traction deposits

**Figure 4.4**: Representative measured sections from the 3 studied mini-basins

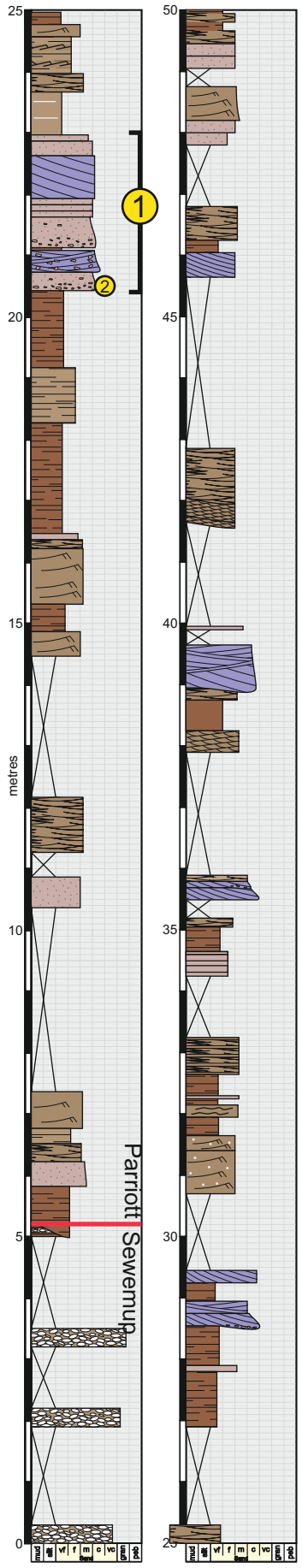


## Big Bend Basin - Big Bend Campsite C

| |
|---|
| **Total Log Thickness: 75 m** |
| **Coordinates: 12 S 631964 / 4279163** |
| **Elevation: 1228 m** |

* Log thickness excludes logged section that correspond to other stratigraphic units.

Outcrop expression of channel belt within the Parriott Member

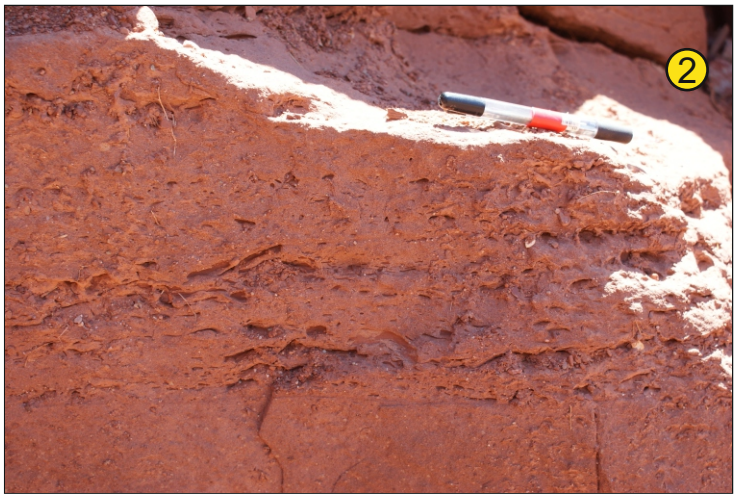


Rip-up clasts within massively-bedded sandstone

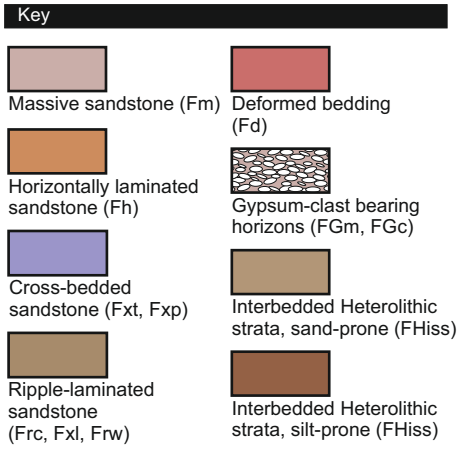


**Figure 4.4 cont.**: Representative measured sections from the 3 studied mini-basins

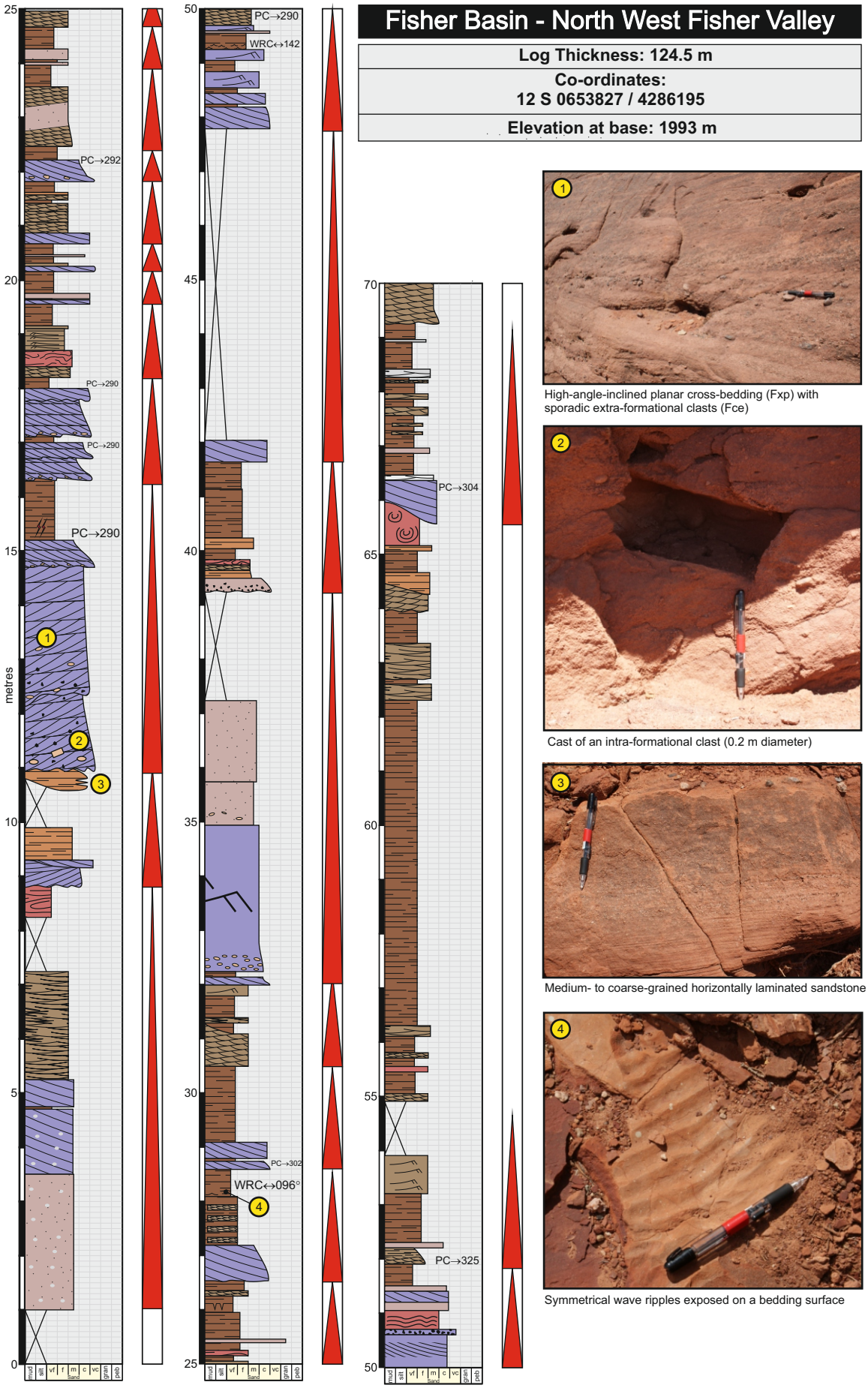


**Figure 4.4 cont.**: Representative measured sections from the 3 studied mini-basins.

| Code | Facies | Colour | Grain size &Texture | Composition | Primary Sed. Structures | Interpretation |
|---|---|---|---|---|---|---|
| **Fm** | Massive | Orange-brown | V.Fine to V.Coarse. Ang to SR | Quartzo-feldspathic sand | Some graded bedding | Rapid deposition from suspension |
| **Fxt** | Trough cross-bedding | Purple-brown to orange-brown | Medium to Coarse. Mod. Sorting, SA-SR | Quartzo-feldspathic sand | Trough cross-bedding | Downstream migration of sinuous-crested dune-scale mesoforms |
| **ha Fxp** | High-angle planar cross-bedding | Purple-brown to orange-brown | Medium to Coarse. Mod. Sorting, SA-SR | Quartzo-feldspathic sand | Trough cross-bedding | Straight-crested or sinuous-crested dunes migrating within a fluvial channel (can be trough cross-bedding rotated through 90 degrees) |
| **la Fxp** | Low-angle planar cross-bedding | Purple-brown to orange-brown | M.Fine to Coarse. Mod. Sorting SA-SR | Quartzo-feldspathic sand | Low-angle planar cross-bedding | Migration of lateral accretion mesoforms |
| **Fxl/Frc** | Cross laminated / climbing ripple strata | Orange-brown to red-brown | V.Fine to Medium. Mod. Sorting, SA - SR | Quartzo-feldspathic sand | Current ripple lamination: sub- to super-critical climb | Unidirectional migration of microforms within channels or unconfined flows under low flow regime. Fxl is the preserved expression of sinuous-crested climbing ripples. Frc may be sinuous- or straight-crested. |
| **Fh** | Horizontally laminated | Orange-brown, red-brown or red-grey | V.Fine to Fine. Mod - Well sorting, SA-SR | Quartzo-feldspathic sand | Primary current lineation; normal grading | Deposition from upper-flow regime, either from channel flow or from non-confined sheet flow |
| **Fci** | Intrafomational clasts | Dark-brown clasts; light-brown matrix | 5mm to 70mm clasts, Fine to Medium matrix | Mudstone clasts and sandstone | Weak imbrication | Represents erosion and re-deposition of locally reworked sediments in channel-belt and floodplain areas |
| **Fce** | Extraformational clasts | Green, purple, reds & white | 5mm to 70mm clasts, Fine to Medium matrix | Basement lithologies | Weak imbrication if matrix supported | Represents transportation of basement clasts into the depositional environment, possibly by a high-energy flood event |

**Table 4.1 : Table of Lithofacies**

| Code | Facies | Colour | Grain size &Texture | Composition | Primary Sed. Structures | Interpretation |
|---|---|---|---|---|---|---|
| **FGm** | Gypsum clasts; matrix supported | White clasts with orange or chocolate-brown matrix | 10mm to 150mm clasts, Fine to Medium matrix | Gypsum and sand matrix | | Generated during episodes of salt-wall breaching at surface. Represents slow rates of salt delivery in areas proximal to salt wall, or location distal from salt wall |
| **FGc** | Gypsum clasts; clast supported | White clasts with minor amount of orange matrix | 10mm to 150mm clasts, Fine to Medium matrix | > 80% gypsum clasts. | Weak imbrication | Generated during episodes of salt-wall breaching at surface. High rates of delivery of salt clasts in areas proximal to the salt wall |
| **Gc** | Crystalline gypsum bed | White to grey | Crystalline | >95% gypsum | May display inclined or horizontal lamination | Clinoforms generated by gypsum aeolian dune form migration (Lawton & Buck, 2006) |
| **Gb** | Gypsum-bound sandstone | Orange-Brown to "Cutler purple"-brown | Usually Fine to Medium. Poor sorting, Angular | Gypsum cement | Usually massive bedding | Origin possibly by post-depositional throughflow of dissolved gypsum resulting in cementation |
| **Fd** | Deformed bedding | Orange-brown to chocolate-brown | V.Fine to Med. grain. Mod to Poor, SA-SR | Quartzo-feldspathic sand | Horizontal lamination; current-ripple lamination | Soft-sediment deformation resulting from loading of unconsolidated sediments and associated water-escape. Slumps may indicate movement of sediment down slope, syn or post deposition |
| **Scls** | Crinkley Laminated sandstones | Orange sst. | Fine to Med. Sandstone SA-SR | Quartzo-feldspathic sand, and silt | Crinkelly laminations: laminations are discordant | Represents disruption of sedimentary structures by ground water movement by capillary action (Goodall *et al.* , 2000) |
| **WR** | Wave ripple strata | Orange to chocolate-brown or grey | V.Fine to M.Fine sandstone. | Quartzo-feldspathic sand | Symmetrical ripple forms | Represents bi-directional flow created by surface waves on shallow-water ponds on the alluvial plain |
| **Fhiss** | Horizontally interbedded silts and sands | Orange sst., with chocolate brown silt | Fine to Coarse sst., and silt. Poor sorting | Quartzo-feldspathic sand, and silt | Can contain Facies **WR, Fm, Frc/Fxl, Fh, rare Fci** | Represents multiple flood events where progressively finer material is deposited with corresponding sedimentary structures from a waning flow. |

**Table 4.1 cont.: Table of Lithofacies**

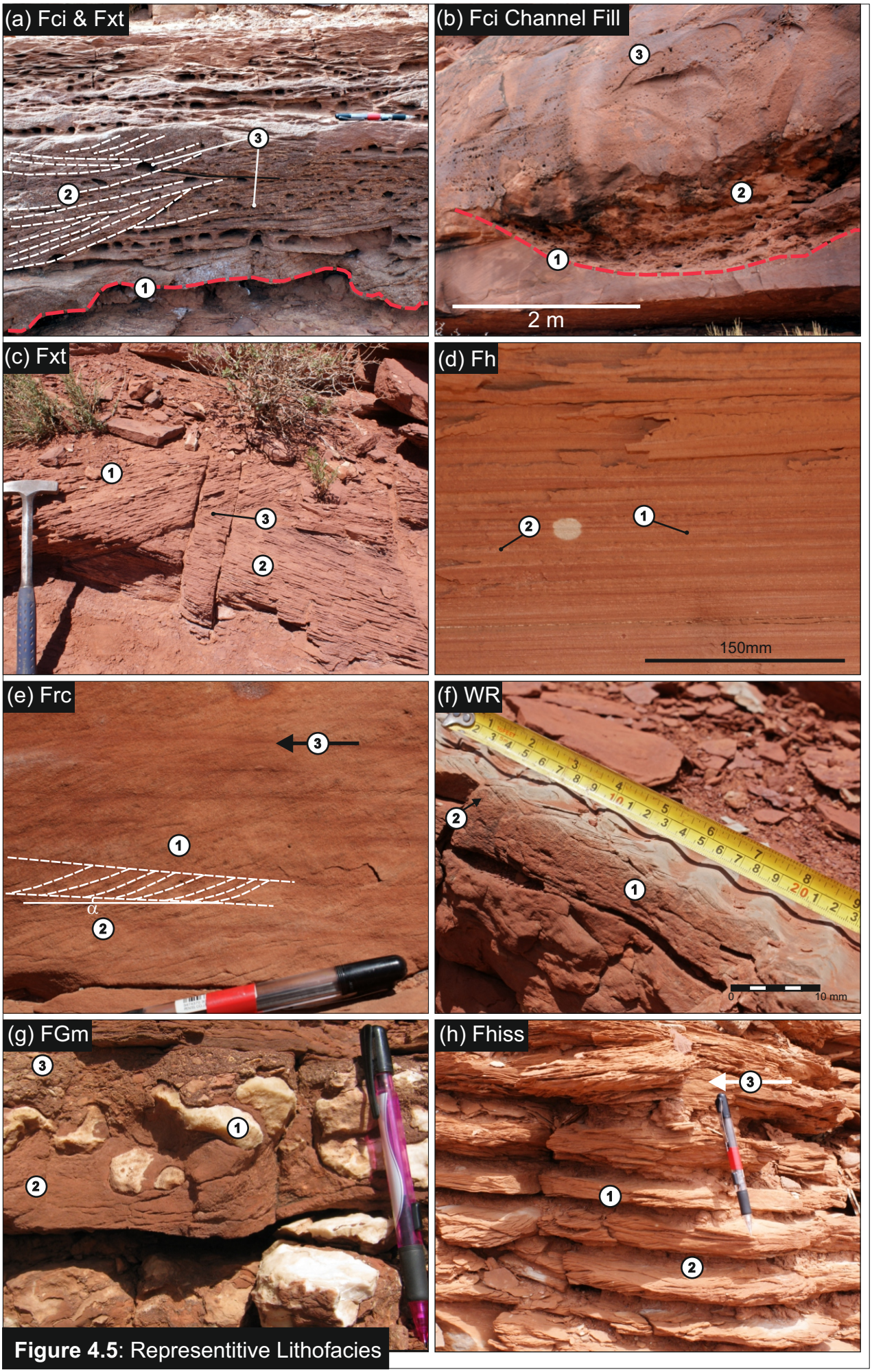


**Figure 4.5**: Representitive Lithofacies

***Figure 4.5:*** *Representative lithofacies of the Moenkopi Formation in the Salt Anticline Region. See Table 1 for explanation of lithofacies codes. (a) Trough cross-bedded sandstone (Fxt) with intraformational clasts (Fci). 1: Underlying erosive base. 2: Medium- to coarse- grained trough cross-bedded sandstone facies with a high proportion of intraformational clasts. 3: Clasts are angular to sub-rounded. (b) Fluvial channel filled with intraformational clasts (Fci). 1: Channel incised into underlying HA Fxp facies. 2: Fluvial channel filled with orthoconglomerate; pebble-grade clasts of intraformational origin (Fci). Matrix is medium- to coarse-grained sandstone. 3: Cross-bedded sandstone set of medium-grained sandstone with isolated pebble-grade clasts of intraformational origin. (c) Trough cross-bedded sandstone (Fxt). 1: Larger-scale cross-bedding is indicative of larger bedforms developed in main channels. 2: Thin foresets within troughs. 3: Intersecting trough cut-offs in sections perpendicular to flow generated by the migration of sinuous-crested dunes with out-of-phase successive bedform crestlines. (d) Horizontally laminated sandstone (Fh). 1: Horizontally laminated sands composed of fine-grained sandstone exhibit thinner laminations than in examples composed of coarse-grained sandstone. 2: Colour mottling and reduction associated with slightly less permeable layers. (e) Climbing ripple strata (Frc). 1: Subcritical climbing ripple stratification in sets composed of fine- to medium-grained sandstone. 2: Positive but subcritical angle-of-climb. 3: Palaeoflow direction. (f) Wave-ripple laminated sandstone (WR). 1: Ripple forms preserved on upper bedding surface seen in section and exhibiting a combination of chevron-style accumulation and draping of foresets onto ripple-crests. 2: Some examples of asymmetric ripples indicate mixed unidirectional and bidirectional flow regime typical of sluggish flow in shallow water influenced by surface wind shear. (g) Gypsum-clast-bearing unit; matrix supported (FGm). 1: Gypsum clasts are sub-angular: indicative of short transport distance. 2: Matrix-supported nature of sets indicates deposition by debris flow or water flow. 3: Pebble-grade clast horizon overlain by coarse-grained granulestone of gypsum micro-conglomerate, indicating disaggregation of larger clasts in higher energy flows, or possibly indicative of longer transport distances. (h) Horizontal interbedded sandstones and siltstones (Fhiss). 1: Subcritical climbing ripple strata in fine-grained sandstone. 2: Thin beds of climbing ripple strata are interbedded with thin sets of siltstone. 3: Palaeoflow direction.*

# Representative Architectural Elements

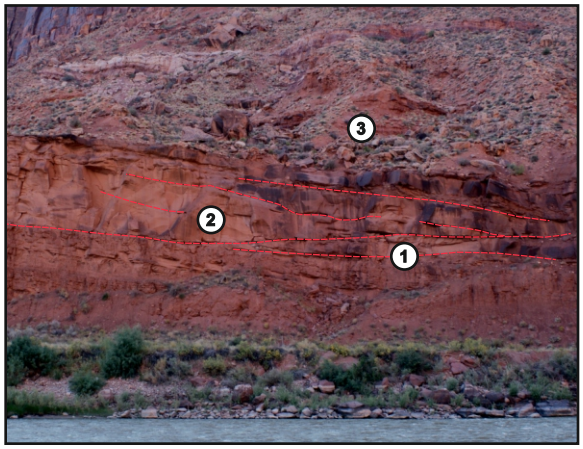


## F1 - Amalgamated Channel Elements

| | |
|---|---|
| Element description | Multi-storey, multi-lateral channel elements |
| Element Type | Confined flow |
| Geometries | Multiple incised and filled channel elements |
| Associated Facies | Fm, Fh Fxt/Fxp, Frc/Fxl, Fce & Fci Lags |
| Vertical Extent | 5 to 10 m |
| Lateral Extent | 500 m to 10s km |

**Key Element Characteristics**

1. Multiple levels of erosive undulating basal contacts.
2. Channel fills are a mixture of Fm, Fxt/Fxp, and Fce & Fci Lags.
3. Amalgamated channel-element complex is superceded by overbank elements.

**Interpretation**

**Represents lateral accretion and vertical stacking of fluvial channel elements over time.**

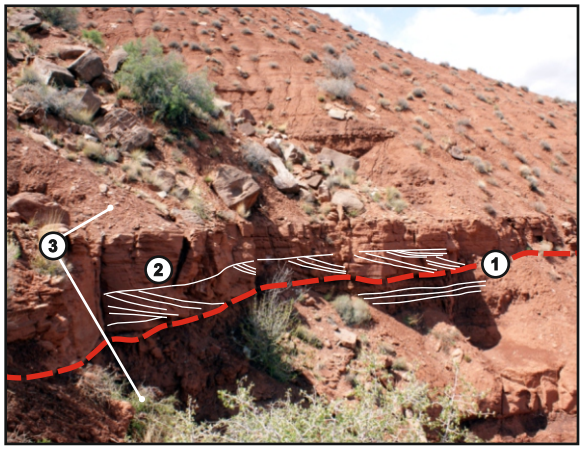


## F2 - Single-Storey Channel Elements

| | |
|---|---|
| Element description | Single-storey, multi-lateral channel elements |
| Element Type | Confined flow |
| Geometries | Channel elements with no vertical stacking |
| Associated Facies | Fm, Fh, Fxt/Fxp, Frc/Fxl, Fce & Fci Lags |
| Vertical Extent | 0.5 to 3 m |
| Lateral Extent | 200 m to 10s km |

**Key Element Characteristics**

1. Erosive undulating basal contact.
2. Trough cross-bedded sandstone (Fxt), with associated climbing ripple-strata (Frc) in channel belt element.
3. Element preceded and superceded by overbank sheet-flood elements (Heterolithic silts and fine sands).

**Interpretation**

**Represents preserved elements created by a single channel or multiple channel migrating laterally on a single horizon.**

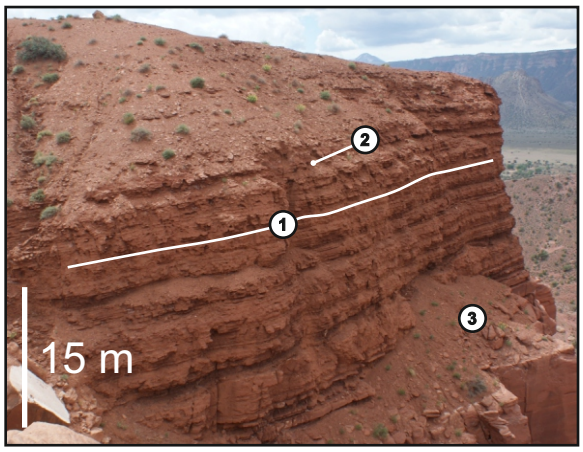


## F3 - Sheet-like Elements (Style 1)

| | |
|---|---|
| Element description | Sheet-like interbedded heterolithic silt and sandstones |
| Element Type | Nonconfined or unconfined flows |
| Geometries | Laterally extensive sheet-like bodies |
| Associated Facies | Fm, Fh, Frc/Fxl, Fci, desication cracks |
| Vertical Extent | 0.2 m to 20 m + |
| Lateral Extent | 500 m to several km's |

**Key Element Characteristics**

1. Very laterally continuous - seen contouring the hill side for several km
2. Can form thick monotonous successions 10s m thick.
3. Friable nature of constituent facies means outcrops tend to weather to scree over any significant distance.

**Interpretation**

**Represents an event where flood water was not confined within channels and sediment transport and deposition happened outside of channel elements.**

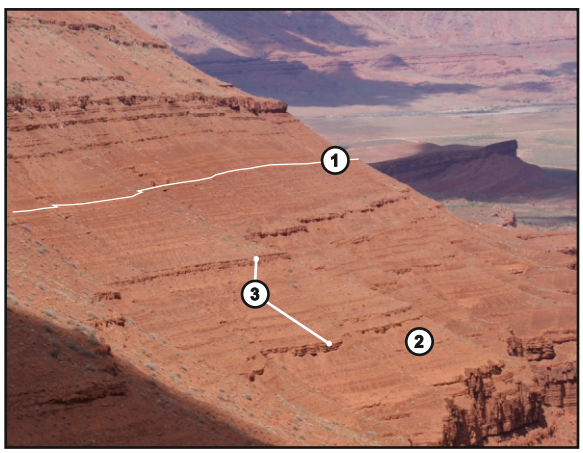


## F3 - Sheet-like Elements (Style 2)

| | |
|---|---|
| Element description | Sheet-like interbedded heterolithic silt and sandstones |
| Element Type | Non or unconfined flows |
| Geometries | Laterally extensive sheet-like bodies, can pinch out |
| Associated Facies | Fm, Fh, Frc/Fxl, Fci, desication cracks |
| Vertical Extent | 0.2 m to 20 m + |
| Lateral Extent | 500 m to several km's |

**Key Element Characteristics**

1. Laterally continuous - seen contouring hill side for several km's.
2. Friable nature of constituent facies means outcrops tend to weather to scree over any significant distance.
3. Channel elements, which are more sand-prone weather proud.

**Interpretation**

**Nature of sheet elements results in these types of elements preferentially degrading to scree, leaving channel elements as short but laterally extensive cliff sections.**

**Figure 4.6**: Representative architectural elements of the Moenkopi Formation, detailing the most common meso-scale elements present in the Salt Anticline Region.

**Figure 4.7a**: Aerial photograph of Fisher Valley and the Onion Creek Diapir. The Onion Creek Diapir is a much younger feature (Pliocene), however has caused deformation within the Undivided Cutler Group. See Fig 4.7b for interpretation.

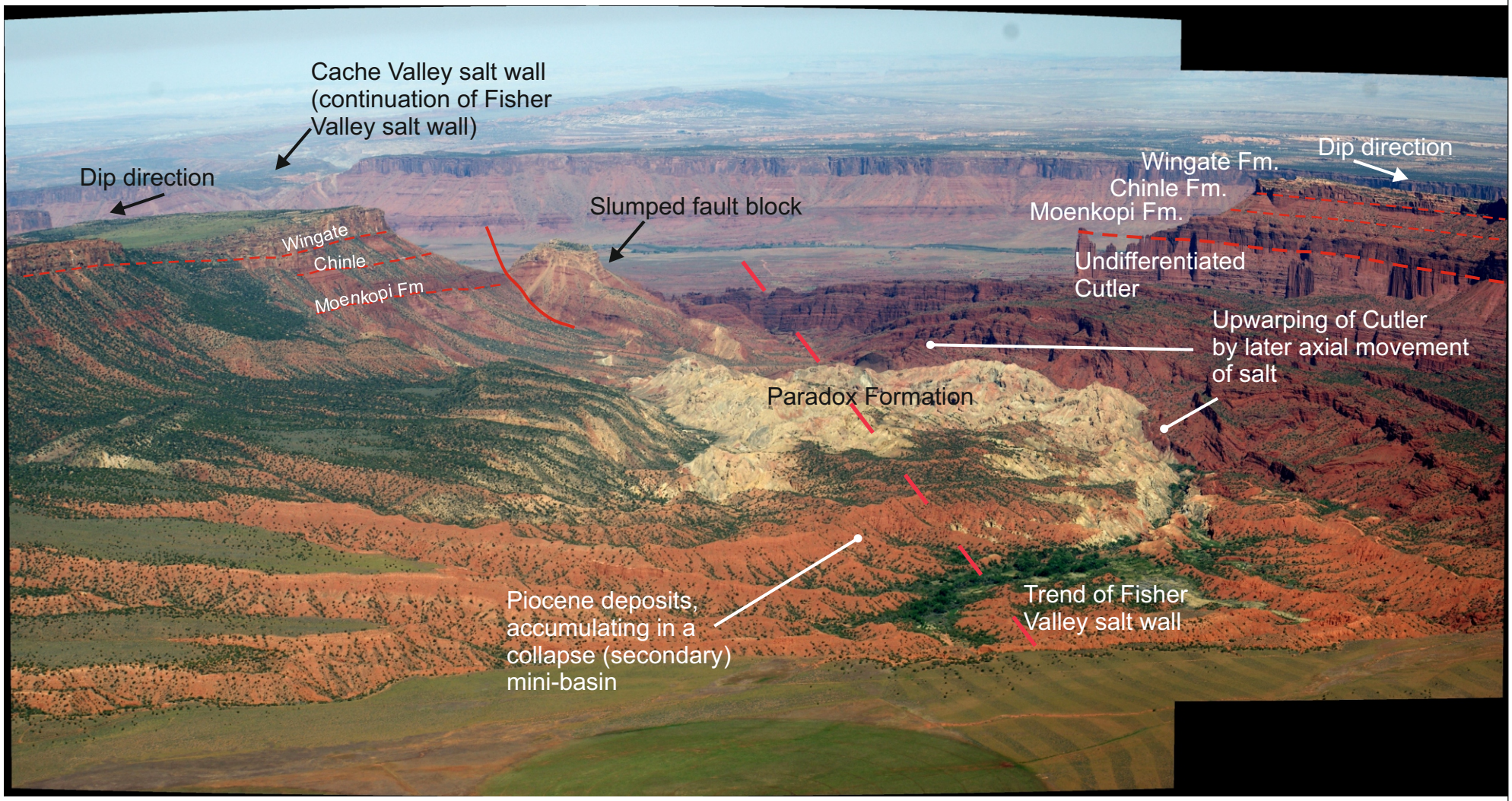


**Figure 4.7b**: Aerial photograph of Fisher Valley and the Onion Creek Diapir. The Onion Creek Diapir is a much younger feature (Pliocene), however has caused deformation within the Undivided Cutler Group.

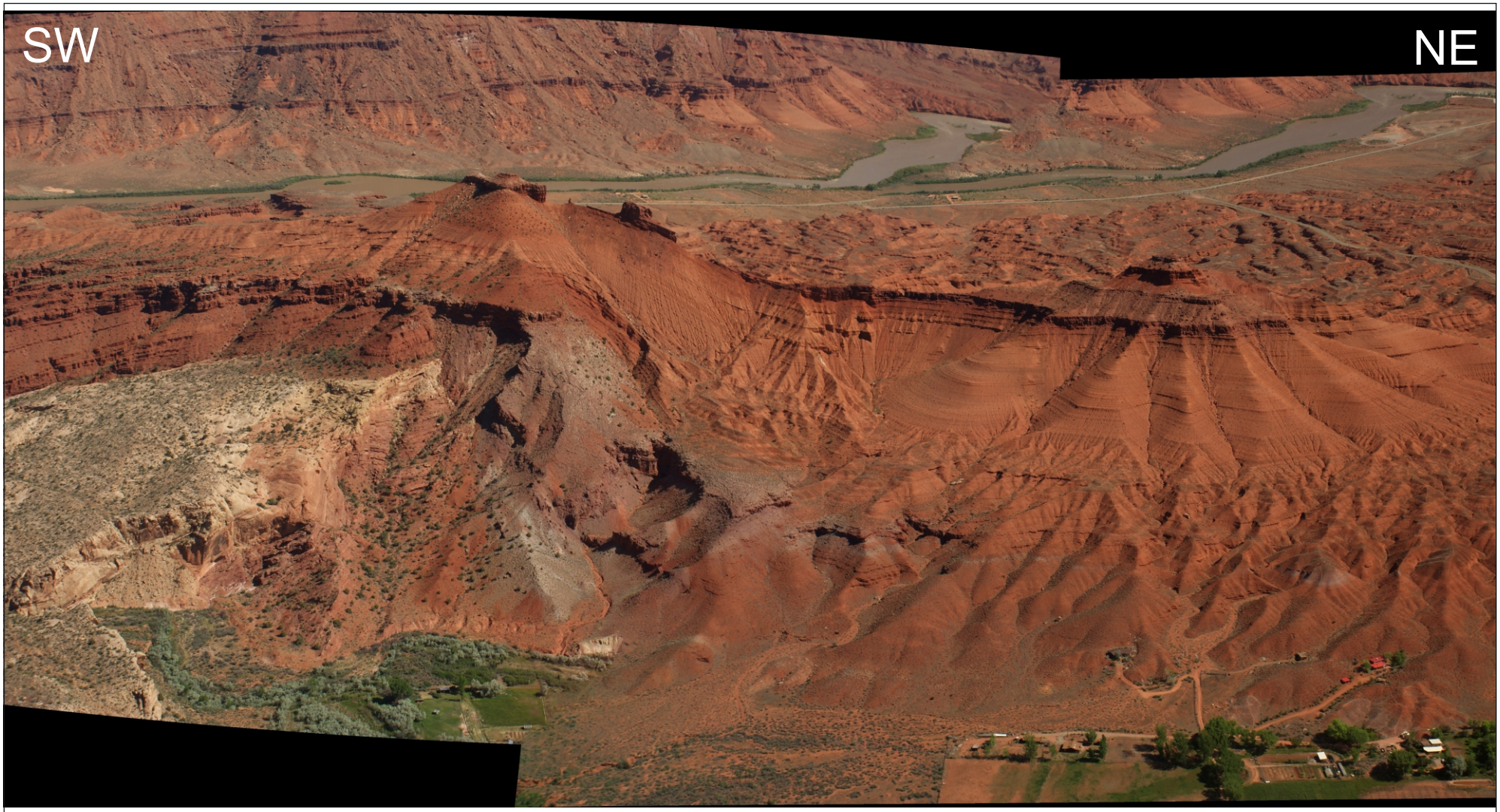


**Figure 4.8a-1**: Aerial photograph of the Red Hills salt-wall collapse structure at the northern end of the Castle Valley salt wall (the so-called “Truck and Boat Structure”). Aerial photograph of the Red Hills (also known as the “Truck and Boat” structure) at the northwest tip of the Castle Valley salt wall. The nature of the uplift is asymmetric, with the western salt-wall flank characterised by a slope geometry and the eastern salt-wall flank characterised by a ramp-flat-ramp trajectory. Note the intraformational unconformity on the west flank of the uplift. See Fig 4.8-2 for interpretation overlay.

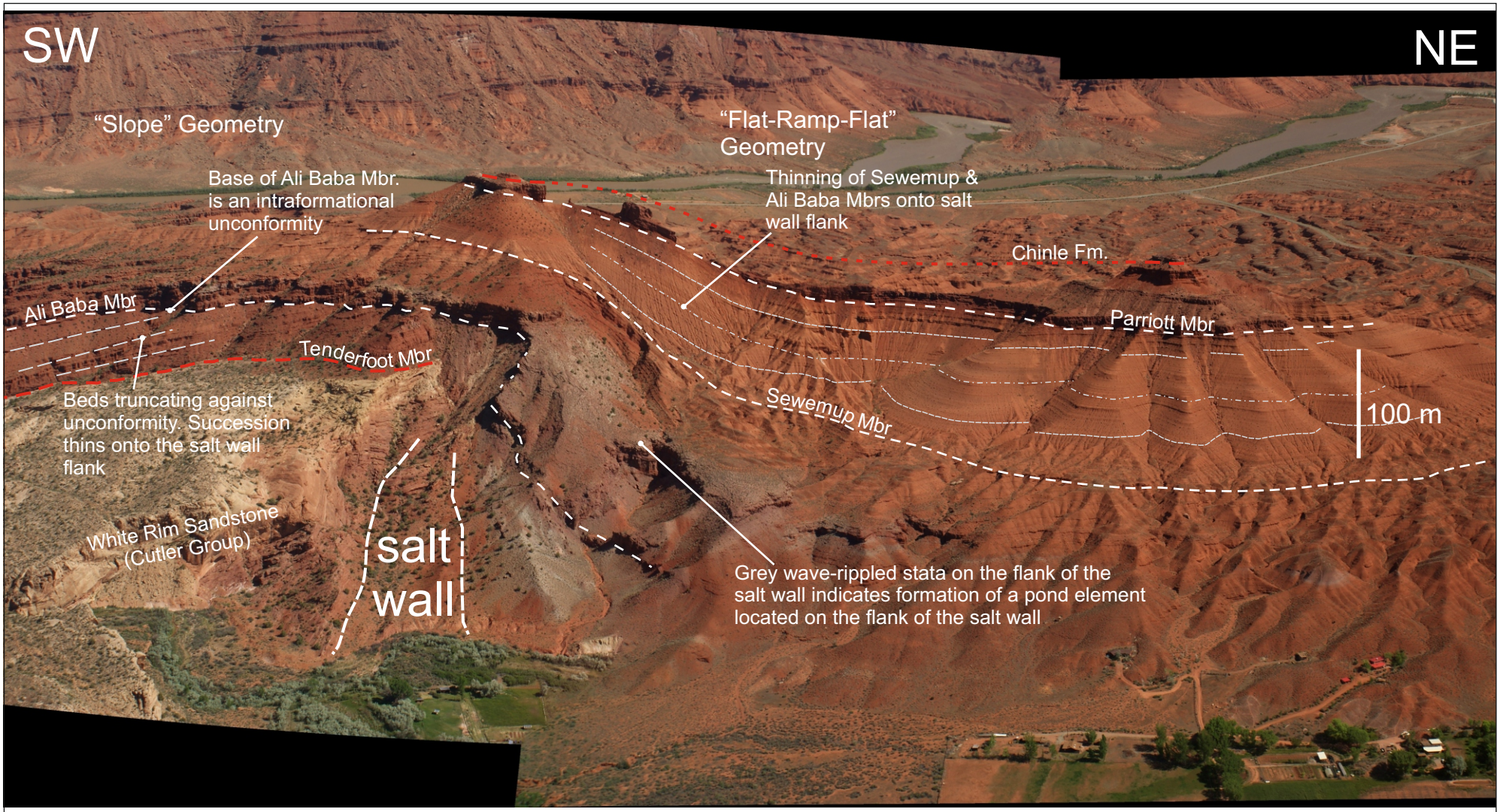


**Figure 4.8a-2**: Aerial photograph with interpretation overlay of the Red Hills salt-wall collapse structure at the northern end of the Castle Valley salt wall (the so-called "Truck and Boat Structure"). Aerial photograph of the Red Hills (also known as the "Truck and Boat" structure) at the northwest tip of the Castle Valley salt wall. The nature of the uplift is asymmetric, with the western salt-wall flank characterised by a slope geometry and the eastern salt-wall flank characterised by a ramp-flat-ramp trajectory. Note the intraformational unconformity on the west flank of the uplift.

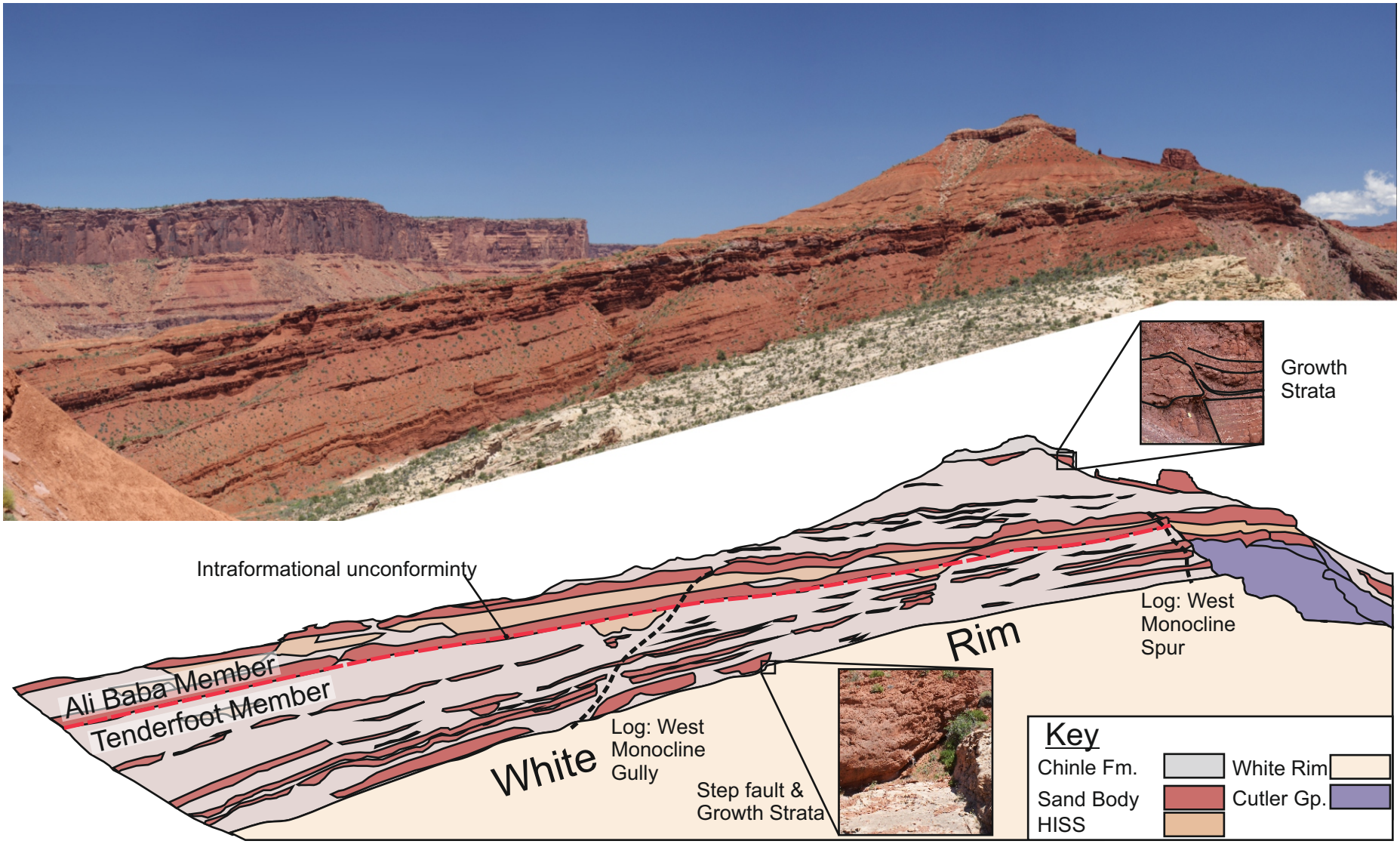


**Figure 4.8b**: Photograph and interpretation panel of the western salt-wall flank slope geometry. Abundance of channel sand-body occurrence decreases upslope toward the crest of the salt wall. The succession thins by 25 m between the two logs, which are situated 270 m apart. High resolution photographs of growth strata depicted in the inserts are available in the on-line supplementary material.

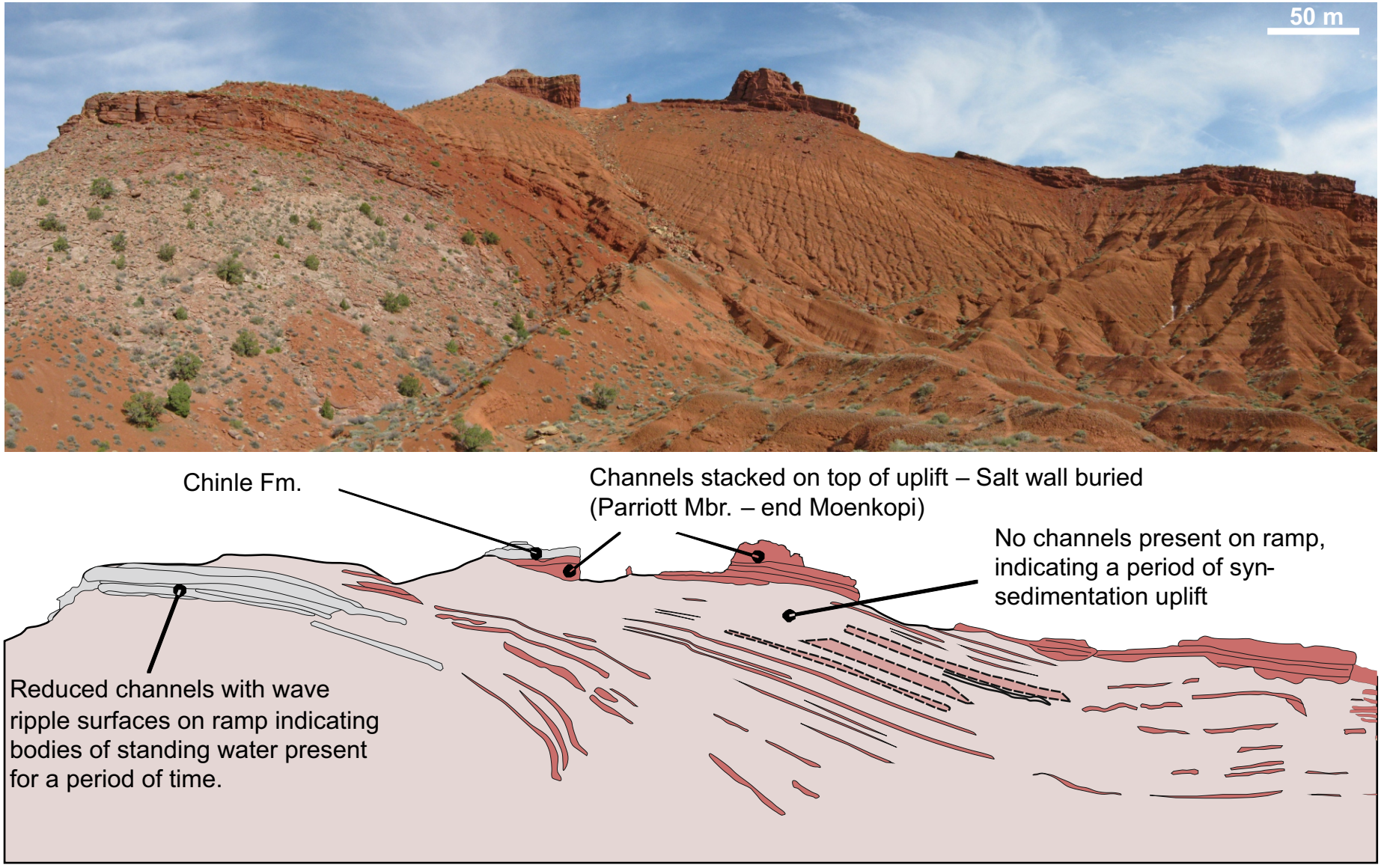


**Figure 4.8c**: Relationship of fluvial strata of the Moenkopi Formation and their thinning against the flat-ramp-flat structure on the south side of the Truck and Boat salt uplift structure, Castle Valley salt wall.

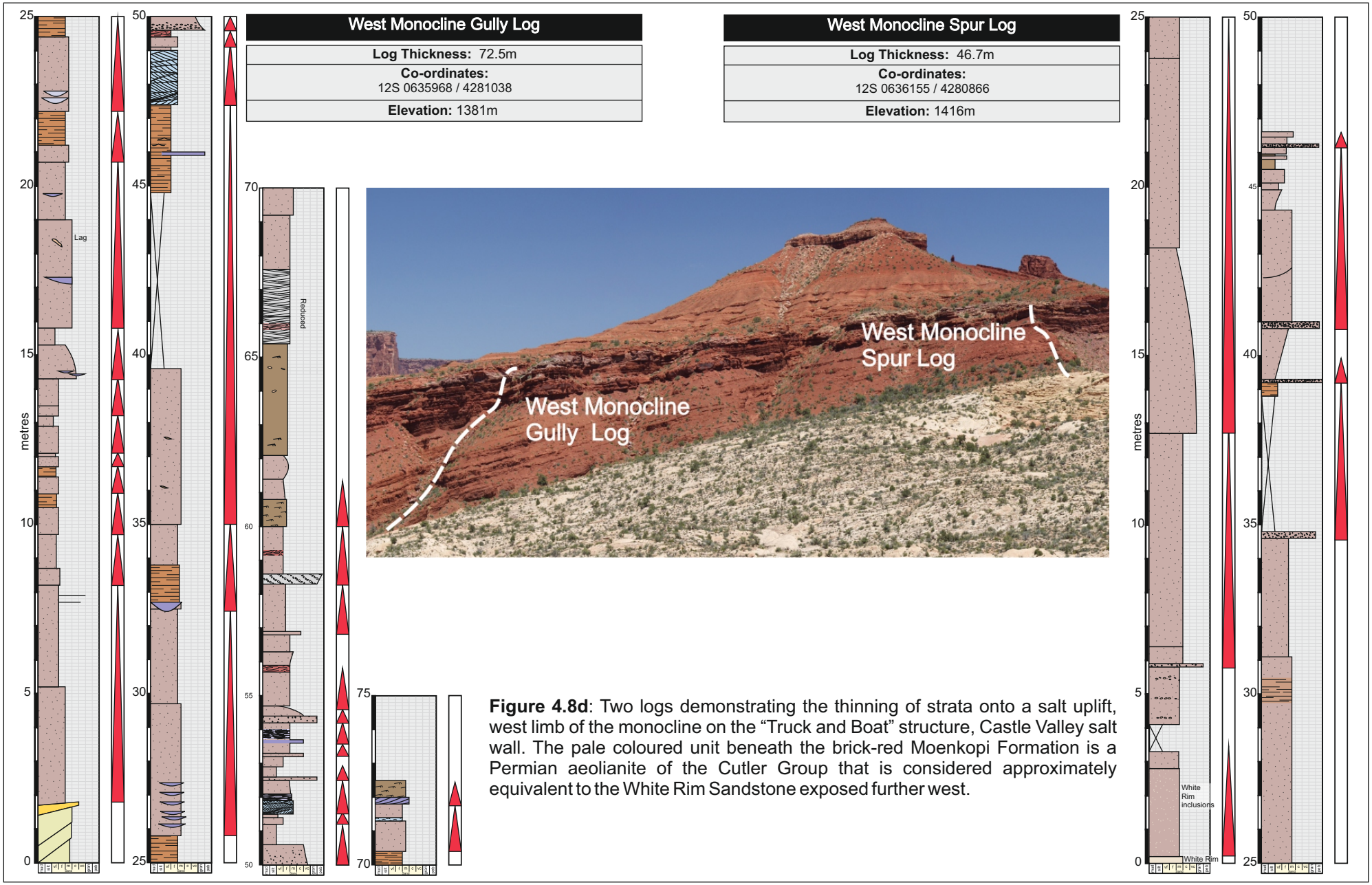


**Figure 4.8d**: Two logs demonstrating the thinning of strata onto a salt uplift, west limb of the monocline on the "Truck and Boat" structure, Castle Valley salt wall. The pale coloured unit beneath the brick-red Moenkopi Formation is a Permian aeolianite of the Cutler Group that is considered approximately equivalent to the White Rim Sandstone exposed further west.

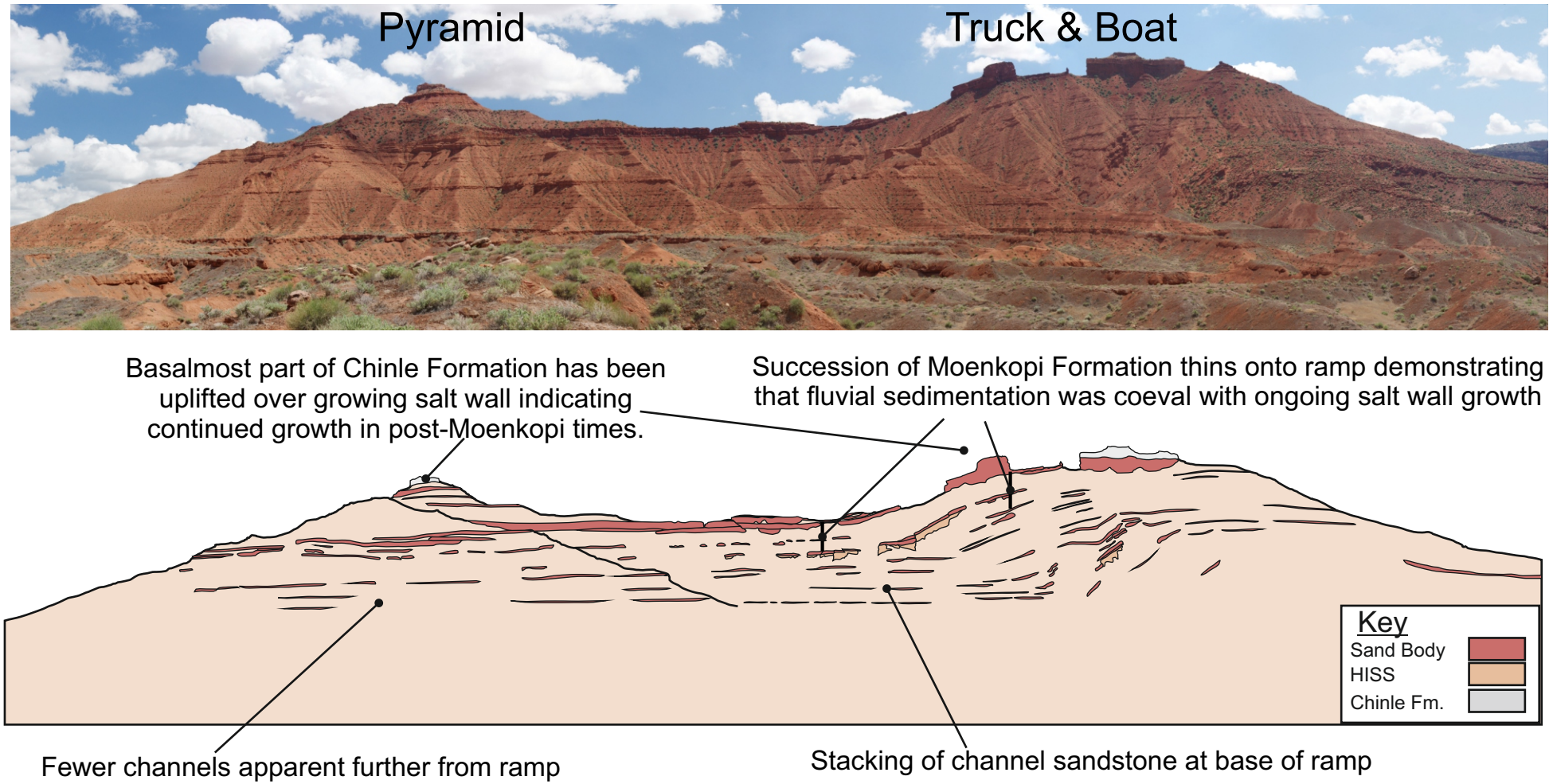


**Figure 4.8e:** Salt wall uplift with a flat-ramp-flat trajectory, Truck and Boat structure, Castle Valley, viewed from the north. Note the progressive thinning of the Moenkopi up the ramp structure. Prominent sand beds become more tightly packed towards the top of the ramp.

the preserved pattern of deposition of coevally active fluvial systems in three studied mini-basins, the Fisher Basin, the Parriott Basin and the Big Bend Basin (Figs 4.2 & 4.3). Tectono-stratigraphic interactions are especially evident in areas adjacent to salt walls (Fig. 4.8a), where fluvial architectural elements of various types ramp onto, or terminate against salt-wall uplifts. Correlations of the four members of the Moenkopi Formation, both within individual mini-basins and between adjacent mini-basins (Fig. 4.9a, b, c), demonstrate the basin-scale architecture of the fluvial fill, relationships within which document the history of accumulation.

### 4.4.1 The Fisher Basin

*Description*

The Fisher Basin, which is situated adjacent to the Uncompahgre Front, is filled predominantly with 4,000 m of sediment of the Pennsylvanian to Permian Honaker Trail Formation and Cutler Group (Trudgill, 2011). The thickest development of the Moenkopi Formation in the Fisher Basin is ~125 m, which is the thinnest preserved succession of Moenkopi Formation in the studied mini-basins of the Salt Anticline Region. An angular unconformity at the base and a disconformity at the top of the Moenkopi Formation are well exposed in the Richardson Ampitheater area and at Fisher Towers. The thickest preserved accumulation of Moenkopi Formation in the Fisher Basin is in a rim syncline developed on the north side of the Fisher Valley salt wall, development and infilling of which occurred predominantly during the Permian (Doelling, 2002a; Trudgill & Paz, 2009).

The basal-most Tenderfoot Member In the Fisher Basin is 30 to 40 m thick and is characterised by massive beds of medium-grained sandstone that are present across the entire basin, with little variation in thickness over 10 km. Associated crinkly laminated units of medium-grained sandstone of uncertain origin are additionally present at some locations within the mini-basin. Channel elements are difficult to discern as the member is largely homogeneous with respect to grain-size. A prominent but regionally restricted, 1.5 m-thick gypsum bed is present 5 m above the base of the Moenkopi

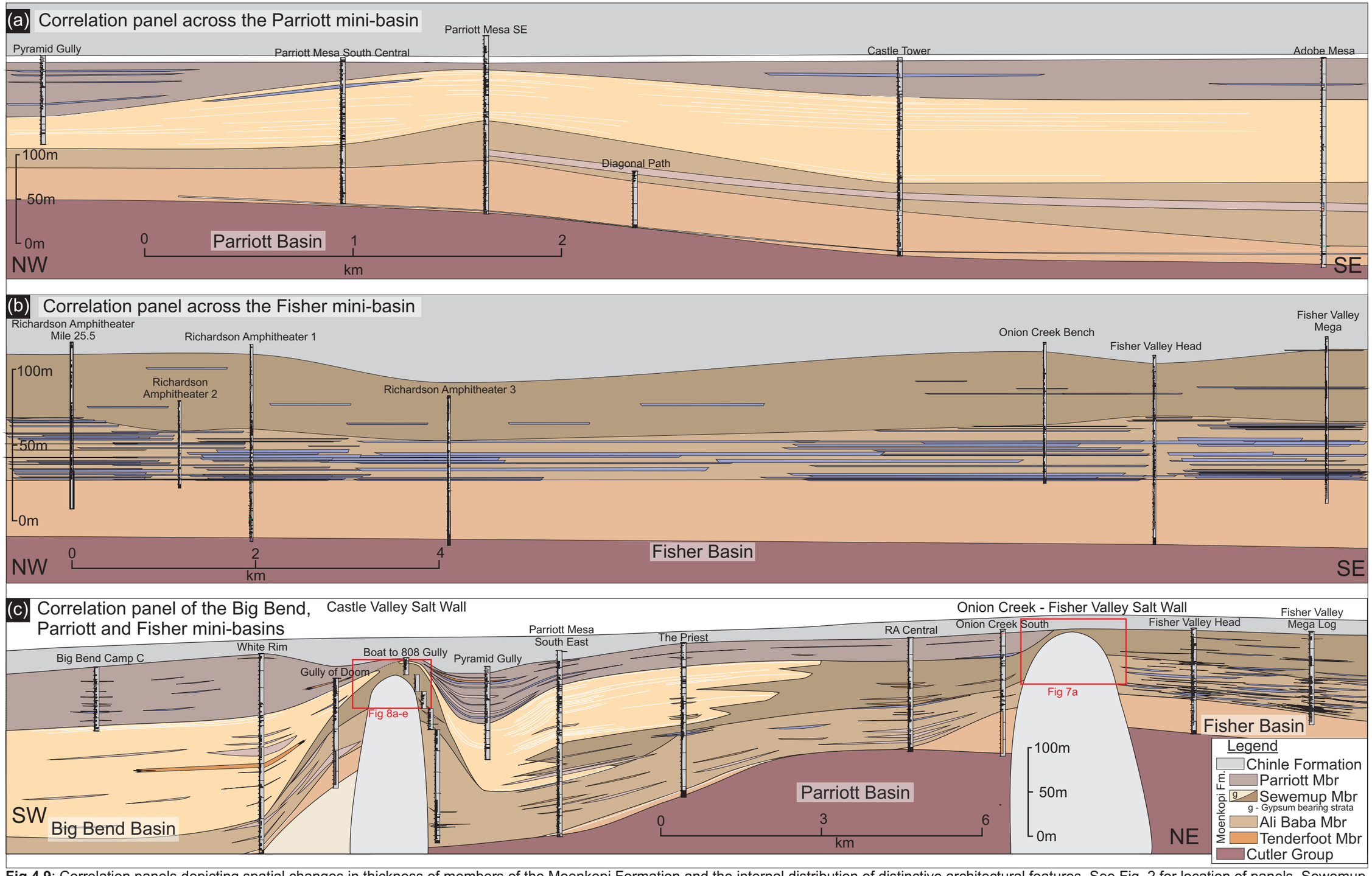


**Fig 4.9**: Correlation panels depicting spatial changes in thickness of members of the Moenkopi Formation and the internal distribution of distinctive architectural features. See Fig. 2 for location of panels. Sewemup Member is divided into gypsum-bearing facies and non-gypsum-bearing facies. (a) Correlation panel for the Parriott basin depicting the thinning of the Moenkopi Formation towards the tip of the Castle Valley salt wall. (b) Correlation panel for the Fisher basin depicting near-constant thickness of the members. Note, however, the significant relief on the disconformity at the base of the overlying Chinle Formation. (c) Correlation panel across all 3 studied mini-basins. Note the asymmetric style of the basin profile in the Parriott basin, and the absence of the Parriott Member from the Fisher basin.

Formation in the Cottonwood Canyon area, but elsewhere in the basin has been largely removed by erosion.

The overlying Ali Baba Member is 50 to 70 m thick and is characterised by multi-lateral and multi-storey, amalgamated channel-fill elements of medium- to coarse-grained sandstone and conglomerate that represent the coarsest-grained units of significant thickness in the Moenkopi Formation of the Salt Anticline Region. Amalgamated channel elements (F1; Fig. 4.6) are composed of planar and trough cross-bedded strata (Fxp & Fxt). The basal-most part of the member is composed of crudely cross-bedded paraconglomerates (Fxt & Fce) with clasts of extraformational origin. The middle part is composed of medium- to coarse-grained, cross-bedded sandstone (Fxt/HA Fxp), beds of which contain intra- and extraformational clasts (Fci/e) as either basal lags or as floating clasts. The upper part is characterised by increasing occurrences of sheet-like elements (F3) composed of climbing-ripple strata (Frc) and heterolithic strata (Fhiss), especially in the uppermost 5 to 20 m of the succession, where channel elements are scarce.

Although the Sewemup Member is present in the Fisher Basin, it lacks gypsum-clast-bearing beds (FGc/m) that are a diagnostic feature in other mini-basins; it is instead characterised by heterolithic siltstones and sandstones expressed as sheet-like elements (F3), with only rare and vertically isolated single-storey channel elements (F2; Fig. 4.6).

The Parriott Member is absent across the Fisher Basin; the disconformity at the top of the Moenkopi Formation incises up to 25 m into the top-most part of the Sewemup Member (Fig. 4.8b). Palaeocurrent readings (n = 88) taken from all members in the Fisher Basin record a vector mean of 305° (vector magnitude = 90.8%), indicating that palaeoflow was aligned parallel to the axis of the salt wall throughout duration of Moenkopi deposition.

*Interpretation*

The majority of the Fisher basin is filled by the deposits of the Honaker Trail Formation and the Undifferentiated Cutler Group, the coarse-clastic detritus, was likely exclusively sourced from the adjacent Uncompahgre Front, with no salt-walls having been present to divert or impede the delivery of pebble- and cobble-grade detritus into the mini-basin via proximal fluvial systems (Trudgill, 2011; Venus *et al.*, 2014). The relatively thin accumulation of the Moenkopi Formation in the Fisher Basin compared to that of the Parriott and Big Bend basins (described later) arose in part because subsidence of the Fisher Basin ceased relatively early in the history of the halokinetic evolution of the area: the rim syncline of the Fisher Basin adjacent to the Fisher Valley salt wall had grounded or was close to grounding on the pre-salt strata by the onset of accumulation of the Moenkopi Formation (Trudgill & Paz, 2009). This resulted in a slow rate of subsidence for the Fisher Basin during the early Triassic, whereby only ~120 m of accommodation was generated and infilled. The source of the fluvially derived sediment filling the basin during accumulation of the Moenkopi Formation was likely a combination of sediment derived from the Uncompahgre Front to the northeast and from the San Luis uplift in the south (Carter, 1970; Stewart *et al.*, 1972). The prominent gypsum bed likely accumulated as a precipitate from an evaporating brine pool that developed in the embayment formed by the developing mini-basin, or developed as a sabkha type deposit, with salt from the underlying wall acting as the source of the salt. In the majority of the basin, significant parts of this bed were eroded by fluvial incision and dissolution prior to renewed sedimentation. Throughout the episode of time represented by the accumulation of the Moenkopi Formation, the Fisher Basin apparently evolved from a sand-prone to a progressively sand-poor basin, as demonstrated by an upward decrease in the sand content of the succession. This change in basin-fill style was likely principally driven by a progressive reduction in the rate of sediment supply from the gradually denuding Uncompahgre Uplift. By the time of accumulation of the Parriott Member, the Uncompahgre Uplift was largely denuded (Blakey & Ranney, 2008; Blakey, 2009) and was no longer a significant source of sediment to the Fisher Basin. The originally accumulated thickness of the Parriott Member in the Fisher Basin remains unknown, though the unconformity at the base of the overlying Chinle Formation has regional relief

of no more than 25 m (Fig. 4.9a), which constrains the maximum likely thickness of the Parriott Member in the Fisher Basin. However, the inferred reduced rate of sediment delivery to the basin could have precluded deposition of the Parriott Member completely.

### 4.4.2 The Parriott Basin

*Description*

The thickness of Moenkopi Formation in the Parriott Basin varies from 140 m adjacent to the Onion Creek – Fisher Valley salt wall, to 180 m in the centre of the mini-basin at the Priest and Nuns mesas, to 220 m in a rim syncline developed adjacent to the Castle Valley salt wall (Fig. 4.9c). The succession thins to less than 30 m directly adjacent to the nose of the Castle Valley salt wall itself (Fig. 4.9b). Two rim synclines formed in the Parriott Basin: one in the northeast, adjacent to the southwest flank of the Fisher Valley salt wall, and another to the southwest, adjacent to the northeast of the Castle Valley salt wall (Doelling, 2002a; Trudgill 2011). In the north eastern rim-syncline (adjacent to Fisher Valley salt wall), the Moenkopi Formation exhibits neither thickening of the succession nor any variations in lithofacies or architectural-element distribution. In the south western rim-syncline (adjacent to Castle Valley salt wall), the Moenkopi Formation thickens by 30 m into the local depocentre and is characterised by an increased abundance of fluvial channel elements in the Ali Baba and Parriott members compared to the equivalent intervals in the centre of the mini-basin.

The accumulated succession in the Parriott Basin is dominated by sheet-like architectural elements (F3), composed of laterally extensive, horizontally interbedded siltstones and sandstones (Fhiss), with minor occurrences of massively bedded sandstones (Fm). The basal-most Tenderfoot Member is characterised by a distinctive 1.5 to 2.5 m-thick gypsum bed, which is also present in part of the Fisher Basin and in the Big Bend Basin. This gypsum horizon is laterally continuous throughout the Parriott Basin, being well exposed on both the Castle Valley and Fisher Valley sides of the basin. The gypsum horizon is characterised by a saccharoidal, crystalline texture and in several places contains deformed internal stratification, though elsewhere is

massive (no internal structure), or is characterised by sigmoidal cross-bedding (Lawton & Buck, 2006).

Interbedded facies associations are particularly notable in the Sewemup Member where they are associated with ubiquitous pebble- and cobble-grade gypsum-clast-bearing beds (FGc/m). These gypsum-clast-bearing units are unique to the Sewemup Member and are most prevalent in areas within 4 km of the margins of the Castle Valley salt wall but are absent from areas adjacent to the Fisher Valley salt wall.

The Parriott Member is characterised by single-storey, multi-lateral channel elements (F2) that are preferentially clustered immediately adjacent to the Castle Valley salt wall in the rim-syncline. The member is of uniform thickness across much of the basin but it doubles in thickness from 30 m to 60 m in the area adjacent to the Castle Valley salt wall where the pronounced rim syncline is developed (Trudgill, 2011). Palaeocurrent indicators throughout the Moenkopi Formation in the Parriott Basin indicate fluvial transport toward a mean vector of 303° (vector magnitude = 85%; n = 57), indicating a dominant palaeoflow that was parallel to the trend of the axis of the mini-basins.

*Interpretation*

The variation in thickness of the Moenkopi Formation in the Parriott Basin demonstrates that the basin underwent an asymmetric pattern of subsidence during accumulation of both the underlying Cutler Group and the overlying Moenkopi Formation. During accumulation of the Cutler Group, transport and deposition occurred in a south westerly direction (Cain & Mountney, 2009; Venus *et al.*, 2014), with overall sediment transport generally being in a direction perpendicular to the trend of the developing salt walls. This indicates that the rate of fluvial sedimentation generally outpaced the rate of salt-wall uplift such that fluvial systems of the Undifferentiated Cutler Group were not influenced by salt-induced surface topography throughout much of their evolution (Venus *et al.*, 2014).

Increased subsidence rates in the rim synclines of the Parriott Basin were driven by loading from a thicker overburden deposited by the prograding fan of the Undifferentiated Cutler Group. Accelerated salt withdrawal resulted in the development of rim synclines on both the Fisher Valley and Castle Valley sides of the Parriott Basin. These rim synclines continued to develop throughout accumulation of the Cutler Group before subsidence in the north eastern rim syncline (adjacent to the Fisher Valley salt wall) ceased, apparently before salt-weld formation occurred (Trudgill & Paz, 2009; Trudgill, 2011). By contrast, the south western rim syncline (adjacent to the Castle Valley salt wall) continued to subside throughout the period represented by accumulation of the Moenkopi Formation, resulting in the development of an asymmetric style of basin-fill (Fig. 4.9c).

During accumulation of the Moenkopi Formation, subsidence rates were greater in the Parriott Basin than in the Fisher Basin, which enabled the former to accommodate a significantly thicker accumulation of Moenkopi succession: a maximum of 220 m versus a maximum of only 125 m in the Fisher Basin. The gypsum bed in the Tenderfoot Member likely accumulated in either a restricted tidal-flat (sabkha) setting or within an embayment with restricted opening that was subject to repeated flooding and desiccation (Stewart *et al.*, 1972). In places, sediment from this gypsum bed has been interpreted to have been partially reworked to form a cross-bedded aeolianite (Lawton & Buck, 2006). Palaeocurrent data demonstrate fluvial flow occurred parallel to the axis of the mini-basin (to the northwest), indicating that the Parriott Basin was isolated from much of the detritus being shed from the Uncompahgre Front during Moenkopi deposition, either because fluvial systems emanating from the remnant Uncompahgre highlands did not extend this far into the Paradox Basin or, more likely, because uplift of the Fisher Valley and Sinbad Valley salt walls generated a surface topography that was sufficient to prevent such fluvial systems reaching the Parriott Basin (Fig. 4.1). This limited the primary source of sediment for the Parriott Basin to that of the San Luis range to the southwest (Cadigan & Stewart, 1971). The likely isolation of the Parriott Basin from the Fisher Basin by elevated salt-wall topography, meant that the rate of sediment delivery to the former was limited

and the rate of filling of accommodation was therefore likely low relative to rate of basin subsidence during early- to mid-stages of accumulation of the Moenkopi Formation, resulting in a basin fill characterised by argillaceous, sheet-like elements (F3) interbedded with only minor sandstone elements (F2) in the Ali Baba, Sewemup and Parriott Members (Fig. 4.6).

High rates of basin subsidence, and associated ensuing high rates of salt-wall uplift at the basin margins relative to the low rate of filling of accommodation in the central parts of the basin culminated in the uplift of the Castle Valley salt wall to a level where it breached the land surface during accumulation of the Sewemup Member, whereupon it acted as a local source of gypsum detritus, which was re-worked into the strata surrounding the Castle Valley salt wall as discrete gypsum-clast-bearing beds (Lawton & Buck, 2006). The absence of gypsum clasts from the Moenkopi succession at the margins of the Fisher Valley salt wall demonstrates that this halokinetic feature did not breach the land surface during deposition of the Moenkopi Formation (Fig. 4.9c). The confinement of gypsum pebbles and cobbles to within 7 km of the Castle Valley salt wall (with orthoconglomerate beds occurring closer to the salt wall) indicates that alluvial processes were not able to distribute the detrital gypsum clasts evenly over the entire basin floor (Fig. 4.8c). During accumulation of the Parriott Member, preferential subsidence during the final phase of salt withdrawal adjacent to Castle Valley salt wall (Trudgill, 2011) resulted in the renewed development of a rim syncline and the preferential preservation of single-storey channel elements (F2) in this local depocentre (Fig. 4.9c ).

### 4.4.3 The Big Bend Basin

*Description*

Deposits in the Big Bend Basin are not as well exposed as those in the other studied mini-basins, with the full thickness of the Moenkopi Formation succession (235 m) only exposed along the south western flank of the Castle Valley salt wall, and the succession thinning to less then 30 m thick adjacent to the nose of the Castle Valley salt wall (Fig. 4.8a, b). The base and top of the Moenkopi Formation are not seen at other single geographic localities in

the Big Bend mini-basin and the true maximum thickness of the Moenkopi Formation in this basin is therefore uncertain.

On the south western flank of the Castle Valley salt wall, a prominent angular intraformational unconformity with a discordance of ~6° is present between the Tenderfoot and Ali Baba members (Fig. 4.8b). The basal gypsum unit is not present in the Tenderfoot Member immediately adjacent to the salt wall, though it is present elsewhere in the Big Bend Basin. Toward the centre of the basin, near the Big Bend campground, only the upper part of the Sewemup Member and the full succession of the Parriott Member are exposed. Gypsum-clast-bearing beds are present in the Sewemup Member at the Big Bend campground locality, a distance of 2.8 km from the Castle Valley salt wall. The Parriott Member at Big Bend Campsite C has a thickness of 70 m, which is the thickest observed preserved succession of Parriott Member in the study area.

Adjacent to the Castle Valley salt wall, at the north east edge of Matt Martin Point (Fig. 4.2), a series of well-developed channel elements are preserved as overlapping multi-lateral and twin- or multi-storey channel complexes (F1). Toward the centre of the mini-basin, near the Red Cliff Lodge road section, the Parriott Member comprises amalgamated channel elements (F1 & F2) composed internally of trough- (Fxt) and planar-cross bedded (Fxp) sets with intraformational clasts (Fci). These elements overlie a succession of interbedded siltstones and sandstones (Fhiss) with a sheet-like geometry (F3), and are themselves overlain by thin interbedded sandstone and siltstone heterolithic sheet-like elements (F3), the upper parts of which are cut-out by the disconformity at the base of the Chinle Formation.

*Interpretation*

The presence of the intraformational unconformity between the Tenderfoot and Ali Baba members demonstrates a temporary cessation in sedimentation, during which time salt-wall uplift was ongoing. During accumulation of the Ali Baba Member, the fluvial system aggraded and encroached onto the flanks of the salt wall, locally reworking the uplifted succession of the Tenderfoot

Member and generating the angular unconformity. A rim syncline had developed in the Big Bend mini-basin immediately adjacent to the flank of the Castle Valley salt wall by the time of accumulation of the Parriott Member (Fig. 4.9); this resulted in the preferential stacking and clustering of vertically and laterally amalgamated channel elements (F1) adjacent to the Castle Valley salt wall, but their absence in central parts of the basin (e.g. Big Bend Campsite C). The gypsum-clast-bearing horizons observed in the Sewemup Member toward the basin centre indicate that gypsum detritus was shed into the Big Bend Basin (in addition to the Parriott Basin) from the actively uplifting Castle Valley salt wall. The presence of gypsum clasts throughout the central part of the Big Bend mini-basin demonstrates that this detritus was reworked and re-distributed by fluvial systems in the mini-basin. The thickness of the preserved Sewemup Member succession is similar in both the Parriott and Big Bend mini-basins, demonstrating that the basins on either side of the Castle Valley salt wall underwent similar rates of subsidence. The different styles of preserved sedimentary architecture of the Parriott Member in the Big Bend and Parriott basins indicates that the fluvial systems were isolated from each other by the Castle Valley salt wall.

## 4.5 Styles of salt-wall and sediment interaction

### 4.5.1 The Fisher Valley salt wall and Onion Creek salt diapir

Due to recent erosion, little direct evidence remains with which to demonstrate the style of interaction between the pattern of sedimentation in the Moenkopi Formation and the synchronous evolution of the Fisher Valley salt wall. To the north of this salt wall, near-horizontally bedded outcrops are largely inaccessible where they form sheer cliffs at Fisher Towers (1.5 km from the edge of the Fisher Valley salt wall). To the south of the Fisher Valley salt wall, the closest outcrop of the Moenkopi Formation is 600 m from the margin of the salt wall and here beds are again near-horizontal. Thus, deformation of the accumulated strata by the uplifting salt wall was restricted solely to the immediate margins of the wall (Fig. 4.7a, b).

### 4.5.2 The Castle Valley salt wall

*Description*

Well exposed outcrops that demonstrate direct evidence for the interaction between sedimentation in the Moenkopi Formation and synchronous salt-wall growth are present in the Red Hills area (known locally as the “Truck and Boat”) at the northern margin of the Castle Valley salt wall (Fig. 4.8a). The style of salt-wall uplift is asymmetric in nature, with the Pre-Triassic sediments of the Cutler Group having been uplifted to a greater height on the western side of the salt wall than on the eastern side. The asymmetric nature of the uplift is further demonstrated by the geometries of the uplifted salt-wall flanks: the eastern flank of the uplift, which forms the bounding edge of the Parriott Basin, exhibits a horizontal-inclined-horizontal geometry, whereas the western flank, which forms the bounding edge of the Big Bend Basin, exhibits a simpler, wedge-like geometry (Fig. 4.8b).

The horizontal-inclined-horizontal geometry that characterises the eastern flank of the Castle Valley salt wall (Fig. 4.8a; east side) is related to a narrow zone of deformation. Two inflection points, a convex bend adjacent to the crest of the salt wall and a concave bend at the down-dip margin of the feature at a point where the succession moves off the salt-wall flank, define a monocline (Lawton & Buck, 2006). The sedimentary succession on top of the salt wall is near-horizontal, whereas inclined strata on the flank of the salt wall dip away from the crest at an angle up to 23° toward 114°. Figures 4.7a demonstrate the extent of the thinning onto the Castle Valley salt wall: the thickness of the succession between the middle of the Ali Baba Member and beds in the upper part of the Parriott Member thins by 30 m over a distance of 445 m from the crest of the salt wall, eastwards to a point at the limit of salt-wall-related deformation, giving an approximate rate of thinning of 1 in 14. The aforementioned beds in the upper part of the Parriott Member have been uplifted by 76 m on to the crest of the salt wall relative to their lateral equivalent beyond the zone of salt-wall deformation. Within the accumulated strata on the eastern flank of the Castle Valley salt wall, sand-prone fluvial channel elements ramp up onto the salt wall, thinning or pinching-out as they

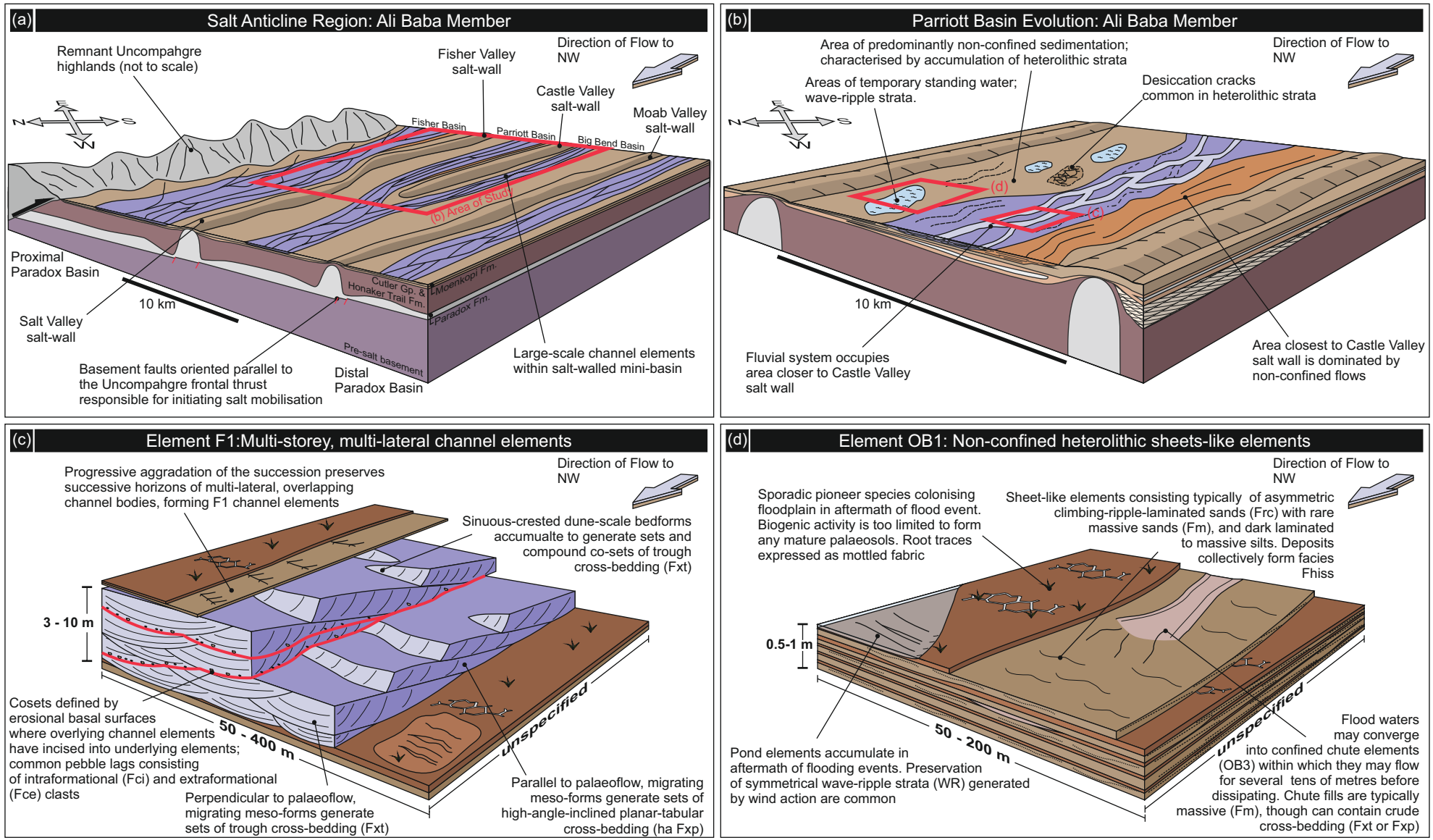


**Figure 4.10**. (a) Model for Salt Anticline Region depicting deposition of the Ali Baba Member. (b) Detailed stratigraphic model for the Parriott basin. (c & d) Examples of fluvial architectural elements F1 & F3, which are two of the main elements composing the majority of the basin fill.

onlap onto the upper flanks of the structure (Figs 4.8b, c & 4.10b). On the eastern flank of the Castle Valley salt wall, beds of the Ali Baba Member with a distinctive grey colouration due to reduction of beds with wave-rippled surfaces are present (Fig. 4.10b). In the upper part of the Sewemup Member and the lower part of the Parriott Member, shearing of some of the sand-prone channel elements is present adjacent to the salt wall (Fig. 4.10b).

The slope geometry that characterises the western flank of the Castle Valley salt wall dips gently towards the west into the Big Bend Basin and is characterised by fanning growth strata that thin onto the crest of the salt wall (Fig. 4.8b). At the unconformity between the underlying sediments of the Cutler Group and the base of the Moenkopi Formation, a series of 3 growth-faults, each of which exhibit displacement of up to 2.5 m, are developed in the strata that form the uppermost part of the Cutler Group (preserved locally as a distinctive white-coloured aeolianite that might be equivalent to the White Rim Sandstone present in more distal parts of the Paradox Basin – Venus *et al*., 2014). These faults, which strike at 197°, parallel to the uplift at the end of the salt wall, have displacements of 1 to 2 m, have hanging-walls that dip away from the salt-wall and are filled with poorly bedded medium-sandstone (Fm) of the Tenderfoot Member.

Two sedimentary sections recording laterally equivalent parts of the Tenderfoot and basal-most Ali Baba Member on the west flank (Fig. 4.8b, d) demonstrate thinning of 30 m over a lateral distance of 270 m, from 72 m at the West Flank Gully log located part-way down the flank of the salt wall, to 42 m at the West Flank Spur log close to the crest of the salt wall (Fig. 4.8b, d), yielding an average rate of thinning of 1 in 9. The top of the succession adjacent to the salt wall has been elevated by 21 m relative to the equivalent part of the succession in the log 270 m away. The density of occurrence of single-storey channel elements (F2) filled with massive sandstone (Fm) systematically decreases with increasing proximity to the salt wall (Fig. 4.8b, d). Several major channel elements that are laterally continuous in the Big Bend rim syncline thin and pinch-out as they onlap onto the upper flank of the

Castle Valley salt wall. Around the rest of the valley, other inferred onlap relationships are not well preserved due to erosion.

*Interpretation*

The Castle Valley salt wall formed an elevated topographic feature that acted to effectively partition and isolate the Parriott and Big Bend mini-basins throughout the majority of the episode of sedimentation represented by the Moenkopi Formation; the margin of the Big Bend Basin is sand-prone whereas the margin of the Parriott Basin is relatively sand-poor. The overall thinning of the strata onto the flanks of the Castle Valley salt wall demonstrates that uplift occurred synchronously with sedimentation. Present-day differences in height between known stratigraphic levels recorded in the logged sections demonstrate continued post-depositional salt-wall uplift. The thinning and pinch-out of channel elements onto the upper flanks of the salt wall indicate that fluvial systems were actively diverted by the uplifted salt wall for significant episodes during accumulation of the Moenkopi Formation. The effective partitioning of the Parriott and Big Bend basins during accumulation of the Parriott Member is demonstrated by differences in basin-fill style either side of the salt wall: the Parriott Member is significantly more sand prone in the Big Bend mini-basin, where multi-storey channel elements (F1) are preserved adjacent to the salt wall but at an equivalent stratigraphic level in the Parriott Basin, only thin and isolated single-storey channel elements (F2) occur intercalated with heterolithic sheet-like elements (F3). Preserved wave-ripple forms on bedding surfaces in the Ali Baba Member on the east flank of the Castle Valley salt wall are indicative of standing water on this now uplifted section of salt wall. This likely indicates that, at some point during Ali Baba deposition, the Castle Valley salt wall was present only in the sub-surface and the topographic expression of the salt wall was sufficiently subdued to allow water to pond in the area directly above the salt wall. In the upper part of the Sewemup Member and the lower part of the Parriott Member, shearing of some sand-prone channel elements in a style indicative of growth-fault development indicates that the salt wall was still growing after accumulation of these members (Fig. 4.10b). The orientation of the growth faults present on the western flank of the Castle Valley salt-wall, together with their style of

displacement, required early cementation and brittle deformation of strata of the White Rim Sandstone in which these features are developed. Displacement was likely associated with phases of salt-wall uplift or mini-basin subsidence, as demonstrated by down-throw on the basinward side, with the generated space subsequently being filled by sediment younger sediment of the Moenkopi Formation. This indicates either that salt-wall uplift was responsible for elevating the growth-fault footwalls, or that salt evacuation in the developing rim syncline was responsible for lowering the hanging walls, or a combination of both.

### 4.5.3 Cache Valley salt wall

The Cache Valley salt wall (Fig. 4.2) is thought to have been linked to the Fisher Valley salt wall by a section of salt swell with subdued relief present only in the subsurface (Shoemaker, 1955). This subdued segment of the salt wall running between the end of Onion Creek and Cache Valley is overlain by a small uplifted outcropping section of the Moenkopi Formation. The structural feature that links these salt walls might be the expression of a relay ramp that joined two pre-salt fault systems, and which was responsible for accumulating differential thicknesses of salt on either side of the structure; such a feature might have served as a trigger for the initiation of salt-wall growth (cf. Hodgson *et al.*, 1992; Doelling, 2002a).

## *4.6 Tectono-stratigraphic model*

Based on observations regarding the sedimentology and stratigraphy of the preserved succession and its relationship to the various subsiding mini-basins and uplifting salt walls, the tectono-stratigraphic evolution of the Moenkopi Formation in the studied part of the Salt Anticline Region has been reconstructed. Detailed relationships established from analysis of field-derived data have enabled a suite of models describing the evolution of the province as a whole to be reconstructed (Fig. 4.11a); tectono-stratigraphic relationships within individual mini-basins have been established (Fig. 4.11b), and the character of individual fluvial architectural elements has been discerned (Fig. 4.10c, d). Furthermore, a series of spatio-temporal evolution models has been developed for the three studied mini-basins and their bounding salt walls; the

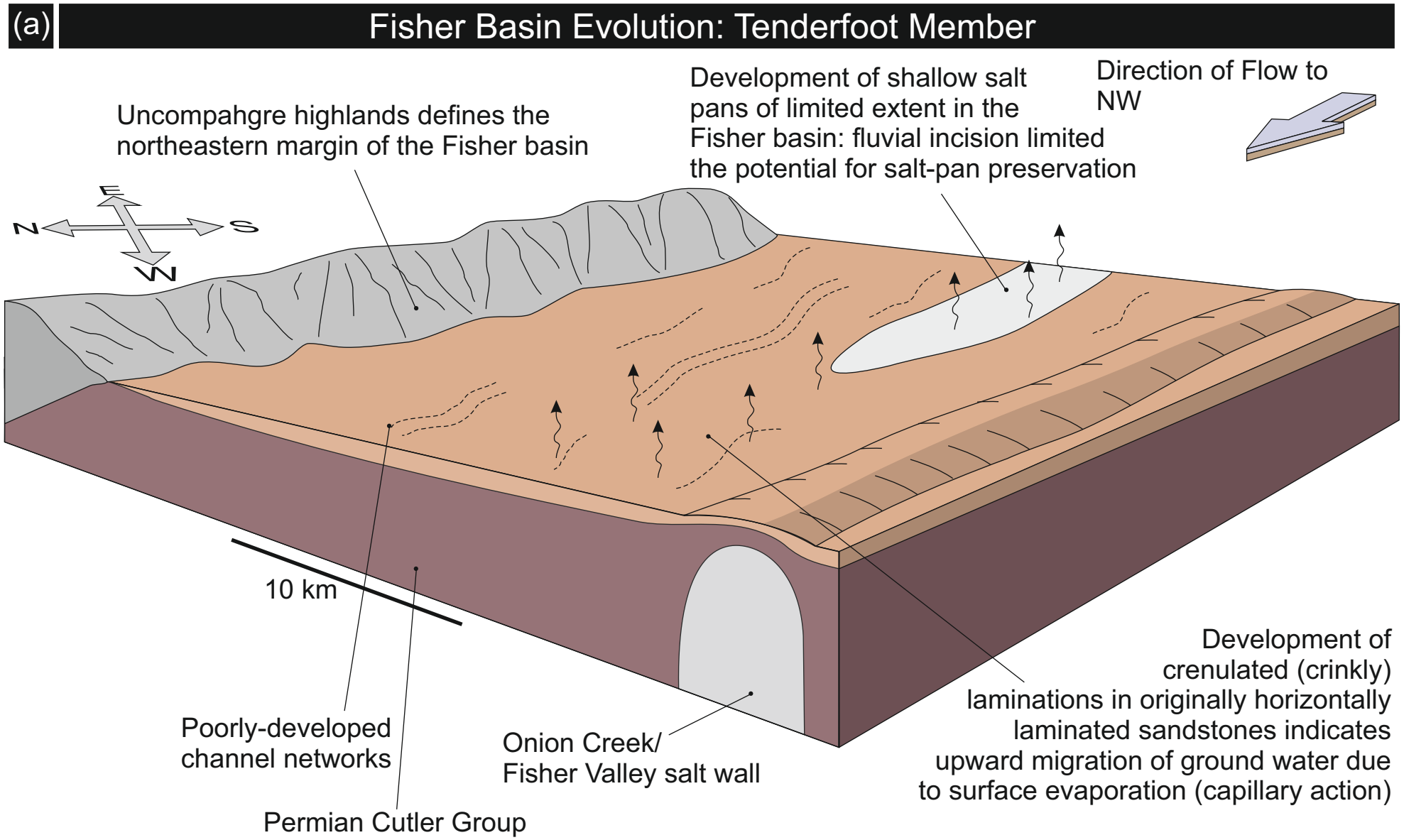


**Figure 4.11a**: Model to account for the temporal evolution of the Tenderfoot Member in the Fisher Basin.

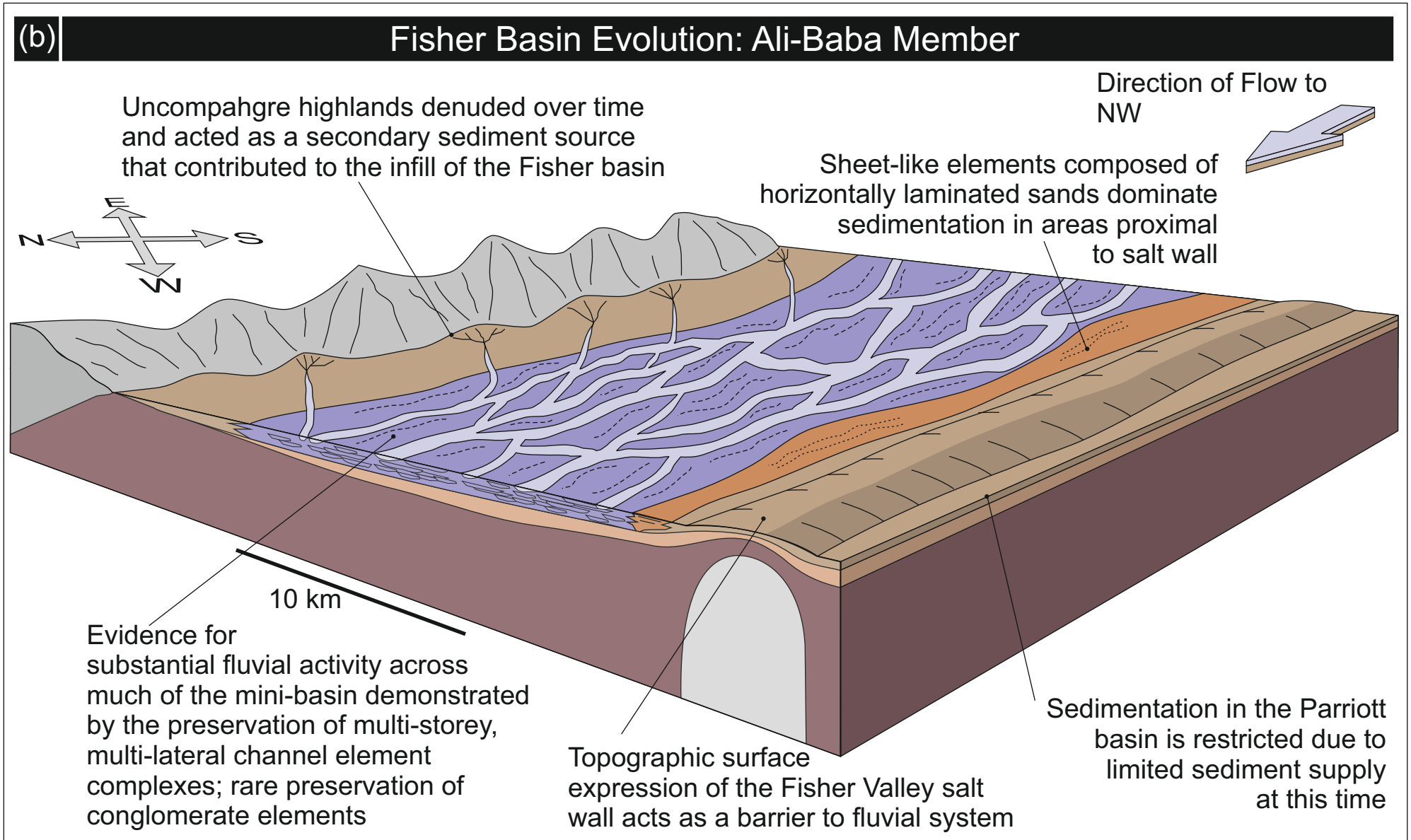


**Figure 4.11b**: Model to account for the temporal evolution of the Ali Baba Member in the Fisher Basin.

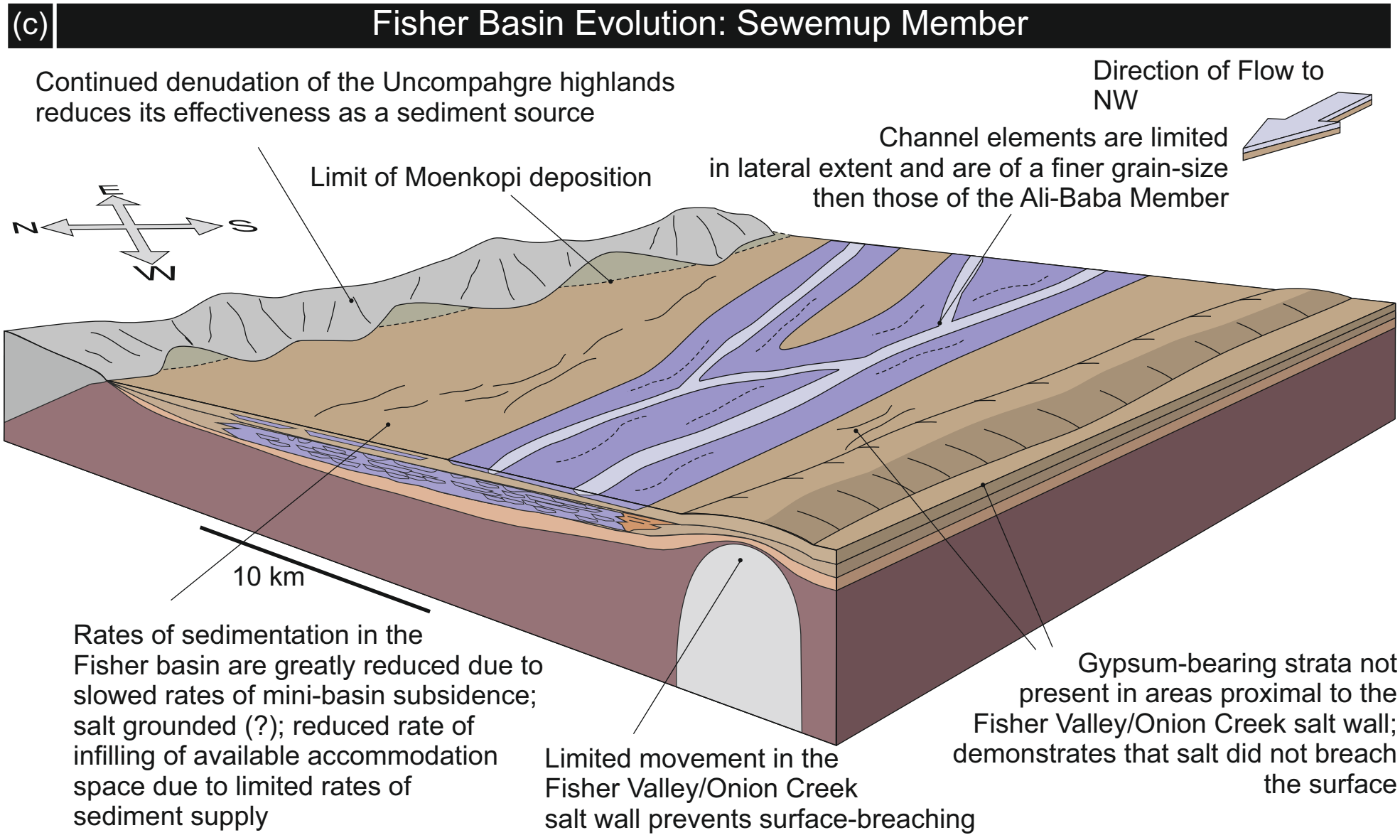


**Figure 4.11c**: Model to account for the temporal evolution of the Sewemup Member in the Fisher Basin

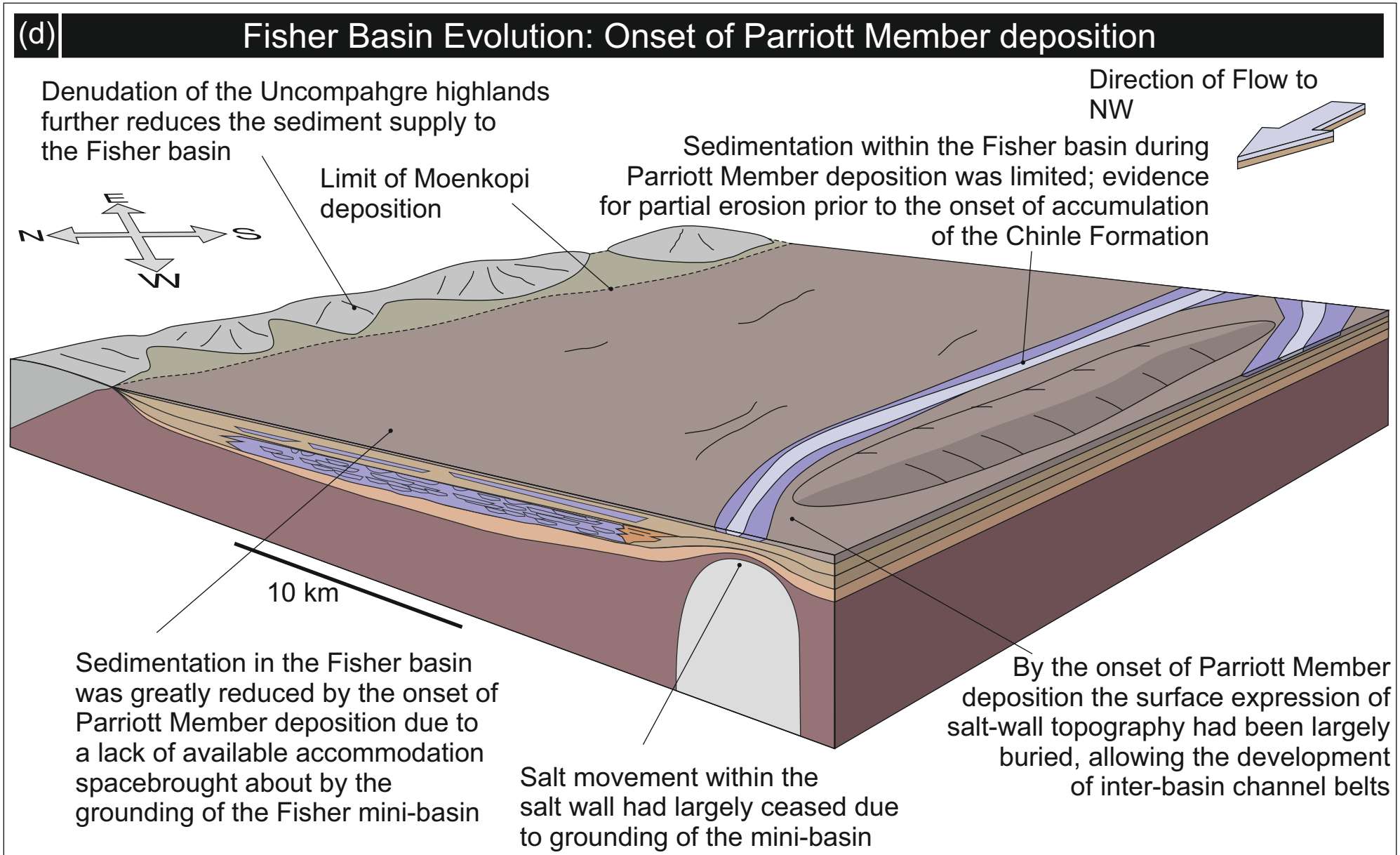


**Figure 4.11d**: Model to account for the temporal evolution of the Fisher Basin at onset of Parriott Member deposition.

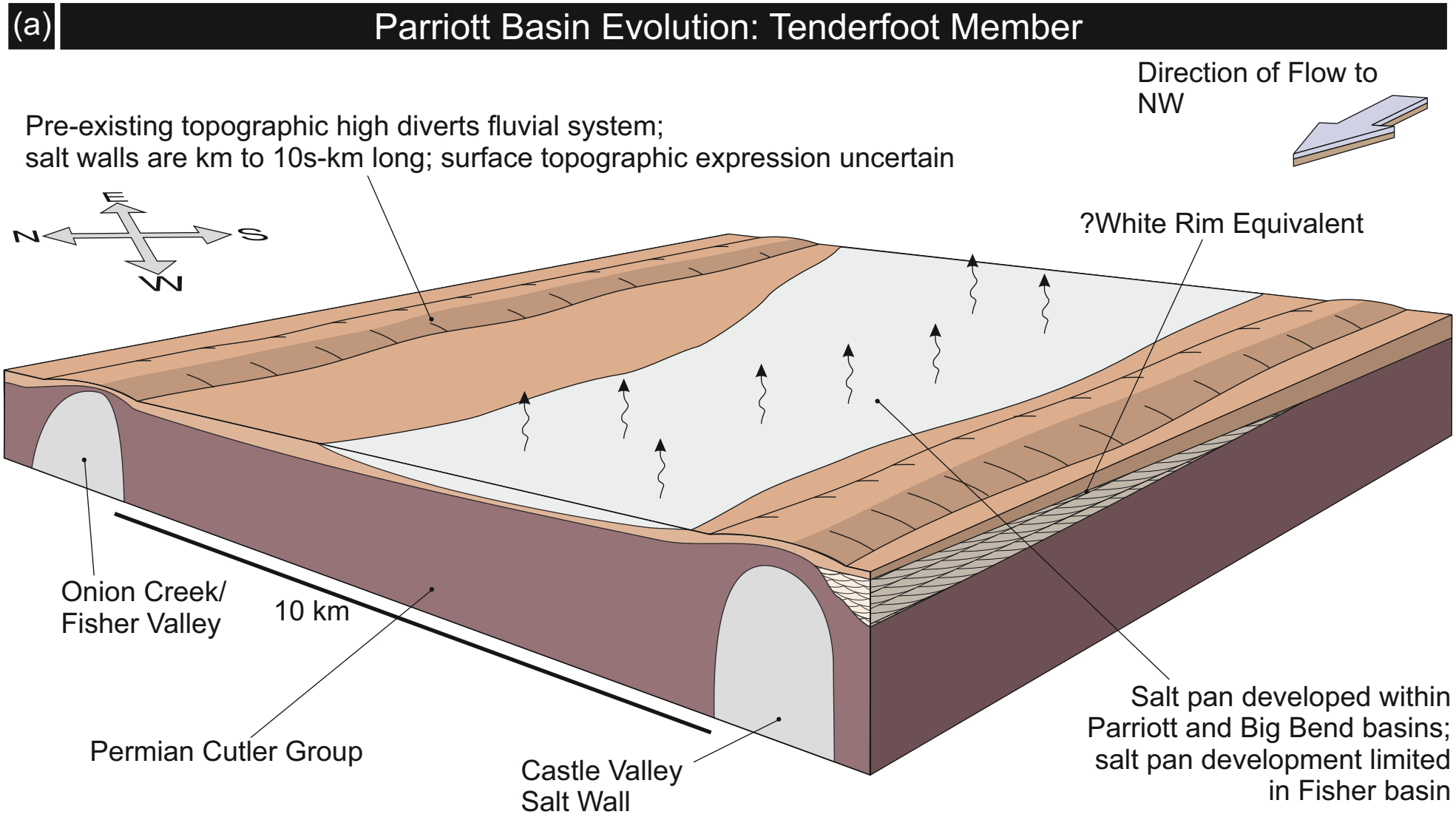


**Figure 4.12a**: Model to account for the temporal evolution of the Tenderfoot Member in the Parriott Basin

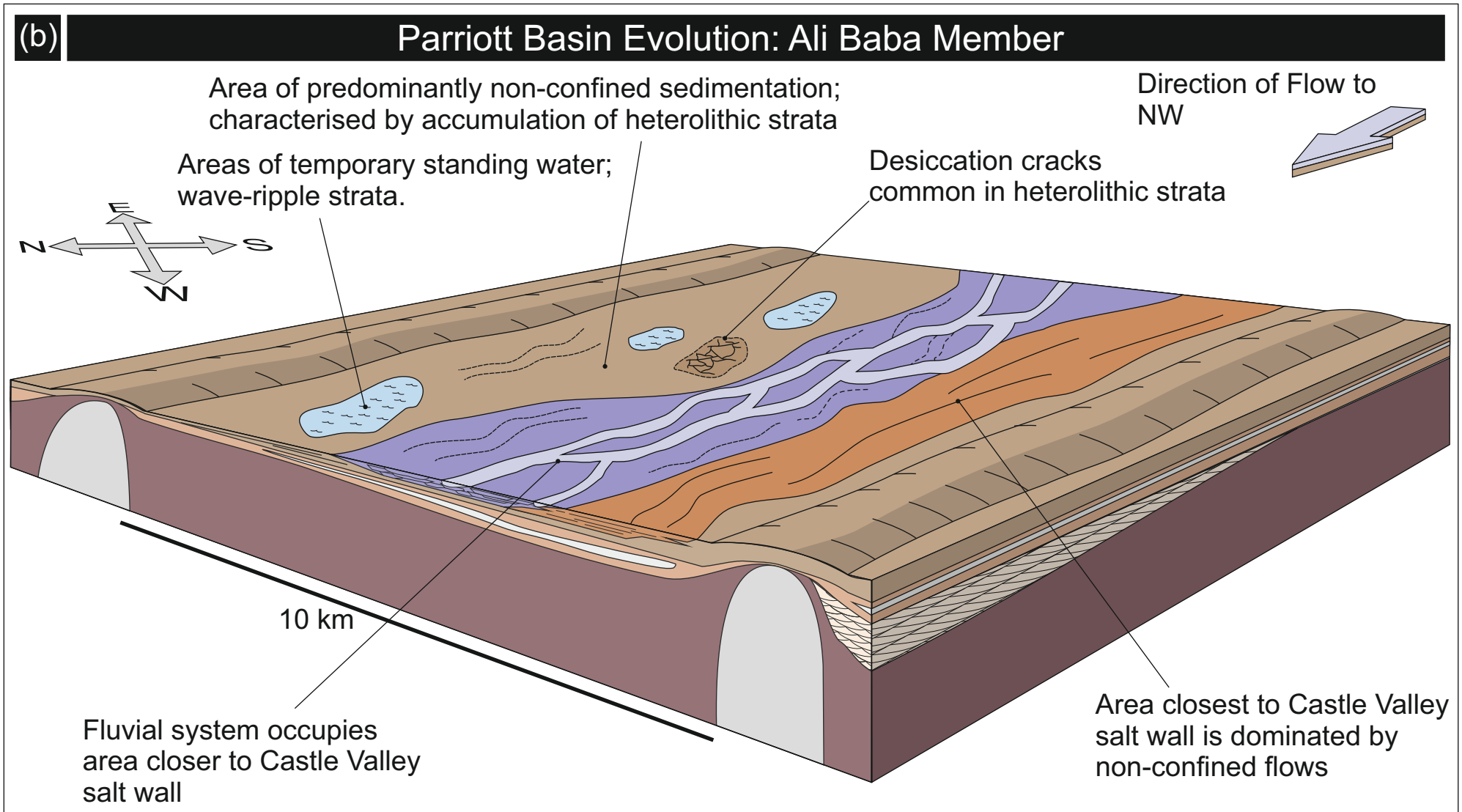


**Figure 4.12b**: Model to account for the temporal evolution of the Ali Baba Member in the Parriott Basin.

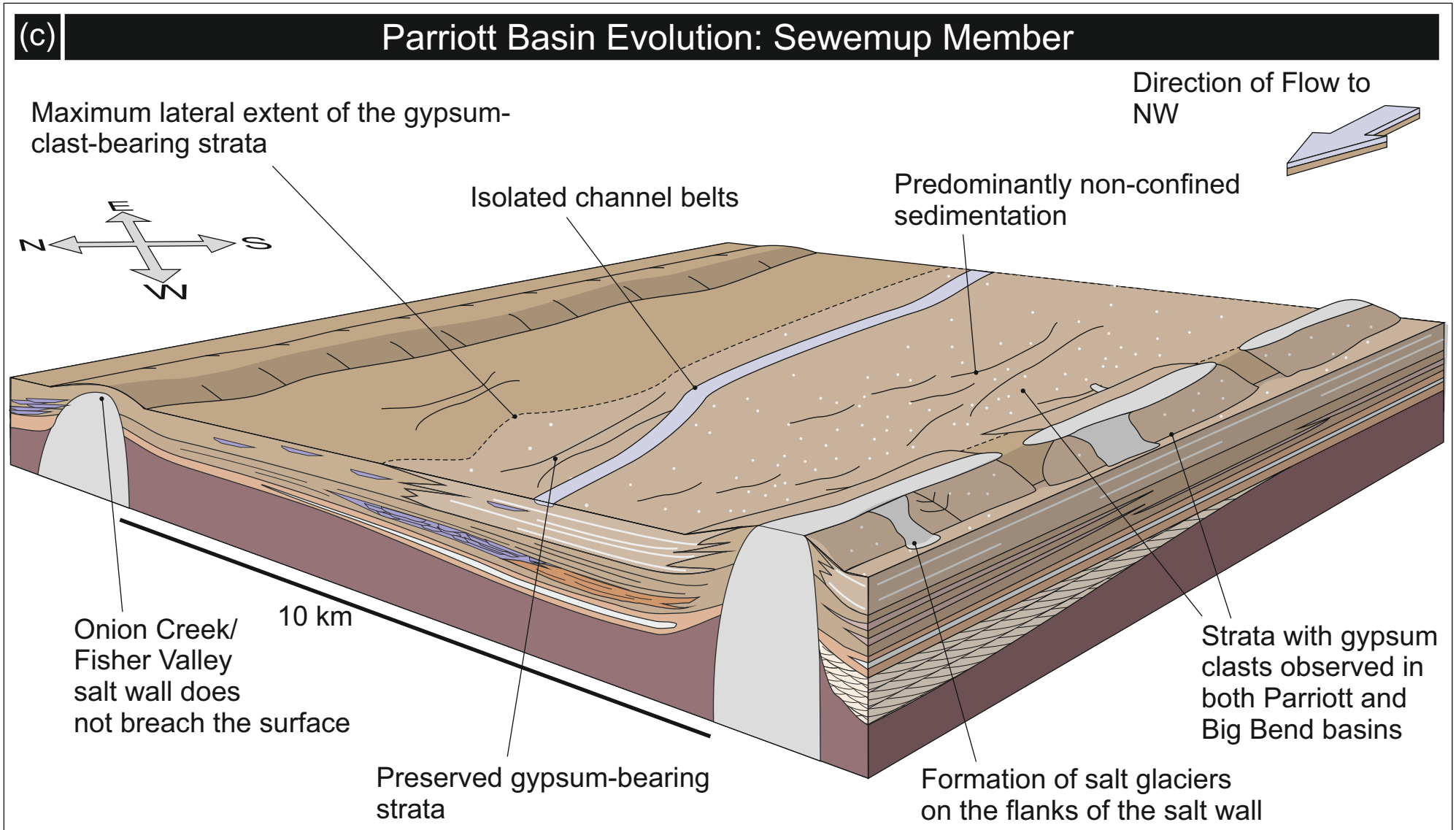


**Figure 4.12c**: Model to account for the temporal evolution of the Sewemup Member in the Parriott Basin.

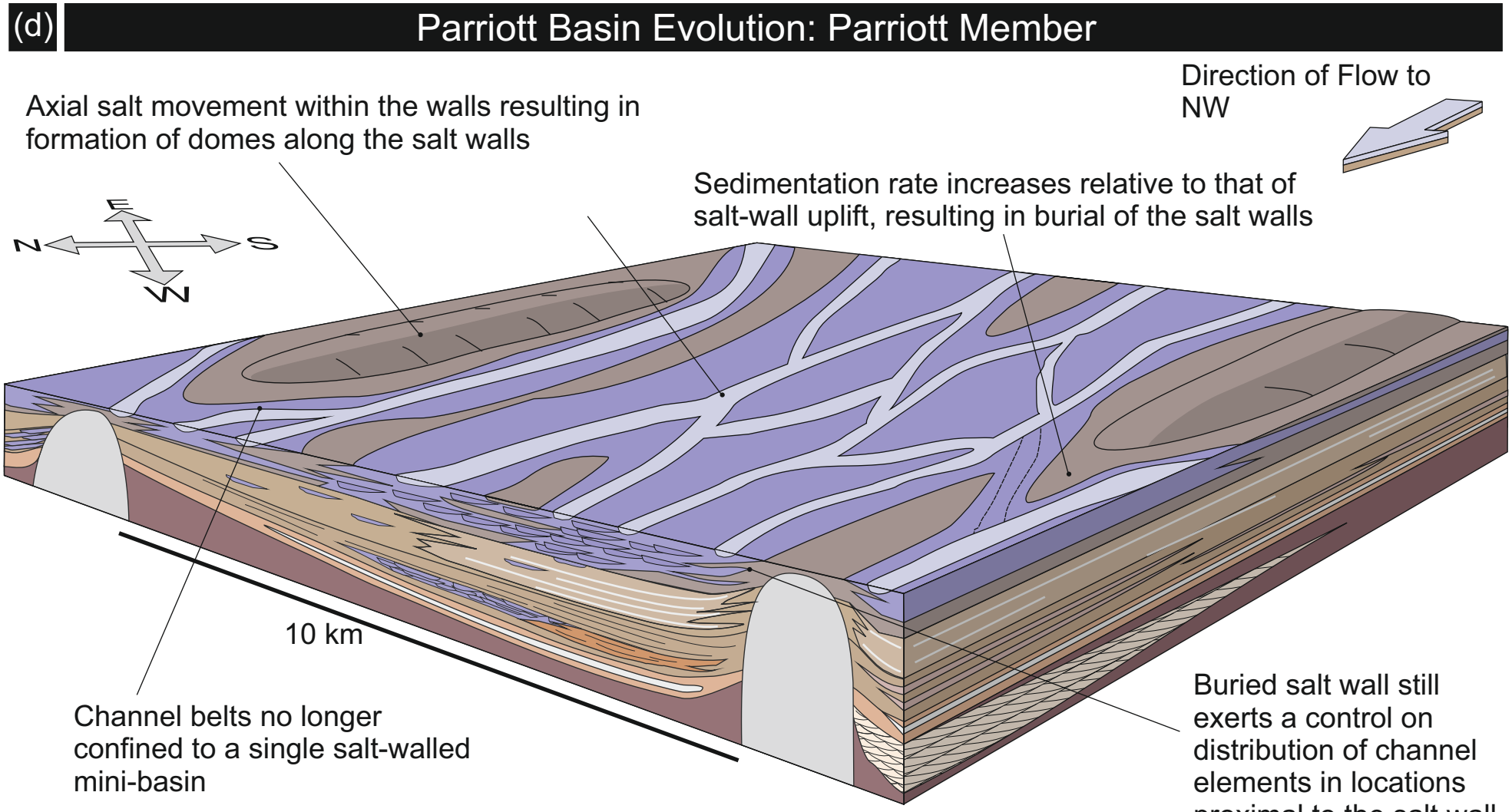


**Figure 4.12d**: Model to account for the temporal evolution of the Parriott Member in the Parriott Basin.

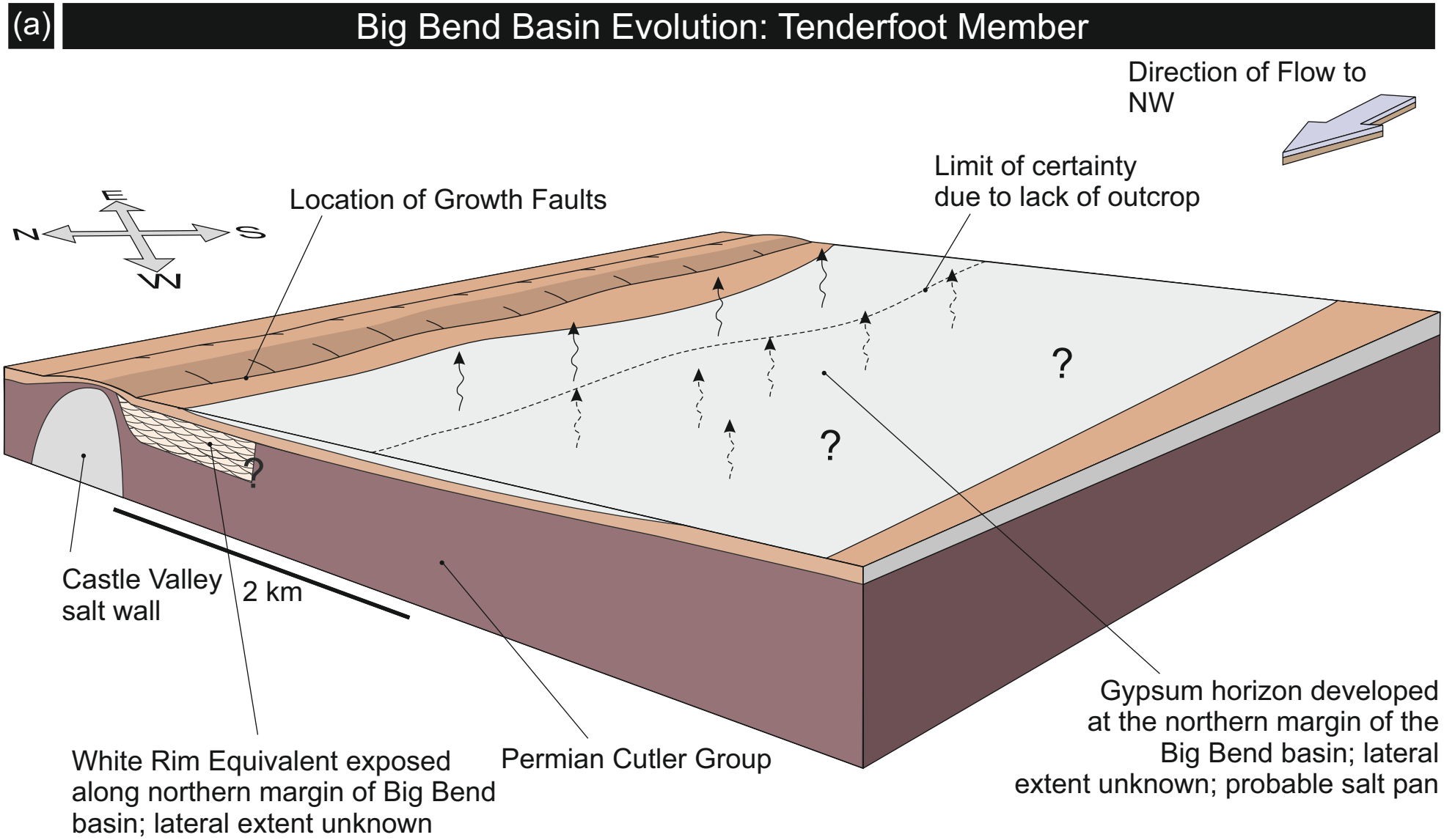


**Figure 4.13a**: Model to account for the temporal evolution of the Tenderfoot Member in the Big Bend Basin.

Left: Growth fault in White Rim Sandstone, and growth strata in the Tenderfoot Member.

Below: Multi-storey and multi-lateral channel element (F1) complex with sheet-like overbank elements (OB1) in the Parriott Member.

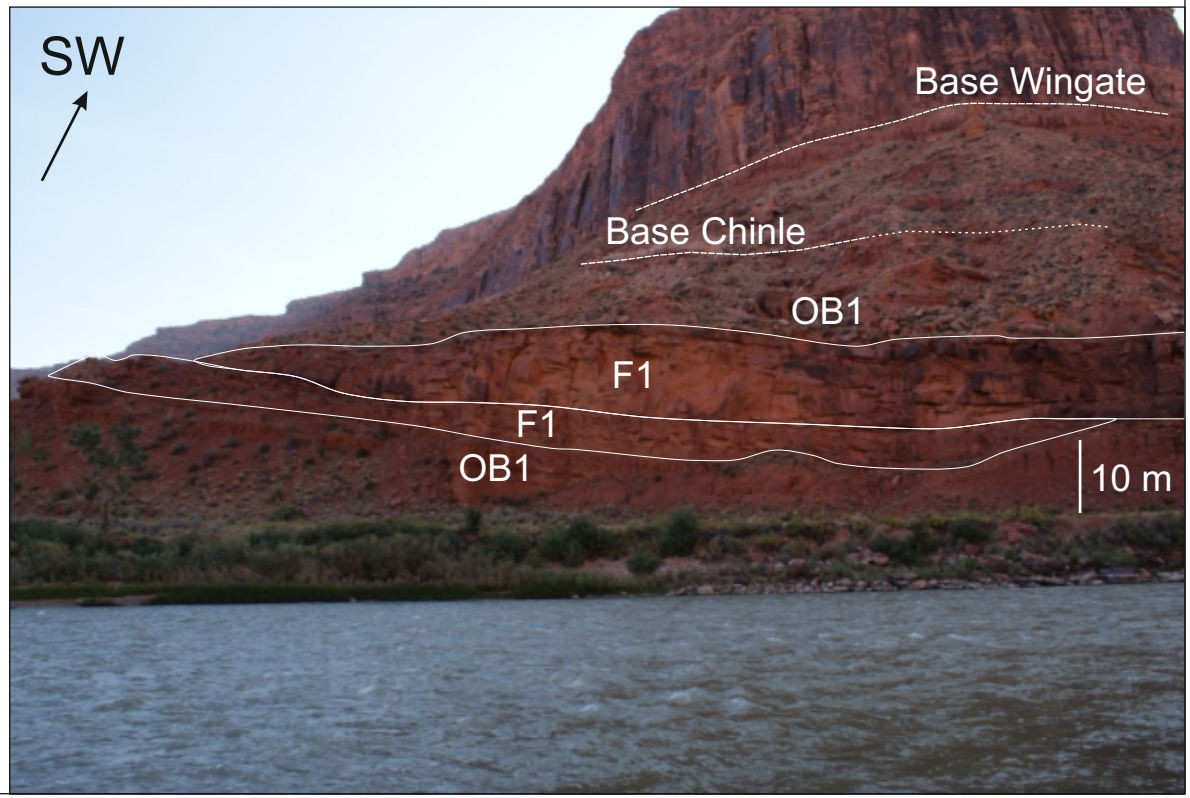


**Figure 4.13b**: Photographs of key sedimentological and structural features within the Big Bend Basin.

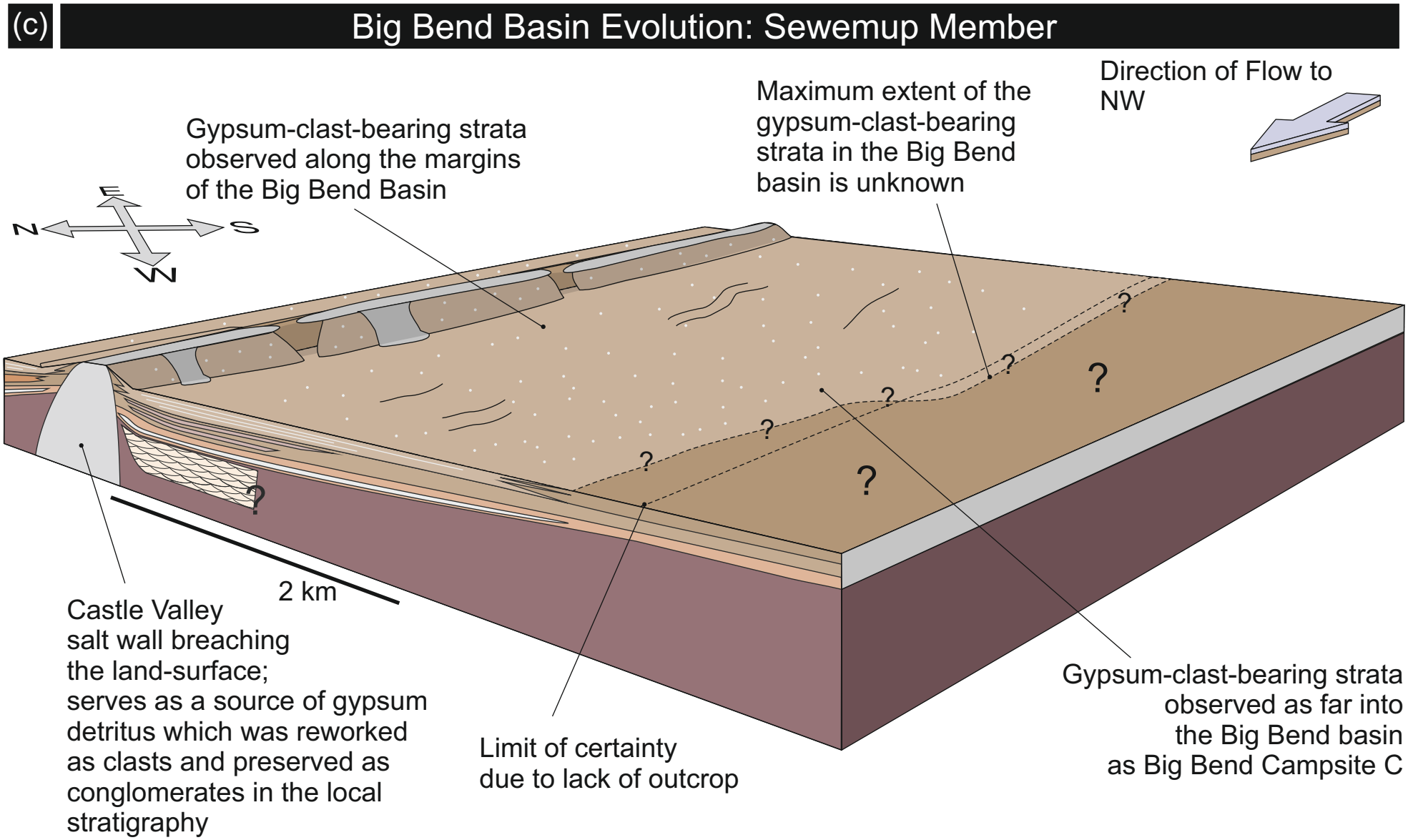


**Figure 4.13c**: Model to account for the temporal evolution of the Sewemup Member in the Big Bend Basin.

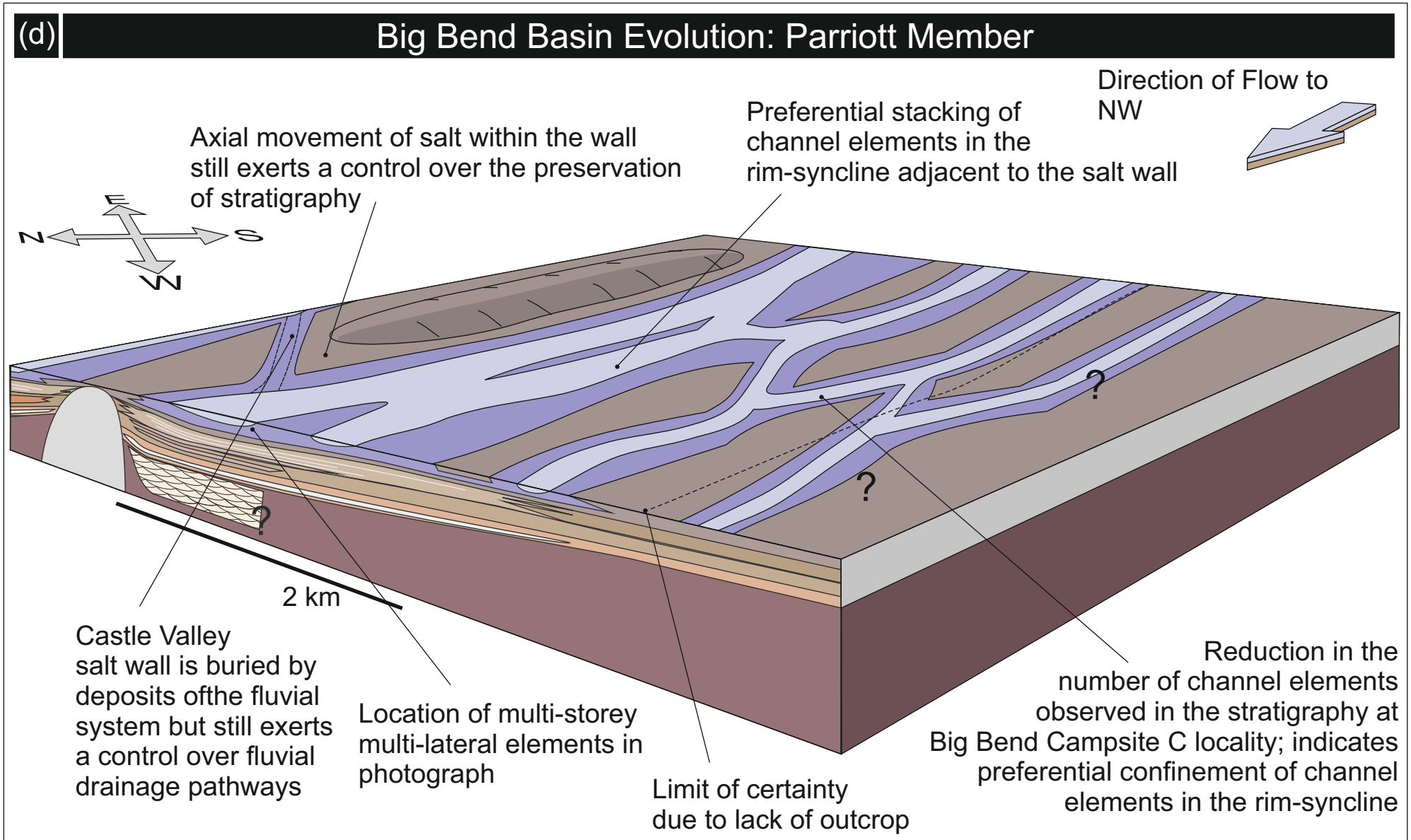


**Figure 4.13d**: Model to account for the temporal evolution of the Parriott Member in the Big Bend Basin.

proposed models account for the distinctive styles of basin fill (Figs 4.11, 4.12, 13), such that differences in preserved fluvial architectural style can be attributed to the dynamic interplay between rates of sediment delivery and accumulation, rates of mini-basin subsidence, and rates and styles of associated salt-wall uplift.

### 4.6.1 Tenderfoot Member

During accumulation of the Tenderfoot Member, sedimentation in the three studied mini-basins was dominated by the accumulation of structureless sandstones, accumulation of which was influenced by evaporite precipitation as indicated by the presence of the distinctive 1.5 to 2.5 m-thick gypsum bed in all thee basins, albeit in only a partially preserved state in the Fisher Basin (Figs 4.11a, 4.12a, 4.13a). The origin of the gypsum could be via (i) precipitation from a super-saturated brines in evaporating salt pans in the restricted basins (Sloss, 1969), or (ii) dissolution of gypsum from within the salt wall, with gypsum-brine then being drawn to the ground surface by capillary action, whereupon evaporation and precipitation led to the accumulation of a sabkha-like pan deposit (Selley, 1988). The deposit was apparently locally reworked by the wind to form a gypsum aeolianite in the Parriott Basin (Lawton & Buck, 2006). In the Fisher Basin, where the gypsum bed was either only sporadically deposited, or was subsequently removed by erosion associated with fluvial activity, crinkly laminated sandstones are present, indicating disturbance of the sediment by ground water being drawn upward by capillary action and evaporation at the ground surface (cf. Goodall *et al.*, 2000). Similar sandstone deposits are present in the Parriott Basin directly above the gypsum horizon, where precipitated gypsum forms a weak sandstone cement.

In the Big Bend Basin, growth strata are present at the base of the Tenderfoot Member in small faults at the very top of the aeolianite at the top of the Cutler Group (Fig. 4.13b). This indicates that the aeolianite (possibly equivalent to the White Rim Sandstone) in this locality had lithified to a point where brittle deformation could take place, and sediment of the Tenderfoot Member accumulated as growth strata within the growing fault-bounded hanging-walls.

The prominent intraformational unconformity present locally at the top of the Tenderfoot Member in the Big Bend Basin indicates a hiatus in sedimentation between deposition of the Tenderfoot and Ali Baba Members, during which time salt-wall uplift continued (Fig. 4.7b).

### 4.6.2 Ali Baba Member

The sedimentary style of the Ali Baba Member is indicative of an episode of significantly increased fluvial activity in all three mini-basins, which is recorded as a series of multi-storey, multi-lateral channel elements (F1) in the Fisher Basin, and single storey channel elements, with sand-prone sheet-like heterolithic units in the Parriott Basin. Paraconglomerates in the Fisher Basin with their characteristic composition of a range of distinctive basement-clast lithology types derived from the Uncompahgre Uplift, are confined solely to the Fisher Basin; no clasts of Uncompahgre affinity are present in the succession in the other mini-basins. This demonstrates that uplift of the Fisher Valley salt wall resulted in the development of a surface topographic expression at this time that was effective in acting as a barrier to fluvial flow, thereby serving to limit the supply of sediment within the Parriott and Big Bend basins to detritus being shed from the San Luis Uplift in the southeast (Cadigan & Stewart, 1971; Stewart *et al.*, 1972).

In the Parriott Basin, the Ali Baba Member is characterised mainly by sheet-like heterolithic elements (F3) with the middle part of the member consisting of a series of vertically and horizontally amalgamated channel elements (Figs 4.11b, 4.12b). A similar arrangement of architectural elements is also present in the Big Bend Basin on the southwest flank of the Castle Valley salt wall, above the intraformational unconformity. The overall change in the style of accumulated elements between the Tenderfoot and Ali Baba members could reflect a change in climate from relatively arid to more humid conditions, resulting in increased channelised fluvial activity, and the absence of evaporitic deposits.

### 4.6.3 Sewemup Member

The preserved succession of the Sewemup Member in all three mini-basins is represented predominantly by sheet-like heterolithic elements (Fhiss; F3),

with only scarce, isolated single-storey channel elements (F2) present throughout the member. The presence of gypsum-clast-bearing horizons (FGc/m) indicates that the relative rate of uplift of the Castle Valley salt wall exceeded the rate at which the adjacent basins were being infilled, resulting in the salt wall breaching the land surface such that gypsum detritus was shed into the adjacent basins and locally reworked by fluviatile processes (Figs 4.12c, 4.13c; Lawton & Buck, 2006). The absence of major channel elements and the preservation of relatively soluble gypsum clasts indicate increased climatic aridity relative to that which prevailed at the time of Ali Baba Member deposition. The absence of gypsum clasts around the vicinity of the Fisher Valley salt wall and their complete absence from the Fisher Basin demonstrate that this salt wall did not breach the surface during Moenkopi deposition (Figs 4.11c, 4.12c). The sheet-like heterolithic elements (F3) represent the preserved deposits of ephemeral, non-confined floods, which swept across the basin floor (Tunbridge, 1981; Marriott *et al.*, 2005), locally reworking gypsum-clast debris.

The Sewemup Member records an upward decrease in the abundance of sand-filled channel elements (F2) and an associated systematic increase in the occurrence of sheet-like heterolithic elements (F3), which could reflect the preserved expression of a temporal reduction in sediment supply rate (Stewart *et al.,* 1972) or a shift to more arid climatic conditions.

### 4.6.4 Parriott Member

During the final stages of accumulation of the Moenkopi Formation in the Salt Anticline Region, the incidence of channelised fluvial sedimentation once again increased in the Parriott and Big Bend basins relative to that indicated by deposits of the Sewemup Member. This is expressed as an increase in the occurrence of single-storey channel elements (F2) in the Parriott Basin and multi-storey channel elements (F1) in the Big Bend Basin. The Parriott Member is absent from the preserved succession in the Fisher Basin, where the disconformity at the base of the Chinle Formation incises into the top of the Sewemup Member throughout the basin. This suggests that little or no sedimentation occurred during Parriott Member accumulation in the Fisher

Basin, which likely indicates the ultimate exhaustion of the sediment derived from the Uncompahgre Uplift (Fig. 4.11d) and the lack of an effective sediment delivery pathway from a southerly source into the Fisher Basin. In the Parriott and Big Bend mini-basins, accumulation of the Parriott Member was mostly confined to rim synclines that had developed along both margins of the Castle Valley salt wall. The fill of the rim syncline on the Parriott Basin side of this salt wall is characterised by non-confined sheet-like (F3) elements intercalated with single-storey, multi-lateral channelised (F2) elements (Fig. 4.12d). The fill on the Big Bend Basin side of the Castle Valley salt wall, is significantly more sand prone, containing a series of multi-storey, multi-lateral channel elements, which are confined solely to the rim syncline directly adjacent to the uplifting salt wall (Fig. 4.13b, d), where enhanced accommodation was locally generated by preferential salt evacuation directly adjacent to the salt wall.

## *4.7 Discussion*

The balance between the relative rates of sediment accumulation and basin infilling, and basin subsidence and associated salt-wall uplift is controlled by a number of factors, some of which are inherently linked to other processes involved in the development of the salt-walled mini-basins (Fig. 4.14). The rate of generation of accommodation within evolving mini-basins is ultimately dictated by the mechanical properties of the salt, including its initial composition and its anisotropic stratification (Hite, 1962), and the rate at which the salt can flow, which in turn depends on dynamic variables such as changes in rate at which sediment accumulates in an overlying mini-basin (Gee & Gawthorpe, 2006; Matthews *et al.*, 2007), and changes in ground-water levels and geothermal gradient. An increase in the rate of sediment loading acts to accelerate the rate of basin subsidence (Stewart & Clarke, 1999; Matthews *et al.*, 2007). Similarly, an increase in the geothermal gradient and the presence of meteoric water both act to decrease viscosity, resulting in faster rates of salt movement (Carter & Heard, 1970; Jackson & Talbot, 1986; Davison *et al.*, 1996b). Other, fixed variables that control mini-basin evolution include initial salt thickness, style and type of stratification in salt-prone units, the location of and offset across basement faults, pre-salt basement

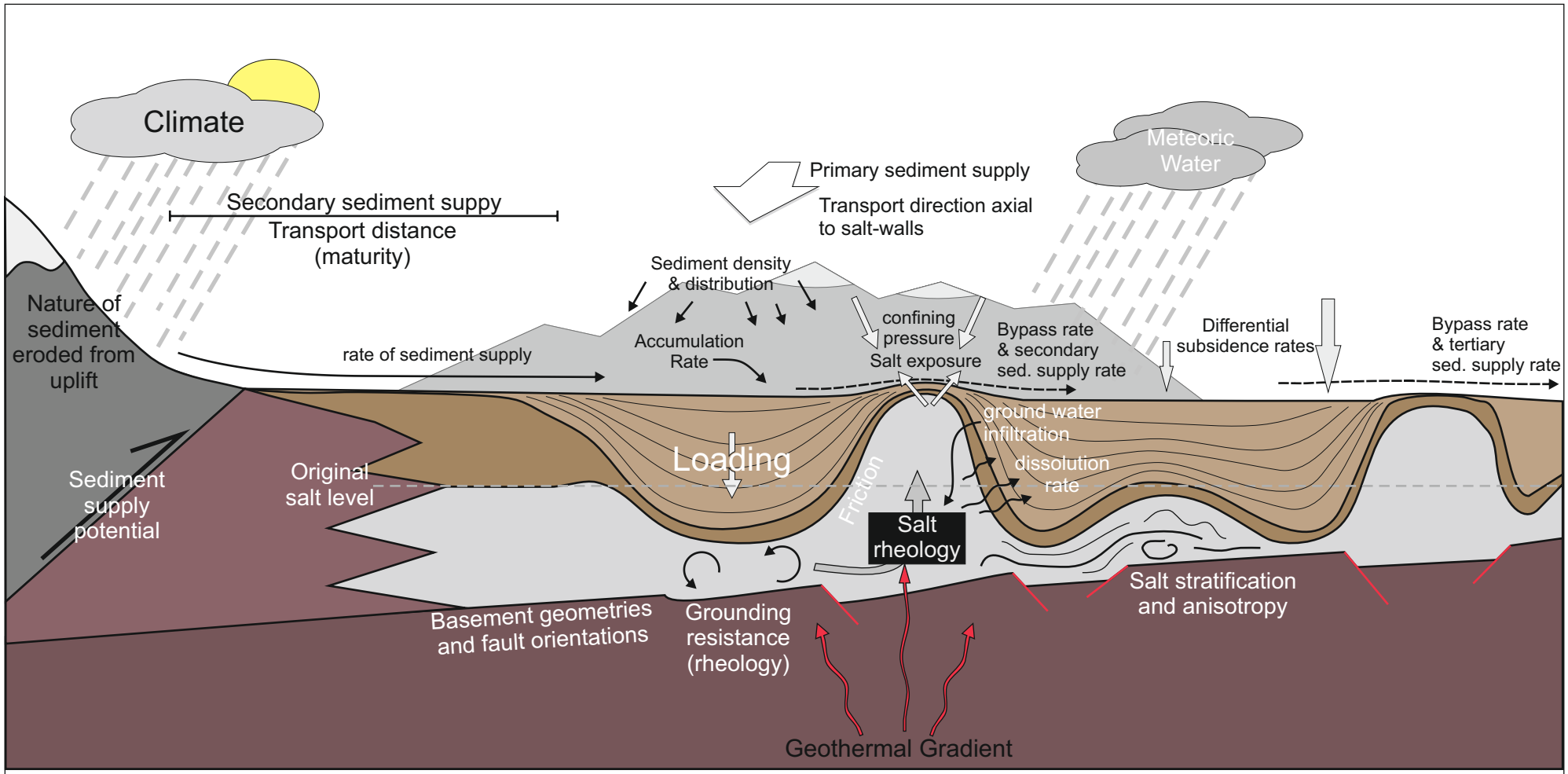


**Figure 4.14**: Conceptual diagram depicting the interaction of the main parameters that either directly or indirectly affect rates of sedimentation, basin subsidence and salt-wall uplift. See text for explanation.

geometries, and inherited pre-existing basin-fill state, each of which combine to exert a series of direct and indirect controls on the style of mini-basin evolution, the generation of accommodation, the orientation and spacing of salt-walls, and local anomalies in rates of salt movement within salt bodies (Hudec *et al.*, 2009, Fuchs *et al.*, 2011). The inertia of a buoyant, rising salt wall can also dictate the style and timing of both the generation of surface topography and surface breaching of the salt wall itself, which can then serve as a local sediment source; momentum forces dictate that an already rising salt wall will continue to rise even after it has attained a buoyancy equilibrium with the surrounding strata (Hudec *et al.*, 2009). The interplay between the parameters that govern salt kinematics can induce positive feedback cycles, which can in turn dictate rates and styles of sediment accumulation within parts of evolving basins, or sediment bypass (via diversion of sediment systems) in other parts. Increased rates of sediment supply and sedimentation generate increased loading and favour accelerated rates of salt withdrawal. This in turn can increase the rate of sediment capture within an individual basin, thereby driving the entire process of sediment accumulation and differential loading at a faster rate via a positive feedback mechanism. This process can occur within an individual basin where differential rates of subsidence occur at different points in the same mini-basin, resulting in locally increased or decreased rates of salt withdrawal and accommodation generation. Associated increased rates of salt-wall uplift might be expressed in the sedimentary record as the increased presence of intraformational clasts (Fci), derived locally from the reworking of strata eroded from above the uplifting salt walls. In cases where the salt walls breach the surface, reworked clasts of salt would be expected, especially in cases where an arid climatic regime prevents dissolution.

The thickness of salt through which the mini-basins subsided throughout their development defines the maximum potential depth of a mini-basin and the total potential accommodation. The configuration of the Paradox Basin allowed the accumulation of thicker deposits of salt of the Paradox Formation in the foredeep area where the thickest accumulations of sediment are accommodated within the salt-walled mini-basins of the Salt Anticline Region

(Kluth & DuChene, 2009; Trudgill & Paz, 2009; Trudgill 2011). Prior to the onset of sedimentation of the Moenkopi Formation, the basin-fill state of the studied mini-basins, in terms of the extent to which accommodation was filled by fluvial, shallow-marine and aeolian strata of the Honaker Trail Formation and Undifferentiated Cutler Group, drove the main phase of mini-basin subsidence and infilling. This defined the geometry of the basins at the time of accumulation of the Moenkopi Formation.

In the Fisher basin, the pre-Triassic basin-fill is the thickest of any mini-basin in the Salt Anticline Region and this basin was apparently already close to grounding on sub-salt basement by the onset of Moenkopi deposition (Trudgill & Paz, 2009). This resulted in slow subsidence rate throughout the episode of accumulation of the Moenkopi Formation in the Fisher basin and, coupled with relatively higher rates of sediment delivery and accumulation during deposition of the Ali Baba Member, accommodation in the Fisher basin was rapidly filled by a sand-prone interval composed of a complex of multi-storey channel elements (F1). Toward the end of the episode of accumulation of the Sewemup Member, rates of delivery of sand-grade sediment to the Fisher basin slowed dramatically as the sediment source area of the Uncompahgre Uplift was denuded, resulting in the accumulation of a sand-poor interval composed of sheet-like heterolithic elements (F3).

The Parriott basin was filled to a lesser degree by pre-Triassic sediment (Trudgill & Paz, 2009; Trudgill, 2011), meaning there was significant inherited accommodation available for filling during deposition of the Moenkopi Formation. This, combined with a higher rate of ongoing subsidence than that experienced by the Fisher Basin, resulted in the accumulation of a thicker succession of Moenkopi Formation in the Parriott basin. The rate of sediment delivery to the Parriott basin was low relative to that of the Fisher basin and major channel complexes did not develop, resulting in the accumulation of a thick but generally sand-poor succession, with minor sand-prone intervals present only in the Ali Baba and Parriott Members, the latter arising from the preferential diversion of channels into a developing rim syncline.

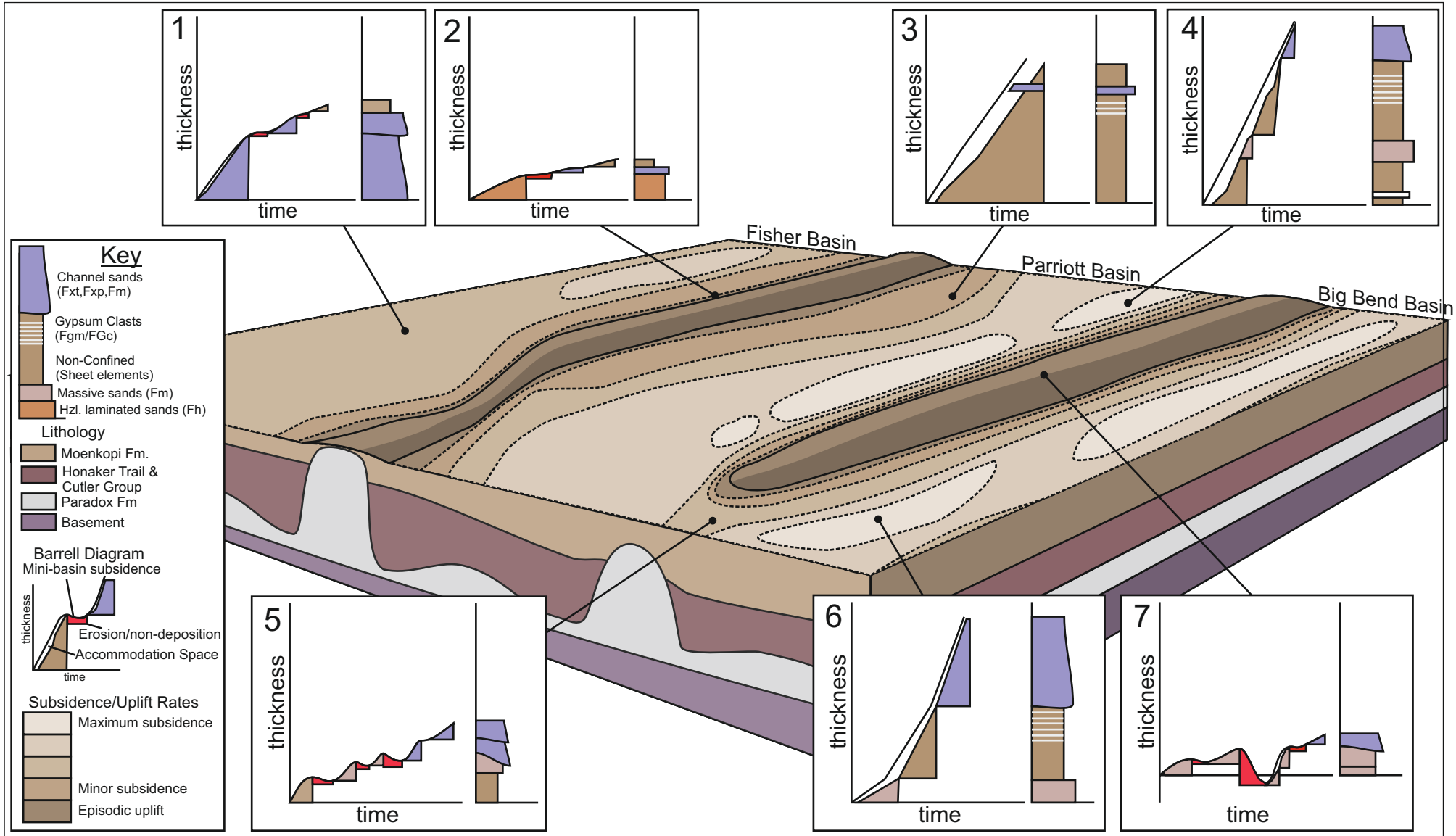


**Figure 4.15**: Model depicting the effects of differential rates of subsidence and accommodation generation on basin-fill style in a salt-walled mini-basin. Barrell diagrams to show basin subsidence rates and sedimentation rates for various locations in an evolving mini-basin. In areas where rates of sedimentation and subsidence are balanced, sand-prone successions tend to accumulate, whereas where rates of subsidence outpace rates of sediment delivery, heterolithic, sand-poor successions tend to accumulate and basins remain partly unfilled. Note that changes in sediment type and supply rates can result in complex changes in sedimentary architecture.

Models developed to predict the spatial and temporal distribution of sedimentary architectural elements in response to graben or half-graben formation using sequence stratigraphy (i.e. Leeder & Gawthorpe, 1987; Gawthorpe *et al.*, 1994; Howell & Flint, 1996; Gawthorpe & Leeder, 2000) have been used as a basis for developing a model to predict architecture distribution in response to halokinetics. This is possible due to the generation of similar surface topographic expressions, despite being caused by different subsurface mechanisms. The philosophy governing these models (particularly Howell & Flint, 1996) in turn, has been used to develop models to predict spatio-temporal distribution of fluvial architectural elements in salt-walled mini-basins.

The rate of generation of accommodation and its rate of filling by accumulating fluvial systems can be explained in terms of a series of Barrell diagrams (Barrell, 1917) for different areas within each mini-basin (Fig. 4.15). In locations where rates of subsidence outpaced rates of sediment delivery, the accumulating stratigraphy became dominated by a relatively argillaceous succession (Fig. 4.15; log 3) of heterolithic sheet-like elements (F3). In locations where rates of subsidence and sedimentation were balanced, sand-prone successions tended to accumulate (Fig. 4.15; log 1) and multi-storey multi-lateral channel elements (F1) and single-storey multi-lateral channel elements (F2) dominated the succession. In locations where rates of sedimentation outpaced rates of subsidence, erosion and sediment by-pass ensued and stacked multi-storey, multi-lateral channel elements (F1) containing abundant intraformational conglomerate (Fci) lags accumulated (Fig. 4.15; log 5) as fluvial systems repeatedly reworked older deposits as they migrated across the filled basin floor. Locations that experienced uplift, such as salt-wall flanks, experienced localised bypass and/or erosion and intraformational unconformities developed as a result of later fluvial incision (Fig. 4.15; log 7).

## *4.8 Conclusions*

1. The Moenkopi Formation demonstrates that the preserved expression of fluvial systems in salt-walled mini-basins is directly controlled by: (i) the

distribution of available accommodation (i.e. space yet to be filled) inherited from earlier basin-fill episodes, as demonstrated by the spatial variations of stratigraphic thickness both between and within mini-basins; (ii) the prevailing climate and rate and pathway of sediment delivery, which dictate fluvial processes and the pattern and distribution of architectural elements between and within mini-basins; (iii) the rate of ongoing salt-induced subsidence beneath evolving mini-basins and the rate of uplift of bounding salt walls, which together dictate the rate of generation of additional accommodation.

2. Sediment within individual mini-basins accumulated contemporaneously throughout the duration of Moenkopi Formation deposition, as demonstrated by the similar characteristic features of each of the members present across all three studied mini-basins.
3. Pre-existing basin-fill architectures inherited from the pre-Triassic sediment-fill state of the mini-basins exerted a significant control on subsequent subsidence during accumulation of the Moenkopi Formation. The Fisher basin (closest to the Uncompahgre Uplift) underwent greater subsidence and sediment filling during the Permian than the Parriott and Big Bend mini-basins, mainly a result of the direction of sediment delivery. The megafan responsible for the accumulation of the undifferentiated Cutler Group delivered sediment across the salt walls, such that the Fisher basin became preferentially filled and subsided to a point close to grounding on the pre-salt strata early in its history. As a consequence, the Moenkopi Formation in the Fisher basin is relatively thin, the succession experienced only slow rates of subsidence and sediment accumulation. Higher rates of mini-basin subsidence and accumulation of strata of the Moenkopi Formation characterised the basins further away from the Uncompahgre Uplift.
4. Subsurface salt-wall growth acted to uplift overlying strata to generate a surface topography, the growth of which was effective in diverting fluvial drainage pathways, especially in areas where salt-wall uplift culminated in surface breaching by the growing salt wall. During deposition of the Moenkopi Formation, preferred fluvial flow pathways were aligned parallel to the trend of the elongate salt walls, which served to effectively partition

neighbouring mini-basins. Where salt walls breached the surface (e.g. Castle Valley salt wall), gypsum detritus was shed as clasts into the surrounding mini-basins and locally reworked by fluvial processes before being preserved in the basin-fill.

5. The point-of-entry of a major fluvial drainage system into a subsiding mini-basin and its preferred flow pathway within the basin dictate the rate and style of accumulation. This is recorded in the preserved fluvial succession whereby fairways of major fluvial activity are preserved as single-storey or multi-storey, multi-lateral channel elements.
6. Salt-wall uplift served to isolate fluvial systems and confine them within their respective mini-basins. As a result of this confinement and isolation, each fluvial system within a specific mini-basin could theoretically be supplied from a different source area. As a result, the preserved expression of the fluvial architecture generated by each isolated fluvial system might vary considerably between adjacent mini-basins. In the Moenkopi Formation, this is expressed as the accumulation of relatively sand-poor intervals at the same stratigraphic levels as relatively sand-prone intervals in adjacent basins. Examples in the Salt Anticline Region include: (i) the difference in sand content between the Ali Baba Member in the Parriott basin versus the Fisher basin; and (ii) the difference in sediment architecture between the Parriott Member in the Parriott and Big Bend basins.
7. Spatial variations in both mini-basin subsidence rate and sedimentation delivery rate act as primary controls on fluvial system accumulation style. Packages of sand-prone strata can be preserved in one part of a mini basin at apparently the same stratigraphic level as packages of sand-poor strata elsewhere in the same mini-basin (e.g. northeast side versus the southwest side of the Parriott Basin).

# 5. Discussion

*This chapter aims to provide a conceptual synthesis of the relationships between fluvial sedimentation and coeval salt-walled mini-basin evolution considered in detail in chapters 2 to 4. It has three main objectives: (1) to distil the observations and interpretations discerned from the Moenkopi Formation – and more generally the Paradox Basin – to demonstrate how the stratigraphic expression of the Moenkopi Formation was controlled by inherited basin-fill state, subsidence rate, sediment supply rate, climate, and fluvial system behaviour such as drainage capture; (2) to apply the lessons learned from the detailed study of the Moenkopi Formation and other reviewed fluvial successions that accumulated in other halokinetic provinces so as to develop a series of generic models with which to predict how interacting variables are likely to control ensuing fluvial stratigraphic styles; (3) to apply these generic models to issues relating to hydrocarbon exploration and to demonstrate how such models can improve our understanding of mechanisms of sediment delivery, sediment routing and accumulation within salt-walled mini-basins known only from the subsurface.*

## *5.1 Moenkopi Formation and Paradox Basin*

The results of the detailed sedimentological study of the Moenkopi Formation presented in chapters 3 and 4 of this thesis demonstrate how an array of factors and their styles of interaction act to control the mechanism of accumulation of a fluvial succession in a series of salt-walled mini-basins. In this chapter, the factors that acted to control the accumulation of the Moenkopi Formation are considered in general terms. These factors include salt-wall geometry, inherited basin-fill style (inherited from the Permian Cutler Group accumulation in the case of the Triassic Moenkopi Formation), rate and style of sediment supply, nature of sediment routing pathways, rate of subsidence and climate, all of which interact to control the basin fill-style indicated by the preserved outcrop expression observed in the Salt Anticline Region.

### 5.2.1 Paradox Basin Geometry

The Paradox Basin is interpreted to be a flexural foreland basin, which developed in response to loading of the crust by the Uncompahgre Uplift, resulting in flexural down-warping of the crust adjacent to the site of loading (Barbeau, 2003). The asymmetric profile (i.e. increasing thickness of the basin toward the foredeep) played an important role in influencing the formation and development of the Salt Anticline Region: as salt layers of the Paradox Formation accumulated during the Pennsylvanian, a thicker accumulation of salt developed in the foredeep, thinning toward the distal margin of the basin to the southwest. This change in thickness of accumulated salt across the basin controlled the maximum potential basin subsidence, limiting the scope for development of deep mini-basins to the foredeep area of the Paradox foreland basin. The uplifted Uncompahgre Highlands, which lay in close proximity to the area of maximum thickness of salt within the foredeep, acted as the principal source for clastic detritus that was delivered into the foreland basin and which was responsible for the differential loading that initiated halokinesis (Doelling, 1988; Barbeau, 2003; Kluth & DuChene, 2009; Paz & Trudgill, 2009; Trudgill, 2011).

### 5.2.2 Cutler Group Basin Fill

Pre-existing basin-fill geometries, which resulted from the accumulation of the Permian Cutler Group strata, imposed a significant control on the ensuing basin subsidence style throughout the history of accumulation of the Moenkopi Formation. Throughout the duration of accumulation of Cutler Group, sediment derived from the Uncompahgre Highlands, were transported and delivered in an orientation perpendicular to the northwest-to-southeast trend of the evolving salt walls (Trudgill, 2011; Venus, 2013). As a result, sediment was preferentially delivered and accumulated in the mini-basins most proximal to the Uncompahgre Front, and this process of mini-basin filling was enhanced by episodic salt-wall uplift which acted to block and impede cross-salt-wall drainage pathways; thus, sediments preferentially accumulated in the foredeep of the Paradox Basin (Fig. 5.1). This pre-existing basin-fill style, resulted in the asymmetric and sequential filling of successive mini-basins, resulting in diminished basin-fill potential for successive episodes of

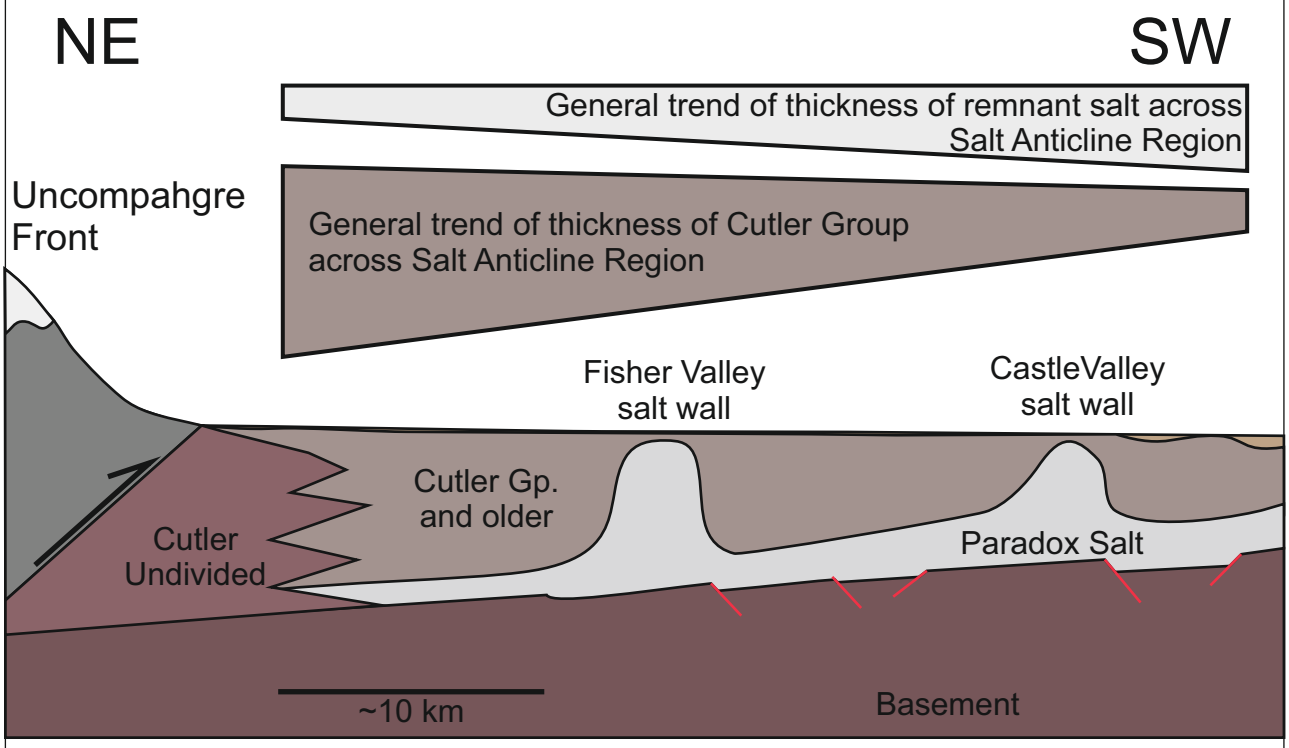


**Figure 5.1**: Schematic illustration depicting the fill state of salt-walled mini-basins in the Salt Anticline Region at the onset of the episode of accumulation of the Moenkopi Formation. Wedges indicate remnant thickness of salt (grey) which is the approximate remnant basin fill potential. The wedge represents the general changes in thickness of Cutler Group across the Region.

sediment accumulation with increasing proximity to the Uncompahgre Front, and increased basin-fill potential away from the Uncompahgre Front. The inheritance of this fill state was an important factor in controlling the later basin-fill style during the ensuing accumulation of the Moenkopi Formation (Banham & Mountney, 2013a).

The basin-fill style of the Cutler Group succession in the Salt Anticline Region is typically characterised by coarse-grained sandstone bodies that contain an abundance of conglomerate beds composed of pebbles and cobbles of extraformational origin. However, the basin-fill style of the Cutler Group shows a progressive reduction in mean sediment calibre with increasing distance from the Uncompahgre Front (Venus, 2013) such that fluvial deposits in the Cane Creek Anticline region rarely exceed granule grade. The basin-fill style of the Cutler Group was further modified by episodic salt-wall uplift, which temporarily diverted drainage pathways toward orientations parallel to the growing salt walls (and therefore impacted on regional sediment supply and delivery patterns). Further, salt-wall growth additionally caused temporary ponding of sediment on the upstream side of growing salt walls (Venus, 2013).

Climatic signature and resultant changes in the rate and style of sediment supply can be discerned in the basin-fill style of the Cutler Group. This is demonstrated by changes in the distribution of coarse- to fine-grained packages of sediment from the proximal to the distal parts of the Paradox Basin. This climatic signature was discussed by Cain (2009) and Cain and Mountney (2009, 2011) in the time equivalent Organ Rock Formation, a terminal fluvial fan which terminated in a dune field in the distal (i.e. downstream) part of the Paradox Basin. Increased channelised fluvial activity whereby channelised fluvial elements are greater in number and stacked into multi-storey and multi-lateral complexes are linked to relatively more humid episodes, whereas relatively more arid episodes are signified by few and less amalgamated channelised sand bodies and an associated expansion of deposits representing aeolian dune fields. Although more common in more distal parts of the Paradox Basin, accumulations of aeolian dune elements are preserved in the Salt Anticline Region, most notably in the lee of the Castle Valley salt wall. This might indicate a shift toward a more arid climate or could

reflect opportunistic preservation of such deposits in a salt-wall lee slope that was shielded from reworking via fluvial processes (Venus, 2013).

### 5.2.3 Moenkopi Basin Fill Evolution

The style of the stratigraphic accumulation of the Moenkopi Formation varied significantly both between and within mini-basins at the same stratigraphic height, and also temporally (i.e. vertically within the succession). These variations have been shown to have been controlled by a combination of factors including climatic variations, diversions of drainage pathways, and changes in rates of basin subsidence associated with differential rates of underlying salt withdrawal and salt-wall growth (Banham and Mountney, 2013a).

| Thickness (m) | Fisher Basin | Parriott Basin | Big Bend Basin |
|---|---|---|---|
| **Parriott** | None preserved | 40 | 70 |
| **Sewemup** | 40 | 110 | 110 |
| **Ali Baba** | 50 | 40 | 30 |
| **Tenderfoot** | 40 | 30 | 30 |
| **TOTAL** | 125 | 220 | 235 |

**Table 5.1: Thicknesses of the various members of the Moenkopi Formation in the three studied mini-basins.**

**Subsidence rates** are demonstrated to vary between the studied mini-basins by the differences in basin-fill thickness between adjacent mini-basins (Table 5.1). Subsidence rates were in part controlled by the pre-existing basin-fill states inherited from the earlier accumulation of the Cutler Group, where the basins were preferentially in-filled by sediments derived from the Uncompahgre Front with increasing proximity to the foredeep (Trudgill, 2011, Banham & Mountney, 2013a). These variable subsidence rates played a part in generating the contrasting basin-fill styles between the Fisher, Parriott and Big Bend Basins. The Fisher Basin, with a generally low rate of subsidence throughout its evolution accumulated a generally sand-prone succession, especially for episodes also associated with higher rates of sediment supply such as experienced during accumulation of Ali-Baba Member. The Parriott Basin, which experienced a higher rate of subsidence compared to that of the Fisher Basin, preferentially accumulated a succession that was relatively sand

poor, especially for episodes also associated with relatively low rates of sediment supply such as experienced during accumulation of the Sewemup Member.

**Drainage diversion and changes in sediment supply pathways** are interpreted to have controlled sediment distribution between the three studied mini-basins throughout evolution of the Moenkopi Formation. The influence of these factors can be discerned through analysis of changes in basin-fill style between mini-basins for successions present at similar stratigraphic levels. A good example is that of the Ali-Baba Member. Within the Parriott Basin, the succession is sand-poor, whereas in the Big Bend Basin, the succession at the same stratigraphic level contains substantially higher proportions of sandstone elements. In the Fisher Basin, the Ali-Baba Member is composed of a succession characterised by a high proportion of extraformational clasts that are not present in adjacent mini-basins. The dominant palaeodrainage direction suggests that sediment was supplied principally from the San Luis Uplift, although drainage networks could have entrained Cutler Group sediments from the southeast (Stewart *et al.,* 1972; Blakey, 1974; Banham & Mountney, 2013a & b). the most probable origin for the extraformational clasts in the Fisher Basin is a secondary supply originating in the Uncompahgre highlands to the northeast, which, although severely denuded by this time, were still exposed throughout the early history of accumulation of the Moenkopi Formation. Clasts from this Uncompahgre source are only found in the Fisher Basin, suggesting that the uplifted Fisher Valley salt wall acted to deflect drainage pathways originating from the Uncompahgre, thereby preventing delivery of sediment form this source into successively more distal basins in the Salt Antlicline Region.

| Fill-style | Fisher Basin | Parriott Basin | Big Bend Basin |
|---|---|---|---|
| **Parriott** | None preserved | Slightly underfilled | Filled |
| **Sewemup** | Underfilled | Underfilled | Underfilled |
| **Ali Baba** | Filled/overfilled | Slightly underfilled | Slight underfilled |
| **Tenderfoot** | Filled | Underfilled | Underfilled |

**Table 5.2: Fill styles within Moenkopi Formation.**

**Climate** controls are demonstrated to effect sediment delivery across the Salt Anticline Region and the effect of climate variations can be discerned from those of halokinetically-driven subsidence or drainage pathway diversion by observation of the basin-fill style across multiple mini-basins and also by comparison with equivalent successions in areas beyond the limit of halokinetic influence. Typically, changes in halokinesis that lead to drainage diversion will influence just a single basin. However, variations in climate tend to operate over broader geographic regions and will therefore influence multiple mini-basins across the province. Thus climatic variations manifest in the preserved record will typically be recorded by similar changes in the depositional style across multiple basins rather than just a single basin for a common stratigraphic level (Banham & Mountney, 2013b). An example of a regional palaeoclimatic control on the style of accumulation is the relative shift in depositional style between the mini-basins during accumulation of the Ali-Baba Member and Sewemup Member (Table 5.2). This is expressed as a relative decrease in proportion of channelised elements across all three basins observed between these members. Subsequently, when conditions became more humid during later accumulation of the Parriott Member, the proportion of channelised elements increased once again in the Parriott and Big Bend Basins. The environment in the Fisher Basin at this time cannot be judged because the Parriott Member is not preserved in this basin, probably due to it being eroded prior to the onset of accumulation of the overlying Chinle Formation.

## Moenkopi Formation Discussion

The complex interplay between ongoing subsidence, the development of drainage pathways and climate variations had a profound influence on the style of the preserved stratigraphic architecture of the Moenkopi Formation in the Salt Anticline Region. At a fundamental level, climate variations controlled the overall net sediment flux into the region, whereas halokinesis controlled the distribution of sediment within the evolving mini-basins. Figure 5.2 portrays a series of schematic logs which were synthesised from the stratigraphic sections recorded in the study area. These synthetic logs

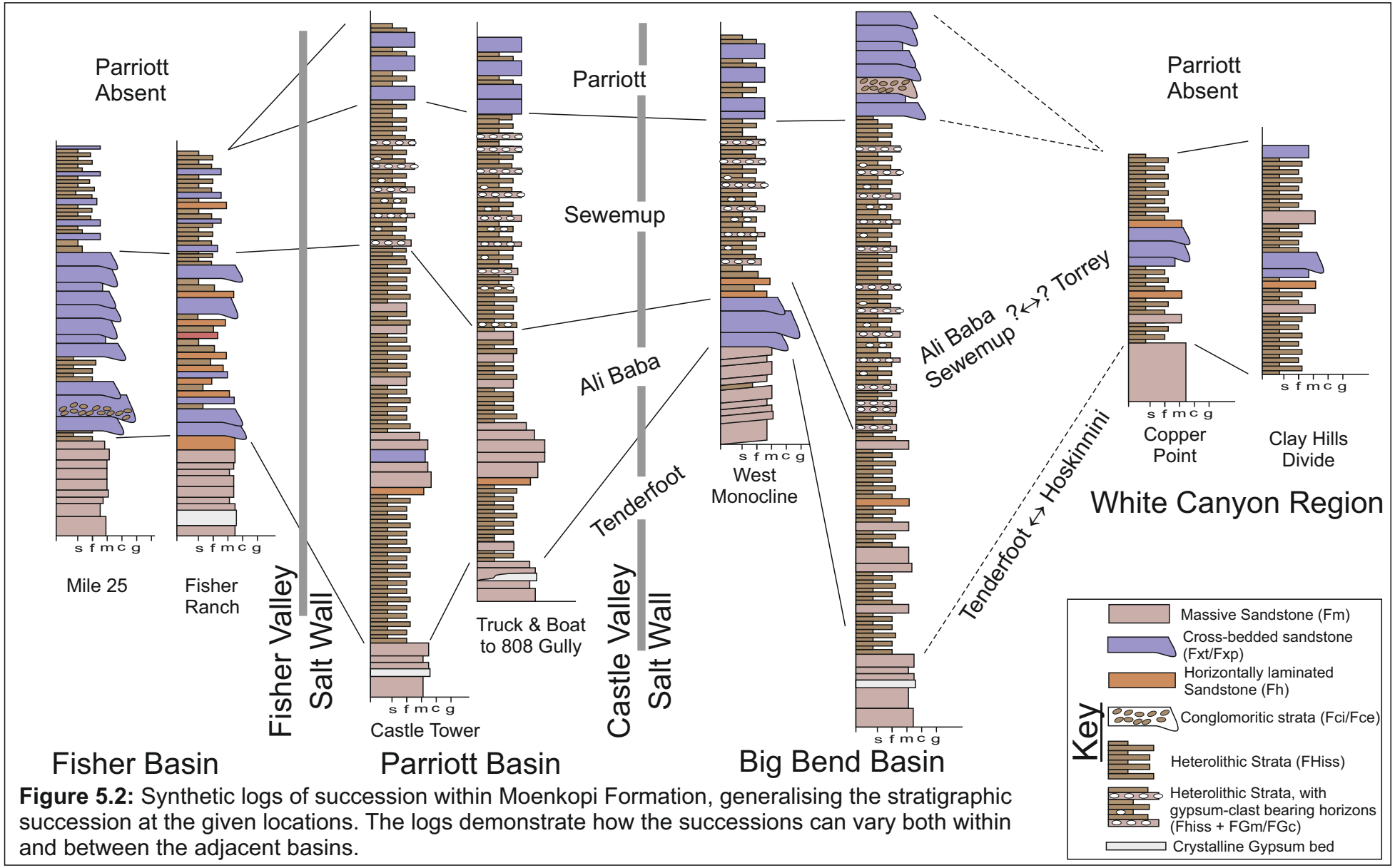


**Figure 5.2:** Synthetic logs of succession within Moenkopi Formation, generalising the stratigraphic succession at the given locations. The logs demonstrate how the successions can vary both within and between the adjacent basins.

demonstrate the variability of the stratigraphic succession both between and within each of the mini-basins and in areas outside of the influence of halokinesis (White Canyon Region). The logs demonstrate the variations in thickness of the succession controlled by varying rates of salt tectonics and the interplay of sediment supply, which is expressed as variations in the facies preserved at a certain location. The temporal and spatial variations in facies can be explained in part by figure 5.3, which depicts how basin-fill styles changed over the course of accumulation of the Moenkopi Formation in relation to the influence of both climatic and halokinetic controls. General trends expressed across all three studied mini-basins can be interpreted in terms of a likely climatic control whereby all three mini-basins became progressively more sand-poor at the onset of accumulation of the Sewemup Member. Superimposed on this general trend are differences in basin-fill styles arising as a likely outcome of halokinesis, including the effects of changes in sediment routing and subsidence rate, such as the Parriott Member being absent from Fisher Basin due to a lack of accommodation brought about by a reduction in the rate of mini-basin subsidence to zero or negligible toward the end of the episode of accumulation of the Moenkopi Formation as a consequence of grounding of the mini-basin (Banham and Mountney, 2013a).

Figure 5.4 depicts the distribution of drainage pathways and their origin throughout deposition of the Moenkopi Formation, and shows how drainage pathways and climate acted jointly to control changes in the rates of sediment supply to the separate mini-basins throughout evolution of the Moenkopi Formation.

During accumulation of the Ali Baba Member, which occurred during an episode of relatively humid conditions (see chapter 3), sediment was delivered from the San Luis Uplift and adjacent areas (to the southeast) and from the Uncompahgre Uplift (to the northeast) into the Salt Anticline Region. The geometries of the salt walls resulted in preferential diversion of the drainage pathways from the San Luis Uplift around the up-stream opening of the Parriott Basin and into the Fisher and Big Bend Basins. In addition, the surface topographic relief associated with the on-going uplift of the Fisher

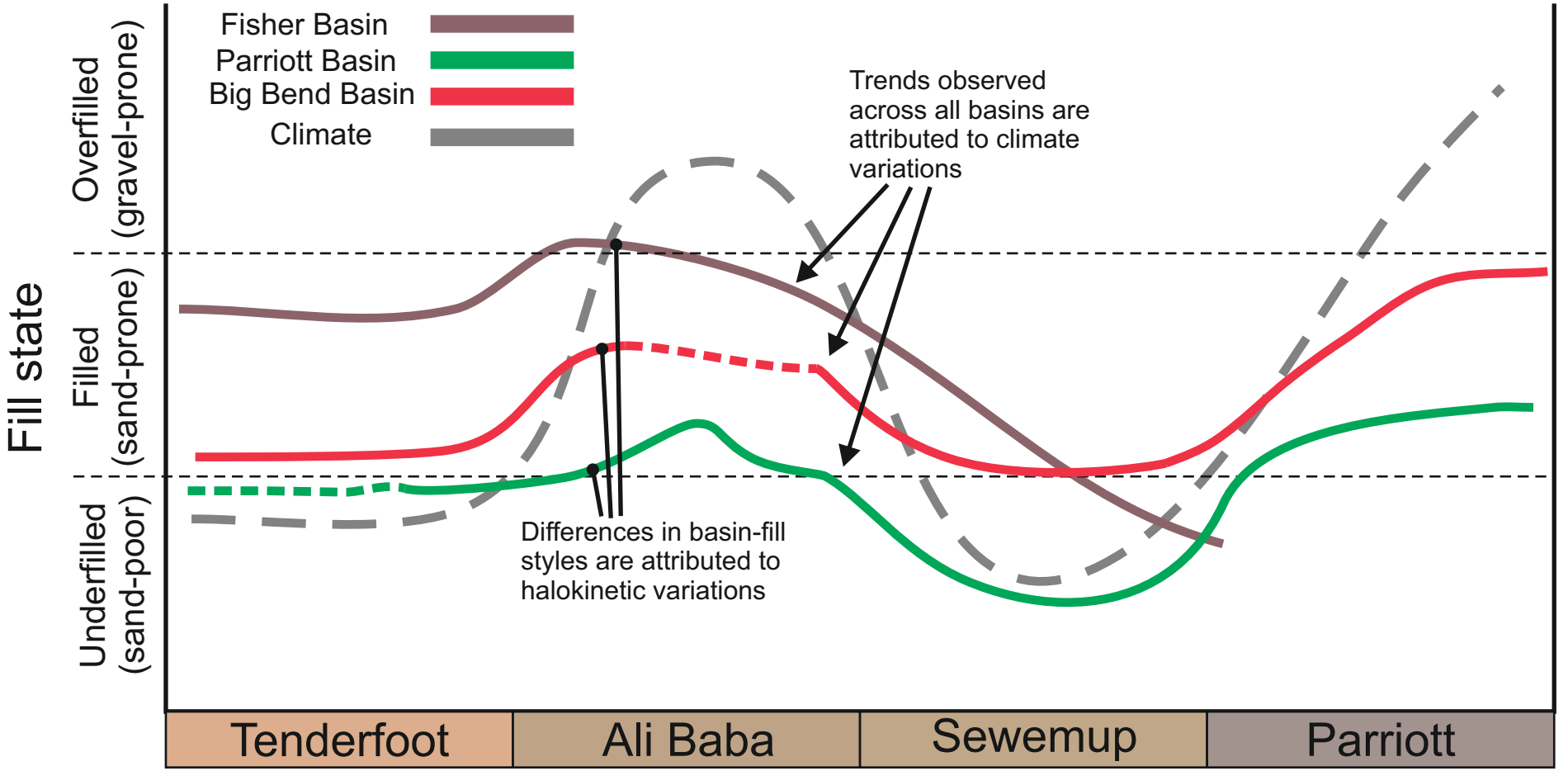


**Figure 5.3**: Inferred changes in basin-fill styles of the three studies mini-basins over the duration of accumulation of deposits of the Moenkopi Formation. The signature of fill state is an indicator of the collective role of climate and halokinesis in moderating the preserved stratigraphic record.

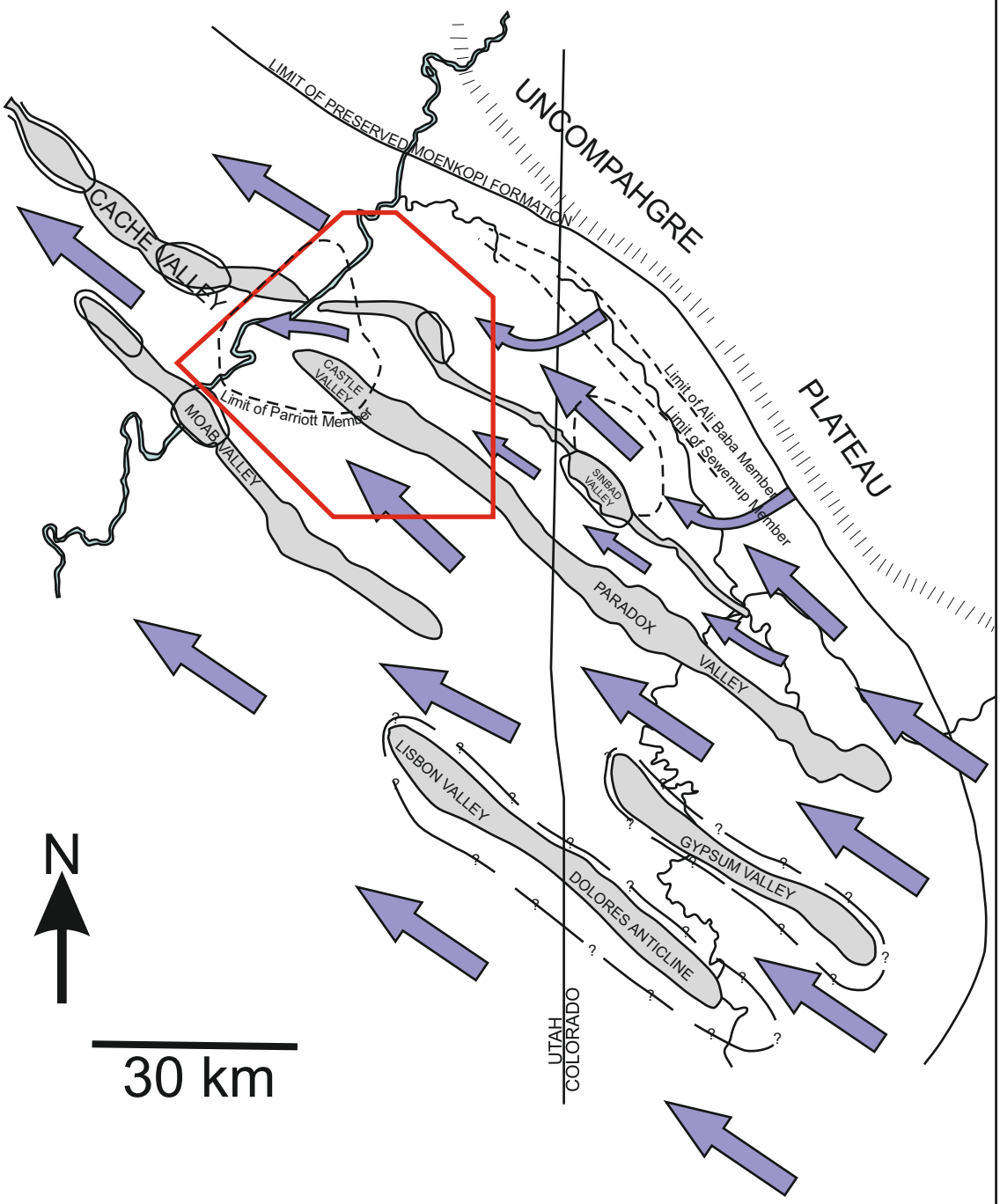


**Figure 5.4a**: Distribution of fluvial drainage pathways during accumulation of the Ali-Baba Member across the Salt Anticline Region. Note that clastic material is delivered into the Fisher Basin from the Uncompahgre Front to the northeast and from the San Luis Uplift to the southwest. Arrow size indicates approximate fluvial activity in basin. Red border indicates limits of the study area.

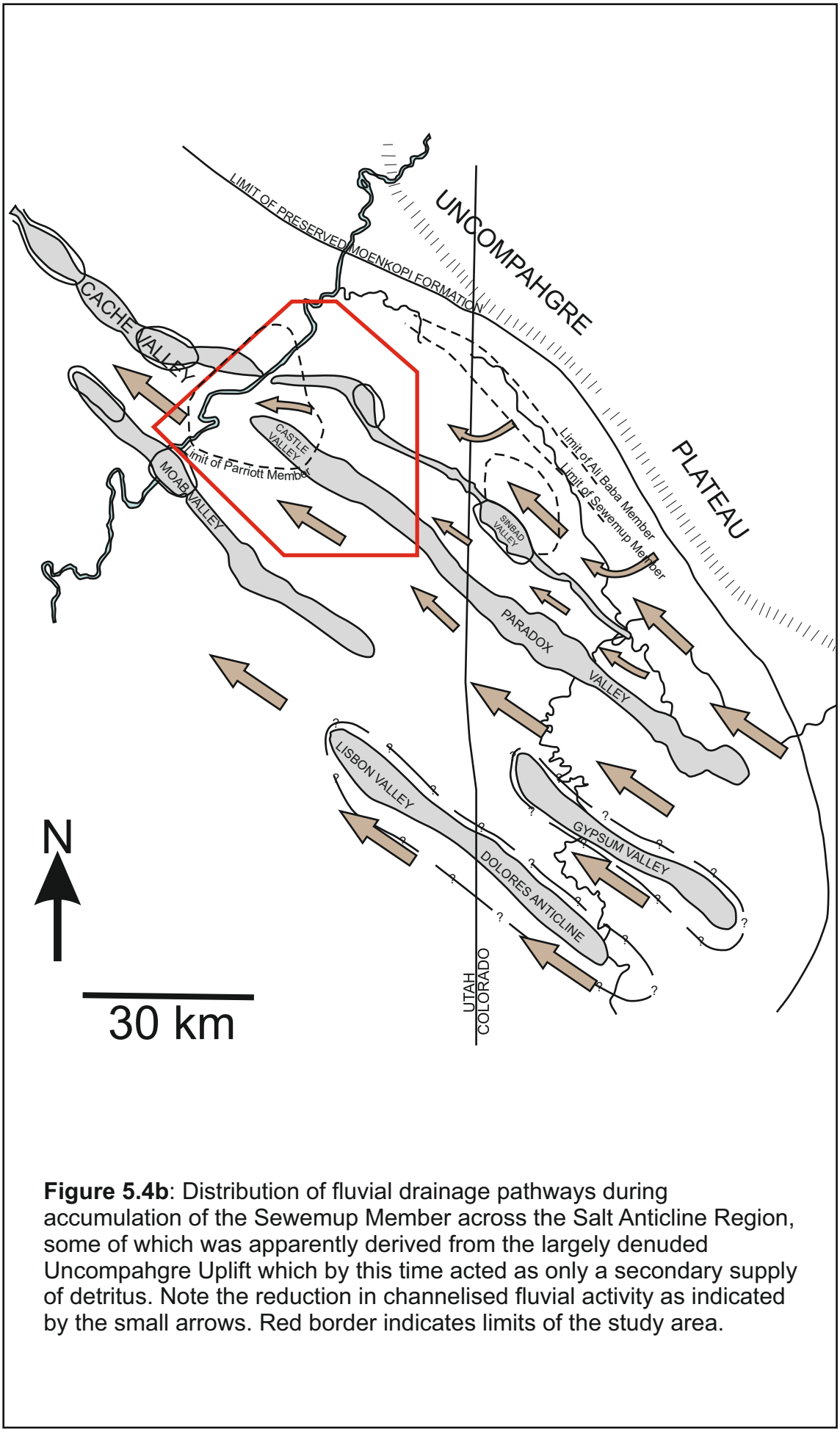


**Figure 5.4b**: Distribution of fluvial drainage pathways during accumulation of the Sewemup Member across the Salt Anticline Region, some of which was apparently derived from the largely denuded Uncompahgre Uplift which by this time acted as only a secondary supply of detritus. Note the reduction in channelised fluvial activity as indicated by the small arrows. Red border indicates limits of the study area.

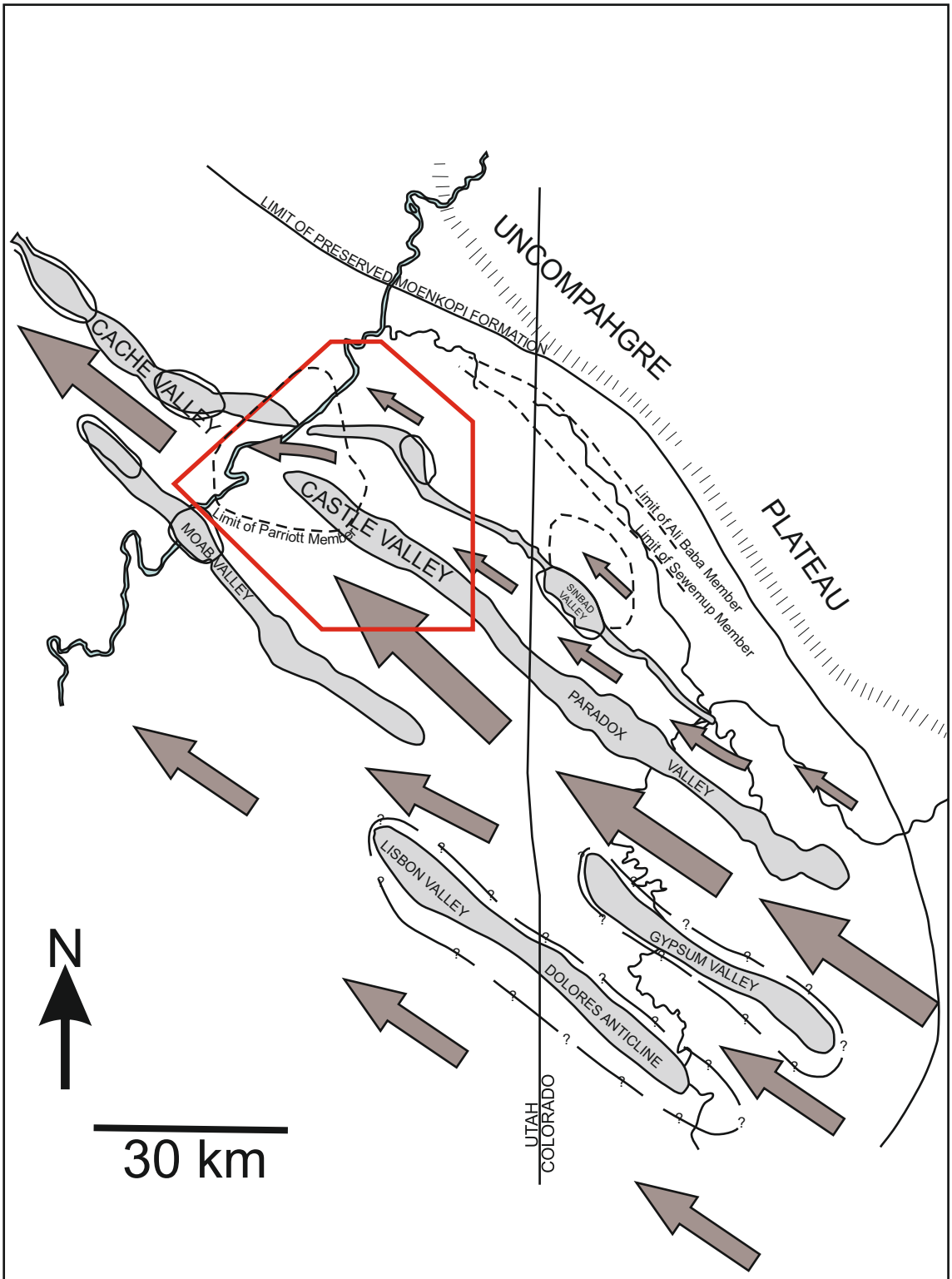


**Figure 5.4c**: Distribution of fluvial drainage pathways during accumulation of the Parriott Member across the Salt Anticline Region. Note that channelised fluvial activity has all but ceased in the Fisher Basin by this time. The principal drainage pathway is axially along the Basin Bend mini-basin. The Uncompahgre Uplift was virtually denuded at this time and no longer acted as a significant source of detritus. Arrow size indicates approximate fluvial activity in basin. Red border indicates limits of the study area.

Valley – Sinbad Valley salt wall likely acted to divert sediment derived from the Uncompahgre Uplift along the axis of the Fisher Basin.

During accumulation of the Sewemup Member (Fig. 5.4b), which occurred during an arid episode, diminished rates of sediment supply from both the southeasterly source and from the Uncompahgre source resulted in the accumulation of fewer channelised elements than during accumulation of older deposits of the Ali Baba Member. In addition, continued degradation of the Uncompahgre Uplift resulted in the reduced supply of sediment from this secondary source region throughout accumulation of the Sewemup Member.

By the onset of accumulation of the Parriott Member, (Fig. 5.4c), climate once more reverted to relatively more humid conditions. At this time, the Uncompahgre Font had been denuded to the point where it was no longer a significant source of sediment for the region. Sediment was almost exclusively derived from the San Luis Uplift area in the southwest. During accumulation of the Parriott Member, the most sand-prone succession accumulated in the Big Bend Basin in an area adjacent to the Castle Valley salt wall where a rim-syncline developed toward the end of the episode of accumulation of the Moenkopi Formation (Banham & Mountney, 2013a). The Parriott Member in the Parriott Basin was more sand-prone than the preceding Sewemup Member, which is interpreted to be a climatic control variation of sediment delivery. This is in contrast to the fill style difference of the Parriott Member between the Parriott and Big Bend Basins, where diversion of drainage pathways resulted in the accumulation of a sand-poor succession within the Parriott Basin relative to that of the neighbouring Big Bend Basin. Had any sediment accumulated in the Fisher Basin during the episode represented by the accumulation of the Parriott Member in other parts of the region, it was subsequently eroded before the onset of accumulation of the overlying Chinle Formation.

## *5.3 Generic Implications*

The observations from the Moenkopi Formation have been used to develop a series of generic models depicting how various aspects of halokinesis can control the distribution and style of accumulation of fluvial architectural elements across a series of salt-walled mini-basins. This section

discusses the following aspects of salt-sediment interactions: controls on the style of basin fill and the interplay between rates of sediment supply and subsidence; mechanisms of basin segregation and the interplay between rates of sediment supply and salt-wall uplift; the role of climate in influencing regional sediment distribution patterns.

### 5.3.1 Basin Fill

The style of basin fill is determined by numerous parameters, including: the inherited basin-fill geometry at the time of onset of accumulation; remnant subsidence potential (controlled by pre-existing basin-fill state); spatial and temporal variations in subsidence rate, both between and within a single mini-basin; mechanisms of sediment delivery and the orientation of delivery pathways relative to the trend of salt walls; spatial and temporal changes in the rates of sediment delivery that are deemed to have been controlled by allogenic factors such as climate and provenance; and calibre of delivered sediment as controlled by factors such as transport distance, climate, and provenance (Banham & Mountney, 2013a,b).

### 5.3.2 Basin-fill geometries

Observations from the Salt Anticline Region (Chapter 3 and 4) and from case study reviews (Chapter 2) demonstrate that broad-scale basin-fill geometries are typically expressed by two common forms, where either a “heel-toe” geometry or a “turtle-back” geometry develops through the evolution of a single mini-basin. Discussion of the kinematics that lead to the evolution of these two separate basin-scale geometric styles is beyond the remit of this study, but factors such as salt-wall spacing, initial sediment delivery orientation into the basins relative to the trend of growing salt walls, and the development of linear or polygonal salt-wall geometries are all important controls (cf. Paradox Basin and Pre-Caspian Basin).

**Heel-toe geometries and structures** form where one side of a salt-walled mini-basin subsides initially, with grounding potentially occurring at one side of the basin before the other side begins subsiding (Kluth & DuChene, 2009; Trudgill, 2011). The style of evolution typically creates one or more intra-basin unconformities, where fluvial elements accumulated during a later

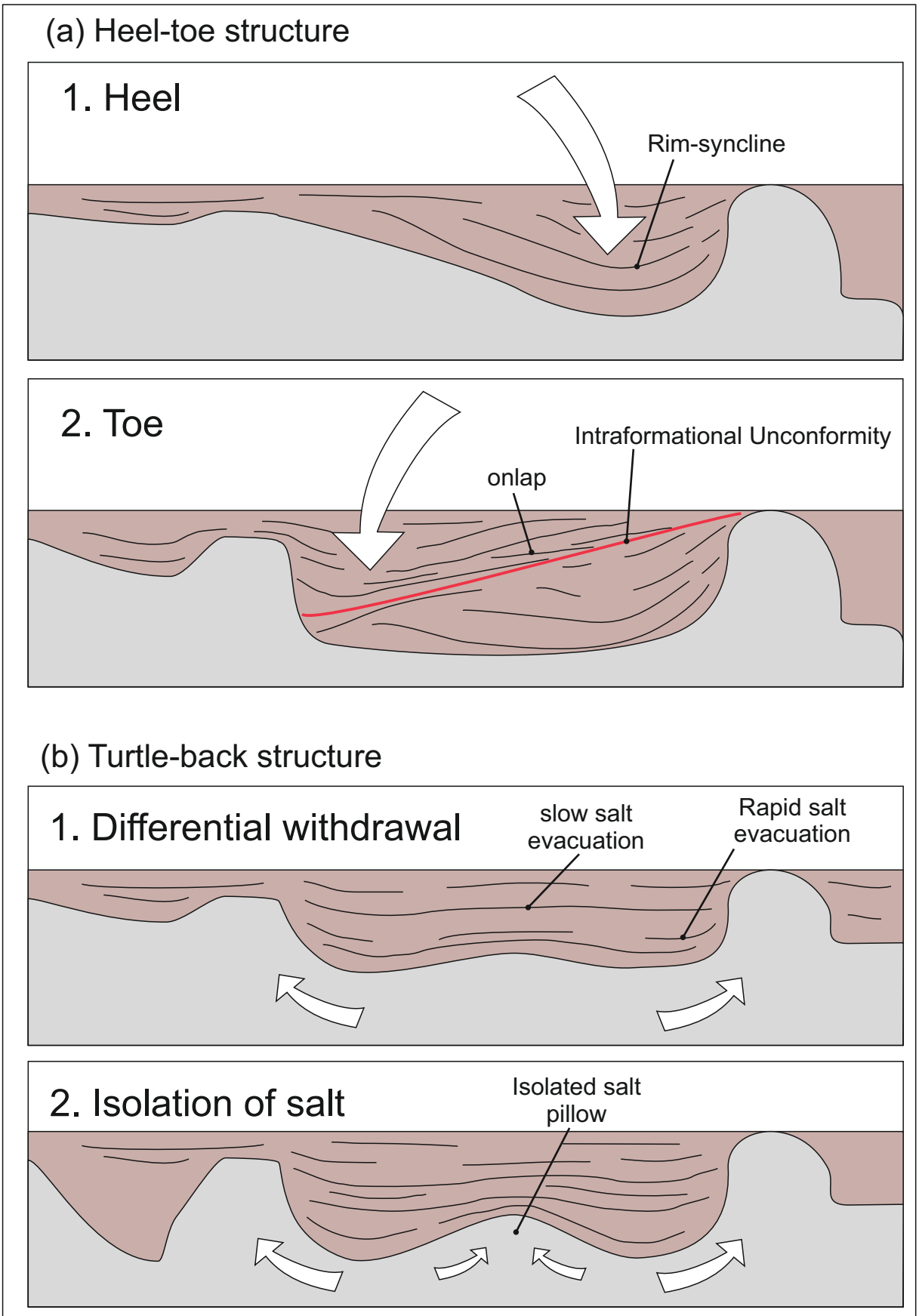


**Figure 5.5**: Schematic diagram of the formation of “Heel-toe” structures and “turtle-back” structures. (a) Heel-toe structure, where rim-synclines develop sequentially (b) Turtle-back structure, where rim-syncline subside simultaneously. Drainage orientation can be transverse or axial to the salt walls.

phase of mini-basin evolution onlap onto a grounded (or near grounded) older sediment wedge (Fig. 5.5). the most rapid rates of subsidence tend to occur in positions adjacent to the salt walls, and therefore channelised fluvial systems will typically migrate to occupy and accumulate sand bodies in the area closest to the salt wall at the locus of subsidence. Channelised fluvial elements will pinch-out onto the previously deposited rim-syncline on the opposite side of the basin (Fig. 5.4). This will result in stacked channels preferentially stacking in a position where the rate of subsidence is greatest. The distance across the basin that channel elements will accumulate will depend on the ratio between aggradation rates versus subsidence rates, with higher aggradation rates relative to subsidence favouring expansion of the active alluvial plain and a more widespread occurrence of fluvial architectural elements across the developing mini-basin

**Turtle-back geometries and structures** form where both sides of the basin subside simultaneously (Fig. 5.5), trapping a ridge of salt in the centre of the basin (Barde *et al*., 2002a). Formation of turtle-back structures can have implications for drainage segregation within a single mini-basin, where one side of the basin can become more sand prone than the same stratigraphic level on the opposite side of the basin, perhaps due to drainage diversion, or differential rates of subsidence in developing rim synclines. Development of rim synclines adjacent to the salt walls will cause preferential migration of fluvial fairways to preferentially trap the majority of channelised fluvial elements in the rim synclines and away from the basin centre, resulting in the accumulation of predominantly non-channelised fluvial architectural elements in the centre of the basin above the developing turtle back. This however, may be mitigated if aggradation rates are sufficiently high to allow burial of the relative high of the turtle-back structure. The distribution of fluvial channel elements across mini-basins with developing turtle-back structures is controlled subtly by spatial variations in rates of halokinesis, as both sides of the mini-basin subside simultaneously.

### 5.3.3 Basin-fill style

The nature of the basin-fill style in terms of whether the accumulation is sand-prone or sand-poor is controlled by, among other things, the interplay

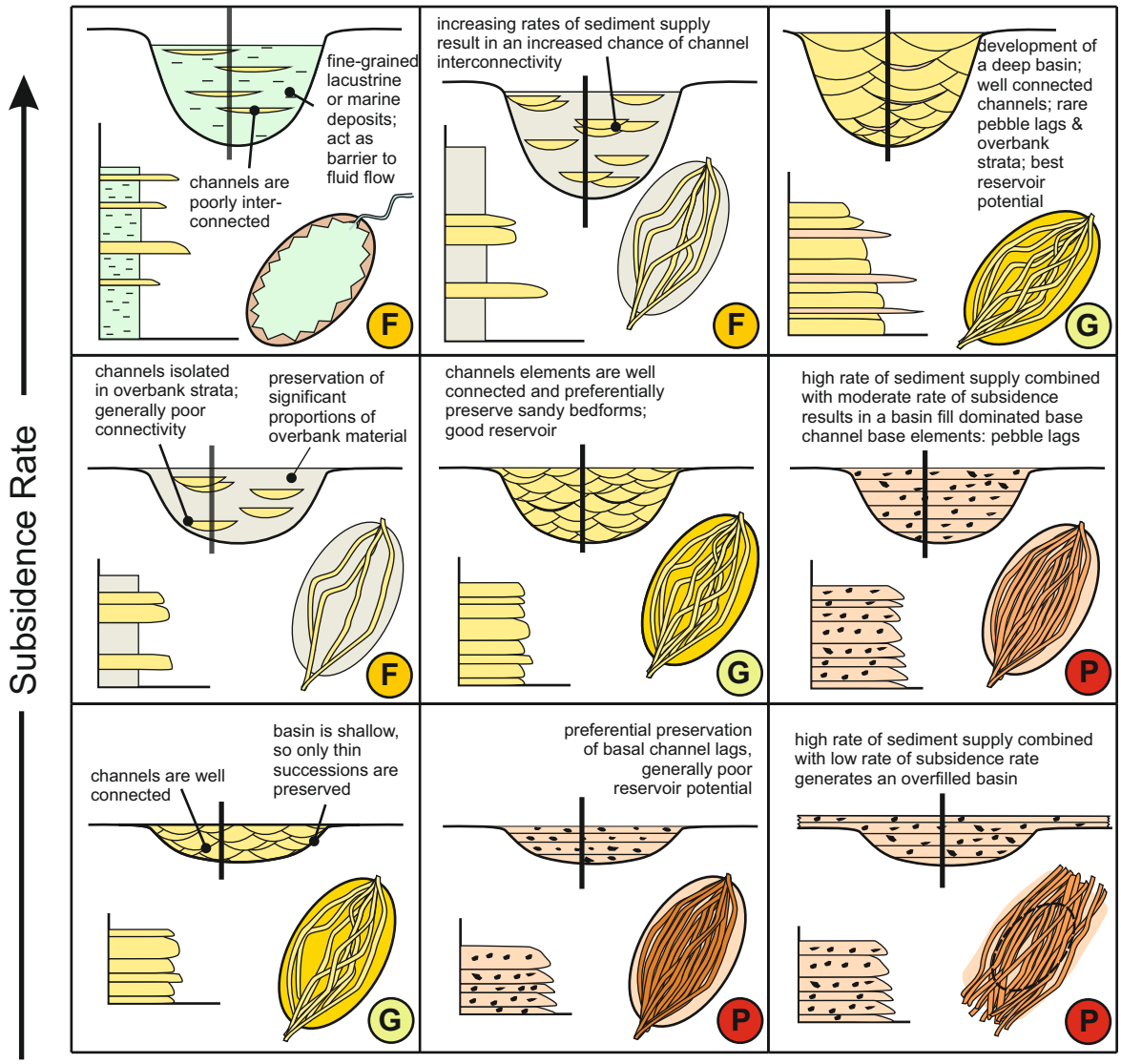


very poorly sorted; clay-pebble

moderately to well sorted; sand

poor to moderately sorted; clay-silt

moderately sorted; silt-fine sand

G good reservoir potential

F fair reservoir potential

P poor reservoir potential

Matrix displays likely basin-fill architectures associated with various rates of sediment supply and subsidence.

Overfilled basins tend to occur when rates of sedimentation outpace rates of subsidence

Underfilled basins tend to occur when rates of subsidence outpace rates of sediment supply and the available accommodation space remains partly unfilled.

Filled Basins occur when the rates of sediment supply and subsidence are balanced.

**Figure 5.6**: Conceptual model demonstrating how the interplay between rates of subsidence and sediment supply act to control the developing basin-fill style. Balanced rates of subsidence and sediment supply generate filled (sand-prone) basins; in cases where the rate of subsidence outpaces the rate of sediment supply, under-filled basins with argillaceous fills tend to develop and available accommodation may remain partially unfilled; in cases where the rate of sediment supply outpaces the rate of subsidence, over-filled basins with gravel-prone fills tend to develop and accommodation is filled leading to downstream bypassing of excess sediment. See text for further explanation.

between the rates of subsidence and sediment supply in the receiving basin. In terms of hydrocarbon prospectivity, for a succession with good reservoir potential to develop, sedimentation rates and subsidence rates need to be balanced to allow the optimum amount of reworking of argillaceous overbank material, without significant reworking of the sandy channel elements (Fig. 5.6). If subsidence rates decrease or sediment input by fluvial systems increases, the fluvial system will have sufficient time to continually rework the accumulated fluvial strata, removing most of the overbank material and the sandy facies which typically compose the upper parts of channel elements, leaving only the coarse pebbly lags that form the bases of the channel elements. This will lead to the development of a gravel-prone succession (or overfilled basin-fill style), and this typically makes for poor quality reservoirs, due to later diagenesis of clay minerals trapped within the matrix. By contrast, where subsidence rates are high, or sediment input is low, the fluvial systems will have insufficient time to avulse and rework the overbank area to remove the typically argillaceous overbank material. This will result in the increased chance that channel elements will be isolated within the overbank succession, decreasing connectivity of the reservoir. This will result in the accumulation of a relatively sand-poor basin (or underfilled basin-fill style).

An additional factor which can exert a control on the distribution of basin-fill styles is the direction of sediment delivery pathways relative to the trend of developing salt walls. Where sediment delivery is perpendicular to the trend of uplifting salt walls (e.g. Salt Anticline Region during accumulation of the Cutler Group, where drainage pathways crossed salt walls within the Pre-Caspian Basin), basin fills typically become successively finer grained with increasing distance from the hinterland. As sediment is delivered into the initial mini-basin, sediment loading typically increases the rate of subsidence, and the mini-basin acts as a sediment sink that traps and accumulates most of the coarse-calibre material entering the halokinetic province. The next basin downstream in the system will preferentially trap the next-coarsest fraction of sediments that bypassed the initial basin, whereas finer-grained material will be transported on into successive mini-basins. This will result in the development and infilling of a series of mini-basins each characterised by a progressively more sand-poor style of fill.

Where sediment delivery pathways are oriented parallel to the trend of linear salt walls, the sediment-fill styles of the evolving mini-basins can be randomly distributed, with gravel-prone basins accumulating adjacent to basins with argillaceous styles of fill. One potential cause for this contrast in basin-fill styles is that the up-stream salt wall geometries are such that they preferentially divert drainage pathways into a single basin. In elongate, linear mini-basins for which axis-parallel drainage pathways dominate, the main factors governing the distribution of the basin-fill style are: potential for drainage pathway capture or diversion by evolving mini-basins or rim synclines, and localised changes in rates of subsidence or salt-wall uplift. Additional factors may also come into play, such as the configuration of salt-wall geometries at the up-stream opening of the mini-basins, which may preferentially divert drainage pathways into or away from a particular mini basin (Hazel, 1994; Matthews et al 2007; Banham & Mountney, 2013a)

## 5.4 Basin segregation

The rate and style of salt-wall uplift can determine the degree of basin isolation – the degree to which fluvial activity is confined to a given basin throughout evolution of a mini-basin province. Figure 5.7 depicts various states of basin isolation resulting from the interactions between the rate of salt-wall uplift and rate of sediment supply. When salt-wall uplift is intermittent, the fluvial system may be able to migrate unrestricted across the salt-wall crest in cases when accumulation has reduced any surface topographic expression to nil. With decreasing rates of sediment supply relative to subsidence, the basin will become partially isolated; scenarios may be envisaged whereby channelised fluvial systems may be deflected by the uplifting salt walls but non-channelised elements may overtop the salt walls during extremely flood events. With increasing continuity of salt wall uplift, the topographic surface expression of the growing salt wall will become more pronounced, limiting potential for inter-basin drainage. Established cross-wall drainage pathways may be able to resist diversion by down-cutting notches into the uplifting salt wall. The ability of antecedent fluvial systems to maintain their course will be dependent on the rate of fluvial down-cutting, relative to the rate of salt-wall uplift, and also on the mechanical properties of the

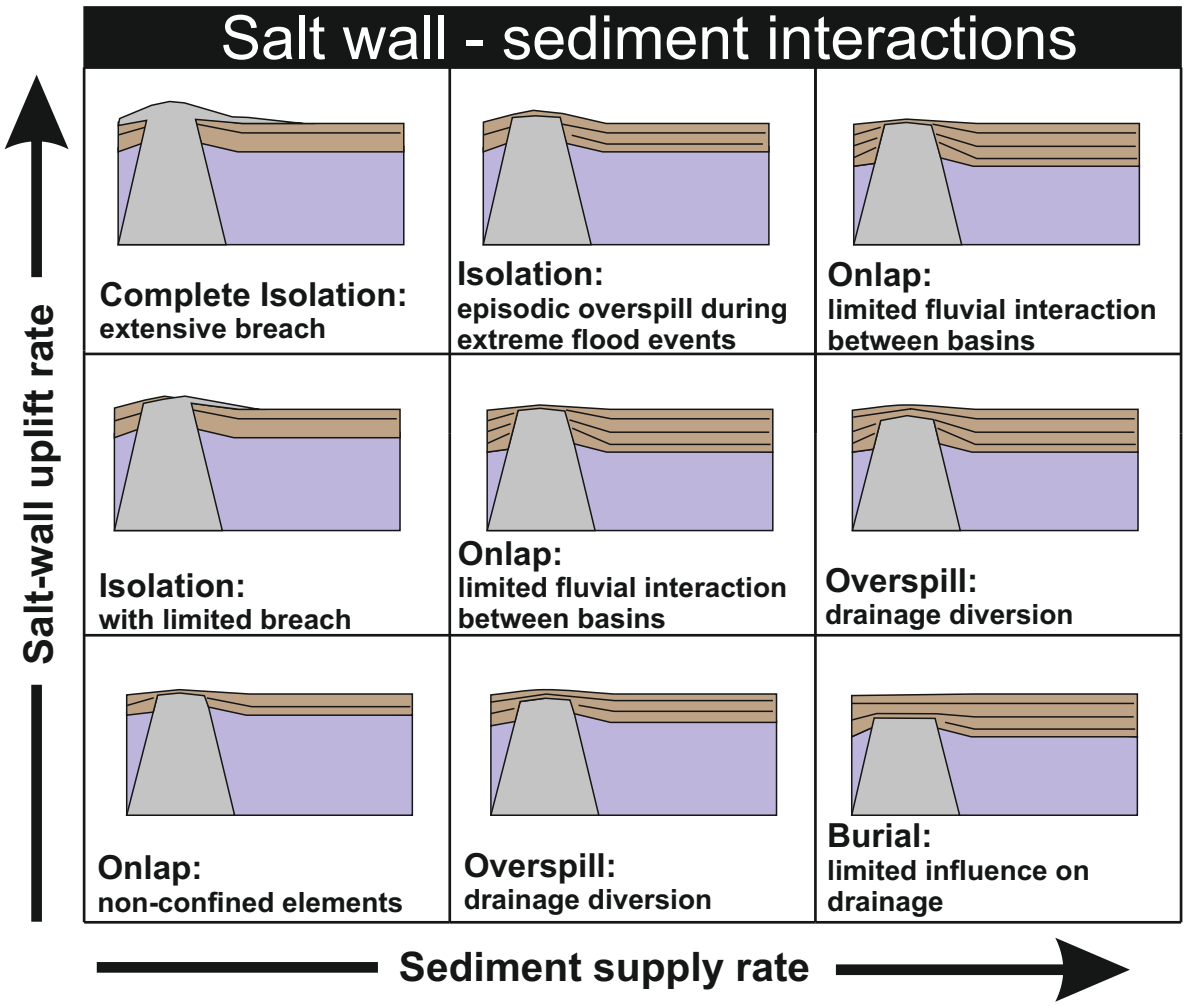


**Figure 5.7a**: Conceptual model demonstrating how the interplay between rates of salt-wall uplift and sediment supply act to control the style of sediment accumulation on salt wall flanks.

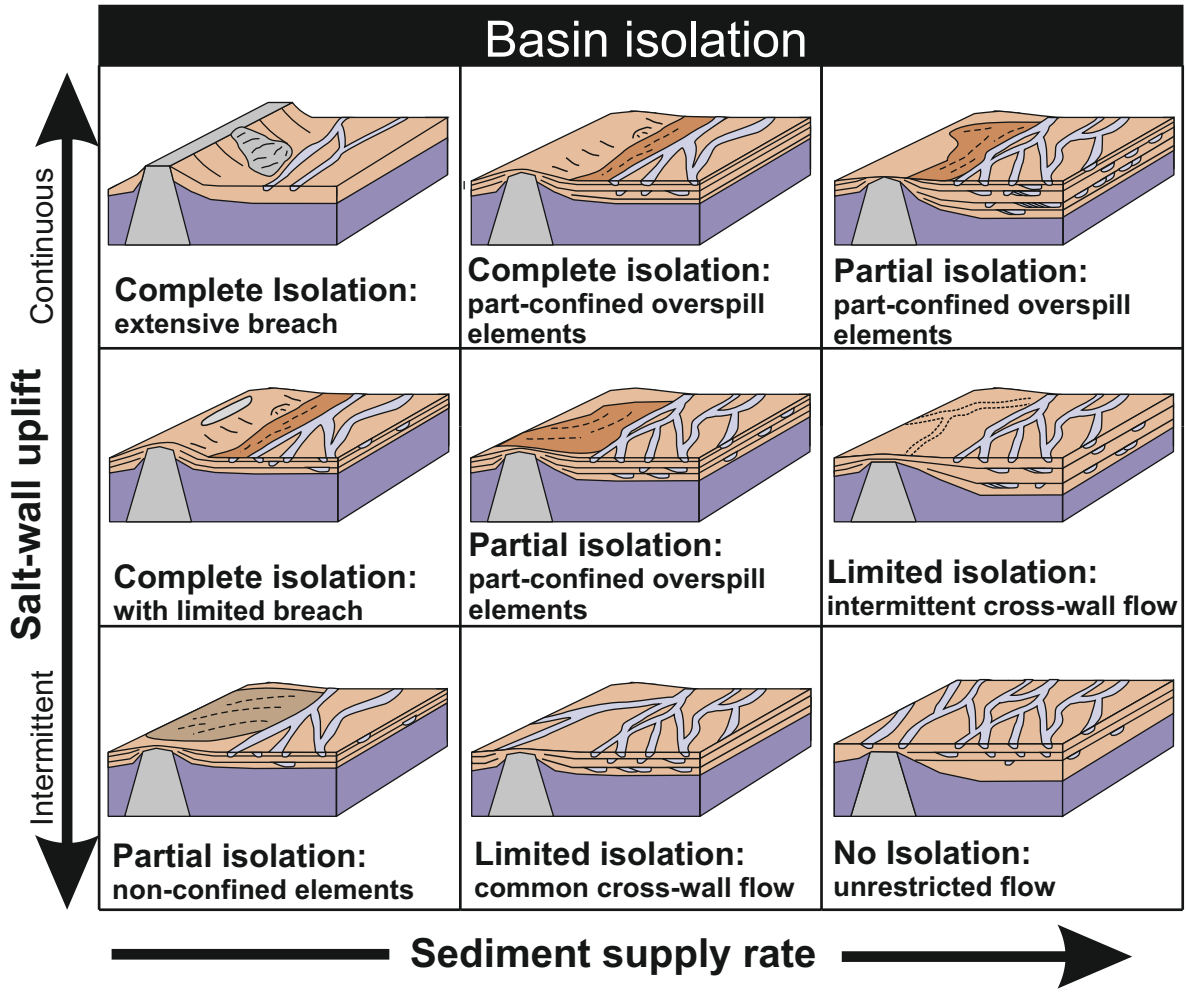


**Figure 5.7b**: Conceptual model demonstrating how the rates of salt-wall uplift and sediment supply control the evolution of fluvial drainage pathways.

uplifting strata overlying the salt wall. Even with high rates of sediment supply, cross-wall drainage will be limited, and with low rates of sediment supply, the salt wall may actually breach the land surface, potentially forming salt glaciers which may be reworked by subsequent fluvial activity (e.g. Zagros Mountains in Iran, Bruthans *et al*., 2009). Where salt-wall uplift is continuous and on-going, cross-wall drainage will be severely restricted, and drainage reversal may ensue. Alternatively, partially confined overbank elements may accumulate in locations where flood-waters pond (Banham & Mountney, 2013b). In addition, where sediment supply is limited, extensive surface breaches may occur, resulting in the reworking of discrete horizons of diapir-derived detritus into the surrounding strata (e.g. Lawton & Buck, 2006; Banham & Mountney, 2013a, b).

Where salt walls breach the ground surface, evaporitic material can flow down the flanks of the uplifted salt wall (Ala, 1974) which can, in-turn be eroded and reworked as clastic detritus into the accumulating stratigraphy. By observing the temporal distribution and the nature of reworked diapir-derived detritus, it may be possible to determine the relationship between rates of salt-wall uplift and sediment supply rate (where the rate of supply of salt detritus is a function of the rate of salt-wall uplift; Fig 5.8). Where the rate of sediment supply is greater than the rate of salt-wall uplift, the salt wall will be buried, with little surface expression exhibited. With increasing rates of salt-wall relative to that of sediment supply, a surface breach by the salt wall may occur such that detrital material from the salt wall will be readily available for reworking by fluvial systems. With lower rates of salt-wall uplift relative to that of sediment supply, limited amounts of detritus will be available for reworking, which will be expressed as rare salt clasts within the accumulating strata (principally gypsum as halite is too soluble for long-term preservation as detrital clasts). With a further increase of the rate of salt-wall uplift, salt clasts will become more abundant, forming discrete beds of matrix-supported gypsum conglomerate, with such clast-supported salt conglomerate beds being best developed with high rates of salt wall uplift or in close proximity to the salt wall and the site of reworking. Where salt-wall uplift rates are high, coupled with low rates of sediment supply, salt glaciers and evaporitic

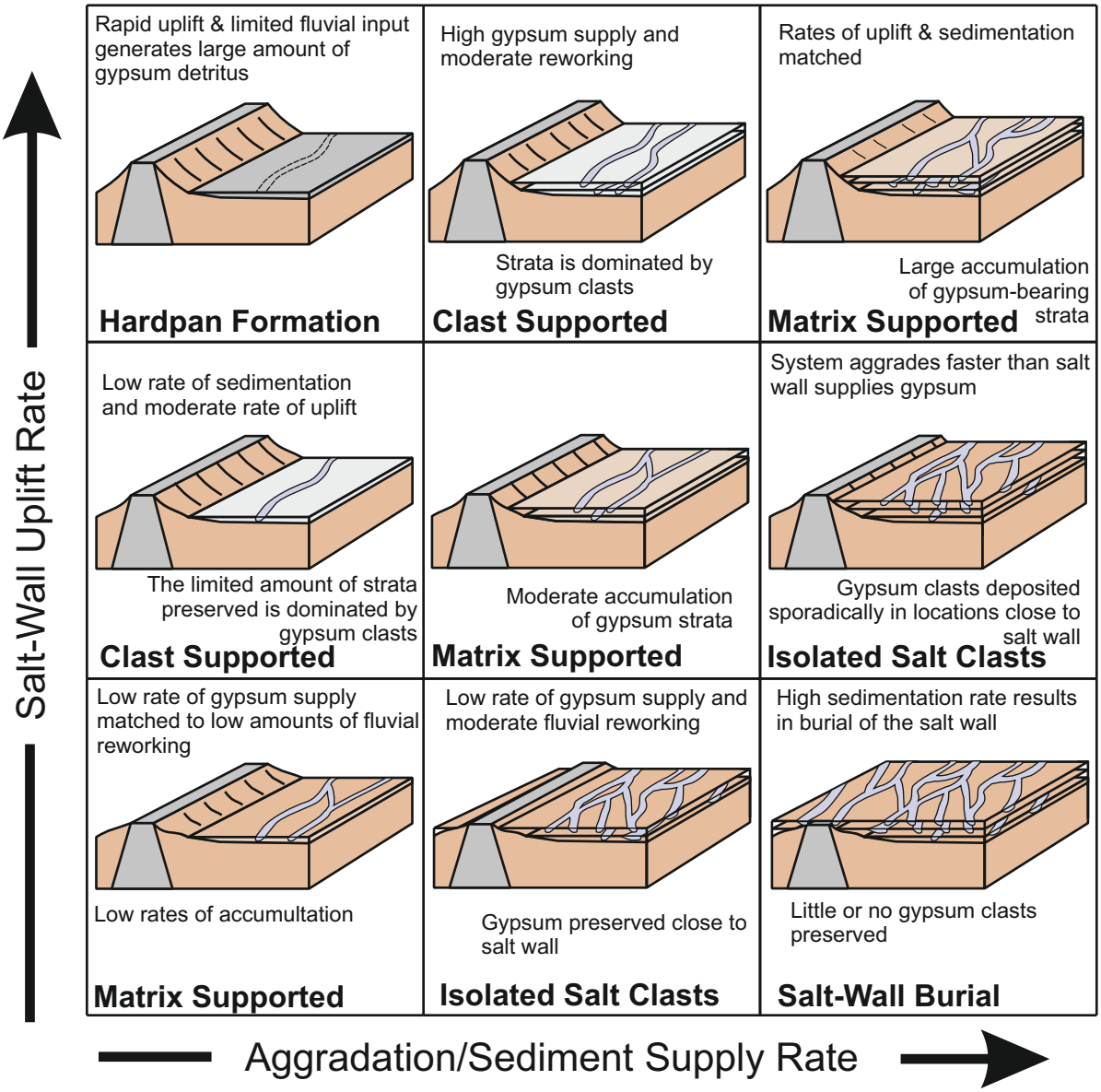


**Figure 5.8:** Conceptual model demonstrating how the rates of salt-wall uplift and sediment supply can control the accumulated stratigraphy when the salt wall breaches the land surface.

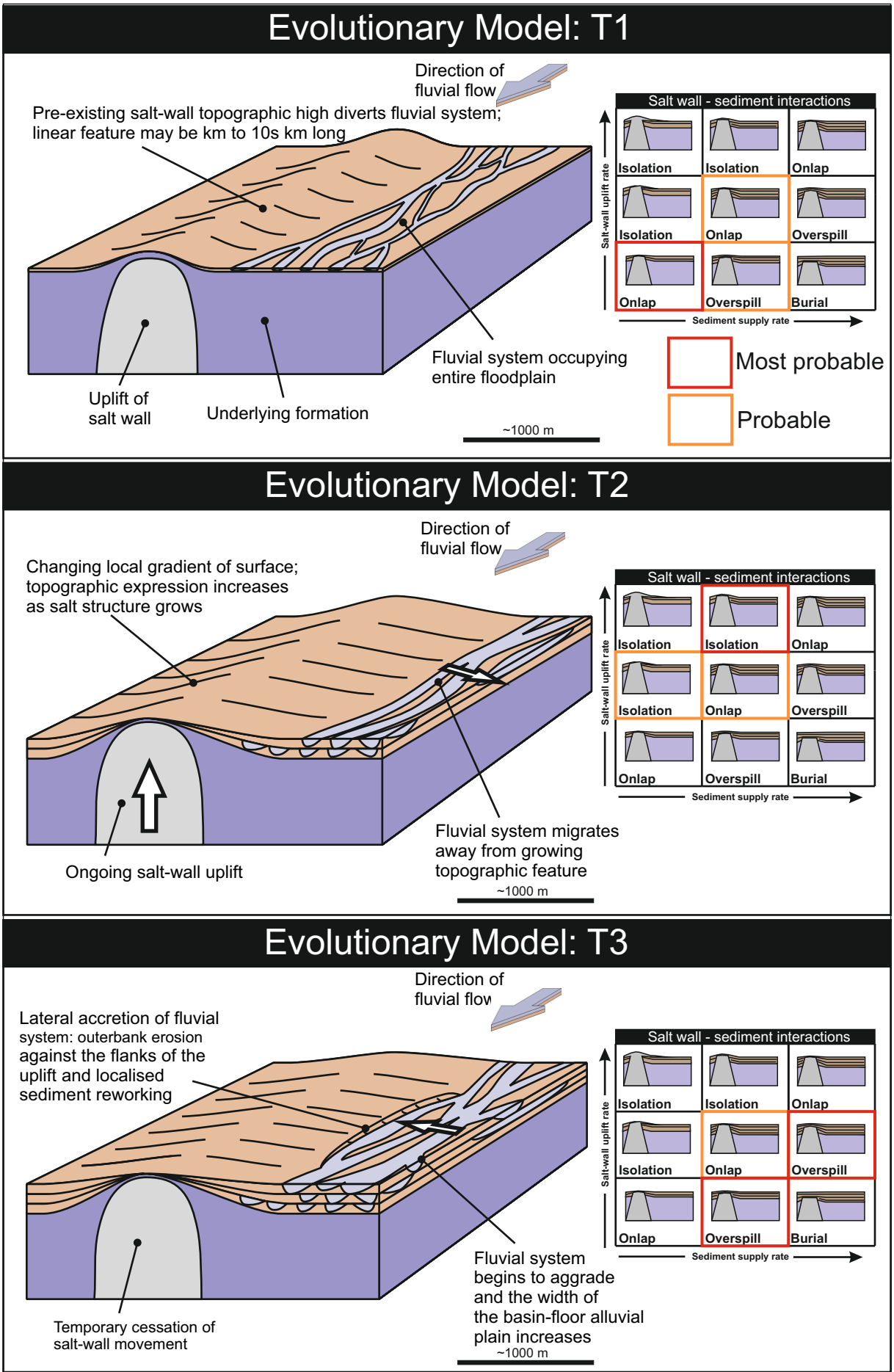


**Figure 5.9**: Evolution of drainage pathways and stratigraphy around a growing salt wall.

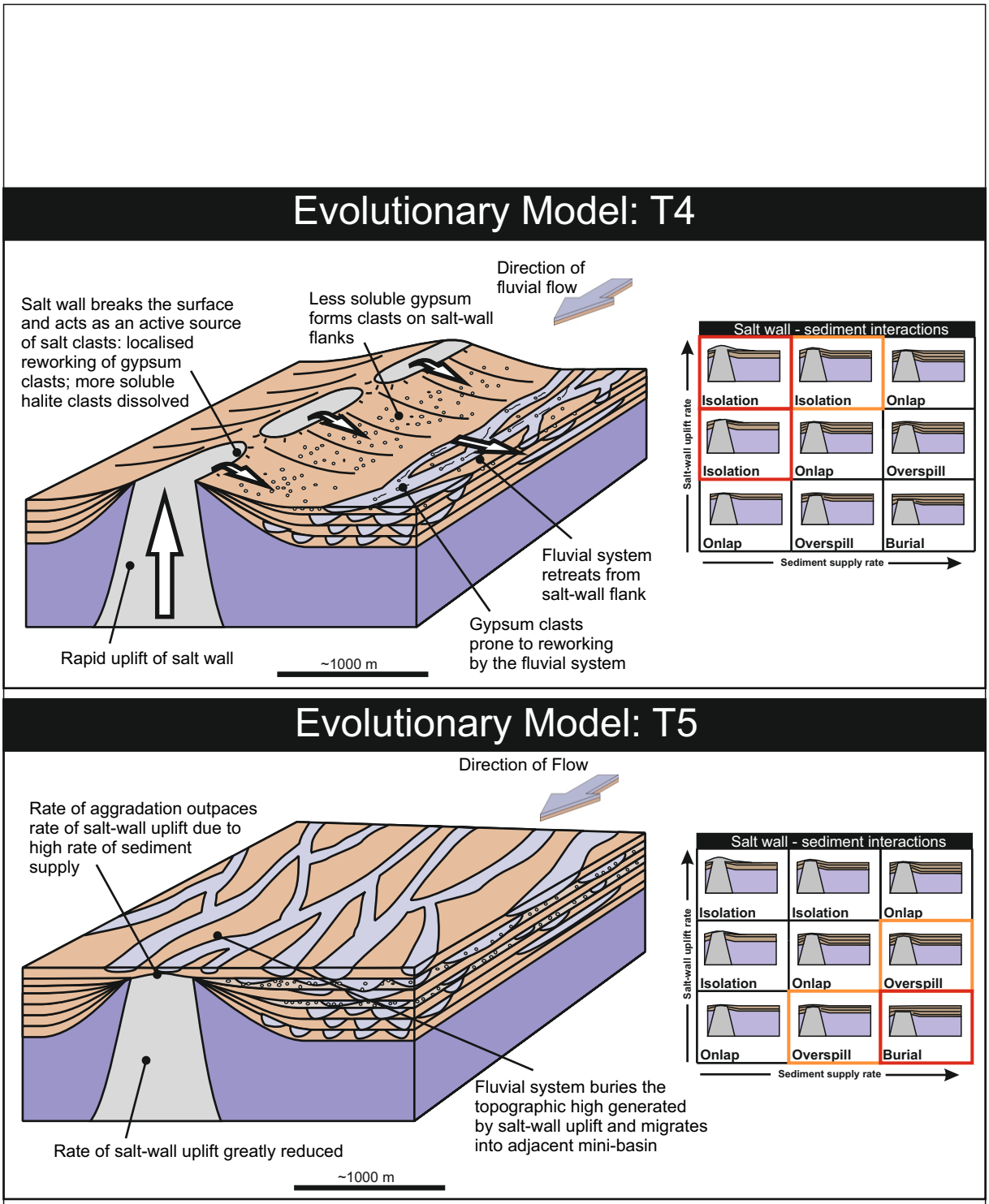


**Figure 5.9 cont.**: Evolution of drainage pathways and stratigraphy around a growing salt wall.

hardpans may develop adjacent to the salt walls and across the basin over prolonged periods (Ala, 1974; Lawton & Buck, 2006; Buck & Lawton 2010).

The nature of interactions between fluvial systems and uplifting salt walls can vary over the episode of evolution of a mini-basin, as illustrated by a series of schematic evolution models depicting such relationships for a scenario where drainage is aligned in an orientation parallel to the axis of the developing salt walls (Fig. 5.9). Adjacent to each model is a matrix diagram (Fig. 5.7) depicting the relation between the rates of salt-wall uplift and sediment supply, where the red indicates most likely relationship, and orange indicates possible relationships. **Initially** (T1), (Fig 6.9) fluvial systems will flow adjacent to salt walls, and can potentially onlap onto the salt wall flanks. If the rate of sediment supply increases, flood waters may overspill into an adjacent basin. A phase of **minor salt-wall uplift** (T2) relative to the level of the accumulating alluvial basin-floor plain would result in the increase of the topographic expression of the salt wall, upwarping the surrounding ground surface. This would result in the deflection of drainage pathways away from the flanks of the salt wall, resulting in basin isolation with only limited onlap of fluvial strata onto growing salt-wall flanks. With a temporary **cessation of salt movement** (T3) or an increased rate of sediment **aggradation** the fluvial system will begin to encroach on the salt-wall flanks, again resulting in onlap, and potential overspill of flood waters into adjacent basins. During a phase of **major-salt wall uplift** (T4) (or an episode of aridity, where the rate of sediment supply is diminished) the salt wall may breach the land surface, forming salt glaciers (or namikers Ala, 1974), which can subsequently be reworked into the adjacent stratigraphy. During these episodes, basin isolation will be the most probable sceneario. Where **salt-wall uplift abates** or **stops completely** (T5), the fluvial system will aggrade, onlap and eventually over-spill the salt wall feeding sediment into the adjacent basin, potentially eventually burying the salt wall. Salt-wall burial typically occurs after the mini-basins ground, and no additional salt is displaced into the salt walls (Hodgson *et al.*, 1992; Banham & Mountney, 2013a).

## 5.5 Climatic Signature

Variations in climate will exert a significant control on the rates of weathering, and sediment transport in the provenance region, ultimately controlling the rate and style of sediment supply to the receiving basin (Fig. 6.9). In addition, climate will influence (i) transmission losses through evapotranspiration (if the floodplain is vegetated), and evaporation, (ii) dissolution of salt through increased infiltration and percolation of meteoric waters and (iii) increased rates of erosion of the uplifted salt-wall flanks, increasing the availability of intra-formational clasts derived form the reworking of uplifted strata, and reworked diapir-derived detritus, where the salt wall has breached the ground surface.

Discerning the preserved stratigraphic signatures of climatic variations from those of drainage diversion can be difficult and requires understanding of the stratigraphy from some or most of the basins across a halokinetic province. Typically, climate controls the sum total of sediment entering the halokinetic province, whereas halokinesis controls distribution (through drainage diversion) and accumulation rates (through subsidence) to individual mini-basins separately. Therefore, when a change in climate reduces the net sediment input into the basin, this will be expressed as a decrease in the proportion of channelised elements throughout the province. Halokinesis will control the localised distribution such that one mini-basin may become more sand-prone at the same time that an adjacent mini-basin becomes relatively sand-poor.

## 5.6 Expression of Climate and Halokineis

The interaction between the rates of halokinesis and climate-controlled sediment-supply are fundamental in controlling the preserved stratigraphic expression within salt-walled mini-basins, especially in axial draining systems which are isolated from adjacent basins for most of their evolution. A series of models depicting the evolution of these types of mini-basins has been developed to demonstrate how the ratio between the rates of sediment supply and halokinetic-controlled subsidence ($^{sed}/_{subs}$) control basin-fill style. These models depict how sediment supply can vary between basins (Fig. 5.11).

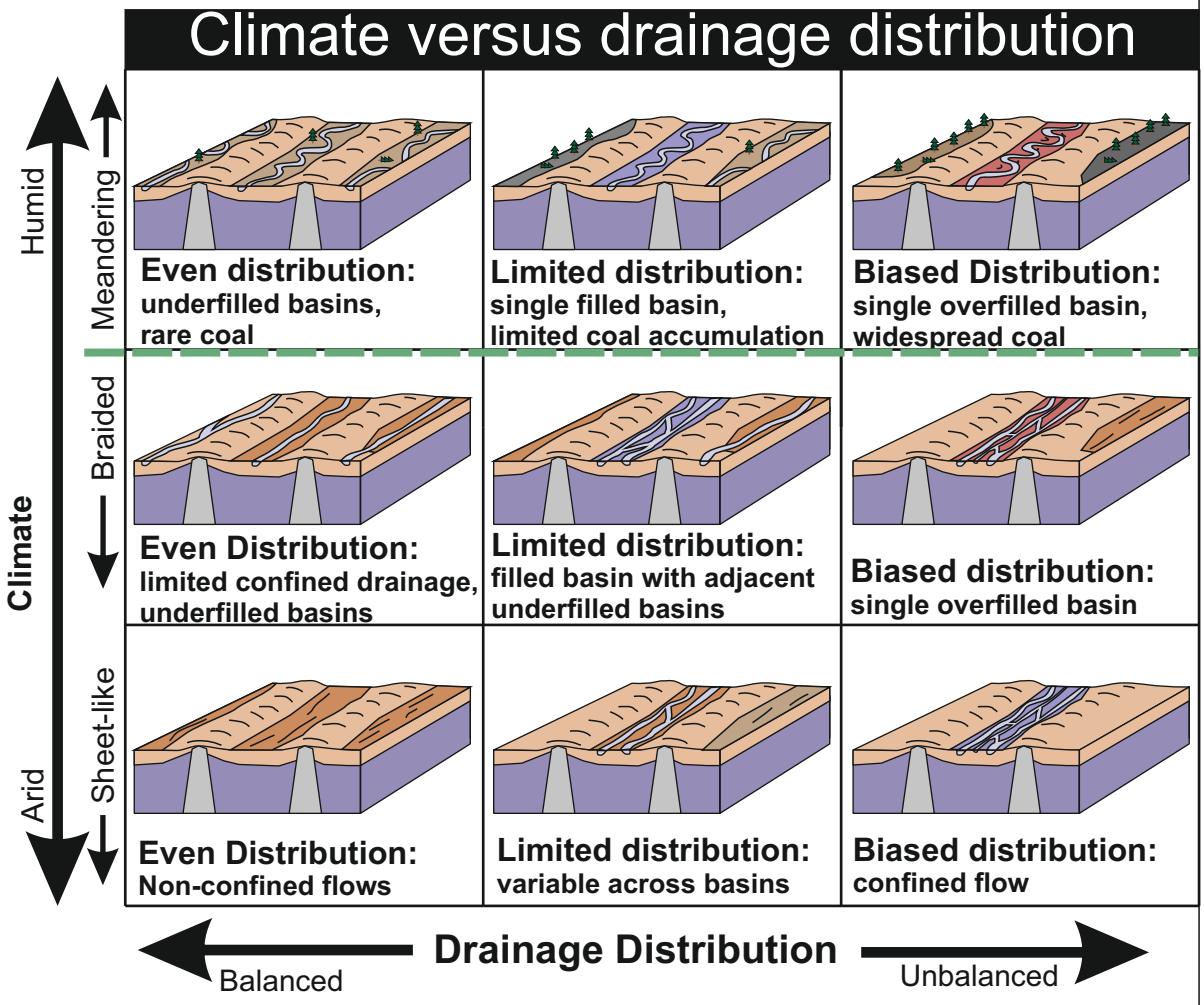


**Figure 5.10b**: Schematic diagram depicting the interplay between climate and drainage distribution, and how this can be expressed in a series of mini basins. This version depicts a greater range of climates from arid sheet-like, through braided systems, to meandering systems.

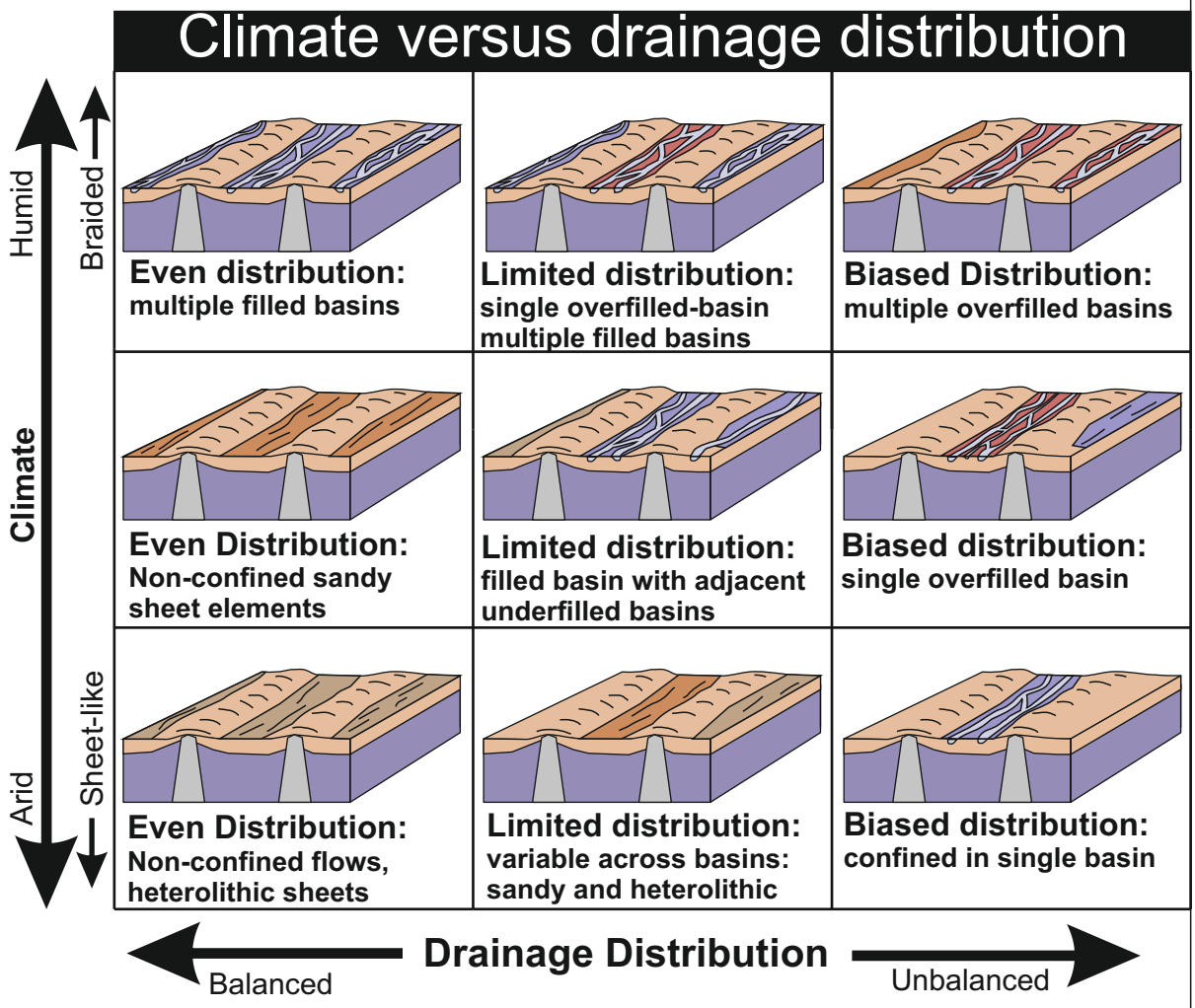


**Figure 5.10a**: Schematic diagram depicting the interplay between climate and drainage distribution, and how this can be expressed in a series of mini basins. See text for further explanation.

# Differential basin-fill style: T1

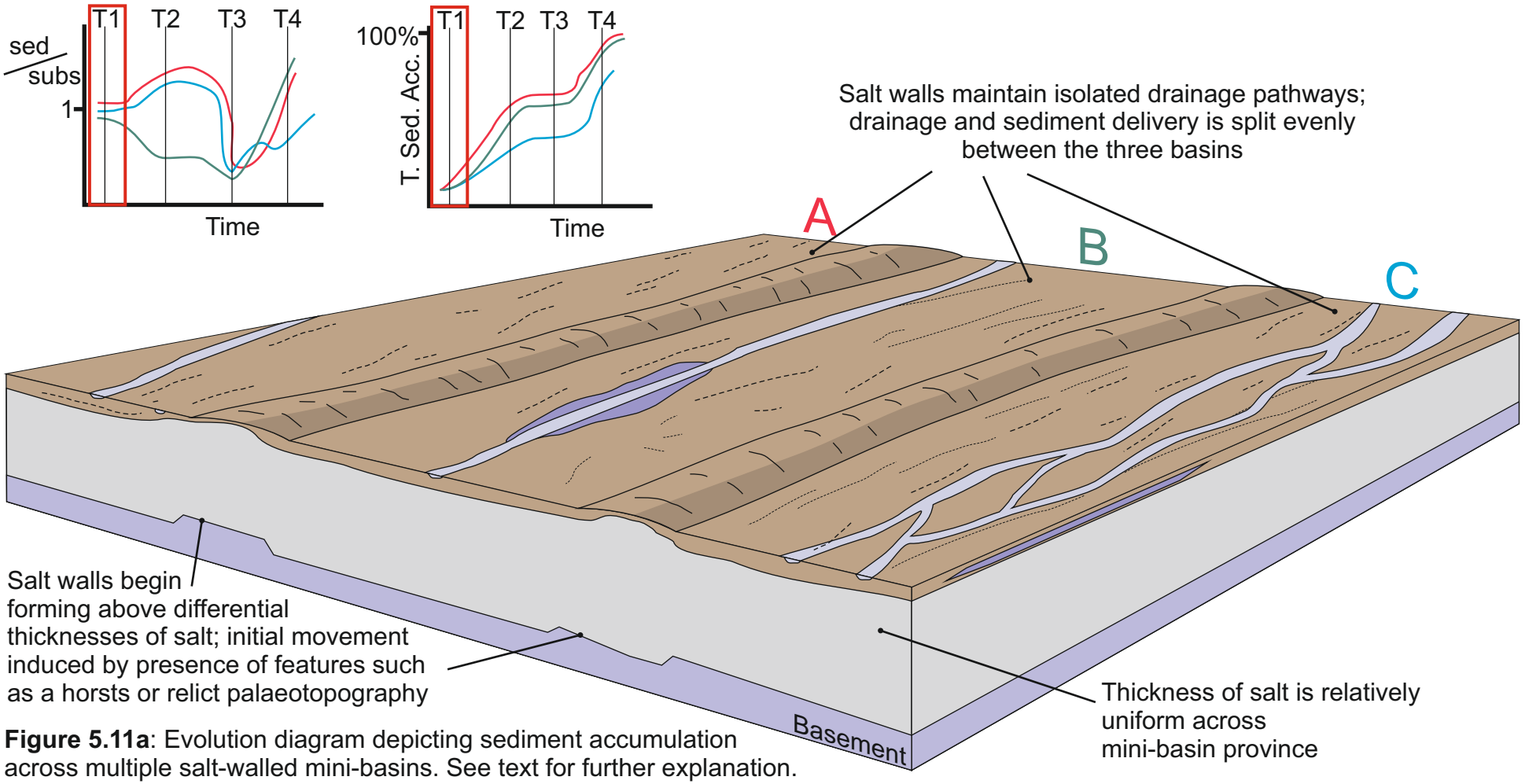


**Figure 5.11a**: Evolution diagram depicting sediment accumulation across multiple salt-walled mini-basins. See text for further explanation.

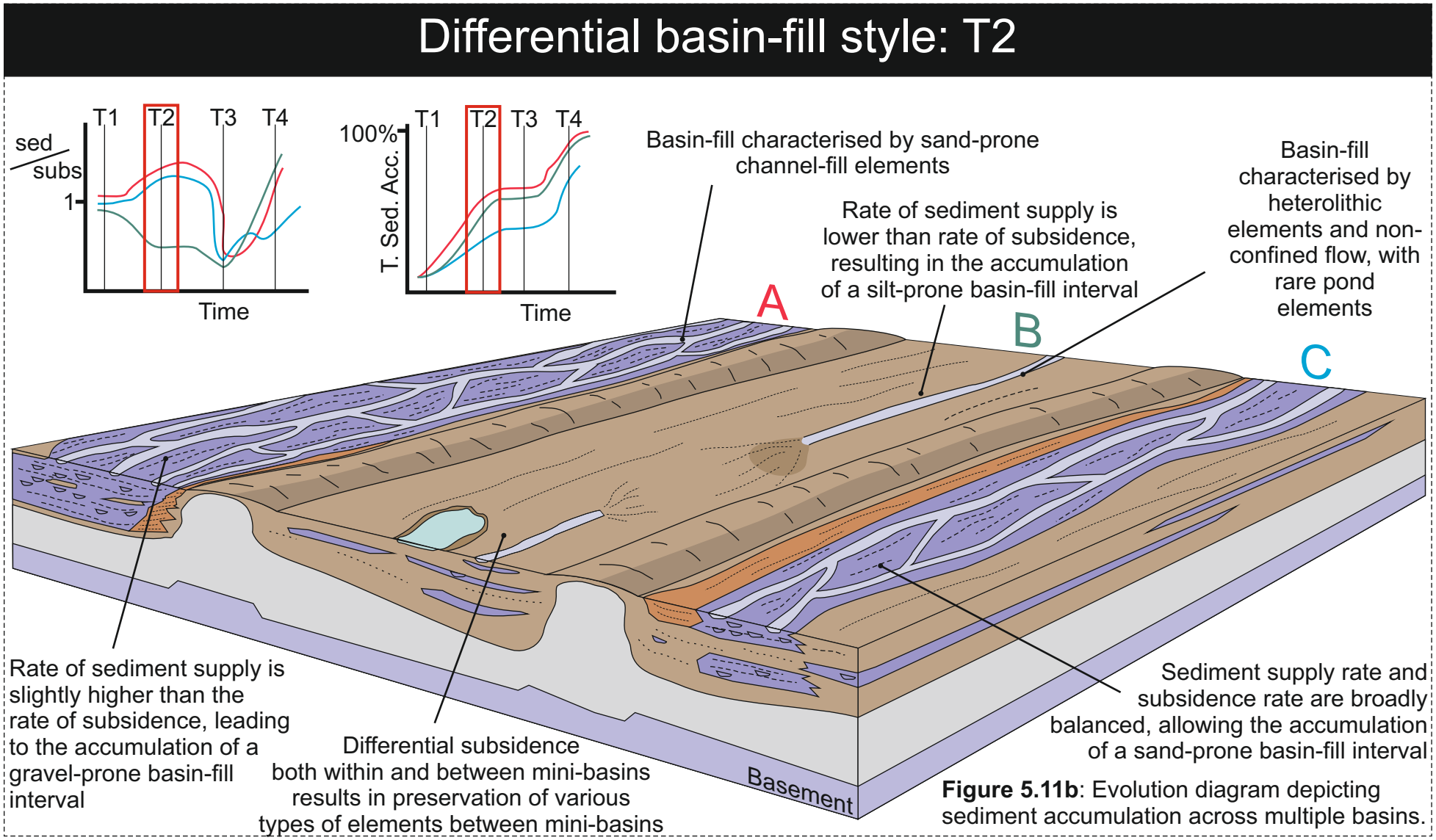


**Figure 5.11b**: Evolution diagram depicting sediment accumulation across multiple basins.

# Differential basin-fill style: T3

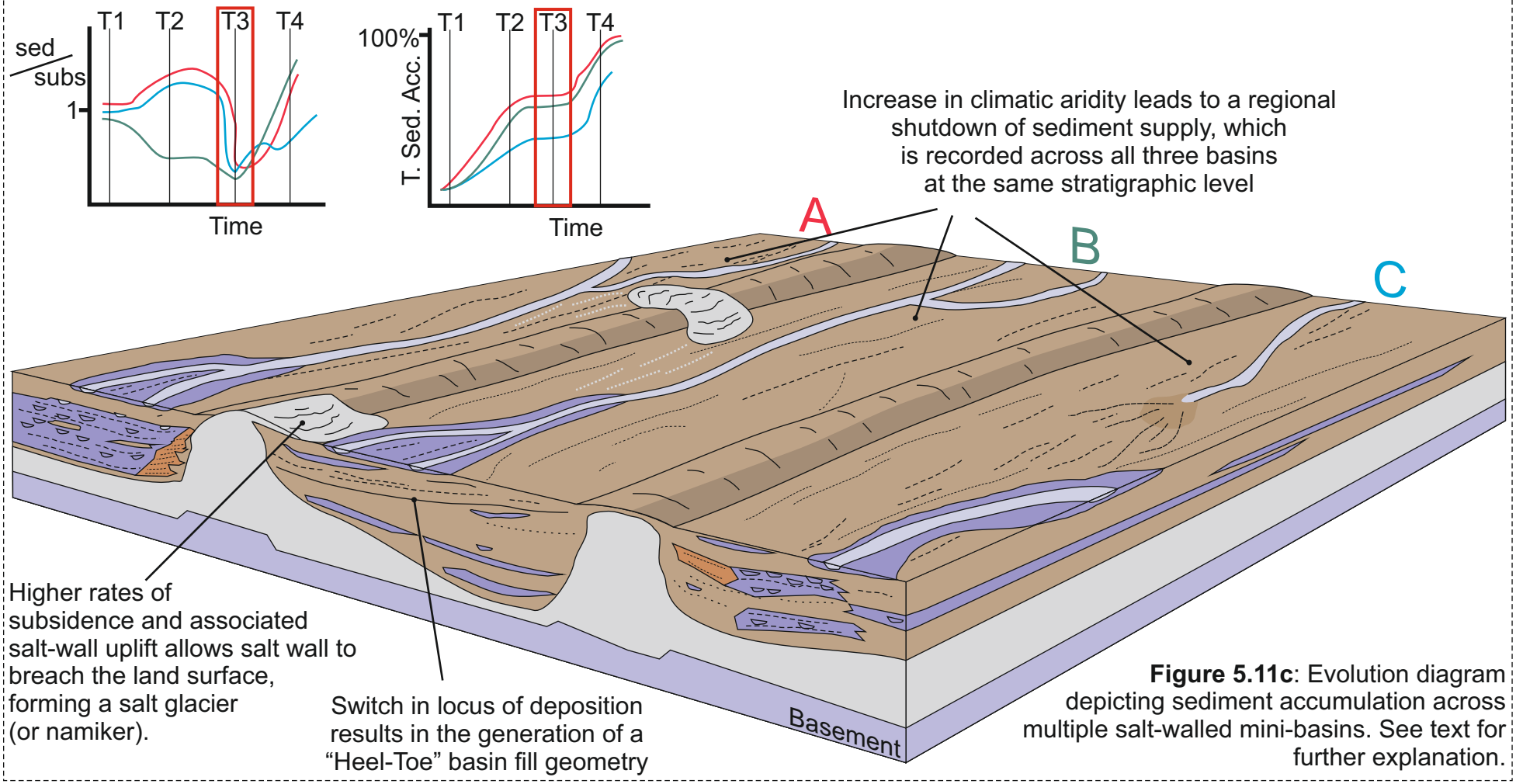


**Figure 5.11c**: Evolution diagram depicting sediment accumulation across multiple salt-walled mini-basins. See text for further explanation.

# Differential basin-fill style: T4

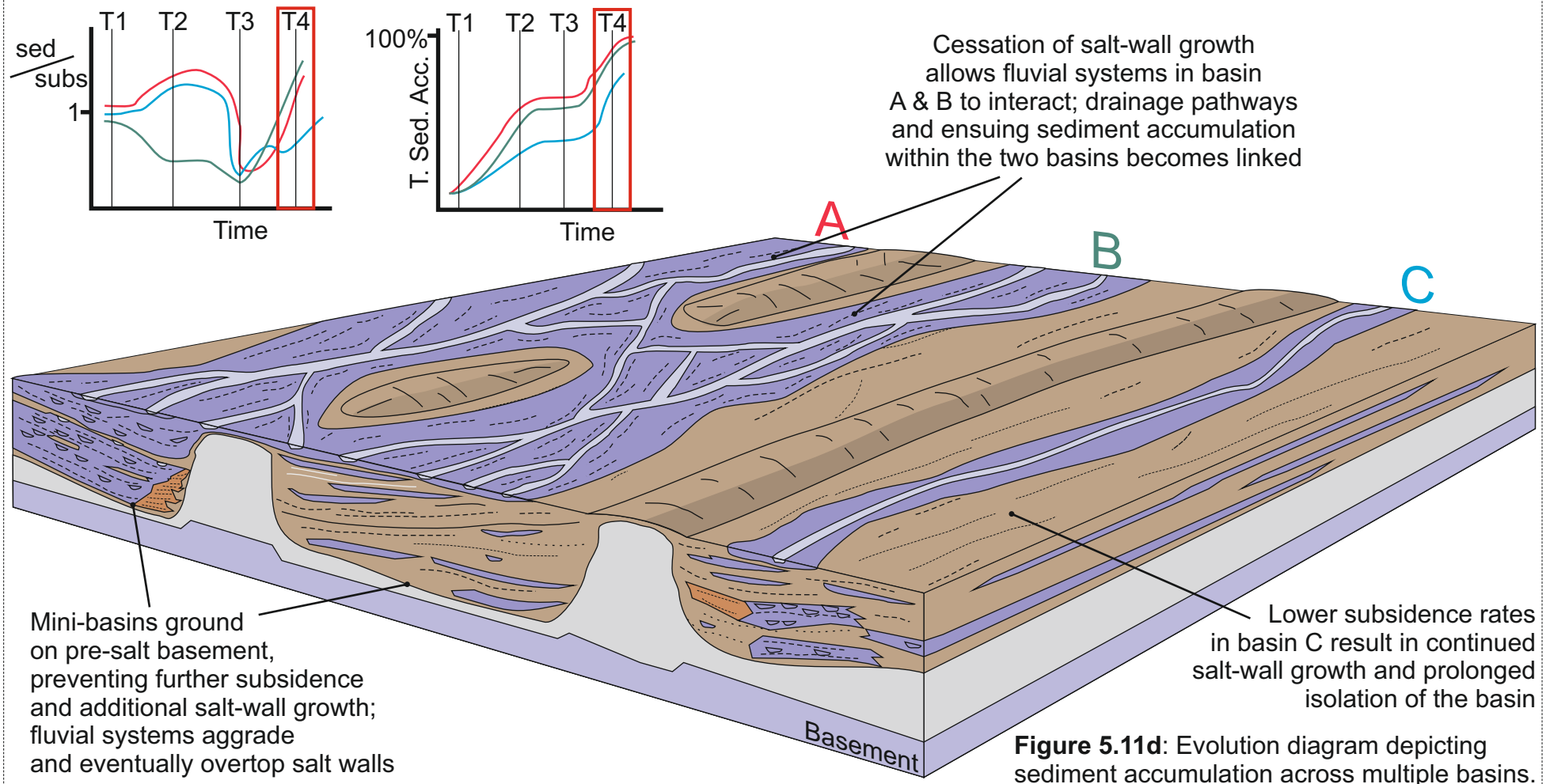


**Figure 5.11d**: Evolution diagram depicting sediment accumulation across multiple basins.

For T1, sediment supply rates and subsidence rates are balanced ($^{sed}/_{subs}$=1) across all three basins (A, B, & C) and total sediment accumulation is low. Salt walls have formed above basement structures which has resulted in differential thicknesses of salt, although the triggering mechanism is not specified (cf. Hudec & Jackson, 2009; Ings & Beaumont, 2010). Salt walls have uplifted to a sufficient height to isolate the drainage pathways between the adjoining mini-basins.

At T2, drainage pathways have been preferentially diverted into basins A & C, largely bypassing basin B. Perennial, or more regular ephemeral drainage pathways are established, delivering greater amounts of detritus to these basins. In basin B, which is largely devoid of established drainage pathways, the main mechanism for delivering sediments into the basin is via non-confined flows. For basins A & C, $^{sed}/_{subs}$ are >1, resulting in the accumulation of sand-prone basin-fills. Sediment loading in these basins also increases subsidence rates, resulting in higher rates of sediment accumulation (positive feedback). The styles of accumulated fills in basins A & C are both characterised by amalgamated channel-fill elements, with associated partially confined sheet-like elements accumulated adjacent to salt-wall flanks. In basin B, $^{sed}/_{subs}$ is <1, resulting in the accumulation of a sand-poor basin-fill interval. The succession in this basin is characterised by heterolithic sheet-like elements, with rare pond elements. Flood waters may converge to form minor chute elements, before dissipating back into non-confined flow. As a result of enhanced rates of sediment supply and loading of the salt, basins A & C are filling faster than basin B. Preferential drainage and accumulation of sediments on one side of the basin (basin B in the example) can lead to asymmetric subsidence and the generation of a “heel-toe” geometry in the basin-scale fill-style.

At T3 sediment supply into the basin is diminished significantly by a regional increase in aridity, which is reflected in the basin-fills across the halokinetic province. Consequently, the $^{sed}/_{subs}$ ratio for all three basins has dropped significantly below 1, resulting in the accumulation of a silt-prone (underfilled) basin-fill style for this episode. Reduced rates of sediment accumulation, coupled with a steady rate of salt-wall uplift have resulted in the breach of the land surface by the uplifting salt wall. Salt extruded from the

subsurface has flowed down the flank of the salt wall and is being eroded and reworked by ensuing fluvial activity during episodic flood events to form discrete horizons of diapir-derived detritus. Accumulated salt-clast-bearing beds are typically associated with heterolithic sheet-like elements.

At T4, the climatic regime has once again returned to a more humid style, resulting in an increase in the rate of sediment supply. Basins A & B have begun to ground on the sub-salt basement, preventing further subsidence of the basins, increasing $^{sed}/_{subs}$ ratio to >1, although sediment accumulation rates remain low overall; as a result the basins are effectively filled. In addition, cessation of the flow of salt into the adjacent salt walls has prevented the further growth of salt walls by salt withdrawal. Salt walls may begin to collapse as a result of axial salt movement within the wall, or dissolution of the salt by meteoric water. Salt diapirs may grow along the axis of the salt wall as a result of secondary basin subsidence where salt-wall collapse occurs (c.f. Coleman, 1983; Hodgson et al., 1992). As subsidence rates abate due to grounding, the succession forming the upper part of the mini-basin fills may become progressively sand-prone, although this part of the succession will likely be vulnerable to reworking, post-grounding (as demonstrated in basin B) (cf. Parriott Member's absence in the Fisher Basin – Banham & Mountney, 2013a, b). Basin C continues to subside, as drainage pathway diversion earlier in the development of the basin reduced the rate of sediment input into this mini-basin, reducing loading induced rate of subsidence, allowing prolonged basin subsidence.

## *5.7 Applications to industry*

The development and exploitation of hydrocarbon reservoirs in sedimentary basins influenced by halokinesis has been on-going since the late 1950s (Sherwin, 1973; Kelling *et al.*, 1978; Fiduck *et al.*, 2004). Developments of hydrocarbon plays in fluvial stratigraphic successions accumulated within active halokinetic provinces has been-ongoing since the 1980s (e.g. Jade Field, 1984, (Hodgson *et al.*, 1992; Smith *et al.*, 1993; Barde *et al.*, 2002b; Goldsmith *et al.*, 2003; Jones, 2005; McKie& Audretsch, 2005; Newell *et al.*, 2013).

Although research has been conducted into gross-scale basin architecture using seismic and well data, these studies are limited by the resolution of the seismic data, which cannot resolve the spatial and temporal distribution of architectural elements and is typically of notably low resolution adjacent to salt walls (Stewart & Clarke, 1999; Barde, 2002a; Trudgill, 2011). This research is designed to augment available primary seismic and well data for hydrocarbon provinces by developing a series of predictive models with which to demonstrate the most probable style of distribution and location of sand-prone fluvial elements that potentially might yield sand bodies of reservoir quality, both within and between mini-basins. The models developed throughout this thesis can potentially be used to populate both conventional and stochastic models for the prediction of likely sand-body distribution and connectivity.

### 5.7.1 Predicting sand distribution

The evolutionary tectono-stratigraphic models presented within the previous chapters can be used to predict the distribution of channel elements within non-outcropping halokinetic provinces.

Where heel-toe structures form, various channel complexes within the basin could potentially make good reservoir sandstones: channel complexes can thin and pinch-out onto the salt-wall flanks; vertically amalgamated channel complexes can stack in rim synclines; channel complexes can potentially accumulate and pinch out on an upward dipping intra-basin unconformity (Fig. 5.12). As these basins evolve, deposition and accumulation will typically become focused into one rim syncline until the initiation of grounding, whereupon a switch to the opposite side of the mini-basin may take place, potentially focusing more sediment transport within this now subsiding depocentre, and resulting in a more sand-prone fill of that portion of the basin.

Where a turtle-back structure forms due to the simultaneous subsidence of rim synclines on both sides of a mini-basin, determining the location of sandy fairways can be problematic due to intra-basin drainage diversion. The topographic expression of the turtle-back structure can potentially run the length of the mini-basin, dividing the mini-basin in two. This

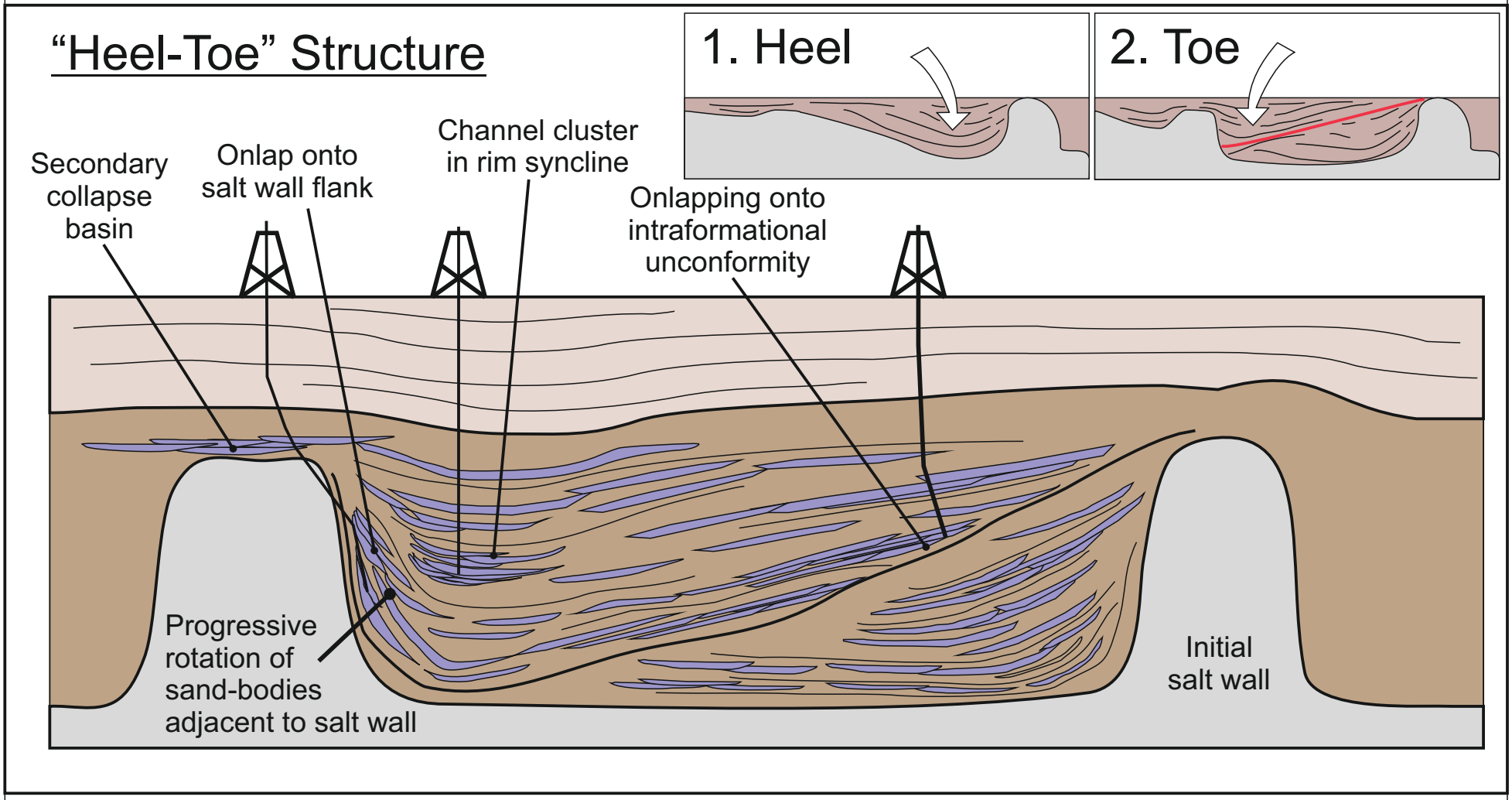


**Figure 5.12:** Prospects within a basin with a heel-toe fill geometry.

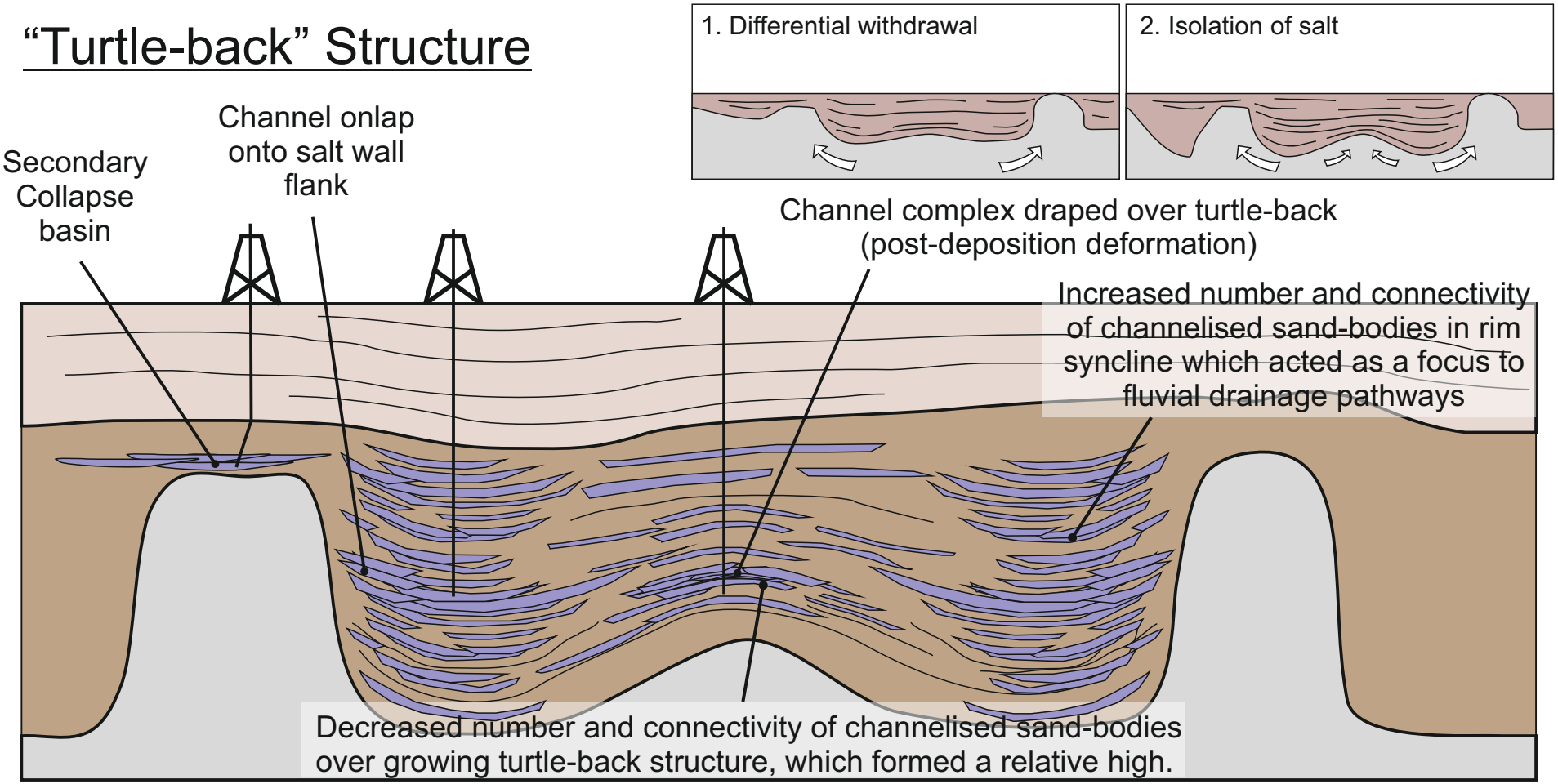


**Figure 5.13**: Prospects within a basin with a turtle-back structure.

may result in drainage isolation within the basin during episodes of diminished fluvial activity. However, the expression of the turtle-back structure may merely act to deflect drainage at certain times. Indeed, fluvial channel elements draping the turtle-back structure may become a favourable target for hydrocarbon exploration (Fig. 5.13). Rim synclines within mini-basins have potential for accumulating amalgamated channel-fill complexes, however caution is required, as drainage may be divided between the two resulting in the accumulation of sub-optimal (isolated) reservoir sands, or alternatively it may preferentially concentrate drainage within a single depocentre, resulting in the preferential accumulation of sand in one rim syncline, leaving the other relatively devoid of sand.

### 5.7.2 Interpreting climate change in wells

Climate change can be discerned within 1D well data by comparing the fill style of a number of basins across the halokinetic province (Fig. 5.14). By comparing intervals at the same stratigraphic level, the regional climate may be interpreted. If all the basins observed demonstrate a shift from deposition of high proportions of channelised elements to more sheet-like elements, this may be interpreted as change in climate to a more arid phase of deposition (Fig. 5.13). If sand proportions rise in a single basin and decrease in another basin, then a halokinetic control on drainage diversion is the most likely cause.

It must be noted that climate variations may not be the only mechanism that can instigate province wide changes in basin-fill style. Factors which can change this include: shutdown of a major regional provenance area due to denudation (c.f Uncompahgre Front throughout evolution of the Paradox basin); regional tectonics (salt unrelated); or a salt uplift at a critical location, such as across the upstream entrance to the halokinetic province. Additional checks, such as: petrographic study (or heavy mineral analysis) to determine provenance; and regional-scale structural observations, may be required to determine if large scale tectonic events are responsible for abatement or diversion of drainage pathways. Complexities can arise when the effects of drainage diversion and climate change are overprinted, making differentiation between the relative roles more difficult. However, analysis of wells data from

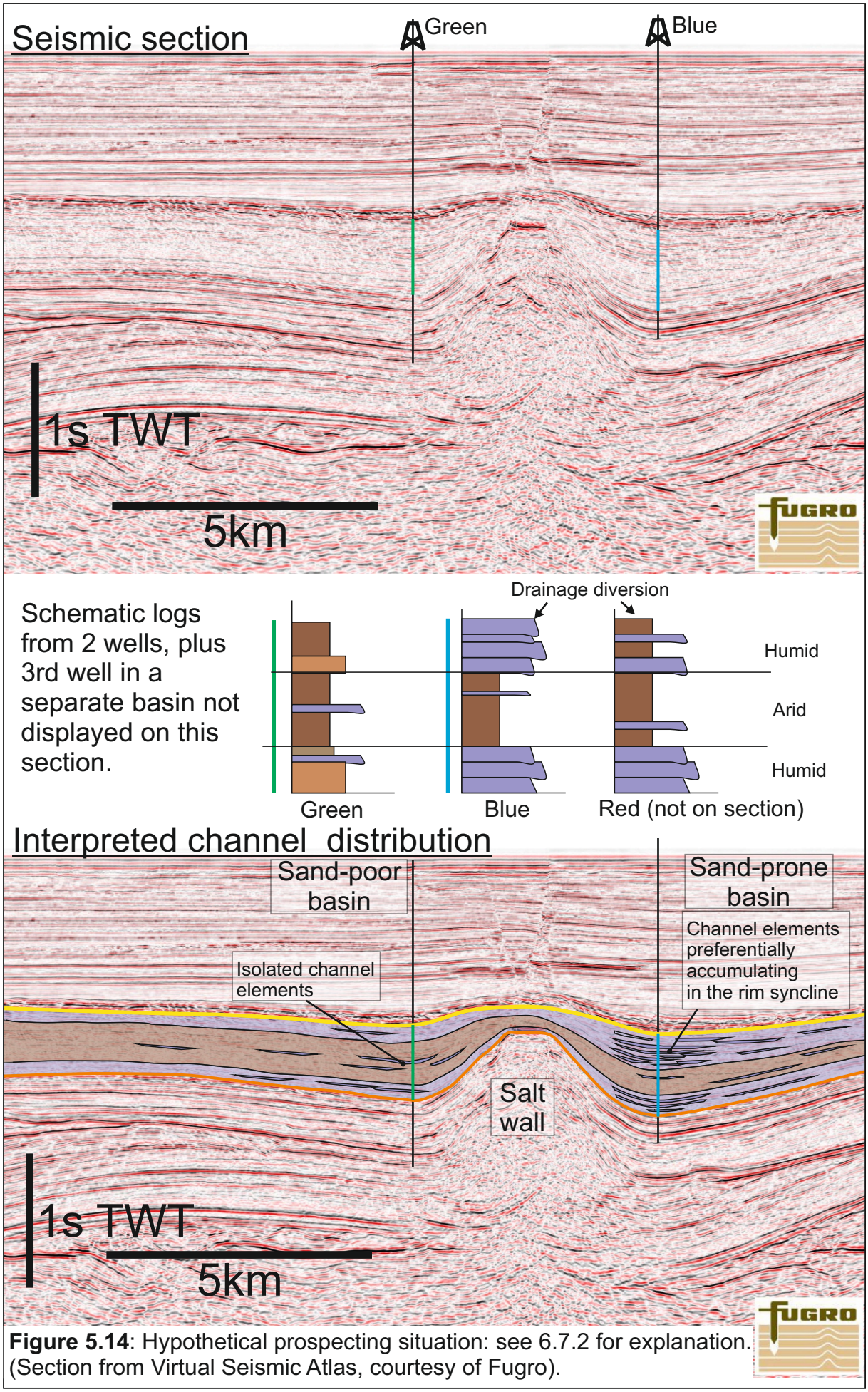


**Figure 5.14**: Hypothetical prospecting situation: see 6.7.2 for explanation. (Section from Virtual Seismic Atlas, courtesy of Fugro).

multiple adjoining mini-basins can help increase confidence in distinguishing the two factors.

## *5.8 Conclusions*

This chapter demonstrates how the combined interplay between a suite of key controlling factors, including halokinesis, climate, and drainage orientation, interact to influence the style of the sedimentary succession that accumulates and becomes preserved within a series of salt walled mini-basins. Key findings are as follows:

1. The Moenkopi Formation demonstrates convincingly how syn-sedimentary halokinesis plays a primary role in governing fluvial sediment accumulation in a series of developing mini-basins. This is manifest in the following ways:
    a. the partitioning and isolation of drainage pathways;
    b. the impact of differential rates of subsidence as a control on the accumulated basin-fill style;
    c. the role played by multiple sources of sediment supply in enhancing sediment delivery to a single mini-basin;
    d. the effects of differential subsidence in controlling the distribution of channel-fill elements within a single basin;
    e. the form of interactions between drainage pathways and salt-wall uplift on the flanks of developing mini-basins.
    f. That the development of rim-synclines can act to capture drainage pathways, resulting in the accumulation of a sand prone succession adjacent to an actively uplifting salt wall.
    g. how variations in climate are expressed within salt-walled mini-basins.
2. The concepts demonstrated within the Moenkopi Formation, and other examples of fluvial systems which accumulated in salt-walled mini-basins have been used to create a series of generic models demonstrating how basin-fill geometries, basin segregation and climatic effects could be expressed in the preserved sedimentary architecture of a series of salt walled mini-basins.

3. The generic models developed from field observations made as part of this study can be applied in strategies for the exploration, appraisal and development of hydrocarbon fields in terms of the development of predictive models with which to account for the distribution of sand both within a single mini-basin and across multiple mini-basins. This has implications for predicting the net-to-gross ratio in these types of basins.

# 6. Conclusions & Further Work

This section reviews the key research questions proposed in Chapter One, summarizes how these questions have been addressed through this study and considers how this work has improved our understanding of the relationship between fluvial system evolution and accumulation, and the development of salt-walled mini-basins. Further this chapter proposes a series of additional research questions that have arisen as an outcome of this study and could be considered in future research programmes.

## *6.1 Research Questions*

This section summarises how each of the key research questions proposed in Chapter 1 have been addressed as a direct outcome of this study.

### *6.1.1 What is the sedimentary expression of the Moenkopi Formation of SE Utah, the preserved sedimentary record of a low relief, dryland fluvial system which accumulated in an arid to hyper-arid continental setting?*

The sedimentary expression of the Moenkopi Formation in the Salt Anticline Region and the White Canyon Region of South East Utah is that of a fluvial succession represented by partially channelized and partially non-confined fluvial architectural elements. Notably, the succession is characterised by laterally extensive architectural elements that can be traced across the study regions for up a few 10s km in some instances and these demonstrate accumulation across a generally low-relief alluvial plain. Individual channel forms within these elements typically have poorly defined margins, have high width-depth ratios, and typically amalgamate laterally to form the multi-lateral channel-fill complexes which represent the preserved expression of braid belts formed by the largely confined flow of water within channelized conduits. These elements are dominated by trough cross bedded facies (**HA Fxp** and **Fxt**), the style of arrangement of which indicate a predominance of down-stream accreting macro-forms. Low-

angle-inclined (asymptotic based) planar styles of cross bedded sets (**LA Fxp**), which are interpreted to form by lateral (cross stream migration) are relatively rare in the succession, suggesting limited lateral migration of barforms within the channel belts.

Non-confined elements (F5-F7) which in some locations constitute over 90% of the observed stratigraphic succession, are interpreted to be the expression of deposition of sediment from suspension and traction during the waning stages of non-confined flood events. The stacked nature of these relatively thin, fining-up cyclic packages (typically fine-grained sandstones with climbing ripple strata fining into homogeneous or laminated argillites – facies frc/fx; and Fhiss) suggests repeated short-duration flooding events. The flows responsible for these deposits are shown to have been flashy, short lived and lack capacity to transport coarser-grained sediment, which is reflected by the fine-grained nature of the facies forming these element. This excludes chute elements, which represent the temporary convergence and dissipation of flood water, where increased water velocity allows transport and preferential accumulation of coarser grade sediments. The very high width-to-thickness ratio (typically 1:500 or higher) of these non-confined elements indicates a largely unconfined flow, which supports the notion that the system accumulated in a low-relief setting. Within the overbank sub-environment, pond elements formed in the aftermath of flood events, and these are characterised by the presence of wave-rippled fine sandstone facies (WR), interpreted to have formed by agitation of the shallow water column caused by wind-generated waves on the surfaces of the ponds. The wave-rippled facies are typically overlain by argillaceous beds containing desiccation cracks indicative of the drying out of these temporary shallow ponds. The origin of the argillaceous sediments overlaying the wave-rippled sandstone beds is uncertain, however is likely to be wind-derived loess delivered from elsewhere on the drying alluvial plain. The arid nature of the climate is demonstrated by the architecture of the non-confined elements, which imply a flashy flow regime typical of ephemeral systems (Picard and High, 1973). This interpretation is supported by

numerous observations of specific and diagnostic lithofacies, including abundant examples of primary evaporite minerals (e.g. thin gypsum beds) preserved within the succession, and the widespread occurrence of desiccation cracks on bedding throughout the succession.

### *6.1.2 What influence did syn-sedimentary halokinesis have on the distribution of fluvial drainage pathways and the ensuing style of accumulation and preservation of the fluvial succession?*

In salt basins filled with continental clastic deposits, synsedimentary halokinesis has the effect of controlling the distribution of fluvial drainage pathways and therefore influences the genesis and geometry of fluvial architectural elements within a halokinetic province. In the case of the Moenkopi Formation, where drainage pathways were aligned parallel to the trend of the linear salt walls, the topography generated by the uplifting salt walls, and development of rim-synclines structures adjacent to the salt walls were each effective in controlling the spatial location of the principal fluvial drainage pathways within the developing mini-basins. Halokinesis within the Salt Anticline Region apparently exerted a subtle control on the preserved fluvial architecture: salt-wall topography and availability of diapir-derived detritus resulted in the formation of some niche architectural elements (i.e. elements that typically only form adjacent to uplifted salt walls) such as partially-confined overspill elements and detrital gypsum-clast-bearing elements and the increased prevalence of single-storey unilateral intraformational clast-filled channel elements for which clasts can be shown to have been reworked from sediment cover lying atop uplifting salt-wall flanks.

The geometry, internal facies composition and distribution of fluvial elements within the basin, together with their relationship to neighbouring elements (i.e. stacking pattern), was dependent on the interplay between the rate of sediment supply and the rate of salt movement leading to subsidence within evolving mini-basins and uplift of adjacent salt walls. Together, these factors controlled fluvial drainage distribution and therefore the pattern of sedimentation. The

mechanism of sediment delivery (i.e. supply) into the halokinetic province was controlled in part by halokinetic processes such as spatial and temporal changes in the pattern of salt-wall uplift, and spatial and temporal changes in rates of mini-basin subsidence. The distribution of the sediment supply within the evolving mini-basins acted to either enhance or diminish the distribution of sand- and granule-grade detritus into individual mini-basins. Within a single mini-basin, subsidence due to progressive withdrawal of underlying salt effectively controlled the ensuing style of fluvial system accumulation: high rates of subsidence favoured “high accommodation” conditions, where rapid aggradation in response to generation of accommodation space results in the accumulation of a higher proportion of sediment entering the basin, including argillaceous material entering the basin. Balanced rates of subsidence and sediment supply will allow sufficient time for channel-belts to avulse and rework the overbank succession, resulting in the accumulation of sand-prone succession. Finally, low rates of subsidence and high rates of sediment supply will favour preservation of gravel-lags where repeated winnowing of the already accumulated channel-belt elements will typically result in just the preservation of the more gravelly channel-element bases. Notwithstanding the role of halokinesis in controlling preserved sedimentary style, the ultimate style of sediment accumulation within mini-basins is also highly dependent on the calibre and and type of sediment delivered into the halokinetic province from the source area and the role of source-region weathering and transport processes represent addition important factors that govern the depositional style.

### *6.1.3 Can the signature of climatic controls be discerned from the signature of halokinetic controls?*

The signature of halokinesis can be deciphered from the signature of climate if the stratigraphic succession can be observed across a number of basins (Chapter 3). It is important to observe the stratigraphy within several mini-basins as not to confuse the changes associated with a change in the distribution of drainage pathways with

those of regional climate change. If a single vertical succession (i.e. a single well) within a single basin is the only data available, it may potentially be difficult to discern the difference both temporal and spatial variations of drainage diversion or temporal variations of climate, as the expression of drainage diversion and climate can look virtually the same in a single vertical sequence. Climate change is typically expressed as the simultaneous change in fluvial style across several mini-basins whereas halokinetic drainage control is usually expressed as a redistribution of drainage pathways and sediment distribution from one mini-basin into another mini-basin, which will be expressed as successions within certain becoming more sand-prone, while others may become sand-poor, or express no change in the stratigraphic succession. Additionally, observations from outside the halokinetic province can assist with elucidation of climatic controls, as the succession will not have been subjected to halokinetic controlled drainage diversion. One pitfall of this is that the preserved stratigraphic successions may bare limited resemblance to one and other due to significantly different rates of basin subsidence. This has been demonstrated by comparison of the Moenkopi Formation and it's outcrop expression observed between the Salt Anticline Region and the White Canyon Region: tentative links can be made between the observed stratigraphic styles preserved within the two regions, however it is difficult to correlate the members due to significant differences in subsidence rates, and slightly different sediment provenance areas.

### *6.1.4 Can the synthesis of data from questions 1-3, plus the synthesis of findings from other studies be used to develop a suite of predictive models for both axial- and transverse-draining fluvial systems accumulated in salt-walled mini-basins?*

Numerous tectono-stratigraphic models have been developed to demonstrate the potential architectural relationships of depositional sequences arising from the evolutionary history of a series of halokinetic mini-basins, based on studies of systems characterised by

different mini-basin configurations: (i) axial-draining linear systems (this study; Hazel, 1994; Matthews *et al.*, 2007; Andre *et al.*, 2012; Banham & Mountney, 2013a, b); (ii) transverse-draining linear systems (Venus, 2013); and (iii) polygonal systems (Hodgson *et al.*, 1992; Smith *et al.*, 1993; Barde *et al.*, 2002a,b; Newell *et al.*, 2012). Within this thesis, these studies have been distilled to propose a series of models with which to account for the generic evolution of various types of successions, as proposed conceptually (Chapter 2), and as supported by the detailed study of the Moenkopi Formation presented herein (Chapter 4), and the model for a generic axial-draining system with which to account for complex routing of sediment delivery (Chapter 5). In addition, several models have been developed to demonstrate the interplay between attributes of halokinesis and sediment supply, and their ensuing stratigraphic expressions.

## *6.2 Summary of Principal Findings Arising From This Study*

This study demonstrates the role played by syn-sedimentary halokinesis in controlling the pattern of fluvial drainage and the resultant fluvial stratigraphic expression preserved in the mini-basins which formed as a result of salt movement and deformation. The following key findings have arisen from this study:

- Halokinesis can effectively control the distribution of fluvial drainage pathways both within and between a series of evolving mini-basins, thereby exerting a primary control on resultant stratigraphic architecture in the preserved fluvial succession.
- Variations in the rate of halokinesis both within and between basins can lead to the accumulation of either sand-prone or sand poor successions, both between adjacent mini-basins and within a single salt-walled mini-basin.
- Climate ultimately acts as a primary control on the style and rate of sediment input into a halokinetic province, and the form of the fluvial system (i.e. non-confined sheet-like system versus braided system versus meandering system) which is expressed across a broad region, regardless of of the degree of drainage diversion exherted by salt wall

uplift. This can be observed within members of the Moenkopi Formation across of Salt Anticline Region where each member has a common outcrop expression across a series of segregated mini-basins, despite variations in the proportions of fluvial elements observed within the respective successions.

- The interplay between the rate of sediment supply to mini-basins and the rate of mini-basin subsidence is a key control on resultant basin-fill style. Both rates must be balanced to result in the accumulation of amalgamated channel fill elements, without too much winnowing of sand grade material, which is more favourable for the development of economic hydrocarbon reservoirs.
- The orientation of fluvial drainage relative to the trend of the salt wall is a key control on the style of evolution of salt-walled mini-basins: for axial-draining fluvial systems, drainage pathways can be distributed non-uniformly between the mini-basins, allowing for the potential accumulation of relatively sand-starved mini-basins adjacent to sand-prone mini-basins; by contrast, for transverse-draining fluvial systems, mini-basins situated in locations more proximal to the sediment source typically tend to be more sand-prone, with proportion of sandy elements decreasing systematically with increasing distance from the sediment source. This is typically because coarse calibre sediments preferentially accumulate in the basins closest to the point-of-entry of the fluvial systems.
- Stochastic modelling of channel-belt connectivity within salt-walled mini-basins demonstrate that potentially economic reservoirs can develop within these basins, even where sediment supply is relatively low due to increased aridity at time of deposition
- This study had drawn together most of the thinking over the last 20 years to develop a series of generalised models depicting the evolution of fluvial systems within salt-walled mini-basins. These models account for various scenarios, including: drainage diversion; variations in climate; change in drainage orientation to the salt walls; and various salt-wall geometries.

## *6.3 Further Work*

### Axial subsidence and uplift

Although this study has considered the influence of differential rates of subsidence along the axes of linear mini-basins (Chapter 4: Banham & Mountney, 2013a), further work detailing the fluvial response to these subtle intra-basin styles of behaviour could yield further details on architectural element distribution. For example, micro-topographic highs could act as a local source of detritus within a mini-basin, resulting in the accumulation of intraformational conglomerates in locations well away from salt-wall flanks (cf. Chapter 3: single-storey, unilateral intraformational clast-filled channel-elements), or in the case of micro-topographic lows, the locus for formation of lacustrine pond elements with argillaceous fills in an otherwise sand-prone basin, or as an inflection point where decrease in gradient allows flooding out of confined flows and deposition of non-confined elements.

### Collapse Basins (secondary basin) evolution

Collapse basins, which form over the crestal structures of collapsing salt-walls following a cessation of salt withdrawal from beneath mini-basins have been discussed by Hodgson *et al.* (1992), and Smith *et al.* (1993), but have received relatively little attention in exposed outcropping settings, aside from a limited study by Coleman (1983) on the Tertiary sediments which accumulated over the collapsing Fisher Valley salt wall of South East Utah where the uplifting Onion Creek salt diapir acted to dam and divert the course of the Dolores River. The style of sediment fill of these secondary collapse basins is dependent on sediment supply from beyond the limits of the halokinetic province, as well as on the style of sediment reworking arising from erosional processes operating in adjacent mini-basins, which would form relative topographic highs as salt is progressively removed from the wall. The rate at which the salt walls undergo collapse due to axial withdrawal and dissolution may vary both spatially along the length of the wall and also temporally. Additional factors to consider include: orientation of drainage pathways relative to the trend of the collapsing salt walls; locus of uplifting diapirs (caused by axial salt movement), which may act as sediment point sources; and areas of salt withdrawal, which will act as a depocentres.

Gaining an improved understanding of the evolutionary history of these secondary mini-basins and their fills will be crucial to understanding fluid flow across the crests of collapsed salt walls: the elements accumulating within these collapse basins could act as important conduits for hydrocarbon flow in reservoir settings or may impede migration, depending on the style of sediment accumulation.

## Relay ramps and their control on salt wall growth

The outcrop of the Moenkopi Formation expressed in the transition zone between the Fisher Valley salt wall and the Cache Valley salt wall indicates limited influence of salt-withdrawal or salt-wall uplift in this region. This may indicate a change in the sub-salt basement geometry in this vicinity, creating conditions which retarded salt migration. Possible basement geometries which may cause this may include fault escarpments, or relay ramps (Doelling,1998; Trudgill, 2011), which would affect salt migration. Such areas of limited salt movement may form important sediment routing pathways for supplying sediments into adjacent basins and therefore be important in other salt-influenced provinces.

## Sedimentation in Polygonal basins

Sediment accumulation in salt-walled mini-basins arranged into polygonal patterns are yet to receive detailed outcrop study, due in-part to limited outcrop availability. The establishment of pathways for the transport of sediments into these basins is of key importance, and it is crucial to understand the nature of the sediment preserved within such mini-basins for understanding potential for development of hydrocarbon reservoirs.

Where these basins are isolated from adjacent basins, successions characterised by loessites, non-confined flow elements or lacustrine successions may develop, which may make sub-optimal to poor reservoirs Alternatively, entrenched fluvial systems which are confined to a series of these polygonal salt-walled basins may create a fairway of amalgamated channel-fill elements which would be favourable for reservoir development.

## Style of sediment accumulation in areas of changing salt wall geometry (Polygonal – linear transition) (North Sea issue)

Salt-wall trends in the Central North Sea region transform spatially from more linear basins in the east to more polygonal basins in the west of the Central Graben region. The cause of this trend is currently unknown, and will potentially have a significant effect on the style and distribution of sedimentary facies and architectural elements accumulating at the time of deposition.

## Three-dimensional modelling using LiDAR or photogrammetry

As discussed by Venus (2013), the Salt Anticline Region of Utah would make an ideal location for collection of high resolution three-dimensional digital outcrop data with which to supplement the findings of recent studies (Lawton & Buck, 2006; Protchnow *et al.*, 2006; Matthews *et al.*, 2007; Paz & Trudgill, 2009; Trudgill, 2011; Venus, 2013; Banham & Mountney, 2013a,b,c; Gough & Clarke, *in press*) The benefit of collecting data within this region is that the Cutler Group, Moenkopi Formation, Chinle Formation and Kayenta Formation are vertically stacked successions that are each well exposed and studied and understood and which each exhibit relatively contrasting styles of fluvial sedimentary architecture, making acquisition of larger data sets quicker and cost-effective. LiDAR could be used to discern and relate subtle differences and distributions of fluvial architectural elements and relate them spatially and temporally to larger scale halokinetic processes. The resultant datasets could be used as a framework for building detailed reservoir models or developing more realistic stochastic models.

## Cross salt-wall drainage study

Although the salt-walls in the Salt Anticline Region can be shown to have been effective in diverting fluvial drainage pathways during accumulation of the Triassic Moenkopi Formation to the extent that their development influenced the style of fluvial sediment accumulation in adjacent mini-basins, it remains uncertain whether the walls acted as a complete barrier to drainage, or whether there was limited cross-wall drainage. To determine this, a detailed study of provenance and palaeocurrent analysis could be undertaken to identify potential sites for cross-wall drainage due to salt-wall breaching.

Formation are vertically stacked successions that are each well exposed and studied and understood and which each exhibit relatively contrasting styles of fluvial sedimentary architecture, making acquisition of larger data sets quicker and cost-effective. LiDAR could be used to discern and relate subtle differences and distributions of fluvial architectural elements and relate them spatially and temporally to larger scale halokinetic processes. The resultant datasets could be used as a framework for building detailed reservoir models or developing more realistic stochastic models.

### Cross salt-wall drainage study

Although the salt-walls in the Salt Anticline Region can be shown to have been effective in diverting fluvial drainage pathways during accumulation of the Triassic Moenkopi Formation to the extent that their development influenced the style of fluvial sediment accumulation in adjacent mini-basins, it remains uncertain whether the walls acted as a complete barrier to drainage, or whether there was limited cross-wall drainage. To determine this, a detailed study of provenance and palaeocurrent analysis could be undertaken to identify potential sites for cross-wall drainage due to salt-wall breaching.

# 7.0 References

**Abdullatif, O.M.** (1989) Channel-fill and sheet-flood facies sequences in the ephemeral terminal River Gash, Kassala, Sudan. *Sed. Geol.* **63**, 171-184.

**Ala, M.A.** (1974) Salt Diapirism in Southern Iran. *Am. Assoc. Petrol. Geol. Bull.*, **58**, 1758-1770.

**Allen, J.R.L** (1968) Current Ripples: Their relation to patterns of water and sediment motion. *North-Holland Publishing Company, Amsterdam.*

**Al-Zoubi, A., Ten Brink, U.S.** (2001) Salt diapirs in the Dead Sea basin and their relationship to Quaternary extensional tectonics. *Mar. and Petrol. Geol.*, **19**, 779-797.

**Andrie, J.R., Giles, K.A., Lawton, T.F., Rowan, M.G.** (2012) Halokinetic-sequence stratigraphy, fluvial sedimentology, and structural geometry of the Eocene Carroza Foramation along La Popa salt weld, La Popa Basin, Mexico. In: *Salt Tectonics, Sediments, and Prospectivity* (Ed. by I.G. Aslop, S.G. Archer, A.J. Hartley, N.T. Grant & R. Hodgkinson). Spec. Publ. Geol. Soc. London, **363**, 59-79.

**Aschoff, J.L., Giles, K.A.** (2005) Salt diapir-influenced shallow-marine sediment dispersal patterns: Insights form outcrop analogs. *Am. Assoc. Petrol. Geol. Bull.*, **89**, 447-469.

**Ashley G.M. (Chair Person)** and **Others** (1990) Classification of Large-Scale Subaqueous bedforms: A new look at an old problem**.** *J. Sed. Petrology*, **60**, 160-172.

**Baars, D.L.** (1966) Pre-Pennsylvanian paleotectonics – key to basin evolution and petroleum occurrences in Paradox basin, Utah and Colorado. *Am. Assoc. Petrol. Geol. Bull.*, **50**, 2082-2111.

**Baker, A.A., Dobbin, C.E., McKnight, E.T., Reeside, J.B**. (1927) Notes on the Stratigraphy of the Moab region, Utah. *Am. Assoc. Petrol. Geol. Bull.*, **11**, 785-808.

**Baker, A.A., Reeside, J.B.** (1929) Correlation of the Permian of southern Utah, northern Arizona, northwest New Mexico, and southwestern Colorado. *Am. Assoc. Petrol. Geol. Bull.*, **13**, 1413-1448.

**Baker, AA, Dane, C.H., Reeside, J.B.** (1933) Paradox Formation of Eastern Utah and Western Colorado. *Am Assoc. Petrol. Geol. Bull.* **8**, 963-980.

**Baldwin, E.J.** (1983) The Moenkopi Formation of North-Central Arizona: and Interpretation of Ancient Environments based upon Sedimentary Structures and Stratification types. *J. Sed. Petrol.* **43**, 92-106.

**Banham, S.G., Mountney, N.P.** (2013a). Controls on fluvial sedimentary architecture and sediment-fill state in salt-walled mini-basins: Triassic Moenkopi Formation, Salt Anticline Region, SE Utah, USA. *Basin Research*. **25**, 709-737.

**Banham, S.G., Mountney, N.P.** (2013b). Climatic versus halokinetic control on sedimentation in a dryland fluvial succession. *Sedimentology, **61**, 570-608.*

**Banham, S.G., Mountney, N.P.** (2013c). Evolution of fluvial systems in salt-walled mini-basins: A review and new insights. *Sedimentary Geology*, **296**, 142-166.

**Barbeau, D.L.** (2003) A flexural model for the Paradox basin: implications for the tectonics of the Ancestral Rocky Mountains. *Basin Res.*, **15**, 97-115.

**Barde, J-P., Garalla, P., Harwijanto, J.,** and **Marsky, J.,** (2002a). Exploration at the eastern edge of the Precaspian basin: Impact of data integration on Upper Permian and Triassic prospectivity. *Am. Assoc. Petrol. Geol. Bull.*, **86**, 399-415.

**Barde, J. P., Chamberlain, P., Galavazi, M., Gralla, P., Harwijanto, J., Marsky, J., van den Belt, F.** (2002b). Sedimentation during halokinesis: Permo-Triassic reservoirs of the Saigak field, Precaspian basin, Kazakhstan. Petroleum Geoscience, **8**(2), 177-187.

**Barrell, J.** (1917) Rhythms and the Measurement of Geologic Time. *Bull. Geol. Soc. Am.*, **28**, 745-904.

**Barton, D.C.** (1933) Mechanics of formation of salt domes with specific reference to Gulf Coast salt domes of Texas and Louisiana. *Am. Assoc. Petrol. Geol. Bull.*, **17**, 1025-1083.

**Bentham, P.A. Talling, P.J., Burbank, D.W.** (1993) Braided stream and flood-plain deposition in a rapidly aggrading basin: the Escanilla formation, Spanish Pyrenees. In: *Braided Rivers* (Eds. J.L. Best, C.S. Bristow), *Geol. Soc. London Spec. Publ.* **75**, 177-194.

**Benvenuti, M., Carnicelli, S., Ferarri, G., Sagri M.** (2005) Depositional processes in latest Pleistocene and Holocene ephemeral streams of the Main Ethiopian Rift (Ethiopia). In: *Fluvial Sedimentology VII* (Eds M.D. Blum, S.B. Marriott, S.F. Leclair) *IAS Spec. Publ.*, 35, 277-294.

**Billi, P.** (2007) Morphology and sediment dynamics of ephemeral stream terminal distributary systems in the Kobo Basin (northern Welo, Ethiopia). *Geomorphology*, **85**, 98-113.

**Blair, T.C.** (2000) Sedimentology and progressive tectonic unconformities of the sheetflood-dominated Hell's Gate alluvial fan, Death Valley, California. *Sed. Geol*, **132**, 233-262.

**Blakey R.C., Ranney W.** (2008) Ancient Landscapes of the Colorado Plateau. *Grand Canyon Association, Grand Canyon, Arizona.*

**Blakey, R.C.** (1973) Stratigraphy and Origin of the Moenkopi Formation (Triassic) of Southeastern Utah. *The Mountain Geologist*, **10**, 1-17.

**Blakey, R.C.** (1974) Stratigraphy and Depositional Analysis of the Moenkopi Formation, Southeastern Utah. *Utah Geological and Mineral Survey Bulletin* **104**.

**Blakey, R.C**. (1989) Triassic and Jurassic Geology of the southern Colorado Plateau. In: *J.P. Jenny, S.J. Reynolds, Geological evolution of Arizona, Tuscon, Arizona Geological Society Digest.* **17**, 369-396.

**Blakey, R.C.** (2009) Palaeogeography and geologic history of the western ancestral rocky mountain, Pennsylvanian-Permian, southern Rocky Mountains and Colorado Plateau In: *The Paradox Basin Revisited – New Developments in Petroleum Systems and Basin Analysis* (Ed. by W.S. Houston, L.L. Wray, & P.G. Moreland), pp. 222-264. Rocky Mountain Association of Geologists, Denver, CO.

**Blakey, R.C., Gubitosa, R.** (1984) Controls on sandstone body geometry and architecture in the Chinle Formation (Upper Triassic) Colorado Plateau. *Sed. Geol.*, **38**, 51-86.

**Blum, M.D., Tornqvist T.E.** (2000) Fluvial responses to climate and sea-level change: a review and look forward. *Sedimentology*, **47**, 2-48.

**Bridge, J.S.** (2003) Rivers and Floodplains: forms, processes and sedimentary record. *Blackwell Science, Oxford.*

**Bridge, J.S.**, **Tye, R.S.** (2000) Interpreting the dimensions of ancient fluvial channel bars, channels, and channel belts from wireline-logs and cores. *Am. Assoc. Petrol. Geol. Bull.*, **84**, 1205-1228.

**Bristow, C.S., Best, J.L.** (1993) Braided rivers: perspectives and problems. In: *Braided Rivers* (Eds J.L. Best, C.S. Bristow). *Spec. Publ. Geol. Soc. London,* **75**, 1-11.

**Bromley, M.H.** (1991). Architectural features of the Kayenta Formation (Lower Jurassic), Colorado Plateau, USA: relationship to salt tectonics in the Paradox Basin. Sediment. Geol., **73**, 77-99.

**Brown, A.R.** (2004) Interpretation of Three-Dimensional Seismic Data, sixth ed. AAPG Memoir 42/SEG Investigations in Geophysics, No.9. *American Association of Petroleum Geologists and the Society of Exploration Geophysicists.*

**Brown, D., Alvarez-Marron, J., Perez-Estaun, A., Gorozhanina, Y., Puchkov, V.,** (2004). The structure of the south Urals foreland fold and thrust belt at the transition to the Precaspian basin. *Journal Geological Society, London*, **161**, 813-822.

**Brun, J.-P., Fort, X.,** (2003). Compressional salt tectonics (Angolan margin). *Tectonophysics*, **382**, 129-150.

**Bruthans, J., Filippi, M., Asadi, N., Zare, M., Slechta, S. Churackova, Z.** (2009) Surficial deposits on salt diapirs (Zagros Mountains and Persian Gulf Platform, Iran): Characterization, evolution, erosion and the influence on landscape morphology. *Geomophology,* **107**, 195-209.

**Buck, B.J., Lawton, T.F., Brock, A.L.,** (2010). Evaporitic paleosols in continental strata of the Caroza Formation, La Popa Basin, Mexico: record of Paleogene climate and salt tectonics. *Geol. Soc. America Bull*. **122**, 1011-1026.

**Bull, W.B.** (1979) Threshold of critical power in streams. Geol. Soc Am. Bull, **90**, 453-464.

**Byrd, T., Kristian, M., Jaffey, N., Vines, J., Buddin, T., Ekstrand, E.,** (2004). 3D Structural Restoration of Ponded-Basin Turbidite Reservoirs in a Linked Extensional-Compressional Salt Basin, Holstein Field, Deep-Water Gulf of Mexico. In: Post, P., Olson, D., Lyons, K., Palmes, S., Harrison, P., Rosen, N. (Eds), *Salt sediment interactions and Hydrocarbon Prospectivity; Concepts, Applications, and Case Studies for the 21st Century*. GCSSEPM 24th Annual Conference, pp. 965-996.

**Cadigan, R.A., Stewart, J.H.** (1971) Petrology of the Triassic Moenkopi Formation and Related Strata in the Colorado Plateau Region. *Department of the Interior, United States Geological Survey Professional Paper*, **692**.

**Cain, S.A.** (2009) Sedimentology and stratigraphy of a terminal fluvial fan system: the Permian Organ Rock Formation, South East Utah. *PhD Thesis,* Keele University.

**Cain, S.A.**, **Mountney, N.P.** (2009) Spatial and temporal evolution of a terminal fluvial fan system: the Permian Organ Rock Formation, South-east Utah, USA. *Sedimentology,* **56**, 1774-1800.

**Cain, S.A., Mountney, N.P.** (2011) Downstream changes and associated fluvial-aeolian interactions in an ancient terminal fluvial fan system: the Permian Organ Rock Formation, SE Utah. In: *From River to Rock Record* (Ed. by S. Davidson, S. Leleu, and C .North), SEPM Spec. Publ., **97**, 165-187.

**Carter, F.W.** (1970) Geology of the Salt Anticline Region in Southwestern Colorado. *Department of the Interior, United States Geological Survey Bulletin*, **637**.

**Carter, N.L., Heard, H.C.** (1970) Temperature and rate dependent deformation of halite. *Am. J. Sci.*, **269**, 193-249.

**Chan M.A.** (1989) Erg margin of the Permian White Rim Sandstone, SE Utah. *Sedimentology*, **36**, 235-251.

**Colman, S.M., Choquette, A.F., Rosholt, J.N., Miller, G.H., Huntley, D.J.,** (1986). Dating the upper Cenozoic sediments in Fisher Valley, southeastern Utah. *Geological Society of America Bulletin*, **97**, 1422-1431.

**Colombera, L., Felletti, F., Mountney, N.P.**, **McCaffrey, W.D.** (2012) A database approach for constraining stochastic simulations of the sedimentary heterogeneity of fluvial reservoirs. *Am. Assoc. Petrol. Geol. Bull.* **96**, 2143-2166.

**Condon, S.M** (1997) Geology of the Pennsylvanian and Permian Cutler Group and Permian Kaibab Limestone in the Paradox Basin, Southeastern Utah and Southwest Colorado. *Department of the Interior, U.S. Geological Survey Bulletin 2000-P*

**Craggs, S., Keighley, D., Park, A., Waldron, J.W.F.** (2013). Stratigraphy and salt tectonics of Mississippian-Pennsylvanian strata of the northern Cumberland Basin, Maringouin Peninsula, southeastern New Brunswick. *Atlantic Geology*, **49**.

**Dane, C.H.** (1935) Geology of the Salt Valley anticline and adjacent areas Grand County, Utah. *Department of the Interior, United States Geological Survey Bulletin*, **863**.

**Darton, N.H.** (1910) A reconnaissance of parts of northwestern New Mexico and northern Arizona. Department of the Interior, United States Geological Survey Bulletin, **435**.

**Davison, I., Alsop, I.G., Blundell, D.** (1996a) Salt tectonics: some aspects of deformation mechanics. In: *Salt Tectonics* (Ed. by I.G. Alsop, D.J. Blundell & I. Davison), Spec. Publ.Geol. Soc. London, **100**, 1-10.

**Davison, I., Bosence, D., Alsop, I.G., Al-Aawah, M.H.** (1996b) Deformation and sedimentation around active Miocene salt diapirs on the Tihama Plain, northwest Yeman. In: *Salt Tectonics* (Ed. by I.G. Alsop, D.J. Blundell & I. Davison), Spec. Publ.Geol. Soc. London, **100**, 23-39.

**Dickinson, W.R., Lawton, T.F.,** (2001). Carboniferous to Cretaceous assembly and fragmentation of Mexico. Geological *Society of America Bulletin*, **133**, 1142-1160.

**Dodd, T.J.H., Clarke, S.M** (2011) Salt Controls on sedimentation in a marginal-marine to continental setting: Implications for facies development and hydrocarbon entrapment. *Unpublished M.Sc. Thesis*, Keele University.

**Doelling, H. H.** (1988). Geology of Salt Valley Anticline and Arches National Park, Grand County, Utah. Salt deformation in the Paradox region, Utah: Utah Geological and Mineral Survey Bulletin, 122, 1-60.

**Doelling, H.H.** (2002a) *Geologic Map of the Fisher Towers 7.5' Quadrangle, Grand County, Utah.* Utah Geol. Surv. Geologic Map 183, p.22.

**Doelling, H.H.** (2002b) Geological map of the Moab and eastern parts of the San Rafael Desert 30' x 60' quadrangles Grand and Emery Counties, Utah and Mesa County, Colorado. Utah Geol. Surv. Geologic Map 180.

**Doelling, H.H** and **Chidsey, T.C.** (2009) Deadhorse State Park and Vicinity Geologic Road Logs, Utah. In: *The Paradox Basin Revisited: New Developments in Petroleum Systems and Basin Analysis* (Eds W.S. Houston, L.L. Wray and P.G. Moreland). *Rocky Mountain Association of Geologists Spec. Publ.*, 635-672.

**Dubiel, R.F., Stanesco, J.D.**, **Huntoon, J.E.** (1992) Clastic sabkha facies and paleogroundwater flow in the Hoskinnini Member of the Moenkopi Formation (Triassic Paradox Basin) – Implications for Hydrocarbon Emplacement. *SEPM – Rocky Mountain Section Newsletter,* **12**, 2.

**Dubiel, R.F.** (1994). Triassic deposystems, paleogeography, and paleoclimate of the Western Interior. *Mesozoic systems of the Rocky Mountain region, USA*, Rocky Mountain SEPM, 133-168.

**Dubiel, R.F., Huntoon, J.E., Stanesco, J.D., Condon, S.M.** and **Mickelson, D.** (1996) Permain-Triassic depositional systems, paleogeography, paleoclimate, and hydrocarbon resources in Canyonlands, Utah. Colorado Geological Survey, Open-File Report 96-4, Field Trip 5.

**Dyson, I.A.,** (2004). Interpreted shallow and deep-water depositional systems of the Beltana mini-basin in the Northern Flinders Ranges. South Australia. In: Post, P., Olson, D., Lyons, K., Palmes, S., Harrison, P., Rosen, N. (Eds), *Salt sediment interactions and Hydrocarbon Prospectivity; Concepts, Applications, and Case Studies for the 21st Century*. GCSSEPM 24th Annual Conference, pp. 593-614.

**Elston, D.P.**, **Shoemaker, E.M., Landis, E.R.** (1962) Uncompahgre front and salt anticline region of the Paradox Basin, Colorado and Utah. *Am. Assoc. Petrol. Geol. Bull.*, **46**, 1857-1878.

**Fiduk, J.C.** (1995) Influence of submarine canyon erosion and sedimentation on allochthonous salt body geometry: the pathway of Bryant Canyon in Garden Banks. In: *Salt, Sedimentation, and Hydrocarbons* (Ed. by C.J. Travis, B.C. Vendeville, H. Harrison, F.J. Peel, M.R. Hudec & B.E. Perkins). GCSSEPM Foundation 16th Annual Research Conference, 41-51.

**Fiduk, J.C., Brush, E.R., Anderson, L.E., Gibbs, P.B., Rowan, R.G.** (2004) Salt deformation, magmatism, and hydrocarbon prospectivity in the Espirito Santo Basin, offshore Brazil. In: *Salt-Sediment Interactions and Hydrocarbon Prospectively: Concepts, Applications and Case Studies for the 21st Century. Gulf Coast State Society of Economic Paleontologists and Mineralogists Foundation, 24th Bob F. Perkins Research Conference Proceedings* (CD-ROM) (Ed. by P.J. Post), 370-393. Gulf Coast Section SEPM Foundation, Huston, Texas.

**Field, J.** (2001) Channel avulsion on alluvial fans in southern Arizona. *Geomorphology*. **37**, 93-104.

**Fillmore, R.** (2011) *Geological evolution of the Colorado Plateau of Eastern Utah and Western Colorado.* University of Utah Press.

**Fisher, J.A., Nichols, G.J.**, (2007). Interpreting the stratigraphic architecture of fluvial systems in internally drained basins. *Journal of the Geological Society, London,* **170**, 57-65.

**Fisher, J.A., Krapf, C.B.E., Lang, S.C., Nichols, G.J.** and **Payenberg, T.H.D.** (2008) Sedimentology and architecture of the Douglas Creek terminal splay, Lake Eyre, central Australia. *Sedimentology*, **55**, 1915-1930.

**Flores, R.M.**, **Pillmore, C.L.** (1987) Tectonic Control on Alluvial Paleoarchitecture and of the Cretaceous and Tertiary Ration Basin, Colorado and New Mexico. In: *Recent Developments in Fluvial Sedimentology, Spec. Publ. SEPM,* **39**, 311-320.

**Friedman, J.D., Case, J.E., Simpson, S.L.** (1994) Tectonic trends of the northern part of the Paradox Basin, southeastern Utah and southwestern Colorado, as derived from Landsat multispectral scanner imaging and geophysical and geologic mapping. *U.S. Department of the Interior, U.S. Geological Survey Bulletin,* **2000-C**.

**Frostick, L.E., Reid, I., Layman, J.T.** (1983) Changing size distribution of suspended sediment in arid-zone flash floods. In: *Modern and Ancient Fluvial Systems* (Ed. by J.D. Collinson & J. Lewin) *Spec Publ. Int. Ass. Sediment. **6**, 97-106.*

**Fuchs, L., Schmeling, H., Koyi, H.** (2011) Numerical models of salt diapir formation by downbuilding: the role of sedimentation rate, viscosity contrast and initial amplitude and wavelength. *Geophys. J. Int.*, **186**, 390-400.

**Gawthorpe, R.L., Fraser, A.J., Collier, R.E.L.** (1994) Sequence Stratigraphy in active extensional basins: implications for the interpretation of ancient basin-fills. *Marine and petroleum Geoscience.* **11**, 642-658.

**Gawthorpe, R. L., Leeder, M. R.** (2000). Tectono-sedimentary evolution of active extensional basins. *Basin Research*, **12**, 195-218.

**Leopold, L.B., Wolman, M.G., Miller, J.P.** (1964) *Fluvial Processes in Geomorphology*, San Francisco, W.H. Freeman and Co., 522p

**Ge H., Jackson, M.P.A., Vendeville B.C**. (1997) Kinematics and dynamics of salt tectonics driven by progradation. *Am. Assoc. Petrol. Geol. Bull.*, **81**, 398-423.

**Gee D.M., Anderson, M.G., Baird, L.** (1990) Large-scale floodplain modelling. *Earth Surf. Process. Landf.*, **15**, 513-523.

**Gee, M.J.R., Gawthorpe R.L.** (2006) Submarine channels controlled by salt tectonics: Examples from 3D seismic data offshore Angola. *Mar. Petrol. Geol.*, **23**, 443-458.

**Geehan, G., Underwood., J.** (1993) The use of length distributions in geological modelling. *The geological modelling of hydrocarbon reservoirs and outcrop analogues*, Spec. Publs int. Assoc. Sedimentologists, **15**, 205-212.

**Gibling, M.R.** (2006) Width and thickness of fluvial channel bodies and valley fills in the geological record: A literature compilation and classification. *Journal of Sedimentary Research,* **76**, 731-770.

**Glennie, K., Higham, J., Stemmerik, L.,** (2003). Permian. In: Evans, D., Graham, C., Armour, A., Bathurst P. (Eds.), *The Millennium Atlas: Petroleum Geology of the Central and Northern North Sea*, 91-103. Geological Society, London.

**Glennie, K.W.** (1970) Desert Sedimentary Environments. *Developments in Sedimentology 14,* Elsevier Publishing Company, Amsterdam.

**Goldhammer, R.K., Oswald, E.J., Dunn, P.A**. (1991) Hierarchy of stratigraphic forcing: Examples from the Middle Pensylvanian self carbonates of the Paradox basin. *Kansas Geol. Surv. Bull.,* **233**, 361-413.

**Goldsmith, P.J., Rich, B., Standring, J.,** (1995). Triassic correlation and stratigraphy in the South Central Graben, UK North Sea. In: Boldy, S.A.R. (Ed.), *Permian and Triassic Rifting in Northwest Europe*. Special Publication, **91**. Geological Society, London, pp. 123-143.

**Goldsmith, P.J., Hudson, G., Van Veen, P.,** (2003). Triassic. In: Evans, D., Graham, C., Armour, A., Bathurst P. (Eds.), *The Millennium Atlas: Petroleum Geology of the Central and Northern North Sea*, 105-127. Geological Society, London.

**Gomez-Gras, D., Alonso-Zarza, A.M.** (2003) Reworked calcretes: their significance in the reconstruction of alluvial sequences (Permian and Triassic, Minorca Balearic Islands, Spain) *Sed. Geol.*, **158**, 299-319.

**Goodall, T.M., North, C.P. Glennie, K.W.** (2000) Surface and subsurface sedimentary structures produced by salt crusts. *Sedimentology*, **47**, 99-118.

**Gough, A. Clarke, S.M.** [In Press] Interaction between proximal and distal sedimentation in arid continental basins: subsequent implications for fluid flow Gough & Clarke 2014. *Sedimentology*.

**Gralla, P., Marsky, J.,** (2000). Seismic reveals new eastern Precaspian target. *Oil & Gas Journal*, **98**, 86-89.

**Gregory, H.E.** (1917) Geology of the Navajo Country: A reconnaissance of parts of Arizona, New Mexico, and Utah. Department of the Interior, United States Geological Survey Professional Paper **93**.

**Halfar, J., Riegel, W., Walther, W.** (1998) Facies architecture and sedimentology of a meandering fluvial system: a Palaeogene example from the Weisselster Basin, Germany. *Sedimentology*, **45**, 1-17.

**Hall, D.J., Thies, K.J.** (1995) Salt kinematics, depositional systems, and implications for hydrocarbon exploration, Eugene Island and Ship Shoal south additions, offshore Louisiana. In: *Salt, Sedimentation, and Hydrocarbons* (Ed. by C.J. Travis, B.C. Vendeville, H. Harrison, F.J. Peel, M.R. Hudec & B.E. Perkins). GCSSEPM Foundation 16th Annual Research Conference, 83-94.

**Hampton, B.A., Horton B.K.** (2007) Sheetflow fluvial processes in a rapidly subsiding basin, Altiplano plateau Bolivia. *Sedimentology,* **54**, 1121-1147.

**Hardgrove, C., Moersch, J., Whisner, S.,** (2010). Thermal imaging of sedimentary features on alluvial fans. *Planetary and Space Science*, **58**, 482-508.

**Harrison, J.C., Jackson, M.P.A.,** (2013). Exposed evaporate diapirs and minibasins above a canopy in central Sverdrup Basin, Axel Heiberg Island, Arctic Canada. *Basin Research*, Doi: 10:1111/bre.12037.

**Harrison, T.S.** (1927) Colorado-Utah salt domes. *Am. Assoc. Petrol. Geol. Bull.*, **11**, 111-113.

**Hartley, A.J., Weissmann, G.S., Nichols, G.J.** & **Warwick, G.L.** (2010) Large distributive fluvial systems: characteristics, distribution, and controls on development. *J. Sed. Res.* **80**, 167-183.

**Hazel, J.E.** (1994) Sedimentary Response to Intrabasinal Salt Tectonism in the Upper Triassic Chinle Formation, Paradox Basin, Utah. *U.S. Geological Survey Bulletin 2000-F*.

**Hinds, D.J., Aliyeva, E., Allen, M.B., Davies, C.E., Kroonenberg, S.B., Simmons, M.D., Vincent, S.J.** (2004) Sedimentation in a discharge dominated fluvial-lacustrine system: the Neogene productive series of the South Caspian Basin, Azerbaijan. *Mar. Petrol. Geol.*, **21**, 613-638.

**Hintze, L.F., Axen, G.J.** (1995) Geology of the Lime Mountain Quadrangle, Lincoln Country, Nevada. Nevada Bureau of Mines and Geology Map 129.

**Hite, R.J.** (1968) Salt deposits of the Paradox Basin, Southeast Utah and Southwest Colorado. In: *Saline Deposits – A Symposium based on Papers from the International Conference on Saline Deposits, Houston, Texas, 1962.* (Ed. by: R.B Mattox, W.T. Holser, H. Ode, W.L. McIntyre, N.M. Short, R.E. Taylor & D.C. Van Siclen) Geol. Soc. Am. Spec. Pap., **88**, 319-330.

**Hjulstrom, F** (1935) Studies of the morphological activity of rivers as illustrated by the River Fyris. *Bull. Geol. Inst. Uppsala,* **25**, 221-527.

**Hodgson, N.A., Farnsworth, J., Fraser, A.J.** (1992) Salt-related tectonics, sedimentation, and hydrocarbon plays in the Central Graben, North Sea, UKCS. In: *Exploration Britain: Geological insights for the next decade* (Ed. R.F.P. Hardman), *Spec. Publ. Geol. Soc. London*, **67**, 31-63.

**Hogg, S.E.** (1982) Sheetfloods, sheetwash, Sheetflow, or … ? *Earth-Science Reviews*, **18**, 59-78.

**Howel, J.A., Flint, S.S.** (1996) A model for high resolution sequence stratigraphy within extensional basins. In: *High resolution sequence stratigraphy: Innovations and Applications* (Ed. by J.A. Howell, J.F. Aitken), Geol. Soc. London Spec. Publ. **104**, 129-137.

**Hubert, J.F., Hyde, M.G.** (1982) Sheet-flow deposits of graded beds and mudstones on an alluvial sandflat-playa system: Upper Triassic Blomidon redbeds, St Mary's Bay, Nova Scotia. *Sedimentology,* **29**, 457-474.

**Hudec, M.R.** (1995) The Onion Creek salt diapir: an exposed diapir fall structure in the Paradox Basin, Utah. In: *Salt, Sedimentation, and Hydrocarbons* (Ed. by C.J. Travis, B.C. Vendeville, H. Harrison, F.J. Peel, M.R. Hudec & B.E. Perkins). GCSSEPM Foundation 16th Annual Research Conference, 125-134.

**Hudec, M.R., Jackson, M.P.A.** (2007) Terra infirma: Understanding salt tectonics. *Earth Sci. Rev.*, **82**, 1-28.

**Hudec, M.R., Jackson, M.P.A., Schultz-Ela, D.D.** (2009) The Paradox of minibasin subsidence into salt: Clues to the evolution of crustal basins. *Geol. Soc. Am. Bull.*, **121**, 201-221.

**Ings, S.J., Beaumont, C.** (2010) Shortening viscous pressure ridges, a solution to the enigma of initiating salt 'withdrawal' minibasins. *Geology*, **38**, 339-342.

**Jackson, M.P.A., Talbot, C. J.** (1986). External shapes, strain rates, and dynamics of salt structures. *Geological Society of America Bulletin*, **97**, 305-323.

**Jackson, M.P.A., Cornelius, R.R., Craig, C.H., Gansser, A., Stocklin, J., Talbot, C.J.** (1990) Salt diapirs of the Great Kavir, Central Iran. *Geol. Soc. Am. Mem. **177.***

**Jackson, M.P.A., Vendeville, B.C., Schultz-Ela, D.D.** (1994) Structural dynamics of salt systems. *Annu. Rev. Earth Planet. Sci.* **22,** 93-117.

**Johnson, H.S., Thordarson, W.** (1966) Uranium Deposits of the Moab, Monticello, White Canyon, and Monument Valley Districts Utah and Arizona. U.S. Department of the Interior, Geological Survey Bulletin **1222-H**.

**Jones, A. D., Auld, H. A., Carpenter, T. J., Fetkovich, E., Palmer, I. A., Rigatos, E. N., Thompson, M. W.** (2005). Jade Field: an innovative approach to high-pressure, high-temperature field development. In Geological Society, London, Petroleum Geology Conference series (Vol. 6, pp. 269-283). Geological Society of London.

**Jones, R.W.** (1959) Origin of Salt Anticlines of the Paradox Basin. *Am. Assoc. Petrol. Geol. Bull.*, **43**, 1869-1895.

**Jordan, O.D., Mountney, N.P.** (2010) Styles of interaction between aeolian, fluvial and shallow marine environments in the Pennsylvanian-Permian Lower Cutler Beds, southeast Utah, USA. *Sedimentology*, **57**, 1357-1385.

**Jordan, O.D., Mountney, N.P.** (2012) Sequence stratigraphic evolution and cyclicity of an ancient coastal desert system: the Pennsylvanian-Permian lower Cutler beds, Paradox Basin, Utah, USA. *J. Sediment. Res.*, **82**, 755-780.

**Kane, I.A., McGee, D.T., Jobe, Z.R.** (2012). Halokinetic effects on submarine channel equilibrium profiles and implications for faces architecture: conceptual model illustrated with a case study from Magnolia Field, Gulf of Mexico. In: *Salt Tectonics, Sediments, and Prospectivity* (Ed. by I.G. Aslop, S.G. Archer, A.J. Hartley, N.T. Grant & R. Hodgkinson). Spec. Publ. Geol. Soc. London, **363**, London, 289-302.

**Kelling, G., Maldonado, A., Stanley, D.J.** (1979). Salt tectonics and basement fractures: key controls of recent sediment distribution on the Balearic Rise, Western Mediterranean. *Smithsonian Contributions to the Marine Sciences*, **3**.

**Kernen, R.A., Giles, K.A., Rowan, M.G., Lawton, T.F., Hearon, T.E.** (2012) Depositional and halokinetic-sequence stratigraphy of the Neoproterozoic Wonoka Formation adjacent to Patawarta allochthonous salt sheet, Central Flinders Ranges, South Australia. In: *Salt Tectonics, Sediments, and Prospectivity* (Ed. by I.G. Aslop, S.G. Archer, A.J. Hartley, N.T. Grant & R. Hodgkinson). Spec. Publ. Geol. Soc. London, **363**, 81-105.

**Kluth, C.F., Coney, P.J.** (1981) Plate tectonics of the Ancestral Rocky Mountains. *Geology,* **9**, 10-15.

**Kluth, C.F.**, **DuChene, H.R.** (2009) Late Pennsylvanian and early Permian structural geology and tectonic history of the Paradox Basin and Uncompahgre uplift, Colorado and Utah. In: *The Paradox Basin Revisited: New Developments in Petroleum Systems and Basin Analysis* (Eds W.S. Houston, L.L. Wray and P.G. Moreland). *Rocky Mountain Association of Geologists Spec. Publ.*, 178-197.

**Kneller, B., McCaffrey, W.D.,** (1995). Modelling the effects of salt-induced topography on deposition from Turbidity Currents. In: Travis, C.J., Vendeville,

B.C., Harrison, H., Peel, F.J., Hudec, M.R., Perkins, B.E. (Eds), *Salt, Sedimentation, and Hydrocarbons*. GCSSEPM Foundation 16th Annual Research Conference, pp. 137-145.

**Lawton, T.F., Buck, B.J.** (2006) Implications of diaper-derived detritus and gypsic paleosols in Lower Triassic strata near Castle Valley salt wall, Paradox Basin, Utah. *Geology*, **34**, 885-888.

**Lawton, T.F., Vega, F.J., Giles, K.A., Rosales-Dominguez, C.,** (2001). Stratigraphy and Origin of the La Popa Basin, Nievo Leon and Coahuila, Mexico. In: Bartolin, C., Buffler, R.T., Cantu-Chapa, A. (Eds) *The western Gulf of Mexico Basin: Tectonics, sedimentary basins, and petroleum systems*. AAPG Memoir 75, 219-240.

**Leeder M.R., Gawthorpe R.L.** (1987) Sedimentary models for extensional tilt-block/half-graben basins. In: *Continental Extensional Tectonics* (Ed. by M.P. Coward, J.F. Dewey, P.L. Hancock) Geol. Soc. London Spec. Publ. **28**, 139-152.

**Leeder, M.R., Harris, T.**, **Kirkby, M.J.** (1998) Sediment supply and climate change: implications for basin stratigraphy. *Basin Res.*, **10**, 7-18.

**Lindholm, R.** (1987) *A practical approach to Sedimentology, 1st Ed.,* Allen & Unwin, Inc, Massachusetts.

**Mack, G. H., Rasmussen, K.A.** (1984) Alluvial-fan sedimentation of the Cutler Formation (Permo-Pennsylvanian) Near Gateway, Colorado. *Geol. Soc. Am. Bull.,* **95**, 109-116.

**Mackey, S.D.**, **Bridge, J.S.** (1995) Three-dimensional model of alluvial stratigraphy: theory and application. *J. Sed. Res.* **65B**, 7-31.

**Mange-Rajetzkey, M.A.,** (1995). Subdivision and correlation of monotonous sandstone sequences using high-resolution heavy mineral analysis, a case study: the Triassic of the Central Graben. In: Dunay, R.E., Hailwood, E.A. (Eds) *Non-biostratigraphical Methods of Dating and Correlation*. Geological Society Special Publication **89**, London, pp. 23-30.

**Marriott, S.B., Wright, V.P., Williams, B.P.J** (2005) A new evaluation of fining upward sequences in a mud-rock dominated succession of the Lower Old Red Sandstone of South Wales, UK. *Fluvial sedimentology VII, Int. Assoc. Sedimentol. Spec. Publ.*, **35**, 517-529.

**Matthews, W.J., Hampson, G.J., Trudgill, B.D., Underhill, J.R.** (2007) Controls on fluvio-lacustrine reservoir distribution and architecture in passive salt diapir provinces: insights from outcrop analogue. *Am. Assoc. Petrol. Geol. Bull.* **91**, 1367-1403.

**Mattox, R.B.** (1968) Salt Anticline Field Area, Paradox Basin, Colorado and Utah. In: *Saline Deposits – A Symposium based on Papers from the International Conference on Saline Deposits, Houston, Texas, 1962.* (Ed. by: R.B Mattox, W.T. Holser, H. Ode, W.L. McIntyre, N.M. Short, R.E. Taylor & D.C. Van Siclen) Geol. Soc. Am. Spec. Pap., **88**, 5-16.

**McKee E.D., Crosby, E.J., Berryhill, H.J.** (1966) Flood deposits, Bijou Creek, Colorado, June 1965. *J. Sed. Petrol.*, **37**, 829-851.

**McKie T., Williams, B.** (2009) Triassic palaeogeography and fluvial dispersal across the northwest European Basins. *Geol. J.* **44**, 711-741.

**McKie, T.** (2011) Architecture and Behaviour of Dryland Fluvial Reservoirs, Triassic Skagerrak Formation, Central North Sea. In: *From Rivers to Rock Record* (eds S.K. Davidson, S. Leleu, and C.P. North) SEPM Spec. Publ. ***97, 189-214.***

**McKie, T., Audretsch, P.** (2005) Depositional and structural controls on Triassic reservoir performance in the Heron Cluster, ETAP, Central North Sea. In: *North-West Europe and Global Perspectives – Proceedings of the 6th Petroleum Geology Conference*, 285-297.

**McKie, T., Jolley, S.J.**, **Kristensen, M.B.** (2010) Stratigraphic and structural compartmentalization of dryland reservoirs: Triassic Heron Cluster, Central North Sea. *Geol. Soc. London Spec. Publ.* **347**, 165-198.

**Miall, A.D.** (1985) Architectural-Element Analysis: A New Method of Facies Analysis Applied to Fluvial Deposits. *Earth Sci. Rev.* **22**, 261-308.

**Miall, A.D.** (1996) *The Geology of Fluvial Deposits*. Springer, Berlin.

**Morales, M.** (1987) Terrestrial fauna and flora from the Triassic Moenkopi Formation of the Southwestern United States. *J.Arizona-Nevada Acad. Sci.* **22**, 1-19.

**Mullens, T.E.** (1960) Geology of the Clay Hills Area, San Juan County, Utah. *U.S. Geological Survey Bulletin* 1087-H.

**Newberry, J.S.** (1861) Geological Report. In Ives, J.C., Report upon the Colorado River of the West: U.S. 36th Cong. 1st Sess. *Senate and House Ex. Doc*, **90**, pt. 3, 154.

**Newell, A.J., Tverdokhlebov, V.P., Benton, M.J.,** (1999). Interplay of tectonics and climate on a transverse fluvial system, Upper Permian, Southern Uralian Foreland Basin, Russia. *Sedimentary Geology*, **127**, 11-29.

**Newell, A.J., Benton, M.J., Kearsey, T., Taylor, G., Twitchett, R.J., Tverdokhlebov, V.P.** (2012) Calcretes, fluviolacustrine sediments and subsidence patterns in Permo-Triassic salt-walled minibasins of the south Urals, Russia. *Sedimentology*, **59**, 1659-1676.

**Nichols, G.J., Fisher, J.A.,** (2007). Processes, facies, and architecture of fluvial distributary system deposits. *Sedimentary Geology*, **195**, 75-90.

**North, C.P., Nanson, G.C., Fagen, S.D.** (2007) Recognition of the sedimentary architecture of dryland anabranching (Anastomosing) Rivers. *J. Sed. Res.* **77**, 925-938.

**Nuccio, V.F., Condon, S.M.** (1997) Burial and thermal history of the Paradox Basin, Utah and Colorado, and petroleum potential of the Middle Pennsylvanian Paradox Formation. In: *Geology and Resources of the Paradox Basin* (eds A.C. Huffman, W.R. Lund, and L.H. Godwin), Utah Geol. Assoc. Guidebook 25.

**O'Hearn, T., Elliott, S., Samsonov, A.,** (2003). Karachaganak Field, Northern Pre-Caspian Basin, Northwest Kazakhstan. In: *Giant oil and gas fields of the decade 1990-1999* (Ed. by M.T. Halbouty), Memoir **78**, American Association of Petroleum Geologists, pp. 237-250.

**O'Sullivan, R.B., MacLachlan, M.E.** (1975) Triassic Rocks of the Moab-White Canyon Area, Southeastern Utah. *Four Corners Geol. Soc. Guidebook*, 8th Field Conf., Canyonlands, 129-141.

**Ohlen, H.R. McIntyre, L.B.** (1965) Stratigraphy and tectonic features of the Paradox Basin, four corners area. *Am. Assoc. Petrol. Geol. Bull.*, **49**, 2020-2040.

**Owen, G.** (1987) Deformation processes in unconsolidated sands. In: *Deformation of sediments and sedimentary rocks* (Eds M.E. Jones, and R.M.F. Patterson), *Spec. Publ. Geol. Soc. London*, **29**, 11-24.

**Owen, G.** (1996) Experimental soft-sediment deformation: structures formed by the liquefaction of unconsolidated sands and some ancient examples. *Sedimentology*, **43**, 279-93.

**Pairazian, V.V.,** (1999). A review of the petroleum geochemistry of the Precaspian Basin. *Petroleum Geoscience*, **5**, 351-369.

**Paz, M., Trudgill, B., Kluth, C.** (2009) Salt system evolution of the Northern Paradox Basin. *Search and Discovery Article #30078*.

**Peacock, D.C.P.** (2004). The post-Variscan development of the British Isles within a regional transfer zone influenced by orogenesis. *Journal of Structural Geology*, **26**, 2225-22231.

**Picard, M.D., High, L.R.** (1973) Sedimentary structures of ephemeral streams. *Developments in sedimentology* **17**, Elsevier Sci. Publ. Co., Amsterdam, Netherlands.

**Prather, B.E. (**2000). Calibration and visualization of depositional process models for above-grade slopes: a case study from the Gulf of Mexico. *Marine and Petroleum Geology*, **17**, 619-638.

**Prather, B.E., Booth, J.R., Steffens, G.S., Graig, P.A.,** (1998). Classification, lithologic calibration, and stratigraphic succession of seismic facies of intraslope basins, deep-water Gulf of Mexico. *Am. Assoc. Petrol. Geol. Bull.*, **82**, 701-728.

**Prochnow, S.J., Atchley, S.C. Boucher, T.E., Nordt, L.C., Hudec, M.R.** (2006) The influence of salt withdrawl subsidence on palaeosol maturity and cyclic fluvial deposition in the Upper Triassic Chinle Formation: Castle Valley, Utah. *Sedimentology*, **53**, 1319-1345.

**Prommel, H.W.C.** (1923). Geology and structure of portions of Grand and San Juan counties, Utah. *Am. Assoc. Petrol. Geol. Bull.* **4**, 384-399.

**Rahn, P.H.** (1967) Sheetfloods, Streamflood, and the formation of Pediments. *Ann. Assoc Am. Geog.* **57**, *593-604.*

**Rasmussen, L., Rasmussen D.L.** (2009) Burial History Analysis of the Pennsylvanian Petroleum System in the Deep Paradox Basin Fold and Fault Belt, Colorado and Utah. In: *The Paradox Basin Revisited: New Developments in Petroleum Systems and Basin Analysis* (Eds W.S. Houston, L.L. Wray and P.G. Moreland). *Rocky Mountain Association of Geologists Spec. Publ.*, 24-94.

**Reid, I., Laronne, J.B., Powell, D.M.** (1998) Flash-flood and bedload dynamics of desert gravel-bed streams. *Hydrol. Process.*, **12**, 543-557.

**Rodríguez-López, J.P., Lies, C.L., Van Dam, J. La Fuente, P., Arlegui, L., Ezquerro, L., De Bore, P.** (2012) Aeolian construction and alluvial dismantling of a fault-bounded intracontinental aeolian dune field (Teruel Basin, Spain); a continental perspective on Late Pliocene climate change and variability. *Sedimentology*, **59**, 1536-1567.

**Rowan, M.G., Lawton, T.F., Giles, K.A.,** (2012). Anatomy of an exposed vertical salt weld and flanking strata, La Popa Basin, Mexico. In: Alsop, G.I., Archer, S.G., Hartley, A.J., Grant, N.T., Hodgkinson, R. (Eds.) *Salt Tectonics, Sediments and Prospectivity*. Geological Society, London, Special Publication 363, pp. 33-57.

**Rumsby, B.T., Macklin, M. G.** (1994) Channel and floodplain response to recent abrupt climate change: the Tyne Basin, Northern England. *Earth Surf. Process. Landf.,* **19**, 499-515.

**Rust, B.R.** (1981) Sedimentation in an arid-zone anastomosing fluvial system: Cooper's Creek, Central Australia. *J. Sedim. Petrol.,* **51**, 745-755.

**Rust, B.R., Legun, A.S.** (1983) Modern anastomosing-fluvial deposits in arid Central Australia, and a Carboniferous analogue in New Brunswick, Canada. In: *Modern and Ancient Fluvial Systems* (Ed. by J.D. Collinson & J. Lewin) *Spec Publ. Int. Ass. Sediment.* ***6****,* 385-392.

**Schamel, S., Pilifossov, V.M., Votsalevsky, E.S.,** (1995). Geological controls on style of salt piercements in the Pricaspian Basin, Kazakhstan: contrasts with the Gulf of Mexico. In: Travis, C.J., Vendeville, B.C., Harrison, H., Peel, F.J., Hudec, M.R., Perkins, B.E. (Eds) Salt, Sedimentation, and Hydrocarbons. GCSSEPM Foundation 16th Annual Research Conference, pp. 253-255.

**Selley, R.C.** (1988) *Applied Sedimentology*. Academic Press Limited, London.

**Senseny, P.E., Hansen, F.D., Russell, J.E., Carter, N.L., Handin, J.W.** (1992). Mechanical Behaviour of Rock Salt: Phenomenology and Micromechanisms. *International Journal of Rock Mechanics and Mining Sciences & Geomechanics Abstracts*, **29**, 363-378.

**Sherwin, D.F.** (1973) Scotian Shelf and Grand Banks. In: *Future Petroleum Provinces of Canada, Their Geology and Potential* (Ed. by I.H. Cram) Canadian Society of Petroleum Geologists, Memoir **1**, 519-559.

**Shoemaker, E.M.** (1955) Structural features of the central Colorado Plateau and their relation to uranium deposits. In: *Contributions to the Geology of Uranium and Thorium by the United States Geological Survey and Atomic Energy Commission for the United Nations Commission for the United Nations International Conference on Peaceful Uses of Atomic Energy, Geneva, Switzerland.* Department of the Interior, Geological Survey Professional Paper 300.

**Shoemaker, E.M., Newman, W.L.** (1957) Notes on the Moenkopi Formation in the Salt Anticline Region of Colorado and Utah. U.S. Department of the Interior, U.S. Geological Survey Trace Elements Investigations Report **681**.

**Shoemaker, E. M., Newman, W. L.** (1959). Moenkopi Formation (Triassic? and Triassic) in salt anticline region, Colorado and Utah. *Am. Assoc. Petrol. Geol. Bull.*, **43**, 1835-1851.

**Sirocko, F., Szeder, T., Seelos, C., Lehne, R., Rein, B., Schneider, W.M., Dimke, M.** (2002) Young tectonic and halokinetic movements in the North-German-Basin: its effect on formation of modern rivers and surface morphology. *Netherlands Journal of Geoscience*, **81**, 431-441.

**Sloss, L.L.** (1969) Evaporite Deposition from Layered Solutions. *Am. Asoc. Petrol. Geol. Bul.* **53**, 776-789.

**Smith, D.B., Taylor J.C.M.,** (1992). Permian. In: Cope, J.C.W., Ingham, J.K., Rawson, P.F. (Eds) *Atlas of Palaeogeography and Lithofacies*. Geological Society, London, Memoir **13**, 87-95.

**Smith, R.I., Hodgson, N. Fulton, M.** (1993) Salt controls on Triassic reservoir distribution, UKCS Central North Sea. In: *Petroleum Geology of Northwest Europe: Proceedings of the 4th Conference* (Ed. J.R. Parker)*, Geol. Soc. London*, 547-557.

**Soreghan, G.S., Soreghan M.J., Sweet, D.E., More, K.D.,** (2009). Hot fan or cold outwash? Hypothesized proglacial deposition in the upper Paleozoic Cutler Formation, western tropical Pangea. Jou*rnal of Sedimentary Research*, **79**, 495-522.

**Srivastava, K.K., Merchant, H.D.,** (1973). Thermal expansion of alkali halides above 300°K. *Journal of Physics and Chemistry of Solids*, **34**, 2069-2073.

**Stanesco, J.D., Dubiel, R.F. Huntoon, J.R.** (2000) Depositional Environments and Palaeotectonics of the Organ Rock Formation of the Permian Cutler Group, Southeastern Utah. In: D.A. Sprinkel, T.C. Chidsey Jr., P.B. Anderson (eds) *Geology of Utah's Parks and Monuments, Utah Geological Association Publication 28.*

**Stewart J.H.** (1959) Stratigraphic relations of Hoskinnini Member (Triassic?) of Moenkopi Formation on Colorado Plateau. *Am. Assoc. Petrol. Geol. Bull.*, **43**, 1852-1868.

**Stewart J.H., Poole, F.G., Wilson, R.F. Cadigan, R.A.** (1972) Stratigraphy and Origin of the Triassic Moenkopi Formation and Related Strata in the Colorado Plateau Region. *Geological Survey Professional Paper 691*.

**Stewart, S.A.** (2007) Salt tectonics in the North Sea Basin: a structural style template for seismic interpreters. In: *Deformation of the Continental Crust: The Legacy of Mike Coward* (Ed. by A.C. Ries, R.W.H. Butler, R.H. Graham), *Spec. Publ. Geol. Soc. London,* **272**, 361-396.

**Stewart, S.A., Clarke, J.A.** (1999) Impact of salt on the structure of the Central North Sea hydrocarbon fairways. *Petroleum Geology Conference series*, **5**, 179-200.

**Stokes, W.L.** (1987) *Geology of Utah.* Utah Geological and Mineral Survey, Occasional Paper **6***.*

**Sundborg, A.** (1956) The River Klaralven: a study of fluvial processes. *Geogr. Annlr.* **38**, 127-316.

**Talbot, C.J.** (1998) Extrusion of Hormuz salt in Iran. In: *Lyell: the past is the Key to the Present.* (Ed. by D.J. Blundell, & A.C. Scott), *Spec. Publ. Geol. Soc. London,* **143**, 315-334.

**Talbot, C.J., Aftabi, P.** (2004) Geology and models of salt extrusion at Qum Kuh, central Iran. *J. Geol. Soc. London*, **161**, 321-334.

**Thaden, R.E., Trites, A.F., Finnell, T.L.**(1964) Geology and ore deposits of the White Canyon area, San Juan and Garfield Counties, Utah. *U.S. Geol. Surv. Bull.* **1125**.

**Thamó-Bozsó, E., Kercsmár, Z., Annamária, N**. (2002) Tectonic control on changes in sediment supply; Quaternery alluvial systems, Körös sub-basin, SE Hungary. In: *Sediment flux to Basins: Causes, Controls and Consequences (Eds.* S.J. Jones and L.E. Frostick). *Geol. Soc. London, Spec. Pub*, **191**, 37-53.

**Tooth, S.** (1999a) Floodouts in central Australia. In*: Varieties of Fluvial Form* (Eds A.J. Miller and A. Gupta), pp. 219–247. John Wiley & Sons, New York.

**Tooth, S.** (1999b) Downstream changes in floodplain character on the Northern Plains of arid central Australia. *Spec. Publs. Ass. Sediment.* **28**, 93-112.

**Tooth, S.** (2000) Downstream changes in dryland river channels: the Northern Plains of arid central Australia. *Geomorphology*, **34**, 33-54.

**Trudgill B.D., Paz, M.** (2009) Restoration of Mountain Front and Salt Structures in the Northern Paradox Basin, SE Utah. In: *The Paradox Basin Revisited: New Developments in Petroleum Systems and Basin Analysis* (Eds W.S. Houston, L.L. Wray and P.G. Moreland). *Rocky Mountain Association of Geologists Spec. Publ.*, 132-177.

**Trudgill, B. D**. (2011). Evolution of salt structures in the northern Paradox Basin: controls on evaporite deposition, salt wall growth and supra-salt stratigraphic architecture. *Basin Research*, **23**, 208-238.

**Trudgill, B., Banbury, N., Underhill, J.** (2004) Salt-evolution as a control on structural and stratigraphic systems: northern Paradox foreland basin, SE Utah, USA. In: *Salt-Sediment Interactions and Hydrocarbon Prospectively: Concepts, Applications and Case Studies for the 21st Century. Gulf Coast State Society of Economic Paleontologists and Mineralogists Foundation, 24th Bob F. Perkins Research Conference Procedings* (CD-ROM) (Ed. by P.J. Post) pp. 132-177. Gulf Coast Section SEPM Foundation, Huston, Texas.

**Trusheim, F.** (1960) Mechanisms of salt migration in northern Germany. *Am. Assoc. Petrol. Geol. Bull.* **9**, 1519-1540

**Tunbridge, I.P.** (1981a) Old Red Sandstone Sedimentation – An example from the Brownstones (highest Lower Old Red Sandstone) of South Central Wales. *Geol. J., **16**, 111-124.*

**Tunbridge, I.P.** (1981b) Sandy high-energy flood sedimentation – some criteria for recognition, with an example from the Devonian of SW England. *Sediment. Geol.* **28**, 79-95.

**Vendeville, B.C. & Jackson, M.P.A.** (1992a) The fall of diapirs during thin-skinned extension. *Mar. Petrol. Geol*., **9**, 354-371.

**Vendeville, B.C. & Jackson, M.P.A.** (1992b) The rise of diapirs during thin-skinned extension. *Mar. Petrol. Geol.*, **9**, 331- 353

**Venus, J.H.** (2013) Tectono-stratigraphic evolution of fluvial and aeolian systems in a salt mini-basin province during changing climatic conditions: Permian Undiferentiated Cutler Group, South East Utah, USA. Unpublished *PhD Thesis,* University of Leeds*.*

**Venus, J.H., Mountney, N.P., & McCaffrey, W.D.** (2014) Synsedimentary salt diapirism as a control on fluvial system evolution: an example from the Permian Cutler Group, SE Utah, U.S.A. *Basin Research.* DOI: 10.1111/bre.12066.

**Volozh, Y.A., Volchegurskii L.F., Groshev V.G., Yu.Shishkina T.** (1997) Types of salt structures in the Peri-Caspiandepression. *Geotectonics*, **31**, 204–217.

**Volozh, Y., Talbot, C., Ismaili-Zadeh, A.** (2003) Salt structures and hydrocarbons in the Pricaspian basin. *Am. Assoc. Petrol. Geol. Bull.*, **87**, 313-334.

**Waldron, J.W.F., Rygel, M.C.** (2010). Evaporite tectonics, transpression and transtension in the development of the Maritimes Basin, Atlantic Canada. *Salt Tectonics, Sediments and Prospectivity*, GSP-SEPM Conference Abstract, 20-22 January 2010, 16.

**Waltham, D.** (1997) Why does salt start to move? *Tectonophysics*, **282**, 117-128.

**Ward, L.F.** (1901) Geology of Little Colorado Valley. *Am. J. Sci.*, **12**, 401-413.

**Weismann, G.S. Hartley, A.J. Nichols G.J., Scuderi, L.A., Davidson, S.K., Owen, A.** (2011) Predicted progradational signatures of distributive fluvial systems (DFS). *Am. Geophys. Union*, #EP21B-0702.

**Weissmann, G.S., Hartley, A.J., Nichols, G.J., Scuderi, L.A., Olson, M.E., Buehler,H.A., Massengill, L.C.** (2011). Alluvial facies distributions in continental sedimentary basins—distributive fluvial systems. *In* Davidson, S.K., Leleu, S., and North, C.P. (eds.), The Preservation of Fluvial Sediments and Their Subsequent Interpretation: SEPM, Special Publication, **97**, 327–355.

**Werner, W.G.,** (1974). Petrology of Culter Formation (Pennsylvanian-Permian) near Gateway, Colorado, and Fisher Towers, Utah. *Journal of Sedimentary Petrology*, **44**, 292-298.

**Williams G.E.** (1970) The Central Australian Stream Floods of February-March 1967. *J. Hydrol.* **11**, 185-200.

**Williams G.E.** (1971) Flood deposits of the Sand Bed Ephemeral Streams of central Australia. *Sedimentology*, **17**, 1-40.

**Williams, M.R.** (1996) Stratigraphy of Upper Pennsylvanian Cyclical Carbonate and Siliciclastic Rocks, Western Paradox Basin, Utah. In: *Paleozoic systems of the Rocky Mountain Region* (Ed. by M.W. Longman & M.D. Sonnenfield) Rocky Mountain Section, SEPM, 283-304.

**Williams, M.R.** (2009) Stratigraphy of Upper Pennsylvanian cyclic carbonate and siliciclastic rocks, western Paradox Basin, Utah. In: *The Paradox Basin Revisited – New Developments in Petroleum Systems and Basin Analysis* (Ed. by W.S. Houston, L.L. Wray, & P.G. Moreland), pp. 381-435, Rocky Mountain Association of Geologists, Denver, CO.

**Williams, P. F., Rust, B. R.** (1969). The sedimentology of a braided river. Journal of Sedimentary Research, **39**, 649-679.

**Williams-Stroud, S.** (1994) The evolution of an inland sea of marine origin to a non-marine saline lake: the Pennsylvanian Paradox salt. In: *Sedimentology and Geochemistry of Modern and Ancient Saline Lakes* (Ed by R.W. Renaut & W.M. Last*), S*EPM Spec. Publ., **50**, 293-306.

**Wu, S., Bally, A.W., Cramez, C.** (1990) Allochthonous salt, structure and stratigraphy of the north-eastern Gulf of Mexico. Part II: Structure. *Mar. Petrol. Geol.,* **7**, 334-370.

**Ziegler, P.A.,** (1975). Geologic Evolution of the North Sea and its Tectonic Framework. *Am. Assoc. Petrol. Geol. Bull.* **59**, 1073-1097.

# 8.0 Appendices

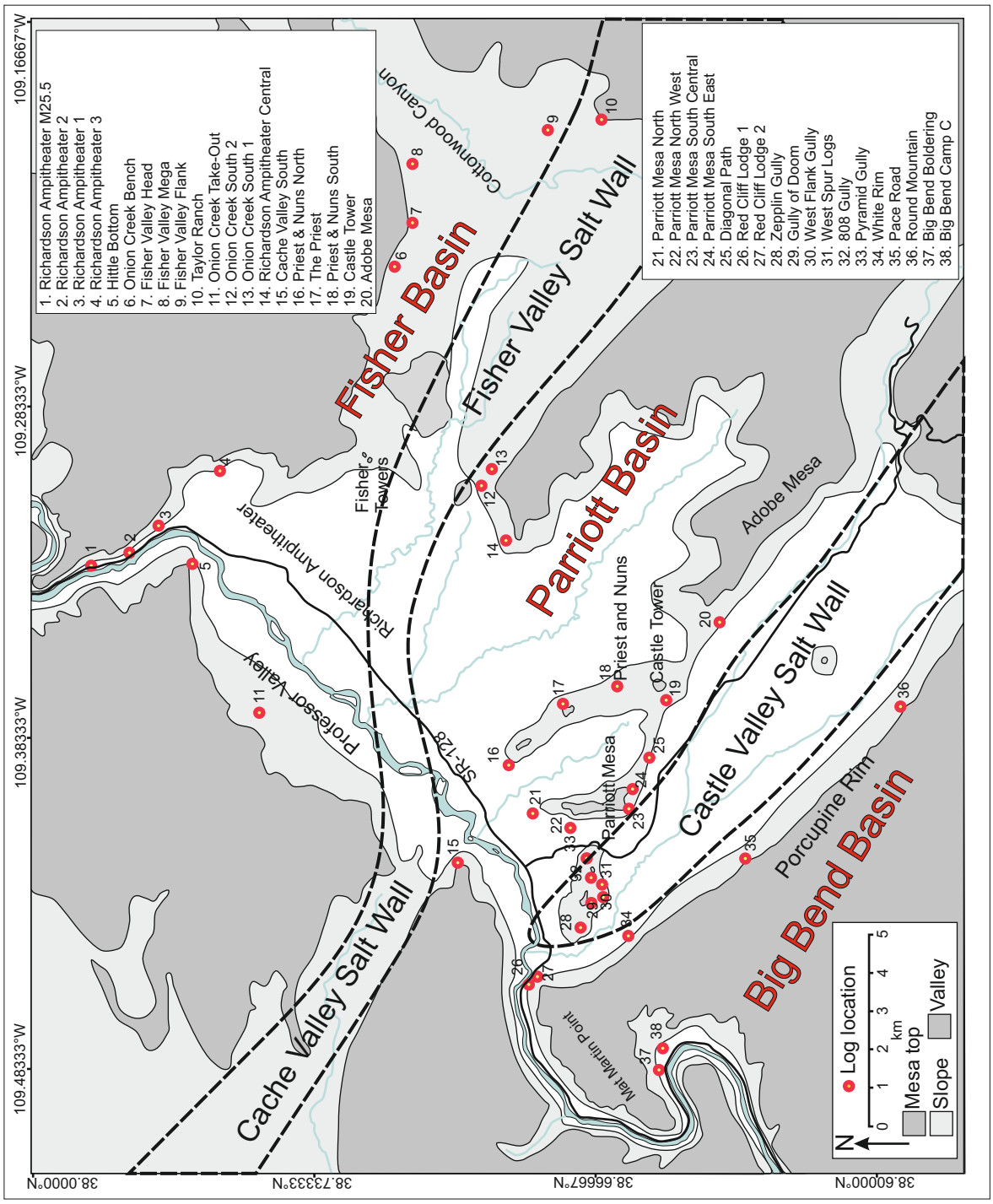


Overview location maps. Salt Anticline Region study area map depicting the location of salt walls and mini-basins in relation to the present-day topography. Map centre: 38.70°N, 109.324°W, geodesic system: WGS 84

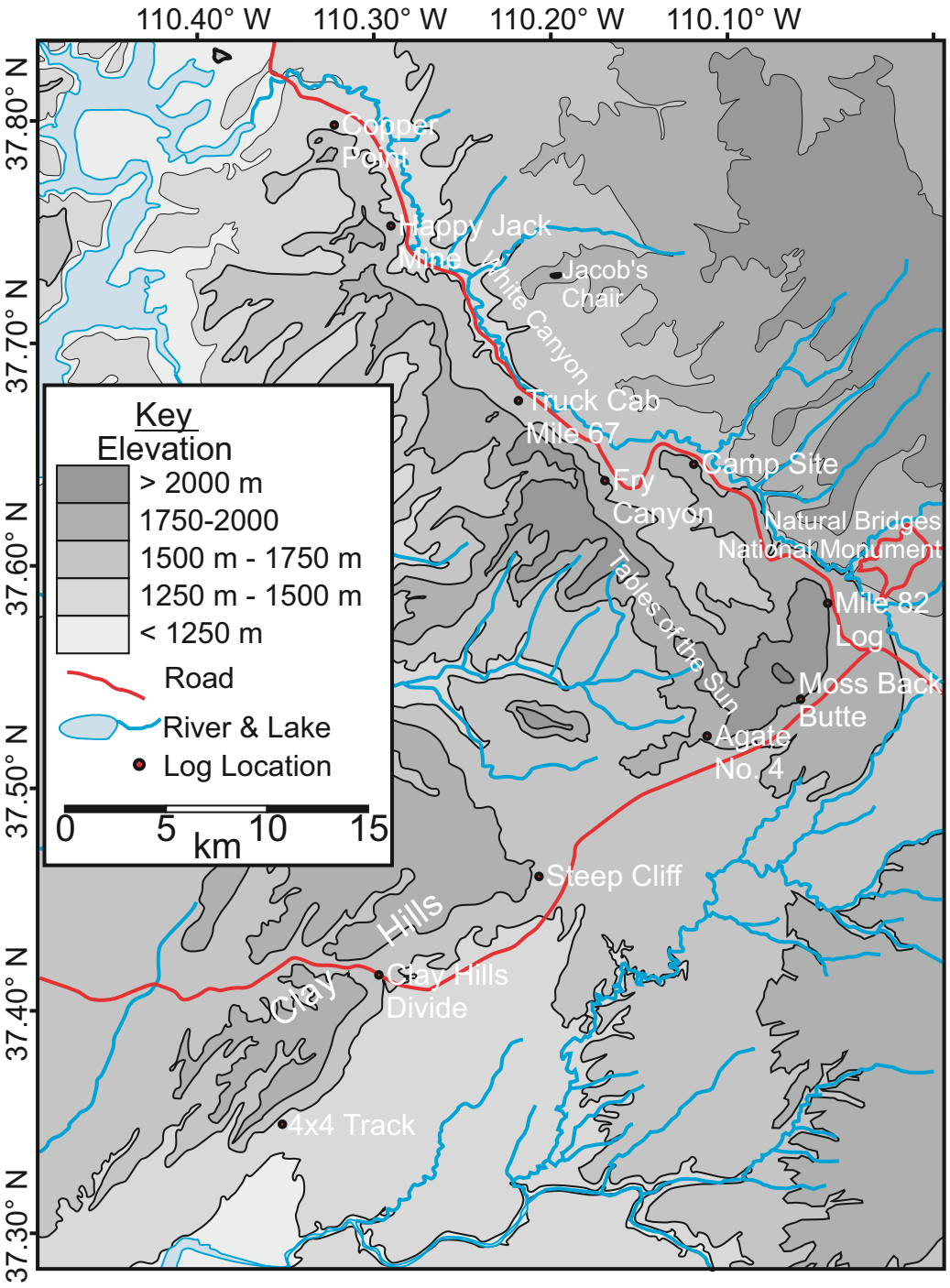


Overview location maps. White Canyon Region study area map. Map centre 37.566°N, 110.233°W, geodesic system: WGS 84. The location of measured vertical log profiles is indicated.

## Key

Massive sandstone (Fm)

Deformed bedding (Fd)

Horizontally laminated sandstone (Fh)

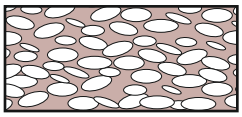

Gypsum-clast bearing horizons (FGm, FGc)

Cross-bedded sandstone (Fxt, Fxp)

Interbedded Heterolithic strata, sand-prone (FHiss)

Ripple-laminated sandstone (Frc, Fxl, Frw)

Interbedded Heterolithic strata, silt-prone (FHiss)

# Castleton Tower Log: 1 of 2

**Log Thickness:** ~220 m

**Coordinates:**
12S 641636 / 4278982

**Elevation:** 1581m

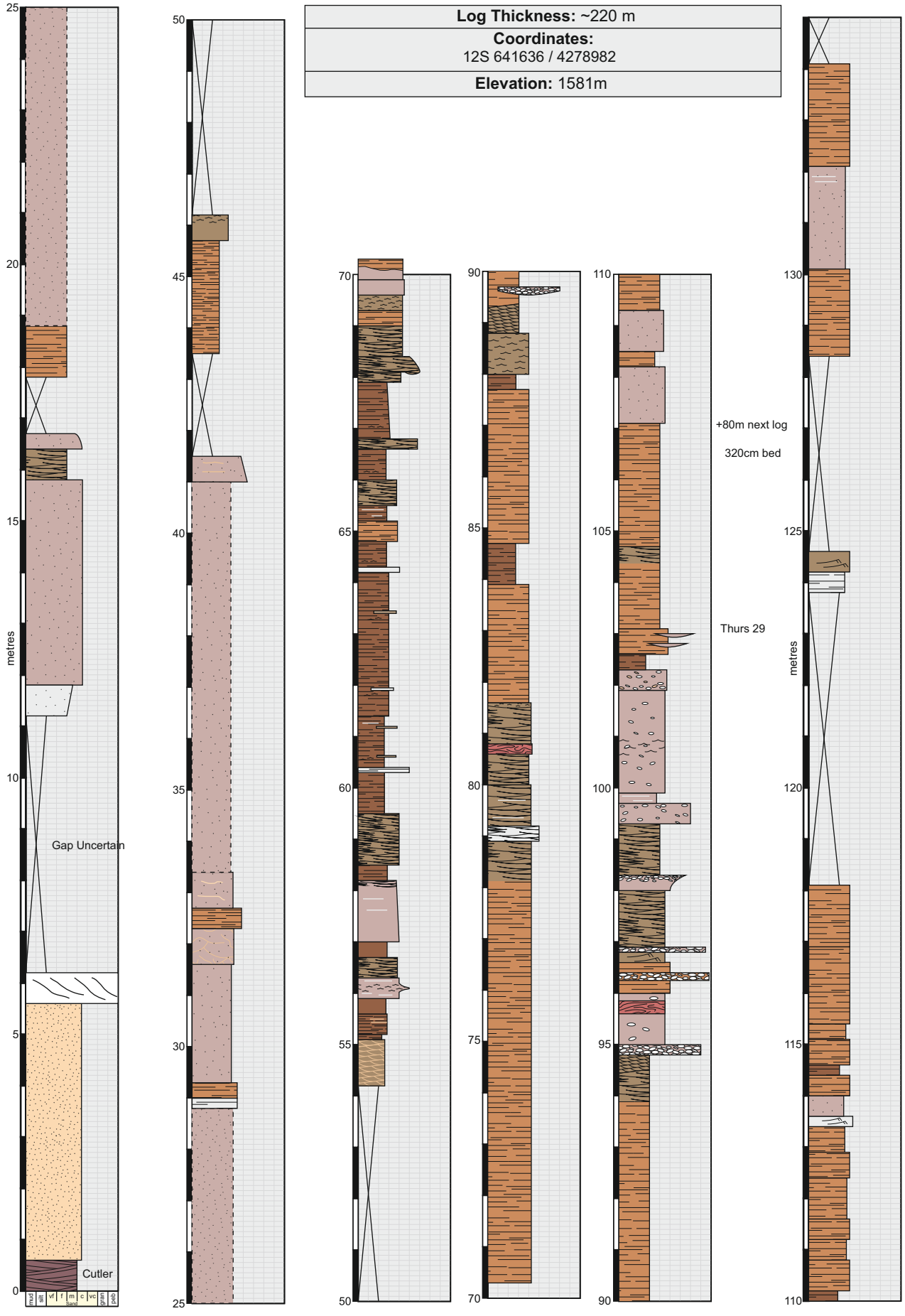

# Castleton Tower Log: 2 of 2

**Log Thickness:** ~220 m

**Coordinates:**
12S 641636 / 4278982

**Elevation:** 1581m

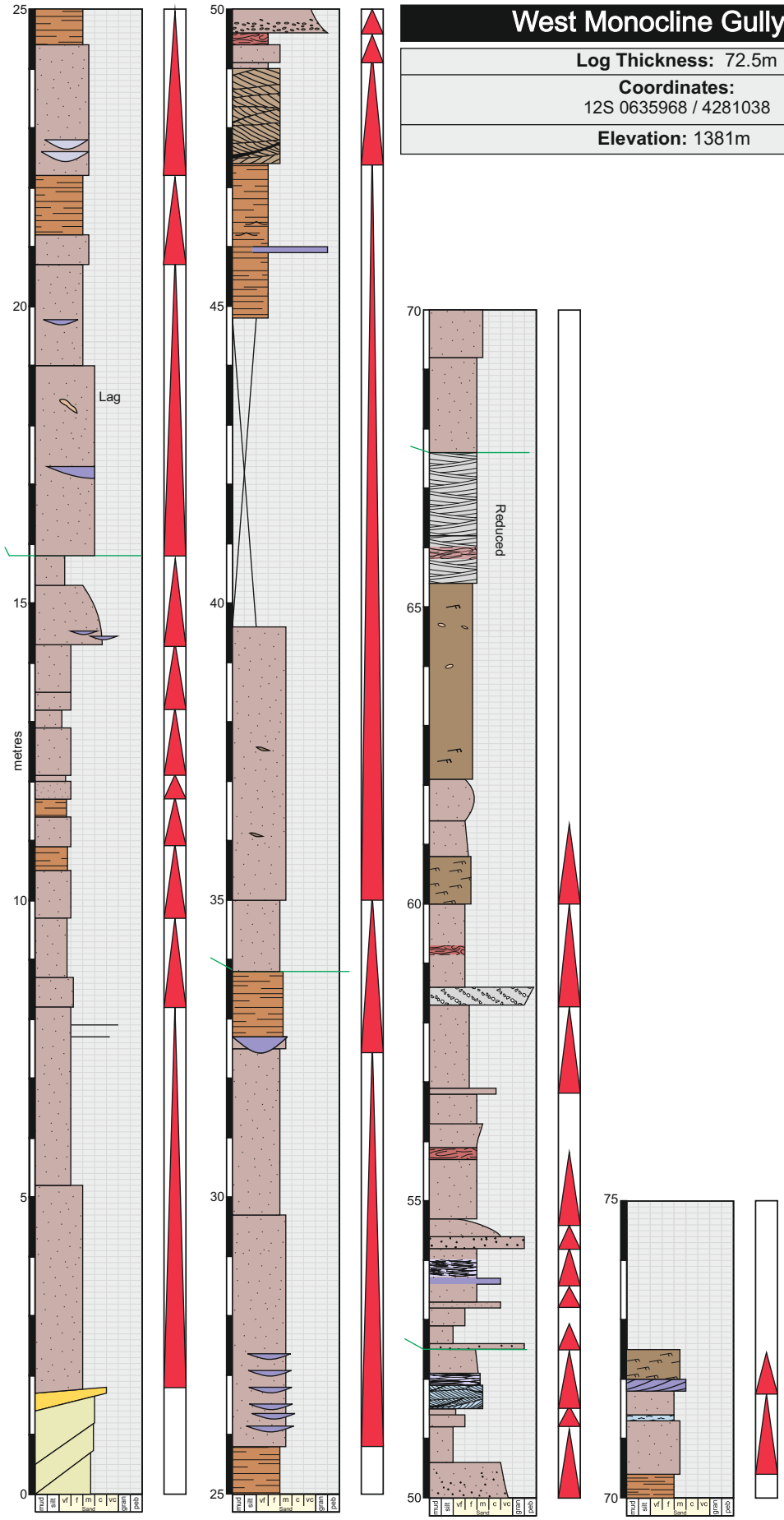
West Monocline Gully Log
Log Thickness: 72.5m
Coordinates:
12S 0635968 / 4281038
Elevation: 1381m
metres
Lag
Reduced
mud
silt
vf
f
m
c
vc
gran
peb
Sand

# Parriott Mesa SE Log: 1 of 2

**Log Thickness:** ~220 m

**Coordinates:**
12S 639295 / 4279722

**Elevation:** 1475 m

# Parriott Mesa SE Log: 2 of 2

| |
|---|
| **Log Thickness:** ~220 m |
| **Coordinates:** 12S 639295 / 4279722 |
| **Elevation:** 1475 m |

# Parriott Mesa South Central Log: 2 of 2

| |
|---|
| **Log Thickness:** ~200 m |
| **Coordinates:** 12S 638650 / 4279754 |
| **Elevation:** 1427 m |

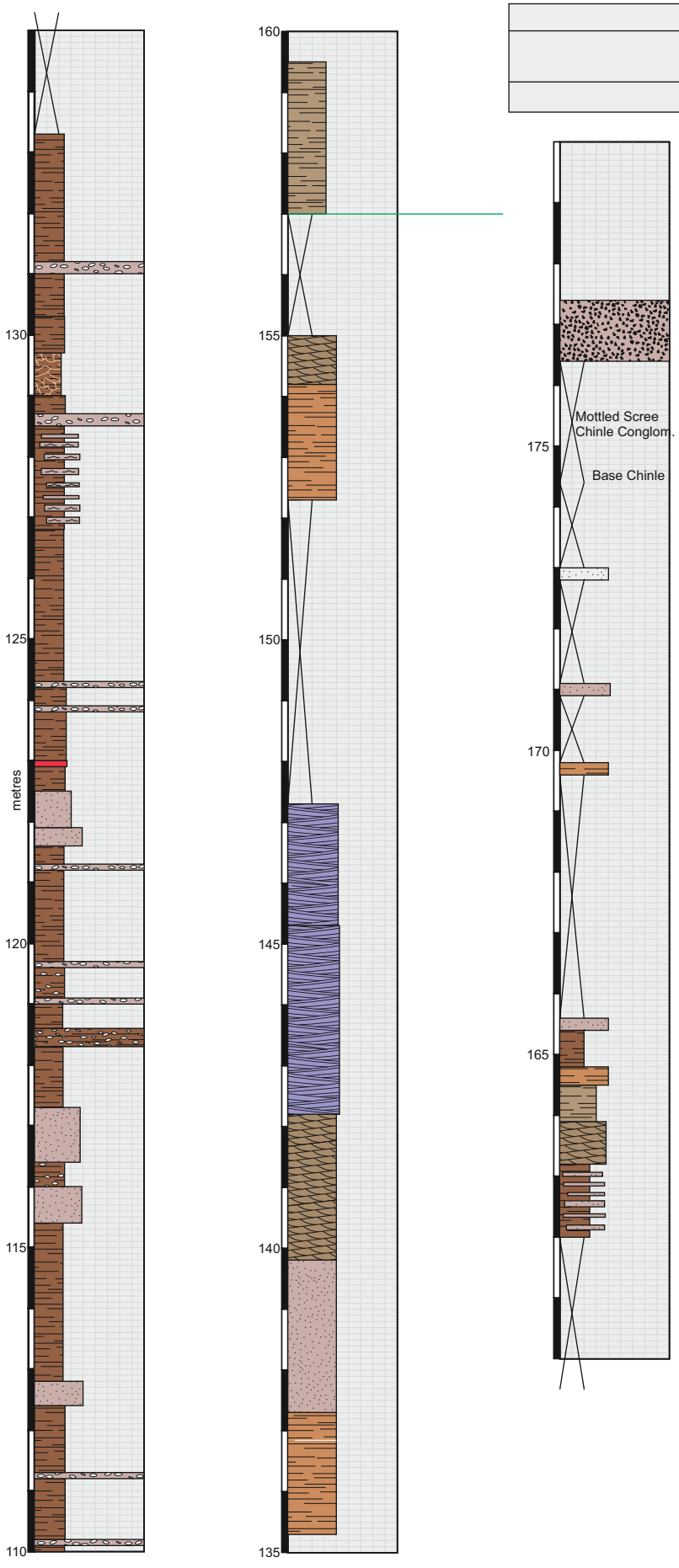

# Parriott Mesa South Central Log: 1 of 2

**Log Thickness:** ~200 m

**Coordinates:**
12S 638650 / 4279754

**Elevation:** 1427 m

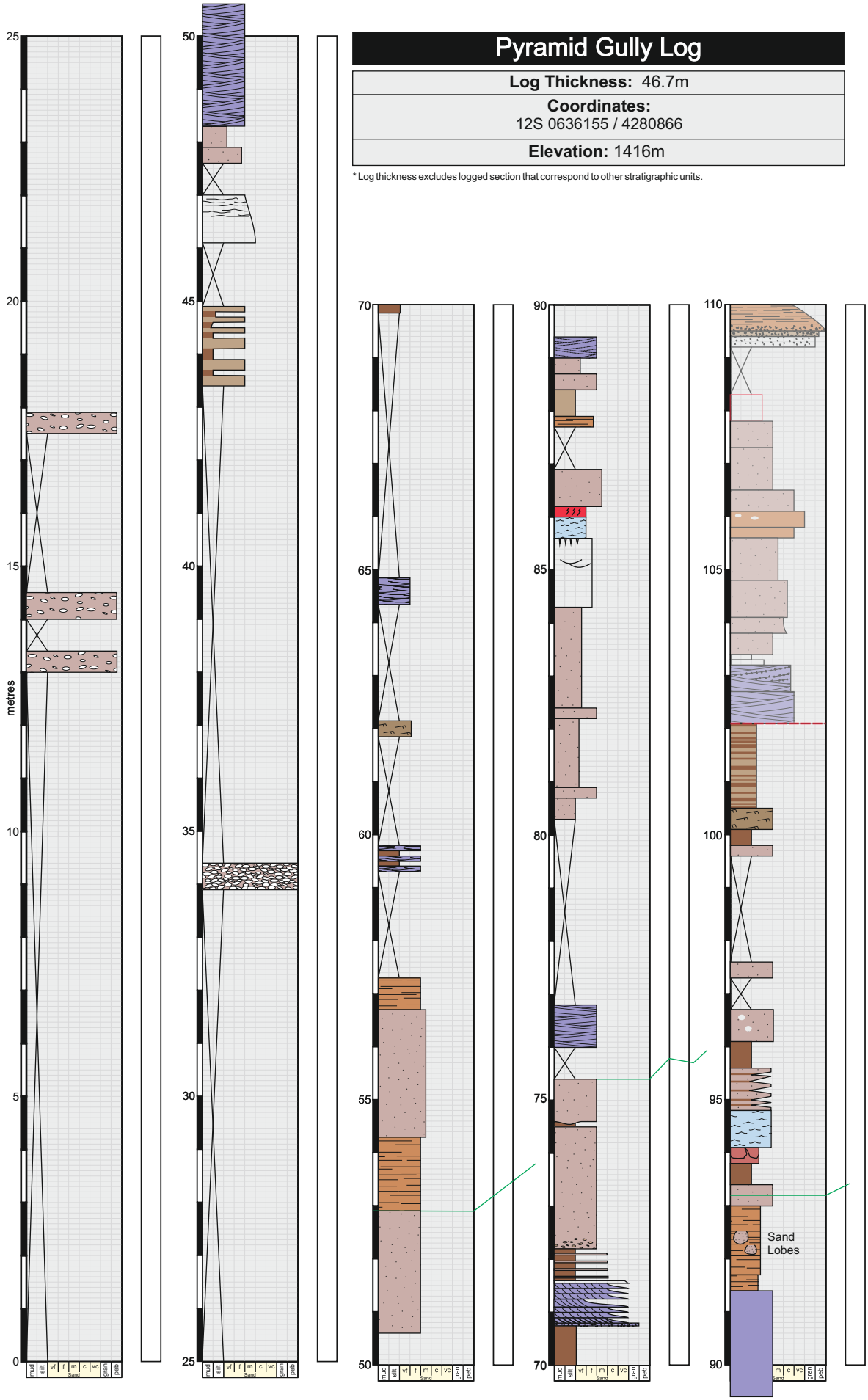
Pyramid Gully Log
Log Thickness: 46.7m
Coordinates:
12S 0636155 / 4280866
Elevation: 1416m
* Log thickness excludes logged section that correspond to other stratigraphic units.
metres
Sand Lobes

# Diagonal Path Log

**Log Thickness: ~70 m**

**Coordinates:**
**12S 640121 / 4279547**

**Elevation: 1491 m**

* Log thickness excludes logged section that correspond to other stratigraphic units.

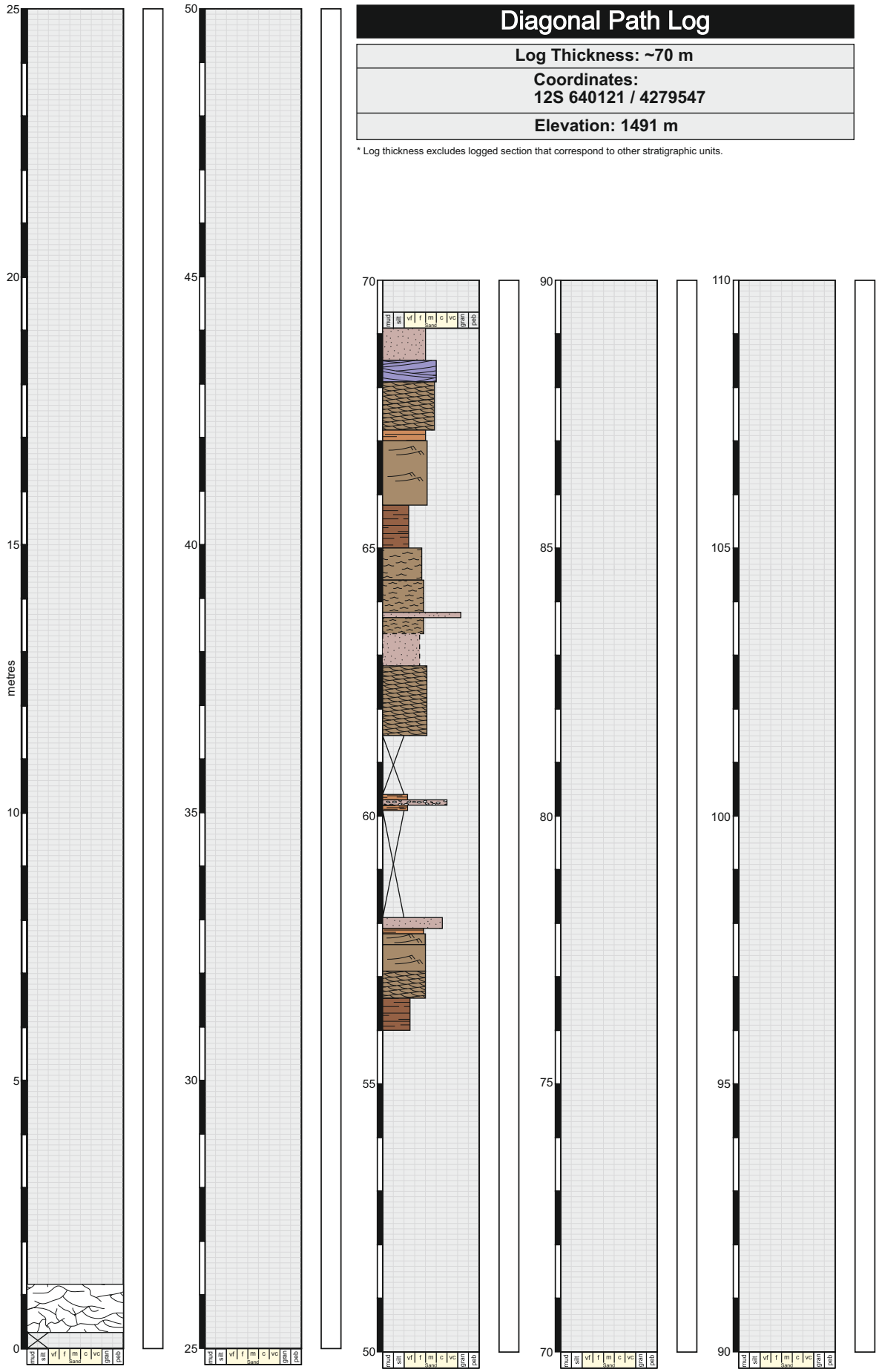

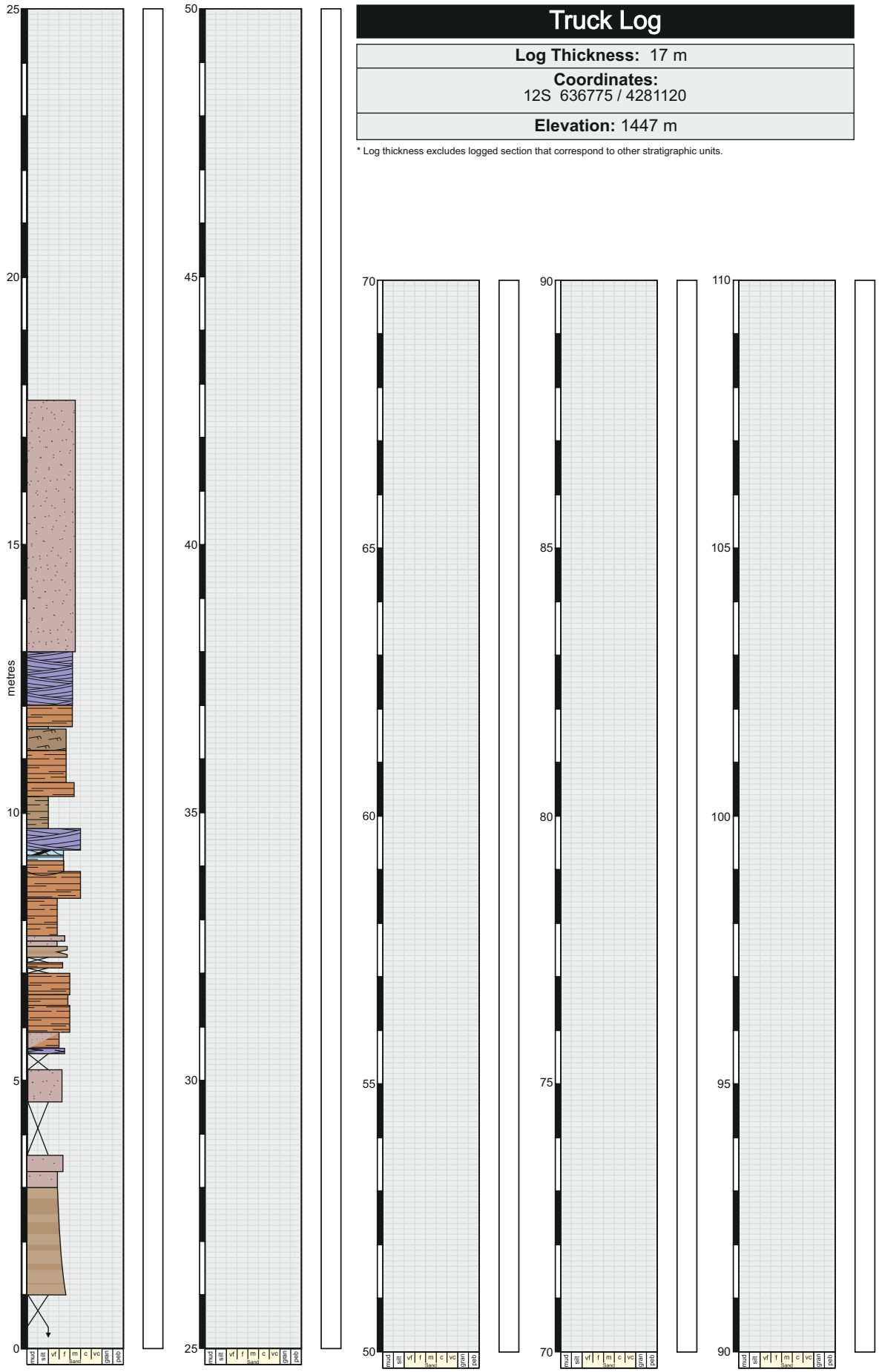


# Truck Log

**Log Thickness:** 17 m

**Coordinates:**
12S 636775 / 4281120

**Elevation:** 1447 m

* Log thickness excludes logged section that correspond to other stratigraphic units.

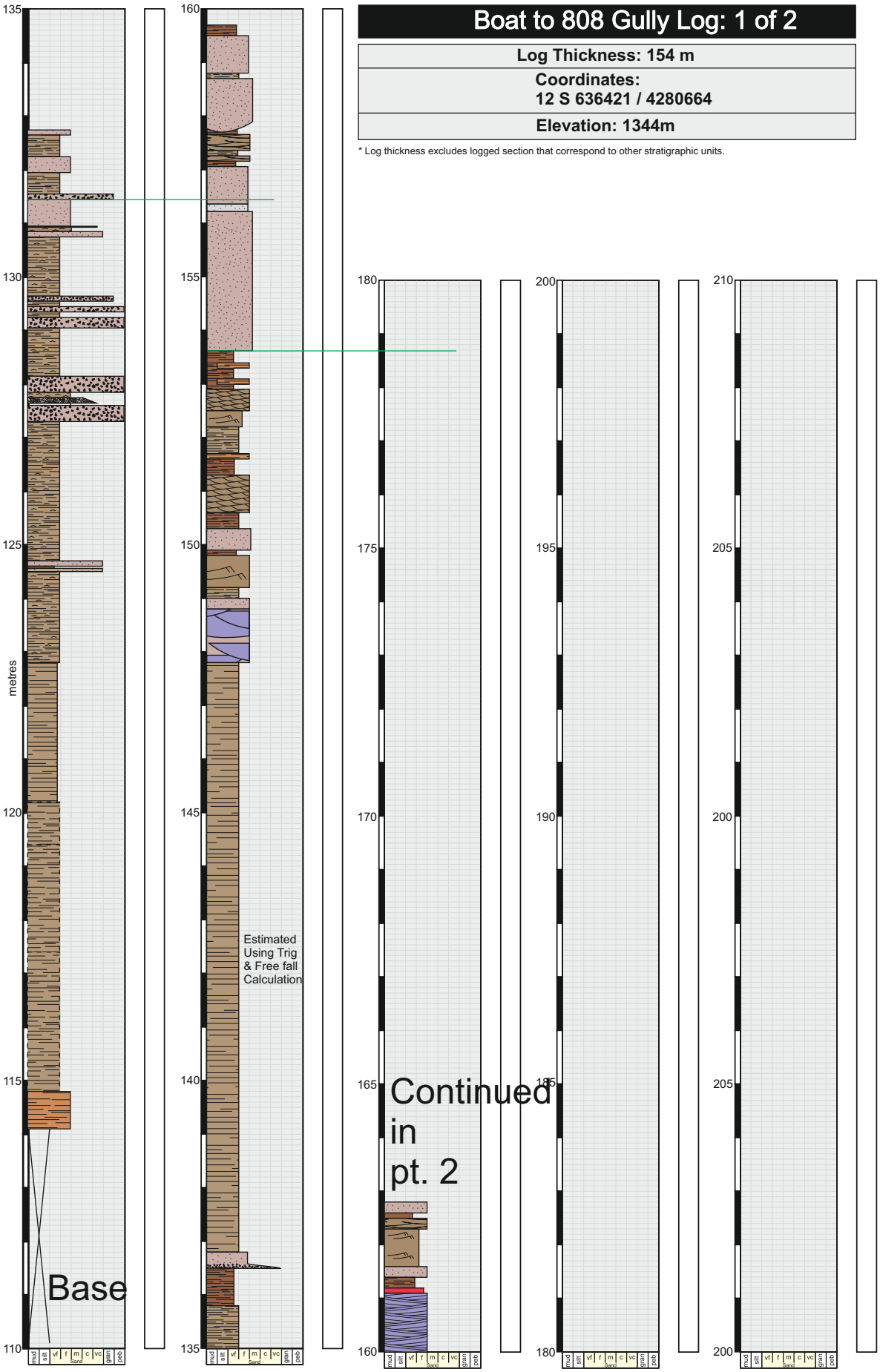
Boat to 808 Gully Log: 1 of 2
Log Thickness: 154 m
Coordinates:
12 S 636421 / 4280664
Elevation: 1344m
* Log thickness excludes logged section that correspond to other stratigraphic units.
metres
Base
Estimated
Using Trig
& Free fall
Calculation
Continued
in
pt. 2
mud
silt
vf
f
m
c
vc
gran
peb
Sand

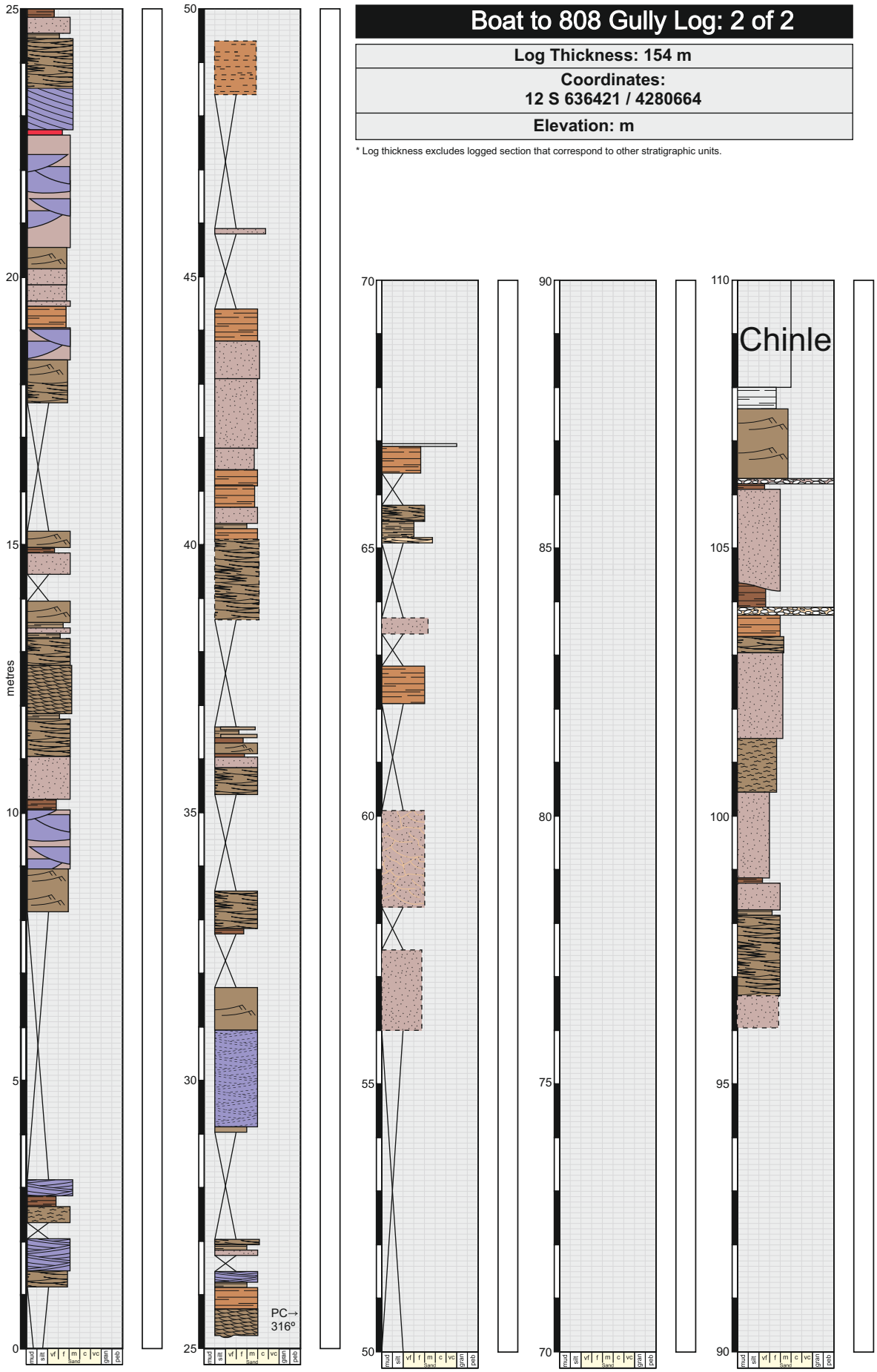
Boat to 808 Gully Log: 2 of 2
Log Thickness: 154 m
Coordinates:
12 S 636421 / 4280664
Elevation: m
* Log thickness excludes logged section that correspond to other stratigraphic units.
metres
PC→
316°
Chinle
mud
silt
vf
f
m
c
vc
gran
peb
Sand

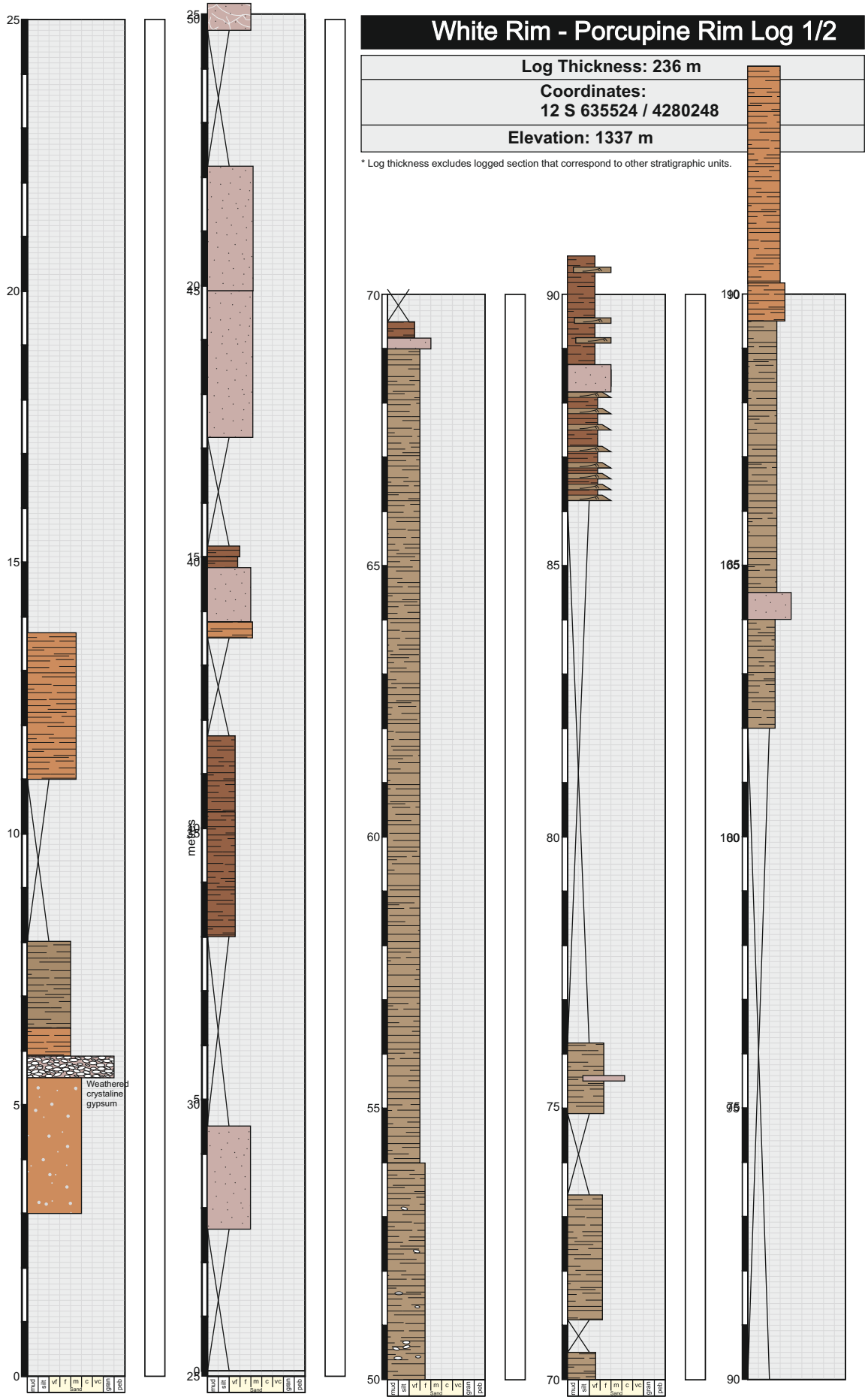
White Rim - Porcupine Rim Log 1/2
Log Thickness: 236 m
Coordinates:
12 S 635524 / 4280248
Elevation: 1337 m
* Log thickness excludes logged section that correspond to other stratigraphic units.
meters
Weathered crystaline gypsum
mud
silt
vf
f
m
c
vc
gran
peb
Sand

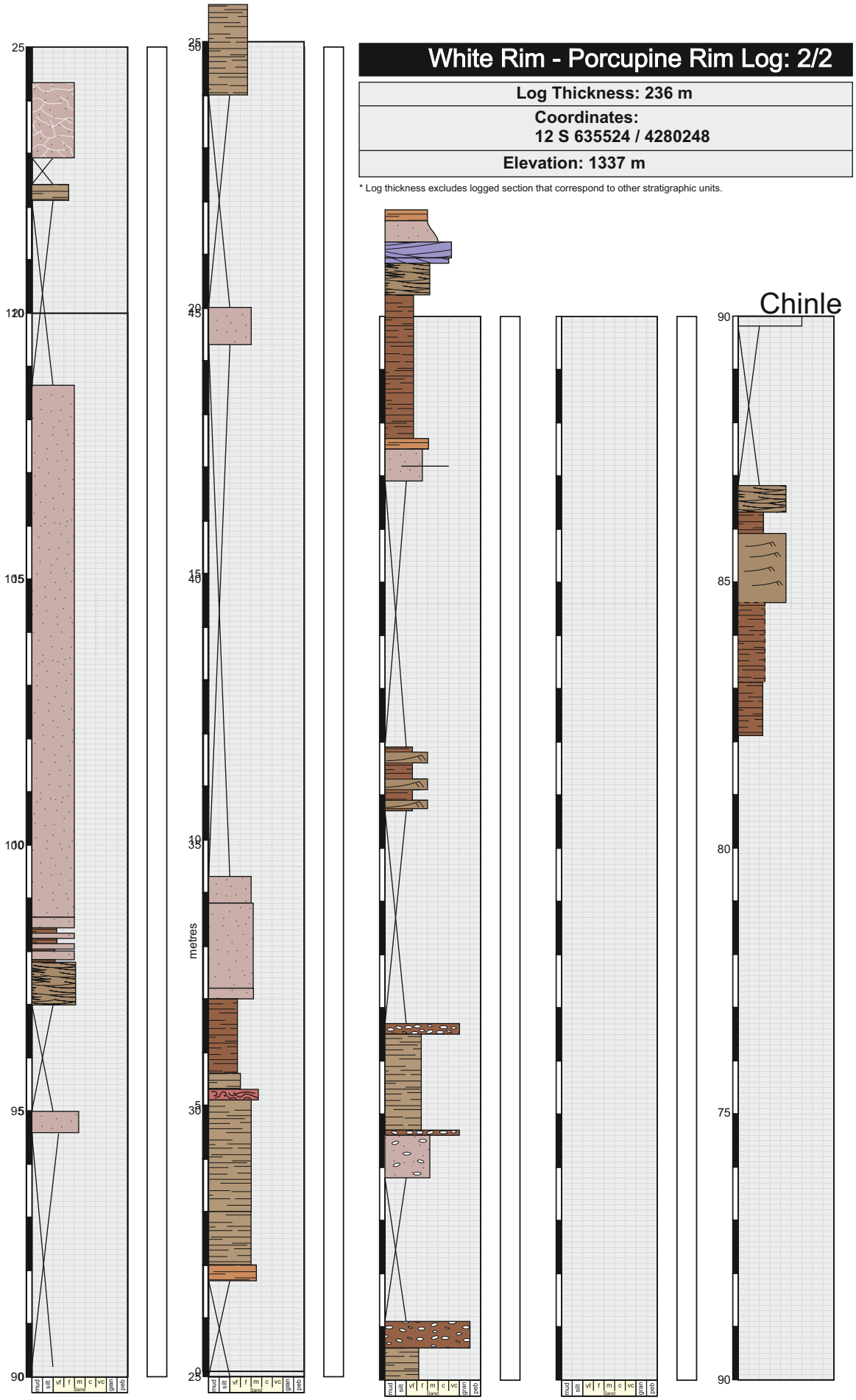
White Rim - Porcupine Rim Log: 2/2
Log Thickness: 236 m
Coordinates:
12 S 635524 / 4280248
Elevation: 1337 m
* Log thickness excludes logged section that correspond to other stratigraphic units.
Chinle
metres
mud
silt
vf
f
m
c
vc
gran
peb
Sand

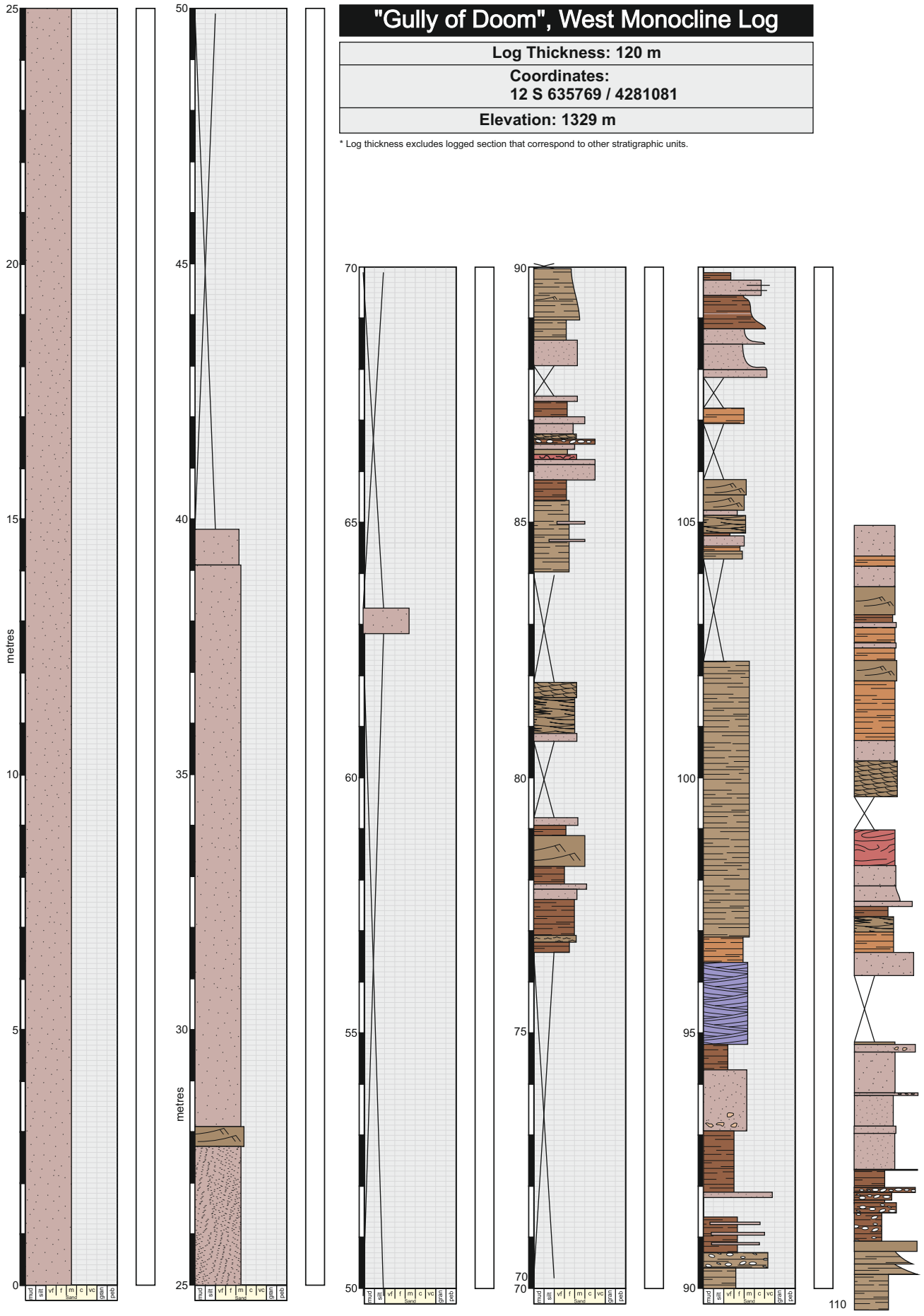
"Gully of Doom", West Monocline Log
Log Thickness: 120 m
Coordinates:
12 S 635769 / 4281081
Elevation: 1329 m
* Log thickness excludes logged section that correspond to other stratigraphic units.
metres
mud
silt
vf
f
m
c
vc
gran
peb
Sand

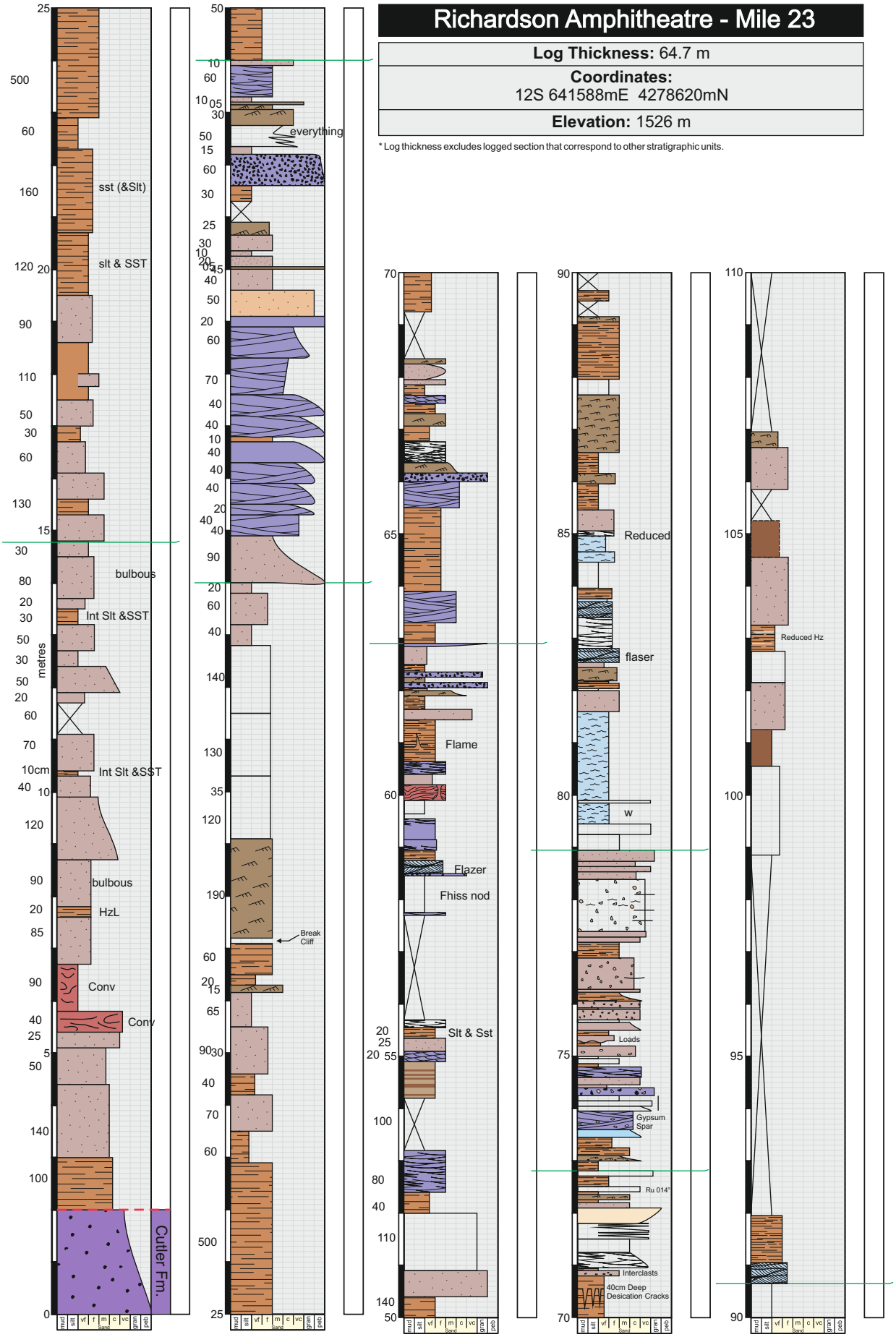
Richardson Amphitheatre - Mile 23
Log Thickness: 64.7 m
Coordinates:
12S 641588mE 4278620mN
Elevation: 1526 m
* Log thickness excludes logged section that correspond to other stratigraphic units.
metres
sst (&Slt)
slt & SST
bulbous
Int Slt &SST
Int Slt &SST
bulbous
HzL
Conv
Conv
Cutter Fm.
everything
Break Cliff
Flame
Flazer
Fhiss nod
Slt & Sst
Reduced
flaser
w
Loads
Gypsum Spar
Ru 014"
Interclasts
40cm Deep Desication Cracks
Reduced Hz
mud
silt
vf
f
m
c
vc
gran
peb
Sand

# Richardson Amphitheatre - Mile 23: 2/2

| |
|---|
| **Log Thickness:** 64.7 m |
| **Coordinates:** 12S 641588mE 4278620mN |
| **Elevation:** 1526 m |

* Log thickness excludes logged section that correspond to other stratigraphic units.

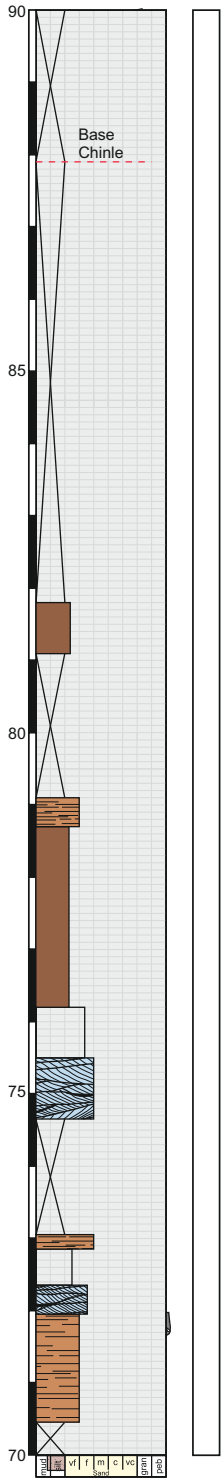

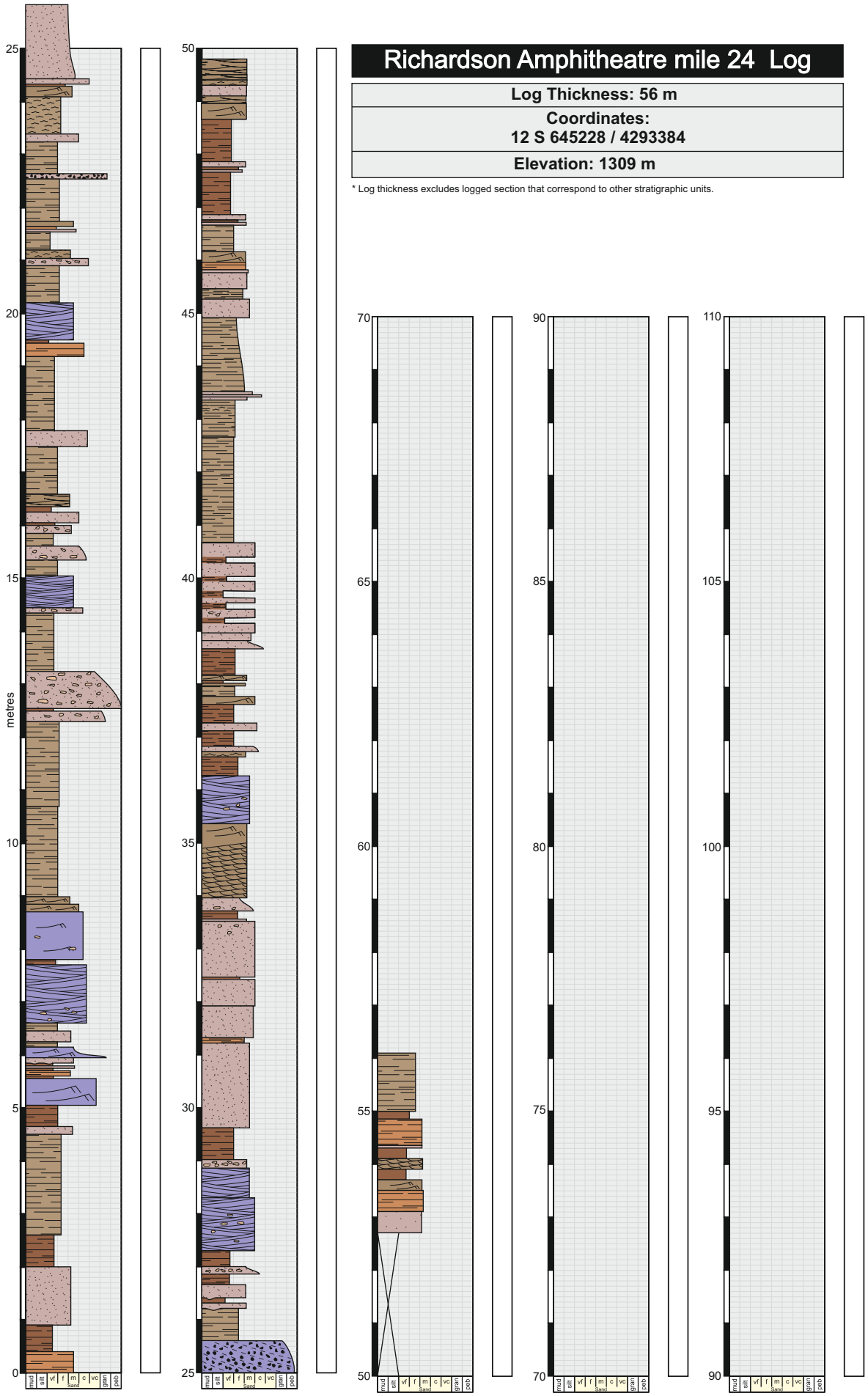


# Richardson Amphitheatre mile 24 Log

**Log Thickness: 56 m**

**Coordinates:**
**12 S 645228 / 4293384**

**Elevation: 1309 m**

* Log thickness excludes logged section that correspond to other stratigraphic units.

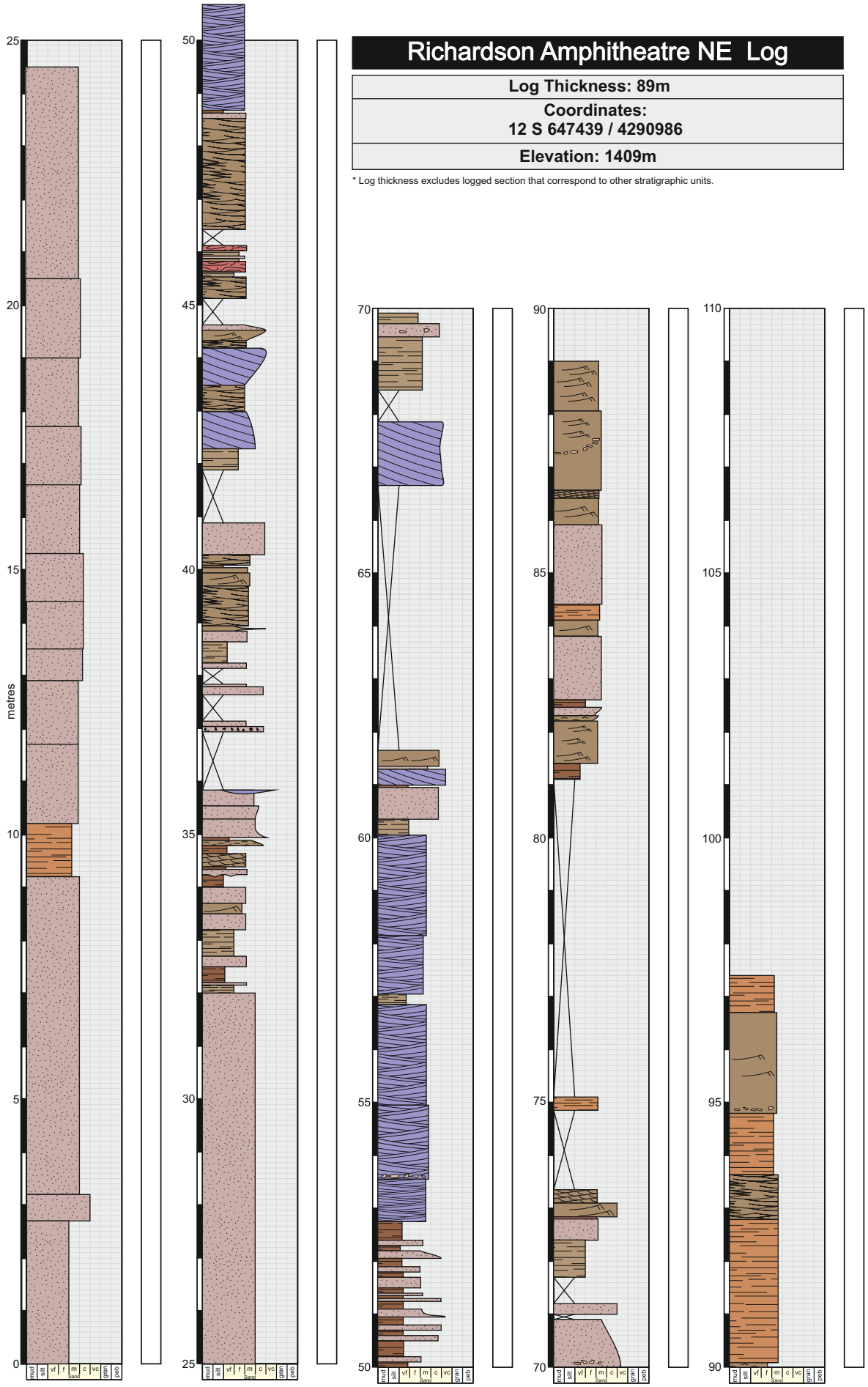
Richardson Amphitheatre NE Log
Log Thickness: 89m
Coordinates:
12 S 647439 / 4290986
Elevation: 1409m
* Log thickness excludes logged section that correspond to other stratigraphic units.
metres
mud
silt
vf
f
m
c
vc
gran
peb
Sand

# Priest and Nuns North Log

**Log Thickness:** ~90 m

**Coordinates:**
12 S 639740 / 4283329

**Elevation:** 1370 m

* Log thickness excludes logged section that correspond to other stratigraphic units.

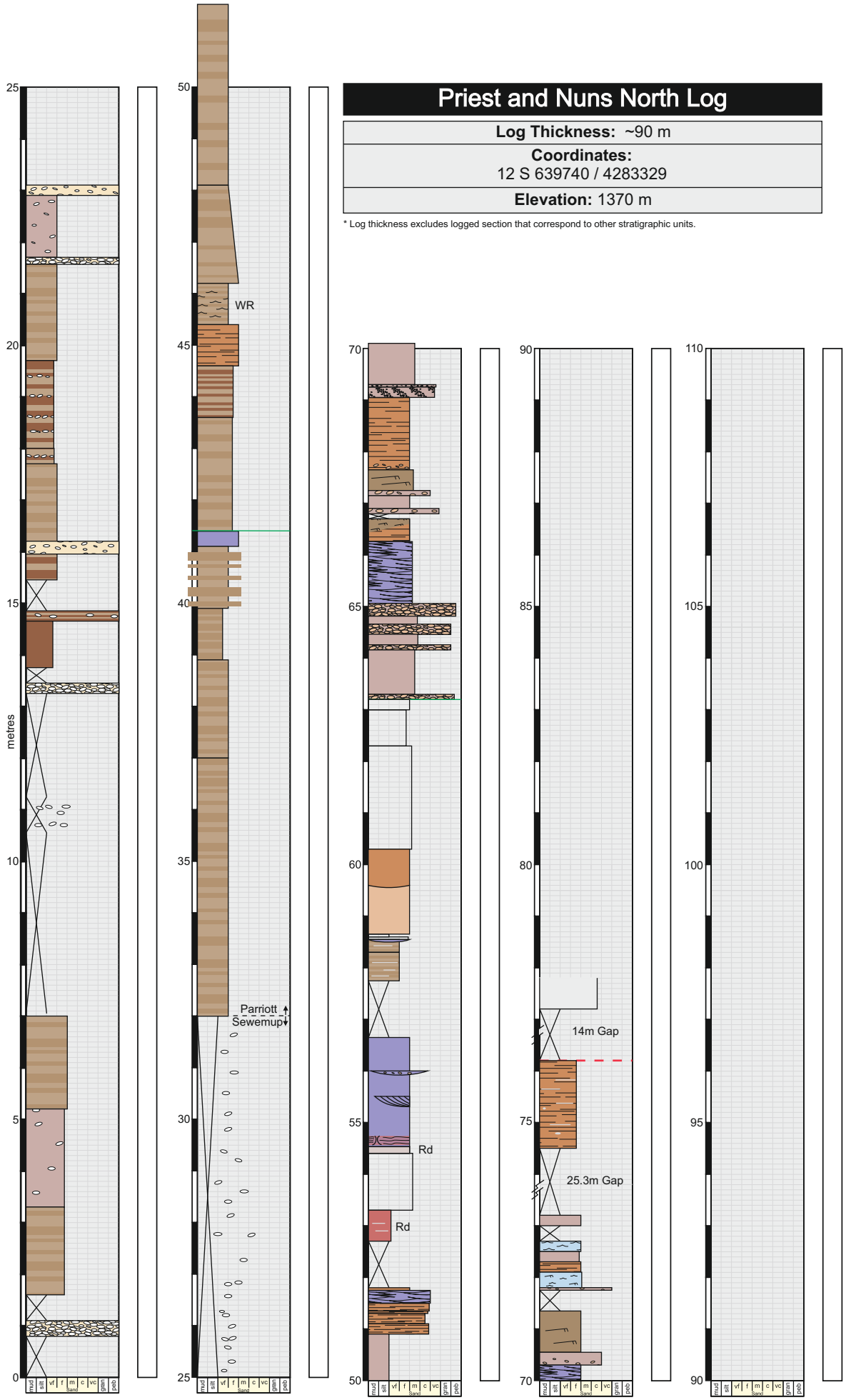

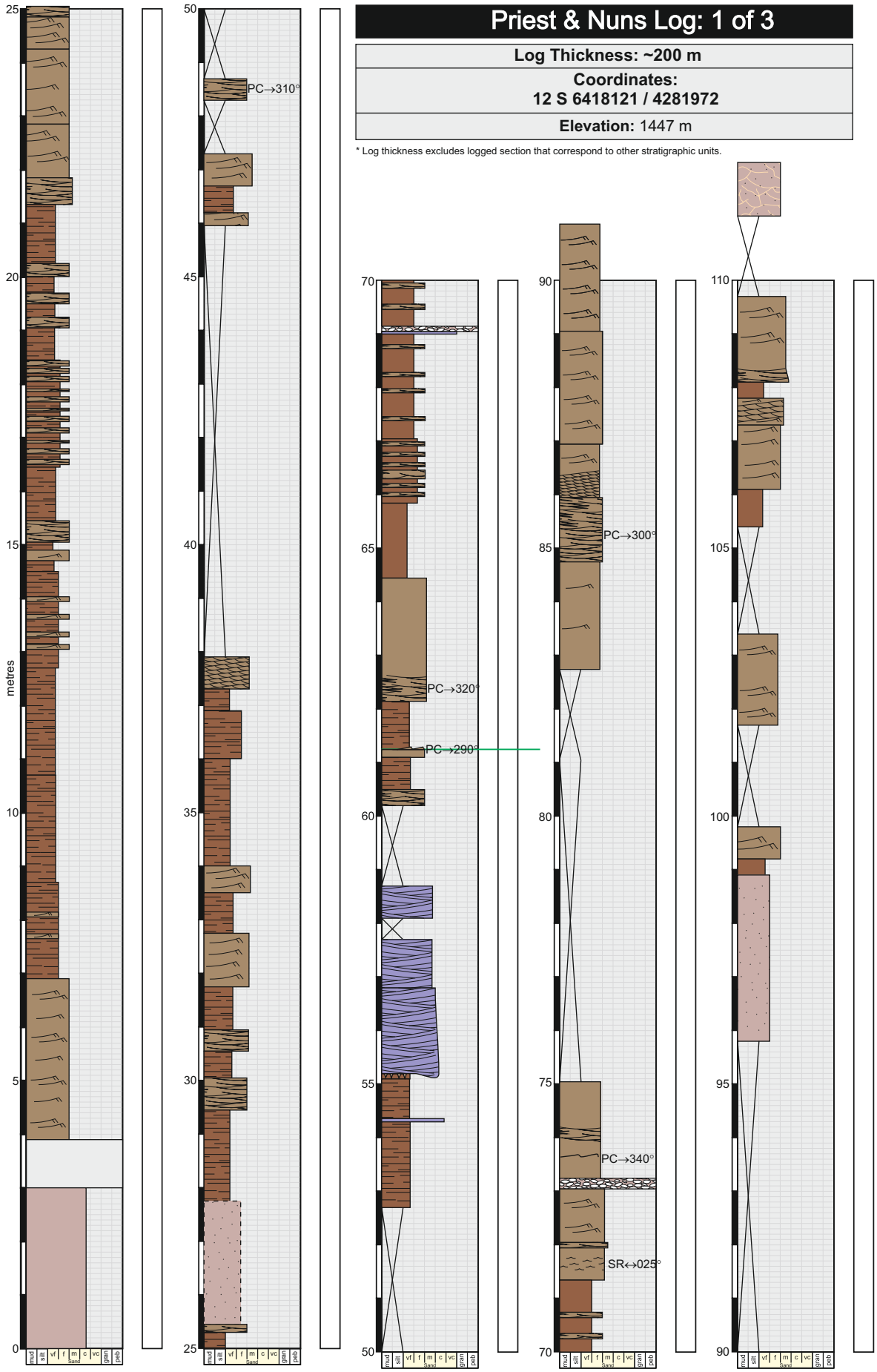
Priest & Nuns Log: 1 of 3
Log Thickness: ~200 m
Coordinates:
12 S 6418121 / 4281972
Elevation: 1447 m
* Log thickness excludes logged section that correspond to other stratigraphic units.
metres
PC→310°
PC→320°
PC→290°
PC→300°
PC→340°
SR↔025°
mud
silt
vf
f
m
c
vc
gran
peb
Sand

Priest & Nuns: 2 of 3
Log Thickness: ~200 m
Coordinates:
12 S 6418121 / 4281972
Elevation: 1447 m
* Log thickness excludes logged section that correspond to other stratigraphic units.
metres
PC→320°
PC→290°
PC→340°
SR↔025°
PC→300°
mud
silt
vf
f
m
c
vc
gran
peb
Sand

Priest & Nuns: 3 of 3
Log Thickness: ~200 m
Coordinates:
12 S 6418121 / 4281972
Elevation: 1447 m
* Log thickness excludes logged section that correspond to other stratigraphic units.
metres
mud
silt
vf
f
m
c
vc
gran
peb
Sand
Mottled
Scree

# The Priest 1 of 2

**Log Thickness: 182 m**

**Coordinates:**
**12 S 642149 / 4280564**

**Elevation: 1573 m**

* Log thickness excludes logged section that correspond to other stratigraphic units.

# The Priest 2 of 2

**Log Thickness: 182 m**

**Coordinates:**
**12 S 642149 / 4280564**

**Elevation: 1573 m**

* Log thickness excludes logged section that correspond to other stratigraphic units.

# Onion Creek south 2 (nr. Fault Block) 1of2

**Thickness: ~130 m**

**Coordinates:**
**12 S 647158 / 4284243**

**Elevation: 1742 m**

* Log thickness excludes logged section that correspond to other stratigraphic units.

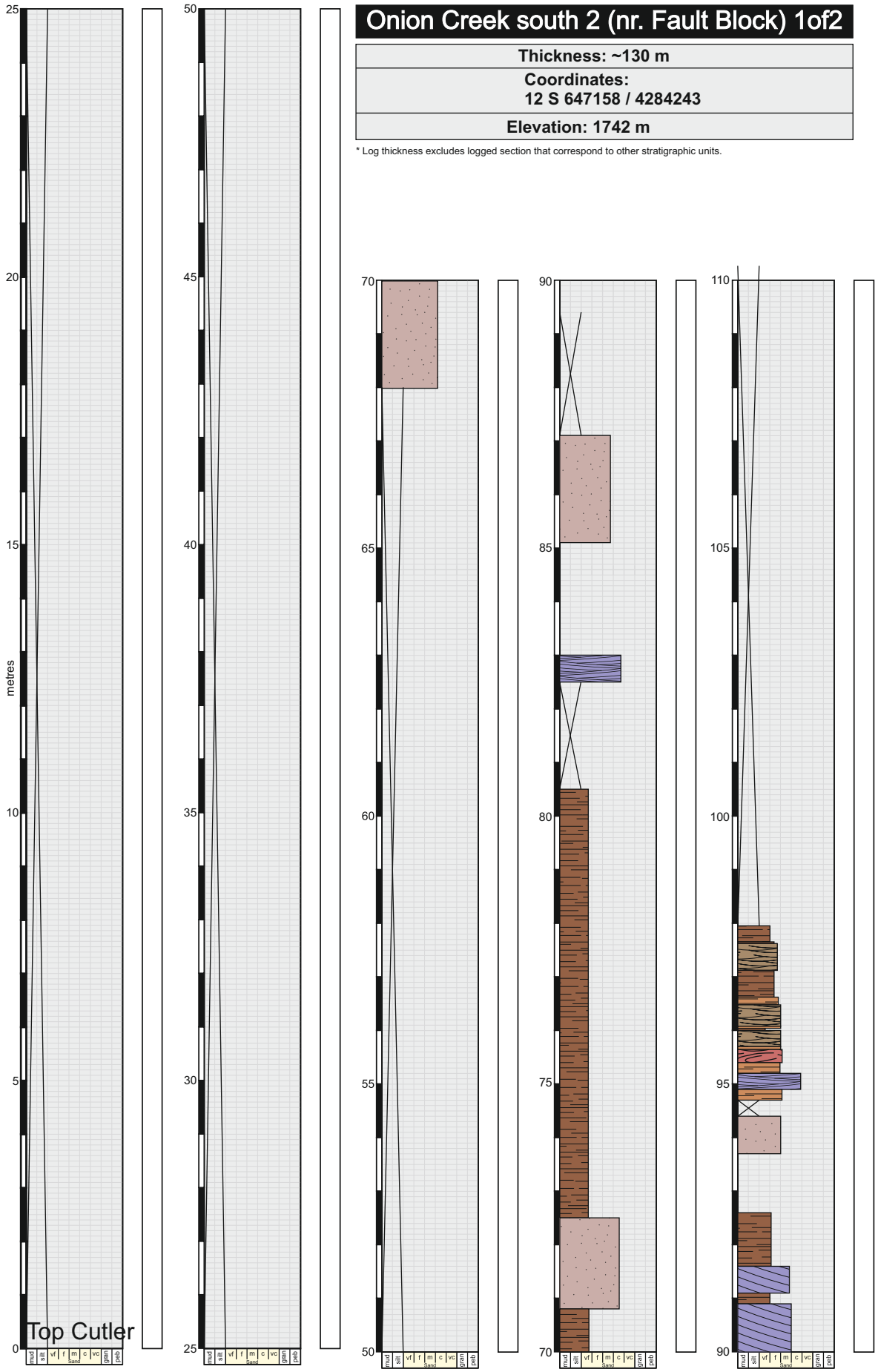

# Onion Creek south 2 (nr. Fault Block) 2of2

**Thickness: ~130 m**

**Coordinates:**
**12 S 647158 / 4284243**

**Elevation: 1742 m**

* Log thickness excludes logged section that correspond to other stratigraphic units.

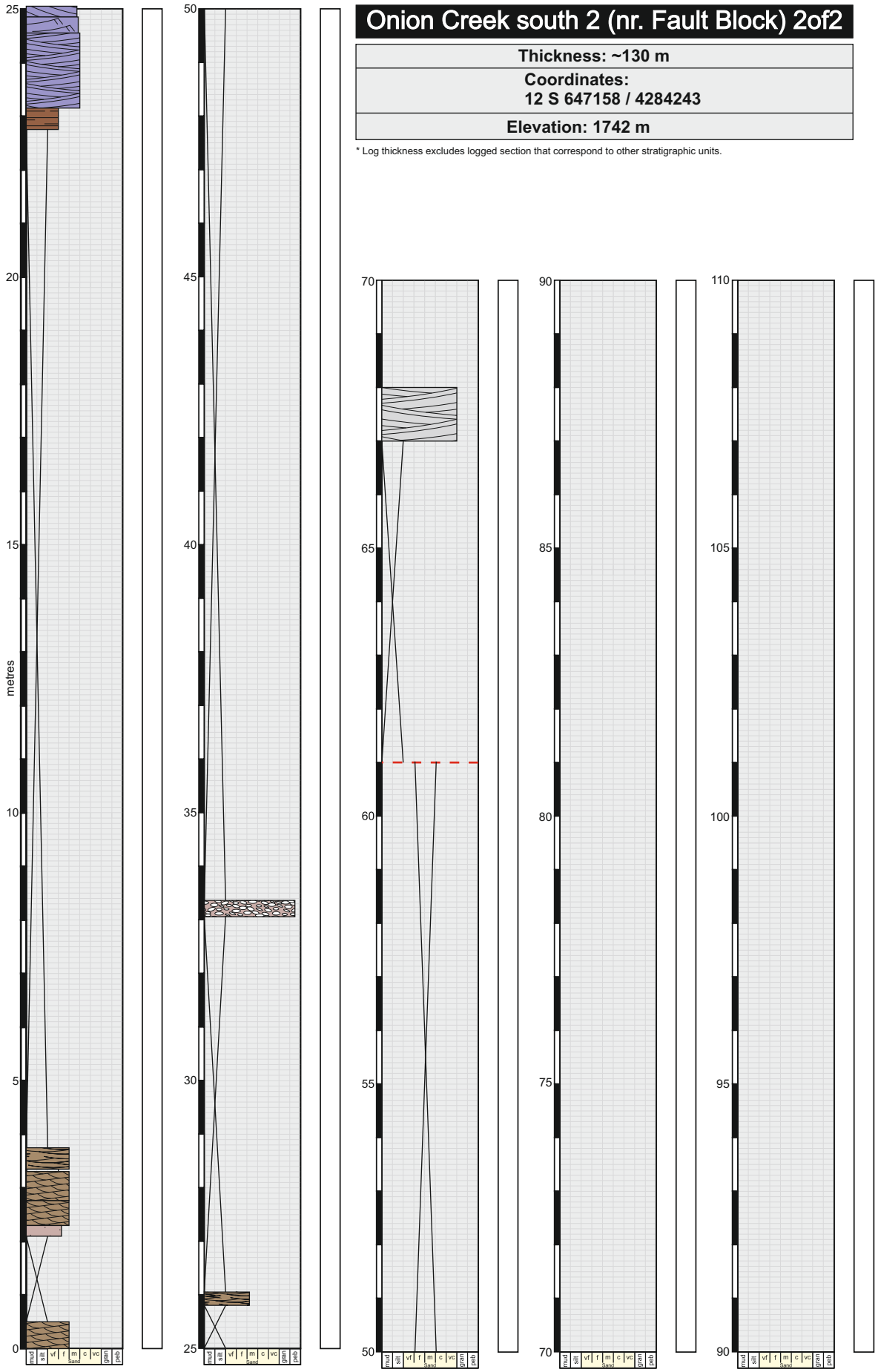

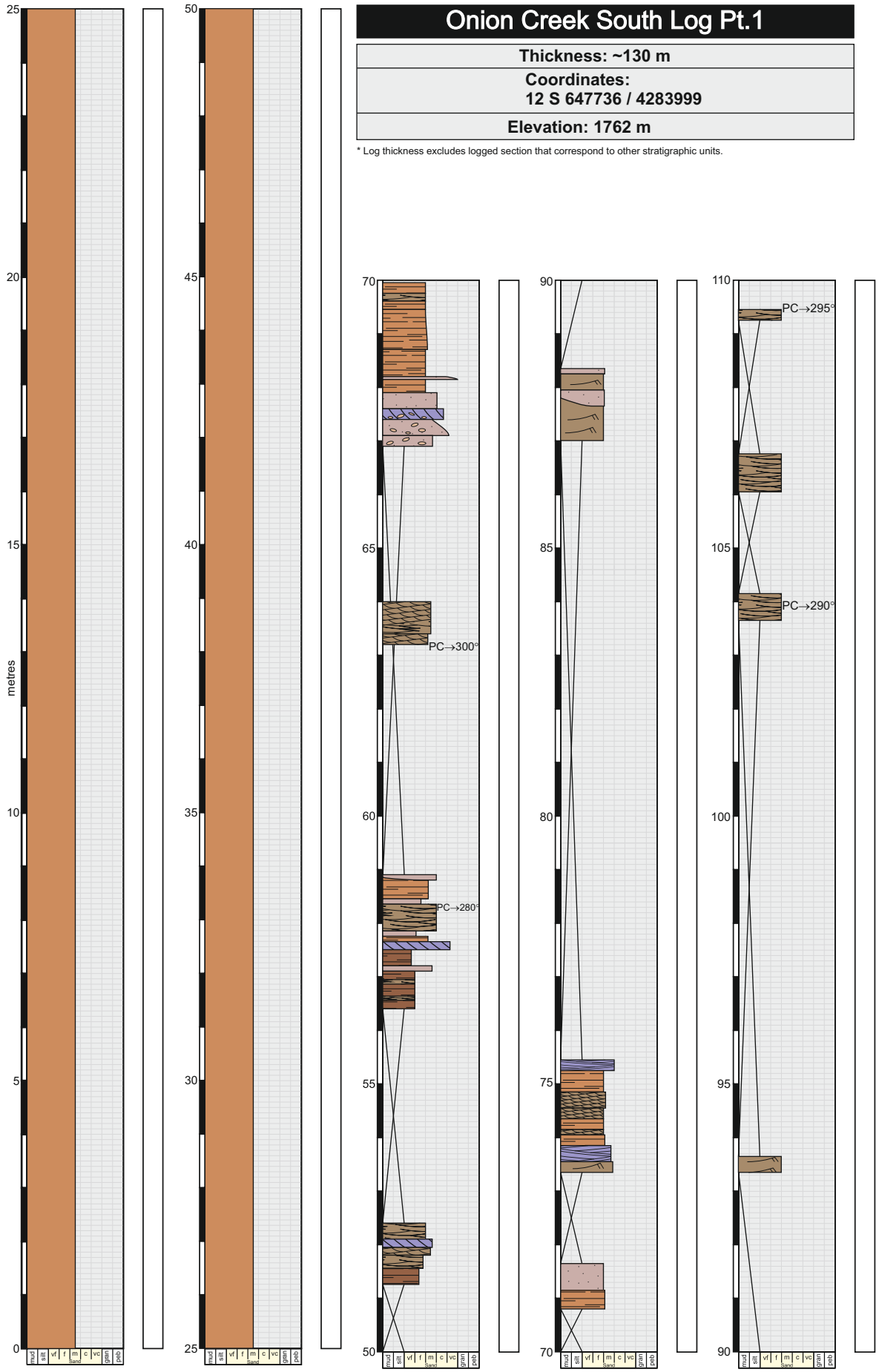
Onion Creek South Log Pt.1
Thickness: ~130 m
Coordinates:
12 S 647736 / 4283999
Elevation: 1762 m
* Log thickness excludes logged section that correspond to other stratigraphic units.
metres
PC→300°
PC→280°
PC→295°
PC→290°
mud
silt
vf
f
m
c
vc
gran
peb
Sand

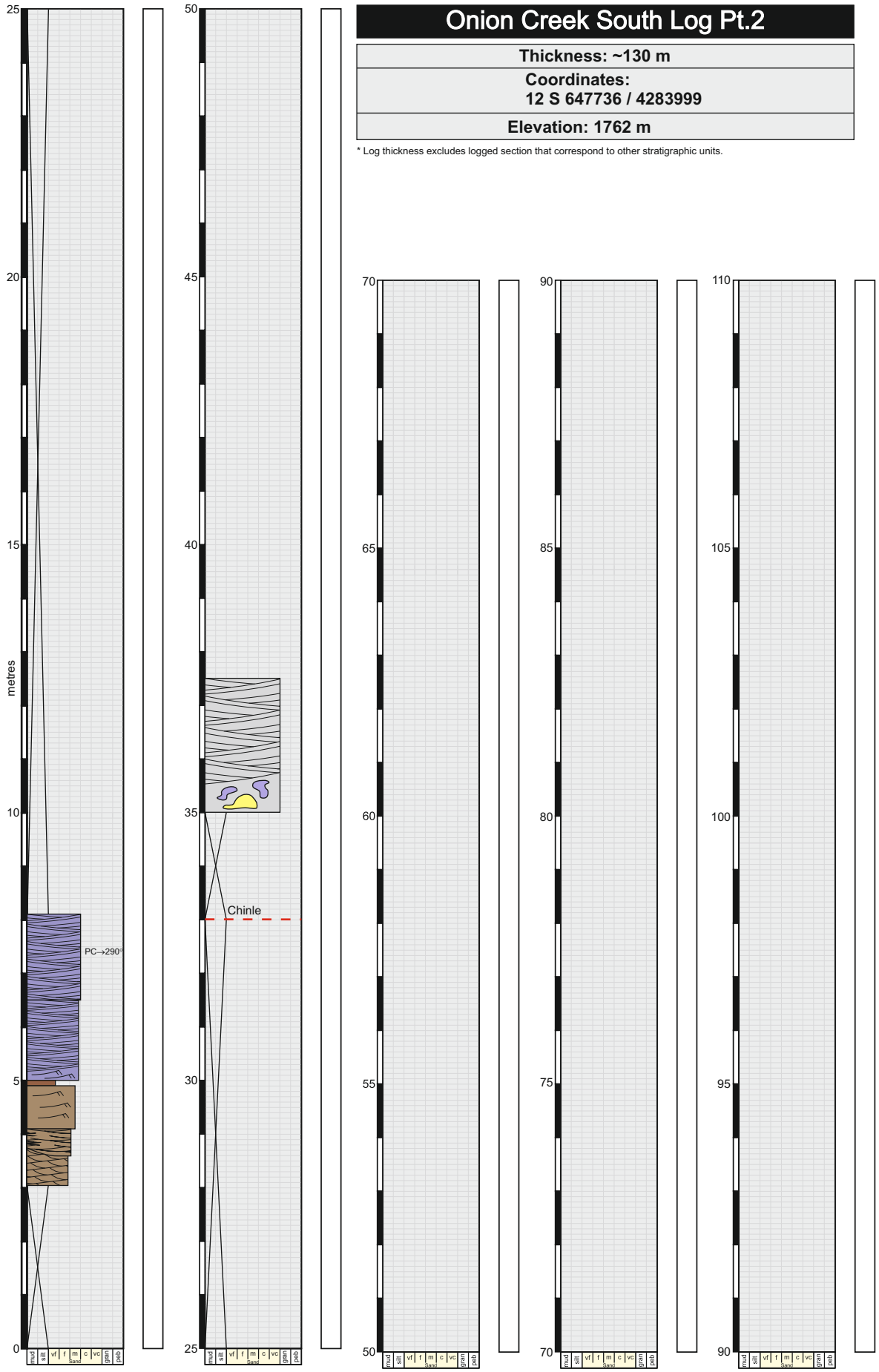
Onion Creek South Log Pt.2
Thickness: ~130 m
Coordinates:
12 S 647736 / 4283999
Elevation: 1762 m
* Log thickness excludes logged section that correspond to other stratigraphic units.
metres
PC→290°
Chinle
mud
silt
vf
f
m
c
vc
gran
peb
Sand

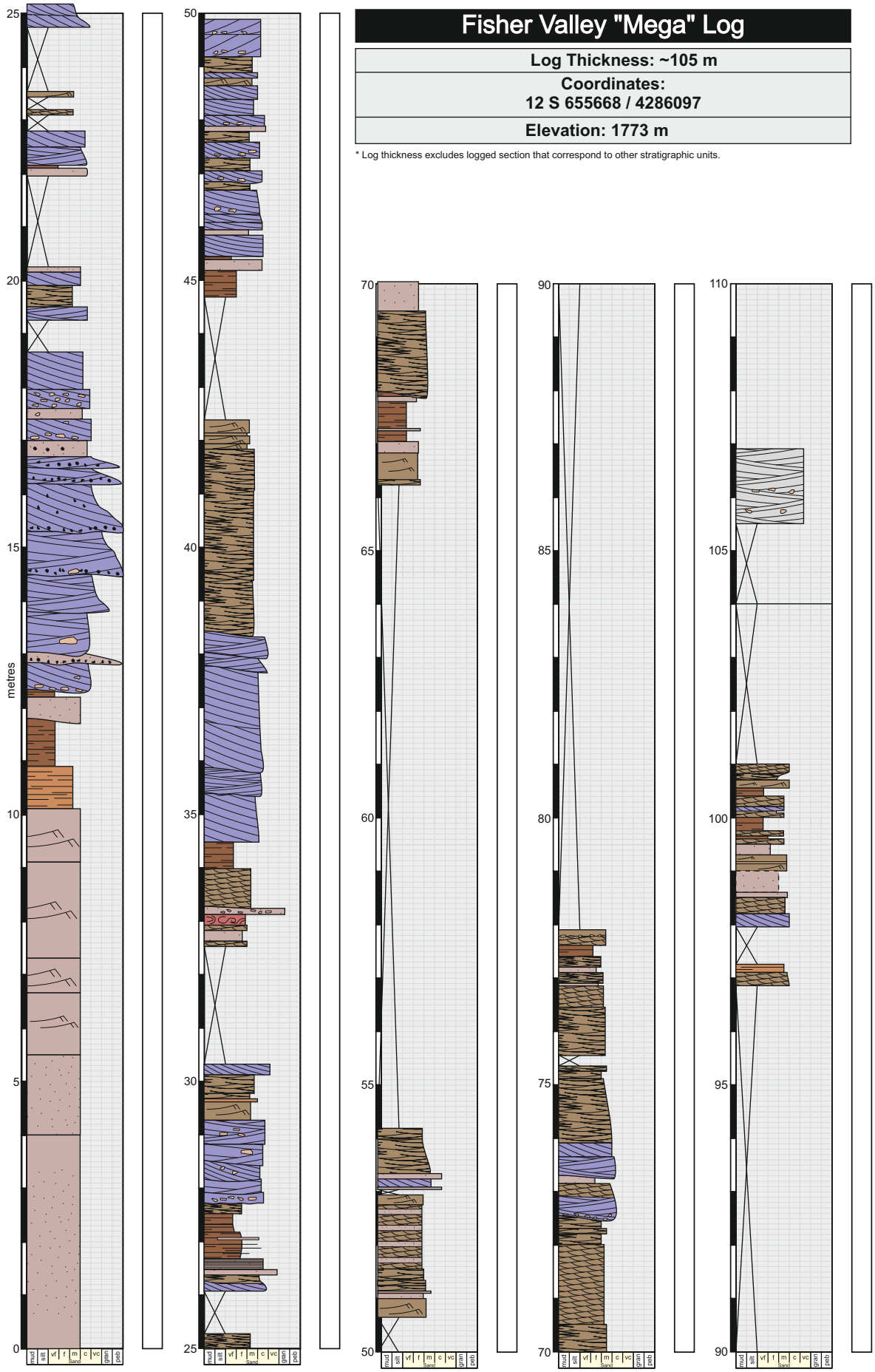
Fisher Valley "Mega" Log
Log Thickness: ~105 m
Coordinates:
12 S 655668 / 4286097
Elevation: 1773 m
* Log thickness excludes logged section that correspond to other stratigraphic units.
metres
mud
silt
vf
f
m
c
vc
gran
peb
Sand

Big Bend Campsite C Log
Log Thickness: 78 m
Coordinates:
12 S 632 467 / 4279125
Elevation: 1254 m
* Log thickness excludes logged section that correspond to other stratigraphic units.
metres
Base not seen
(Within Sewemup)
Chinle
mud
silt
vf
f
m
c
vc
gran
peb
Sand

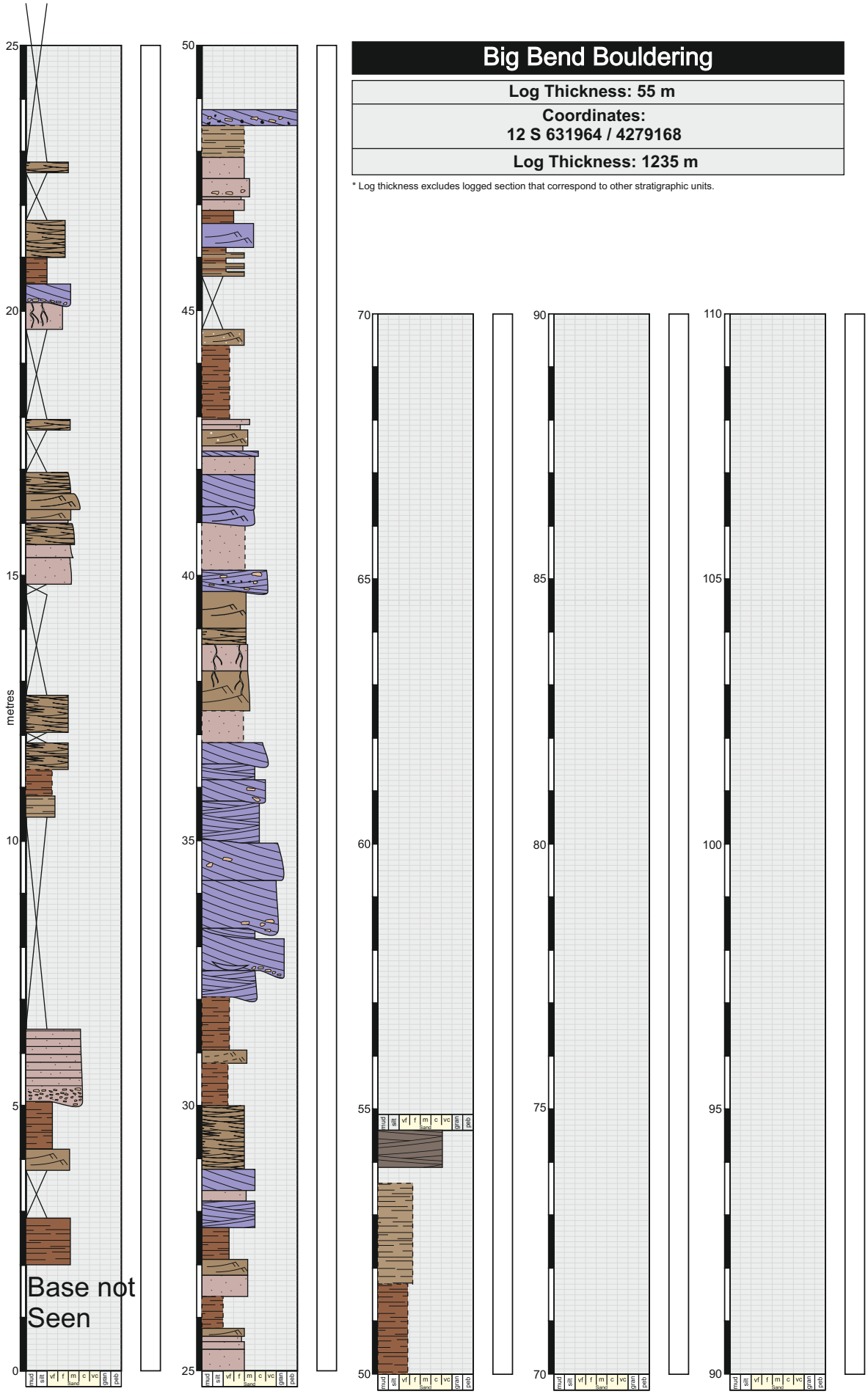
Big Bend Bouldering
Log Thickness: 55 m
Coordinates:
12 S 631964 / 4279168
Log Thickness: 1235 m
* Log thickness excludes logged section that correspond to other stratigraphic units.
metres
Base not Seen
mud
silt
vf
f
m
c
vc
gran
peb
Sand

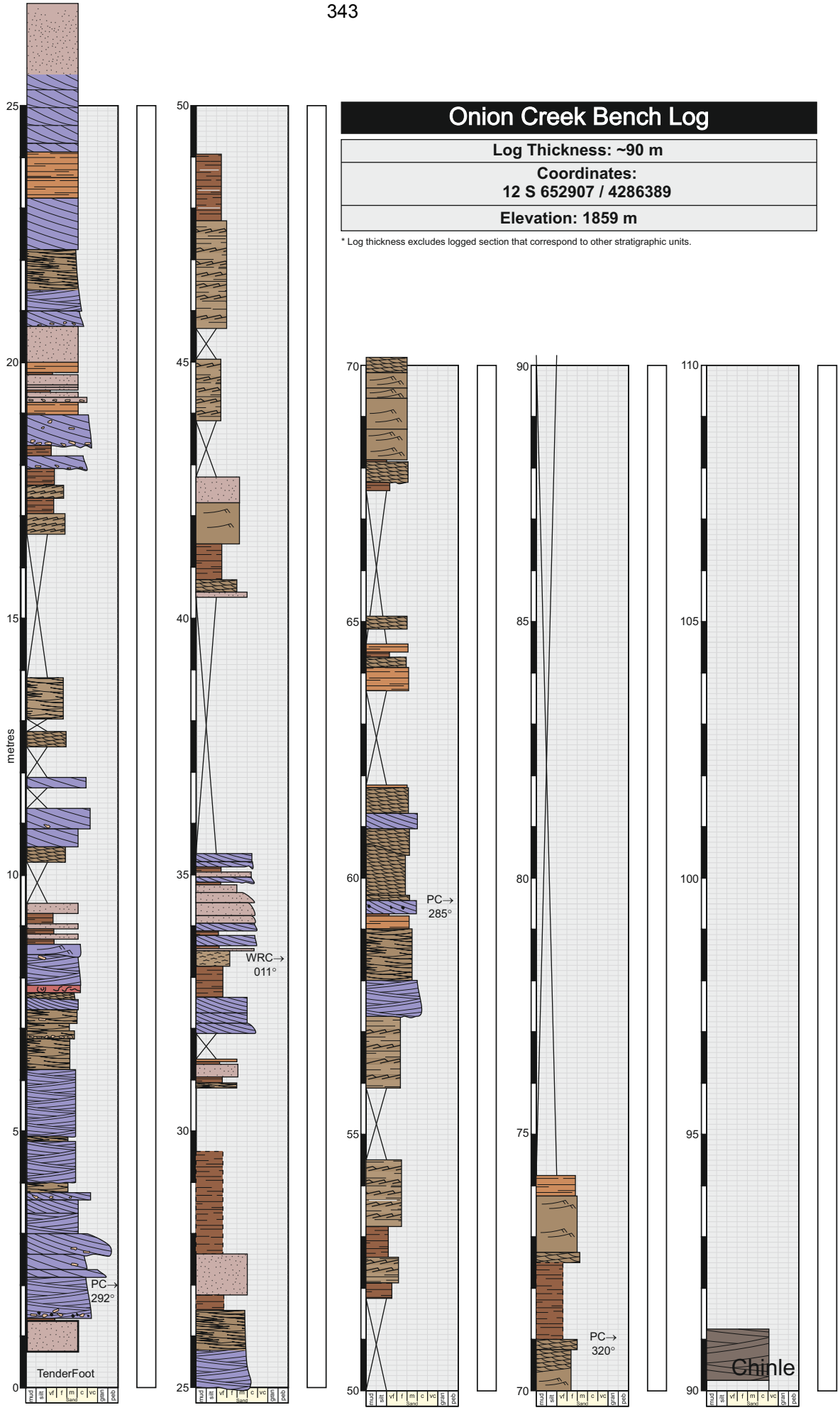
Onion Creek Bench Log
Log Thickness: ~90 m
Coordinates:
12 S 652907 / 4286389
Elevation: 1859 m
* Log thickness excludes logged section that correspond to other stratigraphic units.
metres
TenderFoot
PC→
292°
WRC→
011°
PC→
285°
PC→
320°
Chinle
mud
silt
vf
f
m
c
vc
gran
peb
Sand

Hittle Bottom Log
Log Thickness: 110 m
Coordinates:
12 S 645074 / 4291712
Elevation: 1361 m
* Log thickness excludes logged section that correspond to other stratigraphic units.
metres
Chinle
mud
silt
vf
f
m
c
vc
gran
peb
Sand

# Fisher Valley Head Log

**Log Thickness: ~120 m**

**Coordinates:**
**12 S 653736 / 4286042**

**Elevation: 1848 m**

* Log thickness excludes logged section that correspond to other stratigraphic units.

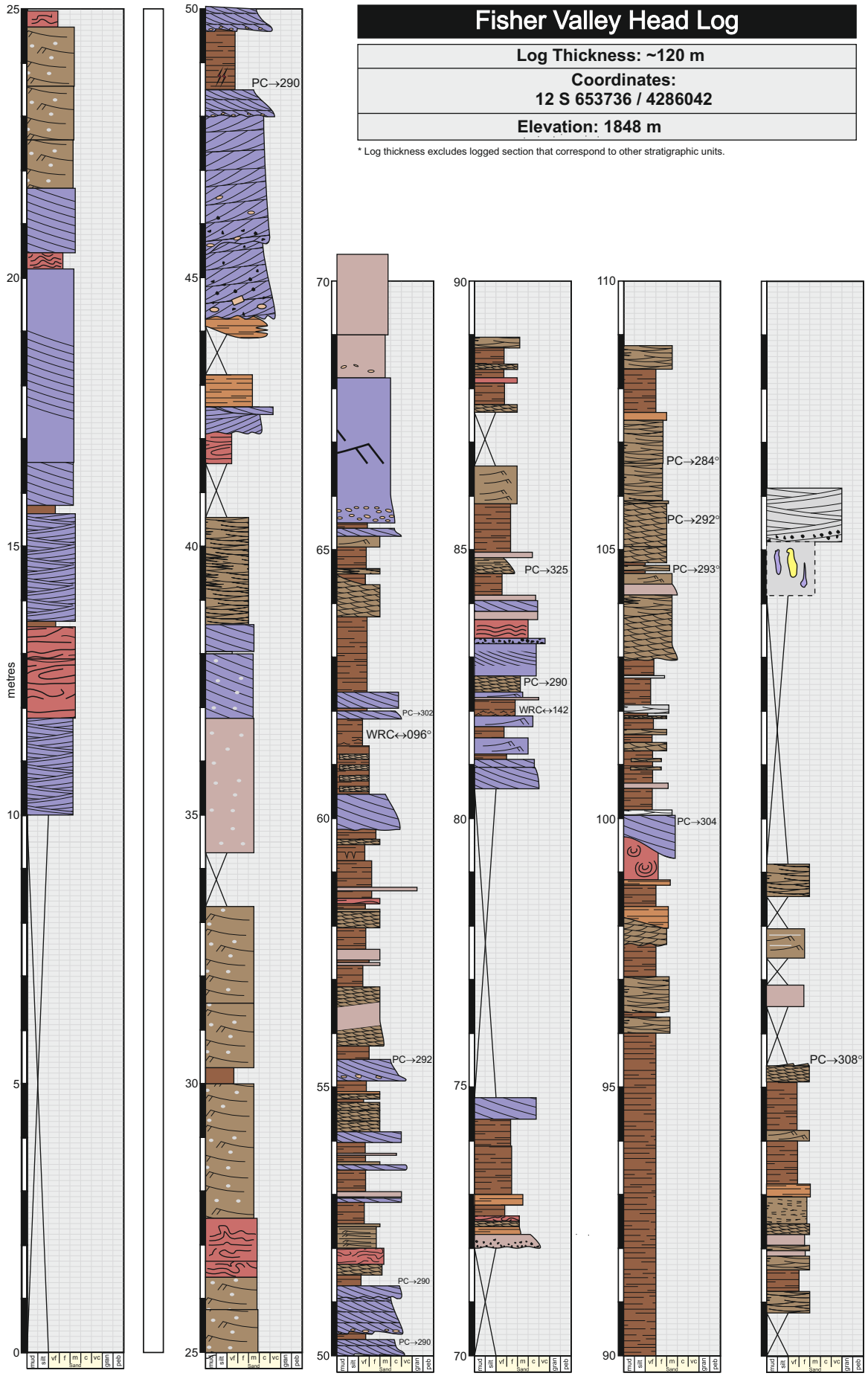

# Fisher Valley Ranch Log

**Log Thickness: 105 m**

**Coordinates:**
**12 S 656845 / 4281152**

**Elevation: 1975 m**

* Log thickness excludes logged section that correspond to other stratigraphic units.

Clay Hills 4x4 Track Log
Log Thickness: 109.95m
Coordinates: 12S
0557511 / 4133659
Elevation: 1380
* Log thickness excludes logged section that correspond to other stratigraphic units.
metres
WRC↔
048°
Tool
Marks
Channel
PC→
348°
Channel
mud
silt
vf
f
m
c
vc
gran
peb
Sand

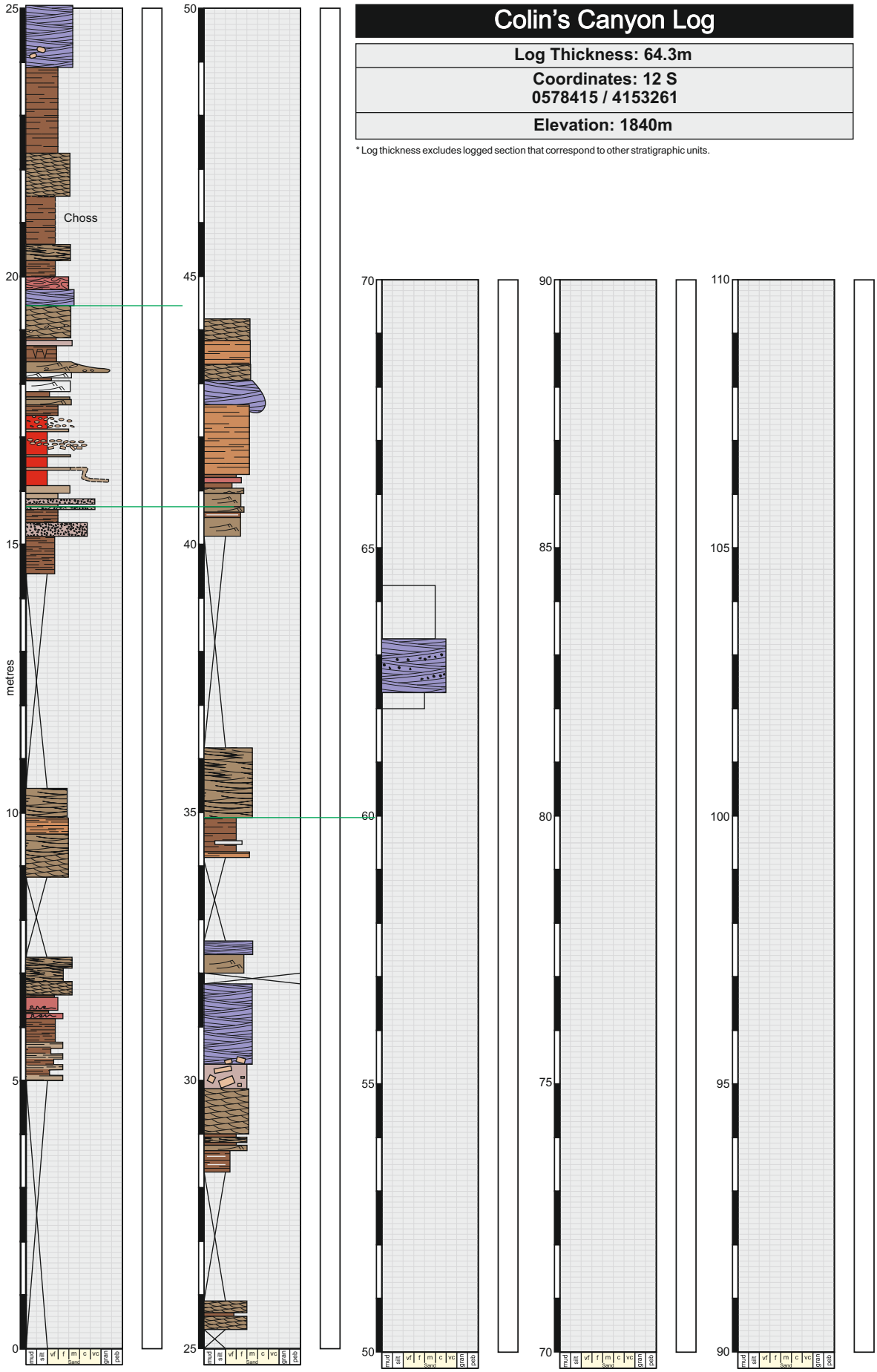
Colin's Canyon Log
Log Thickness: 64.3m
Coordinates: 12 S
0578415 / 4153261
Elevation: 1840m
* Log thickness excludes logged section that correspond to other stratigraphic units.
Choss
metres
mud
silt
vf
f
m
c
vc
gran
peb
Sand

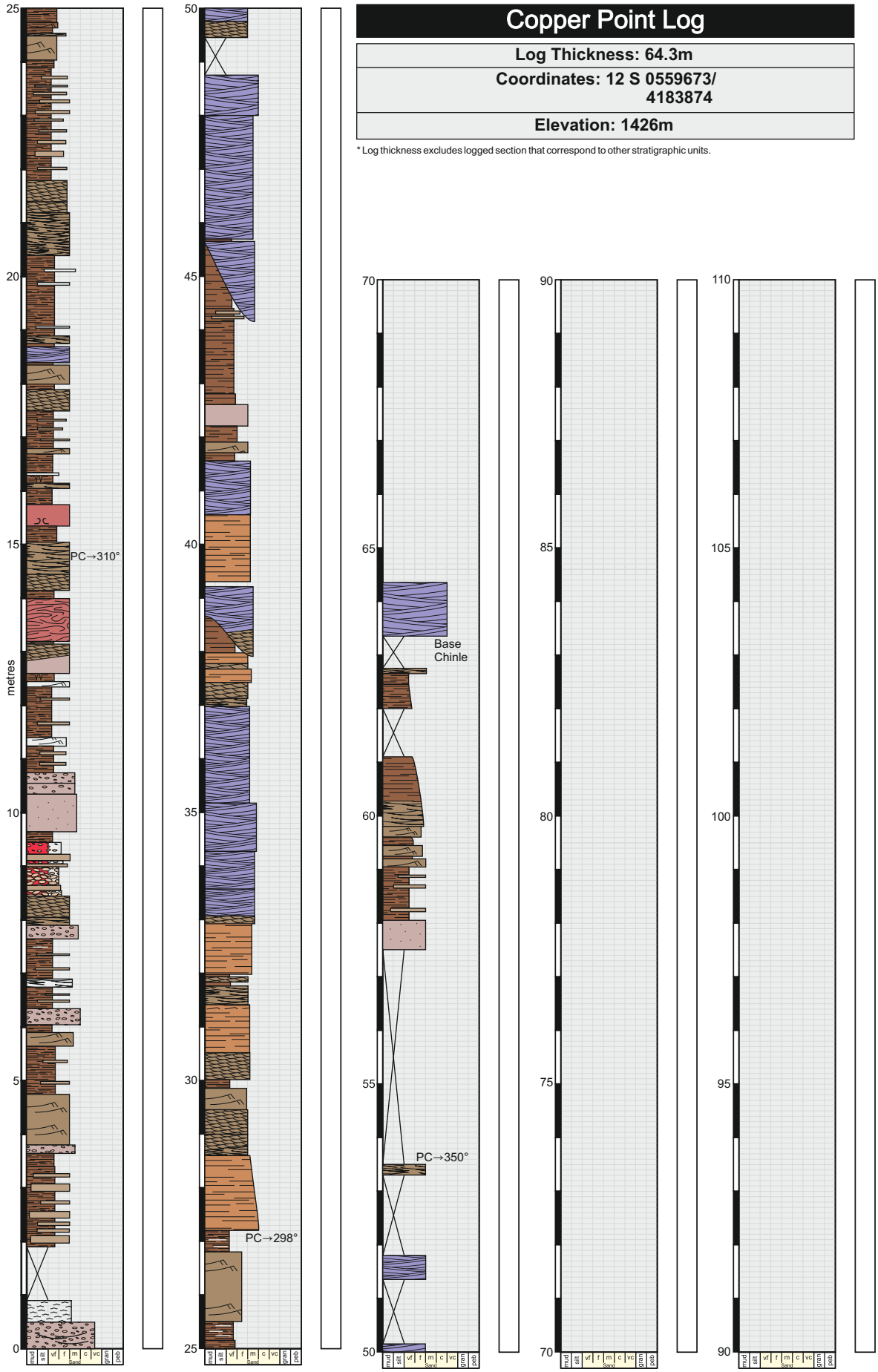
Copper Point Log
Log Thickness: 64.3m
Coordinates: 12 S 0559673/ 4183874
Elevation: 1426m
* Log thickness excludes logged section that correspond to other stratigraphic units.
metres
PC→310°
PC→298°
Base Chinle
PC→350°
mud
silt
vf
f
m
c
vc
gran
peb
Sand

Happy Jack Mine Log
Log Thickness: 50 m
Coordinates:
12 S 562835 / 4178725
Elevation: 1512 m
* Log thickness excludes logged section that correspond to other stratigraphic units.
metres
mud
silt
vf
f
m
c
vc
gran
peb
Sand

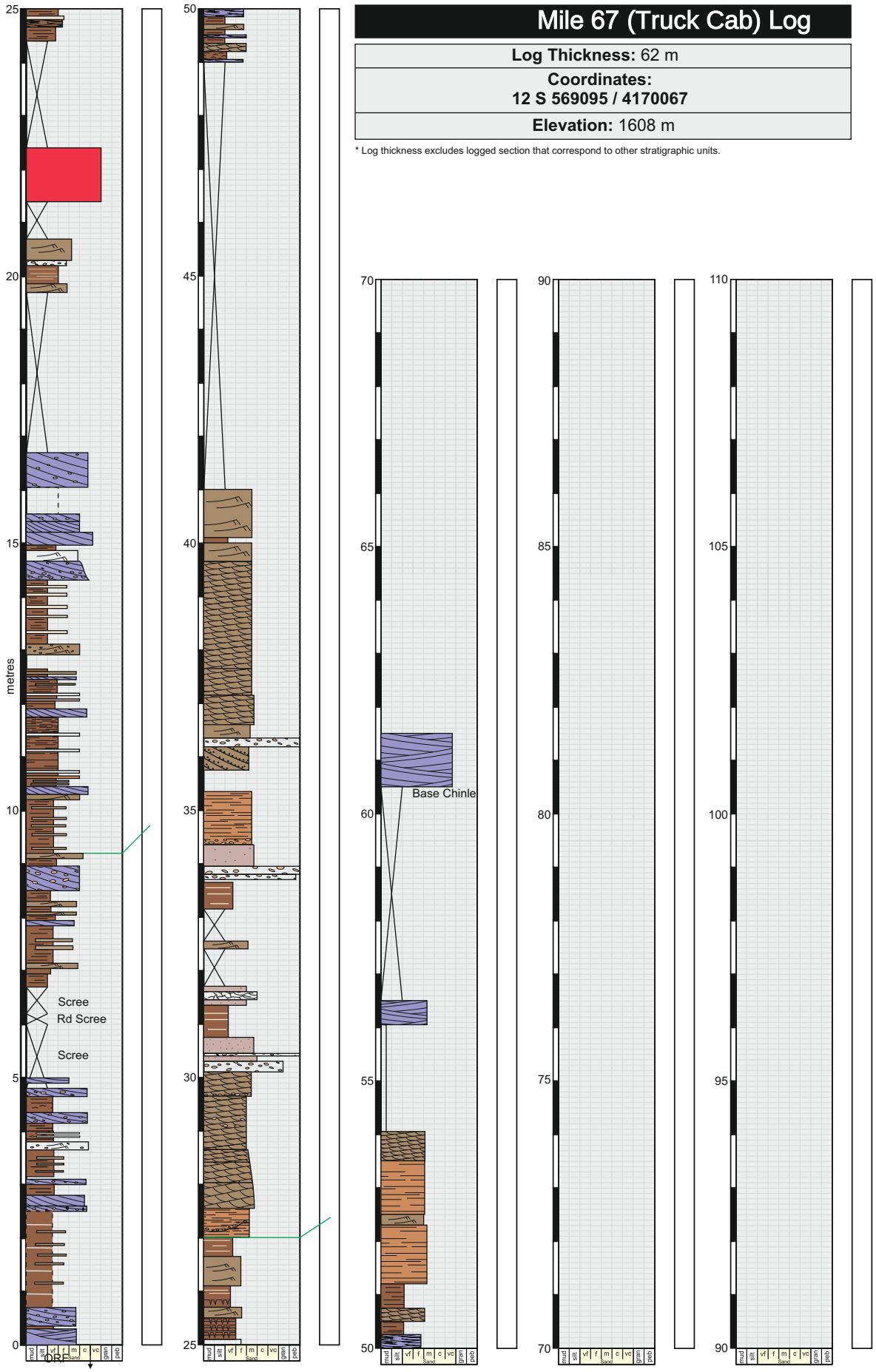
Mile 67 (Truck Cab) Log
Log Thickness: 62 m
Coordinates:
12 S 569095 / 4170067
Elevation: 1608 m
* Log thickness excludes logged section that correspond to other stratigraphic units.
metres
Scree
Rd Scree
Scree
Base Chinle
ORF
mud
silt
vf
f
m
c
vc
gran
peb
Sand

# Mile 71 (Fry Canyon) Log

**Log Thickness:** 80 m

**Coordinates:**
**12 S 573259 / 4166023**

**Elevation:** 1716 m

* Log thickness excludes logged section that correspond to other stratigraphic units.

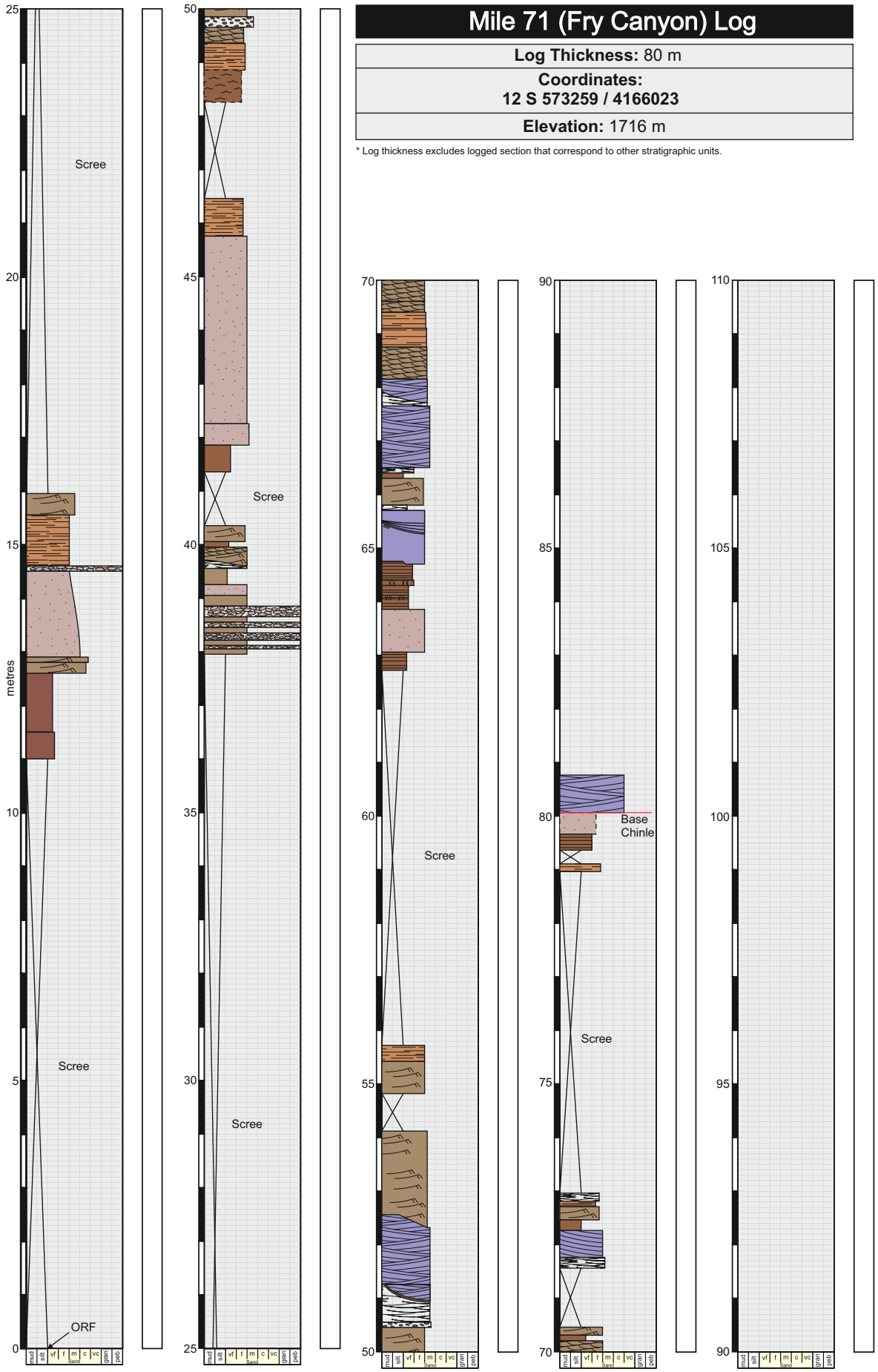

Mile 75 (Camp Site) Log
Log Thickness: 43 m
Coordinates:
12 S 577744 / 4166882
Elevation: 1830 m
* Log thickness excludes logged section that correspond to other stratigraphic units.
metres
PC→ 328°
PC→ 310°
Base Chinle
PC→ ~320°
mud
silt
vf
f
m
c
vc
gran
peb
Sand

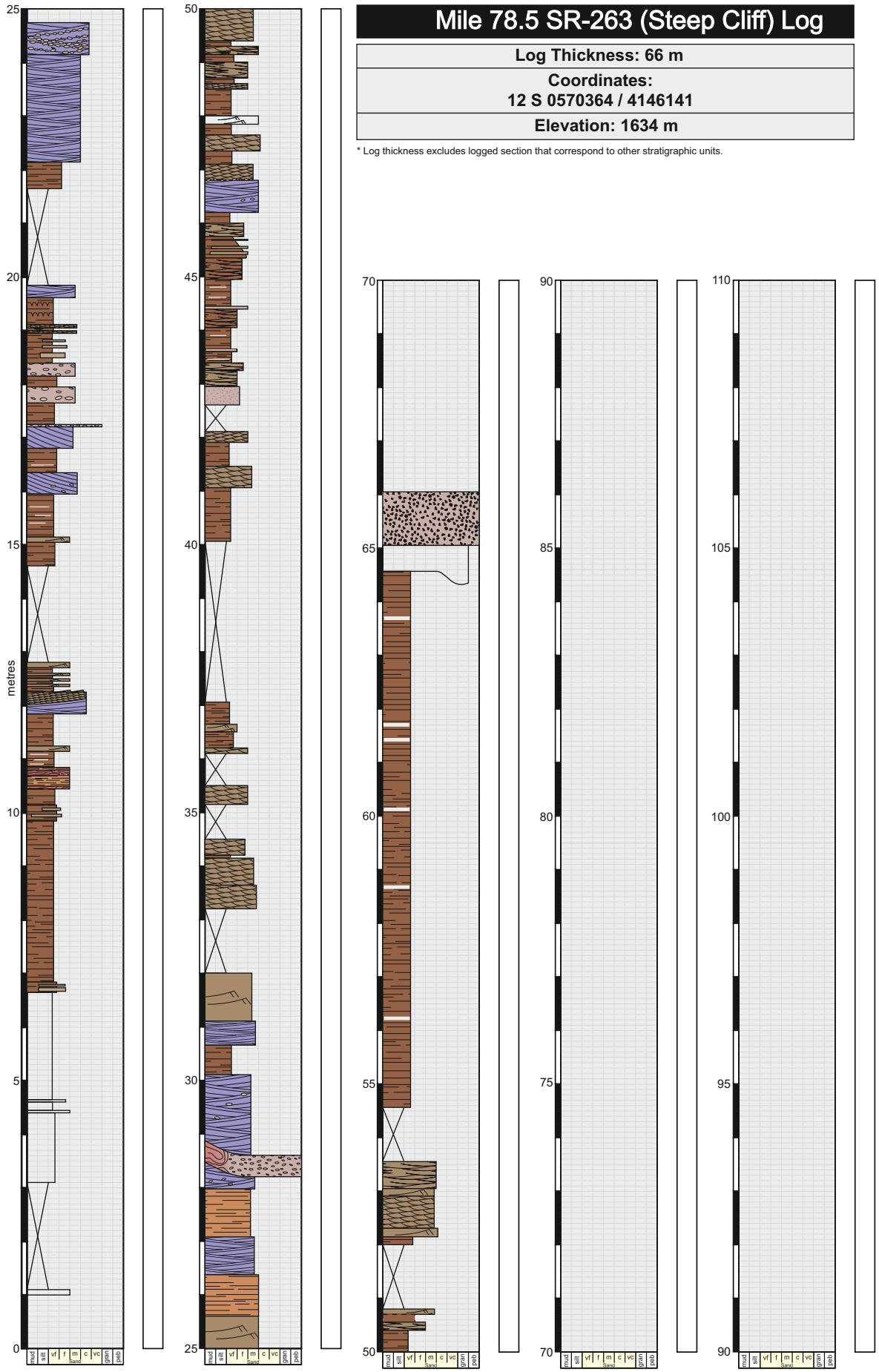
Mile 78.5 SR-263 (Steep Cliff) Log
Log Thickness: 66 m
Coordinates:
12 S 0570364 / 4146141
Elevation: 1634 m
* Log thickness excludes logged section that correspond to other stratigraphic units.
metres
mud
silt
vf
f
m
c
vc
gran
peb
Sand

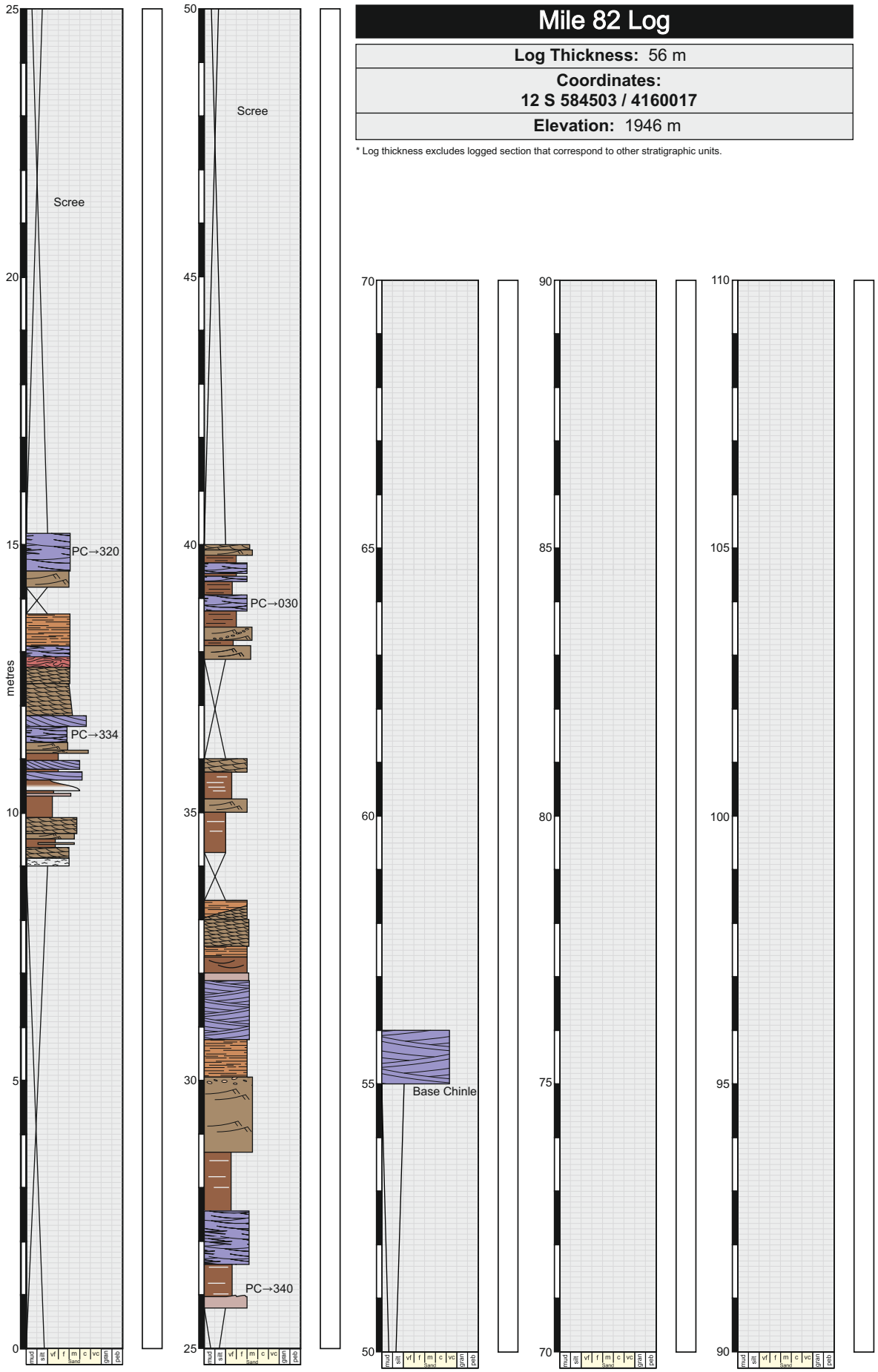
Mile 82 Log
Log Thickness: 56 m
Coordinates:
12 S 584503 / 4160017
Elevation: 1946 m
* Log thickness excludes logged section that correspond to other stratigraphic units.
metres
Scree
PC→320
PC→334
Scree
PC→030
PC→340
Base Chinle
mud
silt
vf
f
m
c
vc
gran
peb
Sand

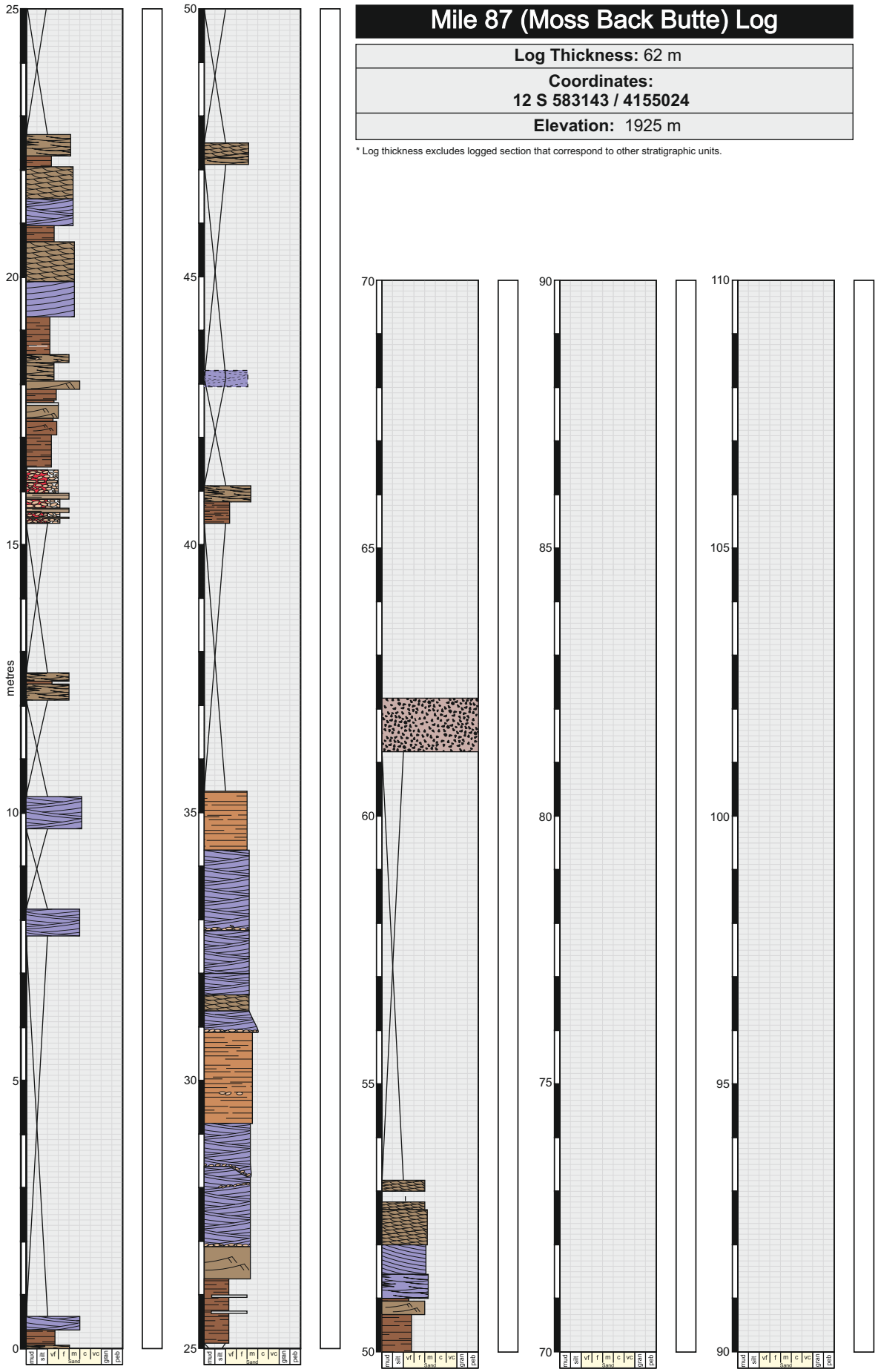
Mile 87 (Moss Back Butte) Log
Log Thickness: 62 m
Coordinates:
12 S 583143 / 4155024
Elevation: 1925 m
* Log thickness excludes logged section that correspond to other stratigraphic units.
metres
mud
silt
vf
f
m
c
vc
gran
peb
Sand

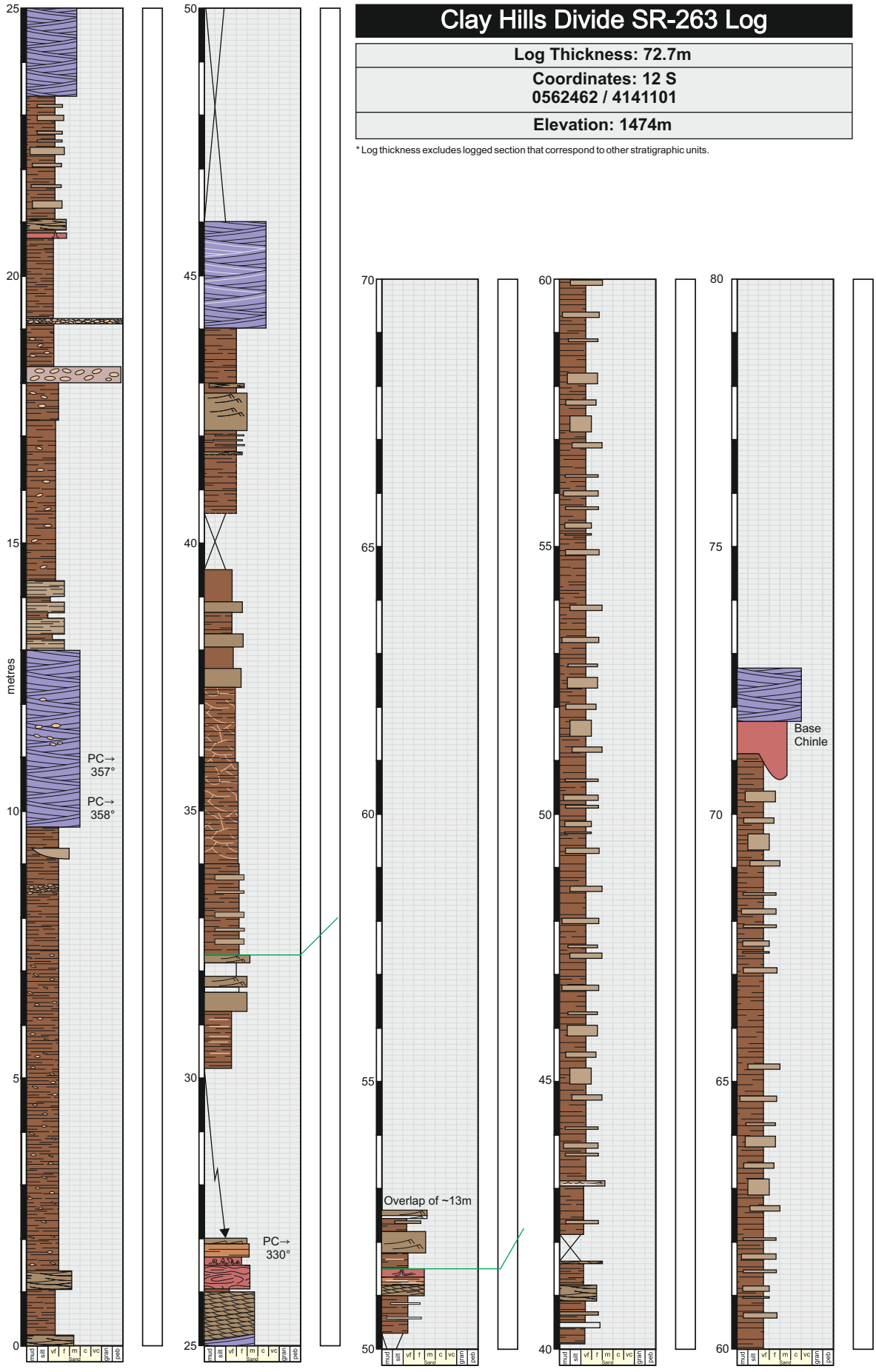
Clay Hills Divide SR-263 Log
Log Thickness: 72.7m
Coordinates: 12 S
0562462 / 4141101
Elevation: 1474m
* Log thickness excludes logged section that correspond to other stratigraphic units.
metres
PC→
357°
PC→
358°
PC→
330°
Overlap of ~13m
Base
Chinle
mud
silt
vf
f
m
c
vc
gran
peb
Sand